STUDY OF NATURALLY OCCURRING RADIONUCLIDES AND STABLE METALS IN SOILS OF WEST MALAYSIA

GHAZWA HATEM TAKLEEF ALZUBAIDI

FACULTY OF SCIENCE
UNIVERSITI MALAYA
KUALA LUMPUR

2022

STUDY OF NATURALLY OCCURRING RADIONUCLIDES AND STABLE METALS IN SOILS OF WEST MALAYSIA

GHAZWA HATEM TAKLEEF ALZUBAIDI

THESIS SUBMITTED IN FULFILMENT OF THE REQUIREMENTS FOR THE DEGREE OF DOCTOR OF PHILOSOPHY

INSTITUTE OF BIOLOGICAL SCIENCES
FACULTY OF SCIENCE
UNIVERSITI MALAYA
KUALA LUMPUR

2022

UNIVERSITI MALAYA

ORIGINAL LITERARY WORK DECLARATION

Name of Candidate: **GHAZWA HATEM TAKLEEF AL-ZUBAIDI**

Matric No: **17056053/1**

Name of Degree: **DOCTOR OF PHILOSOPHY**

Title of Project Paper/Research Report/Dissertation/Thesis ("this Work"):

STUDY OF NATURALLY OCCURRING RADIONUCLIDES AND STABLE METALS IN SOILS OF WEST MALAYSIA

Field of Study: **RADIATION BIOPHYSICS**

I do solemnly and sincerely declare that:

(1) I am the sole author/writer of this Work;
(2) This Work is original;
(3) Any use of any work in which copyright exists was done by way of fair dealing and for permitted purposes and any excerpt or extract from, or reference to or reproduction of any copyright work has been disclosed expressly and sufficiently and the title of the Work and its authorship have been acknowledged in this Work;
(4) I do not have any actual knowledge nor do I ought reasonably to know that the making of this work constitutes an infringement of any copyright work;
(5) I hereby assign all and every rights in the copyright to this Work to the University of Malaya ("UM"), who henceforth shall be owner of the copyright in this Work and that any reproduction or use in any form or by any means whatsoever is prohibited without the written consent of UM having been first had and obtained;
(6) I am fully aware that if in the course of making this Work I have infringed any copyright whether intentionally or otherwise, I may be subject to legal action or any other action as may be determined by UM.

Candidate's Signature Date: 12 APRIL 2022

Subscribed and solemnly declared before,

Witness's Signature Date: 12 APRIL 2022

Name:

Designation:

STUDY OF NATURALLY OCCURRING RADIONUCLIDES AND STABLE METALS IN SOILS OF WEST MALAYSIA

ABSTRACT

Linking scientific information to environmental parameters that influence radionuclide dispersion in response to chemical, physical, and biological responses within the soil profile is still lacking, particularly in the tropics. Bearing in mind the likelihood that nuclear energy will be a substantial component of social and economic development across the tropics in future decades due to climate change, this study sought to evaluate the behavior of radionuclides in the tropical environment. The primary objective of this study was to investigate the vertical distribution of the activities of natural radionuclides ^{226}Ra, ^{232}Th, and ^{40}K, and chemical elements in different areas of tropical soils in order to obtain a common understanding of the reactive environment factors associated with the reactions of radionuclides, as well as, assessing radiation risks according to this activity. A total of 228 soil samples were collected randomly at depths of 0-10, 10-20, 20-30 and 30-40 cm, from August 2013 to October 2017 from six agricultural regions of Peninsular Malaysia. In addition, 40 soil samples were collected at one depth of 0-40 cm from a paddy field in Kedah, Malaysia, to study seasonal changes that may have a potential impact on radionuclides behavior, 20 samples were collected during the wet season or growing season (March-April) and 20 samples during the dry season or harvest season (June-August). In all the examined study areas, the mean concentration values of ^{226}Ra, ^{232}Th, and ^{40}K were comparable higher than the global averages provided by the United Nations Scientific Committee on the Effects of Atomic Radiation (UNSCEAR). The study areas did not show clear spatial divergence in the calculated values of radionuclide and chemical element concentrations. The study of the distribution patterns of radionuclides and elements were affected by the same

mechanisms and factors within the soil profile and adopted a consistent behavior within the interactive environment of tropical soils. The calculated mean values of the radium equivalent activity (Ra_{eq}) for the study areas did not exceed the acceptable safe limit of 370 $Bq.kg^{-1}$ recommended by UNSCEAR. The calculated values of the mean absorbed dose rate (D) for the study areas were higher than the overall global value of 60 n Gy h^{-1}, where the mean values ranged from 103.26 to 113.30 n Gy h^{-1}. The measured mean values of the annual effective dose equivalent (AEDE) for the study areas fall within the recommended levels by the International Committee on Radiological Protection (ICRP) which is 1 mSv $year^{-1}$. The measured values of the external hazard index (H_{ex}) for the study areas did not exceed the acceptable safe limit value (less than or equal to one). Radionuclides showed a similar tendency in most of the study areas in their correlations with chemical soil components. These consistent correlations indicate that radionuclide mobility underwent the same migration mechanisms and that its behavior was modified by many unique features of the tropical environment.

Keywords: Radioactivity, Environment, West Malaysia, Heavy metals, Microbial, Tropics, Soil.

STUDY OF NATURALLY OCCURRING RADIONUCLIDES AND STABLE METALS IN SOILS OF WEST MALAYSIA

ABSTRAK

Menghubungkan maklumat saintifik kepada parameter persekitaran yang mempengaruhi penyebaran radionuklid sebagai tindak balas kepada tindak balas kimia, fizikal dan biologi dalam profil tanah masih kurang, terutamanya di kawasan tropika. Dengan kesadaran akan kemungkinan tenaga nuklear menjadi komponen penting dalam pembangunan sosial dan ekonomi di kawasan tropika dalam beberapa dekad yang akan datang disebabkan oleh perubahan iklim, kajian ini berusaha untuk menilai tingkah laku radionuklida di persekitaran tropika. Objektif utama kajian ini adalah untuk menyiasat taburan menegak aktiviti radionuklida semula jadi (^{226}Ra, ^{232}Th, dan ^{40}K) dan unsur-unsur kimia di kawasan tanah tropika yang berlainan, bagi memahami faktor persekitaran reaktif yang berkaitan dengan tindak balas radionuklida, serta menilai risiko radiasi mengikut aktiviti ini. Sebanyak 228 sampel tanah dikumpulkan secara rawak dari kedalaman 0-10, 10-20, 20-30 dan 30-40 cm, antara Ogos 2013 dan Oktober 2017 dari enam kawasan pertanian Semenanjung Malaysia. Selain itu 40 sampel tanah dari satu kedalaman 0-40 cm dari sawah di Kedah Malaysia, dikumpulkan untuk mengkaji perubahan musim yang mungkin berpotensi mempengaruhi perilaku radionuklida, di mana 20 sampel dikumpulkan pada musim hujan atau musim tanam (Mac-April) dan 20 sampel semasa musim kemarau atau musim menuai (Jun-Ogos). Di semua kawasan kajian yang diperiksa, nilai kepekatan min ^{226}Ra, ^{232}Th, dan ^{40}K adalah setanding dan lebih tinggi daripada purata global yang disediakan oleh Jawatankuasa Saintifik Pertubuhan Bangsa-Bangsa Bersatu mengenai Kesan Sinaran Atom (UNSCEAR). Kawasan kajian tidak menunjukkan perbezaan spasial yang jelas dalam nilai kiraan kepekatan unsur radionuklida dan kimia. Kajian corak penyebaran

radionuklida dan elemen menunjukkan pengaruh mekanisme dan faktor yang sama dalam profil tanah dan menerapkan tingkah laku yang konsisten dalam persekitaran interaktif tanah tropika. Nilai min yang dikira bagi aktiviti setara radium (Ra_{eq}) untuk kawasan kajian tidak melebihi had selamat yang boleh diterima iaitu 370 $Bq.kg^{-1}$ yang disyorkan oleh UNSCEAR. Nilai yang dikira dari kadar purata dos yang diserap (D) untuk kawasan kajian adalah lebih tinggi daripada nilai global keseluruhan 60 nGy h^{-1}, di mana nilai min berkisar di antara 103.26 hingga 113.30 nGy h^{-1}. Nilai min yang diukur dari setara dos efektif tahunan setara (AEDE) kawasan kajian adalah dalam tahap yang disyorkan oleh Jawatankuasa Antarabangsa Perlindungan Radiologi (ICRP) yang merupakan 1 mSv year−1. Nilai yang diukur dari indeks bahaya luaran (Hex) untuk kawasan kajian tidak melebihi nilai had selamat yang boleh diterima (kurang dari atau sama dengan satu). Di kebanyakan radionuklida menunjukkan kecenderungan serupa dengan komponen tanah kimia. Korelasi yang konsisten ini menunjukkan bahawa mobiliti radionuklid menjalani mekanisme migrasi yang sama dan tingkah lakunya diubah oleh banyak ciri unik persekitaran tropika.

Keywords: Radioaktiviti, Alam Sekitar, Malaysia Barat, Logam berat, Mikrob, Tropika, Tanah.

ACKNOWLEDGEMENTS

Foremost, I would like to express my sincere gratitude to my supervisor Associate Professor Dr. Fauziah Shahul Hamid for providing invaluable guidance throughout this research. Her dynamism, vision, patience, insightful comments, suggestions and continuous support have deeply inspired me. My gratitude extends to my co-supervisor Professor Dr. Irman Abdul Rahman his invaluable advice, continuous support, and patience during my PhD study.

My gratitude extends to UMRP- Centre of Research Grant Management (PPGP) for the funding opportunity to undertake my study. I would like to express gratitude to Professor Dr. D. A. Bradley for his treasured support which was really influential in shaping my experiment methods and critiquing my results. I also thank Dr. Khandoker Asaduzzaman for his mentorship.

Special thanks to my colleagues in the Microbiology lab Iffa, Jayanthi and Helen for their help and stimulating discussions. My thanks also go to the staffs of Radiation, ICP-MS, and Microbiology laboratories for their various form of technical support during sample preparation and measurement. All support provided by Faculty of Science, University of Malaya is highly respected and appreciated.

Last but not least, I would like to thank my parents, husband and children for their encouragement, support and patience throughout the PhD journey.

TABLE OF CONTENTS

LIST OF FIGURES

LIST OF TABLES

LIST OF SYMBOLS AND ABBREVIATIONS

Al	:	Aluminium
APM	:	Airborne particulate matter
As	:	Arsenic
ATSDR	:	Agency for toxic substances and disease registry
Ba	:	Barium
Bi	:	Bismuth
Ca	:	Calcium
CAC	:	Codex alimentarius commission
Cd	:	Cadmium
CDC	:	Centers for disease control and prevention
CICAD	:	Concise international chemical assessment document
CNS	:	Central Nervous System
Co	:	Cobalt
Cr	:	Chromium
Cu	:	Copper
DNA	:	Deoxyribonucleic acid
DPP	:	Differential Pulse Polarography
EC	:	Electron capture
FAO	:	Food and agriculture organization
Fe	:	Iron

Ge	:	Germanium
GFAAS	:	Graphite furnace atomic absorption spectrometry
HG- FS	:	Hydride generation atomic fluorescence spectrometry
HPGe	:	High purity germanium
IAEA	:	International atomic energy agency
ICRP	:	International commission for radiological protection
IDPH	:	Illinois department of public health
K	:	Potassium
keV	:	Kilo electron volt
MeV	:	Mega electron volt
Mg	:	Magnesium
Mn	:	Manganese
Al	:	Aluminum
OM	:	organic matter
NORM	:	Naturally occurring radioactive material
TENORM	:	Technologically enhanced naturally occurring radioactive material
TF	:	Transfer Factor
UNSCEAR	:	United nations scientific committee on the effects of atomic radiation
WHO	:	World health organization
XRFS	:	X-ray fluorescence spectrometry
Zn	:	Zinc
P	:	Phosphorous

^{40}Ar	:	argon-40
Mn	:	Manganese
Mg	:	Magnesium
α	:	Alpha
B	:	Beta
γ	:	Gamma
ICP-MS	:	Inductively coupled plasma mass spectrometry
IAEA	:	International atomic energy agency
Ca	:	Calcium
Cr	:	Concentration Ratios
Kd	:	Distribution Coefficient
OC	:	Organic Carbon

LIST OF APPENDICES

CHAPTER 1: INTRODUCTION

1.1 Research background

The geographical area of interest includes the vast region of the globe north and south of the equator, apart from the shared feature that the region generally enjoys a warmer climate than the temperate regions of the planet. This region contains many countries with high population density, increasing industrialisation, the current concerns regarding climate change; limitations on the availability of and access to fossil fuels, there a strong expectation that nuclear energy will play a substantial role in the social and economic development of human societies over the next few decades, the knowledge of well-managed nuclear power is one of the cleanest, cheapest, and most reliable means of providing base-load electricity. These variables highlight the need of gaining a better knowledge of radionuclide environmental behaviour in the tropics, which may be influenced by factors such as human activities, the operation of nuclear power reactors and associated facilities, and nuclear waste disposal sites. The anticipated developments will be more pronounced in tropical regions of the planet with the current population levels and predicted growth. Given those assumptions, it is also pertinent to ensure that the possible consequences of a nuclear future are well considered and that the affected populations are well placed to make use of the many advantages that nuclear science has to offer. Hence, knowledge of the nature of radiation in the environment, as well as of the behavior of any radioactivity released into it, is essential to best manage such development.

At the outset, it is important to have an understanding of the basic elements of the radiological environment of the subject before embarking on the journey through the topic, in order to identify and understand the many mechanisms that control the behavior and influence of radioactive materials within the biosphere and use the unique characteristics of radionuclides to trace ecological processes. Knowledge of the

radiological environment is an integrated science that includes components of nuclear physics, chemistry, biology, ecology, physiology, toxicology, and risk assessment.

The amount of energy and the forms of radiation emitted vary tremendously among the radioactive elements. It is because of this variation that the applications of radioactive materials range from powerful tracers of biological, physiological, and geological cycles to healing medicine to weap- ons of mass destruction. Tracking the behavior of radionuclides is of interest for several reasons. It can be used for investigations into environmental processes, or used as a tracking marker or marker of human activity, such as tracking industrial pollution or detecting nuclear weapons tests, as well as, estimating the radiative effect of the presence of the radionuclides themselves, that is, to estimate the dose on humans and non-human biota.

The distribution of radionuclides in the environment is determined by five main factors. First, the source of radionuclides and the mechanism through which they enter Second, the processes of participation of radionuclides in chemical reactions and their association with other molecules. Third, horizontal and vertical mixing mechanisms (primarily perturbed) may cause dilution and dispersion to parts distant from its place of origin. Fourth, wet and dry deposition to the Earth's surface may result in its physical removal. Finally, radioactive decay, quantified by the radionuclide's half-life, acts as another removal mechanism.

The tropical climate is characterised by high temperatures without significant seasonal variation and a relatively constant day length, which remains close to 12 hours throughout the year. Typically, rainfall is concentrated during monsoon season. As described by Wambeke, (1992), tropical soils are considered the products of interactions between this unique climate and the parent geological materials of the Earth's crust. A full range of parent materials occurs in the tropics, including very young basalt and serpentine landscapes. Landscapes in the tropics can be placed in four broad categories

that are useful when considering soil types and radionuclide behavior: (1) old and tectonically stable regions, (2) young and tectonically active regions, (3) tropical karst, and (4) tropical coasts (Reading, Thompson & Millington, 1995; Twining & Baxter, 2012). Tropical coasts are frequently fringed by extensive fluviomarine features, such as sediment plains, formed by the deposition of material eroded due to high-intensity rainfall. Other coastal geomorphologies that lead to distinctive soil properties are the coral reefs and atolls, algal mats, and mangrove mudflat systems (Twining & Baxter, 2012). Weathering within the equatorial climatic regime is the major process contributing to the properties of tropical soils. Due to relatively high temperatures and high-intensity rainfall in parts of the region, weathering is rapid and the strong leaching leads to an abundance of highly stable minerals such as kaolinite and sesquioxides (Naidu *et al.,* 1998). The soil types of the tropics are described, with some variation in categorisation, in several texts. In the classification scheme used by Wambeke, (1992), the soils in the tropical areas consist of approximately 25% oxisols, 20% aridisols, 20% alfisols, 10% of ultisols, and 10% entisols. The oxisols and other highly weathered soil types, including alfisols and ultisols, which predominate in the humid tropics, are important for agriculture and occupy extensive areas of land used for crop and food production. These soils are dominated by low activity sesquioxide minerals (i.e. oxides and hydroxides of iron and aluminium) and 1:1 layer silicates (kaolin), both of which have a variable surface charge (Naidu *et al.,* 1998; Twining & Baxter, 2012). In recent years, models of the behavior of potentially toxic elements in soils have been developed for temperate soils, which tend to have quite different characteristics to those of tropical soils. Typically, temperate soils have much higher concentrations of more active clay minerals, including the 2:1 layer silicates, which possess permanent charge and therefore differ in ion exchange properties from tropical soils. As noted by Rieuwerts, (2007), the major tropical soil types are distinguished by low activity clays, low organic

matter contents, low pH values, and high levels of Fe oxides. In tropical soils, the combination of relatively low pH, low organic matter, and the dominance of kaolinite tends to mitigate against the retention of heavy metals. In contrast, the Fe- oxide content might have a proportionally greater importance in heavy metal retention. For example, it has been reported that iron oxides are important in adsorbing uranium in tropical soils (Payne *et al.,* 1994). The general conclusion is that heavy metals will tend to be comparatively mobile in tropical soils and appear to be relatively bioavailable (Rieuwerts, 2007).

Velasco *et al.,* (2008) identified the two main factors distinguishing tropical soils and affecting radionuclide transfer factors as follows:

- In tropical environments, almost all organic material that reaches the soil surface decomposes rapidly, so the surface accumulation of soil organic matter is minimal. Consequently, there is rapid recycling of nutrients and contaminants into the vegetation. In temperate zones, the decomposition of organic debris is slower and the accumulation of soil organic matter is usually greater than the rate of decomposition, resulting in highly organic surface soil.
- In the tropics, due to the relatively highly aged soils and high mineral weathering rates, clays of low exchange activity, such as kaolinite, are more common than in temperate zones. This leads to soils that, despite having high clay content, have a low exchange capacity.

Understanding the mobility of radionuclides under tropical conditions is a high priority because these soils provide food resources for large populations.

1.2 Problem statement

Peninsular Malaysia is situated at the southernmost part of the Thai/Malay Peninsula, with a total land area is about 130,000 km².

Malaysia, situated near the equator, typically has climatic characteristics of uniform high temperatures, high humidity, and ample rainfall throughout the year, although the geography of Malaysia may cause differences in the microclimate of the country's regions. The wind is generally light, where is located in the equatorial doldrums area (Paramananthan, 2000, Ashraf *et al.,* 2017).

Malaysia is subject to the El Niño impact in the dry season, which reduces rainfall. Climate change is expected to have a major influence on Malaysia, increasing sea level and rainfall (Marshall, 2008).

There are three main type of seasonal variation of rainfall in Peninsular Malaysia. On the eastern coast of the states, November, December, and January are the months with maximum rainfall, while June and July are the driest months in most districts, over the rest of the Peninsula with the exception of the southwest coastal area, the monthly rainfall pattern shows two periods of maximum rainfall separated by two periods of minimum rainfall. The primary maximum generally occurs in October-November, whereas the secondary maximum generally occurs in April-May. Over the northwestern region, the primary is generally occurs in April-May, whereas over the northwestern region, the primary minimum occurs in January-February with the secondary minimum in June-July. Over the southwest coastal area, October and November are the months with maximum rainfalls, and February is the month with the minimum rainfall (Wong, 2009, Ashraf *et al.,* 2017).

Large areas of land are used as palm oil plantations, rubber plantations, and paddy fields. As of 2011, the percentage arable land in Malaysia is 5.44%. Croplands consist of 17.49% while other land uses consists of 77.07% (Ashraf *et al.,* 2017).

Although the climate of Malaysia as characterized by its high temperature and high rainfall exerts a tremendous influence on the weathering and soil forming processes, the parent material is also important in soil genesis in Malaysia.

Natural radioactivity of soils is largely controlled by the mineral composition of the parent material. To a lesser extent, radionuclides are adsorbed onto soil components (organic matter, clays, carbonates, Fe and Mn oxides) that can take part in biogeochemical processes.

Tropical environments have a unique climate that impacts the properties of soils and the mobility of radionuclides due to of the higher temperatures and, in particular, the patterns of rainfall. In many tropical environments there are monsoonal climates, implying intense episodic rainfall events; a fluctuating water table; and cyclic saturation and unsaturation with associated redox changes and flooding. A major implication of the flooded surface environment (such as rice paddies) is that atmospheric radionuclides are often deposited onto standing water rather than onto soil (Choi *et al.,* 2005).

Soils play a major role in biogeochemical cycles of elements and nuclides. Elements are contained within the crystal structure of soil-forming minerals as well as bound to different phases of soil particles by a variety of mechanisms the migration of radionuclides in tropical environments is subject to the same scientific principles as in any other environment. Thus the basic migration mechanisms involve similar hydrological and geochemical parameters. However, the behaviour of radionuclides is also modified by many unique features of the tropical environment, as summarised in the following sections.

Tropical environments have a unique climate that impacts the properties of soils and the mobility of radionuclides due to of the higher temperatures and, in particular, the patterns of rainfall; Where Monsoonal climates may be found in many tropical locations, meaning high episodic rainfall episodes, a changing water table, and cyclic saturation and unsaturation, as well as redox changes and floods.

In the relatively weathered soils of the tropics, clays of low exchange activity, such as kaolinite, are more common than in temperate zones. This leads to soils that, despite having high clay content, have a low exchange capacity. This can lead to greater mobility of radionuclides through the soil layers. This was demonstrated by the studies at Goiânia (Goiânia accident in Brazil 1987), where mobility of ^{137}Cs in the contaminated soils was higher than previously observed in temperate climates.

The majority of organic material in shallow soil horizons of tropical environments decomposes rapidly, and accumulation of soil organic matter is therefore minimal in many cases. In temperate zones, the decomposition of organic debris is slower, and soils often have a higher content of organic matter. This has implications for migration of radionuclides and, depending on the role of organic matter, may increase or decrease their mobility (Twining & Baxter, 2012).

The nutrient status of tropical soils can also be a consideration. Studies suggest there is a direct competition between Cs and K ions indicating a common accumulation mechanism. This implies that the deficiency of nutrients, such as K, could contribute to increasing plant uptake of ^{137}Cs (Kaplan et al., 1995; Carvalho et al., 2006). Similar results were reported by Twining *et al.,* (2004), who suggested that trace nutrient deficiency of tropical soils may be implicated in increased transfer factors of trace metals, such as zinc (Zn), relative to temperate environments.

There is a high degree of environmental change underway in the tropics with ongoing modifications in land use (e.g., urbanisation and the conversion of tropical

forest to plantation), as well as, local impacts of the more general phenomenon of global climate change. Climate change will alter the distribution and delineation of tropical and temperate ecosystems, and it has been speculated that global warming will eventually affect the soil-to-plant transfer factors of radionuclides (Dowdall *et al.,* 2008).

There is considerable diversity among tropical soils, as evidenced by the contrasting roles of organic matter in determining the behavior of some radionuclides (Twining & Baxter, 2012). Some tropical soil types, such as the coral atolls are dominated by carbonate minerals. In such soils, the cycling of radionuclides is highly unusual. For example, in these soils, cesium (Cs) is more mobile than expected in temperate environments, whereas strontium (Sr) appears to be more strongly bound (Robison *et al.,* 2000). The differences amongst tropical soils imply that it is important to consider diverse behavior between soils from different tropical environments and not to erroneously conclude that the behavior of one tropical soil will necessarily be similar to soil from a different environment. Whilst there is an ample evidence of the unique nature of radionuclide migration in the tropics, it is also important to avoid generalisations on the basis of the work undertaken thus far.

Increasing attention has been given to the abundance and distribution of natural radioisotopes in soils. Nevertheless data on biogeochemical behaviour of longlived radioisotopes in soils are still scarce (e.g. de Jong et al., 1994).

The broad objective of this research is to describe radionuclide behaviour in tropical soils, in particular, to highlight similarities and differences between the tropical and the comparatively well-studied temperate environments. As well as providing a contribution to the issues to be considered when considering environmental factors that may be more important in the effect of a potential radionuclide release into the tropics.

1.3 Objectives of the study

1. To determine the concentrations of natural radionuclides ^{226}Ra, ^{232}Th and ^{40}K and stable metals in different regions of tropical soils.
2. To study the vertical distribution of natural radionuclides activities (^{226}Ra, ^{232}Th, and ^{40}K) and stable metals in different agricultural areas of the tropical environment.
3. To investigate the effect of major physical and chemical factors on the behavior of radionuclides in tropical soils.
4. To investigate the spatial distribution of radionuclides and elements in soils of different tropical regions.
5. To investigate the correlations between radionuclide concentrations and soil microbial properties contributed by tropical climate factors.
6. To assess the radiological hazards in different areas of tropical soils.

CHAPTER 2: LITERATURE REVIEW

2.1 Introduction

Radionuclides that emit nuclear radiations are the sources of radioactivity. Intensive experiments undertaken by Marie and Pierre Curie, Rutherford and several other Scientists in the following decades have shown that these pollutants are radioelements that emit ionizing radiation, first classified by Ernest Rutherford according to their penetrating and ionising capacity as alpha particles, beta particles and gamma rays (Eisenbud & Paschoa, 1989).

This chapter deals with early literature reviews on the topic of radioactivity, including the basic concept of radioactivity, environmental sources of radioactivity, radioactive decays together with radioactive equilibrium, nuclear decay processes, gamma-rays interaction with matters, biological effect of low dose radiation, and radioactivity. Moreover, international and local reviews of radioactivity in soil were highlighted.

2.1.1 Environmental sources of radioactivity

Various types of nuclear radiation are available in nature, from different sources in soil, rocks, water, air, and vegetation, where the people are constantly exposed to small amounts of ionizing radiation from the environment as they carry out their normal daily activities; this is known as natural background radiation. The worldwide average natural dose to humans is about 2.4 mSv (240 mrem) per year (UNSCEAR, 1982; Gorycki, 2014). The International Atomic Energy Agency states:

"Exposure to radiation from natural sources is an inescapable feature of everyday life in both working and public environments. This exposure is in most cases of little or no concern to society, but in certain situations the introduction of health protection measures needs to be considered, for example when working with uranium and thorium

ores and other Naturally Occurring Radioactive Material (NORM). These situations have become the focus of greater attention by the Agency in recent years" (IAEA, 2016). There are many elements on the earth's surface and in the interior that contain isotopes, some radiant and the other stable. The discovery of radiation activity in 1896, by Henri Becquerel, was achieved in the uranium ore. In nature there are about 340 isotopes of various elements, 20% of these isotopes have radioactivity, and most the radionuclides are radioactive isotopes of heavy elements with, each element with an atomic number (Z) Z > 82 has radioactive isotopes (Becquerel & Crowther 1948; Allisy, 1996). Natural sources of nuclear radiation on the earth are classified into two types: from outside the earth (cosmic radiation), and from the composition of the earth's crust (terrestrial radiation). While there are four major sources of public exposure to natural radiation: cosmic radiation, terrestrial radiation, inhalation and ingestion, identified by United Nations Scientific Committee on the Effects of Atomic Radiation (UNSCEAR, 2000; Canadian Nuclear Safety Commission). About 82% of the radiation dose received by the human population is from natural sources, and approximately half of it from ^{222}Rn. The origin of these sources can be grouped into two types, namely cosmogenic and terrestrial (UNCSEAR, 2000), as illustrated in Figure 2.1.

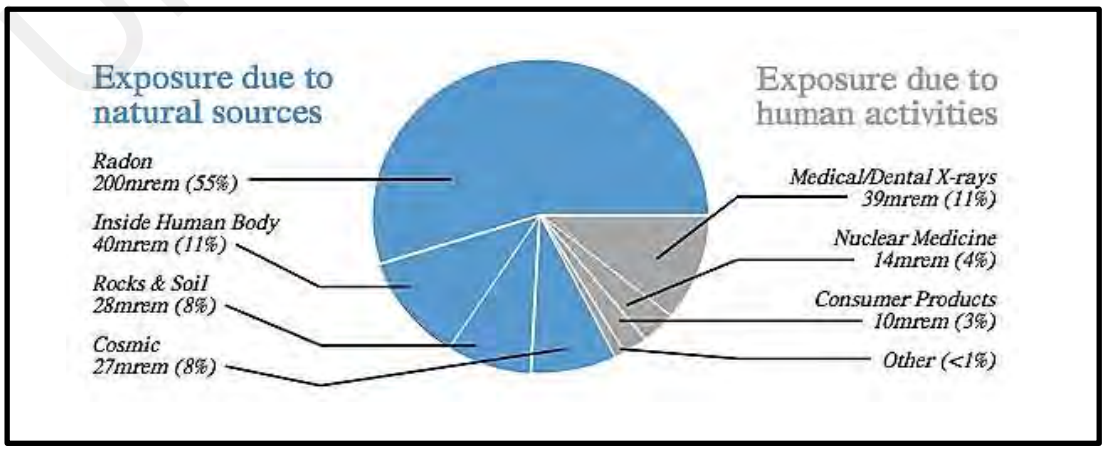

Figure 2.1: Environmental sources of radioactivity (https://serc.carleton.edu)

Figure 2.1 gives a breakdown of the many sources that can expose humans to radiation. Four major groups from which humans receive doses of radiation include radon, sources inside the human body, rocks and soil, and the sun. These are all natural sources. Other sources of radiation include medical diagnostic tools, nuclear medicine, and consumer products (Kathren, 1984; Eisenbud & Paschoa, 1989).

2.1.1.1 **Cosmogenic nuclides cosmic rays**

Cosmic radiation is constantly bombarding the earth's outer atmosphere (Dunai, 2010). Cosmic radiation is made up of fast-moving particles that are present in space and originate from a range of sources, including the sun and other celestial occurrences. Protons make up the majority of cosmic rays, although they can also be other particles or wave energy (Gosse & Phillips, 2001; Dunai, 2010). Natural radiation exposure occurs when ionising radiation penetrates the earth's atmosphere. This radiation reacts with atoms in the atmosphere, resulting in an air shower of secondary radiation, which includes X-rays, alpha particles, electrons, neutrons, protons, muons, and pions. The immediate dosage from cosmic radiation is largely muons, neutrons, and electrons, and it varies throughout the planet due t o elevation changes and the effects of the earth's magnetic field (Möller *et al.,* 2012; Ginzburg & Syrovatskii, 2013; Dunai, 2010; Shahbazi-Gahrouei, 2003).

The two most significant radionuclides produced in this manner are 81Kr from the (n,g) reaction on 80Kr and 14C from the (n, p) reaction on 14N. Extraterrestrial dust and meteorites give additional and minor quantities of radioactivity to the earth's atmosphere, mostly from ^{53,54}Mn, ^{56,57,58,60}Co, ^{48}V, ^{51}Cr, ^{22}Na, ^{46}Sc, ^{59}Mn, and ^{26}Al owing to spallation of heavier minerals. Cosmic radionuclides are elements with half-lives ranging from a few minutes to 2.5 million years with atomic numbers that are typically low.

The earth's geomagnetic shielding to the atmosphere reduces the strength of cosmic radiation from space, enabling only extremely energetic particles to enter at lower geomagnetic latitudes.

Generally speaking, Earth's magnetic field is weakest at the magnetic poles, and therefore the cosmic radiation levels and dose rates are higher in the Polar Regions and lowest at the equator (Grieβmeier *et al.,* 2005; Bagshaw, 2008). Depending on the altitude, latitude and time in the solar cycle, neutrons contribute 40–80% of the total equivalent dose rate at passenger airplane cruising altitudes (UNSCEAR, 2010). The sun is one of determinant of cosmic radiation. With a cycle of approximately 11 years, the Sun's activity varies in a predictable way. Due to the resulting magnetic field of the sun deflecting radiation away from the Earth, the higher solar activity leads to lower cosmic radiation levels and vice versa. Solar flares are another determinant of cosmic radiation, i.e., charged particles erupting from the sun. Solar flares occur very infrequently, therefore, their contribution to the cumulative dose is minimal (Grieβmeier *et al.,* 2005). However, radiation levels are increased by a factor up to one hundred at the time of a strong flare. The radionuclides are transported primarily through gravitational settling and precipitation cycles to the earth's surface. Consequently, not only with altitude, but also due to atmospheric mixing mechanisms and radiological half-lives, cosmogenic radionuclide amounts differ considerably (Darvill, 2013).

From a biological viewpoint, the two most important cosmic radionuclides are ^{14}C and tritium (^{3}H) (Hong, 2002; Yim & Caron, 2006). In living things, sodium (^{22}Na) and beryllium (^{7}Be) and other radionuclides can also be present, but their rates of production, concentration and half-lives combine to make them of little biological significance. C-14 biodynamics can be defined in terms of the carbon cycle. In this

situation, cosmogenic ^{14}C is oxidised to form carbon dioxide (CO_2) used by plants that animals ultimately consume. Organic ^{14}C is put into the marine and terrestrial ecosystem through death and excretory cycles of both plants and animals where it persists in the active repository of the food chain (Kathren, 1984; Shaw, 2007; Abdel, 2012). Table 2.1 lists the natural origins of cosmogenic radionuclides.

Table 2.1: Cosmogenic radionuclides of natural origin

Element	Nuclide	Half-life *	Decay mode and discrete** gamma energy (keV)
Hydrogen	^{3}H	*12.32 (2) years*	*β- (100%)*
Beryllium	^{7}Be	*53.22 (6) days*	*EC (100%) and γ (477 keV*)*
	^{10}Be	*1.51×106 (4) years*	*β- (100%)*
Carbon	^{14}C	*5700 (30) years*	*β- (100%)*
Sodium	^{22}Na	*2.6029 (8) years*	*β+ and γ (1275 keV*)*
Aluminium	^{26}Al	*717 ×103 (24) years*	*EC (100%)*
Silicon	^{32}Si	*153 (19) years*	*β- (100%)*
Phosphorous	^{32}P	*14.268 (5) days*	*β- (100%)*
	^{33}P	*25.35 (11) days*	*β- (100%)*
Sulphur	^{35}S	*87.37 (4) days*	*β- (100%)*
Chlorine	^{36}Cl	*3.013×105 (15) years*	*EC (1.9%), β- (98.1%)*
Argon	^{37}Ar	*35.011 (19) days*	*EC (100%)*
	^{39}Ar	*269 (3) years*	*β- (100%)*
Krypton	^{81}Kr	*2.29×105 (11) years*	*EC (100%)*

Source: *(Kathren, 1998)*

2.1.1.2 **Terrestrial radionuclides**

Radioactive materials that originate from earth's crust are found in nature, occur naturally in the soil, rocks, water, air, and vegetation. The radionuclides that formed from thermonuclear reactions in the heart of a star with other stable nuclei in the process of galactic nucleogenesis are called primordial radionuclides, and then erupted as a supernova and enriched the nucleus cloud from which the sun and the solar system originated (Poschl & Nollet, 2006; Eisenbud & Paschoa, 1989). At a time when the solar system was created around 4 to 5 billion years ago, they were part of the Earth. To date, only half-life radionuclides (greater than around 10^8 years) have been preserved. K-40 is the most abundant primordial radionuclide; the average

content in the crust of the Earth is around 3 $\times 10^{-3}$%, With a half-life of $T_{½}$ = 1.277×10^{9} years, ^{40}K disintegrates to stable isotopes of ^{40}Ar (89%) through β- decay and electron capture to ^{40}Ca (11%).

Another natural primary radionuclide is ^{232}Th, which has a half-life of $T_{½}$ = 1.39 × 10^{10} years and eventually disintegrates into a variety of so-called thorium decay chain radionuclides by γ- decay (i.e., secondary radionuclides) (Osburn, 1965; Kathren, 1998; Derin *et al.,*2012). However, ^{235}U, with a half-life of $T_{½}$ = 7.038 × 10^{8} years, and ^{238} U, with a half-life of $T_{½}$ = 4.468 × 10^{9} years, are the most important natural radionuclides of primary origin in the Earth's crust. All of these uranium isotopes are eventually converted by α-decay into a variety of radionuclides of both uranium decay chains (Poschl & Nollet, 2006).

Most of these sources have been decreasing, due to radioactive decay since the formation of the Earth, because there is no significant amount currently transported to the Earth. Thus, the present activity on earth from ^{238}U is only half as much as it originally was because of its 4.5 billion year half-life, and ^{40}K (half-life 1.25 billion years) is only at about 8% of original activity. But during the time that humans have existed the amount of radiation has decreased very little (Choppin *et al.,* 2002).

A number of secondary radionuclides are continually formed by the decay of primary radionuclides. Natural radionuclides ^{238}U ^{235}U and ^{232}Th decay into nuclei by α and later even β decay, which, like their other radioactive decay chains, are also radioactive (Poschl & Nollet, 2006). In nature, there are three radioactive chains of decay, namely ^{238}U, ^{235}U, and ^{232}Th, all three chains of natural decay are definitely similar. They consist of isotopes of heavy elements mostly of α - radioactivity and a smaller part is also β. Radon (^{222}Rn) tends to be the most stable isotope in the second half of the series; its decay products have a brief half-life and disintegrate with α and

β decay at the same time as each other. Radon is a noble gas, and one of the heaviest radioactive nuclear gases. All three chains of natural decay result in stable isotopes of lead (Cecil & Green, 2000; Choppin *et al.,* 2002).

Many shorter half-life (and thus more intensely radioactive) isotopes have not decayed out of the terrestrial environment because of their on-going natural production. Examples of these are ^{226}Ra (decay product of ^{230Th} in decay chain of ^{238}U) and ^{222}Rn (a decay product of ^{226}Ra in said chain) (Lütz, 2007). Thorium and uranium (and their daughters) primarily undergo alpha and beta decay, and aren't easily detectable. However, many of their daughter products are strong gamma emitters. ^{232}Th is detectable via a 239 keV peak from ^{212}Pb, ^{511}Pb, ^{583}Pb and 2614 keV from ^{208}TI, and ^{911}TI and 969 keV from ^{228}Ac. Uranium-238 manifests as 609, 1120, and 1764 keV peaks of ^{214}Bi (*cf.* the same peak for atmospheric radon). Potassium-40 is detectable directly via its 1461 keV gamma peak (Aldrich & Wetherill, 1958). The level over the sea and other large bodies of water tends to be about a tenth of the terrestrial background. Conversely, coastal areas (and areas by the side of fresh water) may have an additional contribution from dispersed sediment. The dose of radiation varies widely and is influenced by factors such as geographic location, soil and building material with natural radioactive contaminants, and the kinds of materials used in building structures (Schroeyers, 2017).

Some communities situated on soil with high concentrations of granite or mineral sand receive doses many times the average. Examples include coastal areas in Espiritos Santos and Rio de Janeiro in Brazil; Kerala, on the southwest coast of India; and the Guangdong province in China. In Brazil, the black sand beaches are composed of monazite, a rare earth mineral containing 9% radioactive thorium (Gonçalves & Braga, 2019). External radiation dose rates from these sands may be as high as 5 mrem/hr

(0.05 m Sv/hr), where permanent residents experience an average annual dose equivalent of approximately 500 mrem (5 mSv) (NRC, 1990). In Kerala, on the west coast of India, residents receive 1,300–1,500 mrem (13–15 mSv) annually, due to the presence of monazite sand (NRC, 1990). Some dose rates are as high as 3,000 mrem $year^{-1}$ (NRC, 1990; Eisenbud & Gesell, 1997; Barthel & Tulsidas, 2014).

Apart from radiation exposures due to living in close proximity to the earth's crust, people are also exposed to additional radiation when earth crust products (oil, coal, coal ash, minerals) are extracted, refined, and used (Provost & Kohavi, 1998; Mayfield & Lewis, 2013). The naturally occurring radioactive materials in these products are concentrated into what is called technologically enhanced naturally-occurring radioactive materials (TENORM).

2.1.2 Nuclear decay processes

2.1.2.1 Radioactivity

The science of nuclear physics was started in 1886 by Henry Becquerel (1852-1908) while he was studying phosphorescence phenomenon. Becquerel inspired other scientists to follow his studies on rays emitted from elements such as uranium salts and oxides. He found out that if some crystals which were already exposed to sun light; unknown radiation was emitted, accordingly. This radiation is able to darken photographic plates. Further studies were carried out to prove that certain types of salts such as potassium uranyl sulfate is able to cause similar effects on photographic plates even if the plates are kept away from sunlight. This finding indicated that certain salts with known phosphoric properties are able to emit a different type of radiation to x-rays as they do not require external excitation (Tykva & Berg, 2004). Soon after, on 28 December 1898, the combined efforts of the Curies contributed to successful results when Pierre decided to turn to his wife's research work on radiation instead of his own

work on piezoelectricity. The Curies noted more radiation than expected was sent out from the uranium minerals on which they were working. Following rigorous work on chemical separation, the Curies reached the conclusion of the presence of a new radionuclide.

Polonium, the name of the new radionuclide, was given in honour of the native land of the Curies in July 1898. Radioactive as a word after then was mentioned for the first time by Marie and her Husband Pierre Curie upon their continuous work on pitchblende (Tykva & Berg, 2004; Eisenbud & Paschoa, 1989). Later on, scientists found out that there was no effect on radioactivity regarding the physical or chemical processes used in radioisotope separation such as cooling, heating or interacting with other chemical materials. Accordingly, scientists reached a conclusion that such radiation originated from the nucleus, the inner part of the atom. Further details of radioactivity phenomena came into light to reveal that unstable nuclides tend to disintegrate by emitting energy in the form of radiation in order to reach stability. Many isotopes, which have the same mass number but different atomic numbers, disintegrate by emitting either α or β particles. Sometimes both types of particles might be emitted by certain types of radionuclides. Such particles might be directly, or after a certain interval, followed by the emission of γ radiation due to the transition of nuclides from excited to the ground state (Cooper *et al.,* 2003; Tykva & Berg, 2004)

Radioactive decay by the emission of α/ β particles followed by γ radiation is statistical process which is subject to a statistical law of physics. This is because the expectation is true that a certain nucleus will disintegrate at a specific moment in time.

2.1.2.2 **Radioactivity Decay**

The main quantity used for quantification of radioactive source is the activity, which is defined as the quotient of the number of radioactive transformations in a radionuclide *dN*, and the time interval *dt* in which these transformations occurred i.e,

$$A = \frac{dN}{dt} \tag{2.1}$$

In environmental system, the term activity is sometimes used in quite different contexts (e.g., biological activity). Therefore, in relation to quantification of nuclear tr-ansformations, the term radioactivity is often used instead of activity. A nucleus can undergo different nuclear transformations, the main ones being represented by α (alpha) decay – emission of helium nuclei, β (beta) decay either β^- (electrons) or β^+ (positrons), respectively, and emission of γ - rays emission of electromagnetic quanta. In principle, there can be other nuclear transformations, although they are rare, represented by orbital electron capture, internal conversion, isomeric transmission, spontaneous fission, neutron emission and other processes (Cooper *et al.,* 2003; Shleien *et al.,* 1998).

The fundamental law of radioactive decay for a single radioactive nuclear species is given by (Krane & Halliday, 1988; Turner, 2007):

$$A(t) = -\frac{dN(t)}{dt} = -\lambda N(t) \tag{2.2}$$

where *A* is the activity (i.e. the number of decays per unit time) of a given radionuclide species; *N* is the number of radioactive (unstable) nuclei present at time t, and λ the decay constant characteristic for this decay (i.e. the probability of decay per unit time).

If we consider N_0 as the number of atoms present at time $t = 0$, and that no decay products were present initially (at $t = 0$), then:

$$N_A(t=0) = N_0 \tag{2.3}$$

$$N_B(t=0) = N_2(t=0) = \cdots 0 \tag{2.4}$$

Considering the general case during the decay process in which a radioactive daughter was formed from the decay of the parent, then the number of the parent nuclei (N_A) decreases with time according to the following relation:

$$dN_A = -\lambda_A N_A dt \tag{2.5}$$

The number of the daughter nuclei increases due to the parent's decays but also decreases due to its own decay, resulting in the expression

$$dN_B = \lambda_A N_A dt - \lambda_B N_B dt \tag{2.6}$$

after integrating equation (2.6) a very useful equation is obtained for the law of exponential decay:

$$\int \frac{dN_A}{N} = -\int \lambda\, dt \rightarrow N_A(t) = N_A(0)\, e^{-\lambda t} \tag{2.7}$$

where *N(0)* is the original number of nuclei of radioactive nuclei present at the reference time *($t_0 = 0$)*, *N(t)* is their number present at a time *t* later, and *e* is the base of the natural logarithm.

This exponential decay relationship is of fundamental importance in working with radioactive materials. Taking into account equations above can be rewritten in the form

$$A(t) = \lambda N(t) = \lambda N(0) e^{-\lambda t} = A(0) e^{-\lambda t} \tag{2.8}$$

where *A(0)* and *A(t)* represent activity in time *t = 0* and *t*, respectively. In practice, radionuclides are characterized by their half-lives rather than decay constant. The half-life is defined as the time period required for the activity to decrease to just one half of its original value. It is actually the time interval over which the chance of survival of a particular radioactive atom is exactly one-half (Choppin *et al.,* 2002).

$$\frac{1}{2} = e^{-\lambda.T_{1L2}} \tag{2.9}$$

where $T_{1/2}$ is the half-life, for which we get

$$T_{1/2} = \frac{ln2}{\lambda} = \frac{0.693}{\lambda} \tag{2.10}$$

Although the half-life value of a certain radionuclide can be well defined, the instant of disintegration for a particular radionuclide can occur anywhere between $t = 0$ and ∞. However, also a mean life may be used; it can be introduced on the basis of the probability $p(t).dt$ that a radioactive nucleus survives up to time t and decays in the interval t and $t+dt$.,

$$p(t).dt = e^{-\lambda.t}.dt \tag{2.11}$$

From where we can calculate the mean life T_{ml}:

$$T_{ml} = \frac{\int_0^\infty t.p(t).dt}{\int_0^\infty p(t).dt} = \frac{1}{\lambda} \tag{2.12}$$

The mean life time T_{ml}, and the half-life are bound together as:

$$T_{ml} = \frac{T_{1/2}}{0.693} = 1.44 \times T_{1/2} \tag{2.13}$$

The relation between the mean-life T_{ml}, and the half-life $T_{1/2}$, the decay constant and the initial number of radioactive atoms N_0 is graphically illustrated in (Figure 2.2).

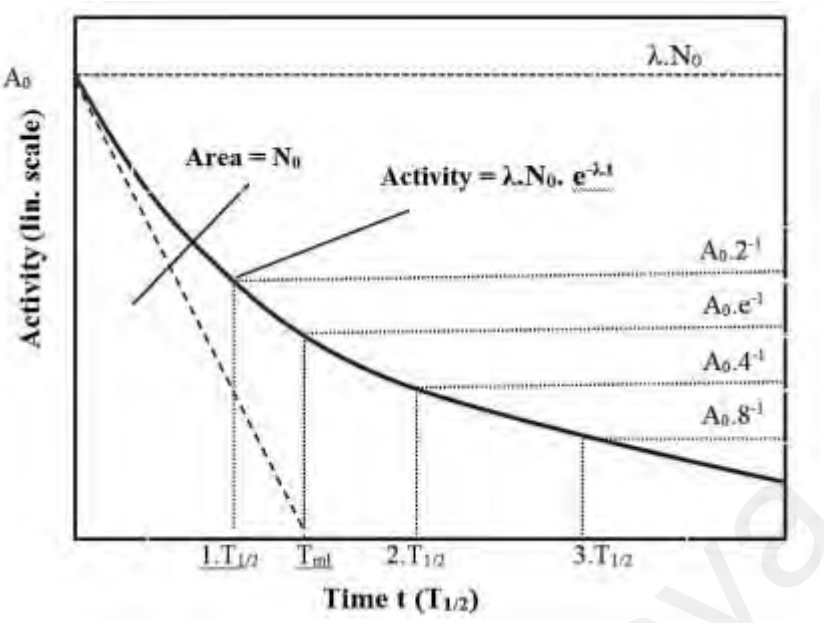

Figure 2.2: Relationships of characteristics in radioactivity decay.

It is very common in the decay of a radioactive atom that the resulting atom (daughter or decay product) is not stable and can again undergo a nuclear transformation. The process may continue in a series until it reaches a stable product. Generally, radioactive nuclide *A* decays to nuclide *B*, which is also radioactive. Then nuclide *B* decays to a radioactive nuclide *C*, and so on. For example, ^{232}Th decays to a series of ten successive radioactive nuclides. For a more complex decay scheme in which the daughter product is radioactive and thus decays to a third nucleus which is also radioactive, and so on; let's assume the initial part of radioactive series consisting of tree radioactive nuclides *A*, *B*, *C* and stable *D* with decay constants λ_A, λ_B and λ_C, i.e.,

$$A \overset{\lambda_A}{\rightarrow} B \overset{\lambda_B}{\rightarrow} C \overset{\lambda_C}{\rightarrow} D \tag{2.14}$$

if, at the beginning, at time $t = 0$, N_{A0} atoms of type *A* are present, the numbers N_A, N_B and N_C of atoms of types *A,B* and *C* which will be present at a later time *t*, are given by the equations (Krane & Halliday, 1988; Tykva & Berg, 2004):

$$N_A = N_{A0} e^{-\lambda_A . t} \tag{2.15}$$

$$N_B = N_{A0} \frac{\lambda_A}{\lambda_B - \lambda_A} \left(e^{-\lambda_A t} - e^{-\lambda_{B2} t} \right) = N_A \frac{\lambda_A}{\lambda_A - \lambda_B} \left(e^{(\lambda_A} - e^{\lambda_{B)} . t} \right) - 1) \tag{2.16}$$

$$N_{BC} = N_{A0} \left(\frac{\lambda_A}{\lambda_C - \lambda_A} \frac{\lambda_B}{\lambda_B - \lambda_A} e^{-\lambda_A t} + \frac{\lambda_A}{\lambda_A - \lambda_B} \frac{\lambda_B}{\lambda_C - \lambda_B} e^{-\lambda_B t} + \frac{\lambda_A}{\lambda_A - \lambda_C} \frac{\lambda_B}{\lambda_B - \lambda_C} e^{-\lambda_C t} \right) \tag{2.17}$$

where the activities of individual radionuclides *A, B* and *C* are given as:

$$A_A = \lambda_A . N_A, \qquad A_B = \lambda_B . N_B, \; A_C = \lambda_C . N_C \tag{2.18}$$

As long as a radioactive parent is initially a pure source whose activity at $t = 0$ is AA_0, the ratio of the activities of the parent *A* and the daughter *B* will change with time according to the equation:

$$\frac{A_B(t)}{A_A(t)} = \frac{\lambda_B}{\lambda_B - \lambda_A} \left(1 - e^{-(\lambda_B - \lambda_A) . t} \right) \tag{2.19}$$

2.1.3 Radioactive Equilibrium

Radioactive equilibrium is the term usually used to explain the state when the members of the radioactive series decay at the same rate as they are produced (Prince, 1979). The three predominant cases of the state of equilibrium can be explained as below.

2.1.3.1 Transient Equilibrium

If the half – life of the parent A is greater than the half – life of its daughter B, i.e., $\lambda_B > \lambda_A$, as *t* increases, the ratio $A_B(t) / A_A(t)$ also increases, but as *t* becomes large, this ratio become a constant greater than one. Consequently, for sufficiently large values of *t*, the daughter will decay with the half – life of the parent, but its activity will be greater than the parent activity by the factor $\lambda_B / (\lambda_B - \lambda_A)$. Such a situation is referred to as a transient equilibrium (Figure 2.3) (Faires & Parks, 1958; Cooper, Randle & Sokhi, 2003). ^{212}Pb, for example, decays to ^{212}Bi with a half-life of 10.64 hours, which has a half-life of 60.55 minutes. The activity of the parent is longer than the daughter in this

instance. The activity of the daughter begins from zero, increases to a maximum value, and then decreases with the same parent's half-life. The overall operation in the framework will be the sum of the actions of parents and daughters. As a consequence, the daughter undergoes transition at the same rate that it is formed and its complete activity then decays at the same rate (at $t = \infty$) as the original parent nuclide. It is said that the two radionuclid species are in in a state of transient equilibrium (Cooper, Randle & Sokhi, 2003; Burcham, 1973).

For $\lambda_B > \lambda_A$ or $(T_{1/2})_B < (T_{1/2})_A$

$$\frac{A_B}{A_B} = \frac{\lambda_B}{\lambda_B - \lambda_A} \tag{2.20}$$

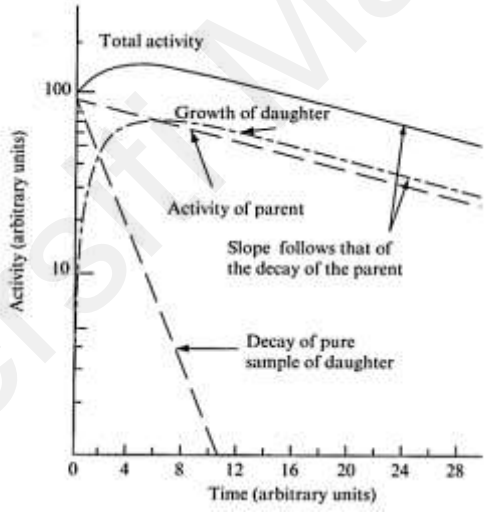

Figure 2.3: The transient equilibrium between a parent and the resulting daughter nuclei. In this case, the half- life of the parent is equal or nearly equal to (greater than) that of daughter. Reported by Kathren, R. L., Radioactivity in the Environment, Figure 3.4, p. 59, Harwood Academic, 1991.

2.1.3.2 **Secular Equilibrium**

If we consider the case of secular equilibrium, where the activity of the parent does not decline measurably over several subsequent half-lives of the nucleus of the daughter, so the chain of *n*, subsequent short-lived radionuclides, may all be in secular

equilibrium with the original long-lived parent (Cooper, Randle & Sokhi, 2003). At the same rate at which they are formed, the daughter nuclides decay, so that:

$$\lambda_A N_A = \lambda_B N_B = \ldots = \lambda_n N_n \quad (2.21)$$

The activity of each member of the chain equals that of the parent while the total activity is *n* times the activity of the original parent. To illustrate this, consider the first three stages of the ^{232}Th (i.e. ^{232}Th → ^{228} Ra → ^{228}Ac) and ^{238}U (i.e. ^{238}U → ^{234}Th → ^{234m}Pa) decay series. In the case of each parent/daughter pair, the half-life of the parent is much greater than that of the daughter and thus a secular equilibrium established between each pair (Cooper, Randle & Sokhi, 2003; L'Annunziata, 2016) (Figure 2.4).

The activity of ^{234}Th and ^{234}Pa $^{+234m}$Pa (based on their respective branching ratios, the activity will be divided between the two nuclides) will be equal to that of ^{238}U and the activity of ^{228}Ra and ^{228}Ac will be equal to that of ^{232}Th. The cumulative activity, respectively, will be three times that of ^{238}U and ^{232}Th. Secular equilibrium occurs because, relative to that of the daughter, the half-life of the parent nuclide is very long. The decay of ^{226}Ra (*T1/2* = 1600 years) to ^{222}Rn (*T1/2* = 3.82 days) in the decay chain of *4n+2* led by ^{238}U is a good example. Here the daughter decays more rapidly than the parent and reaches secular equilibrium after approximately 7 half-lives , such that the activity of the daughter tends to the same ^{238}U series. ^{238}U has a half-life 4.57×10^9 years and decays to ^{234}Th (half-life: 24.10 days).

As ^{234}Th decays into ^{234m}Pa, the concentration of the protactinium and its activity rises until its production rate and decay rates are equal. Thus if the activity of one of the radionuclide in a decay chain can be measured, it can be assigned to the other radionuclides within the chain, i.e. assuming equilibrium (Jaffey *et al.,* 1971).

For $\lambda_B \geq \lambda_A$ or $(T_{1/2})_B \leq (T_{1/2})_A$

we have: $A_B/A_A \approx 1$.

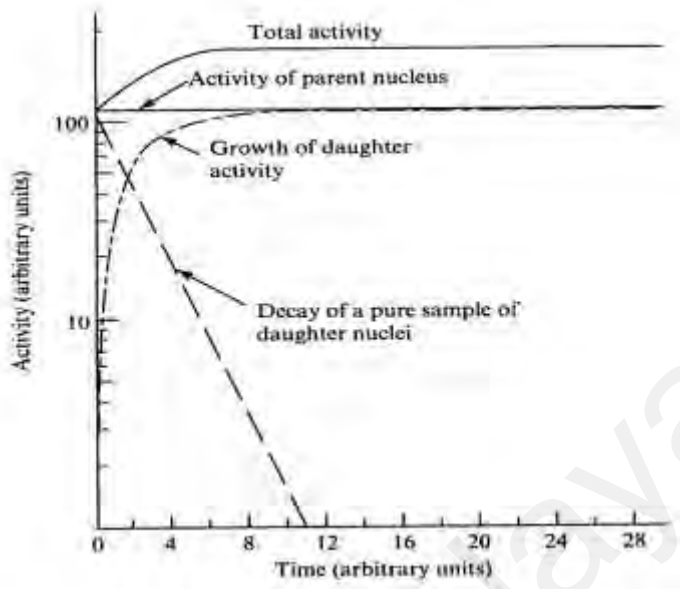

Figure 2.4: A secular equilibrium between a parent and the resulting daughter nuclei. In this case, the half- life of the parent is much greater than that of the daughter. Reported by Kathren, R. L., Radioactivity in the Environment, Figure 3.3, p. 57, Harwood Academic, 1991.

2.1.3.3 **Non-Equilibrium decay**

When the parent has a shorter half-life that that of the daughter; hence the parent will decay, the daughter activity grows to some maximum and then decays with its own characteristic half-life (Cooper *et al.,* 2003; Krane & Halliday, 1988), this is shown in Figure 2.5.

For $\lambda_B < \lambda_A$ or $(T_{1/2})_B > (T_{1/2})_A$

then :

$$\frac{A_B}{A_A} = \frac{\lambda_B}{\lambda_B - \lambda_A}\left(1 - e^{-(\lambda_B - \lambda_A)t}\right) \qquad (2.22)$$

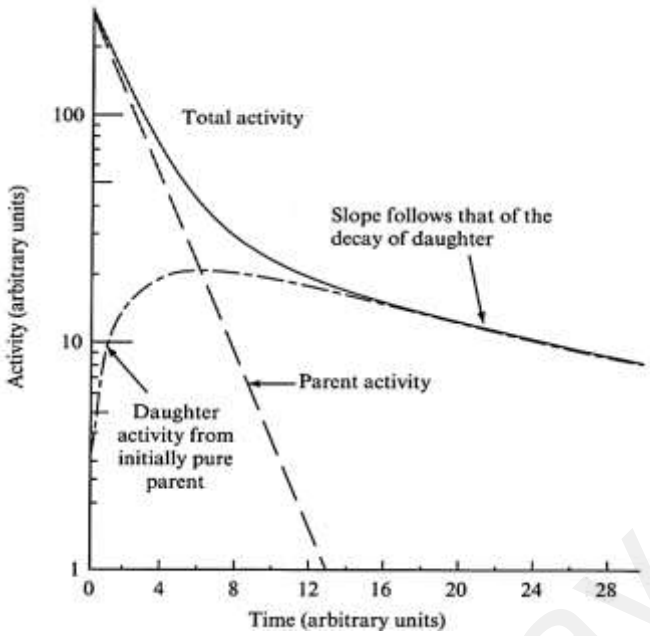

Figure 2.5: **A schematic of no-equilibrium situation between a parent and the resulting daughter nuclei. In this case, the half- life of the parent is less than that of the daughter. Reported by Kathren, R. L., Radioactivity in the Environment, Figure 3.5, p. 60, Harwood Academic, 1991.**

2.1.3.4 **Branching Ratio**

Nuclear decay can occur not only in a single form, but also in some cases through multiple competing processes. The branching ratio gives the relative intensities of these opposing decay modes Krane & Halliday (1988) as illustrated: If λ_{TOT} = the total decay probability of a nuclear state, then

$$\lambda_{TOT} = \sum_{i=1}^{n} \lambda_i \tag{2.23}$$

where λ_i is the partial decay probability associated with a particular mode of decay. The ratio of different decay modes for a nuclide, correspond to the proportions of different (energy) particles that are emitted during the decay process itself. An example is the alpha-decay of ^{226}Ra to the spin/parity ($I^{\pi} = 0^{+}$) ground state of ^{222}Rn with a branching ratio of 94.0 % The branching ratio is frequently expressed by giving the partial decay constant or partial half-life of the nuclide involved (Krane & Halliday, 1988). The

competing alpha decays to the first excited state have a branching ratio of 5.95 hours For example, ^{226}Ac whose half-life is 29.37 hours has a decay constant of

$$\lambda_{Ac} = \frac{0.693}{T_{1l2}} = 0.024\ h^{-1} = 6.6 \times 10^{-6} s^{-1} \quad (2.24)$$

Its partial decay constants for the three observed decay modes can be derived as follows:

$$\lambda_{\beta} = 0.83\ \lambda_{Ac} = 5.5 \times 10^{-6} s^{-1} \quad (2.25)$$

$$\lambda_{\varepsilon} = 0.17\ \lambda_{Ac} = 1.1 \times 10^{-6} s^{-1} \quad (2.26)$$

$$\lambda_{\alpha} = 6\ \lambda_{Ac} = 4 \times 10^{-10} s^{-1} \quad (2.27)$$

Note that that the total decay rate is given $\lambda_{TOT} = \lambda_1 + \lambda_2 + \ldots.+\lambda_n$ and the partial halflives for each decay mode correlate with the partial decay constants for *n-th* mode of decay given as:

$$T_{\frac{1}{2}}(n) = \frac{0.693}{\lambda_n} \quad (2.28)$$

It is clear that beta-emission is more likely than alpha-emission for ^{226}Ac. However, the overall activity will only decay for a total half-life.

In practical terms, thus, ^{226}Ac decays with a total half-life of 29 hours and, for that reason, any gamma-radiation activity calculation of ^{226}Ac for any decay mode should use the total half-life, taking into account the branching ratio of that particular form of decay (Krane & Halliday, 1988).

2.1.4 Types of Decays

There are many types of emitted particles and radiation that radioisotopes produce when they decay. The three principal modes of decay by a radioactive nucleus are alpha and beta, followed by γ-ray emission (Figure 2.6). Alpha decay is seen only in heavier

elements greater than atomic number 52, tellurium. The other two types of decay are seen in all of the elements.

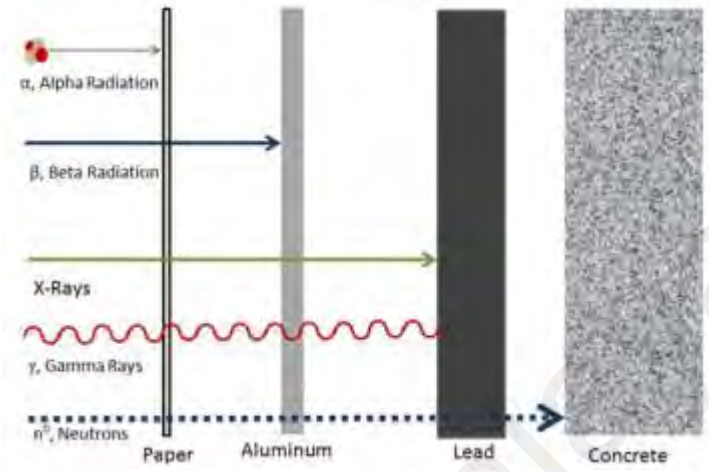

Figure 2.6: Penetration of the modes of decayAlpha particles can be completely stopped by a sheet of paper. Beta particles can be stopped by aluminum shielding. Gamma rays can only be reduced by much more substantial mass, such as a very thick layer of lead.

2.1.4.1 **Alpha Decay**

Alpha α decay is a type of radioactive decay in which an atomic nucleus emits an alpha particle (helium nucleus) and thereby transforms or 'decays' into an atom with a mass number that is reduced by four (A → A – 4) and an atomic number that is reduced by two (Z → Z – 2). An alpha particle is identical to the nucleus of a helium-4 atom, which consists of two protons and two neutrons. It has a charge of +2 *e* and a mass of 4 u (atomic mass unit). For example, ^{238}U decays to form ^{234}Th Alpha particles have a charge +2 *e*, but as a nuclear equation describes a nuclear reaction without considering the electrons a convention that does not imply that the nuclei necessarily occur in neutral atoms the charge is not usually shown.

The emission of alpha particles is commonly the most preferred mode of decay for naturally occurring radionuclide with $Z > 83$ (Gilmore, 2008; Knoll, 2000).

$$^{238}_{92}U \rightarrow {}^{234}_{90}Th + {}^{4}_{2}H + Energy \tag{2.29}$$

The energy released during the decay process is called 'Q_α value' and from conservation law and it must equal the mass-energy difference between the initial and final-decayed products. The transformation energy equals the Q-value and can be deduced from the mass difference as follows (Krane & Halliday, 1988):

$$Q_\alpha = (m_A - m_B - m_\alpha)c^2 \tag{2.30}$$

where m_A, m_B, m_α are the mass of the parent, daughter, and emitted alpha particle, respectively. The Q value is expressed in MeV while the mass is expressed in atomic mass units (or amu). 1 amu = 931.5 MeV/c^2 = 1u, and c is the speed of light. Spontaneous decay can occur when the Q_α value is a positive number (i.e. $Q_\alpha > 0$), indicating that alpha-decay is an exothermic process in such cases.

Assuming the initial condition at rest, then the released energy in alpha decay will appears as kinetic energy transferred to the decayed fragments, shared between the final particles in a definite ratio. The Q_α-value from 2.31 can be re-written in terms of non-relativistic (kinetic) energy as:

$$Q = E_B + E_\alpha = \frac{1}{2} m_B \, (V_\alpha)^2 + \frac{1}{2} m_\alpha \, (V_B)^2 \tag{2.31}$$

where m_B, m_α, V_B, V_α are the masses and velocities for the daughter and alpha particles, respectively (Krane & Halliday, 1988; Lilley, 2013). For linear momentum to be conserved, the daughter product and alpha particle must travel with the same momentum but in opposite direction (Cember, 2009). This requires that

$$m_B V_B = m_\alpha V_\alpha \tag{2.32}$$

The ratio of the (non- relativistic) Kinetic Energy of the outgoing particles can be re-written as:

$$\frac{E_B}{E_\alpha} = \frac{\frac{1}{2}m_d(V_B)^2}{\frac{1}{2}m_\alpha(V_\alpha)^2} \rightarrow \frac{E_B}{E_\alpha} = \frac{(m_B V_B)^2 m_\alpha}{(m_\alpha V_\alpha)^2 m_B} = \frac{m_\alpha}{m_B} \tag{2.33}$$

Using 2.31 and 2.32, the *KE* of the emitted alpha-particle can be expressed in terms of the Q-value as follows (Krane & Halliday, 1988):

$$E_\alpha = Q(\frac{m_B}{m_\alpha + m_B}) \tag{2.34}$$

The alpha particle being less massive than the residual daughter radionuclide carries most of the *KE* which corresponds to ~ 98% of the Q_α-value for $A > 200$, leaving the recoil energy of the massive daughter nuclide to about 2% of the released Q_α- value. The ranges of energy for alpha particles emitted are between 4 to 10.5 *MeV* for members of the U and Th natural decay chains.

2.1.4.2 **Beta Decay (*β* -, *β*+ and *EC*)**

Via a mechanism known as beta decay, atoms release beta particles. In 1900, Henri Becquerel discovered beta particles. Beta decay happens when an atom contains either too many protons or too many neutrons in the nucleus. This is the most frequent form of radioactive decay, and against this type of transition all nuclides not lying in the 'stability valley' are unstable.

The atomic number (Z) and the neutron number (N) of a nucleus change by one unit each in beta decay, but the overall mass number, $A=N+Z$, remains unchanged. Beta decay thus provides a convenient decay mode for an unstable nucleus to increment down a mass parabola of constant A to approach the stable isobar (Lapp & Andrews, 1954; Krane & Halliday, 1988). The beta particle is simply a relativistically energised electron or positron ejected from the nucleus. This process takes place by the emission either of an electron $\beta-$ and an anti-neutrino; positron $\beta+$ and a neutrino υ; or through the competing process of electron capture EC.

(a) ***Negative β-decay***

The first process is negative beta $\beta-$ decay occurs in nuclei that have neutron excess compared to the lowest energy isobar of a given mass A chain. The neutron to proton ratio is reduced inside the nucleus during the decay by converting a neutron into a proton with the anti-neutrino carrying away from the nucleus any excess binding energy above the energy of the beta-particle. This mechanism happens when the ratio of neutrons to protons is larger than the stable ratio for that particular isobaric chain. This process reduces by one the number of neutrons and increases by one the number of protons (Krane & Halliday, 1988). The following example represents a β- decay process:

$$n = \rho^{+} + \beta^{-} + \acute{\upsilon} \qquad (\acute{\upsilon}\ anti - neutrino) \tag{2.35}$$

$$^{210}_{82}Pb_{128} \rightarrow {}^{210}_{83}Bi_{127} + e^{-} + \acute{\upsilon} \tag{2.36}$$

Beta-particles, from zero to the so-called endpoint, have a constant flow of energy. This point is equal to the energy difference between the mother's original and final states and the nucleus of her daughter, respectively. Since β decay is a three-body process, the kinetic energy that is emitted between the β-particle and the antineutrino is exchanged (Krane & Halliday, 1988), β-particles emitted have a continuous distribution of kinetic energies, varying from zero to the limit permitted by the Q_{β} - value (β-end point energy). Figure 2.7 shows a continuous distribution of energy from 0 up to 1.16 MeV from β-particles emitted from ^{210}Bi (Hsue *et al.,* 1966).

In β decay, it is possible to describe the Q-value of β decay as the difference between the original and final nuclear mass energies. The Qβ-value can be calculated from the following Equation if the variations in electron binding energy and electron mass are neglected (Krane & Halliday, 1988):

$$Q_{B^-} = [m\,(^{A}X) - m\,(^{A}\grave{X})]\,c^2 \quad (2.37)$$

$$Q_{B^-} = T_e + E_{\acute{\upsilon}} \quad (2.38)$$

where the masses are neutral atomic masses. The Q value represents the energy shared by the electron and neutrino.

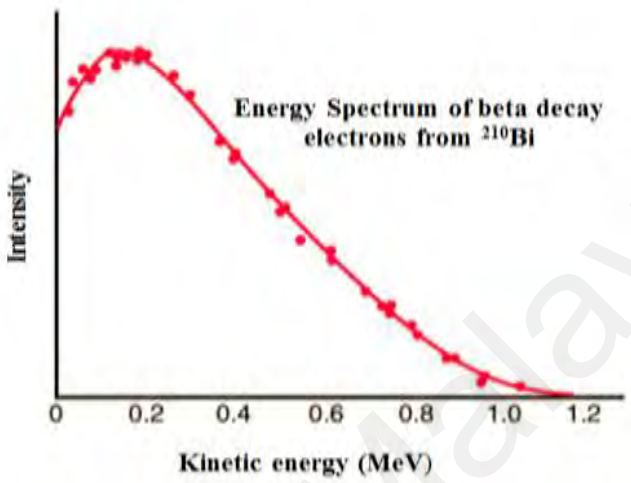

Figure 2.7: Experimental energy spectrum for decay electrons from 210Bi. Emax = Q = 1.16 MeV is the maximum energy. From (Neary, 1940).

(b) ***Positive β-decay***

In the second scenario; positrons or $\beta+$ emission occurs, when there is a proton excess relative to the most stable isobar of that isobaric (constant A) mass chain occurs when the n - p ratio in the nucleus is < 1. This is true for $A < 40$, however positron decay also occur in heavier nuclides where the $N > Z$, i.e. neutron to proton ratio is > 1. The result of such processes is to bring the neutron to proton ratio to a more energetically favorable value for a given A chain. Unlike in alpha decay, beta particle energies are not mono-energetic but rather are emitted with a continuous energy range up to the end-point Q_β – value for that decay.

Beta minus decay changes the neutron number *(N)* by *−1* unit while the total mass number (*A=N+Z*) remains unchanged. Such decays increment down a "mass parabola" of constant A to approach the most stable isobar, and *Z: N* configuration, for constant *A*. Examples of mass parabola of isobaric nuclei.

In this process, a proton is transformed into a neutron, a positron and a neutrino. As a result, the nuclear charge is decreased by one unit. As in *β*- decay, this decay is a three-body process and the positrons are emitted with a continuous range of energies (Hsue *et al.,* 1966). The following example represents β^+ decay process:

$$\rho^+ \rightarrow n + \beta^+ + v \tag{2.39}$$

$$^{25}_{13}Al_{12} \rightarrow {}^{25}_{12}Mg_{13} + e^+ + v \tag{2.40}$$

The *Q*-value must be greater than 0 for this process to be able to occur. The *Q* value of β+ decay is given by (Krane & Halliday, 1988):

$$Q_{B+} = [m\ (^{A}X) - m\ (^{A}\grave{X}) - 2m_e]\ c^2 \tag{2.41}$$

2.1.4.3 **Gamma Decay**

Gamma rays are high-energy electromagnetic radiation that can be produced in one of two ways: by oscillating charge, a changing electric field induces a magnetic field; or by shifting current or magnetic moment, a changing magnetic field induces an electric field. Via charge and current distribution within an atomic nucleus, these two are created (Nelson & Reilly, 1991).

A gamma photon is electrically neutral of a very high energies photons with very short wavelengths and thus very high frequency. Since the gamma rays are in substance only a very high-energy photons, they are very penetrating matter and are thus biologically hazardousand travels at the speed of light. Gamma rays can travel hundreds

of metres in air before they interact and are attenuated. Gamma rays are emitted by unstable nuclei in their transition from a high energy state to a lower state known as gamma decay. In most practical laboratory sources, the excited nuclear states are created in the decay of a parent radionuclide, therefore a gamma decay typically accompanies other forms of decay, such as alpha or beta decay (Noz & Maguire, 2007; Nelson & Reilly, 1991; Krane & Halliday, 1988).

Since γ rays also have no charge or mass, the number of protons and neutrons within the emitting nucleus remains constant following γ–ray emission. Gamma decay processes take place from within the nucleus and typical photon energies range from 10 keV to 10 MeV with the corresponding wavelengths between 10^4 and 100 fm.

Unlike α and β- particles, γ rays have much greater range in matter. However high density materials, such as lead , are effective in attenuatting γ- rays and hence lead regularly used as a shielding material against gamma rays.

2.1.5 Interaction of radiation with matter

Radiation can penetrate into an object, some of the photons interact with the particles of the matter and their energy can be absorbed or scattered. This absorption and scattering is called attenuation. Other photons travel completely through the object without interacting with any of the material's particles. The number of photons transmitted through a material depends on the thickness, density and atomic number of the material, and the energy of the individual photons.

Even when they have the same energy, photons travel different distances within a material simply based on the probability of their encounter with one or more of the particles of the matter and the type of encounter that occurs (Table 2.2). Since the probability of an encounter increases with the distance traveled, the number of photons

reaching a specific point within the matter decreases exponentially with distance traveled. As shown in the graphic to the right, if 1000 photons are aimed at ten 1 cm layers of a material and there is a 10% chance of a photon being attenuated in this layer, then there will be 100 photons attenuated. This leaves 900 photons to travel into the next layer where 10% of these photos will be attenuated. By continuing this progression, the exponential shape of the curve becomes apparent.

$$I = I_0\, e^{-\mu x} \tag{2.42}$$

The factor that indicates how much attenuation will take place per cm (10% in this example) is known as the linear attenuation coefficient, m.

Table 2.2: Classification of radiations

Type	Radiation	Penetrability
Charged	Heavy (alpha)	Range ~ 10^{-5} m
	Light (beta)	Range 10^{3} m
Uncharged	EM (Gamma, X)	d ½ 0.1 m
	Neutrons	d ½ 0.1 m

2.1.5.1 **Gamma-rays interactions with matter**

A beam of γ-rays passing through a substance can interact with atoms of the material either through *absorption* or through s*cattering*. In the absorption process, a photon is removed as a result of interacting with an atom of the material, and in second case the photon is deflected from the original direction of the beam. Both of these processes can be described by the term *attenuation*. The interactions responsible for these processes take place between the photons and the orbital electrons of the atom. The probability of an interaction taking place between an incoming photon and an 'arget' atom is related to the *cross-section* of the interaction. The cross-section reflects the probability of an interaction taking place, and hence, greater the probability of interaction, then larger the

value of the cross-section for that particular interaction. It is obvious that the chances of a projectile striking a target will depend on the area of the target and the number of projectiles. When considering atomic interactions, the cross-section is considered to be the area associated with the atoms with which the photon (projectile) interacts. Typically, atomic cross-sections are of the order of 10^{-28} m^2. Cross-sections are often quoted in units of barns (b) where:

$$1\ b = 1 \times 10^{-28} m^2 \tag{2.43}$$

For a photon beam incident on a material of thickness *dx,* as illustrated in Figure (2-8) the probability of interaction given by the following:

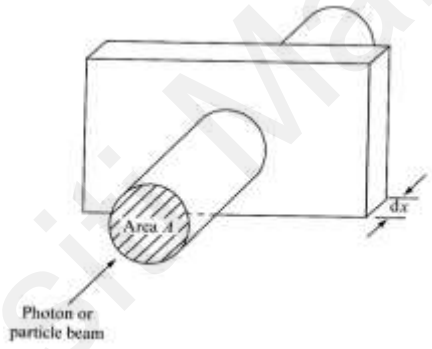

Figure 2.8: A schematic of photon or particle beam of cross-sectional area A incident on a target of thickness dx.

$$\frac{AN\sigma dx}{A} = N\sigma dx \tag{2.44}$$

where A is the area of the incident photon beam, N is the number of atoms per unit volume (m^{-3}), σ is the cross- section of the interaction (m^2) and dx is thickness of the material. For n photons or particles, the number of interactions is given by the following:

$$nN\rho dx \tag{2.45}$$

During these numbers of interactions, *dn* photons will be attenuated or removed from the incident beam and thus:

$$dn = -nN\sigma dx \tag{2.46}$$

$$\frac{dn}{n} = -N\sigma dx \tag{2.47}$$

The n_t photons present in the transmitted beam can now be obtained by integrating Equation (2.46) to give:

$$n_t = n_0 \exp(-N\sigma dx) \tag{2.48}$$

In terms of the intensity of homogeneous incoming photon beam, Equation (2.49) can be written as follows:

$$I = I_0 \exp(-\mu x) \tag{2.49}$$

where I is intensity of beam after passing through the material of thickness x, I_0 is the incident intensity of the incoming beam and μ is the *total linear attenuation coefficient.*

The latter is function of number of atoms per unit volume and the cross-section, σ, of interaction and is given by the following:

$$\mu = N\sigma \tag{2.50}$$

The linear attenuation coefficient represents the fraction of X-rays or γ-rays removed from the incoming beam per unit thickness of the target material. The units of μ are m^{-1}, with this becoming clear from Equation (2.51), namely:

$$m^{-3}(N)m^2(\sigma) = m^{-1}(\mu) \tag{2.51}$$

As μ is proportional to the number of atoms per unit volume of the material with which an incident photon beam interacts, it follows that it is also proportional to the density of the material and thus will have different values for the different phases of the same material (solid, liquid or gas). As there is this dependence on density, *the mass*

attenuation coefficient (μ/ρ) is a more fundamental and practical measure of the attenuation of photons than is the linear attenuation coefficient. This parameter is independent of the density of the absorber material and thus does not depend on its physical state. The units of μ/ρ are as follows:

$$\frac{m^{-1}(\mu)}{kgm^{-3}(\rho)} = m^2kg^{-1}(\mu/\rho) \tag{2.52}$$

The total mass attenuation coefficient thus represents of X-rays or γ-rays removed from a beam of photons with a unit cross-sectional area passing through a medium of unit mass. The parameter μ/ρ are related to the cross-section of interaction through the following expression:

$$\frac{\mu}{\rho} = \frac{N\sigma}{\rho} \tag{2.53}$$

By substituting for N with the expression:

$$N = \frac{N_A\rho}{A} \tag{2.54}$$

we obtain the following:

$$\frac{\mu}{\rho} = \left(\frac{N_A\rho}{A}\right)\left(\frac{\sigma}{\rho}\right) = \frac{N_A\rho}{A} \tag{2.55}$$

where N_A is the Avogadro constant, 6.02×10^{23} mol^{-1} which is the number of units in one mole of any substance. The amount of substance containing this number of entities (such as atoms or molecules) is called *mole* (mol). In the above equation, A is the atomic weight of absorber material. In order to maintain the dimension of the exponential term in Equation (2.49), thickness of absorber (x) is now replaced by the *areal density* (ρx). Thus, Equation (2.49) becomes:

$$I = I_0 \exp(-\frac{\mu}{\rho}\rho x) \tag{2.56}$$

where μ/ρ is dependent upon various interaction processes between the photon the absorbing material.

There are five processes by which γ-rays can interact with matter. These are as follows: The Photoelectric Effect; Compton (Incoherent) Scattering; Pair Production; Elastic (Coherent) Scattering; Photonuclear Interaction. The extent to which γ-rays interact by each of these mechanisms is largely determined by the energy of the γ-rays and the atomic number (*Z*) of the material. The first three processes are the most important in the context of environmental radioactivity and are accompanied by the transfer of energy to an atomic electron which can be ejected from the atom and can then cause further ionization along its track within the absorber. An understanding of these mechanisms is important when considering the biological effects of radiation and in radiation detection techniques such as gamma-ray spectroscopy (Figure 2.9).

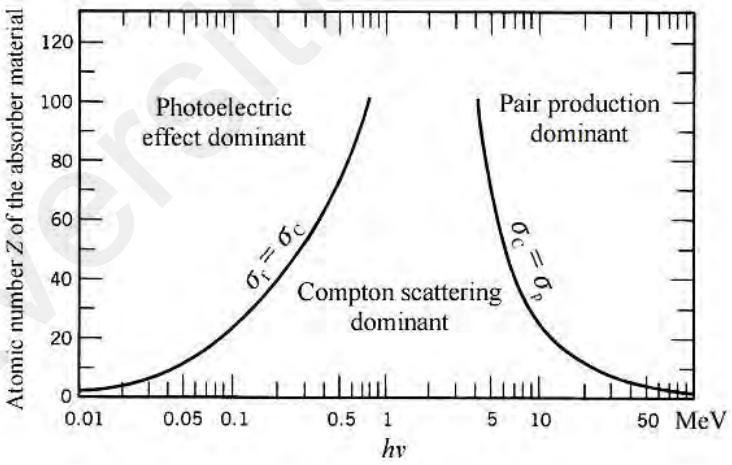

Figure 2.9: The relative importance of various processes of gamma radiation interaction with matter

2.1.5.2 **The Photoelectric Effect**

The photoelectric effect is the most important mechanism by which low-energy photons interact with matter. In this process, the γ-ray photon interacts with the atom during which the photon is completely absorbed and an inner-shell atomic electro is

ejected, as shown in Figure 2.10. The vacancy created this ionizing process is filled by an electron from higher shells, thus leading to the possible emission of X-rays. This process of X-ray production is more clearly illustrated in Figure 2.11. For example, if the k-shell electron is ejected, then the electrons in the higher shells (L and M) can fill this vacancy, so leading to possible emission of K_α or K_β X-ray. These X-rays are characteristic of the absorbed material. Therefore, if a photon of energy E ejects an electron from the K shell with a binding energy E_B, then the energy of the ejected electron from the K shell with a binding energy E_B, then the energy of the ejected electron E_j will be given by the following:

$$E_j = E - E_B \tag{2.57}$$

The recoil energy of the atom is nearly zero and thus can be ignored. In competition to X-ray production, there is a finite probability that the process will result in the emission of an *Auger electron* from the outer shells, rather than X-rays from the inner shells. This process cannot occur unless the energy of the incident photon, E, is greater than the binding energy of the inner shell, that is:

$E > E_B$

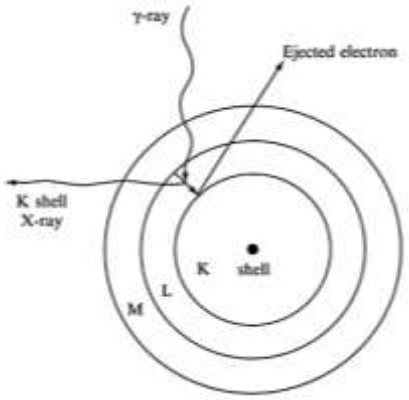

Figure 2.10: Illustration of the photoelectric absorption process where a γ-ray photon is absorbed and a characteristic X-ray are emitted.

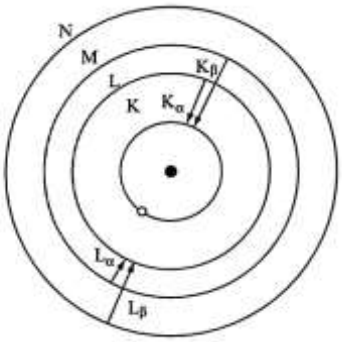

Figure 2.11: Representation of the inner electron shells of an atom and the electronic ransitions that can lead to the emission of characteristic X-ray

The probability of the photoelectric effect taking place is greatest when:

$$E = E_B \tag{2.58}$$

and declines rapidly as the photon energy increases. As the incoming photon is removed or absorbed from the incident beam, the mass attenuation coefficient is referred to as the *mass absorbed coefficient* (τ/ρ), where τ is the photoelectric linear *absorption coefficient*. The rapid decrease in τ/ρ with increasing E is illustrated in Figure 2.12. As the photon energy increases, the absorption due to the individual electronic shells becomes important, but as soon as the energy exceeds a particular shell binding energy then the mass absorption coefficient, which gives a measure of the probability of interaction, falls rapidly. In Figure 2-12, the edges refer to the sudden rise in τ/ρ as the energy of the photon approaches the binding energy of a shell. Beyond the edges τ/ρ decrease rapidly, approximately as $1/E^3$, and increases with atomic number (Z) of the absorber as Z^3, and thus:

$$\frac{\tau}{\rho} \propto \frac{Z^3}{E^3} \tag{2.59}$$

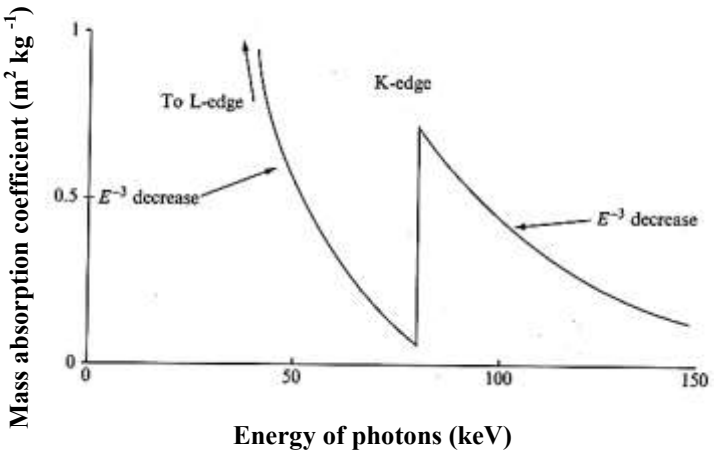

Figure 2.12: Variation with photon energy of the mass absorption coefficient for the photoelectric process

This proportionality is approximately valid for photon energies up to about 200 keV, but at higher energies τ/ρ varies less strongly and decreases as $1/E^2$, and eventually as 1/E. This effect is the dominant interaction mechanism for photons of intermediate and low energies (0.5 to 200 keV). As described by Equation (2.60), the absorption increases rapidly with the atomic number of the absorber and this is the main reason why high-Z materials, such as lead, are used for shielding against γ-rays. Such shielding materials are not only used for protection against radiation but also for the purpose of reducing background signals in techniques like γ-ray spectroscopy.

2.1.5.3 **Compton Scattering**

The elastic and incoherent scattering of γ-quantum on free or only weakly bound electrons is called Compton scattering. Consequently, the photon has less energy than its initial value and the electron is ejected in the process. The energy (E1) and momentum (p1) of the incident photon are given by the following:

$$E_1 = hv_1 \tag{2.60}$$

$$p_1 = \frac{hv_1}{c} \tag{2.61}$$

Where h is the Plank constant, v_1 is the frequency of the incident photons, and c represents the velocity of the light. The energy of the scattered photon (E_2) and the kinetic energy of the recoiled electron (E_e) are given by:

$$E_2 = hv_2 \tag{2.62}$$

$$E_e = hv_1 - hv_2 = h(v_1 - v_2) \tag{2.63}$$

From the law of conservation of momentum and resolving in the horizontal and vertical directions we obtain the following:

$$\frac{hv_1}{c} = \frac{hv_2}{c}cos\theta + p_e cos\Phi \tag{2.64}$$

In the horizontal direction, and:

$$0 = \frac{hv_2}{c}sin\theta - p_e sin\Phi \tag{2.65}$$

Figure 2.13 shows the incoming photon Interact with an electron and is scattered at an angle θ, whereas the electron recoils forward at an angle Φ; λ_1 and λ_2 are the wavelengths for the incident and the scattered photons, respectively.

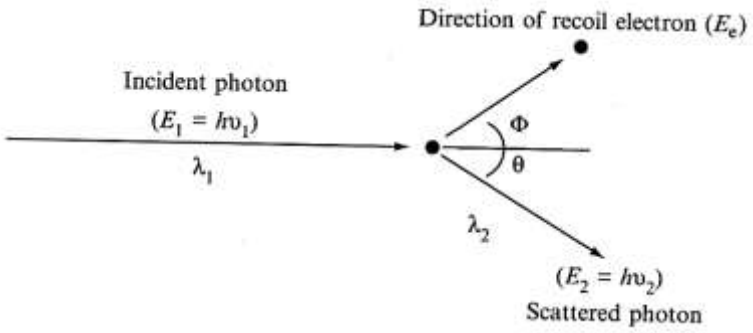

Figure 2.13: Illustration of the Compton scattering process

In the vertical direction: Φ and θ represent the scattering angle for the recoil electron and the scattered photon, respectively. The energy of the recoiled electron (E_e) is related to its momentum through the equation of special relativity, as follows:

$$p_e^2 c^2 = E_e\,(E_e + 3m_e c^2) \tag{2.66}$$

where m_e is the mass of the electron. By eliminating Φ and p_e from Equations (2.64) and (2.65), the equation for the energy of scattered photon (hv_2) can be derived to give:

$$hv_2 = \frac{hv_1}{1 + \frac{hv_1}{m_e c^2}}(1 - cos\theta) \tag{2.67}$$

This equation is easily transformed to give an expression for the Compton wavelength shift (λ_2-λ_1) experienced by the photon as a result of this type of interaction:

$$\lambda_2 - \lambda_1 = \frac{h}{m_e \mathrm{c}}(1 - cos\theta) \tag{2.68}$$

The term $h/m_e c$ (=2.43×10^{-12}m) is known as the Compton wavelength. The energy of the incident photon is distributed between the recoiled electron and the scattered photon and thus depends on the scattering angle and the original energy of the photon (E_1). Compton scattering is termed an inelastic process because the incident photon loses energy in the process, although the total energy is obviously conserved.

From equation (2.68), we can deduce that the Compton wavelength shift is independent of the wavelength of the incident photon and of the scattering material. As the Compton wavelength term ($h/m_e c$) is a constant, the Compton wavelength shift only depends on the scattering angle of the photon (θ). It follows then that for a given angle of scatter the wavelength shift will be a constant. The photon energy (hv_2), given by equation (2.67), is a maximum when $\theta = 180^\circ$.

Compton scattering is particularly important at intermediate γ-ray energies and increases linearly with the atomic number of the absorbing material. This process has particular significance in γ-ray spectroscopy where leads to the so-called attenuation coefficient for Compton scattering medium and the energy of incoming photon. The mass attenuation coefficient, therefore, decreases with increases with increasing photon energy. The electron density can be estimated by using the following simple relationship:

Electron density = Number of atoms per unit mass × Number of electron per atom (2.69)

The first term is the Avogadro constant (N_A) divided by the mass number (A) of the medium, while the second term is simply the atomic number (Z), as the number of electrons for an atom is equal to the number of protons in the atom's nucleus. Thus, the mass attenuation coefficient for Compton scattering is given by the following:

$$\frac{\sigma}{\rho} \propto \left(\frac{N_A Z}{A}\right)\left(\frac{1}{E_1}\right) \tag{2.70}$$

For most elements, the ratio Z/A is about 0.5 it follows that the mass attenuation is of similar magnitude for all substances. Hydrogen is a special case, where the ratio Z/A is unity as $Z = A$ (that is, the hydrogen nucleus only has one proton and no neutron) and thus σ/ρ will be twice the magnitude of the values found for most other substances.

2.1.5.4 **Pair Production**

Pairing can occur when the energy of the gamma quantum is at least equal to twice the resting energy of an electron ($2m_0c^2$=1022 keV). Here, the photon generates a positron electron pair in the coulomb field of a nucleus, where it disappears itself. The unpaired energy of the previously existing photon is split as kinetic energy onto the positron and electron, which move away from the interaction site due to conservation of momentum in opposite directions. Since the positron generally generates annihilation

radiation together with an electron in a short time, two secondary gamma quanta with energy of 511 keV each are formed as secondary particles.

$$E_\gamma = 2mc^2 + T_1 + T_1 \tag{2.71}$$

where E_γ is the gamma-ray photon energy, $T_{1,2}$ are the kinetic energies of the electron kinetic energies of the electron and the positron, respectively, and mc^2 is the rest mass energy for each of the electron and positron, m is the mass of the electron or the positron and c is the speed of light. In terms of energy units MeV, the rest mass of an electron or a positron is 0.511 MeV. A small amount of energy is imparted to the recoiling nucleus which serves to conserve the momentum of the interaction. As each of these particles have a rest-mass equivalent of 0.511 MeV in terms of energy, Equation (2.71) can be written as follows:

$$E_\gamma(M_eV) = 1.02 + T_1 + T_2 \tag{2.72}$$

In practice, this process for absorbing gamma- ray is only important if their energies are greater than about 1.5 MeV and becomes dominant for γ-ray energies of greater than 5 MeV. The positron can annihilate in flight but it is more probable that as it losses its kinetic energy and slows down it will interact with an electron in the absorbing medium and produce two annihilation photons of energy 0.511 MeV (equivalent to mc^2), with each travelling in opposite direction. Since environmentally important radionuclides do not emit γ-rays of these energies, this process is not very significant. The mass attenuation coefficient for pair production, κ/ρ, where κ is the linear attenuation coefficient and ρ is the density of the medium, is given by:

$$\frac{\kappa}{\rho} \propto Z(E - 1.02) \tag{2.73}$$

This equation shows clearly that unlike the other attenuation processes, pair production increases with increasing photon energies. It also increases linearly with the atomic number of attenuating substance.

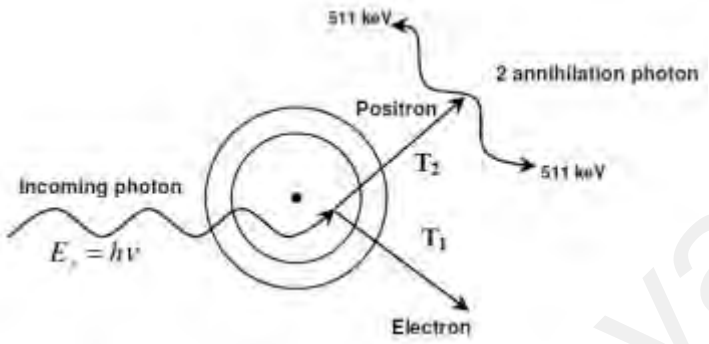

Figure 2.14: Schematic of the pair production process and annihilation

2.1.6 Biological effects of radiation

Early Knowledge of Radiation Effects Reports of radiation injury began to appear in the literature with astonishing rapidity after the announcement on November 8, 1895 of Roentgen's discovery of X-rays. The very first volume of the American X-ray Journal, published in 1897, included a compilation (Scott, 1897) of 69 cases of X-ray injuries reported from laboratories and clinics in many countries of the world (Duggar, 1936; Eisenbud & Paschoa, 1989). In such a brief amount of time, the explanation that so many cases of injuries may have been identified is due to the history of the discovery of X-rays and the sort of study that has already been ongoing for many years. X-ray technology seems to have begun in 1859 when Plücker first reported that on the inner wall of a vacuum tube from which a current circulated under high voltage, an apple green fluorescence was visible (Grubbé, 1933; Duggar, 1936). Plücker's work was followed by a number of experiments in other laboratories, and in 1875, Sir William Crookes made the first high vacuum tube which thereafter bore his name. Crookes discovered that the apple green fluorescence reported originally from a discharge at the

negative end of the tube, and, thus, Plücker inaugurated the word "cathode rays." Heinrich Hertz, who is mostly known for his classic observations of the electromagnetic spectrum and his evidence of the electromagnetic spectrum, evidently discovered the fact that cathode rays contained a portion of radiation that could pass through solid material (Duggar, 1936). According to Grubbé, Roentgen's principal contribution was the observation that he could see the shadow created by the bones of his hand when it was placed between a Crookes tube and a screen covered with fluorescent chemical (Eisenbud & Paschoa, 1989). To this penetrating radiation he gave the name X-rays. The important point is that experimentation with Crookes tubes has been ongoing in many parts of the world, and that many of these tubes have created X-rays unknown to investigators. Grubbé, a physician who was also a manufacturer of Crookes tubes, was researching chemical fluorescence at the same time as Roentgen was performing his classical experiment. When he heard of Roentgen's announcement, Grubbé began immediately to experiment with the newly named X-rays and by January, 1896 developed an acute dermatitis which was followed by skin desquamation and eventual cancer that many years later necessitated amputation of his hand. The early stages of his injuries were discussed at a scientific conference at the Hahnemann Medical College in Chicago on January 27, 1896, at which Dr. Gilman made a fascinating discovery that "any physical agent capable of causing so much harm to normal cells and tissues could give possibilities, if used as a medicinal agent, for the treatment of a pathological disorder in which he was pronounced (Duggar, 1936; Eisenbud & Paschoa, 1989). By 1900 the natural radioactivity contained in uranium ore had been sufficiently concentrated so that the first skin burn was produced on the arm of a Mr. Giesel and shortly thereafter confirmed in an experiment by Pierre Curie using a radium extract he reported as having an activity 5000 times that of metallic uranium (Becquerel & Curie, 1901). By March, 1902, the number of cases reported in the literature totaled at least

147 (Codman, 1902). The estimated number of people who were injured and killed by X-ray and radium prior to the establishment of effective radiation hygiene guidelines will probably never be known. During and immediately following World War I, the use of radium in luminous paints was attended by hazards arising out of ignorance of the effects of this radioelement when ingested (Finkel *et al.,* 1969; Evans *et al.,* 1969). Around 40 staff, mainly women, developed bone cancer and aplastic anemia from the habit of brushing their lips. In addition, during the 1920s, for a number of conditions including arthritis, mental illness, and syphilis, radium was medically prescribed as a nostrum; this procedure caused additional deaths until it was abandoned. More recently, from 1944 to 1951, a compound containing ^{224}Ra (half-life 3.6 days) was injected intravenously into about 2000 German patients with tuberculosis and other diseases. Spiess and Mays, 1970, and by 1969 bone sarcomas had already appeared in 50 of these patients. The dial-painting cases have been studied thoroughly by these several investigators, but the main credit belongs to Evans for having worked out the basic biophysical principles of radium injury in sufficient detail so that safe practices could be adopted.

The mines had been operated for centuries as a source of ores of many metals and, from the beginning of the twentieth century, as a source of pitchblende. When it was realized that cancer could result from chronic irradiation by radionuclides deposited within the body, it was suggested that the high incidence of lung cancer among miners of radioactive ores might be explained by their exposure to radioactive substances in the atmospheres of the mines (Lorenz, 1944; Grosch, 2012). The presence of high concentrations of radon was discovered by mine air tests and this radioactive gas was believed by many to be the etiological cause in the high occurrence of lung cancer. By 1942, when the wartime atomic energy program was initiated in the United States, the

early epidemiological radiation experience had been thoroughly digested, and standards had been developed by 1941 which- served well throughout World War II.

As is well known, ionizing radiation divides into alpha, beta, gamma and neutron radiation. If alpha or beta particles or gamma radiation hit molecules, electrons can be "knocked" out of chemical bonds. The harmful effect of alpha particles is approximately 20 times that of beta particles or gamma radiation. If ionizing radiation hits molecules and "knocks out" electrons, these molecules lose their stability and unstable fragments, so-called radicals, are created. The chance that two such radicals will meet and form stable connections is rather small; instead they disrupt the function of other stable molecules. However, it gets particularly bad when ionizing radiation hits the DNA. This can lead to a break in the DNA strand, which means that the binding properties of the genetic material are disrupted (Grosch, 2012)

It has become undoubtedly now that ionizing radiation causes many damage, not only to human health, but to all living creatures, and that many of these damages are fatal or harmful to the extent that a person suffers from their effects throughout his life, especially after the widespread use of ionizing radiation in many life fields such as medicine, agriculture and industry, generating electrical energy and other various uses, which contributed to the pollution of the atmosphere with radiation and increased the human possibility for it in an additional way, so the effect of ionizing radiation on living cells and methods of protection from them has become an important topic and it has gained the attention of people and government institutions and international as one of the topics that concern all people who share a life on the globe, share its resources and suffer from any pollution that they may be exposed to (Grosch, 2012; Martin, 2018).

The effect of ionizing radiation is divided into two parts, the direct and indirect effect. Most of the damage caused by radiation comes from its biological effect on

living organisms and organic systems. There are two ways in which the radiation affects living organisms; the first way is what is known as the direct effect, where the radiation ionizes part of the atoms involved in the composition of body tissues as a result of these atoms absorbing energy from radiation (Martin, 2018). This can be illustrated by the following example, that absorbing a dose of 4 Gy means that each gram of tissue will obtain an amount of energy of 2.5×10^{16} electron volt, since it takes about 34 electron volts to generate one ionic pair in the tissue, we find that the number of ions generated as a result of the absorption of the previous dose is 7.65×10^{14} ion pair, that is means a dose of 400 rad may cause this number of atoms in per gram of tissue to be ionized. If it is taken into account that for every ionizing atom there are nine other atoms that are excited, then we find that about 7.65×10^{14} atoms per gram have been directly affected as a result of the body's exposure to this lethal dose, but if this number is divided by the number of atoms in one gram of tissue, the ratio is one out of ten million atoms has been affected by radiation, a number that may seem very little at first(Grosch, 2012; Martin, 2018). However, the process of ionizing atoms will lead to the dissolution of the molecules, which these atoms within their structure, and this will have great damage at the level of a single cell or the entire organism. But the process of ionization of atoms will lead to the dissolution of the molecules that enter these atoms within their structure, and this will have great damage at the level of a single cell or the entire organism (Martin, 2018). The most important direct damages to radiation are genetic mutations as well as cell death, for example, a radiation dose of 400 rad represents the lethal radiation dose for half of those exposed to it within 30 days and is symbolized by the symbol 50/30 LD, and it is considered a large radiation dose when given to the whole body, despite its direct effect (Henriksen & Maillie, 2003; Turner, 2008).

The second way that radiation affects living things is the indirect way. In this way, the effect of radiation does not transfer directly to the cells. Rather, the radiation

produces a large number of free radicals within body fluids, especially water. These free radicals in turn form toxic chemical compounds. In this way, the effect of radiation becomes more severe, for example, bacterial chalkboards need a dose of 500,000 rad so that 90% of their cells die, while the same checkboards need about 100,000 rad to have the same effect when they are in the water, this is due to the fact that the radiation creates free radicals in the water, where these free radicals combine to form the oxidized hydrogen peroxide, which works to cause more damage to cells and other important molecules in the body (Turner, 2008; Kiefer, 2012).

Ionizing radiation damages cells and tissues (or any other material) by ionizing the atoms of the irradiated material. These physical interactions result in changes in the chemical bonds in the respective irradiated molecules. This can either happen directly (direct effect) or by interacting with reactive oxidative species (ROS) (indirect effect). ROS (free radicals) arise e.g. through water radiolysis (cells consist of approx. 80% water):

$$H_2O \rightarrow H_2O^{+} + e^{-} \rightarrow HO^{\cdot} + H^{+}$$

In the presence of molecular oxygen (breathing), further ROS are created, such as hyper oxide anion (superoxide anion) and hydrogen peroxide. ROS attack biomolecules and as a result of such chemical reactions altered bio-molecules, including altered DNA, are created. Cells have developed various defense mechanisms to protect against the ROS (which is also constantly caused by cellular respiration) (e.g. to ward off radiation-induced ROS). If cellular defense is no longer sufficient, oxidative stress occurs. Oxidative stress is involved in many pathological processes and disease development: cancer, aging, neurodegenerative diseases and cardiovascular diseases (Turner, 2008; Grosch, 2012; Kiefer, 2012).

2.1.7 Radiation detection

2.1.7.1 Radioactivity in rocks

Natural radioactivity is found in almost all rocks, and it is caused by the decay of radionuclides that are normally present in trace amounts. Natural radiation levels in soil and rock are determined by radionuclide concentrations and specific activity, which is defined as the number of decays per unit time per unit amount of substance (Missimer *et al.,* 2019). Specific activity is an inverse function of the radionuclide's half-life, and it may be determined using the number of decays of either the radionuclide or daughter radionuclides.

Radionuclides of the elements uranium, thorium, and potassium are the principal sources of natural radioactivity in rock and soil, specifically the the ^{238}U, ^{232}Th, and ^{40}K decay chains (Missimer *et al.,* 2019). The decay of the arent radionuclides and their daughter radionuclides produces the radiated radiation. Natural radiation of soil and rock is determined by mineralogical composition. Natural radioactivity is relatively high in rocks composed of minerals with relatively high concentrations of uranium, thorium, and potassium (Schroeyers, 2017; Missimer *et al.,* 2019).

Uranium, which is a predominantly lithophile, appears in igneous rocks, generally associated with rocks containing mainly light elements (Basham & Kemp, 1994). In general, magmatic fractionation increases uranium content (Wedepohl, 1978).

Globally, granitic and rhyolitic rocks have uranium contents ranging from 2 to 15 mg/kg, while silicic alkaline rocks frequently have higher uranium contents, up to 26 mg/kg (Basham & Kemp, 1993; Cumberland *et al.,* 2016). Some granites can be more uraniferous than others (Christophersen *et al.,* 2013), with some Proterozoic granites in Australia containing up to 50 mg/kg U. (Kreutzer *et al.,* 2010). In comparison to granitic or silicic alkaline igneous rocks, metamorphic rocks contain less uranium. According to

Basham & Kemp, (1994), the uranium content in metamorphic rocks is normally between 0.1 to 4 mg/kg, and uranium depletion occurs as metamorphic grade increases. However, this is an oversimplification; the variation in uranium content of metamorphic rocks is quite large, as might be expected for rocks derived from a variety of parent materials and under a variety of physical-chemical conditions. Wedepohl, (1978) data show a much wider range of compositions ranging from 0.1 to 45 mg/kg U, with typical values ranging from 1 to 4 mg/kg U regardless of metamorphic grade.

The uranium concentration in sedimentary rocks varies greatly. There are two major factors that affect uranium content: (1) detrital source mineralogy, and (2) uranium redox-chemistry, which is strongly influenced by the geochemical processes operating during weathering of source rock and sediment transport, within the depositional environment, and during subsequent burial diagenesis (Burns & Finch, 1999).

Uranium is redox-sensitive, and while it can exist in three different oxidation states 3+, 4+, 5+, and 6+, only 4+ and 6+ are important in nature. The mineral wyartite [CaU^{5+} $(UO_2)_2(CO_3)$ $O_4(OH).7H_2O$] has been found to contain pentavalent uranium (U^{5+}) (Burns & Finch, 1999), however it is extremely rare in nature. Consequently, uranium concentrations in sedimentary rocks can be much higher than those found in parent igneous rocks (Cumberland *et al,* 2016). Sandstones normally contain 0.5 to 4 parts per million of uranium; shales and mudrocks often include 1 to 5 mg/kg of uranium; and limestones typically contain around 2 mg/kg of uranium (Wedepohl, 1978), however some more uraniferous limestones have been documented (Milodowski *et al.,* 1989). Much of the uranium in siliciclastic sedimentary rocks (sandstones, shales, mudrocks) is found in detrital heavy minerals (zircon, apatite, xenotime, titanite, monazite, xenotime), which occur as trace components or as inclusions preserved in major detrital minerals like quartz, feldspars, and micas (Wedepohl, 1978; Milodowski

& Hurst, 1989). In carbonate rocks, tiny amounts of uranium are thought to act as a calcium replacement in the lattice. Uranium contents are frequently much higher in organic-rich and phosphatic sediments and sedimentary rocks. Uranium enrichment is common in phosphorites, with up to 700 mg/kg observed in some formations (Wedepohl, 1978; Cumberland *et al.,* 2016). The uranium content in black shales and organic sediments (coals, lignites, and peats) varies greatly 1 to 6000 mg/kg, with some formations reporting extremely high uranium concentrations (Wedepohl, 1978; Cumberland *et al.,* 2016).

Regarding the host uranium metal, as mentioned earlier, uranium is a lithophile element, meaning that all uranium minerals include oxygen, and it does not exist naturally as a native element or as a sulphide mineral when combined with sulphur. There are about 160 minerals in which uranium is a critical component of the crystal structure. In addition, uranium can be found as a minor or trace component in a wide range of other minerals, where it is incorporated intrinsically by substituting major ions within the crystal structure, for example, Ca^{2+} in calcium carbonates; titanite and apatite; for Zr^{4+} in zircon; and rare earth elements, mainly Ce and Y in rare earth minerals such as monazite and xenotime; iron oxides and oxyhydroxides. Uranyl ions can also be adsorbed on clay minerals, zeolites, iron oxides and hydroxides, manganese, and titanium, or they can be adsorbed, reduced, or create organic-metallic species with organic matter.

Moving on to the abundance of thorium in the rocks, thorium is a lithophile and is often associated with alkaline silicic igneous rocks. Granites and granodiorites may contain roughly 10 mg/kg of Th, but syenites are often more enriched, with up to 35 mg/kg of Th in some circumstances (Hazen *et al.,* 2009). Basalts and mafic intrusive rocks generally have 0.1 to 4 mg/kg of Th, but ultramafic rocks may have much less

(Wedepohl, 1978). The concentration of thorium in sedimentary rocks varies greatly. Thorium is a very immobile element that is geochemically isolated from mobile uranium in igneous parent rocks during weathering and alteration of primary minerals (Wedepohl, 1978). As a result, it is concentrated in resistate detrital heavy minerals like zircon, monazite, xenotime and apatite. If it is released during weathering, it is highly sorbed onto clays and iron and manganese oxide alteration products (Wedepohl, 1978). Consequently, residual deposits such as bauxites and heavy mineral placer deposits are generally rich in thorium. According to Wedepohl, (1978), typical values for shales and mudrocks are around 12 mg/kg Th; 1 to 7 mg/kg Th for sandstones; very low values in limestones, because thorium does not enter the carbonate lattice; 1 to 5 mg/kg Th in phosphatic rocks; and > 20 mg/kg in residual deposits such as bauxites and bentonites.

The content of thorium in metamorphic rocks varies significantly and is determined by the consentration of thorium in the parent igneous or sedimentary rock. According to Wedepohl, (1978), thorium concentrations in feldspathic rocks can range from 0.1 mg/kg in marble to > 67 mg/kg in some high-grade feldspathic rocks. Most metamorphic rocks, on the other hand, contain thorium concentrations that are near to the crustal average of 6–10 mg/kg (Wedepohl, 1978).

There are only a few thorium host minerals that contain thorium as an important component. Uranothorite ([Th,U]SiO4), uranothorianite ([Th,U]O_2), thorianite (ThO_2), , Thorite ($ThSiO_4$), and thorogummite ($Th(SiO_4)_{1-x}(OH)_{4x}$. Thorite-uranothorite, thorianite-uranothorianite, and monazite (cheralite) are secondary minerals found in alkaline granitic rocks, syenites, and related pegmatites. Monazite has also been discovered in Lower Palaeozoic mudrocks and low-grade metamorphic rocks in worldwide as a low-temperature concretionary authigenic mineral (Milodowski & Zalasiewicz, 1991). Authigenic monazites, on the other hand, are often deficient in

thorium. They appear to be confined to Lower Palaeozoic rocks in Europe; however they have recently been discovered in Triassic rocks from Iran (Alipour-Asli *et al.,* 2012). Thorogummite is a low-temperature secondary mineral that forms as a result of the weathering, alteration or metamictisation of primary thorite or thorium-rich minerals (Basham & Kemp, 1993).

Potassium concentrations are highest in the more fractionated alkaline silicic rocks and lowest in the silica-poor ultramafic rock types. Its concentration is mostly determined by the presence of significant potassium silicate minerals, which include alkali feldspars (sanidine, microcline, and orthoclase), micas (phlogopite, muscovite, paragonite, and biotite), and feldspathoids, and alkali-bearing amphiboles (Wedepohl, 1978):

- Alkali igneous rocks, such as granites, granodiorite, rhyolite, and trachyte, often contain 2.5 to 4.5 % potassium.
- Syenites and phonolites are more alkali-rich, with potassium contents ranging from 3 to 6 % potassium.
- Syenites and phonolites are more alkali-rich, with potassium contents ranging from 3 to 6%.
- Potassium concentrations in intermediate igneous rocks, such as diorites and andesites, are generally between 1 and 2%.
- Potassium concentrations in mafic igneous rocks, such as gabbros and basalts, are generally in the 0.5 to 1.3 % range.
- The potassium content in ultramafic rocks, which include pyroxenites, anorthosites, dunites, peridotites, and eclogites, is often quite low. Potassium concentrations, on the other hand, vary greatly, ranging from 10 mg/kg in certain dunites and peridotites to around 1% in some anorthosites.

Potassium concentrations in sedimentary rocks vary significantly and are influenced by detrital mineralogy, primary chemically precipitated sedimentary minerals, and sediment burial alteration. Potassium concentrations in carbonate rocks and sediments can range from 0.01% to 5%. The non-carbonate fraction contains the majority of the potassium in these materials. This is mostly made up of detrital silicate minerals such alkali feldspars, micas, and clay minerals (particularly potassium-rich clay minerals such as illite, smectite or mixed-layer illite-smectite).

The clay mineralogy controls the potassium concentration of mudrocks (clays, shales, mudstones, and siltstones), with a little contribution from K-feldspar. Potassium concentration and clay mineral content generally have a high positive association. This is also reflected in wireline gamma-logs of sedimentary sequences, where clay-rich strata are often associated with an elevated gamma response (Hurst, 1990). Illite and micas are the most prevalent and important potassium-bearing clay minerals found in mudrocks. Glauconite, which is often detrital in origin, can also be a significant source of potassium in particular sedimentary sequences. Three minerals primarily govern the potassium concentration of sandstones: K-feldspar, mica, and glauconite. With increasing sediment maturity, the quantity of detrital K-feldspar and mica decreases. During burying diagenesis, glauconite is often produced in situ as an authigenic mineral. The quantity of clay in the sandstone also affects the potassium content: poorly sorted clay-rich sandstones often have more potassium than well-sorted low-clay sandstones.

The presence or absence of potassium-rich salts precipitated from highly developed brines during late-stage severe evaporation determines the potassium content of evaporite rocks. Only tiny or minimal levels of potassium are found in pure gypsum, anhydrite, and halite. The presence of detrital clay minerals has a substantial impact on the potassium concentration in evaporites dominated by these minerals. Potash deposits

generated by the precipitation of potassium salts may be found in late-stage evaporite sequences. There are several potassium salts, but sylvite is the most significant potassium mineral in evaporites in terms of volume (KCl).

The potassium content in metamorphic rocks varies greatly. This is mostly due to the parent igneous or sedimentary antecedent rock's composition. Pelitic rocks formed by the metamorphism of mudrocks, for example, contain a lot of mica and, as a result, a lot of potassium. Quartzite formed by metamorphism of clean quartz-rich sandstone, on the other hand, have little or no potassium.

2.1.7.2 **Radioactivity in phosphate rock**

Phosphorite deposits are formed when nutrient-rich marine waters rise to the surface of a shallow continental shelf with limited circulation. Rock phosphate, also known as phosphate rock or phosphorite, is a non-detrital sedimentary rock that is densely packed with phosphate mineralization, including apatite (Filippelli, 2011). Phosphate rocks are thought to be an unusual source of uranium, particularly in certain deposits where it can reach high concentrations (Gabriel *et al.,* 2013; Emsbo *et al.,* 2015; Wu *et al.,* 2018). Although phosphorite deposits can contain up to 0.065% uranium and the resource is significant, the uranium is also coupled with other elements like Se and As, and the waste would be an environmental issue.

Other elements that could be concentrated in specific phosphate rocks, such as cadmium, radium, and thorium, are currently weighing heavily on their production and transformation. Phosphorus is always combined with other elements in phosphate rocks in the form of phosphate minerals, the most common and widely distributed of which is apatite (Mar & Okazaki, 2012).

Uranium in phosphate rock deposits throughout the world range from 3 to 400 mg kg -1 (Guimond & Hardin, 1989); It has been estimated that 1000 kg of Florida phosphate rock contains about 37 × 10^8 Bq each of ^{238}U and ^{226}Ra and 148 × 10^6 Bq of ^{230}Th (Menzel, 1968). Some of these elements are retained in the H_3PO_4 and the remainder is transferred to the by-products during fertilizer manufacture. For instance it is estimated that 60% of the radioactivity in mined Florida phosphate rock remains with slime and sand tailings during beneficiation (Guimond & Windham, 1975).

Phosphate rock is mined from geological deposits all over the world. The primary constituent of PR is apatite, a calcium phosphate mineral. Sedimentary phosphorites of marine origin are now the primary raw material for phosphate industries, accounting for a sizable proportion of global phosphate rock production 90%. Igneous phosphate rocks account for 10%, with the remainder derived from residual and guano-type sedimentary deposits (Pufahl & Groat, 2017). In terms of chemical quality, geographical distribution, and exploitability, both sources (igneous and sedimentary rocks) offer some advantages and drawbacks.

Phosphates are not currently mined for uranium, however uranium is recovered unofficially from phosphates used in fertiliser manufacturing by numerous countries, and most governments do not report uranium from phosphorites as a resource. Morocco has the most uranium reserves from phosphorite deposits, yet quoted amounts are cautious due to the connotation of uranium being present in commercial fertilisers (Fitzgerald *et al.,* 2014). Recent estimates put the global total at 22 million uranium (OECD/NEA-IAEA, 2008, 2010). Despite the difficulties in extracting uranium and other elements from phosphorites, these deposits represent a significant uranium reservoir that may become more strategic in the near future as environmental demands for uranium removal from phosphates become more pronounced. Recent estimates put

the global total at 22 million uranium (Grancea *et al.,* 2020). Despite the difficulties in extracting uranium and other elements from phosphorites, these deposits represent a significant uranium reservoir that may become more strategic in the near future as environmental demands for uranium removal from phosphates become more pronounced (Fitzgerald *et al.,* 2014).

Phosphate rocks have high scientific value in addition to their economic value. Sedimentary phosphates reveal important details about the ecology and chemistry of the world's past oceans. Indeed, their formation, accumulation, and preservation necessitate specific paleoenvironmental conditions, as well as complex biogeochemical processes during early diagenesis (Föllmi, 1996; Pufahl & Groat, 2017).

Furthermore, because of the relationship between the phosphorus cycle and other biogeochemical cycles, such as C and N, the production of phosphate rocks (phosphogenesis) plays an essential role in climate regulation, as well as nitrogen and oxygen levels in the atmosphere across geological timescales (Föllmi, 1996).

2.1.7.3 **Phosphate Fertilizer**

There is an increasing need to develop and intensify agricultural production in the tropical areas, because of population growth and the growing food demands of other regions. Tropical soil acidity, aluminium and other toxicities associated with it, low levels of major plant nutrients, trace element deficiencies, and disease hazards have all hampered agricultural production intensification on these soils.

Most acid tropical soils have low total P contents, usually below 200 mg/kg (Cabala & Fassbender, 1970; Von Uexkull, 1986). In highly weathered Oxisols and Ultisols, the two most important groups of tropical soils, despite the fact that the P content of organic

materials is relatively low, up to 80% of all P can be in the organic form and hence substantially concentrated in the surface horizon (Von Uexkull, 1986).

As soil pH falls, increasing concentrations of Fe and Al ions, as well as possibly Mn ions, in the soil solution combine with phosphate ions to form compounds with very low solubility. Furthermore, on the exchange complex, phosphate ions combine with Al to form insoluble compounds with the general formula Al $(OH)_2.H_2PO_4$ (Coleman *et al.,* 1960). Applied phosphate can thus precipitate Al and reduce or eliminate Al toxicity. This is commonly referred to as "phosphate liming" but unless an excess of P is applied, P may still be deficient.

Acid tropical soils typically have a low CEC and extremely low base saturation. Although Al or Mn toxicity and P deficiency are the most common causes of poor crop performance on acid soils, Ca, Mg, and K deficiencies are also common. This is especially true for the tropics' Oxisols and Ultisols. Once low pH and P deficiency are corrected, yields begin to improve; available soil K and Mg status frequently become limiting factors (Von Uexkull, 1986).

Phosphate fertilizers are enriched with ^{238}U during its production from phosphate rocks. When processing phosphate rock to make fertilizer, the phosphorous is removed by dissolving the rock in an acidic solution. Phosphategypsum is the name given to the waste that is left behind. This waste contains the majority of the naturally occurring uranium, thorium, and radium found in phosphate rock. Radium is formed when uranium and thorium decay into radium, and radon is formed when radium decays into radon, a radioactive gas. Because of the concentration of the wastes, phosphogypsum is more radioactive than the original phosphate rock (Roessler *et al.,* 1979; Guimond, 1978; NCRP, 1993).

After the ore is treated with sulfuric acid, fertilizers become somewhat enriched in uranium (up to 150% of the ore), while 80% of the ^{226}Ra, 30% of the ^{232}Th and 5% of the uranium are left in the phosphogypsum. Processing of phosphoric rocks can generate radiation emitted by ^{238}U and ^{226}Ra when released into the environment. The use of phosphate fertilizers in agriculture and gypsum in construction materials is another source of possible public exposure (Boukhenfouf, 2018).

The ores generally contain around 1500 Bq/kg of uranium and radium, although some phosphates contain up to 20000 Bq/kg of U_3O_8 (UNSCEAR 2008). In general, phosphate ores of sedimentary origin have higher concentrations of uranium family nuclides. Magmatic minerals, such as those from Kola (Russia) and Phalaborwa (South Africa), have lower concentrations of uranium-family nuclides and higher concentrations of thorium-family nuclides, although the total activity is lower than that of sedimentary minerals. According to Khalifa & El-Arabi (2005), sedimentary phosphate rocks contain relatively high concentrations of ^{238}U and its decay products (U, Th, Ra, Bi, and Pb) due to accumulation of dissolved uranyl complex in sea water during geological formation of the phosphate rocks.

Phosphate rocks vary considerably in their content of U, Ra, and Th, depending on the geographical area from which they were mined. In a survey of phosphate rock samples from all of the major phosphate rock-producing regions of the world at the time, the median contents were 59 mg.kg $^{-1}$ or U, 8 mg.kg $^{-1}$ of Ra (Menzel, 1968). It was estimated that totals of 148×10^5 Bq each of U and Ra and 555×10^3 Bq of Th had been applied per acre in some potato *(Solanum tuberosum* L) fields in Maine over a 45-year period. Such additions of U and Ra are nearly equal to the total amounts naturally occurring in the soils. However, the addition of thorium was much greater than the naturally occurring amount. Most crops are not as heavily fertilized with P as potatoes,

although tobacco *(Nicotiana tabacum* L.) is usually highly fertilized with phosphate (Valkovic, 2000).

The contribution of uranium and radium to agricultural lands owing to the application of phosphate fertilizers does not significantly affect the dose received from the general population (Kirchmann *et al.,* 1980). However, phosphorus, in the form of mineral phosphate rock, is sometimes added to cattle feed and this practice can result in increased levels of uranium and radium in cows' milk. However, continued application of phosphate fertilizers to soil over a period of many years could eventually double the radium and uranium content of the soil, which would result in a corresponding doubling of the dose to bone from this source (Eisenbud & Gesell, 1997).

Spalding & Sackett, (1972) stated that the uranium content of North American rivers is higher than in the past, which they attribute to increased runoff of phosphate fertilizers.

Literature on the radionuclide content of phosphates is rather extensive. Radium, uranium, thorium and members of their decay series are the principal radioelements present in fertilizers. Radium content in fertilizers is extensively discussed by some authors (Guimond, 1990; Roessler, 1990). Several authors have reported on uranium concentrations in phosphates (Cathcart, 1978; Górecka & Górecki, 1984; Paschoa et al., 1984; Vučić & Ilić, 1989). Radioactivity in phosphate rocks due to ^{238}U, ^{226}Ra, ^{232}Th and ^{40}K is discussed by some authors Komura *et al.,* (1985); others discuss U and Th activity as a function of particle size (Baeza *et al.,* 1995; Baeza *et al.,* 1995). Radioactivity released by the use of phosphate fertilizers, accumulation in soil, migration and transfer or radioactivity into plants is extensively discussed (Rutherford *et al.,* 1994; Aswathanarayana, 1988; Guimond & Hardin, 1989; Scholten & Timmermans, 1995; Rothbaum *et al.,* 1979; Shishkunova *et al.,* 1989; Zielinski *et al.,*

(2000); Ahmed & El-Arabi, 2005; Da Conceicao & Bonotto, 2006; Hassan *et al.,* 2016; Lubkowski, 2016). Sedimentary phosphate ores, such as those found in Florida and Morocco, tend to have high concentrations of uranium, whereas the opposite occurs with magmatic ores, such as apatite from Kola. Typical activity concentrations of ^{238}U are 1500 $Bq.kg^{-1}$ in sedimentary phosphate deposits and 70 $Bq.kg^{-1}$ in apatite. ^{238}U is generally found in radioactive equilibrium with its decay products. The activity concentrations of ^{232}Th and of ^{40}K in sedimentary phosphate rock are much lower than those of ^{238}U, and comparable to those observed normally in soil (Papastefanou, 2002).

2.1.7.4 **Fertilizer consumption in Malaysia**

Fertilizer consumption is the amount of plant nutrients consumed per unit of arable land. Fertilizers include nitrogenous, potassium, and phosphate fertilisers, including ground rock phosphate. Traditional nutrients, such as animal and plant manures, are excluded. The FAO defines arable land as land under temporary crops (double-cropped areas are counted once), temporary meadows for mowing or pasture, market or kitchen gardens, and land temporarily fallow. Land that has been abandoned as a result of shifting cultivation is not included.

Malaysia has 2.4 million ha of peat and this type of soil is very poor in phosphorus and needs P application (Rahman et al., 2014).

Mineral fertilisers account for more than 90% of all fertilisers used in Malaysian farming systems. Urea, ammonium sulphate, calcium ammonium nitrate, phosphate rock, super phosphates, ammonium phosphate, potassium chloride, potassium sulphate, and NPK, NP, and PK are the main fertilisers (Goh & Fairhurst, 2003). Due to the rapid expansion in crop production, particularly of plantation crops (rubber, oil palm, and cocoa), has resulted in an increase in fertiliser use. The most significant increase has been seen in potassium fertilisers. This significant increase in potassium fertiliser use is

due to the continued expansion of oil-palm cultivation, which necessitates large amounts of this nutrient. The estimated nutrient removed by oil-palm (producing 25 t/ha fresh fruit bunches (FFB) per year) are 192, 11, 209, 36 and 71 kg/ha per year of P, N, K, Mg and Ca, respectively (Goh & Hardter, 2003).

In 2018, fertilizer consumption for Malaysia was 2,106.5 kilograms per hectare. Fertilizer consumption of Malaysia increased from 175.1 kilograms per hectare in 1969 to 2,106.5 kilograms per hectare in 2018 growing at an average annual rate of 6.82%.

2.1.8 The behavior of natural radionuclides in the environment

Different types of radionuclides or radioisotopes can be found in nature. They tend to be ubiquitous in the biosphere as they can occur naturally or deliberately synthesized. Radioactivity occurs as a result of the accidental disintegration of a parent radionuclide and the creation of a daughter nuclide by releasing γ, β and α radiation in the phase (Malik, 2021). Radionuclides that find their way into environmental spheres may cause adverse effects as radioactive contamination. Furthermore, if not adequately handled, they may also pose an occupational health risk (Kato, Konoplev & Kalmykov, 2020; Saleh & Rahman, 2018).

Radiation may be released from electron excitation and emission. This process occurs by the electron absorbing energy from external sources of electromagnetic radiation. The extra energy that the excited electron consumes is emitted in due course by releasing lower-energy electromagnetic radiation. Hence, the energy of an electromagnetic wave is directly proportional to its frequency and inversely proportional to the wavelength. As a consequence of nuclear instability, radionuclides intrinsically will have excess of energy. Radioactive decay arises because a nuclei is unstable. The ratio of neutron to proton and the total number of nucleons in the nucleus are the two determining factors that help ascertain the degree of stability of an isotope (Saleh &

Rahman, 2018; Kato, Konoplev & Kalmykov, 2020). However, to become more stable radionuclides emit particles or rays. Radiation is the release of energy particles and rays from atoms. Accidental release of radionuclides along with their decay products end up naturally in soil, water and air ecosystems. Many of tnese radionuclides can be anthropogenic generated and accidentally released in the environment leading to associated health risks. United States Nuclear Regulatory Commission (U.S.NRC) reported that on an annual basis a person will typically receive an annual dose of 620 millirem (Saleh & Rahman, 2018; Kato, Konoplev & Kalmykov, 2020). In that regard, natural sources account for 50% of radiation exposure that people generally receive while anthropogenic sources account for the remaining 50%. Radionuclides such as ^{226}Ra, ^{228}Ra, ^{232}Th and ^{238}U are commonly found in various ecosystems. In nature, the radionuclides in some series are approximately in a state of secular equilibrium. This entails that that the activities of all radionuclides within a series are nearly equal. All radium in nature is radioactive. It is found in each of the three natural radioactive series, the thorium series, the uranium series, and the actinium series. However, radium higher solubility and its decay to radon make it a primary environmental concern. As a radioactive gas, radon is colorless, odorless and tasteless. Inhala- tion is the primary route of radon exposure as it seeps into homes viz.; cracks in walls, floors, foundations and through floor drains and sumps. Weathering releases and concurrent speciation of radionuclides and nuclides to water, sediment, soil and air with potential for further distribution and dispersion via dust and biota uptake has to be taken into account in modeling and assessing their mobilization and remobilization. More precise knowledge of the impact of various abiotic components is paramount (Valkovic, 2000; Schroeyers, 2017; Saleh & Rahman, 2018). Interaction of radionuclides with various physical and chemical constituents present in environmental systems represents a key factor in affecting their environmental speciation and mobility. It has been reported that the

migration and mobility of radioisotopes in the presence of mineral surfaces plays a vital role in predicting the environmental impacts in the case of an accidental release. Hence as vitally important in assessing the risk associated with radioactive waste disposal or radioactive contaminated sites. The term adsorption refers to the adhesion of contaminants, termed adsorbate, to a surface, termed adsorbent. Hereafter, the term sorption is used to refer to the combined process of adsorption and absorption processes occurring at the surface of a sorbing material. Many investigations have suggested that sorption-desorption process is one of the most important factors affecting the fate and behavior of radionuclides and contaminants in the environment (Saleh & Rahman, 2018). Varying factors have been reported to influence the process including organic matter content and degree of humification, dissolved organic matter, surface tension of ous phase, level of system pH, buffering capacity and ionic strength, type of clay and content, change in system redox, competition for sorbing sites, characteristics of sorbent and sorbate, precipitation and temperature fluxes, interaction mechanisms and contribution of different types of binding phase, sorbent solubility in a given system boundary, weathering as well as the concentration of the contaminant (Saleh & Rahman, 2018; Kato, Konoplev & Kalmykov, 2020).

2.1.8.1 **Radioactive radium in the environment**

Radium is element number 88 in the Periodic Table and it belongs to the alkaline earth metals. Twenty-five radium isotopes have been identified, each with a different number of neutrons in its nucleus, but the most abundant among the naturally occurring isotopes are ^{226}Ra, an α emitter with a half-life of 1600 years, and ^{228}Ra (mesothorium), a β emitter with a half-life of 5.8 years. They are daughters of the most abundant naturally occurring isotopes of uranium ^{238}U and thorium ^{232}Th, respectively. These two isotopes of radium are also the most radiotoxic (Iyengar, 1990; Campos, 2015).

Radium also became famous. It was a source of radioactivity for medical and industrial radiography and was used for research into radioactivity and the structure of matter. Its luminescent properties, enhanced by mixing with a solid scintillator, such as zinc sulphide, were used to make dials glow in the dark. Its ionizing properties were exploited for static electricity eliminators and electronic valves. In the 1930s, radium mixed with beryllium provided a convenient source of neutrons (Campos, 2015). Within a few years of its discovery in uranium ores, radium was found to occur widely in the natural environment. Many different materials yielded evidence of radioactivity and, in most cases; this could be attributed to its content of the uranium, thorium or actinium series nuclides (Jenkins *et al.,* 1972). None of the early workers appear to have thought that such radioactivity might be hazardous to health. On the contrary, these discoveries added to the perceived curative value of spring water and spas. The discovery that radium is hazardous to humans resulted from a study of occupationally exposed workers and, since the inception of the ICRP, the major concern of the radiation dose limitation system has been such workers. Radium was first identified as a significant environmental pollutant from the uranium industry in the 1950s by Tsivoglou and others working in the Colorado Plateau area of the (Houtermans *et al.,* 1980). The hazard posed by radium pollution of the environment is more difficult to assess than radium contamination of the workplace. The many different transport mechanisms and exposure routes, and the variability of biological uptake and of human behaviour make environmental radiation dose assessment little more than formalized guesswork (De Bortoli & Gaglione, 1972; Campos, 2015).

There are no stable isotopes of radium. There are four naturally occurring radioactive isotopes present in the environment because they are part of decay series of primordial radionuclides, ^{226}Ra is part of the ^{238}U series, ^{223}Ra is part of the ^{235}U series and ^{224}Ra and ^{228}Ra are part of the ^{232}Th series. The only anthropogenic isotope with a significant

half-life is ^{225}Ra ($t_{1/2}$ = 14.9 days) from the ^{237}Np series, where the immediate parent is ^{229}Th ($t_{1/2}$ = 7880 years). This Ra isotope has been used as a yield tracer for Ra chemistry and as the subject of nuclear physics studies, but has not been reported in the environment (De Bortoli & Gaglione, 1972). The nuclear properties of the five main radium isotopes are given in Table 2.2 (Hursh, 1957) and can be summarized as follows:

- ^{226}Ra, ^{223}Ra and the two isotopes, ^{228}Ra and ^{224}Ra, are, respectively, decay products of the uranium (^{238}U), actinium (^{235}U) and thorium (^{232}Th) decay chains (respectively, the $4N^{+2}$, $4iV^{+3}$ and 4JV decay chains);
- ^{225}Ra is an isotope in the ^{237}Np decay chain (4AH-1 chain).

Table 2.3: Naturally occurring and assumed naturally occurring isotopic of Radium

Mass	Common name	Decay series	Half-life	Nature and energy (in MeV) of decay
226	Radium	U-238	1622 a	*α,* 4.79
228	Mesothorium	Th-232	6.7 a	β^-, 0.012
224	Thorium-X		3.64 d	*α,* 5.68, 5.45
223	Actinium-X	U-235	11.2 d	*α,* several 5.4-5.7
225		Np-237	14.8 d	β^-,0.31

Each decay series includes a number of isotopes that have a wide range of half-lives and represent a number of elements that have substantially different characteristics. The concentration of each isotope is controlled by that of the parent and the amount of time since fractionation between the isotope and its parent has occurred. For samples sealed over long timescales, the activity of each isotope (the decay rate) is the same as that of its parent, i.e. it is in secular equilibrium with its parent. For example, for the ^{232}Th decay series,

$$(^{232}Th) = (^{228}Ra) = (^{228}Th) = (^{224}Ra) = \cdots$$

following a standard notation where an isotope in parentheses, e.g. (^{232}Th), denotes the activity of that isotope. There are two important points to note: (a) In secular equilibrium, the distribution of a daughter isotope is controlled by that of the parent isotope, and so ultimately all isotopes in the series are controlled by the long lived parent (here, ^{232}Th); (b) While the activities are equal, the molar abundances are inversely proportional to the decay constants, so that the concentrations of very short lived nuclides are very low (IAEA, 2014).

For the ^{232}Th decay series, the molar ratio at secular equilibrium is:

$$\frac{\boldsymbol{228_{Ra}}}{\boldsymbol{232_{Th}}} = \frac{\boldsymbol{\lambda_{232Th}}}{\boldsymbol{\lambda_{226Ra}}} = \frac{\boldsymbol{228Ra_{t\,1/2}}}{\boldsymbol{232Th_{t\,1/2}}} = 4.0 \times 10^{-9} \tag{2.74}$$

And

$$\frac{224_{Ra}}{232_{Th}} = \frac{224Ra_{t\,1/2}}{232Th_{t\,1/2}} = 7.1 \times 10^{-13} \tag{2.75}$$

For the ^{238}U decay series, the molar ratio is:

$$\frac{226_{Ra}}{238_{U}} = \frac{226Ra_{t\,1/2}}{238U_{t\,1/2}} = 3.6 \times 10^{-7} \tag{2.76}$$

For the ^{235}U series:

$$\frac{223_{Ra}}{235_{U}} = \frac{223Ra_{t\,1/2}}{235U_{t\,1/2}} = 3.1 \times 10^{-8} \tag{2.77}$$

For all natural U:

$$\frac{238_U}{235_U} = 137.88 \qquad \textit{and also}: \frac{238_U}{235_U} = 21.8$$

While there is some variation in the Th/U ratio in rocks and soils, for the continental crust the average ratio is:

$$\frac{232_{Th}}{238_U} = \ 3.8 \qquad and\ also: \frac{232_{Th}}{238_U} = 1.2$$

Therefore, even where U and Th are strongly enriched, Ra isotopes have extremely low molar concentrations. Clearly, Ra is composed predominantly of ^{226}Ra, although Ra activity concentrations due to ^{224}Ra and ^{228}Ra are comparable. ^{223}Ra is a minor constituent, but an important tracer in the marine environment. Each Ra isotope is generated from the decay of a corresponding.

Each Ra isotope produces a chain of daughters that are very short lived and contributes to the overall radiation load of a Ra bearing substance. For ^{223}Ra and ^{224}Ra, the daughter isotopes all have very short half-lives, and so will rapidly grow into secular equilibrium with the parent Ra isotope. For ^{226}Ra, the immediate decay product is the noble gas ^{222}Rn, which may be readily lost prior to decay from non-retentive materials. However, in minerals or large organisms, the ^{222}Rn may not escape before decay, and so will generate a chain of short lived daughter nuclides. If the ^{210}Pb has been recently separated from ^{226}Ra, then this isotope will accumulate over the timescale of its half-life 22.3 years (Choppin, Liljenzin & Rydberg, 2002). Similarly, while the activity of ^{210}Bi will follow that of ^{210}Pb, the isotope ^{210}Po will slowly grow into secular equilibrium with ^{210}Pb as determined by its half-life of 138 days. For ^{228}Ra, the immediate daughter ^{228}Ac will generally be found in secular equilibrium with its parent, while the activity of ^{228}Th will grow into secular equilibrium with ^{228}Ra according to its half-life of 1.9 years. The short lived nuclides further along the decay chain may have activities equal to that of ^{228}Th, depending on the environmental medium. Overall, the impact of the ^{226}Ra and ^{228}Ra daughters will depend upon the retention of ^{222}Rn and the time of separation from ^{210}Pb, ^{210}Po and ^{228}Th (IAEA, 2014).

Radium is an alkaline earth metal, with atomic number Z = 88. It is expected to have similar chemical characteristics to those of the other alkaline earths Table 2.3, as all these elements are only present in nature in the +2 oxidation state. There are various trends in behaviour across the group due to increasing ionic radius with atomic number. The behaviour of Ra is similar to that of Ba due to the similarity of their ionic radii. Therefore, where Ra data are not available, Ba has often been used as a chemical analogue for predicting Ra behaviour. Radium can be readily separated through chemical processes from its parent, Th. Thorium is highly insoluble in natural waters, and strongly adsorbs onto mineral surfaces. It has a strong affinity to humic acids and other organic ligands, and so can be concentrated in organic deposits or transported in organic colloids (Langmuir & Herman, 1980). In contrast, U is highly soluble under oxidizing conditions. It is readily adsorbed onto mineral surfaces, though to a lesser degree than Th and Ra, and can be complexed by organic ligands. Uranium is also incorporated into secondary Fe oxyhydroxides, where daughter nuclides can be retained (Sheppard, 1980; IAEA, 1990; Carvalho, 2014).

Table 2.4: Element characteristics

Alkaline earth elements	Atomic number	Crystal ionic radius (Å)	Hydrated ionic radius (Å)	Electronegativity
Sr	38	1.13	4.12	0.99
Ra	88	1.52	3.98	0.90
Mg	12	0.62	4.28	1.23
Ca	20	0.99	4.12	1.04
Ba	56	1.35	4.04	0.97

(IAEA, 1990)

Due to the very low molar concentrations of Ra in the environment, precipitation of Ra phases is rarely important. Rather, removal from waters can occur by co-precipitation of phases in which Ra forms a solid solution. Barium is typically present in

natural waters and ground waters (Grandia *et al.,* 2008; Felmlee & Cadigan, 1978) in molar concentrations 108 times greater than those of Ra.

The concentrations of Ra in waters and the mobility of Ra through the environment are generally controlled by interaction with surfaces by adsorption through ion exchange. This is commonly described by a partition coefficient (*Kd*), which is defined as:

$$Kd = \frac{concentration\ in\ solid\ phase}{concentration\ in\ solution} \quad (2.78)$$

The concentration in the solid phase is expressed as the amount of adsorbent in a total mass of solid (in e.g. moles/kg), while the concentration in solution is expressed in moles L^{-1}. Therefore, the unit of Kd is in terms of volume of solution to mass of solids (e.g. L/kg). Data for Ra Kd values are limited compared to many other contaminants (IAEA, 2014).

The studies reviewed below indicate that Ra is readily adsorbed to clays and mineral oxides present in soils, especially at near neutral and alkaline pH conditions. For the pH conditions of most natural waters, dissolved Ra will be present primarily as the uncomplexed Ra^{2+} cation. Sorption studies generally confirm the adsorption behavior expected for Ra^{2+} as a function of pH, with negligible adsorption at very acidic pH values and increasing adsorption with increasing pH. As discussed by (Krupka *et al.,* 1999), the pH range at which adsorption of cations begins to increase on mineral surfaces depends on the values of the point of zero charge (PZC) for each type of mineral, when the electrical charge density on a surface is zero. In general, at pH values of less than the PZC, the mineral surface has a net positive charge and strongly adsorbs anions. At pH values greater than the PZC, the surface strongly adsorbs dissolved cations.

Radium is the heaviest of the Group II alkaline earth metals. Like Ba, Sr and Ca, which also belong to Group II, Ra forms insoluble sulphate, carbonate and chromate salts. The chloride, bromide, nitrate and hydroxide salts of Ra are soluble in water. In general, Ra salts are less soluble than are corresponding Ba salts (Moore, 1972).

Discrete Ra minerals such as $RaSO_4$ are not reported in earth materials and the Ra concentrations in water in contact with soil or sediments are reduced by sorption (e.g. by hydrous oxides of Fe, Al and Mn) and co-precipitation reactions (Langmuir & Riese, 1985).

Radium competes with other alkaline earth cations for sorption sites. In comparison to other alkaline earth elements, the relative affinity of this group of elements for ion exchange is: $Ra^{2+} > Ba^{2+} > Sr^{2+} > Ca^{2+} > Mg^{2+}$ (Tesoriero & Pankow, 1996). The adsorption of Ra has been shown to be strongly dependent on ionic strength and concentrations of other competing ions in that adsorption of Ra decrease with increasing ionic strength. Overall, for widespread phases, Ra is less efficiently sorbed onto iron oxides and more efficiently sorbed onto secondary minerals with high cation exchange capacity (CEC) than is U (Ames *et al.,* 1983). Even for specific materials, adsorption constants are strongly dependent upon solution composition (e.g. Eh, pH and other cations), temperature, surface characteristics and degree of alteration (Beneš & Poliak, 1990). The studies discussed below provide a guide to Ra behaviour in the environment, though site specific values will ideally be determined taking into account mineralogy, actual water chemistry and competing ions, mineral chemistry, surface chemistry, availability of active surfaces and variations in site conditions.

Johnston & Gillham, (1980) stated that Ra is present as Ra^{2+} over the pH range 4–8 and does not readily form complex species. Radium could be expected to co-precipitate with BaSO4, carbonates and ferric hydroxides, and the presence of these compounds in

the soil may lead to overestimated Ra Kd values. Since Ra generally occurs in nature as a divalent cation, it therefore has a high affinity for the regular exchange sites of the soil. Johnston & Gillham, (1980) have correlated Kd values with soil CEC.

Arnold & Crouse, (1965) obtained a correlation between Ra adsorption and the CEC. The leaching studies reported by (Havlik *et al.,* 1968) support the view that cation exchange is an important mechanism for Ra adsorption. Nathwani & Phillips, (1978) showed that organic matter and clay play a significant role in the adsorption of ^{226}Ra, with organic matter adsorbing approximately ten times as much Ra as clays.

Haji-Djafari *et al.,* (1981) found sorption of Ra to increase with soil pH (Kd = 12 L/kg and 100 L/kg at pH 4.5 and 7, respectively) and (Rusanova, 1962) monitored desorption decreases with pH 5–10 times higher desorption at pH 3 than at pH 6–10. Calcium concentrations in the soil solution or exchangeable phase significantly affect Kd (Ra) values.

Relative to other alkaline earth elements, Ra is the one most strongly sorbed by ion exchange on clay minerals. Further, clays generally have a high specific surface area due to their fine grained nature. Therefore, in any soils, aquifers or rocks that have been exposed to weathering, these phases have strong effects on Ra migration.

Kaolinite is commonly formed by alteration of aluminosilicate minerals, in particular from feldspars by leaching of Na, Ca and other cations by weathering. It is therefore typically found in granitic rocks, especially those weathered under conditions of relatively low pH. Amongst the common clay groups, kaolinites generally have relatively low CECs (3–15 meq/100g at pH = 7) (Carroll, 1959). Results from (Riese, 1982; Langmuir, 1997) indicate that significant adsorption of Ra occurs on kaolinite over a pH range of 3–9. The adsorption of Ra increases with increasing pH, especially

at pH values greater than 6, and decreases with increasing concentrations of dissolved calcium. However, Beneš *et al.,* (1985) found that adsorption was less than on montmorillonite, and that the pH dependency of Ra adsorption on kaolinite was less than that determined for ferric hydroxide and quartz. For a pH of 7.58, a partition coefficient (Kd) of ~2900 mL/g at low Ra concentrations was found, and generally varied according to a Langmuir isotherm. Ra was easily desorbed by changing solution chemistry, and was strongly affected by competition from other ions. Ames *et al.,* (1983) conducted batch experiments at different temperatures and a wider concentration range, and found a weak dependence of Kd on temperature and concentration, with a Kd of ~500 mL/g at 25°C and 0.05 Bq/L in solution.

Radium has been found to adsorb onto oxidized Fe phases that are widely found as weathering products on rock surfaces, in soils and within aquifers. Fe is contained in various primary minerals, and Fe oxyhydroxides form as fine-grained particles and surface coatings. Beneš *et al.,* (1984) reported that adsorption of Ra onto ferric hydroxide is strongly dependent upon pH, with > 50% adsorption occurring above pH ~8, and is readily reversible. Therefore, the extent of adsorption changes substantially within the pH range of natural waters.

Manganese oxide is known to strongly scavenge Ra, and is routinely used to concentrate Ra from water samples. Manganese oxides commonly occur in sediments as coatings and fine aggregates with large surface areas, and so can be important in controlling Ra behavior even at low bulk compositions. While many Mn minerals have been reported, Mn oxides are typically fine-grained and poorly crystalline and so often remain uncharacterized (Post, 1999). The stability of Mn phases is sensitive to water conditions, with the solubility controlled by redox reactions between soluble Mn (II)

and insoluble Mn (III) and Mn (IV), which may link bulk Ra adsorption to changes in pH and Eh. This has been argued for some ground waters by (Sturchio *et al.,* 2001).

Lima & Penna-Franca, (1988) observed that in farm soils from a highly radioactive region in Brazil, approximately 50% of ^{226}Ra was associated with the residual fraction, 30% with oxides of Fe and Mn, 15% was organically bound, 5% was associated with carbonates and only 3% was in an easily exchangeable form. Similarly, (Bunzl *et al.,* 1995) found that for a soil close to the exhaust of the ventilating shaft of a U mine, 6% of the ^{226}Ra was associated with the exchangeable fraction, 15% each was associated with the organic and oxide fraction and 66% was in the residual fraction. For soils outside the area of impact, no ^{226}Ra was found in the exchangeable and organic fractions, 3% was associated with the oxide fraction and more than 90% was in the residual fraction. In contrast, for two Australian soils. Cooper *et al.,* (1981) found that the majority of Ra was associated with the exchangeable fraction and with iron and manganese oxides.

Only a few studies have been conducted on the adsorption of Ra on organic matter. The results of these studies suggest that Ra may be strongly adsorbed by organic material in soils (Greeman *et al.,* 1999; Nathwani & Phillips, 1978; Nathwani & Phillips, 1979). Nathwani & Phillips, (1978, 1979) used batch equilibration experiments to study ^{226}Ra adsorption by soil with different physicochemical characteristics. The measured ^{226}Ra adsorption followed Freundlich adsorption isotherms over a large range of ^{226}Ra concentrations. Organic matter and clay were determined to be the dominant phases contributing to the adsorption of ^{226}Ra on these soils. Nathwani & Phillips, (1979) suggested that adsorption affinity of the organic matter and clays is primarily due to their CEC. Their results also indicated that organic matter adsorbs approximately 10 times more ^{226}Ra than the clays. Greeman *et al.,*

(1999) determined that Ra is enriched in the organic (humic) matter fraction of selective chemical extraction separations of soils.

Because Ra has four naturally occurring isotopes with half-lives ranging from 3.7 d to 1600 a, it is a powerful tracer of environmental processes. The distributions of these isotopes may be modelled to reveal important information about the environment. Thus, Ra is not only a potential environmental problem, but also a potential environmental problem solver.

The average radium content of rocks in North America and Europe varies from 1×10^{-6} μg/g for sedimentary shales and clays to 1×10^{-8} μg/g for ultrabasic rocks (Vinogradov, 1959). The average radon content varies from 6.9×10^{-12} μg/g to 6.5×10^{-14} μg/g for the same types of rocks; the content of radium (and of uranium and thorium) is higher in granites and other acid rocks than in basic rocks (Vinogradov, 1959). Keefer & Dauer, (1970) reported that the oolitic limestone formation of Miami, Florida contains 5×10 ug Ra/g, and the south Florida sands formed from the weathering of this limestone contain 7×10^{-7} to 7.6×10^{-6} μg Ra/g.

Many salts of radium are soluble in water; therefore surface waters may be enriched in both radium and radon. Radium concentrations of various Russian mineral springs are 1×10^{-5} to 748×10^{-6} μg/g. The radium concentration in tabling material (the residue of uranium extraction) is usually higher than in uranium ore (Gera, 1975). Typical radium concentration in tailings at U.S. mills is about 1×10^{-3} μg/g. However, the radium content is highly dependent on the particle size of the tailing materiel since approximately 30% of the tailings contain 70−80% of the radium (Gera, 1975). The finer tailing material often referred to as slime, can have several nanograms of radium per gram of dry weight.

The Earth's crust consists of a variety of rocks belonging to igneous, sedimentary and metamorphic groups which are 95% magmatites, 4% slate or shale, 0.68% sandstone and 0.32% carbonate rocks (Rösler & Lange, 1965). Concentrations of naturally occurring radionuclides in igneous rocks are usually higher compared to sedimentary ones, excepting shale, deep-sea sediments and phosphate rocks, while metamorphic rocks have concentrations similar to those of the rocks from which they were derived. High silica igneous rocks contain relatively higher U concentrations compared to such basic low silica igneous rocks as basalt. Isotopes of Ra are progeny of the U, Ac and Th natural radioactive decay series of radioactive elements and are therefore widely distributed in the Earth's crust. The estimated average ^{238}U concentration in the continental crust is 32.9 Bq/kg (Taylor, 1964) and, assuming radioactive equilibrium with ^{238}U, the crustal ^{226}Ra activity is expected to be of an equivalent order. Although it can be anticipated that in most igneous rocks Ra isotopes are present in equilibrium concentrations with their precursors, the impact of some environmental factors, such as weathering, can change ratios between ^{226}Ra or ^{228}Ra and their precursors, i.e. ^{230}Th and ^{232}Th, because of the differences in their environmental mobility. The highest ^{226}Ra concentrations were observed in shale, bitumen slate and volcanic and phosphate rocks followed by granites, clay rocks and sandstone and, finally, sedimentary rocks, lime and carbonate (Carvalho, 2014; Saleh & Rahman, 2018). The high ^{226}Ra levels in shale and bitumen slate are likely due to associations of clay rich material of organic origin, while phosphate rocks of sedimentary origin are well known as minerals rich in U. Granites and basalts tend to have nearly similar mean ^{226}Ra concentrations. At the same time, granites have a much wider range of ^{226}Ra occurrences, with especially high concentrations in rocks with a substantial occurrence of U and Th. Data from Conway, in New Hampshire and the Colorado Front Range,

both in the United States of America; illustrate such a phenomenon (Richardson, 1968; Phair & Gottfried, 1968; Carvalho, 2014).

2.1.8.2 **Radium-226 in the Soil**

Concentrations of naturally occurring radionuclides in the soil are heavily influenced by the parent rock properties. Rocks are continuously affected by many environmental factors which result in soil formation such as changes in temperature, water, flora and fauna, etc. In particular, because of its weathering from the host rocks and its further dispersion in the environment, Ra can be transported and deposited as loess, silt placers and tertiary soil (Iyengar, 1990; Carvalho, 2014; Saleh & Rahman, 2018). In the soil, Ra behaves very much like other elements from Group 2 (alkaline earth metals) of the Mendeleev periodic table, namely, Ca, Sr and especially Ba. Ion exchange processes play an important role in the migration of Ra in soil, and in this respect it has a close similarity to Ba owing to its large ionic radius. The ion exchange capacity characteristics of different types of soil vary considerably and this has a significant influence on the distribution of Ra in soil. Radium dissolved in groundwater (or surface water) is transferred with the water flow until it becomes adsorbed in the soil (Iyengar, 1990). Some of the Ra data available for different types of soil are given in Table 2.5.

As Ra is highly electropositive, it reacts readily with many agents; most of these reaction products are insoluble. Radium also co-precipitates with Ba and Sr to form insoluble sulphates. Uptake of the bivalent ^{226}Ra is mostly controlled by factors affecting the soil exchange capacity. Radium has a high affinity for the regular exchange sites of the soil (IAEA, 2009). Organic matter adsorbs almost ten times as much Ra as clay, according to Simon & Ibrahim (1987). Ra concentrations in plants have been observed to be reduced by increased exchangeable Ca, increased pH, and high soil sulphate content.

Many early geochemical/geophysical exploration projects noticed the relationship of Ra with organic matter. In a recent investigation of wetland soils (14–50 % organic matter) in Ireland, activity ratios of $^{226}Ra/^{238}U$ of up to 9.0 were found; the higher ratios reflect a loss of ^{238}U compared to ^{226}Ra, assuming initial isotopic equilibrium in soil (i.e. $^{226}Ra/^{238}U = 1.0$) (Pettersson *et al.,* 1988; Vandenhove et al., 2006; IAEA, 2009).

Table 2.5: Ra-226 concentrations in soils

Landscape	Type of soil	Texture	^{226}Ra Bq/kg	Reference
Tundra	−	−	140 ± 20	Taskayev *et al.,* 1978
Taiga	Soddy-podzolic	Loam	280 ± 70	Taskayev *et al.,* 1978
Taiga	Soddy-podzolic	Loam	14 – 44	Taskayev *et al.,* 1978
Mixed forest	Podzol	Loam	30 ± 3.7	Baranov *et al.,* (1964)
Mixed forest	Soddy-podzolica	Light Loam	22.6 ± 1.0	Drichko & Lisachenko, (1984)
Mixed forest	Grey forest soil	Loam	28.1 ± 0.7	Drichko and Lisachenko, (1984)
Mixed forest	Bog-podzol	Organic	24 ± 4	Baranov *et al.,* (1964)

Because the highest ratios are seen in depth zones that are only saturated at particular periods of the year, this implies that oxidising conditions and percolating soil water leaching of uranyl complexes may cause such disequilibrium. It indicates Ra's relative immobility in comparison to U under oxidising conditions (Vandenhove *et al.,* 2006). The high uptake of radionuclides by lichens and mosses is one of the primary causes explaining the significant accumulation of radionuclides in these species. Most lichens and mosses obtain water and mineral nutrients mainly by foliar absorption. These plants lack a well-developed root system and tend to accumulate contaminants from the atmosphere by entrapping airborne articulates by both passive (which normally dominate) and active mechanisms via extracellular ion exchange activities (Zeichmeister et al., 2003). Many investigations have shown a linear relationship

between radionuclide and heavy metal concentrations in lichens and mosses. The lowest values are specific to temperate environments with low releases of these radionuclides to the atmosphere (e.g., Saskatchewan, Canada), whereas concentrations are three- to fivefold higher in dry industrial areas with higher resuspension and release of naturally occurring radionuclides to the air.

Many fungi species are characterized by a marked ability to accumulate some radionuclides, particularly ^{137}Cs. However, transfer factors for many other radionuclides and heavy metals are also typically higher for fungi than for woody and grassy plants (Balonov *et al.,* 2010). Overall, data on ^{226}Ra concentrations in fungi are generally rather scarce. Baeza et al., (2004) reported data for ^{226}Ra concentrations in 71 fungi species sampled in Spain, with a mean value of 25 ± 22 $Bq.kg^{-1}$ and a range of 13 – 87 $Bq.kg^{-1}$, although ^{226}Ra was above the detection limit only in 38.4% of the samples. Concentrations of ^{226}Ra in saprophytic species 32 ± 27 $Bq.kg^{-1}$ were higher than those in Mycorrhizal species 23 ± 21 $Bq.kg^{-1}$; however, this difference was not identified as statistically significant.

Kribek *et al.,* (1979) reported that the vertical distribution of Ra in soil profiles in an area of U mining depended on the type of soil profile. In flood plain soil significantly contaminated by Ra owing to periodic flooding with river water receiving mine effluents, approximately 79% of the Ra contained in the top 60 cm of the soil was accumulated in the 0 − 10 cm layer and 18% in the 10 - 25 cm layer. The latter conclusion appears to back with the findings of Justyn and Stanek (1968), who computed the rate of radium transfer during water seepage through a soil layer using Boenzi *et al.,* (1965) and Dlouhy (1968) proposed relationships. Using a value of 2000 − 3000 $cm^3. g^{-1}$ for the distribution constant Kp and a ratio of mass to pore volume of the soil of 3 − 5 g. cm^{-3}, they calculated a rate of radium movement equal to or less than 10^{-}

$^{7}-10^{-8}$ cm. s^{-1}. According to the scientists, soil blockage and swelling might delay the migration rate even further. The computation was based on the situation of neutral water seepage and did not take into account the influence of acidity, which might increase radium mobility in soil (Nathwani & Phillips, 1978). Nevertheless, Rapid neutralisation of the wastes in the soil layer or mixing with ground fluids would help to slow the migration of radium released with acid wastes into ground waters (Kaufmann & Bliss, 1977).

Kirchmann *et al.,* (1966) determined an inverse relationship between the log of the ^{226}Ra content in plants and the amount of sorptive material in soil. Lauria *et al.,* (2009) reported a significant inverse correlation between concentration ratios (Cr) – Ra and the soil CEC. According to (Simon & Ibrahim, 1990), organic matter adsorbs about ten times as much Ra as clay, which is more adsorptive than other soil minerals. Vandenhove & Van Hees, (2007) found, in a potted soil experiment with prairie soils, that log-*Cr* for grass and clover were strongly correlated with the soil CEC and with soil organic matter.

It has been documented that alkaline earth metals may compete for adsorption binding sites on the root surface. In the presence of high soil concentrations of alkaline earth cations, the uptake of Ra may be suppressed due to adsorption competition. Some authors have referred to a membrane discrimination mechanism (IAEA, 2009). The observed ratio (OR= Ra/Ca in plants, or Ra/Ca in soil) has been documented to be less than unity in plants, suggesting the existence of a discrimination mechanism of membranes in ion uptake from soils to plants. Several authors found that total soil bivalent cation concentration (IAEA, 2009) and exchangeable Ca and Mg (Gerzabek *et al.,* 1998) suppressed Ra uptake. In a greenhouse experiment with three different soils artificially contaminated with Ra, Vandenhove *et al.,* (2005) found a significantly

negative dependence of concentration ratios Cr − Ra for clover and ryegrass in the concentration of Ca and Mg in soil solution. Subsequently, (Vandenhove & Van Hees, 2007) found a significant negative relation between log-*Cr* and soil solution calcium concentration for both ryegrass and clover, but not with the total bivalent cation concentration (Ca^{2+} + Mg^{2+}) in the soil solution. However, Vasconcellos *et al.,* (1987) and Lauria *et al.,* (2009), who studied Ra transfer in high natural background areas and at conventional and organic farms, respectively, argued that the exchangeable Ca in soils did not seem to influence Ra uptake by plants in a defined way.

Gerzabek *et al.,* (1998) conducted lysimeter studies to determine the uptake of ^{226}Ra by agricultural crops and reported significant negative correlations between *Cr* and pH. The pH effect was explained by the lower Ra availability with increasing pH (Hewamanna *et al.,* 1988). For the IAEA compilation (Moore, 1972; Vandenhove *et al.,* 2009), a significant negative dependency of *Cr* − Ra on pH was only observed for leguminous fodder and grasses. No significant pH effect on *Cr* − Ra was observed by (Vandenhove & Van Hees, 2007). Ra uptake has been reported to be influenced by soil P content. Vandenhove & Van Hees, (2007) found a weak correlation between the ryegrass and clover *Cr* and total soil P. No correlation was found with available P or P concentration in the soil solution. In the study of (Million *et al.,* 1994), P nutrition did not affect Ra uptake.

2.1.8.3 **Radioactive thorium in the environment**

Thorium was discovered in 1828 by the Swedish chemist Jons Jakob Berzelius, but was found to be radioactive in 1898 independently by Gerhard Carl Schmidt and Marie Curie. Although most of the thorium isotopes are naturally occurring, some thorium isotopes can be artificially produced, all of which are radioactive. It is present at very low levels in virtually all rocks, soils and water, and therefore is found in plant and

animals as well. However, it is more abundantly and higher concentrations in crustal rocks, and minerals such as monazite and thorite (thorium silicate) (Sheppard, 1980). Thorianite (mixed thorium and uranium oxides) also is rich in thorium and may be mind for the metal. In general artificial isotopes come from the decay of artificially produced radionuclides, or as a byproduct in nuclear reaction (Atwood, 2013).

Thorium has 25 radioisotopes with the most common being ^{224}Th, ^{226}Th, ^{227}Th, ^{228}Th, ^{229}Th, ^{230}Th, ^{231}Th, ^{232}Th and ^{234}Th. These can be natural and artificially produced. Thorium isotopes have different nuclear properties and half-lives (t ½) of seconds to 10^{10} years. They range in atomic mass from 212 to 236, and have an atomic number of 90 and one main stable oxidation state (+4), under all redox conditions in natural waters (Fry & Thoennessen, 2013).

Thorium is a member of the actinide series of ^{232}Th and U (^{235}U, ^{238}U and ^{234}U) and artificially produced elements such as Pu. There are six thorium isotopes in natural environment, with beta- emitting ^{234}Th (t ½ : 24.10 days) and alpha- emitting ^{230}Th (t ½ : 7.54×10^4 years) in uranium (^{232}U) series, alpha- emitting ^{232}Th (t ½ : 1.41×10^{10} years) and ^{228}Th (t ½ : 1.913 years) in thorium (^{232}Th) series, and beta- emitting ^{231}Th (t ½ : 25.52 h) and alpha- emitting ^{227}Th (t ½ : 18.72 days) in ^{235}U series (Fisica & Divisione Materiali, 1976; Sheppard, 1980). Among these isotopes, ^{232}Th, ^{230}Th, and ^{238}Th are particularly important due to their relatively long half-lives, high natural abundance and activity concentration, and α- particle radiation. Thorium is widely distributed in small with an average concentration of 8 – 12 mg/kg in the earth's crust (at average concentration of 6 mg/kg in soil) (Kabata-Pendias, 2010). This makes it about two times as abundant as uranium. In sedimentary rocks, its concentration is only a few million (ppm), while in acid igneous rocks; its concentration can be 10 times higher (Atwood, 2013; Sheppard, 1980). Thorium is commonly assumed to appear in

the insoluble residue of carbonate rocks, mainly in the clay material. Although insoluble, thorium can form soluble complexes with organic materials and hence is capable on the surface of hematite crystals.

Thorium is an important component of several minerals and contributes to the general background radioactivity. The minerals in which thorium mainly occurs originate from igeoous rocks, as disseminated and discrete minerals. Thorium is also found in minerals that constitute part of the heavy mineral fraction in beach sands, mainly monazite (Sheppard, 1980). Thorium is not as soluble as uranium and is thus not as mobile in the chemical environment, but does move by mechanical processes as discrete resistant mineral grains. Thorium is usually associated with U and the rare-earth elements. It also occurs in similar rocks as uranium such as granite, pegmatite, and gneiss. The more important minerals that contain thorium are monazite (a phosphate of light-weight rare earths), usually associated with silica. Most thorium compounds are obtained as a byproduct of processed monazite for rare-earth elements (Sheppard, 1980). The concentration of thorium oxide in monazite sands is about 3 – 10 %. Thorium is also found in the minerals thorite (thorium silicate), thorianite, uranothorite (mixed thorium and uranium oxides), and thoroqummite. Windblown terrestrial dust and volcanic eruptions are two important natural sources of thorium release into the air (Sheppard, 1980; Östhols, 1994).

2.1.8.4 **Thorium-232 in the soil**

Thorium occurs in nature as tetravalent ions. It cannot be oxidized under geologic conditions to a hexavalent state to form an analogue of the uranyl ion (Adams *et al.,* 1959). In solution it is quickly adsorbed or precipitated as a hydrolysate, because of the very high ionic potential of the tetravalent ion. This is the reason for the low thorium/uranium ratio observed in natural waters. Adams *et al.,* (1959) stated that, like

uranium, thorium is concentrated largely in accessory minerals such as zircon, monazite and xenotime. Because it can be hydrated, thorium is easily precipitated and adsorbed on or held by surfaces. Thorium also forms radiocolloids which attach to other particles and are transported in this manner (Koczy, 1961).

Thorium has generally been considered to be a lithophilic element of low geochemical mobility. Like U^{4+} and Th^{4+} is relatively immobile since it is adsorbed tenaciously on cation-exchange resins and is one of the last elements to be eluted when cation-exchange columns are leached with 3 mol/L HC1 (Hansen & Huntington, 1969). Thorium forms metal complexes with substances such as citric acid, oxalic acid and acetyl acetone, which render it more mobile (Hansen & Huntington, 1969). In a similar manner, thorium can be leached from soils and soil-clay fractions by various solutions.

Thorium is the most abundant of the heavy elements, i.e., elements with atomic number greater than Bi (83). It has a crustal abundance of 9.6 - 12 mg/kg, which is more abundant than Sn and only slightly less than Pb. It is strongly lithophilic, and is more abundant in crustal rocks than in meteorites and mantle-type rocks, such as dunite. It forms several minerals including monazite (Ce, La, Nd, Th) (PO_4, SiO_4), the rarer thorite $ThSiO_4$ and thorianite ThO_2, but is more widely dispersed as an accessory element in zircon, sphene, epidote, uraninite, allanite and apatite in igneous rocks. Although Thorium is a transition element, possessing more than one valency state, its geochemistry is dominated by the Th^{4+} ion, which has an ionic radius of 94 pm, and shows greatest affinity to other M^{4+} elements such as U, Ce and Zr. The minerals of these elements are often isostructural, with replacement and solid-solution gradations between the endmembers, e.g., thorianite ThO_2, cerianite CeO_2 and uraninite UO_2; thorite $ThSiO_4$ and zircon $ZrSiO_4$; and monazite (Ce, La, Th, U) PO_4 (Berger *et al.,* 2008; Kato, Konoplev & Kalmykov, 2020).

Anthropogenic sources of thorium include fertilisers, uranium mining and processing, and coal combustion. The amounts of thorium in the environment may increase as a result of accidental releases of thorium from nuclear processing plants. Thorium has no known biological function. It is chemotoxic, radiotoxic and a carcinogen. In the environment, thorium behaves similarly to the REEs, especially Ce, substituting for Ca in bones and teeth. Long-term exposure to thorium increases the chances of developing lung diseases and lung, pancreas and bone cancer (Reimann & de Caritat, 1998). Thorium has been found to show significant bioconcentration in lower trophic animals in water, but the bioconcentration factors decrease as the trophic level of aquatic animal's increases (Leiterer, Berard & Ménétrier, 2010).

It has been reported that thorium content of soil normally increases with an increase in clay content of the soil (Harmsen & Haan, 1980). Due to the large surface of the clay, is able to adsorb different metals. Moreover, in the case of thorium, the ability of this radio-nuclide to be strongly fixed onto the solid phase of soil is a characteristic feature of the element (Katz *et al.,* 1987).

Manmade sources of thorium contamination in soil are mining, milling and processing operations and uranium, thorium, tin and phosphate fertilizer production (Hu & Kandaiya, 1985; Joshi, 1987; Sill, 1977). The two principal processes that can contaminate soil from these industries are precipitation of airborne dusts and land disposal of uranium or thorium containing wastes.

Thorium is generally higher in granitic than mafic igneous rocks. Since it can enter some rock-forming minerals, such as biotite, it is not as strongly concentrated in the incompatible pegmatite phase like U, although some thcontaining minerals, such as allanite do occur in pegmatite. Granite typically contains 10-40 mg/kg thorium, although there is much local and provincial variation. Intermediate rocks, such as

andesite have about 1– 4 mg/kg thorium, while gabbro usually has less than 3.5 mg/kg, and basalt less than 1 mg/kg. In metamorphic rocks, the thorium content is generally immobile up to the highest grades, but anatexis will result in concentration in the mobile granitic phase. High thorium values, therefore, indicate the presence of felsic rocks, especially intrusives (Ogunsanwo *et al.,* 2019).

Thorium in sedimentary rocks is essentially resistant in character, as its major host minerals, such as monazite and zircon, are highly resistant to both chemical and physical breakdown. Any thorium released by weathering has a transient existence in solution as it is strongly sorbed by clay minerals. Thus, sandstone, arkose and graywacke may have up to 10 mg/kg, and normal shale and mudstone 10–13 $mg.kg^{-1}$. Mielke (1979) cites levels of thorium in shale, sandstone and carbonate rocks as 12, 1.7 and 1.7 mg/kg, respectively. Black shale may have higher thorium levels, but never as high as the uranium content, because of the much stronger affinity of uranium for organic material and the greater mobility of oxidised UO_2^{2+} in solution. Placer deposits, such as monazite sands, however, may be exceptionally rich in thorium and constitute one of the major ores of thorium. Limestone is normally very low in thorium, since Th^{4+} cannot form a stable carbonate, unlike UO_2^{2+}; similarly, thorium is almost completely absent from evaporite deposits. Marine Mn nodules are often enriched in Th (24 – 124 mg/kg) and Atlantic pelagic clay has been noted to contain 30 $mg.kg^{-1}$ (Wedepohl, 1995). The average value for loess is quoted as 11.3 $mg.kg^{-1}$ (McLennan & Murray, 1999).

Thorium has low mobility under all environmental conditions, mainly due to the high stability of the insoluble oxide ThO_2 and the strongly resistant nature of its carrier minerals such as monazite and zircon. Unlike U, thorium cannot be oxidised to a stable cation equivalent to the highly mobile uranyl ion UO_2^{2+}. The soluble species $Th(SO_4)^{2+}$

may form below pH 3, and under oxidising conditions (Brookins, 1988), e.g., in acid mine water. Any thorium released into solution will be rapidly sorbed by clay minerals and hydrolysed to the hydrous oxide Th $(OH)_4$, which will be intimately associated with the clay-mineral fraction, unless it can be mobilised by other inorganic or organic ligands (Hem, 1992). Thus, thorium is essentially insoluble in surface and groundwaters, and levels are extremely low at 0.01 – 1 µg/L (Hem, 1992). Because of this, thorium is a useful pathfinder element in stream sediment for locating uranium deposits associated with magmatic rocks, since almost all the thorium is transported as solid mineral material with minimal loss to solution. The average thorium content in river particulates is given as 14 mg/kg (McLennan & Murray, 1999).

The mobility of thorium in soil is governed by the same principles as that in water in most soils, thorium will remain strongly sorbed and the mobility will be very slow. The presence of ions or ligands $(CO_3)^{-2}$, humic matter that can form soluble complexes with thorium increases its mobility in the soil. The contamination of groundwater through the transport of thorium from soil to groundwater will not occur in most soils, except those that have low sorption characteristics and have the capability to form soluble complexes. Chelating agents produced by certain microorganisms (e.g pseudomonas aeruginosa) present in soils may enhance the dissolution of thorium (Östhols, 1994; Atwood, 2013).

It is well-documented fact that the distribution of a given trace element in soil is strongly influenced by its solubility, parent material of soil, pedogenic processes in the soil and plant recycling (Temgona *et al.,* 2003). Until now, it is widely believed that mobility of uranium in soil is higher than thorium mobility, regardless of the soil type (Titaeva, 1994). Th^{4+} is readily soluble, but at the same time may be quickly adsorbed or precipitated as hydrolysate. It was shown (Syed *et al.,* 1999) that thorium ion is

largely hydrolysed at pH above 3.2, and the hydroxyl complexes are involved in the sorption process. The adsorption of thorium on clays, oxides and organic matter increases with increasing pH and is completed at pH 6.5. On the other hand, it was suggested (Hansen & Huntington, 1969) that mobility of thorium in soil may be less affected by soil pH than by soil organic matter. Tetravalent thorium may be strongly complexed with soil organic matter, thus increasing the mobility of thorium in soil. In particular, (Hansen & Huntington, 1969) reported distinct thorium behaviour in soil horizon immediately below layers with high organic matter content.

Tyuryukanova & Kalugina, (1971) reported that thorium was distributed nonuniformly in the soil profile. The lowest thorium concentration is detected in the surface organic horizons, and the highest concentration is found in the unconsolidated material close to bedrock. Accumulations of thorium are often associated with a gleyed horizon, suggesting that thorium accumulates under reducing conditions. The low thorium content in peaty soils is apparently due to a low biogenesis and weak assimilation by bog plants (Tyuryukanova & Kalugina, 1971). Surface area is a factor influencing thorium content in soil particles less than 100 μm in diameter (Megumi & Mamuro, 1977). Tyuryukanova & Kalugina, (1971) listed thorium content for various soil types, forest floors, and forest vegetation. The values range from 0.2 ug Th/g dry soil for the A-horizon of a peaty-gley soil to 9.5 lag Th/g dry soil at 50-60 cm depth in a gleyed clay soil, with the average thorium content being 4 μg/g dry soils.

It has been reported (Kabata-Pendias, 2010) that surface soils of the U.S. show a relatively small variation in the content of thorium regardless of the soil type. Similar phenomenon was observed for different soils collected by the author in the North-West region of Russia. Concentrations of thorium in the soils sampled in different sites were rather constant. Quite another situation may be observed in soil near uranium mining. In

this case concentrations of both radionuclides uranium and thorium in the soil may be several times higher than those in the background soil.

Vinogradov, (1959) reported an average thorium content of 6.0 μg/g in soil. The thorium content of podzolic sandy soils is approximately twice that in rock. Hansen & Stout, (1968) have shown that thorium leached from organic layers reprecipitates in zones containing less organic matter. Baranov *et al.,* (1963) showed that soils high in organic matter have the lowest Th/Ra ratio.

Hansen & Huntington, (1969) reported that thorium may be subject to cheluviation (complexation with organic substances and transported in solution), but it may have a different pattern of translocation and different conditions for reprecipitation than iron, which is commonly cheluviated. Assuming similar initial concentrations, this could be reflected in a more diffuse profile distribution for thorium than for iron. The thorium distribution in the soil profile is apparently less affected by change in pH than is the iron distribution. The study carried out by Vinogradov, (1959) revealed that no values of ^{232}Th were found in soil solutions.

Tilling, (1969) reported that thorium does not crystallize out of basic magmas; it is enriched in silicic magmas such as granites. It may be present in simple isomorphous substitution for tetravalent zirconium, or as optically continuous inclusions of the isomorphic thorite ($ThSiO_4$). Adams *et al.,* 1959 stated that in well-crystallized, coarse-grained rocks, much of the thorium as well as the uranium may be occluded, adsorbed on crystal imperfections, or fixed in other dispersed sites before being concentrated enough to enter into the stable mineral species. Picciotto, (1952) indicated that thorium and uranium occur in very small mineral or liquid inclusions in quartz. Analysis of quartz in beach sands indicates that about 5% of the thorium and uranium in granite can be expected to be similarly fixed (Murray & Adams, 1958).

Iron and manganese hydrous oxides play an important role in immobilizing thorium through precipitation. Megumi, (1979) stated that 90% of thorium is surface adsorbed, 80% coexists with goethite and 80% is soluble in HCl, when extractions are carried out on separate soil samples. Evidence indicates that the transport of thorium in solution is a very unimportant process. Since a significant amount of the thorium in the environment is adsorbed onto clay-sized particles, or precipitated, the major means of transport are by wind and water erosion, and by mineral and/or organic particles moving through the soil system. Baranov *et al.,* (1963) stated that, unlike uranium, thorium in the natural environment is transported primarily in the colloidal form. Dementyev & Syromyatnikov, (1965) concluded that thorium migrated in groundwater as colloidal particles and as anionic complexes, the latter probably with organic acids.

2.1.8.5 **Radioactive potassium in the environment**

Potassium is an alkali metal belonging to group 1 of the periodic table, which also includes Li, Na, Rb and Cs. The element has an atomic number of 19, withone oxidation state (+1). It has been discovered in 1807 by deriving it from potassium hydroxide KOH. Being an alkali atom it has only one electron in the outermost shell and the charge of the nucleus is being shielded by the core electrons. Potassium has a chemical weight of 39.0983 and appears naturally in three isotopes, ^{39}K, ^{40}K and ^{41}K. These isotopes all have half-lives of less than one day so they are not of concern for environmental Management Institutions. ^{39}K comprises most (about 93.3%) of naturally occurring potassium total mass, and ^{40}K accounts for essentially all the rest. Radioactive ^{40}K comprises a very small fraction (about 0.012%) of naturally occurring potassium (Pratt, 1965; Halperin & Kamel, 1998). The half-life of ^{40}K is 1.3 billion years. The fermionic isotope ^{40}K has two radioactive decay channels. In 89% of the cases it decays through a $\beta -$ decay of 1.311MeV resulting in the stable ^{40}Ar. In the remaining 11% it

decays through electron capture (K-capture) to ^{40}Ca (Ažman, Moljk, & Pahor 1968; Tiecke, 2010).

Potassium-40 is an important radionuclide in terms of the dose associated with naturally occurring radionuclides (Mengel *et al.,* 2001). Potassium is the eighth most abundant element in the Earth's crust with an estimated concentration in the Earth's crust of 1.84% (Manning, 2010), and is a major constituent of many rock-forming minerals, including important silicate minerals such as alkali feldspar, leucite, biotite, muscovite, phlogopite and some amphiboles. It is also a component of many phosphate, halide and sulphate minerals. It forms several minerals in its own right, including sylvite KCl and carnallite $KMgCl_3.6$ (H_2O), which occur in evaporite deposits. Potassium is a major constituent in many igneous rocks, and their petrographic classification is often based on K concentrations or abundances (Rich, 1968). It is progressively concentrated during magmatic fractionation, and is thus enriched in felsic relative to mafic igneous rocks. This is seen in the difference in K content of basalt, commonly 6% (Wedepohl, 1995; Mengel *et al.,* 2001).

Once released through the weathering of feldspar minerals, K is very soluble and occurs as the simple cation K^+ over the entire stability field of natural water (Sheppard, 1980). Although K is an abundant element, its mobility is limited by three processes: it is readily incorporated into clay-mineral lattices because of its large size; it is adsorbed more strongly than Na^+ on the surfaces of clay minerals and organic matter and; it is an important element in the biosphere and is readily taken up by growing plants. As a consequence, K concentrations exceeding a few tens of mg l^{-1} are unusual, except in water with high dissolved solids content or water from hydrothermal systems (Hem, 1992). Sea water contains 390 mg/L potassium on average (Hem, 1992). Fertilisers are the main anthropogenic source of potassium. Many K salts have important chemical and

medicinal applications, including the hydroxide, nitrate, carbonate, chloride, chlorate, bromide, iodide, cyanide, sulphate, chromate and dichromate. However, natural sources are considered to be far more important in the environment than anthropogenic ones (Reimann & De Caritat, 1998).

2.1.8.6 **Postassium-40 in the soil**

Potassium-40 is present as a very small fraction of naturally occurring potassium, which is an element found in large amounts throughout nature. Potassium is the seventh most abundant element in the crust of the earth and the sixth most abundant element in solution in the oceans. It is present in mineral waters and brines, and in various minerals such as carnallite, feldspar, saltpeter, greensand, and sylvite. Radioactive ^{40}K comprises a very small fraction, represents 0.012% of naturally occurring potassium; its concentration in the earth's crust is about 1.8 mg/kg, or 13 picocurie per gram (pCi/g) (Leutz & Wenninger, 1965; Tiecke, 2010). ^{40}K binds preferentially to soil, with the concentration associated with sandy soil particles estimated to be 15 times higher than in the interstitial water in pore spaces between soil particles; it binds more tightly to loam and clay soil, so those concentration ratios are higher, above 50. Together with nitrogen and phosphorous, potassium is a major soil fertilizer, so levels of ^{40}K in soils are strongly influenced by fertilizer use; it is estimated that about 111×10^{12} Bq of ^{40}K are added annually to U.S. soils. The half-life of ^{40}K is 1.3 billion years, and it decays to ^{40}Ca by emitting a beta particle with no attendant gamma radiation, 89% of the time, and to the gas ^{40}Ar by electron capture with emission of an energetic gamma ray, and 11 % of the time (Spiers, 1950; Leutz & Wenninger, 1965). ^{40}K is an important adionuclide in terms of the dose associated with naturally occurring radionuclides.

Potassium-40 behaves the same as ordinary potassium, both in the environment and within the human body it is an essential element for both. Potassium is an important

constituent of fertile soil and is an essential nutrient for plant growth and in the human diet (Vinogradov, 1957). Both nitrogen and phosphorus are constituents of the soil organic matter, but potassium is not. Soil organisms have a much lower requirement for potassium than plants do. Consequently, as organic residues decompose, most of the potassium is quickly released. The behavior of potassium in the soil is determined more by physical than by chemical or biological processes (Mouhamad, Atiyah & Iqbal, 2016).

Two mechanisms limit the leaching of potassium from the soil. One is that the potassium ion is small and may be trapped inside crevices within clay particles, where it is held by crystalline forces. This happens also to ammonium ions. Both are trapped and become unavailable, although they are released slowly if the amount in solution drops. Potassium so held is sometimes called fixed or non-exchangeable potassium (Blake *et al.,* 1999: Arienzo *et al.,* 2009). The second soil mechanism for conserving potassium is cation exchange, which comes about because small clay and humus particles develop a negative electrical charge. The negatively charged particles attract positively charged ions, or cations, which include potassium.

Vinogradov, (1957) stated that the radioactivity of ^{40}K (normally present in organisms) is not connected with any biological reaction or process proceeding under normal conditions in plants and animals, through his investigations on effect of ^{40}K upon the growth and development of *Aspergillus niger*.

Królak & Karwowska, (2010) found that mean concentrations of ^{137}Cs are higher than ^{40}K in soil, as ^{137}Cs is found in larger quantities in the forms available for plants than ^{40}K. Through their analysis of ^{137}Cs and ^{40}K concentrations in the surface layers of arable soil in a selected region of Eastern Poland approximately 20 years after the Chernobyl power plant accident. Santos Júnior *et al.,* (2005) reported that the measured

activities of ^{40}K in the western State of Pernambuco, Brazil are five fold higher than the world mean, and, consequently, while the elemental concentrations and absorbed dose were five fold higher than the world average. Values from 541 to 3572 Bq kg^{-1} were obtained with a mean of 1,827 Bq kg^{-1}. Values allowed the determination of the elemental concentrations as well as the absorbed dose rates in air, 1 m above the ground. Where, the values varied from 1.7 to 11.5% with a mean of 6% and from 23.4 to 154.3 nGy $h^{-1}$with a mean of 79 nGy h^{-1}, respectively. Królak *et al.,* (2008) studied the activities of ^{40}K and ^{137}Cs in forest, cropland and fallow land soils in soil samples were collected from three depths: 0-3, 3-7, 7-12 cm from district Powiat of Garwolin, the Province of Mazowsze. And they reported high concentrations of ^{137}Cs in litter and upper layer of forest soils; while the content of the isotope decreased in deeper layers of the soil. The higher of ^{137}Cs was forest soils; less of this isotope was found in fallow and cropland soils. In forest and fallow land soils, the ^{40}K content did not depend on the depth from which the samples were taken. In arable soil, the largest quantity of ^{40}K isotopes was found, with the lowest in forest soils. The soil content of ^{137}Cs reduced as the soil reaction rose, but increased at a higher level of organic carbon. The ^{40}K isotope concentration was negatively correlated with the soil reaction and the sand fraction content, but correlated positively with the clay fraction content.

A field study was counducted by Zach, Hawkins & Mayoh, (1989) on the transfer of fallout ^{137}Cs and natural ^{40}K in 1978 and 1979 in a boreal environment is presented. They observed that radionuclide concentrations in soils and plants did not vary greatly between areas underlain by limestone and crystalline rock of the Precambrian Shield, with mean concentrations of ^{137}Cs ranging from 0.03 to 0.21 $Bq.g^{-1}$, and of ^{40}K from 0.09 to 0.46 $Bq.g^{-1}$ depending on the soil type.

In Lehliu, Romania, on the sediments of loess (upper pleistocene) where luvisols and sand deposits (lower Holocene) that have been developed that contain carbonate-rich levels, clay minerals and fossil thresholds that influence these geological properties and control the distribution of natural radionuclides in the soil, particularly the distribution of ^{40}K. A study was carried out by Ion, (2014, May) to analyze ^{40}K in 16 soil samples by using HPGe, The specific activity for ^{40}K ranges from 320 to 512 $Bq.kg^{-1}$ which fall within the range specified by UNSCEAR. However, a slight increasing trend of ^{40}K activity was observed in the samples of cultivated soil comparing with grassing soil, these differences may be associated with the presence of fertilizers.

2.1.9 Experimental and field studies of radioactivity in soil

Natural radioactivity in the soil is mainly due to the decay of radionuclides from the uranium and thorium series. Beck, (1972) found that the decay of those isotopes and ^{40}K accounted for 50-80% of the gamma radiation flux at the soil surface. Radiation from natural sources is a major environmental concern where the human exposure to natural radionuclides has increased significantly since the 1960s Baxter, (1991), and more attention has been given to the abundance and distribution of natural radioisotopes in soils (e.g., Kiss *et al.,* 1988; Navas *et al.,* 2002a). The mineral composition of the parent material controls the natural radioactivity of soils. In addition, radionuclides are adsorbed onto soil components (organic matter, clays, carbonates, Fe/Mn oxides) and take part in biogeochemical processes. Soils play a major role in the cycling of radionuclides and their physicochemical properties 3 influence the mobility and bioavailability of these radionuclides in terrestrial ecosystems (Kabata-Pendias & Pendias, 2001). Thus, an understanding of the distribution of radionuclides in soils is essential to many environmental studies (Navas *et al.,* 2007). Furthermore, the knowledge of the radionuclide content of soils is central to the establishment of environmental baselines for various substrates and environments (Jordan *et al.,* 1997).

Data on the distribution and behaviour of long-lived radioisotopes in soils is limited. Understanding the pathways by which radioactivity reaches humans requires an assessment of the soil properties that affect the abundance and distribution of radionuclides. With this purpose most studies have been at the soil profile scale (Sully *et al.,* 1987; Navas *et al.,* 2002a, 2005a; Fujiyoshi & Sawamura, 2004). However, little information exists on the spatial distribution of radionuclides in tropical where the behaviour of natural gammaemitting radionuclides can be approached in an integrated approach based on the soil and the environmental processes operating at the catchment scale. The soil radioactivity is usually important for the purposes of establishing baseline data for future radiation impact assessment, radiation protection and exploration. The dose rates vary from one place to another depending upon the concentration of natural radionuclides such as ^{238}U, ^{226}Ra, ^{232}Th and ^{40}K present in soil. These radionuclides pose exposure risks externally due to their gamma-ray emissions and internally due to radon and its progeny that emit alpha particles.

Evaluation of the concentrations of natural radionuclide activity is particularly important because it embodies an important contribution to the external dose of the population. In this range, the United Nations Scientific Committee on the Effects of the Atomic Radiation (UNSCEAR) provides a direct correlation between the activity of ^{238}U, ^{232}Th and ^{40}K in soils and the external doses absorbed by the population. The radionuclides present in soils can pass on to the food chain and the air, contributing to the internal dose received by the population.

Many countries around the world have a growing interest in assessing their baseline amount of terrestrial radiation (Al-Hamarneh & Awadallah, 2009; Al-Sulaiti *et al.,* 2012; Al-Jundi *et al.,* 2003; Saad & Al- Azmi., 2002; Dawood, 2011; Ramadan *et al.,* 2009). There is no place on earth that has no natural radioactivity. As a consequence,

many areas with high NORM were subjected to dosimetry radiobiological and epidemiological dosimetry trials, as reported by (Sahoo *et al.,* 2010; Marsh *et al.*, 2012; Sorhabi, 1998; Faulkner, 2001, 2010; Zakeri *et al.,* 2011). It may be due to the geological and geochemical nature/ structure of the soil any increase of NORM levels identified in such surveys or by technologically improved radioactivity attributable to human activities. There are many studies conducted around the world to determine NORM and TNORM in the soil. Measurement of natural background radiation and radioactivity in soil has been carried out in many countries to establish base line data of natural radiation levels (Ibrahiem *et al.,* 1993; Quindos *et al.,* 1994; Mireles *et al.,* 2003).

A study was carried out by (Veiga *et al.,* 2006) to measure the natural radioactivity in Brazilian beach sands of ^{40}K, ^{226}Ra and ^{232}Th, were collected along the coast of four Brazilian States: São Paulo (SP), Rio de Janeiro (RJ), Espírito Santo (ES) and Bahia (BA). And the study found out that the values of the annual effective dose rates or γ-ray radiation hazard indices exceed the average worldwide exposure of 2.4 mSv y^{-1}. In order to assess the levels of natural activities of nuclides with values at the standard levels proposed by the Organization for Economic Cooperation and Development (OECD) for building materials. The average values of the radium equivalent activities were evaluated and found to be 696 Bq kg^{-1} in Mambucaba (RJ), 1621 Bq kg^{-1} in Buena (RJ), 2289 Bq kg^{-1} in Anchieta (ES), 10 205 Bq kg^{-1} in Meaipe (ES), 83 425 Bq kg^{-1} in Guarapari (ES), 531 Bq kg^{-1} in Vitória (ES), 2026 Bq kg^{-1} in Serra (ES), 3240 Bq kg^{-1} in São Mateus (ES), 3075 Bq kg^{-1} in Porto Seguro (BA) and 1841 Bq kg^{-1} in Itacaré (BA). These values were above the limit of 370 Bq kg^{-1} recommended for the safe use of building materials for dwellings by OECD (OECD, 1979).

To support soil safety studies and provides input to the collective dose assessment of the population of Vietnam. A study was conducted by by Hien *et al.,* (2002) to establish database on ^{238}U, ^{232}Th, ^{40}K, and ^{137}Cs in 292 surface soils by using gamma spectrometry. The study found that the high rainfall areas in the northern and central parts of the country have received considerable ^{137}Cs inputs exceeding 600 Bq m^{-2}, which is the maximum value that can be expected for Vietnam from the UNSCEAR global pattern (Hien, 2002). The mean activity concentrations of naturally occurring radionuclides ^{238}U, ^{232}Th, and ^{40}K are 45, 59, and 401 Bq kg^{-1}, respectively, which are higher than the corresponding world averages of 40, 40, and 370 Bq kg^{-1}, that involve an average absorbed dose rate in air of 62 nGy h^{-1}, which is around 7% higher than the world average.

A study was carried out by Kurnaz *et al.,* (2007) to determination of radioactivity levels and hazards of soil and sediment samples in Fırtına Valley (Rize, Turkey) using high purity germanium detector. The mean concentrations of the radionuclides ^{238}U, ^{232}Th, ^{137}Cs, and ^{40}K in soil and sediment samples determined were a comparable with literature values. But the ^{137}Cs activity concentrations in some places are higher than the other results, which may be the result of Chernobyl nuclear power plant accident and the atmospheric nuclear weapon tests conducted by several countries as researchers have explained. While the annual effective dose equivalent (AEDE) found to be higher than the world average. Nevertheless, health effect due to natural radiation from soil and sediment of the Fırtına Valley is low and thus, health hazards were insignificant.

A study conducted by Sahoo *et al.,* (2011) reported the geochemical behavior of thorium, uranium and rare earth elements (REEs) are relatively close to one another while compared to other elements in a geological environment of weathered Japanese soil samples, and how the radioactive elements like ^{232}Th and ^{238}U along with their

decay products are present in most environmental matrices and can be transferred to living bodies by different pathways which can lead to the sources of exposure to man. It has been observed that granitic rocks contain higher amounts of U, Th and light REEs compared to other igneous rocks such as basalt and andesites. The researchers suggested further consideration of soil characteristics when investigating the behavior and distribution pattern of radionuclides ^{232}Th and ^{238}U along with REEs in soil samples of weathered acid rock (granite and ryolite) collected from two prefectures of Japan. However, the study concluded that no significant variation with the soil depth profile, there was less than 5% variation in a particular core sample.

High Purity Germanium radiation detector was employed by Darwish *el al.,* (2013) to assess the natural radioactivity and radiological hazards in soils from Qarun Lake and Wadi El Rayan in Faiyum, Egypt. The results showed that the mean activity concentrations of ^{238}U, ^{232}Th in soils of Qarun Lake and Wadi El Rayan are comparable to reported world. The study noticed that there are strong correlations between ^{238}U and ^{232}Th, ^{238}U and ^{40}K, and ^{232}Th with ^{40}K in soil samples from Qarun Lake, which means that the two elements accompanied each other. Samples of Wadi El Rayan showed strong correlation between ^{238}U and ^{232}Th, which means that the two elements accompanied each other, while there is weak correlation between ^{232}Th and ^{40}K, and ^{238}U with ^{40}K. The mean activity concentrations of ^{238}U, ^{232}Th and ^{40}K found to be 0.37, 0.44 and 3.22 times of the world wide average concentrations of these radionuclides 35, 30 and 400 Bq/kg, respectively, (UNSCEAR, 2000).

The Areia Preta beach in Guarapari (Espírito Santo State) is a famous example, visited by tourists for its black radioactive sand, looking for sea swimming and treatment of rheumatoid. Thus, it is important to investigate the radionuclide and mineral activities along the Atlantic coast of Brazil, where many heavy mineral deposits

are found in beaches and sandy ligaments along the coasts. Veiga *et al.,* (2006) addressed in the context of their hypothesis the anomalous behavior of heavy mineral along the Atlantic coast of Brazil by determined the concentrations of ^{226}Ra, ^{232}Th and ^{40}K and their hazard indexes in the study area. Where, they reported the value of 70 mSv at Areia Preta beach (Guarapari) as the highest annual dose rate and the hazard indices reach about 350 times the limit recommended by (OECD, 1979). Although the radium equivalent activity of 82 Bq kg^{-1} were observed in the majority of the beaches, but for some specific beaches these values exceed the limit recommended by OECD, since the enhanced natural radioactivity in these sites may be correlated with the presence of heavy mineral deposits in their sands. Excluding all the anomalous areas observed in their work, the mean activity of ^{226}Ra and the external annual effective dose rates in the beaches of Sao Paulo, Rio de Janeiro and Bahia States were 24 Bq kg^{-1}, 0.07 mSv y^{-1}, respectively, which were comparable with many countries around the world.

An investigation of the distribution of radioactive nuclides in river sediments and coastal soils in Chittagong, Bangladesh was taken by Chowdhury *et al.,* (1999), and showed that the activity concentrations of ^{238}U, ^{232}Th, and ^{40}K were higher than the average world values which are 35, 30, 400 $Bq.kg^{-1}$, respectively. Ahad *et al.,* (2004), revealed that the mean values of ^{226}Ra, ^{232} Th, ^{40}K, and ^{137}Cs activities in soil samples were collected from Bahawalpur, Pakistan are found to be 32.9, 53.6, 647.4 and 1.5 $Bq.kg^{-1}$. A study carried out by Tzortzis *et al.,* (2004) to evaluate the activity concentration levels arising from radionuclides ^{238}U, ^{232}Th and ^{40}K in surface soils in Cyprus, where they reported to be 0.01 to 39.3, 0.01 to 39.8, and 0.04 to 565.8 $Bq.kg^{-1}$, respectively, which are considered very low levels compared to the global average.

Soil and sediments were investigated to assess levels of natural radioactivity in Turkey by Kurnaz *et al.,* (2007), the obtained data covered a wide area in Fırtına Valley,

and the mean values of the radionuclide concentrations ^{238}U, ^{232}Th, ^{137}Cs, and ^{40}K in soil and sediment samples were reported to be comparable with literature values. However, the study revealed high values of ^{137}Cs that could be attributed to the Chernobyl nuclear power plant accident and the atmospheric nuclear weapon tests conducted by several countries. The average concentrations of ^{238}U, ^{232}Th, ^{40}K and ^{137}Cs were reported to be 50, 42, 643, and 85 $Bq.kg^{-1}$ in dry weight, respectively. While the average values of ^{238}U, ^{232}Th, ^{40}K and ^{137}Cs were reported to be 39, 38, 573, and 6 $Bq.kg^{-1}$ in sediment, respectively.

The average value of *the annual effective dose equivalent (AEDE)* was calculated to be 152 $mSv.year^{-1}$ in the Xiazhuang Granite Area, China, in a study carried out by Yang *et al.,* (2005), while, Örgün *et al.,* (2005) reported *the annual effective dose equivalent (AEDE)* as 314.1 $mSv.year^{-1}$ in Eskisehir, Turkey, and 69.8 $mSv.year^{-1}$ the value of AEDE reported by Karahan & Bayulken, (2000) in the soil from Istanbul, Turkey. The average values of the *external hazard index* (H_{ex}) were repoted to be 2.03 for Eastern Desert, Egypt in a study counducted by Arafa, (2004), and the value given by Örgün *et al.,* (2005) to be 0.99 in Eskisehir, Turkey. The reported value of H_{ex} by Yang *et al.,* (2005) was 0.84 in Xiazhuang Granite, China.

Taskin *et al.,* (2009) employed HPGe to evaluate the radionuclides concentrations and radiological hazards in a total of 177 soil samples were selected among 230 sampling stations in Kirklareli regin, Turkey, the estimated average outdoor gamma dose rate was 118 ± 34 nGy h^{-1}, which is higher than the world's average of 60 $nGyh^{-1}$ (UNSCEAR, 2000). While the annual effective gamma dose calculated to be 144 μSv. The mean values of ^{226}Ra, ^{238}U, ^{232}Th, ^{137}Cs, and ^{40}K activities were reported to be 37 ± 18 Bq kg^{-1}, 28 ± 13 Bq kg^{-1}, 40 ± 18 Bq kg^{-1}, 8 ± 5 $Bq.kg^{-1}$ and 667 ± 281 Bq kg^{-1}, respectively. The *annual effective gamma doses* and the excess lifetime risks of cancer

were higher than the world's average. Terrestrial gamma dose rates varied considerably within the study area, even among the closest regions. This variation is associated with the radionuclides' activity concentrations of the soil that varied due to the differences of geological structures the authors concluded. The interesting results of the study lead us for a better knowledge of the physical, chemical, and biological factors that influence radionuclide behavior in soil.

A study carried out by Al-Trabulsy *et al.,* (2011) to investigate the sources of pollution in the Gulf of Aqaba in the Kingdom of Saudi Arabia due to the many activities taking place in the coastal region. Where, phosphate industry has been considered a major source polluting the marine environment in the study area. The activity concentrations of ^{226}Ra, ^{232}Th, ^{40}K and ^{137}Cs in Bqkg^{-1} of the collected samples were analyzed using HPGe and ICP-MS. The mean specific activities of ^{226}Ra, ^{232}Th, ^{40}K and ^{137}Cs were reported to be 11.4 ± 1.5, 22.5 ± 3.7, 641.1 ± 61.3, and 3.5±0.7 Bqkg^{-1}, respectively. The mean value of ^{40}K is reported to be higher than the world average value of 370 Bqkg^{-1}. The mean values of radium equivalent, absorbed dose, annual effective dose, external and internal hazard index and representative level index were determined as 92.9 Bq. kg^{-1}, 45.6 n Gyh^{-1}, 56.0 mSvy^{-1}, 0.13, 0.28 and 0.73, respectively. Pollutants in the Gulf of Aqaba are likely to be involved for a long time with minimal dispersion as a result of the geographical isolation of the Gulf, and thus will have a detrimental effect on marine life. Thus, the identification of sources of pollution, the pattern of environmental distribution of various pollutants, levels of radioactivity and radiation hazard indicators are important as databases in this area.

Al-Jundi & Al-Tarazi, (2008) reported that the concentrations values of ^{238}U and ^{232}Th to be exceeded the permissible values in the top soil due to the existence of phosphate rocks. The mean absorbed dose rate in the study areas was found to be 51.5 n

Gyh^{-1}, which is below the world average value of 60 n Gyh^{-1}, whereas, the mean value of the *annual effective dose equivalent* was 63.2 mSv y^{-1}.

Saleh & Shayeb, (2014) investigated the distribution of natural radioactivity in soil samples collected from southern Jordan, to assess the radiological health hazard of the radionuclides ^{226}Ra, ^{238}U, ^{232}Th and ^{40}K in five agricultural areas, The mean specific activities of ^{226}Ra, ^{238}U, ^{232}Th and ^{40}K found to be 57.7 ± 5.4, 44.9 ± 6.3, 18.1 ± 1.4, 138.1 ± 40.8 Bq. kg^{-1}, respectively. While, the mean absorbed dose rate in air and the annual effective dose equivalent reported to be 37.15 ± 3.53 $nGyh^{-1}$ and 45.59 ± 4.33 Sv y^{-1}, respectively. The variation in the activities of the radionucldies between the regions may be due to the different geological nature of the regions and the agricultural activities as the researcher stated. They also noted that there was an enrichment in the concentration of ^{226}Ra and ^{238}U which could be due to the nature of the native rocks where the soil formed, as well as the intensive application of fertilizers. Radionuclides are subject to numerous biogeochemical processes that essentially decide their mobilisation and ecological process availability (Dragović *el al.,* 2011).

Radionuclides showed homogeneous distribution in six soil profiles were investigated by Dragovic, (2011) in Belgrade, Serbia. The study findings revealed a positive relationship ($P < 0.01$) between ^{137}Cs and both of organic matter and cation exchange capacity. While, the soil density negatively correlated ($P < 0.01$) with ^{137}Cs and ^{40}K, this is in agreement with Ligero *et al.,* (2001) conclusion. Close positive correlations ($P < 0.01$) were found between (^{226}Ra, ^{232}Th) and (Fe, Mn). While, the soil pH negatively correlated ($P < 0.01$) with ^{226}Ra and ^{232}Th, significant relationships between (^{226}Ra, ^{232}Th) and (Fe, Mn) oxides were also reported by Navas *et al.,* (2005). Chakraborty *et al.,* (2013) reported a difference in the pattern of distribution of radionuclides within the soil depth, where the activity concentrations of ^{226}Ra, ^{232}Th,

^{228}Th, ^{40}K and ^{137}Cs decreased with the depth up to 10 cm in a total of 60 agricultural soil samples were collected from Chittagong city in Bangladesh. The study findings of Chakraborty *et al.,* (2013) regarding the vertical distribution of the radionuclides in soils were in agreement with a study has been carried out by Copplestone *et al.,* (2010) in Sellafield, Cumbria, UK. Copplestone and co-workers examined the spatial, temporal and depth distributions of ^{134}Cs, ^{137}Cs, ^{238}Pu, $^{239+240}$Pu and ^{241}Am in soil and in two species of vegetation; *Festuca Rubra* and *Ammophila Arenaria*. The samples showed evidence of the accumulation of radionuclides derived mainly from sea to land transfer. Accumulated deposits of radioactivity (0–10 cm) lie within the range of 1.1–3.4 Bq kg^{-1} (^{134}Cs), 260–440 Bq kg^{-1} (^{137}Cs), 31–40 Bq kg^{-1} (^{238}Pu), 150–215 Bq kg^{-1} ($^{239+240}$Pu) and 190–240 Bq kg^{-1} (^{241}Am), radionuclide activity concentrations in Festuca Rubra. Ammophila Arenaria and Festuca Rubra were similar, with the ranges 20–70 Bq kg−1 (^{137}Cs), 1–5 Bq kg^{-1} (^{238}Pu), 10–30 Bq kg^{-1} ($^{239+240}$Pu) and 10–65 Bq kg^{-1} (^{241}Am). Clear temporal and spatial variations were observed in both species of vegetation, reflecting the weather conditions antecedent to the sampling period and the influence of sea to land transfer. Soil profiles showed greater activity concentrations in their deeper regions. This is attributed to leaching of radionuclides in percolating drainage water accentuated by the coarse texture, low organic matter and clay mineral content of coastal sands. Concerning the soil particle size, it is well known that radionuclides are adsorbed to clay surfaces or fixed within the lattice structure (Vanden Bygaart *et al.,* 1995; Navas *et al,.* 2005; Okedeyi *et al.,* 2015). The composition of the clay and silt was positively associated with particular behaviours of ^{40}K, ^{226}Ra ($P < 0.01$) and ^{137}Cs ($P < 0.05$) specific activities. While, the sand content was negatively correlated ($P < 0.01$) with ^{226}Ra specific activity.

The depth distributions of ^{134}Cs, ^{137}Cs, and ^{131}I in three different types of agricultural fields and a cedar forest were investigated by Ohno *et al.,* (2012), in Koriyama,

Fukushima Prefecture. The study showed that more than 90% of the radionuclides were distributed within 6 cm of the surface at the wheat field and within 4 cm of the surface at the rice paddy, orchard, and cedar forest. Large variations in the concentrations of ^{137}Cs and ^{131}I within the rice paddy were observed. Ohno and co-workers suggested that rain containing radioactive fallout initially formed puddles in the rice field resulting heterogeneities in the distribution of radionuclides. In comparing profiles of ^{134}Cs, ^{137}Cs, and ^{131}I and their ratios in the different agricultural plots, Ohno, observed faster vertical migration of ^{131}I than ^{134}Cs, ^{137}Cs. Because of the smaller dispersion and higher radioactivity, the deposition density of the wheat field is appropriate for an estimate of the overall amount of fallout in region.

Beach sands are mineral deposits that arise as a result of weathering and erosion of igneous or metamorphic rocks. Some natural radionuclides found in rock component minerals contribute to ionising radiation exposure on Earth, they're well-known for having a high background radiation. These locations are inextricably linked to the existence of heavy-mineral resources. Some of the world's most notable regions of high natural radioactivity (HINAR) are found along or near the Brazilian coast (El-Taher *et al.,* 2006).

In southern Brazil, the Serra do Mar geological formation, for example, is found near the coast. Granites and gneisses make up the majority of this formation's rocks. The Serra do Mar formation is a supply of radionuclide-rich minerals to neighbouring coastal ecosystems, due to high ^{232}Th and ^{238}U concentrations in its felsic, acidic rocks, ^{222}Rn levels in groundwater are often high in this location (Santos *et al.,* 2008; Godoy *et al.,* 2006).

Due to rock weathering and erosion, sedimentary deposits of radioactive heavy minerals occur widespread along the coast of Espírito Santo and Rio de Janeiro States.

Iron oxides (ilmenite and magnetite), zirconium silicates, and rare earth phosphates with 4−6 % thorium impurities (monazite) are the principal heavy minerals (Paschoa, 2000). Several researches have looked at the radioactive background of Brazilian beaches, for example (Franca *et al.,* 1965; Sachett, 2002; Freitas & Alencar, 2004; Alencar & Freitas, 2005). According to previous literature, there are regions in the world that have shown abnormally high ionizing radiation background. Such areas are referred to as high background radiation breas (HBRAs), including, the coastal regions of Espirito Santo and the Morro Do Forro in Brazil (Paschoa *et al.,* 2000; Bennett, 1997), Yangjiang in China (Wei & Sugahara; 2000; Luxin *et al.,* 1993), southwest coast of India revealed by (Paul *et al.,* 1998; Mishra, 1993; Sunta, 1993; Sunta *et al.,* 1982), Ramsar and Mahallat in Iran (Sohrabi, 1998; Ghiassi-Nejad, 2002).

One of the key concerns in studies of natural background radiation, according to Ramli (1997), is the necessity to create reference values, particularly in locations where the possibility of radioactive material being released into the environment is considerable. Monazite sands have been pointed out to be the source of such high background radiation levels in certain parts of Brazil, China, Egypt and India (UNSCEAR, 2000; Paschoa, 2000; Ghiassi-Nejad *et al.,* 2002). In parts of Southwest France, uranium minerals form the source of natural radiation (Delpoux *et al.,* 1996). And in Ramsar, the very high amounts of ^{226}Ra and its decay products brought to the surface by hot springs (Sohrabi, 1998; Ghiassi-Nejad, 2002). Monazite, a significant source of radioactive uranium and thorium, becomes a key ingredient in the sand from HBRAs, hence research in these areas has piqued interest largely for geological reasons (Alam *et al.,* 1999; Derin *et al.,* 2012). The beach placer deposits may also contain zircon, ilmenite, rutile, and garnet, in addition to monazite. Furthermore, from both a societal and biological standpoint, the potential influence of natural radiation on the biota has been a source of severe worry. Some of these sites have been studied for

several years in order to identify the hazards and impacts of long-term natural radiation exposure, particularly in relation to human residents (Sohrabi, 1998; Kochupillai *et al.,* 1976; Das, 2010; Derin *et al.,* 2012).

Narayana *et al.,* (1995) studied the distribution of the radionuclides within the soil profile in coastal Karnataka. The results showed that the radionuclides are confined to the top layer (0-10) cm of the soil. The activity concentration of ^{232}Th and ^{238}U are reduced by 35% in the second layer (10–20) cm and remains the same in the subsequent interval (20– 30) cm. Narayana and his colleagues revealed that the activity of ^{40}K in sand increases by 10 Bq.kg^{-1} in each interval 10 cm and decreases in soil.

To understand and compare the behavior of radionuclides in arid and semi-desert soils, a study conducted by Makki *et al., (*2014) to estimate the soil radioactivity in Najaf city, Iraq The activity concentrations of ^{238}U, ^{232}Th, and ^{40}K were analyzed using HPGe and NaI (Tl) detector. The mean values of the radionuclides reported to be 7±17, 58±36 and 250±21 Bq kg^{-1} for ^{238}U, ^{232}Th, and ^{40}K, respectively, the *radium equivalent activity* Ra_{eq} and *gamma activity index* Iγ calculated to be 88.41 Bq. kg^{-1}, 0.31 Sv.yr^{-1}, respectively. The specific activities of ^{238}U, ^{232}Th, and ^{40}K were comparable with those of the international values reported by IAEA. The two studied soil groups showed high mean values of 304.35 ± 78 Bq kg^{-1} (^{238}U) and 572.75 ± 23 Bq. kg^{-1} (^{40}K), the researchers attributed the high concentrations to the geological structure from which the soil originated, without further clarification. Another study in the same area conducted by Almayahi, (2015), showed high concentrations of ^{238}U , ^{232}Th and ^{40}K Bq kg^{-1}, where the mean absorbed dose rate reported to be 163.57±0.56 nGy h^{-1} which is about three times higher than the world average dose rate of 55 nGy h^{-1} (UNSCEAR, 2000). While, the mean value of Ra_{eq} calculated as 339.16 ± 1.25 Bq kg^{-1}, which did not exceed the

recommended maximum level of radium equivalents in soil 370 Bq kg^{-1} that given by (OECD, 1979).

In Malaysia, Tajuddin *et al.,* (1994), measured the radiation levels, due to cosmic sources, naturally occurring radioactive materials and technologically enhanced natural radiation, along the highway of Peninsular Malaysia using NaI (Tl) detector. The findings showed that the maximum gamma dose rate was 1.5 m Gy h^{-1} in Bukit Merah, while in Penang and Kuala Lumpur, respectively, 150 nGy h^{-1} and 125 nGy h^{-1} were recorded.

The results revealed that the highest value of gamma dose rate was 1.5 m Gy h^{-1} in Bukit Merah, whereas 150 nGy h^{-1} and 125 nGy h^{-1} were reported in Penang and Kuala Lumpur, respectively. The gamma dose rate around Penang was stated to be marginally higher than that in Kuala Lumpur. In the southern part of Ipoh and the surrounding area, the value was found to be 40 $nGyh^{-1}$, which is less than that for Penang and Kuala Lumpur, in the Pontian District, Malaysia.

Ramli, (1997) researched the interaction of the environmental terrestrial gamma radiation exposure with the soil type using a NaI (Tl) survey metre. The calculated values for the natural terrestrial gamma ray dose in the Pontian District ranged from 9 to 270 nGy h^{-1} with a mean value of 67 nGy h^{-1}. Omar *et al.,* (2004) examined the distribution of radium in 470 samples using HPGe for different forms of waste from the oil and gas industries. The concentrations of ^{226}Ra on the Malaysian scale were high, but comparable to those reported in other countries, Omar and colleagues reported.

Ramli, (2005a) evaluated the activities of ^{238}U and ^{232}Th in soil, water, grass, moss and oil-palm fruit samples were collected from Palong, Johor, Malaysia. Ramli found that the soil concentration ranged from 58.8 to 484.8 Bq kg^{-1} (^{238}U), 59.6 to 1204 Bq.kg

$^{-1}$ (^{232}Th), in a village covered by the sample field, the terrestrial γ-ray dose was measured as 1440 nGy h^{-1}. Ramli *et al.,* (2005 b) reported the terrestrial gamma radiation dose throughout Melaka, Malaysia using NaI (Tl). The measured gamma-ray dose found to be ranged from 54±5 to 378 ± 38 n Gy h^{-1}. While, the population mean dose rate throughout Melaka was 172±17 nGy h^{-1}. The reported annual effective dose rate value of 0.21mSv found to be higher than recommended value of 0.07mSv.

A study carried out by Yasir *et al.,* (2007) to estimate the radionuclides in rocks used in building materials in Malaysia using gamma ray spectrometry. The activity concentrations of ^{238}U, ^{232}Th and ^{40}K varied from 19 to 42.2 Bq kg^{-1}, 16.5 to 28.8 Bq kg^{-1} and 243.3 to 614.2 Bq kg^{-1} , respectively. While, the estimated radium equivalent activity value found to be high 130.7 ± 42.2 Bq kg^{-1} in bricks made of cement, while it was low 61.3 ± 10 Bq kg^{-1}in marble.

Rahman & Ramli (2007) published their survey that designed to determine the dose rates of terrestrial gamma rays and the concentration levels of ^{238}U and ^{232}Th in Ulu Tiram, Malaysia. By using NaI (Tl) and HPGe, the mean and average values of ^{238}U and ^{232}Th concentrations were reported to be 3.63 ± 0.39 (1.74 ± 0.20 - 4.58 ± 0.48) ppm and 43.00 ± 2.31 ppm (10.68 ± 0.76 - 82.10 ± 4.01) ppm, respectively. The average of terrestrial gamma-radiation dose rates that measured in Ulu Tiram was 200 n Gy. h^{-1}, the Malaysian average is 92 nGy. h^{-1} (UNSCEAR, 2000), while, world average is 59 nGy. h^{-1}. Rahman and Ramli, revealed a close relationship between the rate of terrestrial gamma-radiation dose and the soil type, where the soil profile can be used as a key indicator of the gamma radiation dose rate.

Using HPGe detector, Alias *et al.,* (2008) assessed the radiation hazard of natural radioactivity of ^{226}Ra, ^{228}Ra, and ^{40}K in soil having variety of surface conditions at an oil palm field in Jengka, Pahang, Malaysia. The mean activity concentrations of the

radionuclides ^{226}Ra, ^{228}Ra and ^{40}K in top soils reported as 22.1±1.1, 36.6±13.2 and 243.0±27.0 Bq kg^{-1}, respectively. The mean surface dose rate and radium equivalent activity Ra_{eq} were 0.122 μSvhr $^{-1}$ and 60.3 Bq kg^{-1}, respectively.

A study has been conducted by Ramli *et al.,* (2009 a) in Selama district, Perak, Malaysia. Ramli and co-workers revealed that the mean terrestrial gamma radiation dose rate in Selama was about 3 times higher than the Malaysian average and about 5 times higher than the world average value. The mean value of terrestrial gamma radiation dose rate outdoor in Selama was reported as (273 ± 133) nGy h^{-1} for the habited land, while, the mean values of dose rates outdoor and indoor stated as 205 ± 59 nGy h^{-1} and 212± 64 nGy h^{-1}, respectively. The reported value of fatal cancer risk is 6.4 × 10^{-5} per year to each individual living in habited land of Selama. The world average values for TGR dose rates outdoor is 57 n Gy h^{-1}, while, the declared value of Malaysia is 75 nGy h^{-1} (UNSCEAR, 2000). The measured values were 178 ± 95 Bq.kg^{-1} (57 – 364) Bq kg^{-1} (^{238}U), 353 ± 143 Bq kg^{-1}(207 - 625) Bq kg^{-1} (^{232}Th), and 273 ± 133 Bq kg-1 (26 – 601) Bq kg-1 (^{40}K). Researchers attributed high values of TGR dose rate are associated to granitic origin of the soil. The high terrestrial gamma radiation dose rates are mostly found in areas with soils originating from granitic rocks (Kogan *et al.,* 1969).

The terrestrial gamma radiation dose rate outdoor locations revealed again in high mean value in a study conducted at Kg Sg Durian, Perak, Malaysia by Ramli et al., (2009 b), where the mean value reported to be (458 ± 295) nGy h^{-1}. This value is about 9 times the world average value of 57 n Gy h^{-1} and 5 times the Malaysian average value of 92 nGy h^{-1} (UNSCEAR, 2000). For indoor values, TGR dose rates were measured at 70 locations inside concrete houses, while, the value mean value was estimated to be (286± 95) nGy h^{-1}. The corresponding annual effective dose equivalent average for TGR dose rates indoor and outdoor are (1.39 ± 0.72) mSv and (0.59 ± 0.21) mSv

respectively. The estimated fatal cancer risk to an individual was calculated using the equation below (Alvarez, 1997):

$$\hat{R}_{i=a\sum H_E} \quad or \quad \hat{R} = a(H_{E\,in} + H_{E\,out}) \qquad 2.80$$

Where (a) is the risk factor, that uses the value of 0.05 per sievert (public) for terrestrial gamma radiation dose (ICRP, 1990); H_{Ein} and H_{Eout} are effective dose rates indoor and outdoor respectively. Dose factor for intake rate is 4.50 $\times 10^{-8}$ Sv Bq^{-1} and 2.30 $\times 10^{-7}$ Sv Bq^{-1} for ^{238}U and ^{232}Th respectively for adult members of the public (UNSCEAR, 2000).

The TGR *annual effective equivalent dose* for the study area reported to be 1.98 mSv that is 4 times higher than the reference value of 0.48 mSv (UNSCEAR 2000). This value cause fatal cancer risk of about 9.90×10^{-5} per year each individual in the area. The highest TGR dose rate outdoor of 1039 nGy h^{-1} were reported at locations with soil type that originate mainly from granitic rock. The annual effective dose in the area with 100% outdoor occupancy is 6.37 mSv. This value can cause fatal cancer risk of about 3.19×10^{-4} per year.

In Malaysia, a study carried out by Lee *et al.,* (2009) to measure concentrations and radiological hazards of the radionuclides in Kinta, Perak, which was the largest producer of tin in the world. Over a century of tin mining has produced a large amount of tin tailings that contain large amounts of thorium and uranium and provide high external dose rates in the work place, storage room and to the environment (Hu *et al.,* 1981; Lim, 2004). The area is mainly overlaid by six different types of soil namely Dystric Histosols, Xanthic Ferrasols– Dystric Gleysols , Ferric Acrisols–Ferric Acrisols– Orthic Ferrasol , Haplic Acrisols , Steep land and Urban land were classified by FAO/UNESCO (Paramanthan, 1978). Most of the sedimentary rocks in the valley are Devonian in age. Rocks of Silurian age are present in the northern part, whereas

rocks of Carboniferous underline areas in the southwestern part of the District. Alluvium covers almost the entire valley part of the district (Rajah, 1979). The study results found that the mean activities of ^{238}U and ^{232}Th in soil samples exceed their corresponding values worldwide.

A study was conducted by Saat *et al.,* (2011) to calculate the radioactivity concentrations of ^{226}Ra, ^{228}Ra and ^{40}K in soil collected from National Park, Malaysia using HPGe detector. The measured range and mean values of ^{226}Ra, ^{228}Ra and ^{40}K found to be (61.92 - 141.68) 99.13 $Bq.kg^{-1}$, (99.52 -198.70) 139.98 $Bq. kg^{-1}$ and (33.22 - 881.73) 598.24 $Bq.kg^{-1}$, respectively (Saat *et al.,* 2011). The estimated radium equivalent activity ranged from 173.30 to 486.7 $Bq.kg^{-1}$ with a mean value of 334.49 $Bq.kg^{-1}$, while, *the annual effective dose, external hazard index and the absorbed dose rate* found to be ranged from 0.060 - 0.749 mSv, 0.476 - 1.331 and 49.28 - 607.67 $nGyh^{-1}$ respectively. The reported activities were higher than world mean values, and the radiation hazard indices were slightly greater than unity in four locations.

A study was carried out by Muhammad *et al.,* (2012) to determine the activities of the radionuclide activities in sediments and soil samples from northern Peninsular Malaysia using HPGe and Neutron Activation Analysis (NAA). The average and mean value of the activity concentrations of ^{226}Ra , ^{232}Th and ^{40}K were reported to range (39.96 ± 2.05 - 89.47 ± 4.57) 51 ± 4.3 Bq kg^{-1} , (15.68 ± 1.02 - 37.9 ± 2.44) 22 ± 1.9 Bq kg^{-1}, and (137 ± 6.96 - 331 ± 16.7) 189 ± 16.45 Bq kg^{-}, respectively. The *radium equivalent activity and external hazards index* were obtained to be lower than the recommended values. While, the external dose rate ranged from 24.08 to 53.87 n Gy h^{-1}.

Almayahi *et al.,* (2012 a), carried out a study to evaluate the natural radioactivity and radiological hazards in soil and sand samples were collected from Penang, Malaysia. The activity concentrations of ^{238}U, ^{226}Ra, ^{232}Th and ^{40}K in soil were reported to varied

significantly from (2 – 799) Bq kg^{-1}, (64 – 799) Bq kg^{-1}, (16 – 667) Bq kg^{-1} and (87 – 1827) Bq kg^{-1}, with mean values of 184 ± 11 Bq kg^{-1} , 396 ± 22 Bq kg^{-1} , 165 ± 14 Bq kg^{-1},a nd 835 ± 28 Bq kg^{-1}, respectively. While, the mean values of *radium equivalent activity* Ra_{eq}*, external and internal hazard indices*, *annual effective dose equivalent* and *the absorbed dose rates in indoor air* were reported as 696 ± 99 Bq kg^{-1}, 1.87 ± 0.26, 2.9 ± 0.42, 2.02 ± 0.29 mSv y^{-1}, 315 ± 44 nGy h^{-1}, respectively. The radium equivalent activity Ra_{eq} found to be higher than world average value of 370 $Bq.kg^{-1}$. The activity concentrations of ^{238}U, ^{226}Ra, ^{232}Th and ^{40}K in sand samples were 31 ± 8 Bq kg^{-1}, 62 ± 16 Bq kg^{-1}, 36 ± 6 Bq kg^{-1} and 369 ± 17 Bq kg^{-1}, while, the external gamma dose rate was 66 ± 12 nGy h^{-1}. In the same year Almayahi *et al.,* (2012 b) conducted a study to assess the radiation hazard index in northern peninsula of Malaysia using HPGe gamma ray spectroscopy. The activity concentrations of ^{226}Ra, ^{232}Th and ^{40}K in the collected soil samples ranged from (7 – 222) $Bq.kg^{-1}$, (10 – 158) $Bq.kg^{-1}$, and (104-1225) $Bq.kg^{-1}$, with means values of 57 ± 2 $Bq.kg^{-1}$, 68 ± 3 $Bq.kg^{-1}$, and 427 ± 17 $Bq.kg^{-1}$, respectively. In the water samples the values reported to varied from 0.70 to 7.03 Bq L^{-1}, (0.55 - 8.64) Bq L^{-1} , and (53 – 222) Bq L^{-1}, with mean values of 2.86 ± 0.79 Bq L^{-1} , 3.78 ± 1.73 Bq L^{-1} , and 152 ± 12 Bq L^{-1}, respectively. All measured values reported to be a comparable with those reported in other countries. The mean values of radium equivalent activity, absorbed dose rates, *annual effective dose rates, external hazard index and internal hazard index* for soil samples were found to be 186 $Bq.kg^{-1}$, 88 nGy h^{-1}, 108 mSv y^{-1}, 0.50 and 0.65, respectively, while, in the water samples reported as 20 $Bq.kg^{-1}$, 10 nGy h^{-1}, 13 mSv y^{-1}, 0.05 and 0.06, respectively. The absorbed dose rate in soil and water varied from (29.8 - 188.8) nGy^{-1} and (5 - 14.1) nGy h^{-1}, respectively.

The mining activities in Kelantan may be involved in uranium mobility in the surrounding environment, posing health risks through external and internal exposure to the radioactive elements. Hamzah *et al.,* (2012), targeted the geological map of

Kelantan containing uranium deposits. Soil samples were collected at depth (0 - 45) cm from different locations along Kelantan River to measure the radionuclides concentration using Gamma Spectrometer. The concentrations of ^{226}Ra, ^{228}Ra and ^{40}K were varied (46.2 - 369.4), (49.7 - 390.6) and (741.3 -3053.3) Bq/kg^{-1}, respectively. The absorbed dose rate ranged from (72.4 - 483.2) nGy h^{-1}. While, the radium equivalent activity, annual effective dose and external hazard index were found to be ranged from (154.8 - 1057.4) Bq kg^{-1}, (0.09 - 0.59) mSv y^{-1}, and (0.42 - 2.86), respectively. Hamza revealed high values of activity concentrations in Kuala Krai compared to the average value of Malaysia, and two times higher than the non-granitic region from other places in the world.

A study conducted by Saleh *et al.,* (2013), to assess the natural radioactivity and associated health risk in the Pontian District, Johor Malaysia. The *external dose rate* was reported to be 69 nGy h^{-1}. The Malaysian average value is 92 nGy h^{-1} (UNSCEAR, 2000). The mean values of *radium equivalent activity (Ra_{eq}), external hazard index (H_{ex})*, the population weighted dose rates, and *the annual effective dose* were found to be 136 Bq kg^{-1}, 0.366, 0.891 mSv year^{-1} and 178 μSv, respectively. The mean activity concentrations of ^{232}Th, ^{226}Ra and ^{40}K were reported to be 53 ± 4 Bq.kg^{-1}, 37 ± 3 Bq.kg^{-1} and 293 ± 14 Bq.kg^{-1}, respectively. According to UNSCEAR (2000) the mean and average values of ^{226}Ra, ^{232}Th and ^{40}K in Malaysia are 66 Bq kg^{-1}(49 – 86) Bq kg^{-1}; 82 Bq kg^{-1} (63 – 110) Bq kg^{-1}; and 310 Bq kg^{-1} (170 – 430) Bq. kg^{-1}, respectively (UNSCEAR, 2000).

Apriantoro *et al.,* (2013) carried out a study to evaluate the radioactivity concentrations of ^{238}U, ^{232}Th and ^{40}K in different type of soil were collected from Perak, Malaysia, using HPGe. The reported activity values of ^{238}U, ^{232}Th and ^{40}K were ranged to be 7 – 554, 23 –1806 and 6 – 2522 Bq kg^{-1}, with mean values of 127 ± 97, 304 ± 28

and 302 ± 29 Bq.kg^{-1}, respectively. The *radium equivalent* activity and *external hazard* were ranged from 129 to 1136 and from 0.35 to 3.07 Bq. Kg^{-1}, respectively.

By using neutron activation analysis technique, the radioactivity concentrations of natural radionuclide of ^{238}U and ^{232}Th have been measured by Aswood *et al.*, (2013), in vegetables and soil samples were collected from farms in Cameron Highlands and Penang. The mean values of the activity concentrations of ^{238}U and ^{232}Th reported to be 203.83 Bq kg^{-1} and 186.17 Bq kg^{-1} in Cameron Highlands, 110 Bq kg^{-1} and 130 Bq kg^{-1}, respectively, in Penang. The activity concentrations of ^{238}U and ^{232}Th in the areas studied differed depending on the geological characteristics of each area. The highland farms reported in high concentrations values than the ground farms, and higher than the world values published by (UNSCEAR, 2000). However, they do not constitute a serious health burden on the population.

The concentration of natural radionuclides in soil varies quite widely due to the geographic locations, climatic conditions, hydrological pattern, agricultural history, etc. The use of PFs in agriculture can be a potential source of radiation exposure to the farmers working in the fields and general public living in vicinity of the fields (Khater & Al-Sewaidan, 2008). Potential negative effects of phosphate fertilizers include contamination of cultivated land with trace minerals and some natural radioactive materials (Lambert *et al.,* 2007). Phosphate rock can be of sedimentary, volcanic or biological origin. Generally, for uranium a range of 3 – 400 ppm (37–4900) Bq.kg^{-1} (^{238}U) and for ^{226}Ra a range of (100 – 10,000) Bq.kg^{-1} reported for the different phosphate deposits (Roessler *et al.,* 1979; IAEA, 1994). The concentration of ^{238}U and its decay products tend to be elevated in phosphate deposits of sedimentary origin, where ^{238}U series typical concentration is about 1500 Bq.kg^{-1} (UNSCEAR, 1993). The specific activities of the natural radionuclides in the phosphate based industrial products

are depending on their concentrations in the phosphate raw materials (phosphate rocks and/or phosphoric acid) and on their radiochemical partitioning during manufacture processes, which is affected by manufacturing (wet or thermal) procedure (Hofmann *et al.,* 2000). The manufacture and the use of phosphate-based products can lead to environmental contamination. Santos *et al.,* (1995) studied the concentration of ^{210}Po and ^{210}Pb concentration in urine, hair and skin smear samples from individuals using phosphate fertilizers. Skin smear results indicated contamination by direct contact with dust from fertilizers. Therefore, the agricultural usage of phosphate fertilizers could be a potential source of radiation exposure to the farmers and general public. Human activities, such as adding fertilizer, importing top soil and the like can alter the surface radioactivity. Agricultural history is important in the concentration of nuclides in soils. The uses of fertilizers in various agricultural situations have affected radionuclide concentrations to a large extent. Also, fertilizers may affect the chemical form of natural radionuclides in soils and, thus their physical transport and biological uptake. According to Khater, (2008), the application of phosphate fertilizers has substantially increased in the world. Furthermore, several authors have stated that the cultivated lands may be contaminated with trace metals and some naturally occurring radioactive materials (NORM) by using phosphate fertilizers in the agriculture activities. A determination of the concentration and the distribution of soil radioactivity are essential in establishing reference data, allowing the observation of possible future changes due to future radiological contamination.

Ioannides *et al.,* (1997), analysed the activity concentrations of ^{226}Ra, ^{232}Th, and ^{40}K in fertilized and unfertilized soil of Greece, and their study observed that natural radioactivity concentrations in fertilized soil was higher than the non-fertilized soils. The rise in radioactivity due to the addition of phosphate fertilizers (PFs) in the agricultural farmland has also been reported by many other authors (Sheppard, 1988;

Mazzilli *et al.,* 2002; Ahmed & El-Arabi, 2005; Tufail *et al.,* 2006; Lambert *et al.,* 2007; Khater & Al-Sewaidan, 2008; Lee *et al.,* 2009; Vukasinovic *et al.,* 2010; Alzubaidi *et al.,* 2016). The presence of radioactivity in the farmland is a source of direct and indirect radiation dose. Indirect internal exposure to radioactive elements from food contaminated with radioactive elements boosted by fertilisers applied to agricultural soils can lead to cancer risk (Akhtar & Tufail, 2011). Highly fertilized and unfertilized barren farmlands have been selected by Tufail, 2012, to investigate the enhanced levels of radionuclides due to the intensive application of PF in farmlands close to nuclear institute of agriculture and biology (NIAB) at Faisalabad in Pakistan. In three sites were identified as site 1, 2, 3, the measured concentration levels, were reported to be 662 ± 15, 615 ± 17, 458 ± 20 Bq.kg^{-1} for ^{40}K, and 48 ± 6, 43 ± 5, 26 ± 4 Bq kg^{-1} for ^{226}Ra, while for ^{232}Th, the values reported as 39 ± 5, 37 ± 5 and 35 ± 5 Bq kg^{-1}. Gamma dose rates one meter above the soil surface were 55, 51 and 40 nGy h^{-1} in sites 1, 2, and 3, respectively. External dose rates in mud- bricks rooms made from the soil of sites 1, 2, and 3, were 161, 149, and 114 n Gyh^{-1}, respectively.

Alzubaidi *et al.,* (2016), carried out a study to evaluate the natural radioactivity levels and radiation hazards in agricultural and virgin soil, the activity concentrations of the radionuclides ^{226}Ra, ^{232}Th, and ^{40}K were determined in 30 agricultural and virgin soil samples were randomly collected from Kedah, north of Malaysia. Using HPGe detector, the mean concentration values of ^{226}Ra, ^{232}Th, and ^{40}K were reported to be 102.08 ± 3.96, 133.96 ± 2.92 and 325.87 ± 9.83 Bq kg^{-1}, respectively, in agricultural soils, while in virgin soil the values reported to be 65.24 ± 2.00, 83.39 ± 2.27 and 136.98 ± 9.76 Bq kg^{-1}, respectively. The concentration values in agricultural soils reported to be higher than those in virgin soils, and those reported in other countries. The mean values of *radium equivalent activity (Raeq), absorbed dose rates D (nGy h−1), annual effective dose equivalent, and external hazard index (Hex)* were 458.785

Bq kg^{-1}, 141.62 nGy h^{-1}, and 0.169 mSv y^{-1}, respectively, in agricultural soils, and 214.293 Bq kg^{-1}, 87.47 nGy h^{-1}, and 0.106 mSv y^{-1}, respectively, in virgin soils, with an average of H_{ex} of 0.525. The results of the study were consistent with another study conducted by Ahmad *et al.,* (2015) that reported high concentration values of ^{226}Ra, ^{232}Th, and ^{40}K in the agricultural soil were collected from Sungai Petani, Kedah, Malaysia, the high values may be attributed to the intensive use of chemical fertilizers, since tropical soils characterized by lack of phosphorus (Dabin, 1980).

Many measurements have been performed to measure radioactivity in phosphate fertilizers worldwide. Barišić *et al.*, (1992) conducted a study to measure the activities of ^{226}Ra, ^{228}Ra, ^{235}U and ^{238}U in different types of phosphate fertilizers and waters using HPGe. Surface water, water from drainage channels, shallow groundwater and deep groundwater samples were collected from the Kanovci agricultural and well field area in Eastern Slavonia. The findings indicated high concentrations of uranium in surface water, shallow groundwater and water from drainage channels are caused by phosphate fertilizer application in agriculture on the Kanovci fields. Hussein *et al.,* (1994) reported the activities in super phosphate fertilizer samples, the findings of gamma-ray spectroscopy analysis showed the ^{238}U in concentrations of 523, 473 and 134 Bq kg^{-1}; 514, 301 and 411 Bq kg^{-1}(^{226}Ra); 37, 24 and 19 Bq kg^{-1} (^{232}Th); 19, 3 and 16 Bq kg^{-1} (^{40}K).

A study conducted by Alam *et al.,* (1997) to measure the radioactivity concentrations in different chemical fertilizers, triple superphosphate (TSP); single superphosphate (SSP); diammonium phosphate (DAP); phosphogypsum; muriate of potash (MOP); urea, zinc sulfate; and zinc oxysulfate that applied in agricultural fields in Bangladesh, the activities of ^{226}Ra, ^{228} Th, and ^{40}K were reported to range from 4.8 ± 0.8 to 323.8 ± 24.4 Bq kg^{-1}; 3.4 ± 1.7 to 22.0 ± 2.8 Bqkg^{-1} and 7.9 ± 2.4 to 12628.5 ± 169.0 Bqkg^{-1},

respectively. A study carried out by El-Bahi *et al.,* (2004) to determine the concentration of ^{238}U, ^{232}Th, and ^{40}K in the phosphate fertilizer in Egypt. The measured concentration reported to be from 134.97 to 681.11 Bq kg^{-1}, 125.23 to 239.26 Bq kg^{-1}, and 446.11 to 882.45 Bq kg^{-1} for ^{238}U, ^{232}Th, and ^{40}K, respectively. The *absorbed dose rate* and *external hazard index* were reported to be 177.14 to 445.90 nGy h^{-1} and 1.03 to 2.71 nGy y^{-1}, respectively. Taylor, (2007) assessed the uranium (U) accumulation in four soil groups in New Zealand, by comparing samples collected and archived in 1992 with soil samples collected and archived 36–43 years previously, from the same four sites. The mean levels of total U were found to be increased by 1.30 ± 0.03 μg g^{-1} for soils sampled about 40 years ago compared with 1992 soil samples, an annual increase of 0.033 ± 0.008 μg g^{-1} yr^{-1}. Taylor attributed these increases to the phosphate fertilizer application.

2.1.10 Experimental and field studies of tropical soil

The following review will highlight current understanding of the occurrence and form of soil micronutrients, geochemistry, and mineralogy, as well as some of the critical features whose availability may influence the behaviour of radionuclides and stable elements.

However, previous research on behavior of minerals, radioactive elements, critical loads and limits has focused on temperate soils, primarily in Europe and North America. It is doubtful therefore, whether the present the enviromental models, which are based on temperate datasets, will be applicable in tropical situations. With this in mind, it is critical to collect data from tropical soils; however, the level of current knowledge and data in this context must first be assessed.

Many authors have commented on the scarcity of data and knowledge on stable minerals behaviour in tropical soils, as well as the relative lack of studies in this area.

(Davies, 1997; Kookana & Naidu, 1998; Naidu et al., 1998; Onyatta & Huang, 1999; Mbila *et al.,* 2001; Appel & Ma, 2002; Herpin *et al.,* 2002; Campos *et al.,* 2003; Reeves, 2003; Bertoncini *et al.,* 2004; de Alcantara & de Carmargo, 2004; Udom *et al.,* 2004; Twining *et al.,* (2004). The goal of this review is to compile existing knowledge and gain a better understanding of trace metal behaviour in tropical soils.

2.1.10.1 **Radionuclide behaviour in tropical soils**

This review addresses radionuclide mobility as well as the existence of radionuclides in the tropical environment as a result of natural sources, bomb testing, or accidents. However, the number of case studies is relatively few to the number of incidents and more frequent nuclear facility emissions in temperate environments. One well-known example is the discharge from Sellafield in the United Kingdom and the subsequent poisoning of the Irish Sea (Cook *et al.,* 1997, Batlle *et al.,* 2008). Similarly, the Chernobyl disaster had a severe influence on a large area of mostly temperate and sub-Arctic settings. As previously mentioned, the more recent Fukushima disaster has resulted in widespread radioactive dispersion, although the possible impacts on tropical environments remain to be elucidated. As such, there have been limited opportunities to research the radionuclide behaviour of manmade radionuclides in tropical ecosystems, apart from nuclear weapons testing and small-scale releases like the Goiania accident. This is related to the fact that tropical countries have a comparatively modest number of nuclear power plants. Part of the motivation for this work, is the scarcity of relevant information on these topics. As a result, the studies considered in this review are empirical examinations of the behavior of radionuclides in laboratory or field experiments. These are typically focused to examining the consequences of hypothetical events, such as the performance of future nuclear waste repositories or leaks from potential nuclear accidents. While a great amount of data on radionuclide migration and distribution has been gathered for soils from cool temperate Northern

Hemisphere areas, there has been limited research pertinent to tropical regions, where the usage of nuclear power as an energy source is expected to increase. As nuclear power will become more common in tropical and subtropical locations, an accident at a nuclear power station is a potential that should be considered (Uchida, 2007).

Payne *et al.,* (2004) have highlighted the use of controlled experiments in resolving these issues. The advantages of using radionuclides for studies of environmental processes include the ability to study a wide range of element concentrations in a single experiment; the direct applicability to the behaviour of radioactive waste or fallout; and the ability to study the mechanisms, reversibility, and kinetics of environmental reactions under controlled conditions.

Rahman *et al.,* (2005) hypothesised that organic matter OM improved the availability of ^{137}Cs in an experimental pot study of the dynamics of Cs in tropical environments using soil from Bangladesh. Their results showed that there is a weak nonspecific interaction between Cs and soil OM, and that the OM reduces the affinity of clay minerals for Cs, limiting their potential to immobilise Cs in soils. Therefore, the role of organic carbon in the Bikini Atoll samples was completely different from what Robison *et al.,* (2000) discovered. In the latter situation, the organic content increased the Cs' propensity for soils devoid of silicate clays and dominated by carbonates.

The Kd data collected in laboratory trials with samples of soil gathered from field sites in Australia's Northern Territory is an example of an experimental examination of radionuclide behaviour. Twining *et al.,* (2004) provide a detailed explanation of this work. In the latter situation, the organic content increased the Cs' propensity for soils devoid of silicate clays and dominated by carbonates.

The tracers ^{65}Zn, ^{85}Sr, and ^{134}Cs, which were added as a mixed tracer solution, were used in the experiment. The pH dependency of Cs, Sr, and Zn sorption on soil was investigated experimentally. The pH of the soil–water system's equilibrium was measured, as well as pH values one unit higher and lower than the equilibrium value. Because of the high retention of Cs by clays, its uptake is quite powerful, yet it is not pH dependent. The simple chemistry of the monovalent Cs^+ ion explains this (Cornell, 1993). Strontium has the highest mobility, while Zn has an intermediate mobility and the greatest pH dependence. In general, cations exhibit greater sorption with increasing pH, as demonstrated by Zn and Sr in this work.

To investigate the impact of various experimental factors on radionuclide adsorption, experimental sorption studies can be performed. In addition to pH, ionic strength, redox potential, the presence of complexing ligands, and other chemical factors can all influence sorption. Where uranium is a function of pH in the presence of representative environmental bonds such as sulfate and citrate; the bonds affect the uptake of uranium by kaolinite, a common clay mineral in tropical environments. The findings of Waite *et al.,* (1994) amply demonstrate the important role of pH in uranium mobility, as well as the potential impact of the presence of complexing ligands. In these systems that are equilibrated with atmospheric CO_2, the adsorption of uranium at high pH values is significantly decreased by the presence of stable aqueous phase uranyl carbonate complexes.

The majority of radionuclides emitted into the environment settle in the upper layer of soils or the interstitial system of sediments in aquatic systems (Sawhney & Brown, 1989). The soil is separated into layers, and radionuclides are assumed to be present in the top layer as well as in the solution flow from the upper layer to the second layer.

Depending on the Kd values, different radionuclides are adsorbed in the second layer (Knox et al., 2000; Iskauder, 1992).

The physicochemical properties of soil, such as mineral composition, organic matter (OM) concentration, and chemical reaction environment, are the primary factors influencing soil radionuclide (Koch-Steindl & Pröhl 2001). Rainfall amounts, temperature, and soil management are other factors that can influence the behavior of radionuclides in the soil. Finally, the pH value is a significant parameter which controls the kinetics of soil components and, subsequently, the kinetics of radionuclides. In order to understand the mobility of radionuclides within soils, it is important to research the inorganic and organic composition of soils. In the other hand, biological activity can improve the mobility of radioelements.

The mineral fractions of the soil (silt and clay fractions) can absorb radionuclides. Smectite, illite, vermiculite, chlorite, allophone, and imogolite are the main minerals in these fractions, while luminium, copper, and manganese are other contributors to the absorption process. Soils with a high concentration of illite, smectite, vermiculite, or mica absorb significant amounts of cations within the clay fraction due to their intrinsic negative charge (Koch-Steindl & Pröhl 2001). On the other hand, between pH8 and pH9, anions may be absorbed by aluminium and iron oxides. The formation of stable complexes and the exchange of ligands with aluminium and iron oxides will absorb water-soluble anionic compounds like phosphate, selenite, molybdate and arsenate.

Soil water dynamics, as well as soil texture and structure, have a significant effect on radionuclide speciation. By water flow, chemically unchanged substances can partially be transferred, while gradual penetration favours interaction with the soil matrix and soil solution. The distribution of radionuclides in soil can be studied using the exchangeable fraction, fraction bound to OM, fraction bound to carbonates, fraction

bound to iron and manganese oxides (Spezzano, 2005). In this case, soil samples are homogenized and different particle size fractions are separated by physical procedures such as sieving and settling (Livens & Baxter 1988).

The presence of radionuclides in a given environmental system is fundamentally a transitory phenomenon. Environmental systems in the wider biogeochemical cycling are interconnected, dynamic and heterogeneously unique at the biotic and abiotic elements. Radionuclides are unstable isotopes of metal and non-metal materials that, unlike heavy metals, undergo radioactive processes. It is well known that the transport actions, bioavailability, absorption and toxicity of radioisotopes or radionuclides and heavy metals in various food chains are controlled by chemical and physical properties, primarily by speciation (Laul & Smith 1984; Maiti, Smith & Laul 1989; Greeman *et al.,* 1999).

2.1.10.2 **Soil Mineralogy**

Micronutrient elements can be found in relatively significant quantities yet in a variety of forms in soils. Hodgson, (1963) proposed that they may be precipitated with other soil components to form a new solid phase; occluded during the formation of new solid phases in which the nutrient is not a principal constituent; included in soil minerals during crystallisation of state diffusion; associated with soil surfaces, organic or inorganic; and incorporated in biological systems. According to Loneragan, (1975), the rate of micronutrient release into soil solution from contained forms is extremely slow, but release from soil surfaces is rapid. Cu, Zn, and Mn ions are found in divalent forms M^{2+}, in acid soils, according to Lindsay, (1972). He also suggested that the monovalent hydroxy cation, $M(OH)^{+}$, will be relevant in neutral and alkaline soils. However, several researchers (Hodgson *et al.,* 1966; and Geering *et al.,* 1969) showed that significant quantities of micronutrients were recovered from surface soils as complexes.

In general, they found that about 50% of Zn, and up to 90% of Mn were complexed by organic compounds in the soil.

According to Bingham *et al.,* (1964), montmorillonite has the ability to adsorb Zn or Cu beyond its cation exchange capacity, especially at near-neutral or alkaline pH values.

They ascribed this to the hydrolyzed form adsorbing or the hydroxides, Zn $(OH)_2$ or $Cu(OH)_2$ precipitating. Nelson & Melsted (1955) demonstrated that a portion of Zn adsorbed on clay was acid soluble but not exchangeable. According to Reddy & Perkins (1974), kaolinitic clay fixes less zinc than bentonite or illite, and fixed zinc is not replaced for lattice ions, but is firmly adsorbed. They discovered a negative relationship between CEC and Zn fixation. Earlier, Thomas & Swoboda (1963) showed that pH and CEC were the controlling factors in the quantity of Zn adsorbed by kaolinite, hydrous iron oxides, and clay-iron oxide complexes.

Despite a substantial body of research, much uncertainty remains about the exact impact of common soil properties on trace metal behaviour in temperate soils. The impact of tropical soil attributes is even less well understood, which could be a significant knowledge gap given that several of the major tropical soil types differ significantly from temperate soils in terms of composition and geochemistry.

According to Davies, (1997), whereas the soil chemistry of many tropical soil types is not considerably different from that of temperate soils, this is not true of oxisols and ultisols. The latter, which occupy large areas in the tropics, predominate (Naidu *et al.,* 1997). Much is known about the general properties of tropical soils, and it may be worthwhile to discuss these first in regard to their anticipated influence on trace metal behaviour. The characteristics that distinguish tropical soils from temperate soils are as follows: kaolinite-dominated clay fractions in comparison to 2: 1 clays; low organic

matter (OM) contents; and high amounts of Fe oxides. In general, these properties are the result of intensive and long-term weathering, leaching, and quicker decomposition.

Tropical soils are frequently acidic for a variety of causes, the most common of which being heavy weathering. When combined with the low levels of OM and 2: 1 clay minerals found in oxisols and ultisols, such tropical soils should be predicted to be particularly prone to high bioavailability and leaching.

As a result of relatively high soil temperatures and high precipitation rates desilication occurs as a result of the intense weathering and leaching observed in the tropics, which is defined as "the leaching of Si (silicates) and the enrichment of primary quartz, secondary Al and Fe oxides, and two-layer clay minerals (primarily kaolinite) relative to all other soil constituents" (Wilcke *et al.,* 1999a; Duchaufour, 1977). The dominance of 'low activity' clays like kaolinite in the mineral fraction of many tropical soils, with limited isomorphous replacement, is one cause for their poor cation exchange capacity (CEC) (Davies, 1997). According to Srivastava *et al.,* (2005), there are two types of binding sites in kaolinite that could interact with metal ions: pH-dependent variable charge induced by protonation and deprotonation of surface hydroxyl groups in the alumina sheet and at crystal edges; and permanent charge from isomorphous substitution (Al^{3+} for Si^{4+} in the silica sheet and Fe^{2+} or Mg^{2+} in the alumina sheet). Despite this, it is acknowledged that kaolinite has a low surface charge. Davies, (1997) makes the essential observation that the fine clay fraction in tropical soils other than oxisols and ultisols is dominated by 2: 1 clays with a high permanent charge and a considerable CEC. The Fe (and Al) oxide fractions, which can selectively absorb metals, are another important component of the mineral fraction in tropical soils (de Matos *et al.,* 2001; Mbila *et al.,* 2001). The net negative surface charge of a tropical soil increases with increasing soil pH and OM content, emphasising the relevance of soil

OM in tropical soils for trace metal retention. However, it is generally recognised that tropical soils are poor in OM due to their rapid decomposition (Naidu *et al.,* 1997). In the tropics, humus mineralization is 3 to 4 times higher than in temperate soils, according to Davies, (1997). In summary, as pointed out by Naidu *et al.,* (1997), the low surface charge density of variable charge soils in the tropics creates conditions conducive to increased trace metal mobility.

The majority of published data on the behaviour and mobility of radionuclides in soils reflects patterns found after initial deposition on the soil surface; reflect the radionuclide's physicochemical characteristics, soil properties, including variations in depth from the surface, plant types, hydrology, and underlying geology (Giddings, 1973). Residence periods for radioactive turnover in a particular soil layer are calculated on the basis of total radionuclide concentration rather than specific fractions extractable with defined extracting agents. The mass conservation equation is the most basic equation for describing migration:

$$ds/dr + dC/dt = Dd^2C/dx - VdC/dx + S \quad (2.84)$$

where C is the concentration in solution, S is the concentration in solid phase, T is time, V is the interstitial solution velocity and D is apparent diffusion coefficient (Meriwether *et al.,* 1988; Weber & Miller, 1989; Igwe *et al.,* 2005).

Radionuclides that have been permanently sorbed to soil particles as initial deposited particles or that are present in ion exchange sites on soil particles are prone to particle movement mechanisms.

Most radionuclides generated in nuclear reactors or other nuclear devices have a poor solubility. As a result, the majority of radionuclides released into the environment will eventually collect in the top layer of soils or the interstitial system of sediments in

aquatic systems. In general, Pu and Am travel very slowly in soil. In a few years, neptunium and strontium move over a small distance of roughly 1 cm (Weber & Miller, 1989). Cs migration is very dependent on soil properties; typically, it is extremely firmly adsorbed and migrates less than Sr.

The soil is separated into layers, and radionuclides are considered to be present in the top layer and partially in solution flow from the upper layer to the second layer. Depending on the Kd values, some of the radionuclides are adsorbed in the second layer (Knox *et al.,* 2000; Iskandar, 1992).

Iskandar, (1992) and Kabata-Pendias & Pendias, (1992) discovered that heavy metals are connected with soil solids in four distinct ways employing chemical extractants. A relatively tiny amount is stored in adsorbed or exchangeable forms that can be absorbed by plants. The elements are held together by organic matter in the soil and organic compounds in the sludge. This type has a significant proportion of copper; howover lead is not as strongly attracted. Heavy metals in soil are associated with carbonates and iron and manganese oxides. Organically bound elements are not easily accessible to plants, but can be released over time; heavy metals in soil are associated with carbonates as well as iron and manganese oxides (Igwe, Nnororm & Gbaruko 2005). These forms are less accessible to plants than the exchangeable or organically bound forms, especially if the soils are kept from becoming excessively acidic; the fourth association is known as the residual form, and it is made up of sulphides and other insoluble chemicals that are less accessible to plants than any of the other forms.

Heavy metals are not easily absorbed by soil - plants, and do not leach quickly from the soil. As a result of the metals' immobility, they will accumulate in soils if sludge is applied repeatedly, which is not beneficial for the healthy growth of plants (Igwe *et al.,* 2005).

2.1.10.3 **Soil pH**

Soil acidity is measured in terms of pH. This is a convenient symbol which refers to the negative logarithm of the hydrogen ion concentration expressed in g ions per litre. If the concentration of hydrogen ions is represented by C_{H^+}, then pH = $-\log_{10} C_{H^+}$. Thus, if the concentration of hydrogen ions in a solution is 10^{-2} (1/100) g. ions per litre, then pH = $-\log_{10} 10^{-2} = 2$.

Pure water which is neither acid nor alkaline contains equal amounts of hydrogen (H^+) and hydroxyl (OH^-) ions. In neutral solutions $C_{H^+} = C_{OH^-} = 10^{-7}$. The pH is therefore equal to 7. Just as a preponderance of hydrogen (H^+) ions indicates acidity, so also will an excess of hydroxyl (OH^-) ions indicate alkalinity. In aqueous solutions, the product of the concentrations of hydrogen (H^+) and hydroxyl (OH^-) ions is 10^{-14}, i.e. $C_{H^+} \times C_{OH^-} = 10^{-14}$. If the con centration of hydroxyl (OH^-) ions is 10^{-5}, $CH^+ = 10^{-14}/10^{-5} = 10^{-9}$ and the pH = 9 (Kalpage, 1979).

pH readings less than 7 indicate acidity, those greater than 7 indicate alkalinity, and 7 is the neutral point. Soils in well-drained humid areas are acidic and have low pH values. Well-drained highland soils are often more acidic than valley bottom soils. Certain fertilisers, such as ammonium sulphate, can also cause acidity.

The negative consequences of acid soils are attributable to secondary factors rather than an excess of hydrogen (H^+) ions. Basic ions such as Na^+, K^+, Ca^{++}, and Mg^{++} are low in extremely acidic soils, phosphorus availability and nitrate production are decreased, and Al, Fe, and Mn, which have enhanced solubilities, may be taken up by plants in lethal proportions. Indicator solutions or indicator papers saturated with such solutions can detect soil acidity. The pH of the soil is indicated by changes in colour ranging from violet to all colours of the spectrum to red (Kalpage, 1979).

Determinations can be made on soil moistend with water or suspensions of soil with different amounts of water. For example, a 1:1 ratio of soil to water has been used water suspentions, in which Ph values are likily of fluctuate in the case of certain soils, other extractance like potassium chloride (N KCL) may be used. Values in normal potassium chloride solutions are generally about 1.5 units of pH lower than in aqueous suspension. The pH meter, of which a number of different models are available, is an instrument for the accurate measurement of pH and is widely used to determine the pH of soils.

The pH has a significant effect on the sorption of trace metals in soils. A low pH tends to lead to a decrease in sorption and a consequent increase in the bioavailability and mobility of most trace metal forms. Although there have been few investigations on this topic with tropical soils, comparable results have been reported. For example, King (1988) observed that the majority of the variance in exchangeable Cd, Co, Cu, Ni, and Zn was explained by pH in a study of trace metals introduced as aqueous solutions to 21 soils (A, B, and C horizons) from the southern United States (including ultisols, alfisols, and entisols).

The exchangeable Cr, Pb and Sb were correlated more with the texture of the soil. Cd and Pb adsorption increased with rising pH, according to Appel & Ma (2002), notably in ultisol and oxisol. Interestingly, the ultisol and oxisol zero net charge points (PZNC), where the pH at which the net charge of total particle surface (i.e. absorbent's surface) is equal to zero are 2.3 and 3.7, respectively, and the oxisol retained metals below its PZNC, signifying complexation of the inner sphere or adsorption of permanent charge sites.

Twining *et al.,* (2004) found that between pH 4.4 and 7.3, the Kd for Zn rose from 40 to 3000 ml/g in 'lateritic' soil types in Australia. Cd, Ni, and Zn were quickly mobilised

in soils from a mining location in Togo under low pH and oxidising conditions (Gnandi & Tobschall, 2002).

Some studies have stated that pH has a lower impact on metal sorption in tropical soils. Gomes *et al.,* (2001) studied the effect of soil properties on cation adsorption in Brazilian soils and found that while Cd, Cr and Ni were correlated with pH at a significant relationship, while Cu, Pb and Zn were not correlated with pH.

In general, reducing pH strongly depresses the rates of absorption rates of Boron (B) and Molybdenum (Mo) but promotes the adsorption of the metallic cations when they are present as inorganic ions (Loneragan, 1975). Cu availability is influenced by soil pH, but it does not usually rise significantly until the pH falls below 5.0. According to Norvell & Lindsay (1969), Cu^{2+} predominates in soil solution below pH 7.3, while above this pH, $CuOH^{+}$ is most abundant. Hodgson *et al.,* (1966) believed that substantial complexing of Cu by soil OM is a key component explaining why Cu deficits are not as common as Zn deficiencies on high pH soils, despite the fact that both cations show a similar drop in solubility with increasing pH. The Mn^{2+} ion is the most abundant species in soil solution, and its concentration decreases 100-fold with each unit increase in pH (Lindsay, 1972). Mn solubility in soils varies greatly and is pH dependant (Bohn, 1970). Geering *et al.,* (1969) reported total Mn levels at 0.01 ppm and computed Mn^{2+} at 0.0003 ppm. The higher solubility of Mn in soils could be attributed to the synthesis of Mn oxide coprecipitates with other heavy metals, particularly Fe. According to Lindsay, (1972), the dominating species at pH < 7 is Zn, and its solubility is pH dependant, decreasing 100-fold for each unit increase in pH. A research conducted by Katyal & Sharma, (1991), total Zn and Cu contents in 57 Indian soils were associated with clay content but not pH or other soil parameters.

According to De Matos *et al.,* (2001), Cd, Cu, Pb, and Zn retardation in Brazilian ultisols and oxisols was significantly positively linked with quantity of bases, CEC, and soil Ca but not with pH. However, when the pH of the soils was decreased, retardation increased, which the authors attributed to precipitation at the highest pH levels.

In five semi-arid Indian soils and 7 English soils, Hooda & Alloway, (1998) compared soil properties and the sorption activity of Cd and Pb, while, the English soils had lower pH values (4.7 - 7.55) than the Indian soils (6.3 - 8.42), they retained Cd and Pb more strongly and this was attributed to the higher values for OM, clay and $CaCO_3$ in the English soils.

Fe oxides have a considerable influence on the solubility of Fe in soils. For each unit increase in pH, the Fe^{2+} and Fe^{3+} activity in solution reduces 100 and 1000-fold, respectively (Lindsay, 1972). Amorphous and crystalline Fe phosphates are known to form in acid soils (Lindsay *et al.,* 1962). However, total P in soils is often significantly lower than total Fe, thus even if all P precipitated as Fe phosphates, hydrous Fe oxides may still maintain soil solution soluble Fe levels.

2.1.10.4 **Organic Matter (OM)**

Soil organic matter (OM) is a complex, naturally occurring substance and plays a critical role in soil fertility, the global carbon cycle, and the fate of pollutants in soil.

Soil organic matter consists of plant and animal leftovers at various stages of decomposition. This organic matter fraction also includes soil organisms that live and die in the soil. Organic matter in soil is formed as a result of the breakdown of plant and, to a lesser extent, animal matter.

Hodgson, (1963) proposed three major kinds of soil organic matter-micronutrient complexes. These include: (1) relatively high molecular weight humic substances

containing condensed aromatic nuclei, which have a high affinity for micronutrients but are largely insoluble in soil; (2) low molecular weight organic acids and bases derived primarily from microbial cells and metabolism, which exhibit relatively high solubility in association with micronutrients; and (3) soluble ligands that precipitate upon reaction with micronutrients. Dead organic matter (OM) of the soil is colonized by microorganisms, which obtain energy for growth from the oxidative decomposition of organic molecules (Federle *et al.,* 1986). It is during the decomposition process whereby inorganic elements are converted from organic compounds, a process called mineralization (Nierop *et al.,* 2007). For example, organic nitrogen and phosphorus are mineralized to ammonia and orthophosphate, respectively, thereby providing nutrients for biotic uptake and growth.

To understand the role that organic matter OM plays in its decomposition, Petigara *et al.,* (2002) critically examined the mechanisms of hydrogen peroxide (H_2O_2) decomposition in soils. As they described, its impact could be significant if its decomposition within the soil leads to the formation of OH radical through Fenton-type chemistry:

$$H_2O_2 + Mn \rightarrow OH + OH^- + M^{n+1}$$

The OH radical is a very potent oxidant. As a result, oxidative processes triggered by OH have the potential to profoundly alter the nature and speciation of organic and inorganic constituents in soil. The researchers employed a sensitive approach to investigate the production of an OH radical as a probable decomposition intermediate. They discovered that in surface soils with more organic matter OM, H_2O_2 degraded quickly, with the production of OH radicals accounting for less than 10% of the total H_2O_2 dissolved. Although H_2O_2 decomposed more slowly in soils with lower OM

content, the OH radical was a major product. Ultimately, the yield of the OH radical varied greatly and was affected by a variety of soil factors (Petigara *et al.,* 2002).

Three main types of the transformation of organic compounds in soils are considered: photodecomposition, chemical transformation, and microbiological degradation. Although it is difficult to differentiate simultaneous chemical and microbiological changes in soils, it is generally assumed that the breakdown of most organic compounds in soils involves microbes since soil sterilisation dramatically lowers the rate of degradation of many chemicals (Sanderman & Amundson, 2014).

Clay minerals, metal oxides, metal ions, and soil organic matter are soil components that may drive chemical reactions of organic molecules. Furthermore, the rates of transformation in soils are affected by a variety of other elements such as temperature, humidity, and ambient oxygen.

In the absence of large amounts of soil organic matter, U generally is considered to be mobile and transported as a divalent uranyl (UO_2^{+2}) ion (Schulz, 1965). Uranyl carbonate complexing results in a wide range of U solubility. Hostetler and Garrels, (1962) reported that U is transported in acid oxidizing solutions as (UO_2^{+2}) or $UO_2(OH)^+$ ions, as a $UO_2(CO_3)_2^2$ complex in neutral solutions, and as a $UO_2(CO_3)_3^{-4}$ complex in alkaline solution. In contrast, the reduced tetravalent form of U behaves similarly to immobile tetravalent Th (Hansen & Huntington, 1969). Talibudeen, (1964) suggested that the Th/U ratio may provide information about weathering intensity in soils, since Th is much less mobile than U.

It is well known that soil organic matter has a significant impact on trace metal activity. Soil OM has a broad capacity to exchange surface negative charge cation and elements such as Pb are found to accumulate in the organic, surface horizons rich

(Zimdahl & Skogerboe, 1977). In addition, soluble OM has an important effect on the distribution of elements in the soil profile, particularly for Cu (Temminghoff *et al.,* 1997). In the tropics, though, humus mineralization is quicker and, thus, tropical soils appear to have even fewer OM. Therefore, the assumption may be that OM in tropical soils has a significant influence on the behaviour of trace metals. For example, an adsorption analysis in Brazil (Sodre *et al.,* 2001) showed that the presence of OM strongly influenced Cu adsorption in clayey soils. Haas & Horwitz, (1986) stated that the addition of alginic and humic acid improved Cu binding to kaolinite.

The effect of soil properties on the retardation of Cd, Cu, Pb, and Zn in Brazilian ultisols and oxisols was analysed by De Matos *et al.,* (2001) and found that retardation was strongly associated with OM, but only for Cu and Pb. Organic carbon (OC) was only substantially associated with Cu in an analysis of the effect of soil properties (pH, OC, CEC, clay, Fe oxides) on adsorption of Cd, Cr, Cu, Ni, Pb and Zn in the B horizons of Brazilian soils (Gomes *et al.,* 2001). The authors observed that the soils had low levels of OC of 0.3% to 2.3%. Wilcke *et al.,* (1999a) compared Cd, Cu, Pb and Zn concentrations in external and internal soil aggregate fractions in 18 Costa Rican agricultural soils (Oxisols, Andisols, Mollisols and Inceptisols) obtaining trace metal contributions from fungicide and fertiliser applications and atmospheric deposition. Copper, which was mostly introduced by fungicides into the soils, was believed to be predominantly sorbed into organic matter on aggregate surfaces and within aggregates (and to Fe oxides).

Alexandre *et al.,* (1995) reported that in Sao Paulo, Brazil, OM was partially responsible for maintaining Cu in a tropical soil profile. Udom *et al.,* (2004) reported a comparatively poor correlation between OM and Cu compared to Cd and Zn in a Nigerian, sludge-amended ultisol, in comparison to the studies mentioned above. In

addition, in savannah soils in Nigeria, Munkholm *et al.,* (1993) found no connection between OM and total trace metal concentrations, including Cu. There is no research on the effect of OM in tropical soils on other trace metals.

Twining *et al.,* (2004) recorded greater binding of Zn in a sandy loam than in clay loam in Australia and claimed that this could have been correlated with OM, as well as strong binding of Zn near the surface. Possible contact with OM was attributed to Zimbabwe (Nyamangara & Mzezewa, 1999). Zhang *et al.,* (2006) reported that OM was not a major factor in deciding the distribution of sub-tropical in 260 soil profiles. In addition to the well-documented sorption of certain trace metals by solid-phase OM, soluble types of OM are well known to affect the mobility and distribution of certain trace metals by temperate soil studies (Temminghoff *et al.,* 1997).

Mbila *et al.,* (2001) argued that the enrichment of Cu at depth in sludge-modified ultisols and alfisols in Nigeria indicated the leaching of Cu attached to soluble OM. De Alcantara & de Carmargo, (2004) reported that the movement of Cr in the A horizon of a Brazilian oxisol was greater than in the B horizon and that this may have been attributed to the formation of soluble compounds between metal and fulvic acids.

In an analysis of the leaching of As, Cu, Pb and Zn from soils to lakes and reservoirs in Bangladesh, Islam *et al.,* (2000), organometallic complexes were identified as one of the major processes of control. In a study of leaching of As, Cu, Pb and Zn from soils into lakes and reservoirs in Bangladesh, Islam *et al.,* (2000) listed organometallic complexes as one of the main influencing processes.

2.1.10.5 **Redox potential**

The chemical behaviour of radionuclides is determined by the specific chemical compound and the oxidation status. The most important factors that control chemical

speciation in soil are the pH-value and the redox potential. All redox processes in soil occur in the presence of water and they are, therefore, within the stability field of water. The upper limit of the stability field of water is given by the decomposition of water into oxygen gas Equation (2.81), whereas the lower limit of the stability field is given by the decomposition of water into hydrogen Equation (2.82):

$$1/2\ H_2O_{(1)} \rightarrow 1/2\ O_2 + 2\ H^+ + 2e- \quad (2.81)$$

$$2\ H^+_{aq} + 2e^- \rightarrow H_{2(g)} \quad (2.82)$$

The redox potential and the pH value are negatively correlated, i.e. within the stability field of water, the E_h value decreases with the increase of pH and vice versa. The first reaction produces protons (decrease of pH), whereas the second one consumes protons (increase of pH). The relationship of redox potential and pH is given in the following Equation (2.83):

$$E_h = E^0 - 0.059 \cdot pH \quad (2.83)$$

where E^0 is the standard potential of the half cell in which oxidised species and reduced species have unit activity. In soil, the speciation of a number of elements depends on the redox conditions (Poinssot & Geckeis 2012). These reactions occur simultaneously and determine an average redox potential of the soil. Important redox reactions of the soil are assigned to the typical redox potential and to the soil aeration status. The borderlines of the stability field of water are the theoretical limits for chemical speciation in the soil. The E_h-pH conditions are a result of the oxygen supply that controls the predominating redox reaction in the soil and the chemical speciation. In well aerated soils under acid conditions, E_h is in the range of 200–800 mV, whereas in waterlogged soils with a pH >7, it may decrease to –400 mV and even less. However, the ranges of E_h and pH conditions are limited by agricultural land use (Diener & Neumann 2011; Poinssot & Geckeis 2012).

The redox potential (E_h) of the soil is determined by various factors, such as soil type, distance to the water table, presence of water-impermeable soil horizons and biological activity of the soil. However, it should be noted that even under a very careful soil management which aims at optimised soil conditions, temporary fluctuations of the redox potential will be observed during the year (Poinssot & Geckeis 2012).

In natural systems, the sequence of redox reactions is frequently mediated by microbes and is accompanied by a diminishing energy yield. As a result, a series of distinctive microorganisms may be discovered in various redox zones of natural waters, ranging from eerotrophic oxygen consumers, denitrifiers, Mn and Fe reducers, and sulphate reducers to methane-fermenting organisms. The capacity of these bacteria to oxidise organic carbon is greatly influenced by environmental factors (such as salinity or temperature) as well as organic carbon bioavailability (Poinssot & Geckeis 2012; Diener & Neumann 2011).

Solubility and mobility of thorium and uranium in soils may vary strongly depending on soil type and physicochemical properties (Ahmed *et al.,* 2012). Soil solution distribution coefficients, Kd, can describe the mobility of elements in soils and rocks range in different environments from 0.03 in sandy soils to 20 000 in clayey soils (Sheppard *et al.,* 1989; Sheppard & Thibault, 1990; Willett & Bond, 1995). Chemical speciation of U (VI) in soils is highly dependent on soil composition and on the pH in the soil solution (Giblin & Swaine, 1981). Complex reactions that control the fate of U (VI) in the soil systems. Hydrolysis of the uranyl ion according to soil pH, results in the formation of different complexes with varying affinities for the soil solid phase (Morrison *et al.,* 1995). Sorption of U (VI) onto soil matrix is higher at lower pH values in soils and decreases strongly with increasing pH (Giblin & Swaine, 1981; Morrison *et*

al., 1995). This relationship is valid in aerated environments within the range of pH 4–9 (Giblin *et al.,* 1981; McKinley *et al.,* 1995). This is the range that is observed for a large majority of cultivated soils (Echevarria *et al.*, 2001). Furthermore, the presence of carbonates in the solution decreases strongly the sorption of U(VI) onto soil matrix by forming carbonate complexes that are negatively charged such as $UO_2(CO_3)_2^{2-}$ Dement'ev and Syromyatnikov, (1968) or $UO_2(CO_3)_3^{4-}$ (Giblin *et al.,* 1981). These negatively charged complexes have a much lower affinity for soil minerals such as hematite (Ho & Miller, 1986), and the soil matrix (Armands, 1961), than uranyl and hydroxy-complexes.

2.1.10.6 **Potential role of soil microorganisms**

Microorganisms play an important role in the biogeochemical cycling of radionuclides (Gadd, 1997, 2002; Morris & Raiswell, 2002; Lloyd & Renshaw, 2005) and can affect soil solution composition by a variety of mechanisms (Tamponnet *et al.,* 2001):

- microorganisms can alter the soil pH (e.g., via the production of organic acids and bases) and the pE (via respiration), both of which are known to influence the rate of transfer of radionuclides from the solute to solid phase,
- exudates in the form of low molecular weight organic compounds produced during microbial metabolism can act as potential ligands for radionuclides,
- microorganisms can alter soil structure through the formation of mineral aggregates, thus affecting radionuclide binding sites,
- radionuclides may also become attached to microbial cell walls or to extracellular polysaccharides of bacteria, and
- radionuclides may be actively taken up by microorganisms from soil solution

Microorganisms can modify both the soil structure and geochemical cycles and thus play an important role in maintaining radionuclides in a biological cycle without fixing them in any chemical sense. This phenomenon has been shown to be especially important in organic and acidic soils (e.g., upland soils, peats and forest soils; Shand et al., 1995; Valcke & Cremers, 1994). In such ecosystems, the major source of nutrients for plant uptake is the plant litter on the soil surface with elemental recycling from litter to plants occurring as a result of decomposition and leaching processes (Clint *et al.,* 1992). As with nutrients, litter is likely to be a main source for radionuclide recycling to plants and the role of fully decomposed litter on radionuclide uptake has been studied. Experimental devices were developed to precise the role of microbiological processes in the bioavailability and cycling of radionuclides, to provide mechanistic information on various aspects of soil microbe radionuclide interactions, and to develop an innovative experimental approach, which incorporates microbial activity at optimal conditions of growth, in order to address the role of soil microorganisms on radionuclide sorption/desorption (Sanchez *et al.,* 2000; Parekh & Bardgett, 2002).

The role of different groups of soil microorganisms on radionuclide uptake has been identified in many literatures. The presence of microorganisms may increase radionuclide binding by increasing the surface area for binding in the organic matrix and clay minerals and/or by depleting the medium of competing ions (Parekh *et al.,* 2008).

Fungi play a major role in providing ecosystem services in terrestrial ecosystems (Dighton, 2003) and it is in these systems that their interaction with radionuclides has been most studied. The International Commission on Radiological Protection recommendations on the ecological aspects of radionuclide release (Coughtrey, 1983), highlighted the importance of organic soil horizons and their microbial communities

(fungi and bacteria) as potential accumulators of nutrient elements and radionuclides within terrestrial ecosystems (Heal & Horrill, 1983). Radionuclide accumulation and movement in organic horizons of forest soils may be related to fungal biomass (Osburn, 1967), and where fungal activity is the pivotal regulator in the interaction between ecosystem components (Avila & Moberg, 1999; Steinera *et al.,* 2002). The potential for macro-fruit bodies of higher fungi to hyperaccumulate radionuclides and heavy metals has led to suggestions that they may be agents for bioremediation (Gray, 1998). Despite nearly 50 years of investigation of interactions between radionuclides and fungi, there is still need for greater understanding of the nature of these interactions, particularly from a molecular standpoint and from the point of view of using fungal and plant–fungal interactions in remediation of polluted systems (Zhdanova *et al.,* 2005b).

Saprotrophic fungi present an enormous surface area of hyphae to their surrounding environment, fitting them for absorbing nutrient elements and radionuclides from the environment. Microbial immobilization of radionuclides from decomposing leaf litter and cellophane accumulated almost three times the amount of radio cesium than sterile equivalents (Witkamp & Barzansky, 1968).

Measurement of radio cesium incorporation into the fungus *Trichoderma viride* from plant litters showed that the concentration factor in fungi (ratio of radionuclide concentration in the fungus to the concentration in the resource) decreased as the leaf litters aged (2.36, 0.46 and 0.23 for litters of 4, 16 and 48 months of age) (Witkamp, 1968). The highest concentration factor 4.31 was found from freshly fallen wood (Witkamp, 1968). This provided basic evidence to suggest that fungi could mineralize radionuclides from these resources and translocate them from the resource into their own biomass, thus pointing to the potential significance of fungi in regulating movement of radionuclides in the environment. In general, it is thought that

accumulation of radionuclide elements follows that of nonradioactive elements. However, with the discovery of isotope discrimination for a number of elements by a range of organisms, this may not hold true. The capacity of an organism to discriminate between isotopes has given rise to new branches of ecology, allowing nutrient cycling to be more exact in determining the source of nutrients obtained from a variety of sources (Henn & Chapela, 2001; Ruess *et al.,* 2005; Trudell *et al.,* 2004; Hobbie, 2005). Saprotrophic fungi in grassland soil have a lot of potential for absorbing and storing radio cesium fallout (Olsen *et al.,* 1990; Dighton *et al.,* 1991).

CHAPTER 3: MATERIAL AND METHODS

3.1 Study area

Peninsular Malaysia is located in the southeast of the Asian countinent with coordinates of 4° 12' 37.7424" N, 101° 58' 32.7684" E, covering a total area of 132,090 km^2 and located between Thailand in the north and Singapore in the south. West Malaysia has a total coastline of 2068 km. Peninsular Malaysia is mountainous, with more than half of it over 150 m above sea level (Ashraf *et al.,* 2017). Around half of Malaysia's peninsula is covered by granite and other igneous rocks, another third by stratified rocks older than granite, and the rest by alluvium. Tin deposit is found in Selangor, Kinta valley in Perak, Pahang and Johor. There are significant deposit of gold in Pahang towns of Raub and Kuala Lipis and also Kelantan's district of Gua Musang (Ooi, 1976).

The climate of the peninsula generally belongs to Koppen's Tropical Rainforest Climate (Af) which is defined as having no distinct dry season. The climate of a location is affected by its latitude, terrain, and altitude, as well as nearby water bodies and their currents. Climates can be classified according to the average and the typical ranges of different variables, most commonly temperature and precipitation. Malaysia is categorised as equatorial, it is hot and humid at an average temperature of 27 ° C (Saw, 2007), with an average rainfall of 2500 mm a year. Malaysia is subject to the El Niño impact in the dry season, which reduces rainfall. Climate change is expected to have a major influence on Malaysia, increasing sea level and rainfall (Marshall, 2008).

Malaysia is characterized by a tropical rainforest climate, experiencing warm and humid condition throughtout the year. The variations in the climate of Malaysia are dictated by the states and provinces that occupy definite climatological zones. Local

climate, thus, can be divided into that of the highlands and lowlands, and coastal regions.

Rainfall pattern is the most marked feature in the northwest and the east coast regions. In the northwest coastal plain, rainfall during the northeast monsoon season is quite low in January and February while the highest rainfall occurs in the September-October period. On the east coast, more than 50% of the precipitation occurs in the January February northeast monsoon season and the remainder of the year is relatively dry. Fluctuation of monthly rainfall generally decreases southward, where rainfall tends to be distributed evenly throughout the year. The annual rainfall ranges from 1,700 to 4,200 mm inland of the west Main Range, from 1,900 to 2,400 mm on the west coast, and from 2,800 to 3,100 mm on the east coast (Paramananthan, 2000, Ashraf *et al.,* 2017).

About 40% of the total land area is hilly or mountainous rising above 150 m and more than half of this (23% of the total) extends above the 300 m contour. There are several mountain ranges aligned, generally, in a north-south direction of which the largest (commonly known as the Main Range) is usually considered the backbone of the country, as it more or less divides the peninsula into west and east coast (Ashraf *et al.,* 2017). The land between about 15 to 150 m above sea level can be described as gently to moderately undulating, while large flat areas of peat swamps and alluvia are found along the west coast rising from sea level to about 15 m and extending inland at places to a maximum of 60 km. Along the east coast these flat alluvial areas are not well represented (Paramananthan, 2000).

The mountain ranges and the lower areas of undulating land are mostly composed of granitic rocks as well as old bedded rocks of the Mesozoic and Paleozoic eras. Granitic rocks have the most widespread distribution, underlying almost half of the total surface

area. The older sedimentary rocks consist of repeated series of quartzites and shales with interbedded limestones and volcanic rocks. Rocks younger than the granites occur only in small patches and are of minor importance as soil parent materials (Paramananthan, 2000, Ashraf *et al.,* 2017). Flat land areas along the coast and a part of the undulating hill lands (not exceeding 80 m above sea level) represent the major part of the Quartenary sediments. The older alluvium is comprised of unconsoli dated clays, sands, and gravel. Similar formations are known to occur in other parts of the peninsula at higher levels (up to 80 m above sea level) further inland taking the form of raised terraces or coastal platforms. Lower-level terraces with flat to gently undulating land forms, intermediate in elevation as well as in age, are known to occur in some parts of the peninsula between the older alluvium and recent allu vium. These are composed of predominantly coarse textured "subrecent" alluvium (Paramananthan, 2000, Ashraf *et al.,* 2017).

Recent alluvia occupy the flat low-lying land along the coast and in intermontane valleys. Flow rates of Malaysian rivers decrease very rapidly at the foot of mountains where elevations are less than 30 m above sea level. As a result there is a reduction in the carrying capacity of the rivers and much of the coarse and medium grained materials is de posited at the landward margins of the coastal alluvial plain in a fresh water condition. Finer grained materials carried by sluggishly meandering rivers are deposited later in a brackish water milieu or in a marine condition at the mouths of rivers and along the coastal stretches. This zoning of marine and river sediments, roughly parallel to the coast line, is typically seen on the west coast. In some of the larger stretches of alluvia along the west coast permanent swamp conditions in the centers have built up thick peat layers (Paramananthan, 2000, Ashraf *et al.,* 2017).

3.2 Sampling sites

A total of 228 soil samples were collected randomly at depths of 0-10, 10-20, 20-30 and 30-40 cm, between August 2013 to October 2017 from six agricultural regions of Peninsular Malaysia. This include 40 soil samples from Alor Setar in Kedah, 35 from Selangor, 38 from Malacca, 40 from Johor, 75 from Pahang (Raub and Lanchang).

Forty samples were collected separately from an agricultural paddy field in Kadah to study seasonal changes that may have potential impact on radionuclides behavior. 20 samples were collected during the wet season or growing season (March-April) and 20 samples during the dry season or harvest season (June-August). Figure 3.1 illustrates the sampling sites for the study.

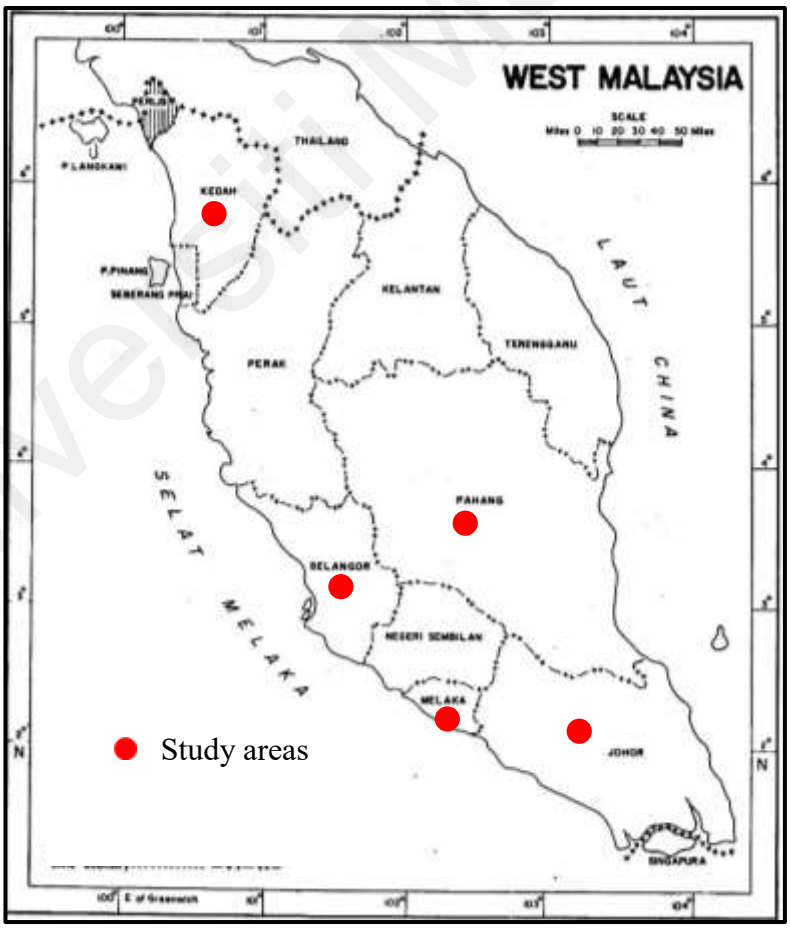

Figure 3.1: Map showing the selected study areas in Peninsular Malaysia

3.2.1 Study area in Kedah State

A total of 40 soil sample were collected randomly at the depths of 0- 10, 10-20, 20-30 and 30-40 cm, from paddy fields in Alor Setar, with latitude, 6° 7' 29.28" N100° 22' 4.1556" E (Figure 3.2). Approximately 115 km^2 plots were selected where the samples were collected, the distance between sampling points was 1- 4 km, in order to ensure a spatial correlation in the geostatistical analysis. Forty samples of soil were collected separately from the same field to study seasonal changes that might have potential impact on radionuclide availability within a depth of 0-40 cm, divided into 20 samples during the growing season or wet season and 20 samples during the harvest season or dry season. GPS coordinates for collected samples and the soil texture of the study area are provided in Appendix A.

Alor Setar is located in the north-western part of Peninsular Malaysia that features a tropical monsoon climate under the Köppen climate classification. Alor Setar has a very lengthy wet season from April to December, and short dry season from December to April, with average high temperatures around 32 °C and average low temperatures around 23 °C. The average of precipitation per year is approximately, 2300 mm.

The geology in Kedah belongs to Quaternary and Carboniferous period. The state is located on marine and continental deposits: clay, silt, sand, peat with minor gravel of Quaternary age that was formed in Holocene period about 15000 years ago (Hussein, 1997). Generally, Alor Setar soil includes the marine clay that consists of mixture of clay, silt and little sand content. The geology of the area was formed from sedimentary rocks and is derived from by the accumulation or deposition of mineral or organic particles at the Earth's surface, such as phyllite, slate, shale and sandstone where argillaceous rocks are commonly carbonaceous (Department of Minerals and Geosciences Malaysia (JMG) https://www.jmg.gov.my/en/).

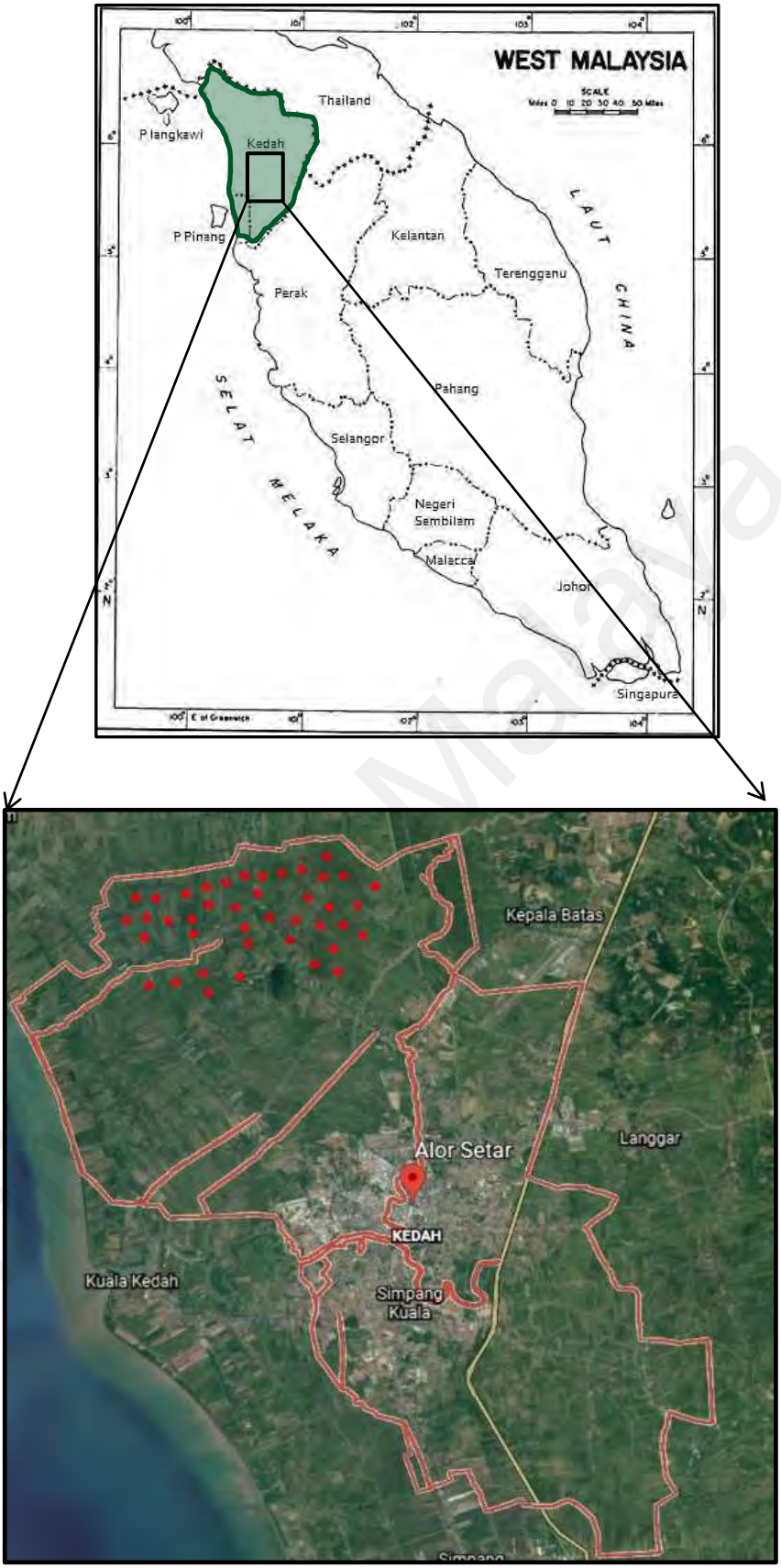

Figure 3.2: Sampling area in the state of Kedah

3.2.2 Study area in Selangor State

A total of 35 soil samples were collected randomly from oil palm plantation in Sungai Tengi, Selangor, Malaysia at the depths of 0-10, 10-20, 20-30 and 30-40 cm. Selangor is located on the west of Peninsular Malaysia, 3° 4' 25.8168" N101° 31' 6.0564" E (Figure 3.3). Approximately 200 km^2 study plots were established where the samples were collected, the distance between sampling points was 1- 4 km, in order ensure spatial correlation in the geostatistical analysis. GPS coordinates for collected samples and the soil texture of Selangor is listed in Appendix A.

As in the rest of Malaysia, Selangor has a tropical rainforest climate bordering on a tropical monsoon climate. It has high average temperature and high average rainfall. The temperature of Selangor is between 29 and 32°C and the mean relative humidity is 65 to 70%. The highest temperature is between April to June, while the relative humidity is lowest in June, July, and September. Soils in Selangor belong to Quaternary and Carboniferous period. Where, the state is located on marine and continental deposits with clay, silt, sand, peat and minor gravel of quaternary, and Phyllite, slate and shale with subordinate sandstone and schist. The eastern parts of Selangor located on igneous rocks intrusive rocks, mainly granite with minor granodiorite (Department of Minerals and Geosciences Malaysia (JMG) https://www.jmg.gov.my/en/). Although the area belongs to the western coastal belt of the Peninsular Malaysia and the soil is derived from the same sedimentary rocks in Kedah. Selangor was chosen in this study considering the amounts of rain and some climatic factors, as well as, vegetation requirements and the type of roots may contribute to spatial divergence in the values of the target parameters.

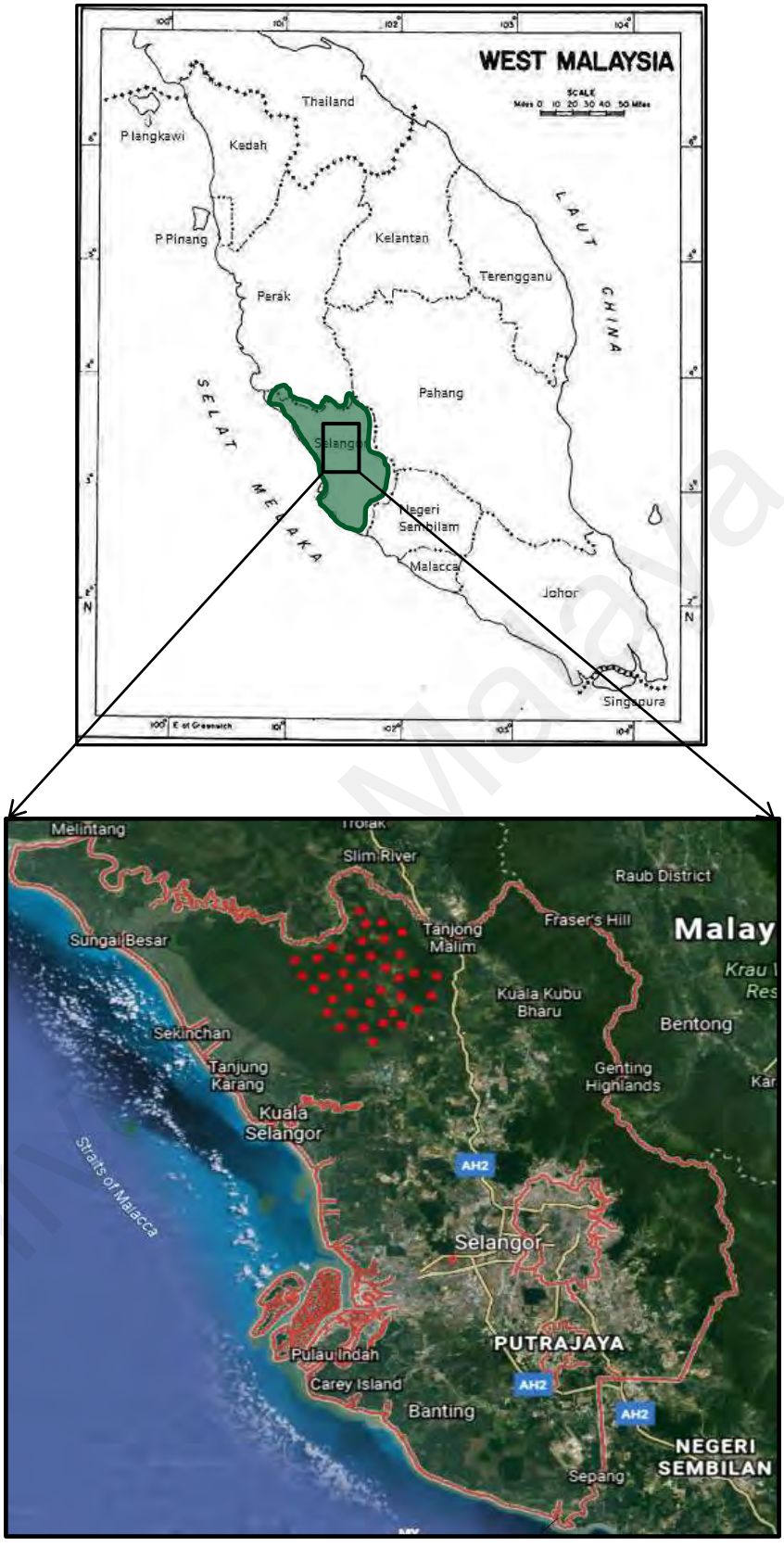

Figure 3.3: Sampling area in the state of Selangor

3.2.3 Study area in Malacca State

A total of 38 soil samples were collected randomly from 0-10, 10-20, 20-30 and 30-40 cm, from tropical fruit fields in Sungai Udang in Malacca, Malaysia, having latitude and longitude of 2.2915° N, 102.1329° E, respectively (Figure 3.4). Approximately 30 km^2 plots where the samples were collected, the distance between sampling points was 0.5 km. The GPS coordinates for collected samples and the soil texture of Malacca are given in Appendix A.

Malacca is situated 148 km (92 mi) south of Kuala Lumpur and commands a central position on the Straits of Malacca. With the exception of some of its small hills, Malacca is generally a lowland area with average elevation below 50 meters above sea level. Temperature ranges generally between 30-35 °C during daytime and between 27-29 °C during night time.

Soils in Malacca belong to the Devonian, a geologic period and system of the Paleozoic, spanning 60 million years from the end of the Silurian, 419.2 million years ago, to the beginning of the Carboniferous. Soil is formed in Malacca from sedimentary rocks which are types of rock that are formed by the accumulation or deposition of mineral or organic particles at the Earth's surface, such as phyllite, slate, shale and sandstone are locally prominent. Some interbeds of conglomerate, chert and rare volcanics, while, the southern parts of the state belong to the Permian Jurassic era. The soil evolved in these parts of igneous rocks that are formed from intrusive rocks, mainly granite with minor granodiorite (Department of Minerals and Geosciences Malaysia (JMG) https://www.jmg.gov.my/en/).

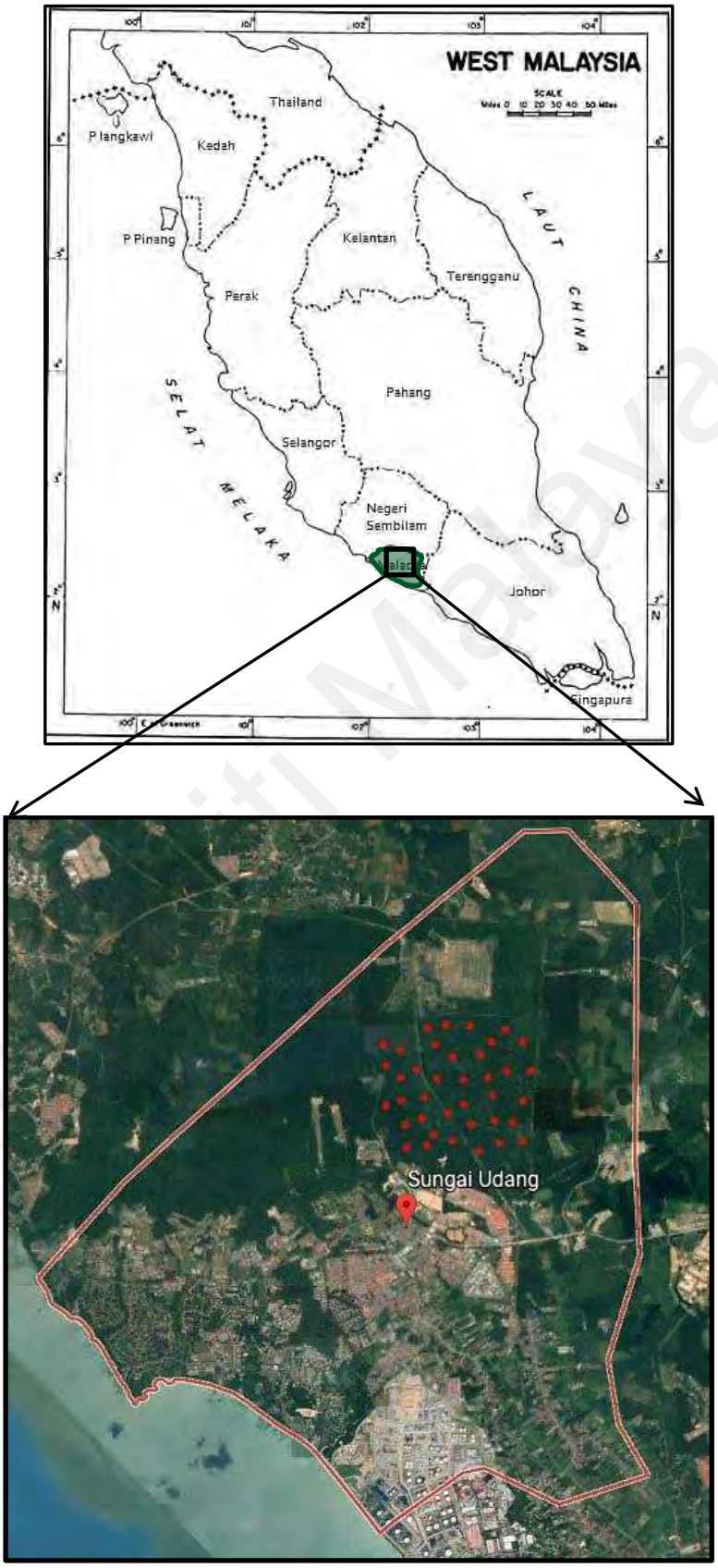

Figure 3.4: Sampling area in the state of Malacca

3.2.4 Study area in Johor State

A total of 40 soil samples were randomly collected at the depths of 0-10, 10-20, 20-30 and 30-40 cm from oil palm plantation in Segamat, Johor. Segamat is located at the south of Peninsular Malaysia between latitudes, longitude of 2.5035° N, 102.8208° E, respectively (Figure 3.5). Approximately 150 km^2 plots were chosen where the samples were collected, the distance between sampling points was 1- 3km. The GPS coordinates for collected samples and the soil texture of Johor are recorded Appendix A.

Johor is situated in the southern part of Peninsular Malaysia. Most of the land in the state is utilized for agriculture, mainly oil palm and rubber plantations. It covers a total land area of 19,210 km^2 (Department of Statistics Malaysia, 2010). The soils of Johor can be classified, according to their parent material, into three broad groups' namely sedentary, alluvial and miscellaneous soils. On the basis of similar characteristics, of which the parent material is the most important, these soils have been differentiated into soil series and associations. The distribution pattern of these soil series and associations reveals a close relation with those of different geological lithologies within the state (Department of Agriculture Peninsular Malaysia, 1973). Geological formations of Segamat district are Acid Intrusive, Permian and Cretaceous-Jurassic.

Johor is located on the central belt called the golden belt of Peninsular Malaysia, which consists of three geological belts (Suntharalingam, 1968; Khoo & Tan, 1983; Ramli & Samsudin, 2014). The soil was formed from sedimentary rocks and derived from interbedded sandstone, siltstone and shale; widespread volcanics, mainly tuffs of rhyolitic to dacitic composition in Central Peninsular, Conglomerate and chert are locally prominent in a group of soils dating back to the Triassic period. Soil within the geological classification that dates back to the Jurassic period is derived from continental deposits of thick, cross-bedded sandstone with subordinate conglomerate

and shale/mudstone. The geological classification that extends to the Tertiary period, soils belonging to sedimentary rocks that derived from isolated continental basin deposits of Late Tertiary, that include shale, sandstone, conglomerate and minor coal seams and volcanics in the Segamat area. The soil was formed in the eastern parts of the state from igneous rocks that derived from intrusive rocks, mainly granite with minor granodiorite (Department of Minerals and Geosciences Malaysia (JMG) https://www.jmg.gov.my/en/; Khoo & Tan, 1983).

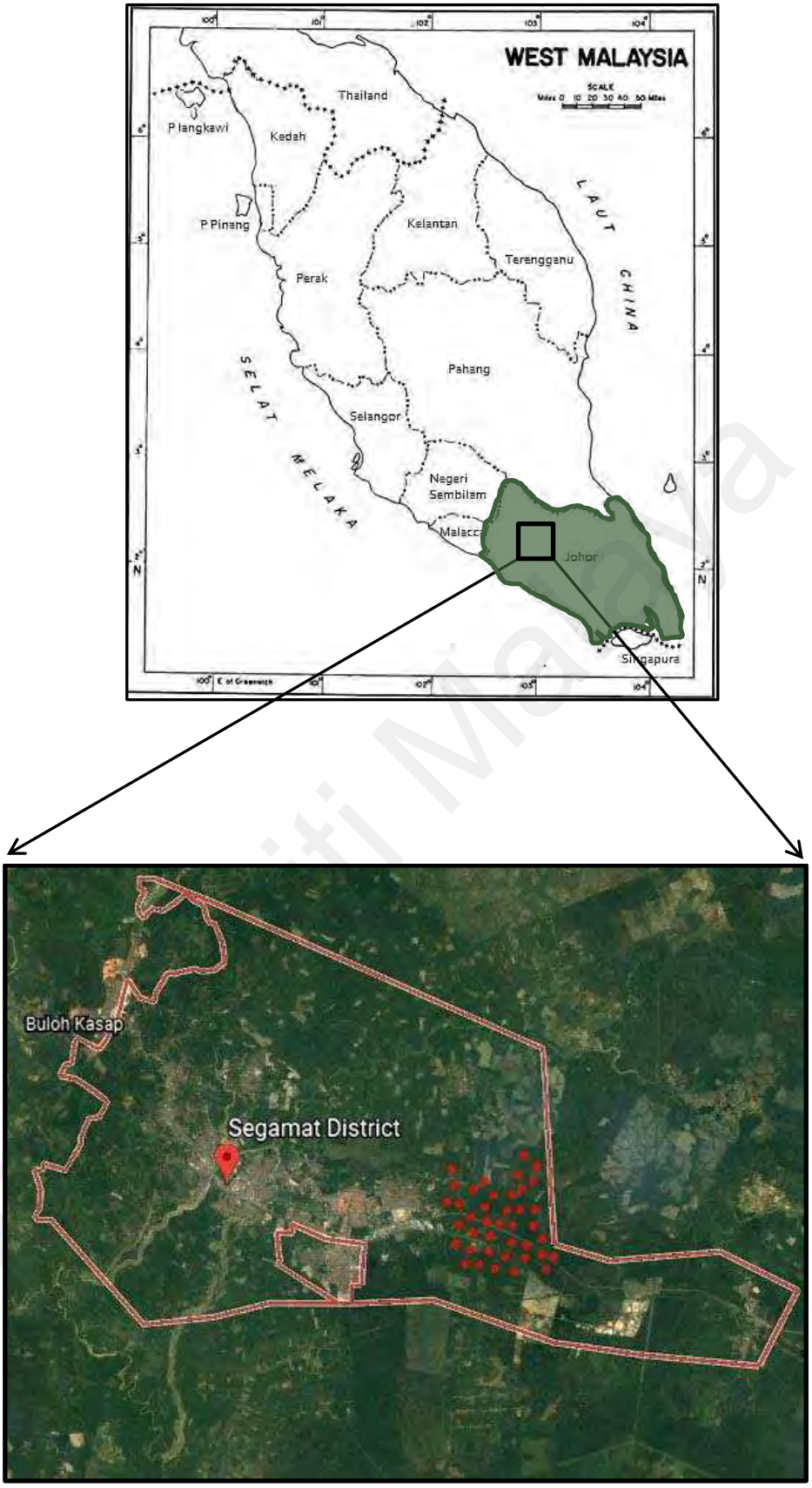

Figure 3.5: Sampling area in the state of Johor state

3.2.5 The study area of Raub in Pahang state

A total of 40 soil samples were collected randomly at the depths of 0-10, 10-20, 20-30 and 30-40 cm from durian farms in Raub, Pahang located at 3.7935° N, 101.8575° E. The area occupies the vast Pahang River basin, which is enclosed by the Titiwangsa Range to the west and the eastern highlands to the north. About 200 km^2 plots were established where the samples were collected, the distance between sampling points was 1- 5 km (Figure 3.6). The GPS coordinates for collected samples and the soil texture of Raub are recorded in Appendix A.

Pahang has a tropical geography with an equatorial climate and a year-round of humidity of no less than 75%. It is warm and humid throughout the year with temperatures ranging from 21 °C to 33 °C. The rainfall here averages at 200 mm monthly. Precipitation is the lowest in March, with an average of 22.25 mm. In October and November, the precipitation reaches its peak, with an average of 393 mm.

The geological region of Raub district dates back to the periods of Triassic, Devonian Permian. Raub district is located on sedimentary rocks of interbedded sandstone, siltstone and shale. Widespread volcanics, mainly tuffs of rhyolitic to dacitic were found in central the Peninsular. Limestone prominent in lower part of the succession, and Phyllite, schist and slate with limestone and sandstone are locally promfriefit together with some interbeds of conglomerate, chert and rare volcanics, Schist, phyllite, slate and limestone of Devonian (Department of Minerals and Geosciences Malaysia (JMG) https://www.jmg.gov.my/en/).

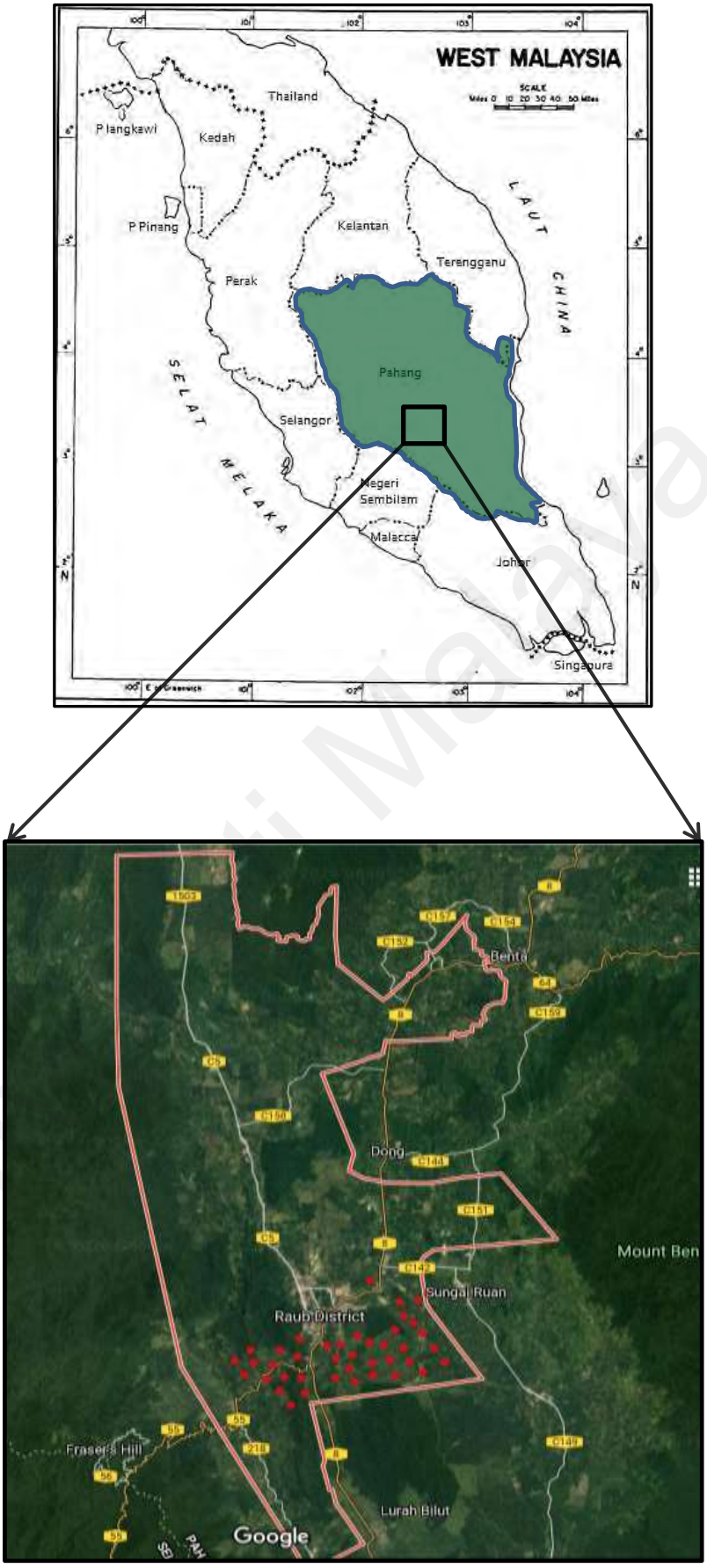

Figure 3.6: The sampling area of Raub in Pahang

3.2.6 The study area of Lanchang in Pahang state

A total of 35 soil sample were collected randomly at the depths of 0-10, 10-20, 20-30 and 30-40 cm from oil palm plantation in Lanchang, Pahang located at 3.4979° N, 102.1911° (Figure 3.7). About 200 km^2 plots were established where the samples were collected, the distance between sampling points was 1- 5km. GPS coordinates for collected samples and the soil texture of Lanchang are provided in Appendix A.

The geological region of Lanchang district dates back to the periods of Triassic and Permian. While the geology of the western strip of the province belongs to the Devonian period. Raub district is located on sedimentary rocks of interbedded sandstone, siltstone and shale where widespread volcanics, mainly tuffs of rhyolitic to dacitic composition in central Peninsular. Soil, which evolved from igneous rocks, is derived from intrusive rocks, mainly granite with minor granodiorite. In the western regions of the district the soil was formed from phyllite, slate, shale and sandstone where argillaceous rocks are commonly carbonaceous. Volcanics of acid to intermediate composition are locally present. Phyllite, schist and slate; limestone and sandstone are locally promfriefit with some interbeds of conglomerate, chert and rare volcanics (Department of Minerals and Geosciences Malaysia (JMG) https://www.jmg.gov.my/en/; Khoo & Tan 1983).

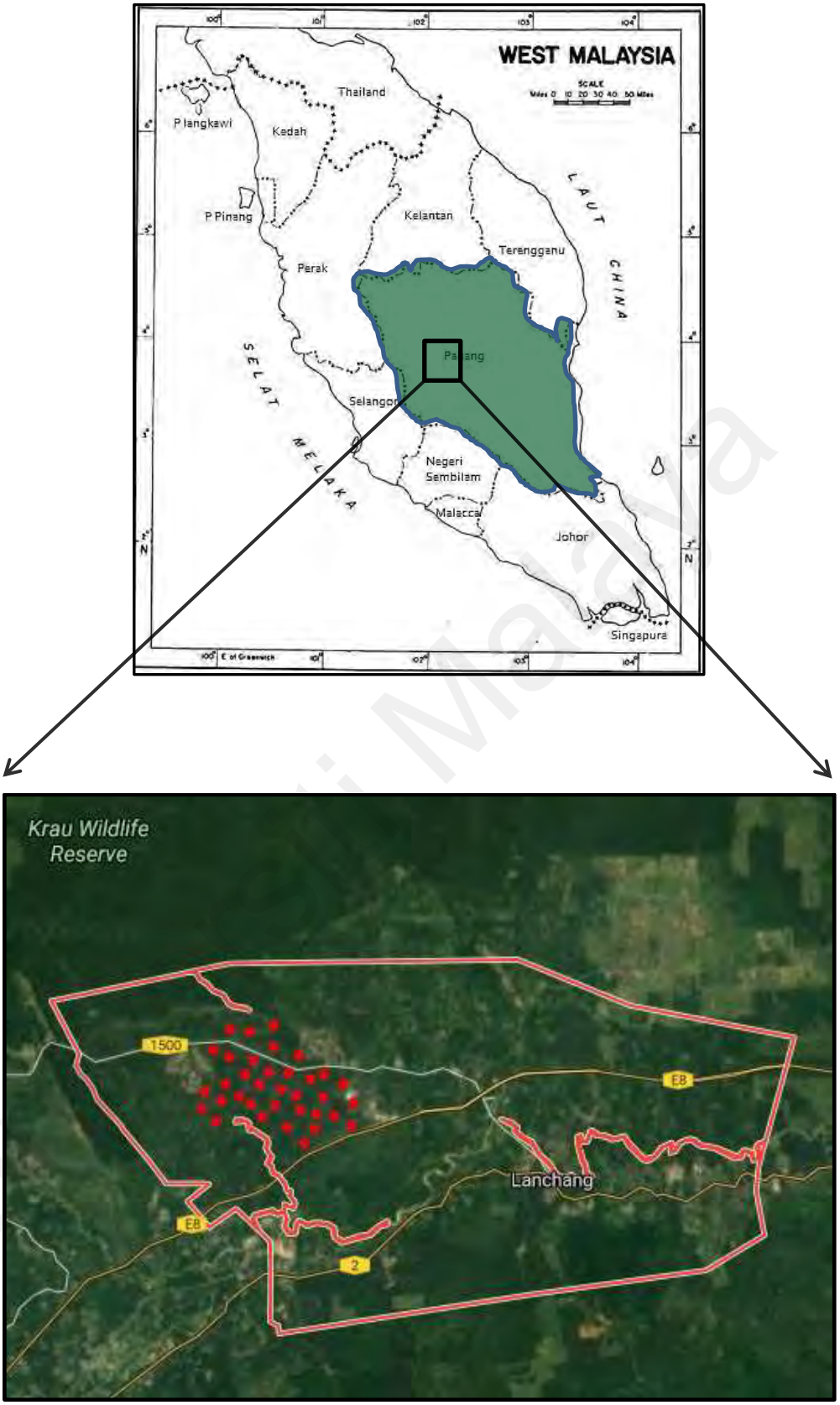

Figure 3.7: The study area of Lanchang in Pahang

3.3 Sampling strategy

1. A random sampling approach was applied to collect samples in all study areas, which is applicable when the selected area is small, homogeneous and readily available. Each sample point is selected independently from all other points, where all subsets of the frame are given an equal probability. Each element of the frame thus has an equal probability of selection. All the study areas were agricultural and homogeneous, where each region showed very similar climatic conditions and management practices. Therefore, it is assumed that the variance of the sample mean is insignificant.
2. The selected sites were without or with a little background information, where the obvious contaminated area does not exist. Another factor that gives preference to random sampling approach include those to reduce bias errors, thus, avoid collecting too large sample size, and taking cost into consideration.
3. Given the homogeneity of the selected agricultural areas, any variation caused by factors affecting radionuclide distribution will be clearly evident, so the vertical distribution was considered as a potential variation factor between the study groups. The vertical distribution can be one of the factors affecting the bioavailability of radionuclides, microorganisms, oxidation states, mineral distribution, soil pH, as well as, various organic fractions. Seasonal changes can also be a potential variation factor as they provide materials that undergo decomposition and vertical and horizontal distribution in the soil. Thus to obtain a good idea of what is happening and identify the causes of the variability.
4. Yet, the microorganisms, biomass, organic matter and related traits may change in short range scale. So, that means organic matter in the soils between plant rows should be highly different due to root development and plant debris addition into the soil. The distance between sampling point and plants has a

critical importance. Since we need more flexibility in site selection, the random approach choice was the most appropriate method in this case than the systematic grid, where we can keeping a constant distance between the sample site and the plant at all sampling points with the random approach.

5. The work did not have to pick a wide region for each category of soils where the position of the environment does not differ. It involved micro-climatic and micro-environmental factors such as variation in moisture content of the soil, grain size distribution, parent material shifts, topography and drainage, homogeneity, temperature and environmental conditions.
6. High purity germanium (HPGe) gamma ray spectrometry was employed to analyse the activities of ^{226}Ra, ^{232}Th, and ^{40}K in the samples, due to the low background, and to place and compare the findings in the context of the larger scientific community.

3.4 Sample collection

The following steps were taken to collect soil samples from six agricultural areas:

1. A total of at least 1– 2 kg of soil was collected at 0 to 40 cm depth levels at each random spot, with an extended surface of 15 cm, using soil sampling probe, shovel and scoop. A soil probe provides more information on the soil's landscaping. It aids in effectively reaching the vertical deeps of numerous layers of soil, and even if it soaks in too deep past the reach of plant roots. Since the presence of extraneous materials which are not relevant for the soil samples may introduce an error in the analytical results (IAEA, 2004), glass pieces, twigs, stones, or leaves were eliminated from the soil samples. Each sample was transferred first to a 2 mm sieve fitted in a collecting pan.

2. The post-sieved samples were then filled into labelled polyethylene bags and sealed. The information of each sample was documented separately in prepared labels and covered with a waterproof tape on each sample bag. The labels included soil information including sample ID, location, depth level, sampling date, name of sampler, and any other pertinent remarks.
3. Before leaving the sample location, the sample information, along with any remarks related to, the sample's collection, volume, depth, the soil's condition, general observations and difficulties were documented carefully in the field notebook.
4. Having into accounts that cleaning the sampling tools were done before collecting each new sample to prevent soil-to-soil contamination.
5. The random spot of the samples was identified using a GPS system.
6. Sampling, data collection and statistics were performed by the researcher independently.
7. The final sample preparation and HPGe and ICP-MS measurements, and microorganism's activities were performed in Department of Physics, Institute of Biological Sciences, and Department of chemistry, in Faculty of Science, University of Malaya, Kuala Lumpur, Malaysia.

3.5 Samples preparation for HPGe detector

Prior to final measurement in the laboratories, the samples were placed in a drying oven at 100 ^{o}C for 24 hours to ensure that any significant moisture was removed from the samples. To obtain uniform particle sizes, a 500μm mesh was then used to sieve the samples which were then weighed and transferred to 550 ml labelled Marinelli beakers. Finally, the samples were stored and kept sealed for about one month in order to reach radioactive secular equilibrium.

Sample homogenization ensures that portions of the samples which were filled in the Marinelli beakers are representatives of the entire collected sample and identical in its composition. According to (IAEA-TECDOC-1415, 2004) the homogenization is the mixing or blending of a soil sample in an attempt to provide uniform distribution of contaminants. Incomplete homogenization would increase the sampling error (IAEA-TECDOC-1415, 2004). Soil samples were grind using soil blender to obtain a homogeneous powder.

Gamma spectrometry analysis was performed using a γ- ray spectrometer with a p-type coaxial HPGe γ-ray spectrometer and a p-type Coaxial ORTEC, GEM-25 HPGe gamma ray detector with 57.5 mm-diameter and 51.5 mm-thick crystals. The detector was set under the following conditions: operating voltage, +2800 V; relative efficiency, 28.2%; energy resolution, 1.67 keV; and full-width at half maximum, 1.33 MeV. The detector was coupled with ^{60}Co emission and 16 k Multichannel Analyzers for data acquisition. Genie 2000 software from Canberra was used to analyze the spectra. The detector was covered by a cylindrical lead shield with a fixed bottom and a movable cover to reduce the interference of background radiation from terrestrial and extra-terrestrial sources in the measured spectrum.

An empty Marinelli beaker was counted in the same way to remove the background radiation from the samples. After the measurement, the background radiation was subtracted to determine naturally occurring background distribution in the environment around the detector.

Energy calibration and relative efficiency calibration of the spectrometer were performed using Marinelli calibration sources containing the following: ^{210}Pb (46.54 keV), ^{241}Am (59.541 keV), ^{109}Cd (88.040 keV), ^{57}Co (122.061 and 136.474 keV), ^{123m}Te (159.00 keV), ^{203}Hg (279.195 keV), ^{113}Sn (391.698 keV), ^{85}Sr (514.007 keV),

^{137}Cs (661.657 keV), ^{88}Y (898.042 and 1836.063 keV), and ^{60}Co (1173.22 and 1332.492 keV). The calibration sources were obtained from Isotope Products Laboratories, Valencia, CA 91355, USA.

The efficiency values were determined by the aid of the amplitude spectra acquired using the Gamma vision software, for every radioactive source, namely, from the net area in the region of interest of the energy peak of interest, divided by the activity of the sources, acquisition time and branching ratio of the energy line. The standard radioactive sources were positioned at 11 cm distance from the end cap of the detector, using a special distance piece. The efficiency fitting curve is described by a 6-term polynomial function to fit the natural logarithm of efficiency to the energy:

The measured detection efficiencies were fitted by using a polynomial function as follows:

$$\ln \varepsilon = \sum_{k=0}^{5} a_k \ln(E^k) \tag{3.1}$$

where ε is efficiency at energy E [MeV], a_k fitting coefficients.

The minimum detectable activity (MDA) of the γ-ray measurement system at 95% confidence level was calculated according to the procedure used by Khandaker *et al.,* (2012a). Each sample was counted for 86,000 s (approaching 24h) and background counts for the same counting time were deducted to obtain the net activity.

Each sample and background data were counted for 86400 s. Gamma spectroscopy was used to determine the activities of ^{238}U, ^{232}Th, ^{40}K and ^{137}Cs.

The specific activity of ^{226}Ra was assessed from gamma-ray lines of ^{214}Pb at 351 keV and ^{214}Bi at 609.3 and 1764.5 keV, while, the specific activity of ^{232}Th had been

evaluated from gamma -ray lines of ^{228}Ac at 338.4, 911.1, 968.9 keV, ^{212}Pb at 238.63 keV, and ^{208}Tl at 583.19 keV. The specific activity of ^{40}K was directly determined from its gamma -ray line at 1460.8 keV (Table 3.1).

Table 3.1: Gamma-ray energy and emission rate for ^{238} U, ^{232}Th and ^{40}K radionuclides

Element	Nuclide	Half life	Gamma-ray energy E_g (keV)	Emission rate	Sources/origin
^{238}U	^{214}Pb	26.8 min	351	35.8	^{238}U (^{226}Ra) series
	^{214}Bi	19.9 min	609.3	45.4	^{238}U (^{226}Ra) series
			1764.5	15.3	
^{232}Th	^{228} Ac	6.15 h	338.4	11.4	^{232}Th series
			911.1	25.8	
			968.9	17.4	
	^{212}Pb		238.63	46.6	
	^{208}Tl		583.19	85.0 %	
^{40}K	^{40}K	1.28 x 10^{9}yr	1460.8	10.7	Primordial

3.5.1 Calculate the activity concentrations of radionuclides

Since the counting rate is proportional to the amount of the radioactivity in a sample, the activity concentration (*Ac*) can be derived using Equation 3.2, which can be rewritten for a specific full energy peak as the follows:

$$\varepsilon(E_\gamma) = \frac{C_{net}}{A \times \gamma} \tag{3.2}$$

where C_{net} are the net peak counts, γ is absolute gamma decay intensity for the specific energy peak (including the decay branching ratio information) and $\varepsilon(E\gamma)$ is the absolute full energy peak efficiency of the germanium detector at this particular gamma-ray energy. Then, the activity per mass unit (i.e., the activity concentration) can be defined as follows:

$$AC = \frac{C_{net}}{\gamma \times \varepsilon(E_\gamma) \times m} \tag{3.3}$$

where *m* is the mass of the sample in kg.

Recalling equation 3.3, then, using the activity concentration as calculated above, the number of radioactive atoms of a given radionuclide, *N* can be determined using the expression:

$$N = \frac{A \times T_{1/2}}{ln2} \tag{3.4}$$

where *A* is the activity and $T_{1/2}$ is the half-life of the specific radionuclide. The activity concentration is usually given in Bq/kg. Since the number of atoms in one gram atomic weight of the sample equals Avogadro's number the mass *(m)* in μg of the number of atoms ≡ part per million (ppm), can be used to determine the number of atoms in the sample using the following equation:

$$m = radionuclidemass\ number \times \left[\frac{N}{Avogadro\ s\ number}\right] \tag{3.5}$$

From this expression, it can be shown, for example, that a concentration of 1 ppm of Th and U in a samples corresponds to 4.04 and 12.36 $Bq.kg^{-1}$, respectively, whereas 1% of K_2O corresponds to 252 $Bq.kg^{-1}$ of ^{40}K (Mohanty *et al.*, 2004).

3.6 Uncertainty of measurements

Since the analyte in gamma-ray spectrometry systems are radionuclides, uncertainties in the evaluated nuclear data, such as the adopted decay half-life and absolute gamma-ray emission probabilities, contribute to the overall combined uncertainty of the activity concentrations. In most cases the uncertainty in the half life is generally rather small compared to the other (statistical) sources of uncertainty. The data on decay half- lives and gamma ray transition branching ratios were taken for this

study from evaluated nuclear data information using Evaluated Nuclear Structure Data File (ENSDF) Analysis Programs provided by the National Nuclear Data Center (NNDC) and the related journal, Nuclear Data Sheets.

The most significant sources of uncertainty that should be taken into consideration in measurements of the determination of the activity concentrations of ^{235,238}U and ^{232}Th (and their decay progeny), ^{40}K and ^{137}Cs in soil samples using a high-resolution gamma-ray spectrometry system are summarized in (Table 3.2).

Table 3.2: The significant sources of uncertainty for measurements of activity concentrations of ^{235,238}U and ^{232}Th and their decay progeny, ^{40}K, and ^{137}Cs in soil samples using a high resolution gamma spectrometry system

Sourse of uncertainty	Typical uncertainty rang %	Typical uncertainty value %
Counting (statistaical)	0.1-20	5
Emission probability uncertainry	0.1-11	< 2
Attenuation correction	0.1-5	< 1
Coincidence correction	1-15	< 3
Half-life uncertainry	0.01-1	< 0.2
Detector efficiency	1-5	< 2
Sample weight	0.01-1	< 0.5

Sourse: Dovlete & Povinec, (2004)

Identifying the uncertainty sources in gamma-ray spectroscopy techniques involving soil samples is an essential step for determining high-quality results. The sources of the standard uncertainties can be classified according to their origin into four categories. These standard uncertainties are shown schematically in Appendex D.

3.6.1 Calculation of uncertainties

The estimated contribution from each component described in the previous section to the final uncertainty is a vital step in quantifying the uncertainty. Considering each of

the main correction factors that are usually applied in measurement of activity concentrations of gamma-emitting radionuclides in soil samples using HPGe spectrometry, the activity concentration, A , for radionuclides in a measured sample is calculated using the Equation (3.3) that can be re-written as (Dovlete & Povinec, 2004).

$$A_c = \frac{N}{\varepsilon \gamma t_s m K_1 K_2 K_3 K_4 K_5} \tag{3.6}$$

Where ε is the efficiency at full energy peak energy, t_s is the live time of the sample spectrum collection in seconds, m is the mass (kg) of the measured sample, γ is the emission probability of the specific gamma-ray line corresponding to the peak energy and N is the net peak area of the corresponding full energy peak, given by:

$$N = N_s \frac{t_s}{t_b} N_b \tag{3.7}$$

N_s is the net peak area in the soil sample spectrum, N_b is the corresponding net peak area in the background spectrum and t_b is the live time of the background spectrum collection in seconds. In the measurement of very low activity samples, the sample and background count time should be kept the same (Hurtgen, Jerome & Woods, 2000). K_1 is the correction factor for the nuclide decay from the time the sample was collected to the start of the measurement. This can be evaluated using the expression:

$$K_1 = exp\left(-\frac{ln2.\Delta t}{T_{1/2}}\right) \tag{3.8}$$

where Δt is the elapsed time from the time the sample was taken, to the beginning of the measurement, and $T_{1/2}$ is the radionuclide half -life.

K_2 is the correction factor for the nuclide decay during counting period where:

$$K_2 = \frac{T_{1/2}}{ln2.\, t_r}\left[1 - exp\left(-\frac{ln2.\, t_r}{T_{1/2}}\right)\right] \tag{3.9}$$

where t_r is the elapsed real time during the measurement. Figure 3.8 shows the change in activity during the counting period itself.

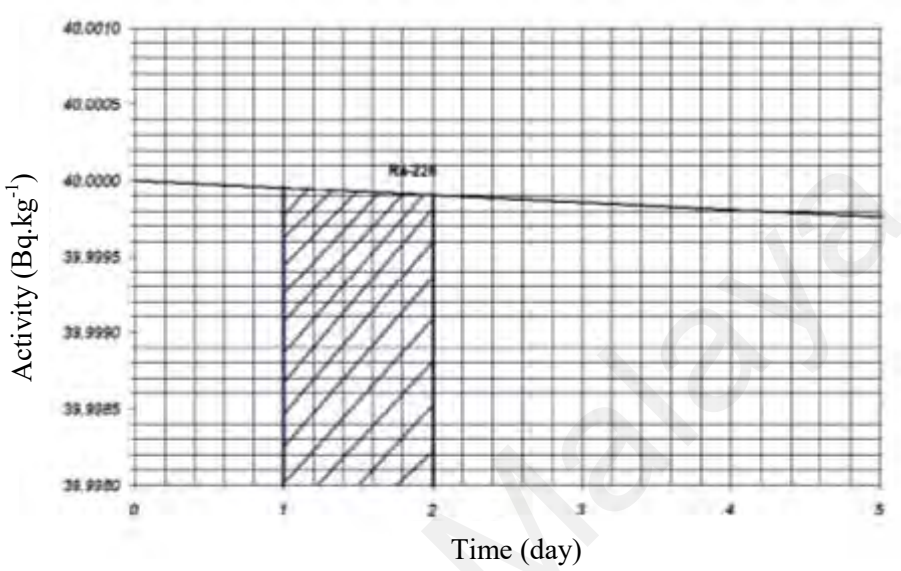

Figure 3.8: Schematic showing the (negligible) reduction in ^{226}Ra activity over a few days, counting time (t_r).

K_3 is the correction factor for a self-attenuation in the measured sample compared with the calibration sample. This is defined as the ratio of the full energy peak efficiency, $\varepsilon(\mu,E)$, for a sample with a linear attenuation coefficient μ and the full energy peak efficiency $\varepsilon\ (\mu_{ref},E)$ for a calibration sample with linear attenuation μ_{ref}. This ratio is represented as follows:

$$K_3 = \frac{\varepsilon(\mu, E)}{\varepsilon(\mu_{ref}, E)} \tag{3.10}$$

K_4 is the correction factor for pulses lost due to random summing (Dovlete & Povinec, 2004). As discussed above, this loss is count rate dependent. This factor is given as:

$$K_4 = \exp(-2R\tau) \tag{3.11}$$

where τ is the resolution time of the measurement system which is approximated to be 20 μs, and *R* is the mean count rate.

K_5 is the coincidence correction factor for those nuclides decaying through a cascade of successive photon emissions, and defined as the ratio of the corresponding apparent efficiency ε_{ap} (E) to the full energy peak efficiency, ε (E) , i.e.,

$$K_5 = \frac{\varepsilon_{ap}(E)}{\varepsilon(E)} \tag{3.12}$$

Table 3.3 represents some values of the correction factors of ^{226}Ra in one of the soil samples.

Table 3.3: Estimated values of the correction factors for ^{226}Ra in a typical soil samples used in the current work

Correction Factor	Value of Correction Factorfor ^{226}Ra
K1 Decay Correction Factor (from collection time to the start of the measurement)	0.99
K2 Decay Correction Factor (during the measurement itself)	0.99
K3 Self-attenuation Correction Factor	1
K4 Random Summing Correction Factor	0.99
K5 Coincidence correction factor	1

From the previous discussion, it can be concluded that not all of the above mentioned uncertainty components will contribute significantly to the combined uncertainty of the final result of the activity concentration. This means that it is possible to eliminate those factors which are not significant from Equation 3.6, which then reduces to:

$$A_c = \frac{N}{\varepsilon \gamma t_s m} \tag{3.13}$$

Each of the quantities in Equation 3.6 has an associated uncertainty. The combined standard uncertainty of the final result can be derived by applying Gauss "error propagation law" (Dovlete & Povinec, 2004). The combined standard uncertainty of *y,* u_c *(y),* is calculated in terms of the component uncertainties, *u(xi),* as follows:

$$u_c\big(y(x_1,..x_n)\big) = \sqrt{\sum_{i=1}^{n}\left(\frac{\partial y}{\partial x_i}\right)^2}\,(u(x_i))^2 \tag{3.14}$$

where $y(x_1, x_2, ..x_n)$ is a function of several quantities x_1 , x_2 ,..x_n. If equation 3.19 is applied to Equation 3.13, the combined standard uncertainty of A, u_c, is calculated in terms of component uncertainties, m, N, γ,ε, t, and K (if required) as follows:

$$\frac{u_c\,(A)}{A} = \sqrt{\left(\frac{um}{m}\right)^2 + \left(\frac{uN}{N}\right)^2 + \left(\frac{u\gamma}{\gamma}\right)^2 + \left(\frac{u\varepsilon}{\varepsilon}\right)^2 + \left(\frac{uK}{K}\right)^2} \tag{3.15}$$

where

$$\frac{u_c\,(K)}{K} = \sqrt{\left(\frac{uK_1}{K_1}\right)^2 + \left(\frac{uK_2}{K_2}\right)^2 + \left(\frac{uK_3}{K_3}\right)^2 + \left(\frac{uK_4}{K_4}\right)^2 + \left(\frac{uK_5}{K_5}\right)^2} \tag{3.16}$$

The unknown value of the activity concentration is believed to lie in the interval $A \pm \Delta A$ where ΔA is the relative expanded uncertainty, $\times \frac{u_c\,(A)}{A}$, with a confidence level of approximately 1σ.

3.7 Mutual peak interference and activity ratio

3.7.1 ^{226}Ra (186.21 keV) and ^{235}U (185.72 keV) Peak Corrections

The activity ratio for a homogenous sample containing natural uranium can be obtained after first determining the counts contribution due to Uranium (^{235}U) (185.72 keV) at the 186.21 keV line for Radium (^{226}Ra). The γ- ray signature of ^{226}Ra decay overlaps with a peak doublet from the decay of ^{235}U at 185.72 keV. This isotope decays to the 2^+ excited state of Radon (^{222}Rn), releasing a gamma-energy of 186.2 keV in the process.

Its analysis, however, is error prone and has to be corrected to remove the contribution of 185.7 keV due to ^{235}U. To obtain unambigous results for the ^{226}Ra, the peak is broken into its components or "deconvoluted" at 185.75 and 186.2 keV for the seperate determination of ^{235}U and ^{226}Ra, respectively (Garcıa-Talavera et al., 2003; Ebaid, 2010; Karangelos et al., 2004; De Corte, 2005).

The excess count at the 186.2 keV peak can be used to determine the activity ratio of ^{235}U and consequently the ^{235}U: ^{238}U, assuming ^{226}Ra is in equilibrium with its parents ^{238}U, the natural isotopic abundance and corresponding half-lives for ^{235}U and ^{238}U Oliver et al., (2007).

are given as:

$^{235}U = 0.72\ \% = N_{235U}\ ;\ 7.038 \times 10^{8}$ *years* and $^{238}U = 99.27\ \% = N_{238U}\ ;\ 4.4683 \times 10^{9}$ *years.*

3.7.2 Interference Peak ratio: ^{226}Ra (186.21 keV) and ^{235}U (185.72 keV)

Recall from the mutual peak interference and activity ratio, A_{235U} and A_{238U} are given by 5.59×10^{5} Bq and 1.23×10^{7} Bq, respectively. Taking into account emission probabilities of 0.0359 for ^{226}Ra and 0.572 for ^{235}U with these activities, the fractional gamma-ray emission for ^{235}U and ^{226}Ra per 100 g of natural uranium at the 186.2 keV peak can be derived as follows:

$N_{\lambda}\ ^{235}U = A_{235U}\ P\gamma \times\ ^{235}U = 5.59 \times 10^{5} \times 0.527 = 2.94 \times 10^{5}$ gamma rays per second.

Similarly,

$N_{\lambda}\ ^{226}Ra = A_{226Ra}\ P\gamma \times\ ^{226}Ra = 1.23 \times 10^{7} \times 0.0359 = 4.41 \times 10^{5}$ gamma-rays per second.

Finally, the individual contributions of ^{235}U and ^{226}Ra to the 186 keV peak can then be calculated as follows:

$$^{235}\text{U} = \frac{(235_U)}{N\,\lambda\,(235_U) + N\lambda\,(226_{Ra})} \tag{3.17}$$

$$^{235}\text{U} = \frac{2.94\times10^5}{(2.94\times10^5) + (4.41\times10^5)} = 0.400 \tag{3.18}$$

and ^{226}Ra

$$^{226}\text{Ra} = \frac{(226_{Ra})}{N\,\lambda\,(226_{Ra}) + N\lambda\,(226_{Ra})} \tag{3.19}$$

$$^{226}\text{Ra} = \frac{4.41\times10^5}{(4.41\times10^5) + (2.94\times10^5)} = 0.60$$

Consequently, the relative contribution of ^{235}U and ^{226}Ra to the 186 keV peak can be expressed as 40% and 60% respectively, assuming the sample is in secular equilibrium.

3.7.3 ^{228}Ac (1459.2 keV) and ^{40}K (1460.8 keV)

The gamma decay of ^{228}Ac with the emission of 1459.2 keV interferes with another γ –ray emission from the decay of Potassium (^{40}K) at 1460.8 energy line (Abusaleem, 2014). Consequently, the contributions to the gross peak at the 1460-keV in a gamma-ray spectrum may be overestimated and therefore need to be corrected. The contribution of the composite peak due to ^{228}Ac at the ^{40}K peak thus needs to be resolved. Since the decay of Actinium (^{228}Ac) also emits other gamma-rays at several other discrete energies and using peak data from the prepared standard ^{232}Th reference source, the ratio between the two discrete gamma-ray emission lines can be determined, since the ratio should also be the same in the samples. The gamma energy yield for the ^{228}Ac at 911 keV is 27.7% and can be compared with the 1459.2 keV to obtain this ratio. The true counts can thus be obtained as follows:

$$\left[\frac{Counts_{1459keV}}{Counts_{911keV}}\right]^{Th} = \left[\frac{Counts_{1459keV}}{Counts_{911keV}}\right]^{Sample} \tag{3.20}$$

such that:

$$Counts_{1459keV} = \left[\frac{Counts_{1459keV}}{Counts_{911keV}}\right]^{Th} = Counts\ _{911keV} = x \tag{3.21}$$

The counts *x* obtained at the 1459 keV shown above can now be substracted from the one recorded at 1460.2 keV to obtain the true count for ^{40}K.

3.8 Samples preparation for ICP-MS and AAS measurements

The metal concentrations were measured using Inductively Coupled Plasma-Mass Spectrometry (ICP-MS) (Agilent Technologies 7500 Series, USA). It is important to thoroughly digest the sample for elemental analysis with ICP-MS. In the microwave digestion system, roughly 0.5 g of soil sample was digested (Multiwave 3000, PerkinElmer, USA). To digest solid samples and primarily move metals into a soluble form for analysis on the inductively coupled plasma mass spectrometry, the samples were dried in an oven at 70–80°C for 24 h, precisely 0.5 g of the dried soil sample was transferred to vessels for acid extraction. The samples was digested within 3 ml of hydrofluoric acid HF and a 9 ml of solution of concentrated nitric acid (HNO_3) mixed, covered with a watch glass, for 15 min using microwave heating 95°C without boiling, the sample is then cooled, 18 ml of boric acid 99.99 % was added to the cooled solution followed by centrifugation. The solution from the centrifugal operation was filtered using filter-paper (Whatman No. 0.45μm), and the volume was topped to 50 ml with deionised water for the measurement of heavy metal concentrations. The preparation procedure described above for metal analyses was based on EPA method 3052 (EPA, 1996; Ilander & Väisänen, 2007; Zhang & Liu, 2002). In all cases, one blank solution and five standards were run under the same conditions with the same reagents used to monitor potential pollution from digestion procedures. Calibration of the ICP-MS was performed using multi-element-element calibration standard 2A solution (10 mg/l of

each element) prepared by adequate mixing and dilution in 5% HNO of five standard solutions (Agilent Technologies, USA, part no. 8500–6940). Concentrations for Na, Mg, Al, K, Ca, Cr, Mn, Fe, Co, Cu, Zn, Cd, As, Se, Rb, Sr, Ba, Hg, Cd, Ni and Pb heavy metals were then determined by using ICP-MS. All the analyses were carried out in several times. The recovered values of all the metals ranged from 88% to 96% of the certified value.

Iron oxides were extracted Fe oxides from soil using an ammonium oxalate solution while, Hydroxylamine chlorhydrate ($HONH_2 \cdot HCl$, 1M, pH=3, 5) used for Mn phases (Schwertmann, 1964). For extracting both the amorphous and well crystallized of Fe and Mn oxides, 2 g homogenized soil, and then sieved (< 2 mm) and air-dried samples were digested with 0.3 M Na-citrate ($Na_3C_6H_5O_7$) solution, 1 M $NaHCO_3$ solution and Na-dithionite ($Na_2S_2O_4$) in a water bath 75 – 80 °C according to the method described by Mehra & Jackson, (1960). The extraction steps were carried out twice. Finally, the soil was washed with 10 ml 0.1 N $MgSO_4$, the supernatant was added to the extract and mixed well. To selectively extract amorphous and poorly crystallized iron oxides 2 g homogenized, sieved (< 2 mm) and air-dried samples were added to a mixture of 0.2 M NH_4-oxalate and 0.2 M oxalic acid at pH 3.25. The suspensions were shaken for one hour in the dark. For both extractions Fe and Mn was determined by atomic absorption spectrometry AAS.

3.9 Soil pH and Organic Matter (OM)

The soil pH (1: 2.5, soil: water suspension) was determined by following the standard procedures of soil pH determination using portable pH meter (Martin, 2008). Where, the soil samples were sieved through a sieve (2 mm mesh) to remove the coarser soil fraction. Approximately 10g were weighed out of the air-dried and sieved soil sample. The soil samples were placed into glass containers and approximately 10 mL of distilled

or deionized water for each sample was added using an automatic pipette or suitable volumetric container. The samples were thoroughly mixed and left standing for an hour. The probes were rinsed with distilled water and the meter was calibrated using pH 4.00 and pH 7.00 buffers before pH measurements.

For soil organic matter determination the *loss of weight on ignition* (Storer, 1984) has been used to calculate the OM by the following equation:

$$LOI\ (\%) = \frac{Weight\ at\ 105^0C - Weight\ at\ 360^0C}{Weight\ at\ 105^0C} \times 100 \qquad (3.22)$$

3.10 Microbiology

To desorb microorganisms from soil particles, a sodium pyrophosphate treatment was utilised. Soil subsamples (15 g) were weighed into sterile Erlenmeyer flasks of 250 mL. At pH 7, 0.1 % tetrasodium pyrophosphate was introduced in a 100 ml aliquot. After shaking for 1 hour at 30°C and allowing the sample to settle, a sub-sample of the solution was collected for further dilution. For all samples, serial dilutions were made using sterile diluent (0:4 g /l $MgSO_4.7H_2O$ + 0.04 g / l K_2HPO_4).

Serial dilutions up to 10^{-8} and aliquots of 10 µl of suitable dilutions were put onto nutritional agar (NA) and malt extract agar (MEA) plates (in triplicate) for dry season (June-August) samples, MEA selects for yeasts and fungi, whereas NA selects for bacteria. For wet season season (March-April) samples, 1.8 ml of diluent was pipetted into individual wells of a microtitre plate, followed by 200 l from each soil solution flask for 1:10 dilution. In a similar manner, serial dilutions up to 10^{-8} were done before being applied to NA and MEA plates. For wet season season (March-April) samples, 1.8 ml of diluent was pipetted into individual wells of a microtitre plate, and then 200 l from each soil solution flask was added to each well for 1:10 dilution. Serial dilutions up to 10^{-8} were performed in a similar manner then applied onto NA and MEA plates.

Individual plate colonies were counted at regular intervals while both sets of plates were cultured at 30°C.

3.11 Radiation risk assessment

3.11.1 Absorbed Dose Rate

The outdoor air-absorbed dose rates due to terrestrial gamma rays at 1m above the ground level can be calculated from ^{226}Ra, ^{232}Th and ^{40}K concentration values in soil assuming that the other radionuclides, such as ^{137}Cs, ^{90}Sr and the ^{235}U decay series can be ignored as their contributions are expected to be negligible to the total dose from environmental background (Kocher & Sjoreen, 1985; Singh, Rani & Mahajan, 2005). The gamma dose rate (D) in the outdoor air at 1 m above the ground level can be calculated by Equation 3.6 (Faheem & Mujahid, 2008):

$$D = \sum_{x} A_x \times C_x \tag{3.23}$$

where Ax (Bq/kg) is the mean activity of ^{226}Ra, ^{232}Th or ^{40}K. C_x (in units of nGyh^{-1}/ Bq.kg^{-1}) are the corresponding dose conversion coefficients which transform the specific activities into absorbed dose. In the current work, the considered dose rate conversion factors for ^{238}U, ^{232}Th and ^{40}K used in all subsequent dose rate calculations in soil are those determined by Saito *et al.,* (1990). These conversion factors have been used previously for related calculations in the report of (UNSCEAR, 1993, 2000). The dose conversion factors used in the calculation for ^{226}Ra, ^{232}Th and ^{40}K were 0.461, 0.623 and 0.0414, respectively (Singh, Rani & Mahajan, 2005). These factors were originally derived from Monte Carlo calculation using mathematical phantoms (UNSCEAR, 1993).

3.11.2 Radium Equivalent Activity

Radium equivalent activity (Ra_{eq}) is used to assess the hazards associated with materials that contain ^{226}Ra, ^{232}Th and ^{40}K in Bq.kg^{-1}, which is, determined by assuming that 370 Bq/kg of ^{226}Ra or 260 Bq.kg^{-1} of ^{232}Th or 4810 Bq.kg^{-1} of ^{40}K produces the same γ dose rate (UNSCEAR, 1982; Beretka & Matthew, 1985; Kumar et al., 2003). The Ra_{eq} of a sample in (Bq.kg $^{-1}$) can be achieved using the following relation (UNSCEAR, 1982):

$$Ra_{eq} = A_K \times 0.077 + A_U + A_{Th} \times 1.43 \tag{3.24}$$

The published maximal admissible (permissible) Ra_{eq} is 370 Bq.kg^{-1}.

3.11.3 The external hazard index

The external hazard index Hex is used to evaluate the danger of natural gamma radiation and its purpose is to restrict the radiation dose to permissible dose equivalent limit of 1mSv.year $^{-1}$ (Ibrahim, 1999; CRP, 1990). Determining this index is based on a model proposed in previous studies and is defined by the equation below (Brekta, 1985; Kumar, 2003; Amrani, 2001).

$$H_{ex} = \frac{A_{Ra}}{370} + \frac{A_{Th}}{259} + \frac{A_K}{4810} < 1 \tag{3.25}$$

where A_{Ra}, ATh, and A_{K} are the specific activities (Bq kg^{-1}) of ^{226}Ra, ^{232}Th and ^{40}K, respectively. The value of this index must be less than unity in order to keep the radiation hazard insignificant. The criterion considered by the model is that the maximum value of the external hazard due to gamma rays corresponds to a maximum radium-equivalent activity of 370 Bq.kg^{-1} for the material (UNSCEAR, 1982; Amrani, 2001).

This model did not take into consideration the wall thickness, and the existence of doors

and windows. Hewamanna, (2001) modified the standard room model in order to take into account the effect of these parameters. The external hazard index equation becomes in this case:

$$H_{ex} = \frac{A_{Ra}}{740} + \frac{A_{Th}}{520} + \frac{A_K}{9620} \leq 1 \tag{3.26}$$

The external hazard index should be below the unity (Al-Hamarneh & Awadallah, 2009).

3.11.4 Annual effective dose equivalent (AEDE)

Annual effective dose should be calculated to assess the health effects of the absorbed dose by using a conversion coefficient (0.7 Sv Gy^{-1}) to transform absorbed dose in air to the effective dose received by humans, with an outdoor occupancy factor (0.2), which is equivalent to an outdoor occupancy of 20% and 80% for the indoors. This factor is suitable for determining the pattern of life in the studied area. Annual effective dose rate (AEDR, in $mSvy^{-1}$) received by the population can be calculated using (UNSCEAR, 1994; Cevik, et al., 2007; Dovlete, 2004):

$$AEDE = D(\frac{10^9 Gy}{h}) \times 24\frac{h}{day} \times 365\frac{day}{y} \times \frac{10^{-6}Gy}{10^9 Gy} \times 0.7\frac{Sv}{Gy} \times 0.2 \tag{3.27}$$

$$AEDE = D \times 1.23 \times 10^{-3} mSvy^{-1}$$

where D (nG/h) is the total air absorbed dose rate in the outdoors; 8760 h is the number of hours in one year; 0.2 is the outdoor occupancy factor; 0.7 Sv Gy^{-1} is the conversion coefficient from absorbed dose in air to effective dose received by adults; 10^{-6} is the conversion factor between nano- and millimeasurements. The world average annual effective dose equivalent (AEDE) from outdoor terrestrial gamma radiation is 460 μSv. $Year^{-1}$ (UNSCEAR, 2000).

3.12 Data analyses

The ANOVA test was used to investigate the fixed effects of soil depth and slope position on soil characteristics, radionuclides, and major and trace elements. To analyse differences between means, the Fisher's LSD test was performed. The correlation matrix was computed for the response variables under consideration. Statistical analysis of the data was performed using the SPSS software package. Pearson correlation significance was computed among various physicochemical parameters of the soil samples at $P < 0.05$ and $P < 0.01$ using a one-way analysis of variance (ANOVA).

CHAPTER 4: RESULTS AND DISCUSSION

4.1 The activity concentrations of radionuclides

4.1.1 The activity concentrations of radionuclides in Kedah

Table 4.1 shows the measured values of radionuclide concentrations in samples obtained from Kedah. The mean concentrations of ^{226}Ra, ^{232}Th, and ^{40}K were measured to be 62.98.1, 74.910.1, and 648.384.5 Bq kg–1, respectively, whereas the range 46.0 – 77.0, 58.0 – 112.0, and 515.0 – 805.0 Bq kg^{-1}, respectively. According to the data released by UNSCEAR, (2000), the worldwide averages of ^{226}Ra, ^{232}Th, and ^{40}K are 35, 30, and 400 Bq kg^{-1}, respectively. The mean concentrations of ^{226}Ra, ^{232}Th, and ^{40}K were higher than the global averages, by 44%, 49%, and 38%, respectively.

In Kedah, the mean activity concentrations of radionuclides are in the order of ^{226}Ra (62.96 Bq kg^{-1}) < ^{232}Th (74.98 Bq kg^{-1}) < ^{40}K (648.33 Bq kg^{-1}).

The gamma spectroscopic analysis revealed that the specific activity due to ^{40}K is the largest contributor to the total activity having a mean activity value of 648.33 Bq kg^{-1}.

In addition, the activity concentration of ^{232}Th is higher than that of ^{226}Ra due to the low geochemical mobility and insoluble nature in water. In other words, ^{226}Ra is relatively more susceptible to be soluble, whereas ^{232}Th is easily adsorbed by soil. The high concentrations of ^{232}Th can also be explained by the high levels of thorium present in certain geological materials such as monazite, which is a raw material for fertilizers production. Intensive use of chemical fertilizer is a common practice for reclaimed agricultural land, where phosphate fertilizers are extensively applied to compensate phosphorus deficiency of acidic soil.

Radium (^{226}Ra) is the main contributor to contamination in phosphate fertilisers and, thus, in fertilised agricultural areas, taking into account that 70 pCi/g radium (0.07 mg Ra) would be found in one ton of phosphate with 0.02 percent uranium (Hodge, 1994). This could explain why it exceeded the recommended levels in the study area. Moreover, Potassium usually binds more tightly to loam and clay soil, and its concentration ratios are higher above 50 (Peterson *et al.,* 2007). This may explains its high concentrations since the study area is dominated by clay and loam soils.

The radioactivity concentrations in current study were found to be higher than similar studies in Pakistan, India, Egypt, Algeria, Greece and Thailand, and those were reported by (UNSCEAR, 2000) (Table 4.2). High radioactivity concentrations of ^{226}Ra, ^{232}Th, and ^{40}K in agriculture soil were also reported in local studies conducted by Ahmad *et al.,* (2015a), Ahmad *et al*., (2015b), Saleh *et al.,* (2013), Almayahi *et al*., (2012), Alzubaidi *et al.,* (2016), as shown in (Table 4.3).

Table 4.1: The activity concentrations of radionuclides (Mean±SD) Bq.kg^{-1} of ^{226}Ra, ^{232}Th and ^{40}K in the soil samples from Kedah

Sample ID	Depth cm	Activity concentrations (Bq.kg^{-1})		
		^{226}Ra	^{232}Th	^{40}K
AS1	10-20	70.5±4.7	74.2±8.5	656.2±7.3
AS2	20-30	58.2±6.6	62.7±3.5	633.2±8.6
AS3	0-10	76.4±4.6	112.3±2.4	740.4±12.5
AS4	10-20	70.5±1.9	82.2±1.8	641.2±6.6
AS5	30-40	56.7±3.3	62.6±1.8	602.5±11.5
AS6	0-10	62.5±3.2	68.5±1.9	778.6±11.7
AS7	10-20	72.4±1.9	83.6±2.2	742.7±11.6
AS8	0-10	75.3±4.7	82.3±2.6	762.5±9.9
AS9	20-30	58.3±4. 8	72.5±0.4	624.4±9.3
AS10	10-20	68.5±6.2	81.6±2.7	642.5±10.4
AS11	0-10	75.4± 1.8	94.3±1.3	804.6±5.6
AS12	10-20	65.5±3.3	78.2±3.2	672.3±11.1
AS13	20-30	68.2±2.9	70.5±2.6	562.2±11.2
AS14	30-40	61.5±9.4	72.4±8.8	602.4±1.3
AS15	0-10	58.2±1.2	65.2±1.1	688.5±7.9
AS16	20-30	54.7±1.1	73.5±1.8	587.3±5.4
AS17	30-40	46.2±3.1	57.5±2.1	522.5±8. 2
AS18	20-30	52.3±1.7	68.2±1.6	644.5±7.2
AS19	10-20	64.0±1.8	74.5±1.7	734.3±6.2
AS20	3040	51.4±6.6	65.4±7.6	580.4±7.5
AS21	10-20	68.2±1.4	72.6±1.5	630.2±12.5
AS22	30-40	56.2±1.4	66.5±1.3	565.5±15.3
AS23	20-30	53.5±1.6	75.2±2.1	602.6±9.0
AS24	30-40	58.2±1.4	67.5±1.4	534.7±12.4
AS25	0-10	68.5±1.2	78.4±1.3	773.6±12.1
AS26	30-40	52.4±1.3	62.6±1.4	564.5±11.0
AS27	10-20	68.6±3.9	76.4±2.7	652.3±8.64
AS28	20-30	55.4±1.3	68.4±1.3	573.3±9.6
AS29	30-40	51.8±2.4	65.5±1.4	514.5±5.4
AS30	20-30	59.5±1.4	74.2±1.3	629.2±7.5
AS31	10-20	61.2±5.3	74.7±6.3	672.6±7.7
AS32	0-10	73.1±1.8	82.4±1.8	784.6±6.6
AS33	10-20	68.2±1.5	81.6±1.6	642.5±1.0
AS34	0-10	77.2±1.2	92.2±9.4	763.5±9.4
AS35	20-30	58.5±2.4	67.4±1.6	642.5±11.3
AS36	30-40	54.6±1.8	72.2±1.8	547.3±6.0
AS37	0-10	74.4±1.6	87.5±1.8	782.6±5.7
AS38	10-20	63.5±2.5	75.2±1.7	573.2±6.9
AS39	0-10	66.5±1.5	74.6±1.9	742.6±7.2
AS40	0-10	62.2±6.5	81.7±7.5	518.4.6±9.5
Mean		**62.9±8.1**	**74.9±10.1**	**648.3±84.5**
Range		**46.0 – 77.0**	**58 – 112.2**	**515.0 – 805.0**

Table 4.2: Mean activity concentrations of radionuclides in soil of other countries around the world established by UNSCEAR, (2000)

Region/ Country	Concentration in soil (Bq kg^{-1})						Absorbed dose rates in air (nGy h^{-1})	
	^{226}Ra		^{232}Th		^{40}K			
	Mean	Range	Mean	Range	Mean	Range	Mean	Range
Malaysia	66	49–86	82	63-110	310	170–430		
United States	40	8-160	35	4-130	370	100-700	47	14-118
Japan	33	6-98	28	2-88	310	15-990	53	35-70
China	32	2-440	41	1-360	440	9-1800	62	2-340
India	29	7-81	64	14-160	400	38-760	56	20-1100
Egypt	17	5-64	18	2-96	320	29-650	32	20-133
Iran	28	8-55	22	5-42	640	250-980	71	36-130
Denmark	17	9-29	19	8-30	460	240-610	52	35-70
Spain	32	6-250	33	2-210	470	25-1650	76	40-120
Poland	26	5-120	21	4-77	410	110-970	45	18-97
Switzerland	40	10-900	25	4-70	370	40-1000	45	15-120
Portugal	44	8-65	51	22-100	470	25-1650	76	40-120
Bulgaria	45	12-210	30	7-160	400	40-800	70	48-96
Romania	32	8-60	38	11-75	490	250-1100	59	21-122
Portugal	44	8-65	51	22-100	470	25-1650	76	40-120
UNSCEAR, 2000	35		30		400		60	53-98

Table 4.3: Mean activity concentrations of radionuclides of agricultural and virgin soils for local and international investigations

Virgin soil							
Region/ Country	Concentration in soil (Bq kg−1)						Reference
	^{226}Ra		^{232}Th		^{40}K		
	Mean	Range	Mean	Range	Mean	Range	
Malaysia (Penang)	396		165		835		Almayahi et al., (2012)
Malaysia (Pontian)	37.0		53		293		Saleh *et al.,* (2013)
Malaysia (Kedah)	51.0		78.44		125.66		Ahmad *al.,* (2015)
Malaysia	65.2	45.1-11.4	83.39	51.8-7.3	136.9	99.2 -72.8	Alzubaidi *et al.,* (2016)
Agriculture soil							
Malaysia (Kedah)	80.63		116.87		200.66		Ahmad *et al.,* (2016)
India	64.0		93		124		Singh *et al.,* (2005)
Pakistan	30.0		56		602		Tufail *et al.,* 2008
Algeria	53.2		50.03		311		Boukhenfouf & Boucenna (2011)
Egypt	66		54		183		Issa, (2013)
Thailand	43.0	11–78	51	7–120	230	7–712	UNSCEAR, (2000)
Malaysia		49–86	82	63–110	310	170–430	UNSCEAR, (2000)
Greece	16±6	12–26	55±14	39–72	305±59	222–376	Ioannides, (1979)
Malaysia	102.0	58.9-166.5	133.9	87.9-180.4	325.8	202.2-529.1	Alzubaidi *et al.,* (2016)

Figure 4.1, 4.2 and 4.3 show the correlation between the measured activity concentrations of ^{226}Ra, ^{232}Th and ^{40}K. A positive correlation R^2=0.65 was obtained between ^{226}Ra, ^{232}Th, indicating similar responses to the soil and environmental processes that affected their distribution. While the correlation was weak (R^2=0.53) between ^{226}Ra and ^{40}K. A strong correlation between radionuclides may indicate that their origin and behavior in soil is consistent. The effect of soil properties on the concentration of radionuclides has been reported in previous studies (Tsai *et al.*, 2011; Fujiyoshi & Sawamura, 2004; Skarlou *et al.,* 1996).

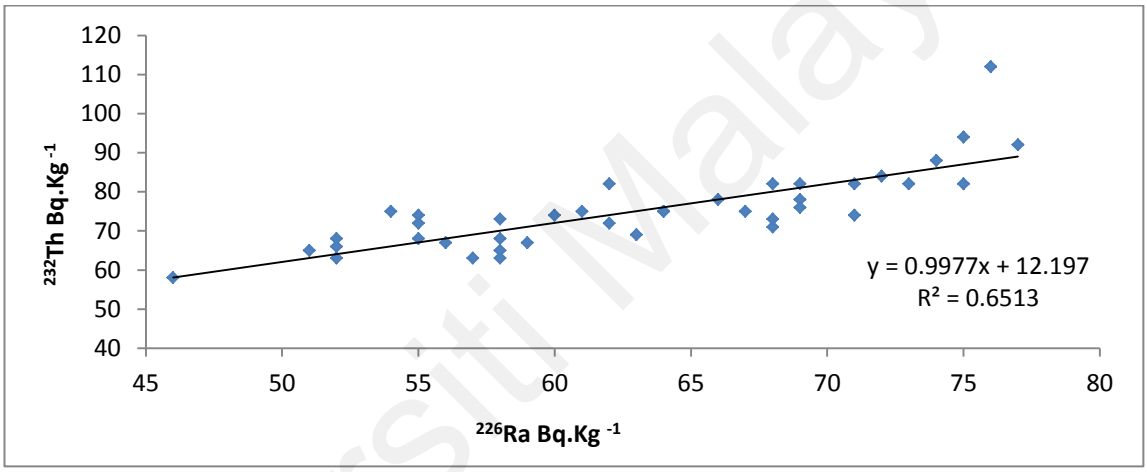

Figure 4.1: The correlation between the concentrations of ^{232}Th and ^{226}Ra for the soil samples from Kedah

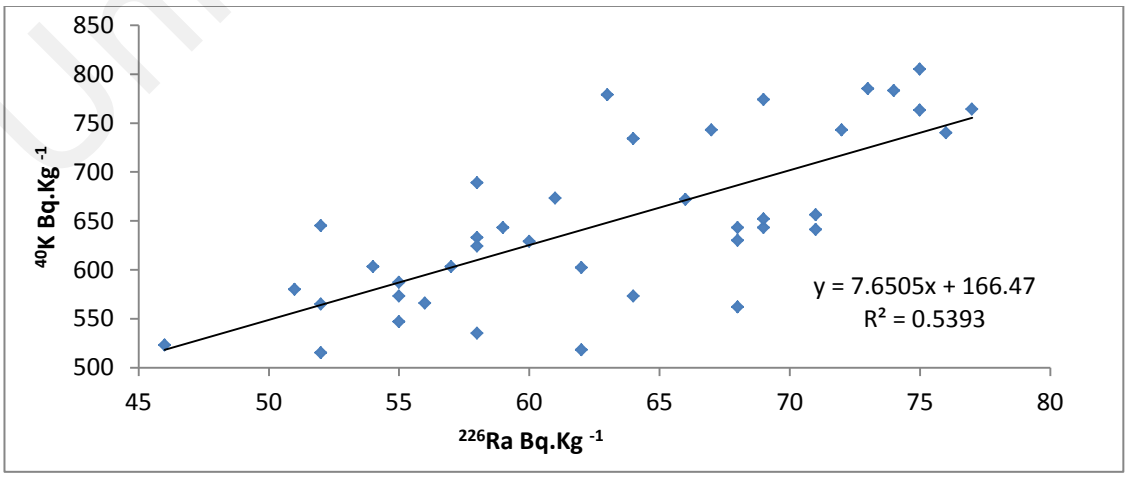

Figure 4.2: The correlation between the concentrations of ^{40}K and ^{226}Ra for the soil samples from Kedah

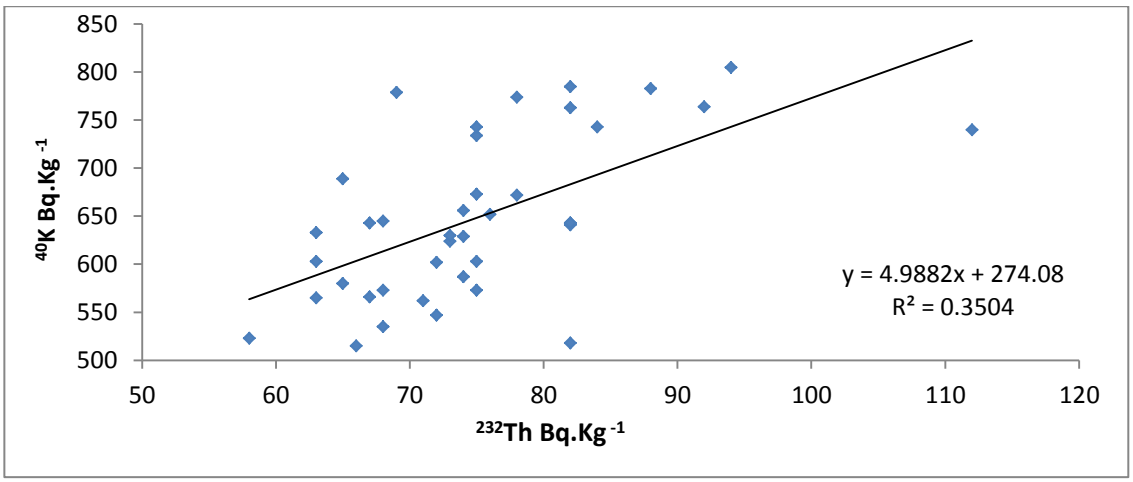

Figure 4.3: The correlation between the concentrations of ^{40}K and ^{232}Th for the soil samples from Kedah

4.1.2 The activity concentrations of in Selangor

The mean values of the radionuclide concentrations in soil from Selangor are shown in Table 4.4. The mean values of ^{226}Ra, ^{232}Th and ^{40}K were found to be 67.5±12.0, 84.7±12.8 and 742.2±145.5 Bq kg $^{-1}$. The ranges were 44 – 95, 60 – 115 and 516 – 1143 Bq kg^{-1}, respectively. The mean concentrations of ^{226}Ra, ^{232}Th, and ^{40}K were greater than the global values given by UNSCEAR, (2000). The concentrations of ^{226}Ra, ^{232}Th, and ^{40}K were 55.6 %, 59.2 %, and 46 % higher than the world averages, respectively.

The mean radionucldies activity concentrations of soils from Selangor follow the order of ^{226}Ra (67.59 Bq kg^{-1}) < ^{232}Th (84.79 Bq kg^{-1}) < ^{40}K (742.28 Bq kg^{-1}). The results showed that ^{40}K is the main soil contaminant, accounting for 83% of the total radioactivity. This may be attributed to the extensive use of NPK fertilizers by farmers to improve crop yield. It was found that the concentration value of ^{226}Ra is comparable to those in Kedah, while, the values of ^{232}Th and ^{40}K are slightly lower with mean values of 84.79±12.8 and 742.28±145.5 Bq kg^{-1}, respectively. The mean activities of the ^{226}Ra, ^{232}Th and ^{40}K in the soil samples of Kedah were comparable to those reported for Malaysia.

The correlation plots between the activity concentrations of ^{226}Ra, ^{232}Th and ^{40}K are shown in Figures 4.4, 4.5 and 4.6. Positive correlations can be observed between the ^{226}Ra and ^{40}K, and between ^{232}Th and ^{40}K. The relationship between ^{226}Ra and ^{232}Th was a positive correlation with $R^2 = 0.88$, indicating similar responses to soil and environmental processes that affected their distribution. This association may suggest similarities in its origin, and thus the soil from which it emerged. The positive relationships between the radionuclides shown by the study are consistent with Sahoo *et al.,* (2012), where the geochemical behavior of thorium, uranium and rare earth elements are relatively close to one another as compared to other elements in a geological environment. This is also consistent with a previous study by Al-Jundi (2002), who found a positive association between ^{40}K and ^{232}Th.

Table 4.4: The activity concentrations of radionuclides (Mean±SD) Bq.kg^{-1} of ^{226}Ra, ^{232}Th and ^{40}K in the soil samples from Selangor

Sample ID	Depth cm	Activity concentrations (Bq.kg-1)		
		^{226}Ra	^{232}Th	^{40}K
S1	0-10	78.5±8.3	91.5±4.5	951.4±11.2
S2	10-20	80.4±3.2	103.6±4.2	1143.4±6.5
S3	0-10	78.2±4.4	92.3±5.6	901.6±12.0
S4	0-10	73.4±2.2	92.7±2.6	917.8±8.5
S5	0-10	74.7±5.2	88.3±3.2	830.4±8.3
S6	10-20	65.5±2.4	83.7±2.2	712.6±7.5
S7	0-10	72.2±2.5	85.5±2.6	625.3±5.3
S8	20-30	58.2± 4.5	72.2±3.5	615.2±8.5
S9	20-30	66.6±3.5	85.4±3.3	833.6±5.5
S10	10-20	71.3±2.5	93.3±2.4	912.5±8.5
S11	20-30	61.5±3.3	85.5±2.5	763.3±5.6
S12	30-40	58.3±5.2	75.5±3.3	657.2±4.5
S13	30-40	52.5± 2.5	68.4±1.2	606.5±8.5
S14	20-30	65.3±2.5	87.5±2.5	653.5±5.2
S15	10-20	72.5±2.5	95.3±2.0	846.3±5.2
S16	30-40	58.2±2.2	77.3±1.5	571.5±7.5
S17	20-30	68.5±7.4	79.5±7.8	695.9±11.6
S18	30-40	44.8±1.6	60.4+2.6	515.9±12.4
S19	10-20	92.5±2.6	115.2±2.0	978.3±12.2
S20	30-40	44.4±3.5	61.5±2.5	557.5±8.2
S21	20-30	54.5±2.5	65.3±0.4	597.5±14.2
S22	30-40	68.5±1.2	86.5±2.0	602.5±8.5
S23	30-40	54.2±2.5	76.2±1.3	684.5±5.5
S24	20-30	65.5±2.5	82.3±2.2	646.2±8.4
S25	0-10	74.5±1.7	97.4±0.5	845.5±8.5
S26	10-20	95.2±0.8	112.3±1.0	884.6±5.2
S27	0-10	83.3±1.3	97.2±0.8	803.8±6.3
S28	10-20	68.3±3.5	84.5±5.5	672.5±7.5
S29	0-10	62.5±2.2	87.5±2.5	683.3±5.3
S30	20-30	72.5±3.2	81.5±3.5	677.5±6.5
S31	0-10	77.2±2.4	87.5±2.2	790.2±9.2
S32	10-20	80.5±2.5	97.5±2.5	903.5 ±8.5
S33	30-40	51.5±3.5	66.5±3.5	651.5±9.5
S34	30-40	54.5±3.3	72.5±4.2	603.5±2.6
S35	10-20	54.5±2.7	72.3±2.8	643.5±13.5
Mean		**67.5±12.0**	**84.7±12.8**	**742.2±145.5**
Range		**44.4 - 95.5**	**60.4 - 115.2**	**516.5 - 1143.4**

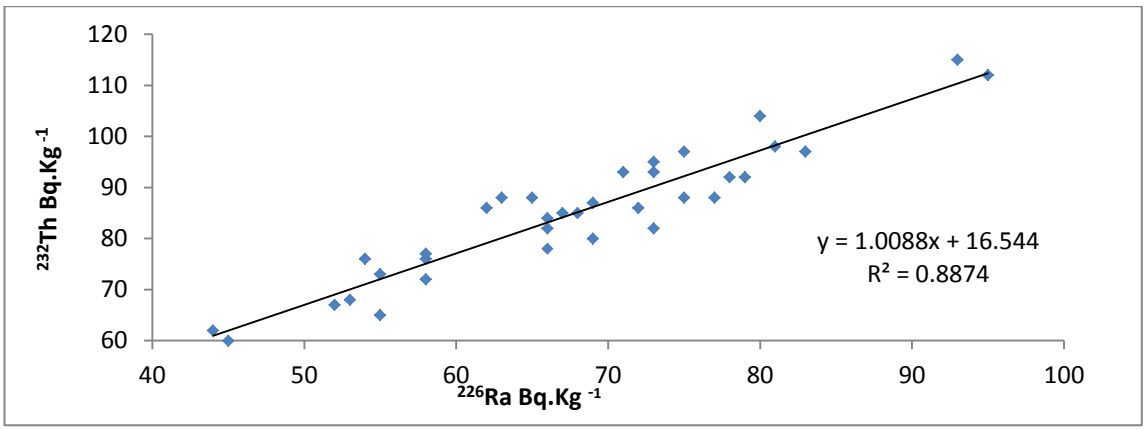

Figure 4.4: The correlation between the concentration of ^{232}Th and ^{226}Ra for the soil samples from Selangor

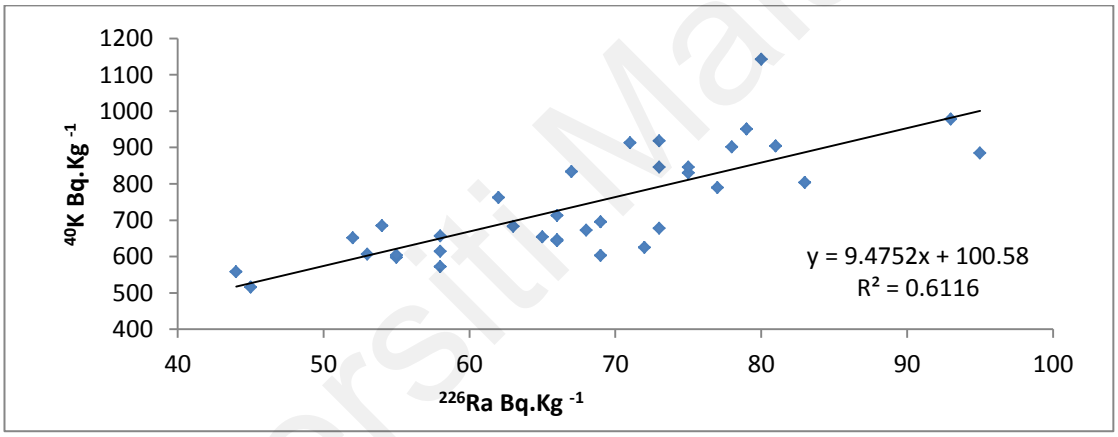

Figure 4.5: The correlation between the concentration of ^{40}K and ^{226}Ra for the soil samples from Selangor

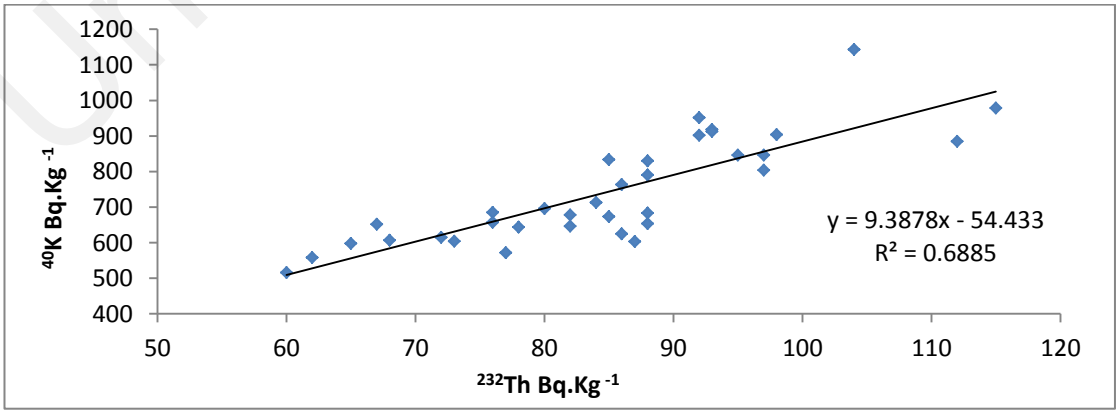

Figure 4.6: The correlation between the concentration of ^{40}K and ^{232}Th for the soil samples from Selangor

4.1.3 The activity concentrations of radionuclides in Malacca

The measured activity concentrations of ^{226}Ra, ^{232}Th, and ^{40}K in soil samples from Malacca are showed in Table 4.5. The mean concentration values of the radionuclides of ^{226}Ra, ^{232}Th and ^{40}K were found to be 62.2±12.8, 79.9±15.0 and 625.1±118.9 Bq kg^{-1}, respectively, whereas, the range varied 370 – 85.0, 51.0 – 105.2 and 404.2 – 891.0 Bq kg^{-1}, respectively. The mean concentrations of ^{226}Ra, ^{232}Th, and ^{40}K were greater than world average values given by UNSCEAR, (2000) by 51.8 %, 56.2 %, and 36%, respectively.

In Malacca, the mean activity values of the radionucldies followed the order of ^{226}Ra (62.27 Bq kg^{-1}) < ^{232}Th (79.97 Bq kg^{-1}) < ^{40}K (625.11Bq kg^{-1}). The results revealed that ^{40}K is the most prevalent soil pollutant, accounting for 82 % of the total. Farmers' extensive use of NPK fertilisers to boost crop production may be to blame for the high levels (Roto *et al.,* 2019; Konoplev & Kalmykov, 2020). However, the activity concentration of ^{232}Th was greater than that of ^{226}Ra. This might be owing to the low geochemical mobility and insoluble nature in water. Furthermore, ^{232}Th concentrations are often greater than ^{226}Ra concentrations in sedimentary rock, which prevails in the research regions of Kedah, Selangor, and Malacca. The measured concentrations of the radionuclides ^{226}Ra, ^{232}Th and ^{40}K were found to be comparable to those in Kedah, and marginally lower compared to Selangor's values. The mean activity values of ^{226}Ra, ^{232}Th, and ^{40}K in Malacca were comparable to earlier local investigations and greater than those reported in other countries. Figure 4.7, 4.8 and 4.9 show the correlation between ^{226}Ra, ^{232}Th and ^{40}K in samples from Malacca. Figure 4.7 indicates strong positive relationship between ^{226}Ra and ^{232}Th at $R^2 = 0.88$. The correlations between ^{40}K and ^{232}Th and ^{226}Ra were a positive $R^2 = 0.67$, $R^2 = 0.60$, respectively. Such associations can display similarities in their origin and thus, their chemical behaviour.

Table 4.5: The activity concentrations of radionuclides (Mean±SD) Bq.kg^{-1} of ^{226}Ra, ^{232}Th and ^{40}K in the soil samples from Malacca

Sample ID	Depth cm	Activity concentrations (Bq.kg-1)		
		^{226}Ra	^{232}Th	^{40}K
M1	20-30	42.5±0.8	55.2±1.0	502.5±7.5
M2	0-10	64.4±0.8	77.5±0.8	612.2±8.0
M3	30-40	54.5±0.7	65.3±0.7	533.6±11.2
M4	20-30	58.5±3.2	68.3±3.5	516.4±5.5
M5	10-20	61.2±1.2	79.2±1.5	686.8±7.5
M6	30-40	48.5±0.5	61.3±0.6	567.6±8.4
M7	10-20	62.4±2.5	77.4±2.5	517.8±6.5
M8	20-30	68.5±0.2	80.5±0.5	632.4± 5.2
M9	30-40	56.2±1.5	69.2±1.5	495.5±5.0
M10	10-20	82.5±0.8	102.3±0.8	708.2±3.5
M11	0-10	72.6±1.2	93.2±1.2	688.4±5.3
M12	20-30	51.7±0.7	67.2±0.7	504.2±8.5
M13	0-10	77.4±2.5	90.5±2.5	840.2±11.2
M14	10-20	75.2±0.8	105.2±1.0	811.5 ±5.8
M15	10-20	72.5±2.2	95.2±2.5	677.2±6.0
M16	0-10	75.7±0.2	91.5±0.5	682.6±5.5
M17	20-30	55.5±8.5	78.4±9.6	584.7±66.8
M18	30-40	51.8±8.6	75.5±8.5	602.5±89.6
M19	30-40	44.2±6.4	68.5±7.8	611.5±48.3
M20	30-40	37.5±0.6	50.6±0.6	476.2±5.5
M21	10-20	73.2±0.5	95.5±0.5	890.5±7.5
M22	10-20	80.4±0.5	102.3±0.5	821.4±8.0
M23	0-10	72.7±0.5	97.5±0.5	607.6±8.5
M24	20-30	57.2±0.2	68.8±0.2	612.1±5.5
M25	30-40	58.2±1.5	70.4±0.7	574.5±7.2
M26	20-30	52.4±0.5	68.3±0.5	452.6±10.3
M27	10-20	84.5±1.5	102.4±1.6	842.2 ±7.0
M28	0-10	77.4±0.6	90.2±0.6	602.5±7.9
M29	0-10	63.2±0.8	76.5±0.9	661.2±14.1
M30	20-30	58.5±0.8	77.8±0.8	605.2±9.0
M31	30-40	36.7±0.7	57.5±0.7	404.2±8.7
M32	0-10	64.2±0.5	88.5±0.5	612.3±7.5
M33	10-20	83.2±0.5	105.2±0.5	818.4±8.1
M34	0-10	73.5±0.7	95.2±0.8	612.4±9.6
M35	10-20	62.4±0.7	87.5±0.8	730.5±11.3
M36	20-30	54.4±5.5	68.5±6.0	514.2±9.2
M37	30-40	48.2±4.9	66.5±5.7	634.2±48.7
M38	30-40	52.5±4.8	68.2±5.6	506.0±25.5
Mean		**62.2±12.8**	**79.9±15.0**	**625.1±118.9**
Range		**37.0-85.0**	**51.0-105.2**	**404.2 -891.0**

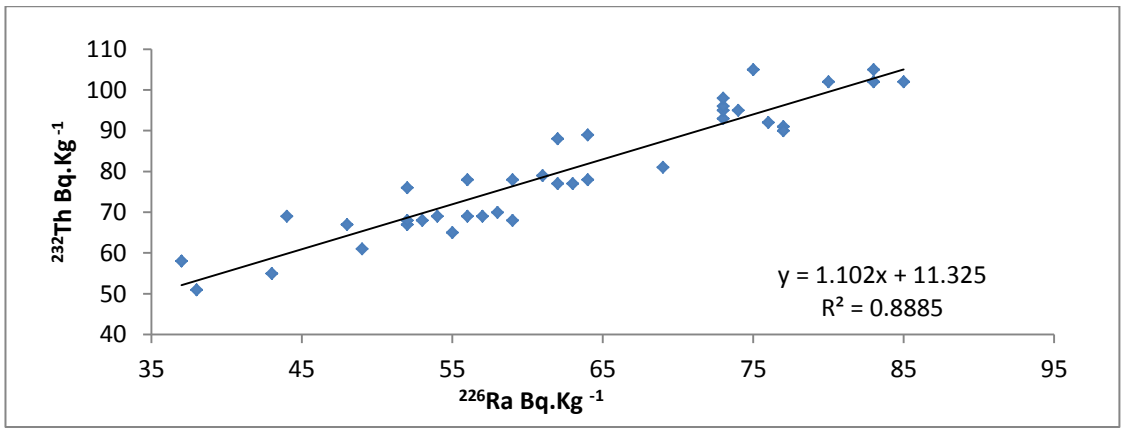

Figure 4.7: The correlation between the concentration of ^{226}Ra and ^{232}Th for the soil samples from Malacca

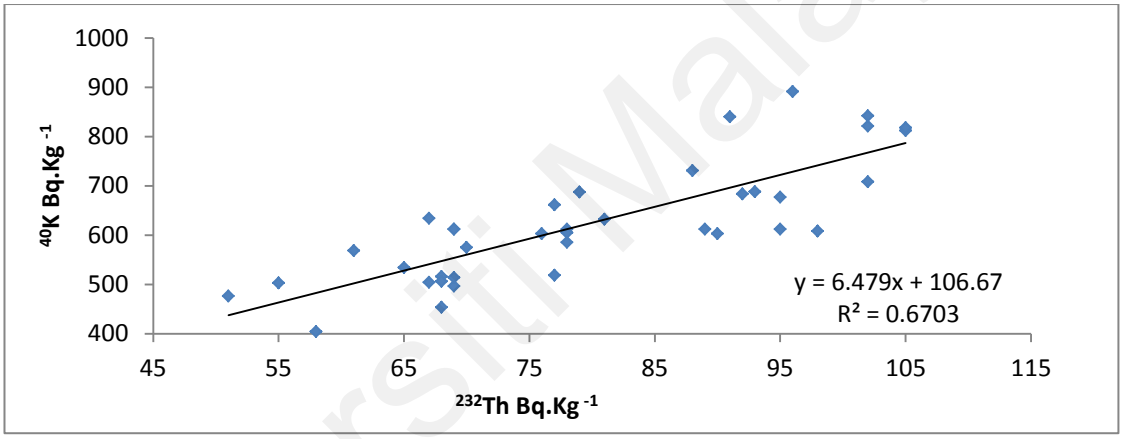

Figure 4.8: The correlation between the concentration of ^{40}K and ^{232}Th for the soil samples from Malacca

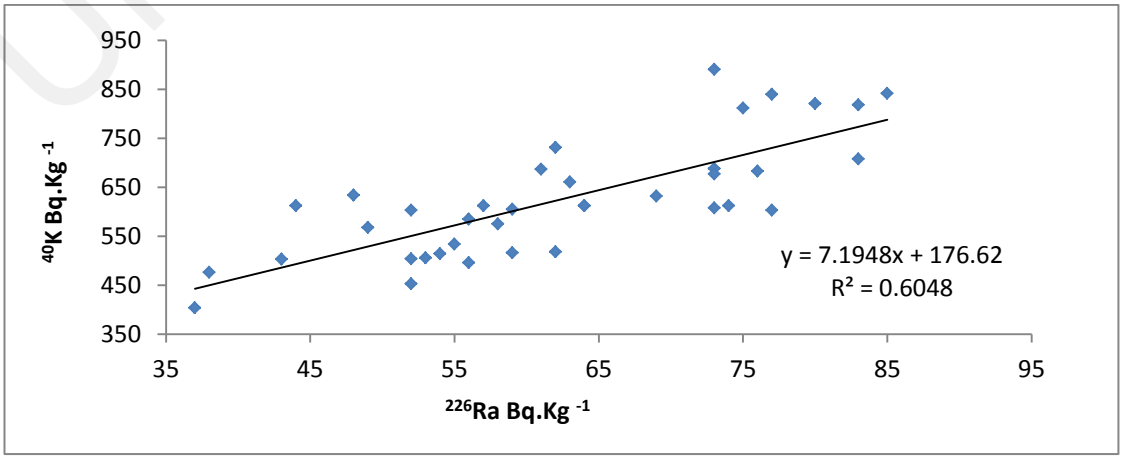

Figure 4.9: The correlation between the concentration of ^{40}K and ^{226}Ra for the soil samples from Malacca

4.1.4 The activity concentrations of radionuclides in Johor

Table 4.6 shows the activity concentrations of radionuclides ^{226}Ra, ^{232}Th, and ^{40}K in soil from Johor. The mean activity concentrations of ^{226}Ra, ^{232}Th, and ^{40}K were determined to be 64.24±11.9, 83.38±12.9 and 759.34±147.3 Bq kg^{-1}, respectively, with a range of 43.4 – 92.3, 62.0 – 116.0, and 517.0 – 1210.0 Bq kg^{-1}, respectively. The mean concentrations of ^{226}Ra, ^{232}Th, and ^{40}K in the chosen area were greater than the world values of UNSCEAR, (2000) by 53.2%, 58 % and 47.3%, respectively.

In Johor, the mean concentration values follow the order of ^{226}Ra (64.24 Bq kg^{-1}) < ^{232}Th (83.38 Bq kg^{-1}) < ^{40}K (759.34 Bq kg^{-1}). The data revealed that ^{40}K was the main contributor. Apart from the fact that potassium is a common element that makes up roughly 2% of the earth's crust, the extensive use of chemical fertilisers in acidic soils may increase radiation levels. The activity concentrations of the radionuclides ^{226}Ra, ^{232}Th and ^{40}K were found to be comparable to those in Selangor, while the ^{232}Th concentration was comparable to that in Kedah and Malacca. The activities of ^{226}Ra, ^{232}Th, and ^{40}K in Johor soil samples were comparable to those reported in local research Table 4.3, and greater than those reported in other countries Table 4.3. Figure 4.10, 4.11 and 4.12 show the correlation between ^{226}Ra, ^{232}Th and ^{40}K in soil samples from Johor. With R^2 = 0.87, a solid connection between ^{226}Ra and ^{232}Th was displayed (Figure 4.10). The association between ^{40}K and ^{232}Th had a significant positive correlation (R^2 = 0.74), with he correlation coefficientas R^2 = 0.71 the relationship between ^{40}K and ^{226}Ra. In areas of relatively homogenous lithology, strong relationships between radionuclides are predicted. The results of Johor soil samples show statistically significant relationships between the members of decay series. Navas *et al.,* 2002 also found substantial connections between radionuclides of different decay series. Strong radionuclide correlations are likely to be discovered in locations with relatively homogenous lithology, this is consistent with the findings of Fairbridge, (1972).

Table 4.6: The activity concentrations of radionuclides (Mean±SD) Bq.kg^{-1} of ^{226}Ra, ^{232}Th and ^{40}K in the soil samples from Johor

Sample ID	Depth cm	Activity concentrations (Bq.kg-1)		
		^{226}Ra	^{232}Th	^{40}K
JB1	0-10	75.5±2.2	92.3±3.6	813.4±7.5
JB2	10-20	80.3± 5.5	104.3±5.2	914.6±8.5
JB3	30-40	57.5±2.5	78.5±0.8	757.5±5.5
JB4	30-40	53.5±1.5	77.3±0.8	622.2±5.7
JB5	20-30	67.2±2.3	82.5 ±1.6	857.5±3.3
JB6	30-40	52.5± 3.2	76.5±1.5	675.5±8.3
JB7	10-20	77.5±5.5	95.5±1.5	827.3±11.2
JB8	10-20	78.5±1.8	97.5±0.5	913.2±7.2
JB9	20-30	55.3±3.4	76.2±3.6	743.7±11.4
JB10	0-10	74.2±3.2	92.7±3.4	865.5±15.2
JB11	20-30	48.4±3.4	64.8±4.5	647.7±11.8
JB12	0-10	63.7±3.4	85.6±3.9	780.2±46.4
JB13	30-40	54.8±1.9	76.5±2.9	649.5±11.2
JB14	30-40	46.7±2.5	61.7±3.2	634.8±12.7
JB15	20-30	64.6±5.2	82.7±5.8	735.3±15.6
JB16	10-20	84.5±1.5	116.5±1.5	1132.1±17.5
JB17	10-20	72.2±1.5	95.3±1.7	863.7±8.0
JB18	20-30	43.4±0.3	66.7±0.3	628.5±7.5
JB19	0-10	62.7±1.7	86.3±1.7	707.2±7.6
JB20	30-40	55.5±2.2	77.8±2.5	612.2±6.5
JB21	10-20	63.2±0.5	83.5±0.5	718.5±5.5
JB22	30-40	57.2± 2.5	67.5± 2.5	586.5±7.0
JB23	20-30	53.6±2.5	68.4±2.5	578.4±5.5
JB24	0-10	61.3±2.2	84.5±2.5	831.3±3.5
JB25	20-30	75.2±0.7	95.5±0.7	922.5±5.2
JB26	0-10	67.3±0.5	87.5±0.5	801.5±4.3
JB27	20-30	55.5±2.2	78.4±2.2	714.6±6.5
JB28	10-20	66.3±1.5	84.8±1.5	732.2±12.0
JB29	10-20	63.5±0.7	78.3±0.7	646.5±2.2
JB30	30-40	48.4±3.8	62.7±4.6	516.5±8.3
JB31	0-10	55.3±1.2	70.6±2.4	617.5±7.8
JB32	20-30	46.2±3.7	64.8±4.6	627.6±8.2
JB33	0-10	74.2±8.3	87.4±10.3	867.2±7.3
JB34	20-30	52.7±2.6	68.8±3.3	609.6±8.7
JB35	0-10	64.4±2.9	87.3±3.8	724.0±7.9
JB36	10-20	92.3±7.3	101.5±8.2	1209.6±6.7
JB37	20-30	74.4±8.3	93.6±9.8	836.4±6.9
JB38	10-20	82.2±7.3	109.4±8.7	995.6±7.2
JB39	0-10	72.8±4.2	85.2±5.2	721.7±7.7
JB40	10-20	75.2±1.8	88.3±2.0	734.3±8.5
Mean		**64.2±11.9**	**83.3±12.9**	**759.3±147.3**
Range		**43.4 – 92.3**	**62.0 – 116.0**	**517.0 – 1210.0**

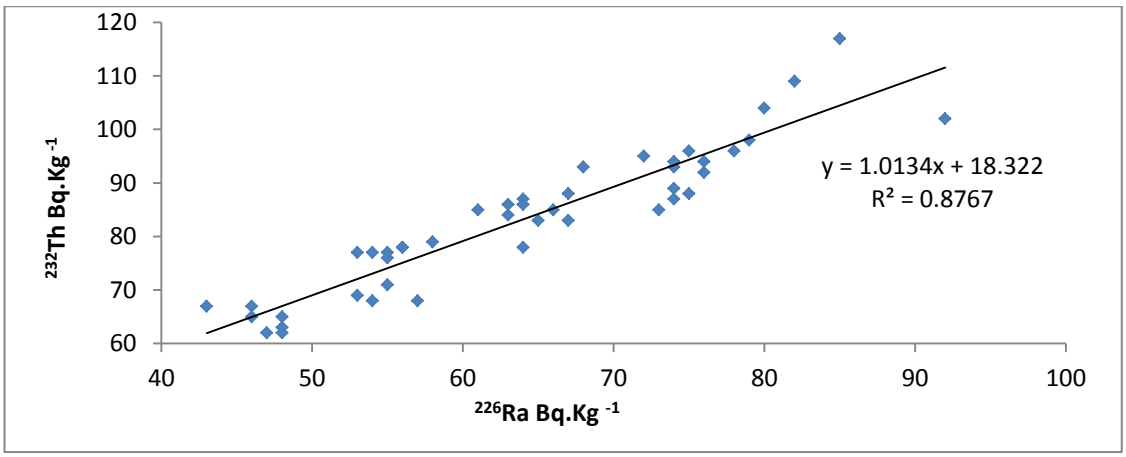

Figure 4.10: The correlation between the concentrations of ^{232}Th and ^{226}Ra for the soil samples from Johor.

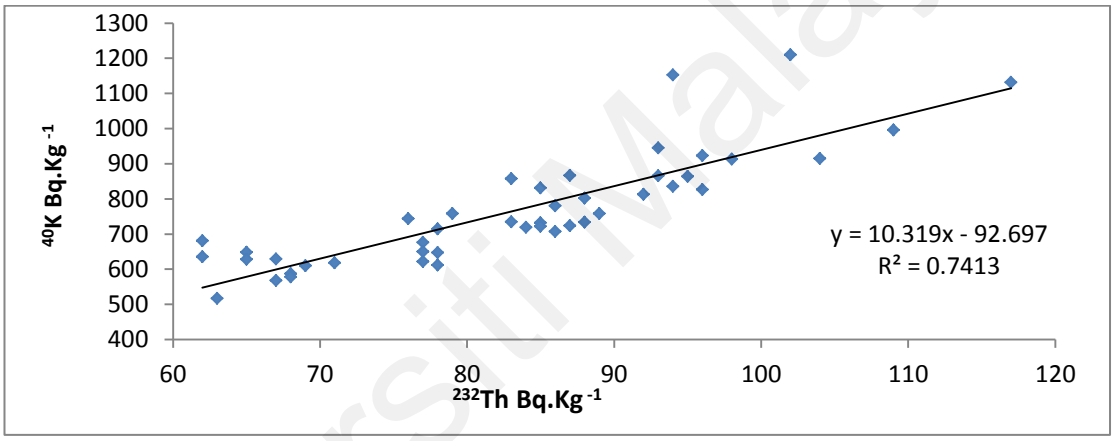

Figure 4.11: The correlation between the concentrations of ^{40}K and ^{232}Th for the soil samples from Johor.

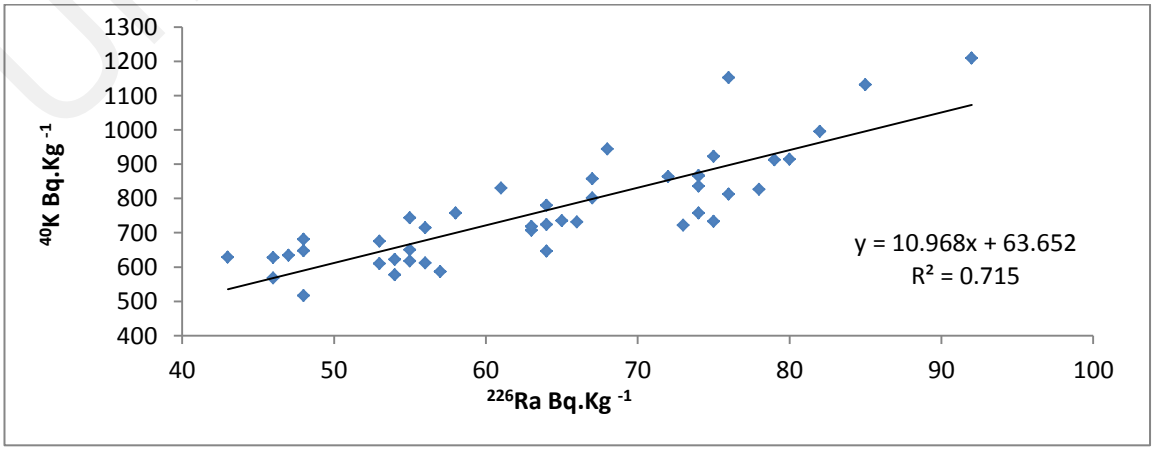

Figure 4.12: The correlation between concentrations of ^{40}K and ^{226}Ra for the soil samples from Johor.

4.1.5 The activity concentrations of radionuclides in Raub

The activity concentrations of radionuclides ^{226}Ra, ^{232}Th and ^{40}K in the soil samples collected from Raub are presented in Table 4.7. The mean values of activity concentrations of the radionuclides ^{226}Ra, ^{232}Th, and ^{40}K were determined to be 61.8±11.8, 81.5±12.3 and 757.6±161.1Bq kg^{-1}, respectively, with a range of 37.0–84.0, 53.0–115.0, and 377.0–1198.2 Bq kg^{-1}, respectively.

The mean concentrations of ^{226}Ra, ^{232}Th and ^{40}K were higher than the global levels published by UNSCEAR, (2000) by 51.4 %, 57 % and 47.2 % respectively.

The mean values of the activity concentrations follow the order of ^{226}Ra (61.83 Bq kg^{-1}) < ^{232}Th (81.56 Bq kg^{-1}) < ^{40}K (757.63 Bq kg^{-1}). The results revealed that ^{40}K is the main contributor of contamination. The activity concentrations of ^{226}Ra, ^{232}Th and ^{40}K were found to be comparable with the findings of Johor, while the ^{232}Th value was comparable to those in Kedah, Selangor, Malacca and Johor. The activity values of ^{226}Ra, ^{232}Th and ^{40}K in Raub were found to be comparable to those reported in earlier local studies (Table 4.3), and higher to those reported in other countries (Table 4.2).

Figure 4.13, 4.14 and 4.15 show the correlations between ^{226}Ra, ^{232}Th and ^{40}K in samples from Raub. A strong positive correlation between ^{226}Ra and ^{232}Th was plotted at R^2 = 0.86 (Figure 4.13). While, the relationship between ^{40}K and ^{232}Th was shown to be a weak R^2 = 0.59 (Figure 4.14), the relationship between ^{40}K and ^{226}Ra was also found to be a weak R^2 = 0.56 (Figure 4.15). According to the correlation coefficient, the activity concentrations of ^{232}Th and ^{226}Ra show equilibrium, as the ratio of ^{232}Th / ^{226}Ra approaches one. While, the estimations show a notable non- equilibrium between the concentration of ^{40}K and ^{232}Th, and also between ^{40}K and ^{226}Ra.

Table 4.7: The activity concentrations of radionuclides (Mean±SD) Bq.kg^{-1} of ^{226}Ra, ^{232}Th and ^{40}K in the soil samples from Raub

Sample ID	Depth cm	Activity concentrations (Bq.kg-1)		
		^{226}Ra	^{232}Th	^{40}K
PR1	30-40	59.7± 2.7	81.0±2.2	606.5±14.7
PR2	30-40	60.2±2.8	93.6±2.3	720.5±8.4
PR3	0-10	49.7±2.3	67.8±2.1	595.6±6.5
PR4	20-30	73.6±2.5	92.4±4.4	835.2±12.6
PR5	30-40	60.3±2.5	82.6±3.6	689.5±12.3
PR6	0-10	76.3±3 3	92.2±1.7	876.8±11.6
PR7	30-40	48.5±2.1	64.6±3.5	655.6±16.8
PR8	10-20	49.7±1.5	75.4±3.9	662.7±12.7
PR9	0-10	78.6±1.9	92.7±2.9	935.8±14.5
PR10	10-20	62.6±2.8	87.4±2.6	748.7±12.2
PR11	10-20	59.5±1.3	78.3±2.6	757.5±14.2
PR12	20-30	60.2±1.8	82.4±2.1	771.5±12.5
PR13	10-20	57.6±3.3	79.5±3.2	651.5±14.6
PR14	20-30	43.5±2.3	64.7±0.7	651.4±12.5
PR15	0-10	72.4±1.4	97.7±0.9	972.8±14.5
PR16	20-30	66.8±1.4	81.4±0.9	778.6±8.6
PR17	10-20	83.5±2.4	101.7±0.4	1012.3±12.3
PR18	20-30	58.5±2.4	78.2±1.7	759.4±11.2
PR19	10-20	75.4±2.1	93.6±1.9	976.4±12.7
PR20	20-30	45.2±1.9	65.3±1.6	575.7±6.8
PR21	30-40	36.8±2.0	52.8±1.9	563.2±8.4
PR22	30-40	54.2±1.8	76.7±2.0	675.5±11.1
PR23	10-20	82.2±1.6	95.4±1.9	1197.6±15.1
PR24	20-30	55.2±1.7	71.3±1.5	680.4±12.1
PR25	30-40	45.8±2.3	68.5±1.6	612.7±6.1
PR26	30-40	49.8±1.6	61.7±1.7	560.8±7.6
PR27	10-20	71.3±3.2	87.5±1.5	687.7±8.5
PR28	20-30	61.6±2.5	83.2±3.2	690.4±11.2
PR29	10-20	70.8±5.6	87.5±6.8	781.5±12.5
PR30	0-10	76.8±6.4	92.7±7.4	843.5±14.4
PR31	0-10	69.2±5.5	80.3±6.4	787.4±12.9
PR32	0-10	83.5±2.3	114.8±3.2	1114.3±15.6
PR33	30-40	60.4±2.2	83.5±4.2	909.4±9.1
PR34	20-30	68.2±3.5	87.2±3.4	377.2±7.1
PR35	30-40	64.8±8.3	87.3±2.8	862.8±11.8
PR36	30-40	47.3±5.3	65.5±2.8	672.7±12.2
PR37	0-10	58.6±4.2	75.8±4.8	705.6±11.2
PR38	20-30	66.8±6.5	87.3±2.6	895.8±12.0
PR39	0-10	51.4±4.3	72.6±3.8	650.2±17.0
PR40	0-10	56.8±3.3	78.4±2.8	802.5±11.5
Mean		**61.8±11.8**	**81.5±12.3**	**757.6±161.1**
Range		**37.0- 84.0**	**53.0 – 115.0**	**377.0 – 1198.2**

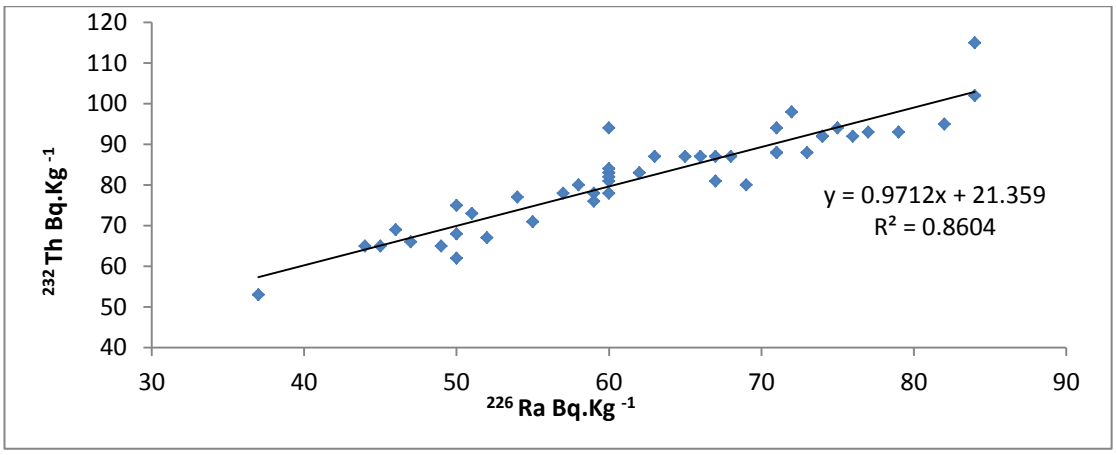

Figure 4.13: The correlation between the concentrations of ^{232}Th and ^{226}Ra for the soil samples from Raub

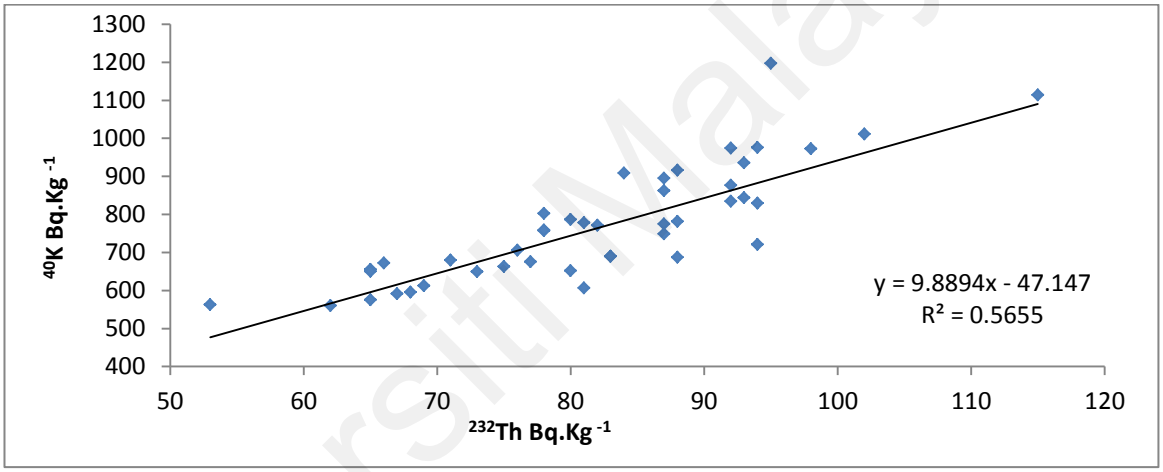

Figure 4.14: The correlation between the concentrations of ^{40}K and ^{232}Th for the soil samples from Raub

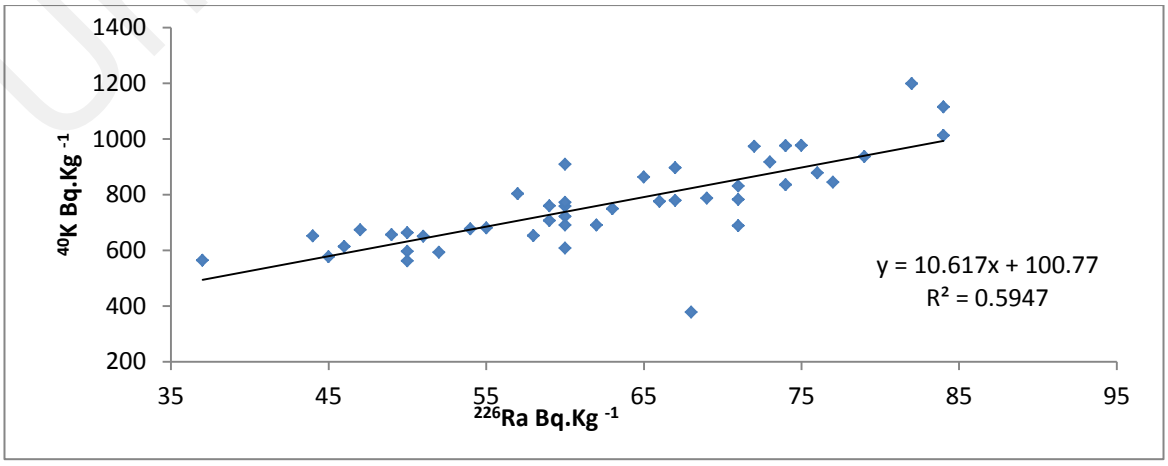

Figure 4.15: The correlation between the concentrations of ^{40}K and ^{226}Ra for the soil samples from Raub

4.1.6 The activity concentrations of radionuclides in Lanchang

The activity concentrations of radionuclides ^{226}Ra, ^{232}Th and ^{40}K in the soil samples collected from Lanchang are presented in Table 4.8. The mean values of the activity concentrations of ^{226}Ra, ^{232}Th and ^{40}K were found to be 64.9±9.7, 84.7±11.2 and 688.9±111.3 Bq kg^{-1}, respectively, whereas the range of value varied 45.0 – 85.0, 63.0 – 112.0 and 493.0 – 951.2 Bq kg^{-1}, respectively. The mean values of ^{226}Ra, ^{232}Th and ^{40}K were higher than the global levels given by UNSCEAR, (2000) by 53.7 %, 58.6 % and 42 %, respectively (Table 4.2).

The mean concentration values in Lanchang follow the order of ^{226}Ra (64.90 Bq kg^{-1}) < ^{232}Th (84.71 Bq kg^{-1}) < ^{40}K (688.95 Bq kg^{-1}). The activity concentrations of the radionuclides ^{226}Ra, ^{232}Th and ^{40}K were found to be comparable to those in Johor and Raub, while the value of ^{232}Th was comparable to the values of Kedah, Malacca, Johor and Raub. The activities of the ^{226}Ra, ^{232}Th and ^{40}K in the soils from Lanchang were comparable those in reported local studies (Table 4.3), and greater than that in other countries (Table 4.2). The statistical analysis of radionuclides activity concentration of Lanchang samples reveals a positive correlation between ^{226}Ra and ^{232}Th with a coefficient of R^2= 0.77, as shown in (Figure 4.16). The different between the soil groups can be observed according to their concentrations ratio ^{232}Th/^{226}Ra. The estimations show a notable non- equilibrium between the concentration of ^{40}K and ^{232}Th, and also between ^{40}K and ^{226}Ra. Raduim ^{226}Ra is usually associated with OM in soil and being the most mobile radionuclide, it can leak into soil with low pH values and high OM. A lack of association between ^{226}Ra and ^{40}K might be attributed to ^{226}Ra's very high solubility and consequently mobility when compared to ^{40}K.

Table 4.8: The activity concentrations of radionuclides (Mean±SD) Bq.kg^{-1} of ^{226}Ra, ^{232}Th and ^{40}K in the soil samples from Lanchang

Sample ID	Depth cm	Activity concentrations (Bq.kg-1)		
		^{226}Ra	^{232}Th	^{40}K
PL1	10-20	73.4±0.8	97.2±0.8	675.5±12.2
PL2	0-10	67.5±0.7	82.5±0.7	588.5±10.9
PL3	10-20	68.7±1.0	81.8±0.9	611.2±13.4
PL4	10-20	73.3±1.2	87.6±1.3	726.8±14.7
PL5	20-30	50.5±1.1	78.7±1.2	671.5±15.9
PL6	10-20	57.8±1.3	83.0±1.3	682.8±16.1
PL7	0-10	66.3±0.7	84.8±0.6	772.2±9.4
PL8	10-20	72.8±0.5	93.4±0.5	702.2±9.6
PL9	0-10	63.4±0.8	85.6±0.8	923.6±14.7
PL10	20-30	55.8±0.6	76.2±0.6	551.3±7.8
PL11	20-30	74.1±1.6	90.3±1.4	746.0±11.4
PL12	10-20	72.7±1.6	94.7±2.1	758.3±15.3
PL13	30-40	45.4±1.0	64.5±1.1	492.8±22.5
PL14	10-20	76.8±1.7	93.0±2.8	810.7±16.7
PL15	20-30	56.4±0.6	73.4±0.6	680.4±22.4
PL16	20-30	68.5±1.5	95.3±1.9	638.3±21.2
PL17	10-20	84.6±8. 3	111.6±2.6	727.5±4.20
PL18	10-20	73.3±7.2	97.5± 2.5	814.4±3.08
PL19	30-40	53.2±0.8	77.7±1.0	548.2±14.9
PL20	30-40	51.7±1.2	73.6±1.5	655.3±15.4
PL21	20-30	62.8±1.4	81.0±1.5	631.5±14.5
PL22	30-40	56.7±1.3	68.4±1.3	585.7±14.8
PL23	10-20	62.2±1.4	84.1±1.3	601.0±13.5
PL24	20-30	62.4±1.4	83.7±1.3	617.4±14.1
PL25	0-10	65.3±1.4	87.3±1.4	658.6±12.3
PL26	0-10	76.4±1.6	94.7±1.5	820.8±14.5
PL27	30-40	56.8±1.2	62.7±1.3	497.5±13.4
PL28	0-10	62.0±1.4	81.8±1.3	694.3±13.3
PL29	0-10	73.7±1.4	88.2±1.3	897.6±13.4
PL30	10-20	82.4±1.3	111.2±1.4	951.2±12.1
PL31	0-10	61.7±1.4	87.5±1.4	758.5±12.9
PL32	30-40	52.6±0.6	68.2±1.3	579.5±14.0
PL33	10-20	76.2±0.6	89.5±0.7	755.2±18.4
PL34	30-40	50.7±1.1	75.7±1.2	661.8±15.4
PL35	20-30	63.5± 8.1	78.4± 2.8	625.2±12.3
Mean		**64.9±9.7**	**84.7±11.2**	**688.9±111.3**
Range		**45.0 – 85.0**	**63.0 – 112.0**	**493.0 – 951.2**

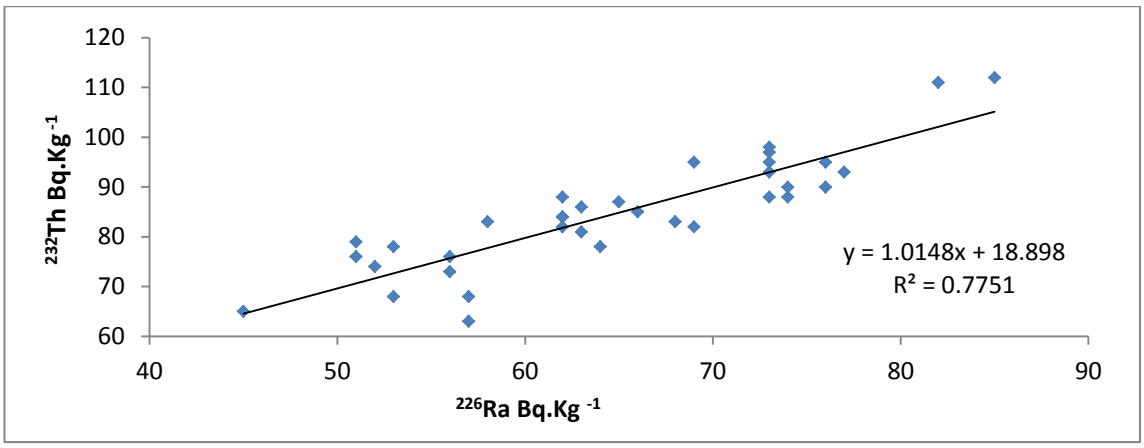

Figure 4.16: The correlation between the concentrations of ^{232}Th and ^{226}Ra for the soil samples from Lanchang

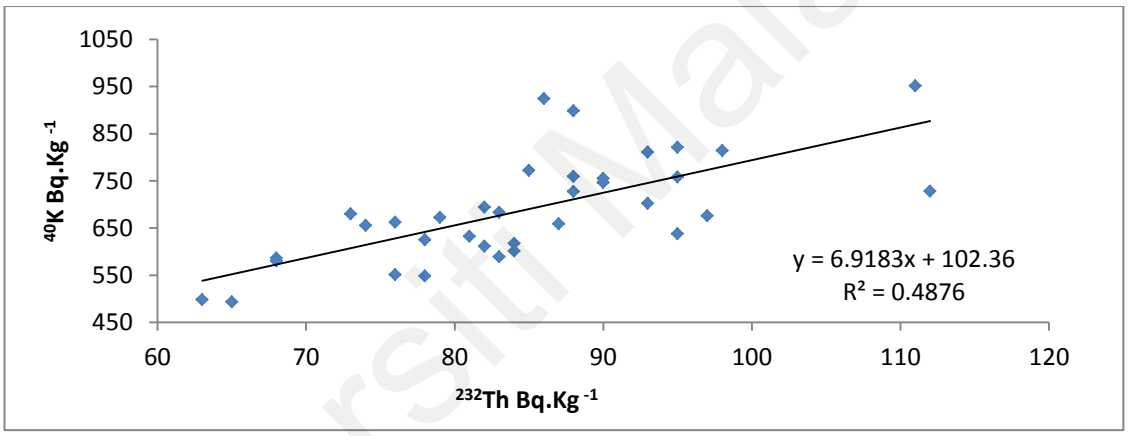

Figure 4.17: The correlation between the concentrations of ^{40}K and ^{232}Th for the soil samples from Lanchang

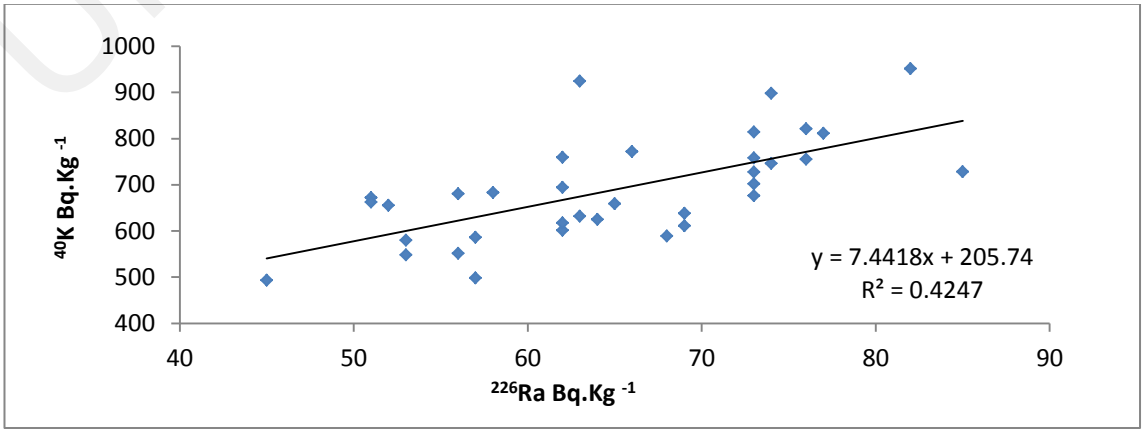

Figure 4.18: The correlation between the concentrations of ^{40}K and ^{226}Ra for the soil samples from Lanchang

The mean values of ^{226}Ra activity concentrations for all the study areas follow the order of Raub (61.8±11.8 Bq.kg^{-1}) < Malacca (62.2±12.8 Bq.kg^{-1}) < Kedah (62.9±8.1 Bq kg^{-1}) < Johor (64.2±11.9 Bq kg^{-1}) < Lanchang (64.9±9.7 Bq.kg^{-1}) < Selangor (67.5±12.0 Bq.kg^{-1}).

The mean values of ^{232}Th activity concentrations for all the study areas follow the order of Kedah (74.9±10.1 Bq kg^{-1}) < Malacca (79.9±15.0 Bq kg^{-1}) < Raub (81.5±12.3 Bq kg^{-1}) < Johor (83.3±12.9 Bq kg^{-1}) < Lanchang (84.7±11.2 Bq kg^{-1}) < Selangor (84.7±12.8.0 Bq kg^{-1}).

The mean values of ^{40}K activity concentrations for all the study areas are follow the order of Malacca (625.1±118.9 Bq kg^{-1}) < Kedah (648.3±84.5 Bq kg^{-1}) < Lanchang (688.9±111.3 Bq kg^{-1}) < Selangor (742.2±145.5 Bq kg^{-1}) < Raub (757.6±161.1Bq kg^{-1}) < Johor (759.3±147.3Bq kg^{-1}) (Figure 4.19).

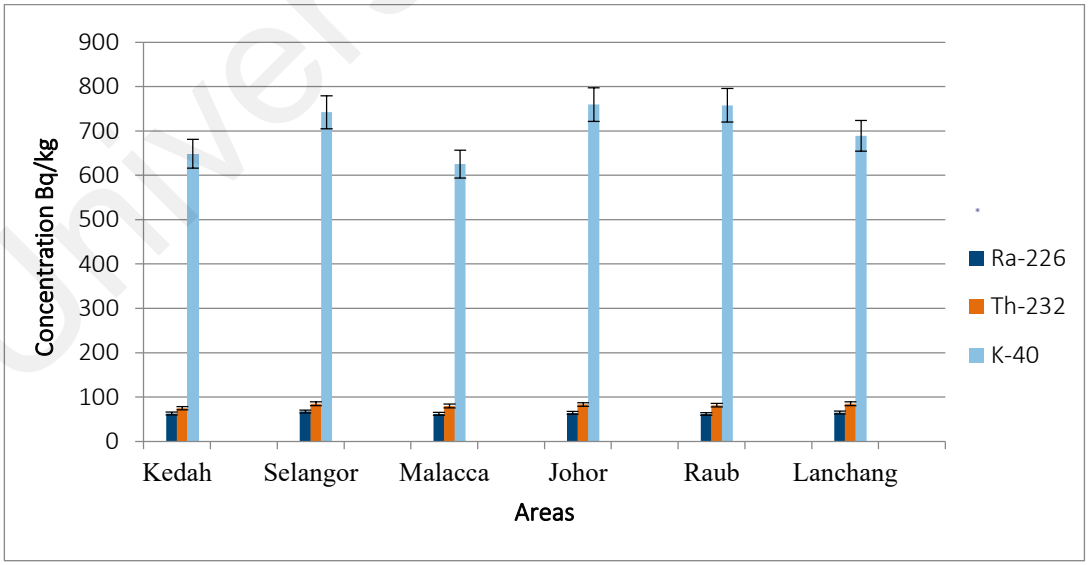

Figure 4.19 The means values of the radionuclides concentration across the study areas

4.2 The vertical distribution of radionuclides in soil

4.2.1 The vertical distribution of radionuclides in Kedah

Table 4.9 depicts the vertical distribution of the ^{226}Ra, ^{232}Th, and ^{40}K activity at the depth profiles. Generally, activity concentrations of ^{226}Ra and ^{232}Th in Kedah show similar trend and regular patterns with the depth. This is owing to their positive association within the soil profile, while ^{40}K showed irregular pattern to ^{226}Ra and ^{232}Th (Figure 4.20). In addition to the regular pattern, soil depth had a distinct decreasing influence on the retention of ^{226}Ra, ^{232}Th, and ^{40}K Bq.kg $^{-1}$. The concentrations of ^{226}Ra, ^{232}Th and ^{40}K tend to decline, with mean values of 67.3, 77.7 and 660.0 Bq.kg^{-1} at the 10 - 20 cm depth, and 57.6, 70.2 and 611.0 Bq.kg^{-1} at the 20-30 cm depth, respectively. At 30-40 cm, the values showed further decrease with mean values of 55.1, 67.3 and 555.2 Bq.kg $^{-1}$. The increase in ^{226}Ra concentrations in the surface layer might be driven by soil bioturbation, which is one of the processes that contribute to the mobility and migration of ^{226}Ra. According to IAEA, (1990), bioturbation may even outperform physicochemical transport in the top 20 cm of soil. Microorganisms, like the roots of plants, can play a significant part in the production of complex elements in huge amounts. The solubility of ^{226}Ra can be greatly increased as a result of this complexity. Furthermore, the ^{226}Ra concentration is linked to OM in the soil's top layer.

The distribution pattern within the soil profile showed that ^{226}Ra does not really migrate through the soil, and that its concentration in the soil depends mainly on the abundance of parent radioactivity in the origin rocks. Vertical distribution of ^{40}K shows a decreasing pattern of the concentrations with the depth (Figure 4.20). Differences in the depth distribution of ^{40}K can generally be attributed to the variability of OM, mineral composition and the soil biological activity including root distribution.

The distribution of ^{226}Ra in the study area agrees with conclusion drawn by Baranov & Morozova (1971), De Jesus *et al*., (1980), Strain *et al.,* (1979), Kaufman *et al.*, (1977), Eadie *et al.,* (1977), De Jesus, (1984), IAstrebov, (1976). Kopp *et al*., (1983) also concluded that ^{226}Ra did not migrate significantly in a particular area of Swiss soil over a period of 45 year.

Table 4.9: The vertical distribution radionuclides ^{226}Ra, ^{232}Th and ^{40}K Bq.kg^{-1} in the soil from Kedah.

Depth cm	^{226}Ra Bq.kg^{-1}	^{232}Th Bq.kg^{-1}	^{40}K Bq.kg^{-1}
0-10	70.75	83.77	762.15
10-20	67.37	77.71	660.00
20-30	57.62	70.29	611.02
30-40	55.12	67.39	555.27
Mean	**62.9±8.1**	**74.9±10.1**	**648.3±84.5**

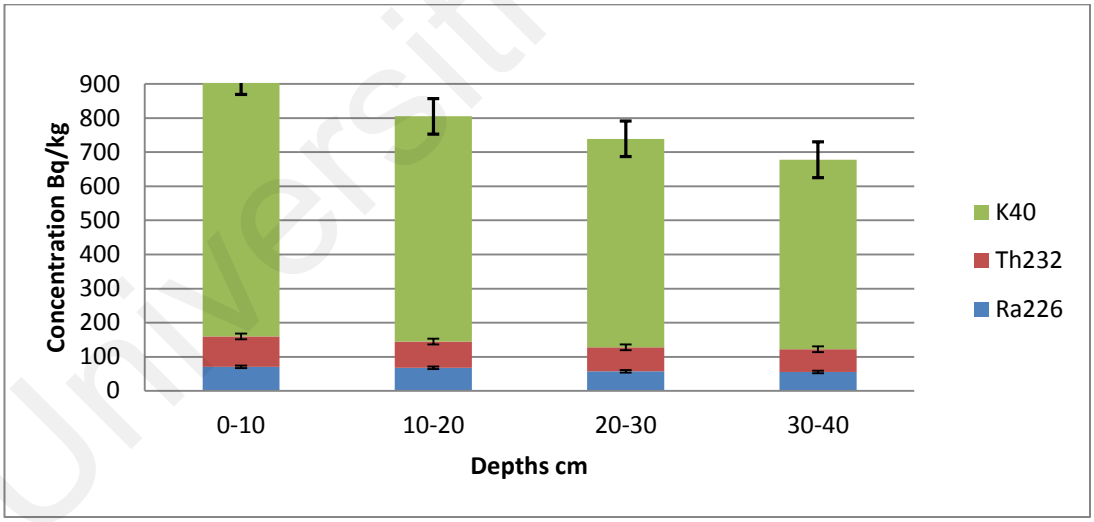

Figure 4.20: The activity concentrations of radionuclides ^{226}Ra, ^{232}Th and ^{40}K at four depths in the soil profile of Kedah

4.2.2 The vertical distribution of radionuclides in Selangor

Table 4.10 shows the vertical distribution of specific activities of radionuclides ^{226}Ra, ^{232}Th and ^{40}K in soil profile of Selangor. ^{226}Ra and ^{232}Th activity concentrations exhibit

a similar trend and consistent pattern with depth. While ^{40}K showed irregular pattern as shown in Figure 4.21. Differences in ^{40}K depth distribution can be ascribed to OM variability, soil mineral content, and biological activity, including root distribution. The ^{226}Ra, ^{232}Th and ^{40}K concentrations tend to decrease at 10-20 cm depth with mean values of 76.87, 95.97 and 855.28 Bq.kg^{-1}, and 64.07, 79.90 and 685.34 Bq.kg^{-1} at 20-30 cm depth, respectively. At the depth of 30-40 cm, the values showed further decrease with mean values of 55.10, 71.64 and 605.58 Bq.kg -1, respectively. Soil depth in Selangor provided a clear decreasing effect on ^{226}Ra, ^{232}Th and ^{40}K concentrations, indicated in Table 4.10.

Table 4.10: The vertical distribution radionuclides ^{226}Ra, ^{232}Th and ^{40}K Bq.kg^{-1} in the soil from Selangor

Depth cm	^{226}Ra Bq.kg^{-1}	^{232}Th Bq.kg^{-1}	^{40}K Bq.kg^{-1}
0-10	74.94	91.10	816.59
10-20	76.87	95.97	855.28
20-30	64.07	79.90	685.34
30-40	54.10	71.64	605.58
Mean	**67.5±12.0**	**84.7±12.8**	**742.2±145.5**

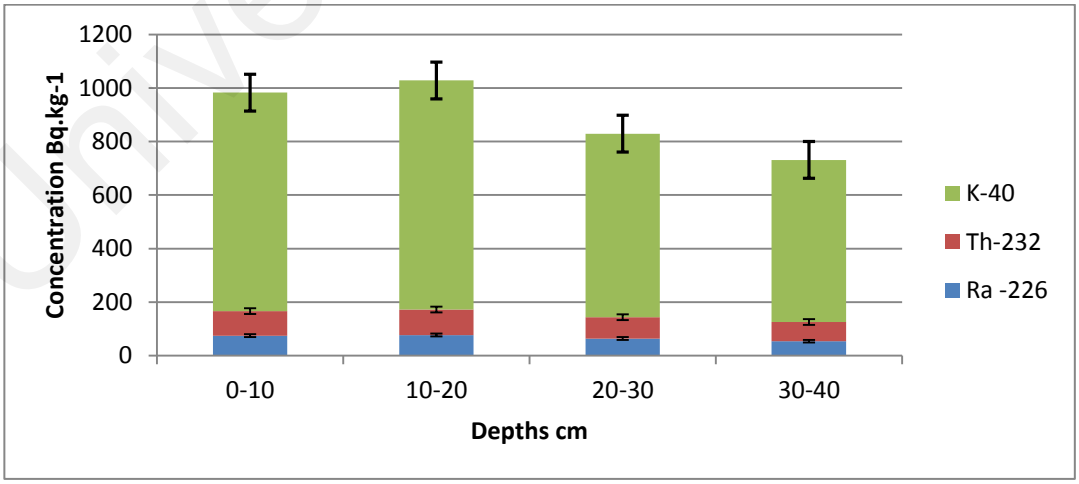

Figure 4.21: The vertical distributions of radionuclide concentrations ^{226}Ra, ^{232}Th and ^{40}K at four depths in the soil profile from Selangor

4.2.3 The vertical distribution of radionuclides in Malacca

Table 4.11 shows the vertical distribution of of the radionuclides activities of ^{226}Ra, ^{232}Th and ^{40}K in soil from Malacca. The activity concentrations of ^{226}Ra and ^{232}Th follow a similar trend and regular pattern with depth, but ^{40}K has an erratic pattern (Figure 4.22).

The vertical pattern of distribution within the soil matrix did not differ substantially from patterns of radionuclide concentrations in Kedah and Selangor soil profiles. This might be because natural radionuclides are more abundant in the fine soil fraction because they bind to clay minerals, as they absorb onto clay surfaces or become fixed within the lattice structure. In the study areas, clays (0.002 mm - 0.06 mm) dominated most the soil groups.

Therefore, the range of values was sufficiently wide to produce strong correlations with the radionuclides. The ^{226}Ra, ^{232}Th and ^{40}K concentrations tend to decrease with mean values of 73.75, 95.22 and 750.45 Bq.kg^{-1} at the depth of 10-20 cm, and 55.47, 70.33 and 547.41 Bq.kg^{-1} at the depth of 20-30 cm, respectively. At 30-40 cm, the values showed further decrease with means of 48.83, 65.30 and 540.58 Bq.kg -1, respectively.

Table 4.11: The vertical distribution radionuclides ^{226}Ra, ^{232}Th and ^{40}K Bq.kg^{-1} in the soil from Malacca

Depth cm	^{226}Ra Bq.kg^{-1}	^{232}Th Bq.kg^{-1}	^{40}K Bq.kg^{-1}
0-10	71.23	88.96	657.71
10-20	73.75	95.22	750.45
20-30	55.47	70.33	547.14
30-40	48.83	65.30	540.58
Mean	**62.2±12.8**	**79.9±15.0**	**625.1±118.9**

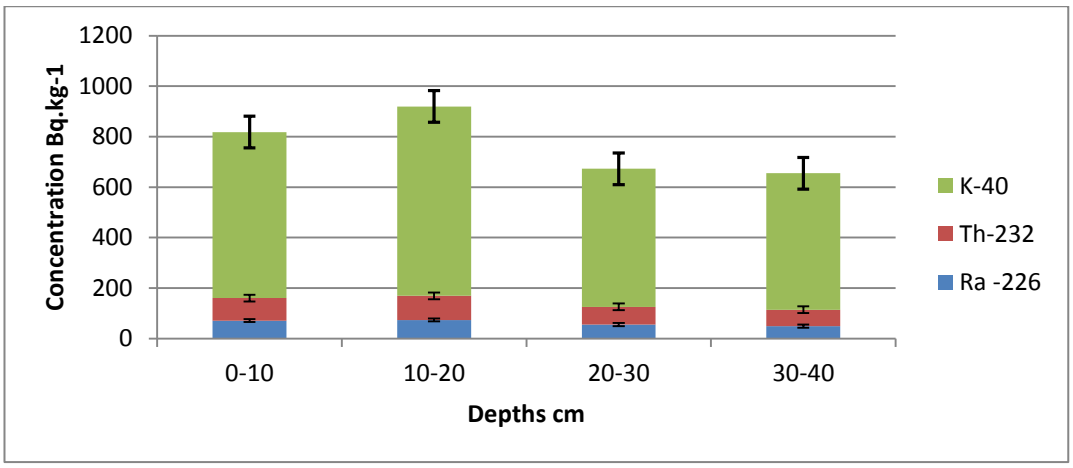

Figure 4.22: The vertical distributions of radionuclide concentrations ^{226}Ra, ^{232}Th and ^{40}K at four depths in the soil profile from Malacca

4.2.4 The vertical distribution of radionuclides in Johor

Table 4.12 depicts the vertical distribution of radionuclide activity ^{226}Ra, ^{232}Th, and ^{40}K in a Johor soil profile. Radionuclide concentrations decreased with depth in the soil profile. The activity concentrations of ^{226}Ra and ^{232}Th exhibit a similar trend and regular pattern with depth; however ^{40}K displayed an erratic distribution pattern (Figure 4.23). The vertical distribution pattern within the soil matrix was not significantly different from the radionuclides behaviour in the soil profiles of Kedah, Selangor, and Malacca. The ^{226}Ra, ^{232}Th and ^{40}K concentrations tend to decrease with mean values of 75.97, 95.90 and 880.69 Bq.kg^{-1} at the depth 10-20 cm, and 56.20, 74.77 and 703.93 Bq.kg^{-1} at the depth of 20-30 cm, respectively. At 30-40 cm, the values showed further decrease with means of 53.26, 72.31and 631.84 Bq.kg $^{-1}$, respectively.

Table 4.12: The vertical distribution radionuclides ^{226}Ra, ^{232}Th and ^{40}K Bq.kg^{-1} in the soil from Johor

Depth cm	^{226}Ra Bq.kg^{-1}	^{232}Th Bq.kg^{-1}	^{40}K Bq.kg^{-1}
0-10	67.14	85.94	772.95
10-20	75.97	95.90	880.69
20-30	57.86	76.58	718.35
30-40	53.26	72.31	631.84
Mean	**64.2±11.9**	**83.3±12.9**	**759.3±147.3**

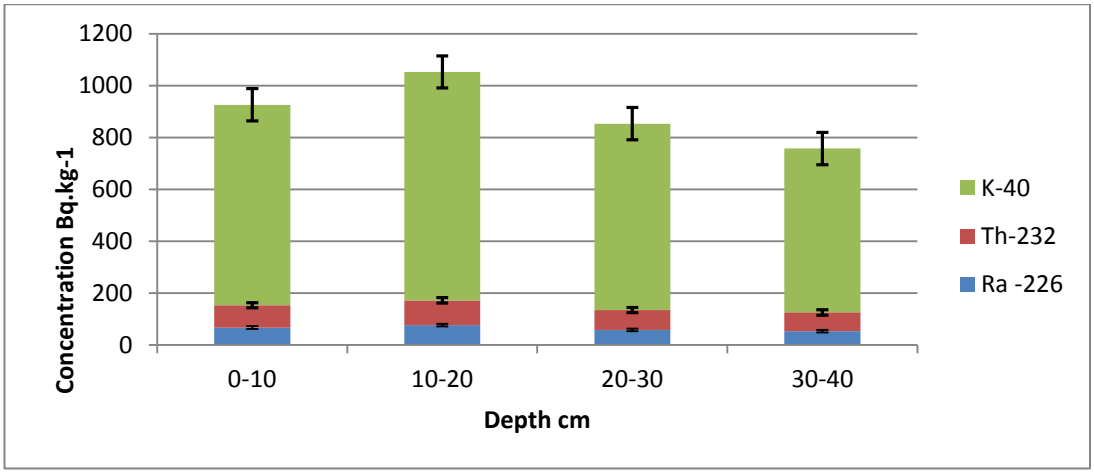

Figure 4.23: The vertical distributions of radionuclide concentrations ^{226}Ra, ^{232}Th and ^{40}K at four depths in the soil profile from Johor

4.2.5 The vertical distribution of radionuclides in Raub

Table 4.13 shows the vertical distribution of radionuclide activites of ^{226}Ra, ^{232}Th, and ^{40}K in Raub soil. The activity concentrations of ^{226}Ra and ^{232}Th followed a similar pattern and trend with soil depths (Figure 4.24). The soil profile revealed declining retention of ^{226}Ra, ^{232}Th, and ^{40}K at lower depths, where concentrations of ^{226}Ra and ^{232}Th decreasing at depths of 20-30 and 30-40 cm, respectively. The vertical profile of ^{40}K, on the other hand, revealed an irregular pattern with depth. At a depth of 10-20 cm, the concentrations of ^{226}Ra, ^{232}Th, and ^{40}K tend to drop, with mean values of 68.07, 87.37, and 830.66 Bq.kg^{-1}, respectively, and 59.96, 79.34, and 701.56 Bq.kg^{-1} at a depth of 20-30 cm, respectively. The values dropped much further at 30-40 cm, with mean values of 53.44, 74.35, and 684.47 Bq.kg $^{-1}$, respectively.

Table 4.13: The vertical distribution radionuclides ^{226}Ra, ^{232}Th and ^{40}K Bq.kg^{-1} in the soil from Raub

Depth cm	^{226}Ra Bq.kg^{-1}	^{232}Th Bq.kg^{-1}	^{40}K Bq.kg^{-1}
0-10	67.33	86.50	828.45
10-20	68.07	87.37	830.66
20-30	59.96	79.34	701.56
30-40	53.44	74.35	684.47
Mean	**61.8±11.8**	**81.5±12.3**	**757.6±161.1**

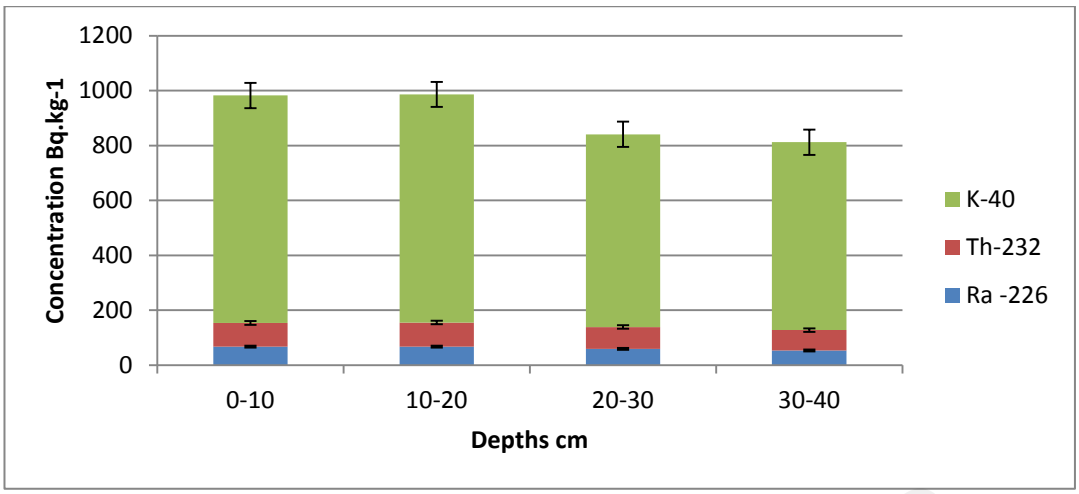

Figure 4.24: The vertical distributions of radionuclide concentrations ^{226}Ra, ^{232}Th and ^{40}K at four depths in the soil profile from Raub

4.2.6 The vertical distribution of radionuclides in Lanchang

Table 4.14 shows the vertical distribution of radionuclides ^{226}Ra, ^{232}Th, and ^{40}K in the Lanchang soil profile. The activity concentrations of ^{226}Ra and ^{232}Th in the investigated region follow a consistent pattern with depth (Figure 4.25). The soil profile exhibited a drop in ^{226}Ra, ^{232}Th, and ^{40}K concentrations at low depths, ^{226}Ra and ^{232}Th concentrations decreasing at depths of 20-30 and 30-40 cm. The vertical distribution of the ^{40}K profile in the soil, on the other hand, suggests an irregular depth pattern. This divergence can be explained by the fact that ^{40}K has a negative association with soil particle size and OM concentration, but ^{232}Th has a positive linear correlation with clay content.

At 10 - 20 cm deep, ^{226}Ra, ^{232}Th, and ^{40}K concentrations tend to drop, with mean values of 72.85, 93.72, and 734.73 Bq.kg^{-1}, respectively, and 61.75, 82.13, and 645.20 Bq.kg^{-1} at 20-30 cm depth. At 30–40 cm, the values dropped even further, to 52.44, 70.11, and 574.40 Bq.kg $^{-1}$, respectively.

Table 4.14: The vertical distribution radionuclides ^{226}Ra, ^{232}Th and ^{40}K Bq.kg^{-1} in the soil from Lanchang

Depth cm	^{226}Ra Bq.kg^{-1}	^{232}Th Bq.kg^{-1}	^{40}K Bq.kg^{-1}
0-10	67.04	86.55	764.26
10-20	72.85	93.72	734.73
20-30	61.75	82.13	645.20
30-40	52.44	70.11	574.40
Mean	**64.9±9.7**	**84.7±11.2**	**688.9±111.3**

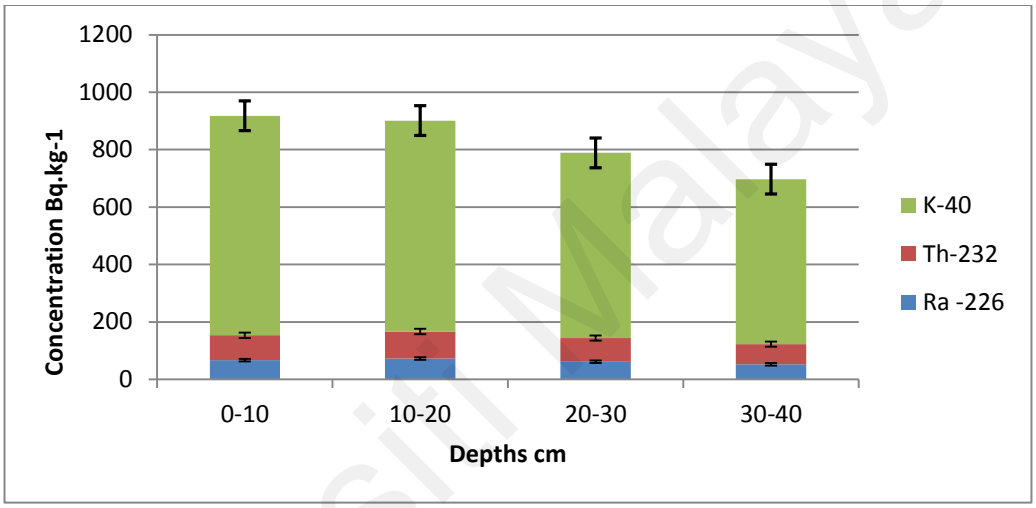

Figure 4.25: The vertical distributions of radionuclide concentrations ^{226}Ra, ^{232}Th and ^{40}K at four depths in the soil profile from Lanchang

The vertical distribution values of the ^{226}Ra at 0-10 cm depth for soil groups follow the order of Lanchang (67.04 Bq.kg $^{-1}$) < Raub (67.33 Bq.kg $^{-1}$) < Johor (68.39 Bq.kg $^{-1}$) < Kedah (70.75 Bq.kg $^{-1}$) < Malacca (71.23 Bq.kg $^{-1}$) < Selangor (74.94 Bq.kg $^{-1}$).

The vertical distribution values of ^{226}Ra at depth of 10-20 cm follow the order of Kedah (67.37 Bq.kg $^{-1}$) < Raub (68.07 Bq.kg $^{-1}$) < Lanchang (72.85 Bq.kg $^{-1}$) < Malacca (73.75 Bq.kg $^{-1}$) < Johor (75.97 Bq.kg $^{-1}$) < Selangor (76.87 Bq.kg^{-1}).

At the depth of 20-30 cm the vertical distribution values of ^{226}Ra follow the order of Malacca (55.47 Bq.kg $^{-1}$) < Johor (56.20 Bq.kg $^{-1}$) < Kedah (57.62 Bq.kg $^{-1}$) < Raub

(59.96 Bq.kg $^{-1}$) < Lanchang (61.75 Bq.kg $^{-1}$) < Selangor (64.07 Bq.kg $^{-1}$), while, the values follow the order of Malacca (48.83 Bq.kg $^{-1}$) < Pahang Lanchang (52.44 Bq.kg $^{-1}$) < Johor (53.26 Bq.kg $^{-1}$) < Pahang Raub (53.44 Bq.kg $^{-1}$) < Selangor (54.10 Bq.kg $^{-1}$) < Kedah (55.12 Bq.kg $^{-1}$), at 30-40 cm depth.

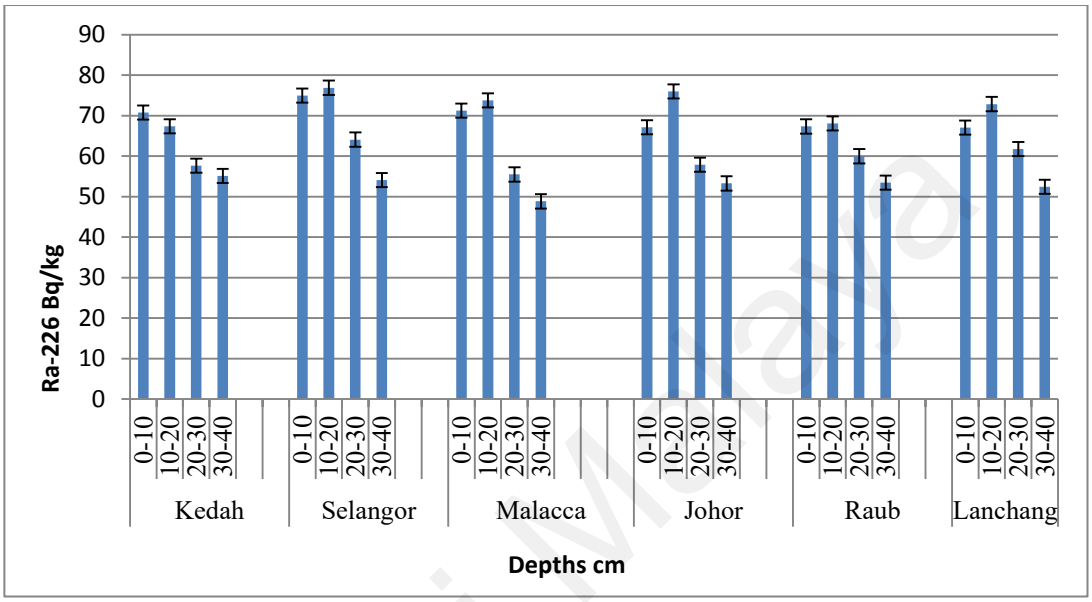

Figure 4.26: The vertical distribution of ^{226}Ra within four depths across the study areas

The vertical distribution values of the ^{232}Th at the depth of 0-10 cm for the study areas follow the order of Kedah (70.75 Bq.kg $^{-1}$) < Raub (86.50 Bq.kg $^{-1}$) < Lanchang (86.55 Bq.kg $^{-1}$) < Johor (87.31 Bq.kg $^{-1}$) < Malacca (88.96 Bq.kg $^{-1}$) < Selangor (91.10 Bq.kg $^{-1}$).

At 10-20 cm depth, the vertical distribution values of ^{232}Th follow the ordre of Kedah (67.37 Bq.kg $^{-1}$) < Raub (67.37 Bq.kg $^{-1}$) < Lanchang (93.72 Bq.kg $^{-1}$) < Malacca (95.22 Bq.kg $^{-1}$) < Johor (95.90 Bq.kg $^{-1}$) < Selangor (95.97 Bq.kg $^{-1}$).

The values of ^{232}Th at 20-30 cm depth follow the order of Kedah (57.62 Bq.kg $^{-1}$) < Malacca (70.33 Bq.kg $^{-1}$) < Johor (74.77 Bq.kg $^{-1}$) < Raub (79.34 Bq.kg $^{-1}$) < Selangor (79.90 Bq.kg $^{-1}$) < Lanchang (82.13 Bq.kg $^{-1}$), whereas, at 30-40 cm depth, they follow

the order of Kedah (55.12 Bq.kg $^{-1}$) < Malacca (65.30 Bq.kg $^{-1}$) < Lanchang (70.11Bq.kg $^{-1}$) < Selangor (71.64 Bq.kg $^{-1}$) < Johor (72.31 Bq.kg $^{-1}$) < Raub (74.35 Bq.kg $^{-1}$).

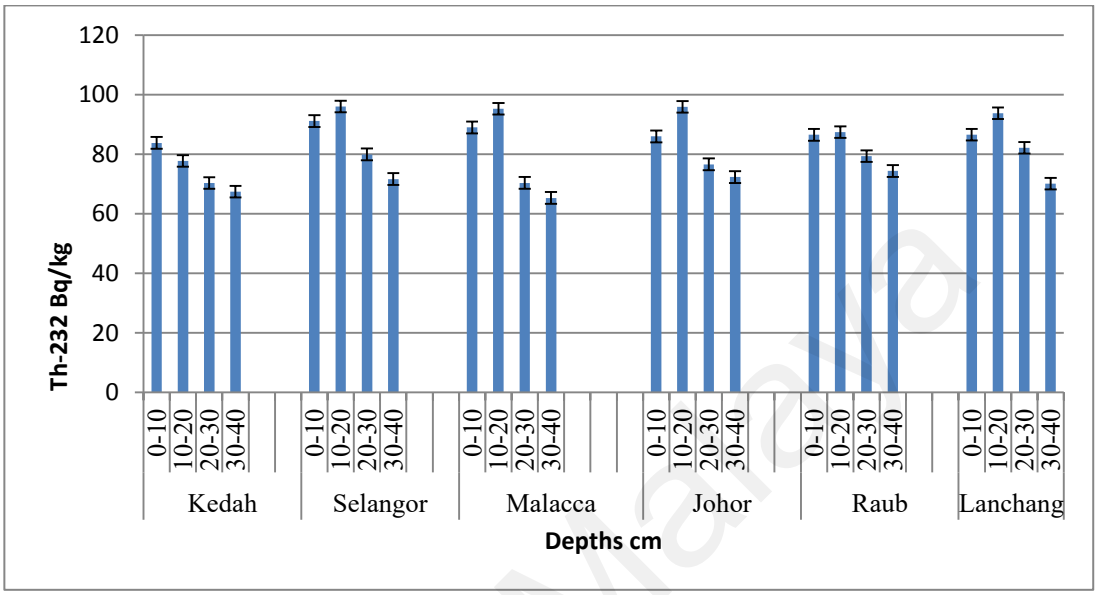

Figure 4.27: The vertical distribution of ^{232}Th within four depths across the study areas

The vertical distribution values of the ^{40}K at 0-10 cm depth for study areas follow the order of Malacca (657.71 Bq.kg $^{-1}$) < Kedah (762.15 Bq.kg $^{-1}$) < Lanchang (764.26 Bq.kg $^{-1}$) < Johor (814.30 Bq.kg $^{-1}$) < Selangor (816.59 Bq.kg $^{-1}$) < Raub (828.45 Bq.kg $^{-1}$).

The values of ^{40}K at 10-20 cm depth follow the order of Kedah (660.00 Bq.kg $^{-1}$) < Lanchang (734.73 Bq.kg $^{-1}$) < Malacca (750.45 Bq.kg $^{-1}$) < Raub (830.66 Bq.kg $^{-1}$) < Selangor (855.28 Bq.kg $^{-1}$) < Johor (880.69 Bq.kg $^{-1}$).

At the depth of 20-30 cm the vertical distribution values of ^{40}K follow the order of Malacca (547.14 Bq.kg $^{-1}$) < Kedah (611.02 Bq.kg $^{-1}$) < Lanchang (645.20 Bq.kg $^{-1}$) < Selangor (685.34 Bq.kg $^{-1}$) < Raub (701.56 Bq.kg $^{-1}$) < Johor (703.93 Bq.kg $^{-1}$), while,

the values follow the order of Malacca (540.58 Bq.kg $^{-1}$) < Kedah (555.27 Bq.kg $^{-1}$) < Lanchang (574.40 Bq.kg $^{-1}$) < Selangor (605.58 Bq.kg $^{-1}$) < Johor (631.84 Bq.kg $^{-1}$) < Raub (684.47 Bq.kg $^{-1}$), for 30-40 cm depth.

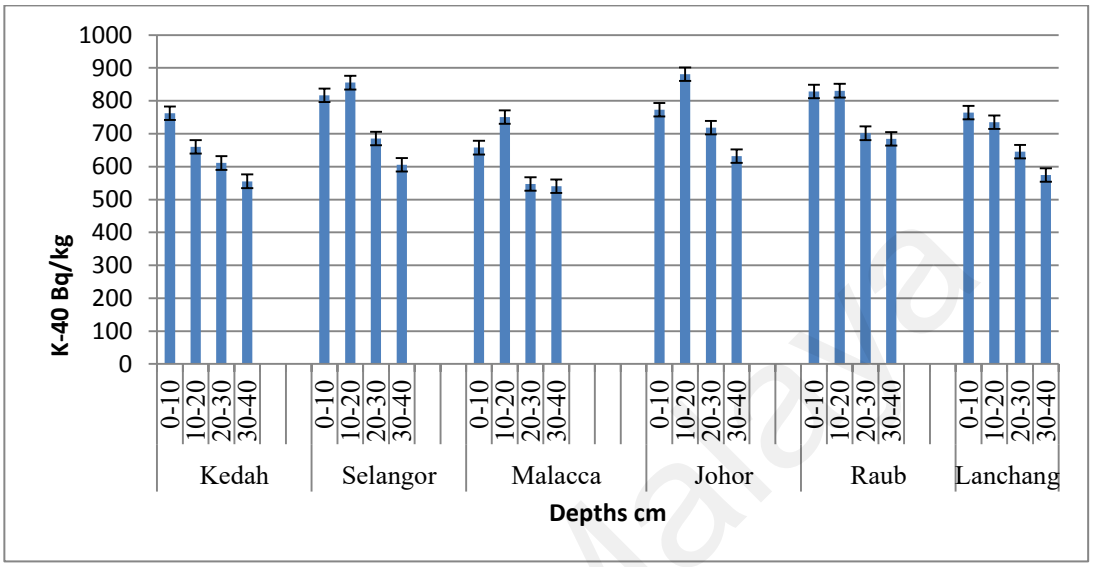

Figure 4.28: The vertical distribution of ^{40}K within four depths across the study areas

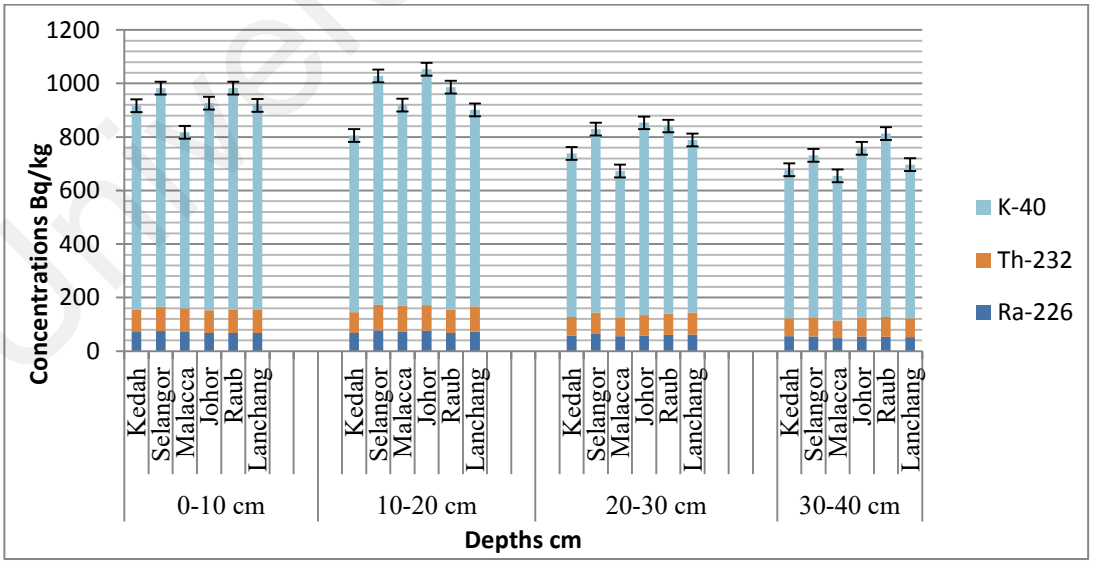

Figure 4.29: The means values of the radionuclides concentration across the study areas

Variation in the movement of radionuclides across the soil matrix may be attributed to the clays of low exchange activity, such as kaolinite, are more common than in temperate zones. This is consistent with Wasserman *et al.,* (2002) suggestion that low exchange capacity of tropics soil can lead to increased mobility of radionuclides through the soil layers. Morever, in tropical conditions, practically all organic material that reaches the soil surface decomposes quickly, resulting in limited soil organic matter accumulating on the surface. As a result, nutrients and pollutants are rapidly recycled into the vegetation, this agrees with Velasco *et al.,* (2008) conclusion.

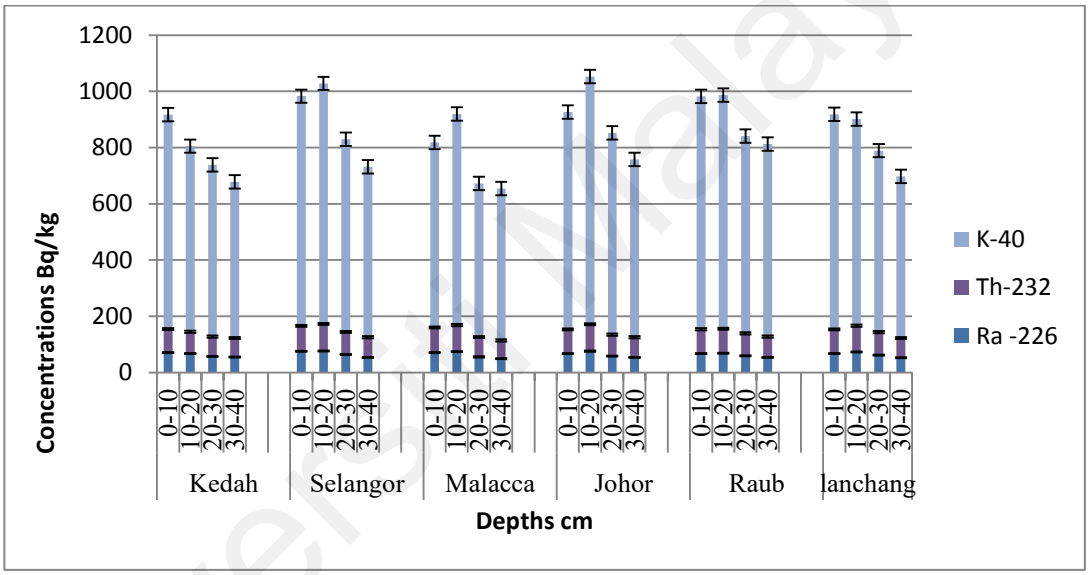

Figure 4.30: The vertical distribution the radionuclides in the soil profile of study areas

Because soils are determined by particular characteristics, such as clay content or organic matter content, the radiometric fingerprint of vertical distribution pattern can be compared to these characteristics. The difference is generally attributed to OM diversity, mineral composition and soil biological activity including root distribution. Radium content in soil is related to organic matter (OM), and because it is more mobile than measured radionuclides, it can seep into soils with low pH and high OM.

The non-similarity in the vertical distribution pattern between ^{40}K and ^{226}Ra may be ascribed to their weak correlation, which is owing to ^{226}Ra's comparatively high solubility and therefore mobility.Soil properties may differentially affect uptake processes, migration, , as well as the biological fixation of these radionuclides in the terrestrial ecosystem. The study found that tropical soils have a diminishing tendency of OM, which is a major regulator of chemical, physical, and biological aspects of the soil. This finding is consistent with earlier researches. Based on these findings, ^{226}Ra and ^{232}Th, which have similar depth distributions, are distinct from the ^{40}K isotope, where they are closely connected to Mn and Fe oxides and maintain a very steady profile down the profiles. Mamouna and Khater (2004), Navas *et al.,* (2005) and Van Henten *et al.,* (2009) also reported that the vertical distribution pattern of ^{40}K differed from that of ^{226}Ra and ^{232}Th. Hamzah *et al.,* (2014) discovered a decrease in ^{226}Ra, ^{232}Th, and ^{40}K concentrations as depth increased.

4.3 Edaphic factors influencing radionuclide distribution in soil

In an effort to determine the chemical properties of soil that would be closely related to the radionuclide behavior, separate samples were obtained in each depth.

As the data were accumulated, it became evident that the chemical environment, climate, as well as human practices differs from site to site, and hence it must be recognized that while patterns can be established through summary data, individual sites may deviate from these trends or be consistent in a uniform response to interaction factors. Tables 4.22 to 4.37 summarise data on essential chemical properties that would be anticipated to have connections with radionuclide distributions.

4.3.1 Distribution of organic matter (OM) and soil pH

4.3.1.1 Distribution of organic matter (OM) and soil pH in Kedah

The calculated values of OM and soil pH in the samples from Kedah are presented in Table 4.15. The measured value of soil pH varied from 3.24 to 4.87, with a mean value of 4.20 $\pm$ 0.4, which falls within the rate of acidic soil. While, the OM values varied from 2.06 to 4.15, with a mean value of 3.01 $\pm$ 0.7%, which lies within the range of OM-poor soils due to the rapid degradation rates of OM in tropical soils.

Figure 4.31 shows the vertical distribution of soil pH and OM within the soil matrix in Kedah, it shows an increase in the level of pH with a decrease in OM values. The difference in the soil pH between depths may be related to the quantities of Al rather than OM. The vertical distribution of pH and OM within the soil matrix is shown in Table 4.16.

The soil pH was slightly lower at the top 0-10 cm with a mean pH of 3.58, while the pH at the depths of 10-20, 20-30 and 30-40 cm, measured to be 4.23, 4.34 and 4.65, respectively. The soil OM value was slightly higher at the top 0-10 cm with pH 3.94, before showing a gradual decrease at 10-20, 20-30 and 30-40 cm depths, with mean pH values of 3.06 2.67 and 2.35, respectively. Figure 4.31 shows the distribution patterns of pH and OM within the soil matrix in Kedah, which showed a different distribution pattern within soil depths. The relationships between pH, OM and the radionuclides activities are presented in Table 4.17. The relationship between soil pH and radionuclides (^{226}Ra, ^{232}Th and ^{40}K) was negatively correlated at ($P \leq 0.01$), while OM was positively correlated at ($P \leq 0.01$) with radionuclides (^{226}Ra, ^{232}Th and ^{40}K) activities. The relationship between OM and soil pH was negatively correlated at ($P \leq 0.01$) in Kedah.

Table 4.15: The soil pH and organic matter (OM) in the soil samples from Kedah

Sample ID	Depth cm	pH	OM%
AS1	10-20	4.15	2.67
AS2	20-30	4.36	2.12
AS3	0-10	3.52	4.15
AS4	10-20	4.17	3.18
AS5	30-40	4.75	2.15
AS6	0-10	3.58	4.12
AS7	10-20	4.17	3.24
AS8	0-10	3.63	3.66
AS9	20-30	4.36	2.75
AS10	10-20	4.34	3.07
AS11	0-10	3.63	3.86
AS12	10-20	4.17	3.04
AS13	20-30	4.32	2.65
AS14	30-40	4.65	2.11
AS15	0-10	3.24	3.88
AS16	20-30	4.38	2.63
AS17	30-40	4.52	4.02
AS18	20-30	4.37	3.67
AS19	10-20	4.15	3.04
AS20	30-40	4.35	2.13
AS21	10-20	4.56	3.05
AS22	30-40	4.87	2.45
AS23	20-30	4.32	2.84
AS24	30-40	4.67	2.06
AS25	0-10	3.62	4.11
AS26	30-40	4.63	2.12
AS27	10-20	4.23	3.11
AS28	20-30	4.38	2.18
AS29	30-40	4.78	2.08
AS30	20-30	4.35	2.32
AS31	10-20	4.26	3.05
AS32	0-10	3.58	4.12
AS33	10-20	4.21	3.05
AS34	0-10	3.64	3.87
AS35	20-30	4.25	2.87
AS36	30-40	4.62	2.14
AS37	0-10	3.63	3.87
AS38	10-20	4.21	3.23
AS39	0-10	3.77	3.76
AS40	30-40	4.66	2.25
Mean		**4.2±0.4**	**3.01±0.7**
Range		**3.24-4.87**	**2.06-4.15**

Table 4.16: The vertical distribution patterns of pH and OM% within the soil matrix in Kedah

Depth cm	Soil pH	Organic Matter OM%
0-10	3.58	3.94
10-20	4.23	3.06
20-30	4.34	2.67
30-40	4.65	2.35
Mean	**4.20±0.4**	**3.01±0.7**
Range	**3.24 - 4.87**	**2.06 - 4.15**

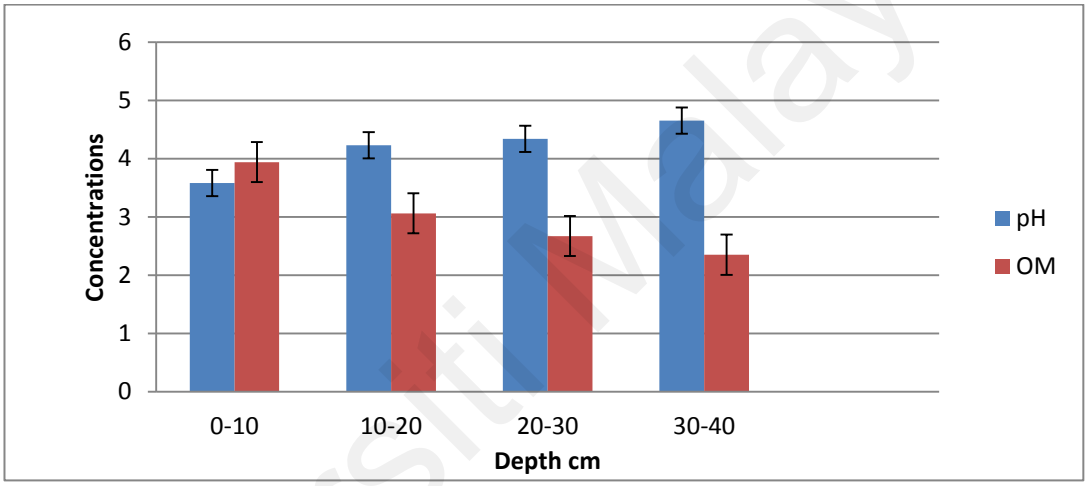

Figure 4.31: The vertical distribution of soil pH and organic matter OM% within the soil matrix in Kedah

Table 4.17: Pearson correlation coefficients between the soil pH and OM% and the radionuclides Bq.kg^{-1} in the samples from Kedah

	^{226}Ra	^{232}Th	^{40}K	pH	OM%
^{226}Ra	1				
^{232}Th	0.812**	1			
^{40}K	0.737**	0.596**	1		
pH	-0.634**	-0.554**	-0.860**	1	
OM%	0.535**	0.495**	0.762**	-0.828**	1

**. Correlation is significant at the 0.01 level (2-tailed).
*. Correlation is significant at the 0.05 level (2-tailed).

4.3.1.2 **Distribution of organic matter (OM) and soil pH in Selangor**

The calculated values of OM and soil pH in the samples from Selangor are presented in Table 4.18. The measured value of soil pH varied from 3.43 to 4.85, with a mean pH value of 4.18±0.4, which falls within the rate of acidic soil. While, the OM values varied from 0.64 to 2.87, with a mean value of 1.43±0.6, due to the accelerated degradation rates of OM in tropical soils, the value falls within the spectrum of soils low in OM.

Table 4.19 shows the vertical distribution of soil pH and OM within the soil matrix in Selangor, it shows an increase in the level of pH in conjunction with a decrease in the values of OM with the depths. The soil pH was slightly lower at the top 0-10 cm with a mean value of 3.54, while the mean values at the depth of 10-20, 20-30 and 30-40 cm given to be 4.09, 4.34 and 4.77, respectively. The soil OM value was slightly higher in the top 0-10 cm with a mean value of 2.38, before showing a gradual decrease at the depths of 10-20, 20-30 and 30-40 cm, with mean values of 1.60, 0.98 and 0.73, respectively. Figure 4.32 shows the distribution patterns of pH and OM within the soil matrix in Selangor, where showed a different distribution direction within soil depths.

The relationships between pH, OM and the radionuclides activities are presented in Table 4.20. The relationship between soil pH and radionuclides (^{226}Ra, ^{232}Th and ^{40}K) was negatively correlated at ($P \leq 0.01$), while OM was positively correlated at ($P \leq 0.01$) with radionuclides (^{226}Ra, ^{232}Th and ^{40}K) activities. The relationship between OM and soil pH is negatively correlated at ($P \leq 0.01$).

Table 4.18: The soil pH and organic matter (OM) in the soil samples from Selangor

Sample ID	Depth cm	pH	OM%
S1	0-10	3.52	2.87
S2	10-20	4.15	1.82
S3	0-10	3.52	2.55
S4	0-10	3.52	2.28
S5	0-10	3.43	2.25
S6	10-20	4.18	1.02
S7	0-10	3.68	2.46
S8	20-30	4.21	0.76
S9	20-30	4.26	0.84
S10	10-20	4.24	1.75
S11	20-30	4.23	0.86
S12	30-40	4.85	0.74
S13	30-40	4.76	0.75
S14	20-30	4.35	1.85
S15	10-20	3.84	1.68
S16	30-40	4.78	0.73
S17	20-30	4.32	0.92
S18	30-40	4.82	0.77
S19	10-20	3.95	1.65
S20	30-40	4.75	0.73
S21	20-30	4.42	0.85
S22	30-40	4.85	0.72
S23	30-40	4.73	0.74
S24	20-30	4.37	0.96
S25	0-10	3.46	2.18
S26	10-20	4.18	1.72
S27	0-10	3.62	2.21
S28	10-20	4.14	1.28
S29	0-10	3.55	2.28
S30	20-30	4.56	0.82
S31	0-10	3.56	2.35
S32	10-20	4.05	1.75
S33	30-40	4.73	0.75
S34	30-40	4.72	0.64
S35	10-20	4.15	1.73
Mean		**4.18±0.4**	**1.43±0.6**
Range		**3.43 - 4.85**	**0.64 - 2.87**

Table 4.19: The vertical distribution patterns of pH and OM% within the soil matrix in Selangor

Depth cm	Soil pH	Organic Matter OM%
0-10	3.54	2.38
10-20	4.09	1.60
20-30	4.34	0.98
30-40	4.77	0.73
Mean	**4.18±0.4**	**1.43±0.6**

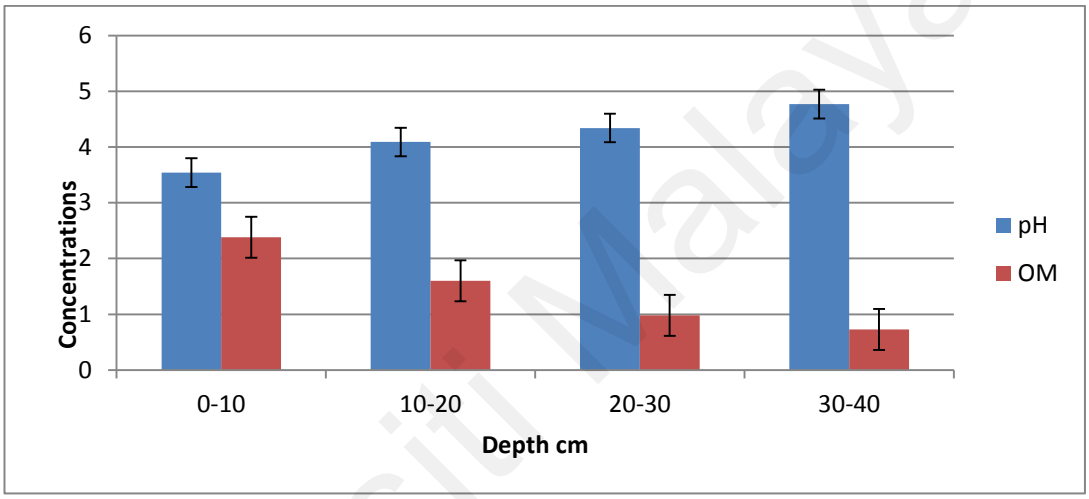

Figure 4.32: The vertical distribution of soil pH and organic matter OM% within the soil matrix in Selangor

Table 4.20: Pearson correlation coefficients between the soil pH and OM% and the radionuclides Bq.kg^{-1} in the samples from Selangor

	^{226}Ra	^{232}Th	^{40}K	pH	OM
^{226}Ra	1				
^{232}Th	0.943**	1			
^{40}K	0.784**	0.831**	1		
pH	-0.654**	-0.613**	-0.608**	1	
OM	0.669**	0.629**	0.616**	-0.904**	1

**. Correlation is significant at the 0.01 level (2-tailed).
*. Correlation is significant at the 0.05 level (2-tailed).

4.3.1.3 **Distribution of organic matter (OM) and soil pH in Malacca**

The calculated values of OM and soil pH in the samples from Malaca are presented in Table 4.21. The measured value of the soil pH varied from 3.25 to 5.57, with a mean value of 4.10±0.4, which falls within the levels of acidic soil. While, the OM values varied from 2.17 to 4.15, with a mean value of 3.12±0.6, this comes within the spectrum of soils poor in OM because of the rapid OM depletion rates in tropical soils. Table 4.22 shows the vertical distribution of pH and OM within the soil matrix. The soil pH was slightly lower at the top 0-10 cm with a mean value of 3.60, while at the depths of 10-20, 20-30 and 30-40 cm, the mean values were given to be 3.91, 4.15 and 4.71, respectively. The soil OM value was slightly higher in the top 0-10 cm with a mean value of 3.88, before showing a gradual decrease at the depths of 10-20, 20-30 and 30-40 cm, with mean values of 3.54, 2.81and 2.29, respectively. The vertical distribution of the soil pH and OM within the soil matrix in Malaca indicates an increase of pH level in conjunction with a decrease in OM values with depth as shown in Figure 4.39. The pH and OM distribution patterns within the soil matrix in Malaca show a different distribution trends within soil depths, as seen in Figure 4.33.

The relationships between pH, OM and the radionuclides activities are presented in Table 4.23. The data showed that relationship between soil pH and radionuclides (^{226}Ra, ^{232}Th and ^{40}K) was negatively correlated at ($P \leq 0.01$), while OM positively correlated at ($P \leq 0.01$) with radionuclides (^{226}Ra, ^{232}Th and ^{40}K) activities. The relationship between OM and soil pH is negatively correlated at ($P \leq 0.01$).

Table 4.21: The soil pH and organic matter (OM) in the soil samples from Malacca

Sample ID	Depth cm	pH	OM%
M1	20-30	4.26	2.18
M2	0-10	3.64	3.72
M3	30-40	4.64	2.25
M4	20-30	3.95	3.38
M5	10-20	3.83	3.55
M6	30-40	4.48	2.25
M7	10-20	3.85	3.44
M8	20-30	4.34	2.42
M9	30-40	4.85	2.25
M10	10-20	3.92	3.57
M11	0-10	3.55	3.61
M12	20-30	4.25	2.34
M13	0-10	3.64	4.15
M14	10-20	3.85	3.53
M15	10-20	3.75	3.62
M16	0-10	3.55	4.12
M17	20-30	4.32	3.32
M18	30-40	4.52	2.17
M19	30-40	5.57	2.24
M20	30-40	4.62	2.17
M21	10-20	3.82	3.55
M22	10-20	3.75	3.61
M23	0-10	3.55	3.87
M24	20-30	4.36	2.86
M25	30-40	4.76	2.51
M26	20-30	3.25	3.42
M27	10-20	4.12	3.51
M28	0-10	3.64	3.72
M29	0-10	3.56	3.75
M30	20-30	4.32	2.72
M31	30-40	4.72	2.45
M32	0-10	3.65	4.06
M33	10-20	3.93	3.55
M34	0-10	3.62	3.97
M35	10-20	4.28	3.55
M36	20-30	4.35	2.72
M37	30-40	4.42	2.38
M38	30-40	4.52	2.27
Mean		**4.10±0.4**	**3.12±0.6**
Range		**3.25 - 5.57**	**2.17 - 4.15**

Table 4.22: The vertical distribution patterns of pH and OM within the soil matrix in Malacca

Depth cm	Soil pH	Organic Matter OM%
0-10	3.60	3.88
10-20	3.91	3.54
20-30	4.15	2.81
30-40	4.71	2.29
Mean	**4.10±0.4**	**3.12±0.6**

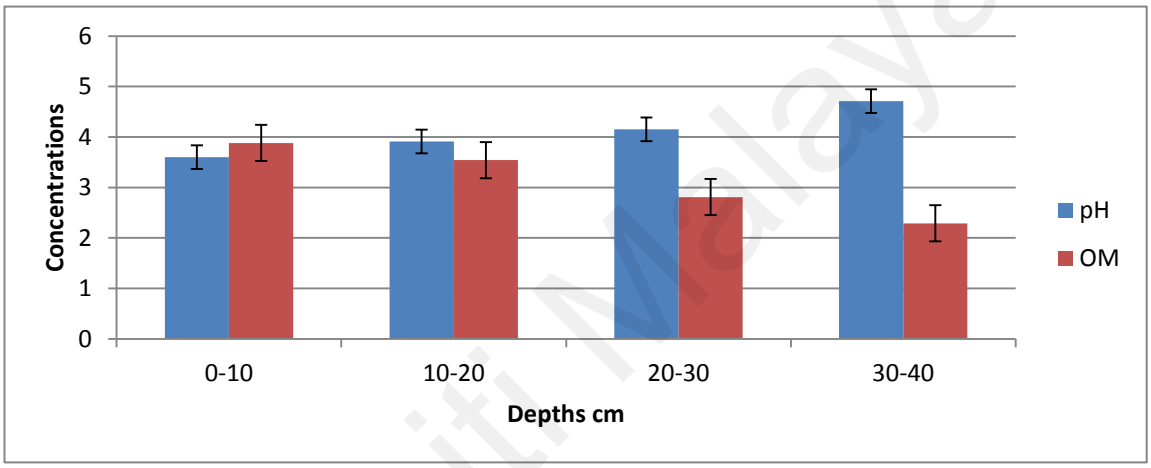

Figure 4.33: The vertical distribution of soil pH and organic matter OM% within the soil matrix in Malacca

Table 4.23: Pearson correlation coefficients between the soil pH and OM% and the radionuclides Bq.kg^{-1} in the samples from Malacca

	^{226}Ra	^{232}Th	^{40}K	pH	OM%
^{226}Ra	1				
^{232}Th	0.946**	1			
^{40}K	0.782**	0.815**	1		
pH	-0.641**	-0.585**	-0.366*	1	
OM	0.773**	0.765**	0.569**	-0.846**	1

**. Correlation is significant at the 0.01 level (2-tailed).
*. Correlation is significant at the 0.05 level (2-tailed).

4.3.1.4 **Distribution of organic matter (OM) and soil pH in Johor**

The calculated values of OM and soil pH in the samples from Johor are presented in Table 4.24. The measured value of the soil pH varied from 3.22 to 5.18, with a mean value of 4.13±0.5, which falls within the levels of acidic soil. While, the OM values varied from 2.24 to 4.97, with a mean value of 3.49±0.8, this falls within the level of soil poor in OM due to the rapid OM depletion rates in tropical soils.

The vertical distribution of pH and OM within the soil depths is shown in Table 4.25. The soil pH was slightly lower at the top 0-10 cm with a mean value of 3.47, while at the depth of 10-20, 20-30 and 30-40 cm, the mean values were given to be 3.87, 4.48 and 4.83, respectively. The soil OM value was slightly higher at the top 0-10 cm with a mean value of 4.49, before showing a gradual decrease at the depths of 10-20, 20-30 and 30-40 cm, with mean values of 3.82, 2.77 and 2.76, respectively.

Figure 4.34 shows the vertical distribution of soil pH and OM inside the soil matrix in Johor, which shows a rise in pH and a drop in OM values with depth. The pH and OM distribution patterns within the soil matrix of Johor indicate a different distribution trends within soil depths, as shown in Figure 4.34.

Table 4.26 shows the connections between pH, OM, and radionuclide activity. The association between soil pH and radionuclide (^{226}Ra, ^{232}Th, and ^{40}K) activities was negatively correlated at ($P \leq 0.01$), whereas OM was positively correlated with radionuclide (^{226}Ra, ^{232}Th, and ^{40}K) activities at ($P \leq 0.01$). The association between OM and soil pH is negatively linked ($P \leq 0.01$).

Table 4.24: The soil pH and organic matter (OM) in the soil samples from Johor

Sample ID	Depth cm	pH	OM%
JB1	0-10	4.05	4.12
JB2	10-20	3.85	3.84
JB3	30-40	4.62	2.24
JB4	30-40	4.62	2.44
JB5	20-30	4.75	2.65
JB6	30-40	5.18	4.92
JB7	10-20	4.17	3.75
JB8	10-20	4.25	3.63
JB9	20-30	4.55	2.85
JB10	0-10	3.54	4.97
JB11	20-30	4.35	2.66
JB12	0-10	3.42	4.54
JB13	30-40	4.75	2.34
JB14	30-40	4.71	3.18
JB15	20-30	4.58	2.43
JB16	10-20	3.87	4.05
JB17	10-20	3.75	3.84
JB18	20-30	4.35	2.85
JB19	0-10	3.26	4.65
JB20	30-40	4.88	2.35
JB21	10-20	3.82	3.87
JB22	30-40	5.12	2.36
JB23	20-30	4.67	3.07
JB24	0-10	3.58	4.11
JB25	20-30	4.23	2.72
JB26	0-10	3.47	4.55
JB27	20-30	4.55	2.68
JB38	10-20	3.72	3.62
JB39	10-20	3.86	3.72
JB30	30-40	4.77	2.32
JB31	0-10	3.22	4.54
JB32	20-30	4.42	3.07
JB33	0-10	3.52	4.43
JB34	20-30	4.26	2.81
JB35	0-10	3.35	4.52
JB36	10-20	3.75	3.85
JB37	20-30	4.65	2.72
JB38	10-20	3.76	3.87
JB39	0-10	3.38	4.56
JB40	10-20	3.82	4.08
Mean		**4.13±0.5**	**3.49±0.8**
Range		**3.22 - 5.18**	**2.24 - 4.97**

Table 4.25: The vertical distribution patterns of pH and OM% within the soil matrix in Johor

Depth cm	Soil pH	Organic Matter OM%
0-10	3.47	4.49
10-20	3.87	3.82
20-30	4.48	2.77
30-40	4.83	2.76
Mean	**4.13±0.5**	**3.49±0.8**

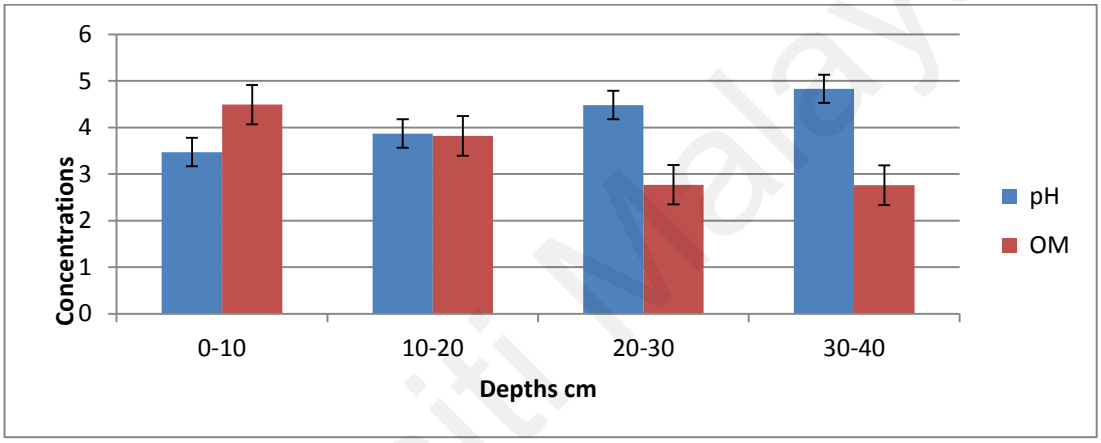

Figure 4.34: The vertical distribution of soil pH and organic matter OM% within the soil matrix in Johor

Table 4.26: Pearson correlation coefficients between the soil pH and OM% and the radionuclides Bq.kg^{-1} in the samples from Johor

	^{226}Ra	^{232}Th	^{40}K	pH	OM
^{226}Ra	1				
^{232}Th	0.936**	1			
^{40}K	0.849**	0.858**	1		
pH	-0.532**	-0.520**	-0.452**	1	
OM	0.487**	0.482**	0.415**	-0.792**	1

**. Correlation is significant at the 0.01 level (2-tailed).
*. Correlation is significant at the 0.05 level (2-tailed

4.3.1.5 **Distribution of organic matter (OM) and soil pH in Raub**

The calculated values of OM and soil pH in the samples from Raub are presented in Table 4.27. The measured value of the soil pH varied from 3.25 to 4.88, with a mean value of 4.15±0.5, which falls within the rate of acidic soil. While, the OM values varied from 1.22 to 3.84, with a mean value of 2.33±0.7, this lies within the level of soil poor in OM due to the rapid OM depletion rates in tropical soils.

Table 4.28 shows the vertical distribution of pH and OM within the soil depths. The soil pH was slightly lower at the top 0-10 cm with a mean value of 3.48, while at the depth of 10-20, 20-30 and 30-40 cm, the mean values were given to be 3.87, 4.55 and 4.61, respectively.

The soil OM value was slightly higher at the top 0-10 cm with a mean value of 3.13, before showing a gradual decrease at the depths of 10-20, 20-30 and 30-40 cm, with mean values of 2.65, 2.03 and 1.60, respectively.

The vertical distribution of the soil pH and OM within the soil matrix in Raub indicates an increase of pH level along with a decrease in OM values with depth, as shown in Figure 4.35. The soil pH and OM distribution patterns within the soil matrix of Raub indicate a different distribution trends within soil depths, as shown in Figure 4.35.29. The relationships between soil pH and radionuclides (^{226}Ra, ^{232}Th and ^{40}K) are negatively correlated ($P \leq 0.01$), and positively ($P \leq 0.01$) with OM. The relationship between OM and soil pH is negatively correlated ($P \leq 0.01$) in Raub.

Table 4.27: The soil pH and organic matter (OM) in the soil samples from Raub

Sample ID	Depth cm	pH	OM%
PR1	30-40	4.26	2.05
PR2	30-40	4.35	1.82
PR3	0-10	3.52	3.25
PR4	20-30	4.42	2.38
PR5	30-40	4.24	1.84
PR6	0-10	3.57	3.14
PR7	30-40	4.83	1.66
PR8	10-20	3.96	2.75
PR9	0-10	3.47	2.85
PR10	10-20	3.74	2.57
PR11	10-20	3.72	2.46
PR12	20-30	4.66	3.84
PR13	10-20	4.12	2.38
PR14	20-30	4.46	1.75
PR15	0-10	3.51	3.78
PR16	20-30	4.84	1.87
PR17	10-20	3.87	2.84
PR18	20-30	4.45	1.83
PR19	10-20	3.62	2.53
PR20	20-30	4.58	1.83
PR21	30-40	4.88	1.22
PR22	30-40	4.74	1.32
PR23	10-20	3.86	2.86
PR24	20-30	4.57	1.83
PR25	30-40	4.85	1.23
PR26	30-40	4.72	1.55
PR27	10-20	4.14	2.75
PR28	20-30	4.46	1.78
PR29	10-20	3.87	2.77
PR30	0-10	3.62	3.22
PR31	0-10	3.48	2.76
PR32	0-10	3.53	3.32
PR33	30-40	4.68	1.54
PR34	20-30	4.48	1.73
PR35	30-40	4.65	1.52
PR36	30-40	4.55	1.87
PR37	0-10	3.25	3.05
PR38	20-30	4.62	1.52
PR39	0-10	3.35	2.68
PR40	0-10	3.58	3.32
Mean		**4.15±0.5**	**2.33±0.7**
Range		**3.25 - 4.88**	**1.22 - 3.84**

Table 4.28: The vertical distribution of pH and OM within the soil matrix in Raub

Depth cm	Soil pH	Organic Matter OM%
0-10	3.48	3.13
10-20	3.87	2.65
20-30	4.55	2.03
30-40	4.61	1.60
Mean	**4.15±0.5**	**2.33±0.7**

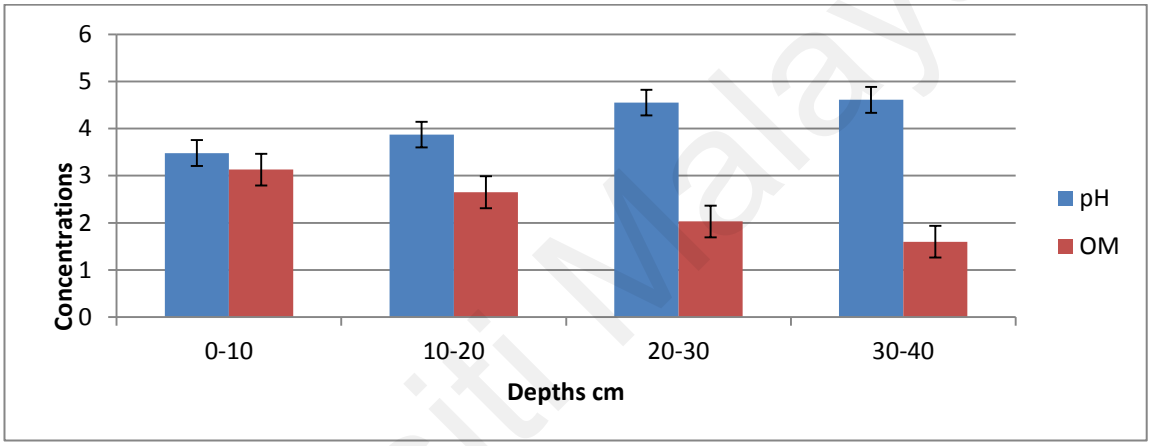

Figure 4.35: The vertical distribution of soil pH and organic matter OM within the soil matrix in Raub

Table 4.29: Pearson correlation coefficients between the soil pH and OM% and the radionuclides Bq.kg^{-1} in the samples from Raub

	^{226}Ra	^{232}Th	^{40}K	pH	OM
^{226}Ra	1				
^{232}Th	0.929**	1			
^{40}K	0.771**	0.753**	1		
pH	-0.521**	-0.487**	-0.464**	1	
OM	0.428**	0.389**	0.368*	-0.670**	1

**. Correlation is significant at the 0.01 level (2-tailed).
*. Correlation is significant at the 0.05 level (2-tailed

4.3.1.6 **Distribution of organic matter (OM) and soil pH in Lanchang**

The calculated values of OM and soil pH in the samples from Lanchang are presented in Table 4.30. The measured value of the soil pH varied from 3.33 to 4.63, with a mean value of 4.03±0.4, which falls within the levels of acidic soil. While, the values of OM varied from 2.24 to 4.58, with a mean value of 3.56±0.7.

Table 4.31 shows the vertical distribution of pH and OM within the soil depths. The soil pH was slightly lower at the top 0-10 cm with a mean value of 3.42, whereas the mean values at the depths of 10-20, 20-30 and 30-40 cm, the mean values given to be 3.95, 4.33 and 4.53, respectively. The soil OM value was slightly higher at the top 0-10 cm with a mean value of 4.35, before decreasing gradually at depths of 10-20, 20-30 and 30-40 cm, with mean values of 4.07, 2.99 and 2.43, respectively. The vertical distribution of the soil pH and OM within the soil matrix in Lanchang indicates an increase of pH level along with a decrease in OM values with depth, as shown in Figure 4.36. The pH and OM distribution patterns within the soil matrix of Lanchang indicate a different distribution trends within soil depths, as shown in Figure 4.36.

The relationships between pH, OM and the radionuclides activities are presented in Table 4.32. The relationships between soil pH and radionuclides (^{226}Ra, ^{232}Th and ^{40}K) were negatively correlated at ($P \leq 0.01$), and positively ($P \leq 0.01$) with OM. The relationship between OM and soil pH is negatively correlated at ($P \leq 0.01$) in Lanchang.

Table 4.30: The soil pH and organic matter (OM) in the soil samples from Lanchang

Sample ID	Depth cm	pH	OM%
PL1	10-20	3.86	4.25
PL2	0-10	3.45	4.42
PL3	10-20	4.11	4.25
PL4	10-20	3.82	3.78
PL5	20-30	4.45	2.72
PL6	10-20	3.98	4.02
PL7	0-10	3.36	4.54
PL8	10-20	3.92	4.16
PL9	0-10	3.36	4.45
PL10	20-30	4.37	3.67
PL11	20-30	4.35	3.16
PL12	10-20	3.85	3.84
PL13	30-40	4.56	2.55
PL14	10-20	4.05	4.22
PL15	20-30	4.24	3.15
PL16	20-30	4.38	2.72
PL17	10-20	4.17	4.05
PL18	10-20	3.92	4.25
PL19	30-40	4.47	2.27
PL20	30-40	4.58	2.24
PL21	20-30	4.36	3.14
PL22	30-40	4.57	2.42
PL23	10-20	3.96	3.84
PL24	20-30	4.24	2.66
PL25	0-10	3.46	4.21
PL26	0-10	3.33	4.32
PL27	30-40	4.63	2.51
PL28	0-10	3.42	4.58
PL29	0-10	3.51	4.38
PL30	10-20	3.85	4.22
PL31	0-10	3.51	3.95
PL32	30-40	4.48	2.25
PL33	10-20	4.00	3.97
PL34	30-40	4.48	2.83
PL35	20-30	4.25	2.75
Mean		**4.03 ± 0.4**	**3.56 ± 0.7**
Range		**3.33 – 4.63**	**2.24 - 4.58**

Table 4.31: The vertical distribution of pH and OM within the soil matrix in Lanchang

Depth cm	Soil pH	Organic Matter OM%
0-10	3.42	4.35
10-20	3.95	4.07
20-30	4.33	2.99
30-40	4.53	2.43
Mean	**4.03±0.4**	**3.56±0.7**

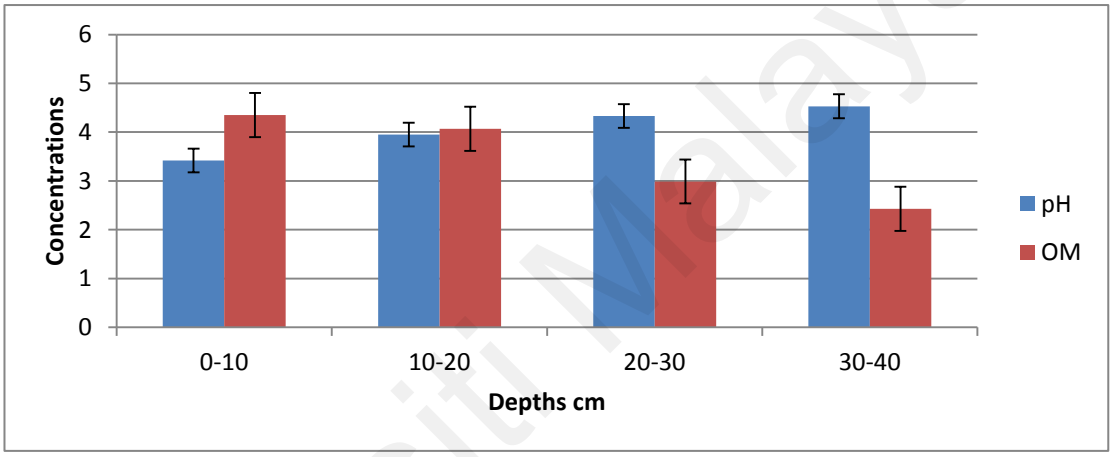

Figure 4.36: The vertical distribution of soil pH and organic matter OM% within the soil matrix in Lanchang

Table 4.32: Pearson correlation coefficients between the soil pH and OM% and the radionuclides Bq.kg^{-1} in the samples from Lanchang

	^{226}Ra	^{232}Th	^{40}K	pH	OM
^{226}Ra	1				
^{232}Th	0.884**	1			
^{40}K	0.658**	0.697**	1		
pH	0-.505**	-0.483**	-0.624**	1	
OM	0.666**	0.627**	0.630**	-0.869**	1

**. Correlation is significant at the 0.01 level (2-tailed).
*. Correlation is significant at the 0.05 level (2-tailed

For all study areas, the mean values of the soil pH follow the order of Lanchage and Kehad (4.03±0.4) < Malacca (4.10±0.4) < Johor (4.13±0.5) < Raub (4.15±0.5) < Selangor (4.18±0.4). The mean values of the soil OM are follow the order of Selangor (1.43±0.6) < Raub (2.33±0.7) < Kedah (3.01±0.7) < Malacca (3.12±0.6) < Johor (3.49±0.8) < Lanchage (3.56±0.7).

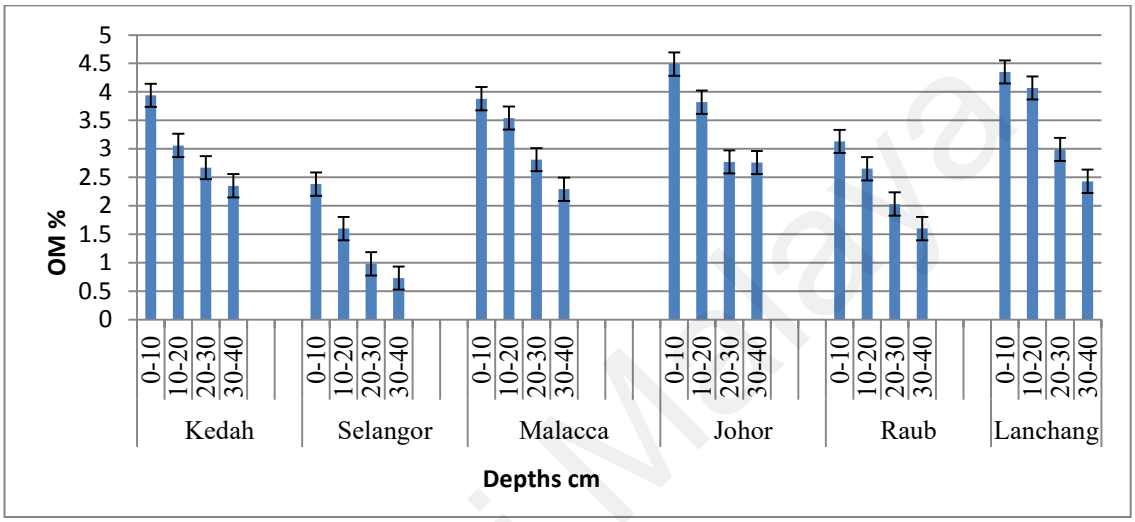

Figure 4.37: The vertical distribution of OM within four depths across the study areas

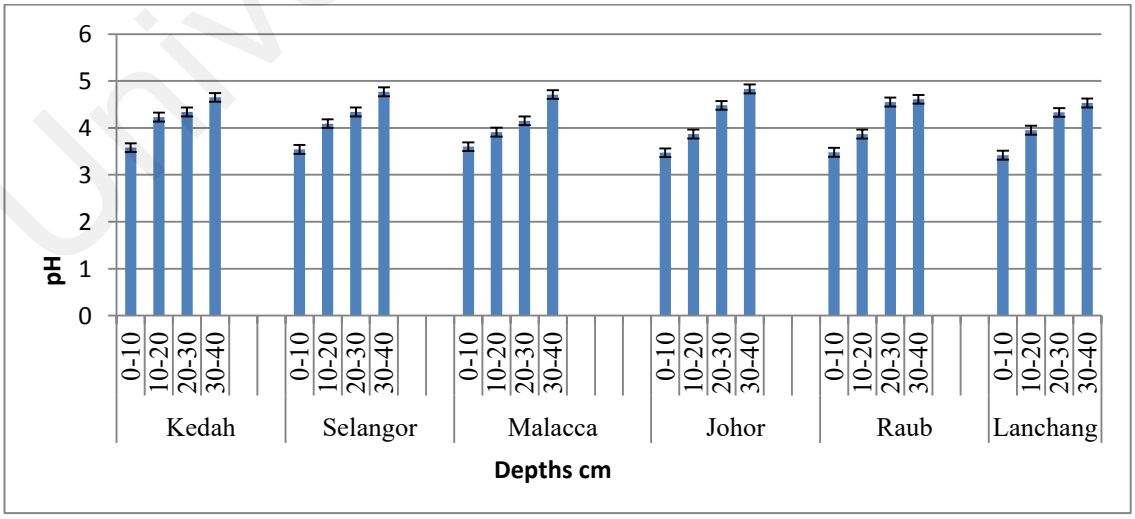

Figure 4.38: The vertical distribution of pH within four depths across the study areas

All the soil groups were acidic with pH values ranging from 4.03±0.4 to 4.18±0.4. No significant differences were found in pH levels between study areas, the slight differences in acidity appeared to be related to OM content where pH decreased appreciably with an increase in OM. Due to the high weathering conditions in the tropics, the electrical conductivity of the soil EC is substantially reduced and thus the ion exchange potential is limited. Cation exchange capability (CEC) can directly affect changes in soil pH, since each time clay particles capture cations; they release H and Al^{3+} ions that acidify soil at high concentrations.

In general, the content of organic matter was low in all study areas that is because practically all organic material OM that reaches the soil surface decomposes quickly in tropical conditions, surface buildup of soil organic matter OM is negligible, this agrees with Velasco *et al.,* (2008) conclusion.

Soil pH values varied with depths and the soil areas. Generally, the soil pH was slightly higher in the top 0 -10 cm than in lower 30-40 cm. The difference in acidity appeared to be related to OM content as evident in soils where pH decreased appreciably with an increase in OM content. The net charge of the OM complex which is higher in the topsoil may contribute to the offsetting of any net positive charge coming from the mineral fractions. Moreover, the pH difference between soil depths may generally be related to greater quatities of Al rather than OM.

The mean values of OM content varied from 2.33±0.7 to 3.56±0.7, the soil OM was higher in the top 0 -10 cm than in lower depth of 30 - 40 cm. these differences may result from the greater accumulations of leaves and litterfall.

In all study areas, the soil pH was negatively correlated ($P \leq 0.01$) with radionuclides (^{226}Ra, ^{232}Th and ^{40}K), while OM was positively correlated ($P \leq 0.01$). Since OM is

extremely heterogeneous and consists of organic acids, lipids, lignin, fulvic and humic acids, there are a large number of possible reactions and interactions of radionuclides with organic matter. Organic matter contains functional groups that can form complexes with radionuclides. This complexation affects radionuclide mobility, adsorption to soils and bioavailability. This explains the positive correlations between radionuclides and OM in soil groups of the study areas.

The negative correlations between the pH and the radionuclides ^{226}Ra, ^{232}Th, and ^{40}K, were also reported by Tsai *et al.,* (2011), Navas *et al.,* (2005), Dragović *et al.,* (2011) and Navas *et al.,* (2011). A negative correlation between pH and ^{232}Th in soil was also stated by Belivermis *et al.*, (2010). The important relationship between OM and the radionuclides was reported by (Elejalde *et al.,* 1996; Navas *et al.,* 2002; Ligero *et al.,* 2001; Dragović *et al.,* 2012).

Figures 4.39, 4.40, and 4.41 illustrate the percentage trend of radionuclides and pH value contributes across depth in the soil samples from Kedah.

The radionuclides showed sensitivity to the soil pH level in the soil, as the concentration of the radionuclides ^{226}Ra, ^{232}Th and ^{40}K increased at low pH levels. This trend appeared in all study areas. As the most of the radionuclides in soil exist in the cationic form, decrease in pH, clay content, and CEC lead to an increase in pollutant mobility including the radioactive.

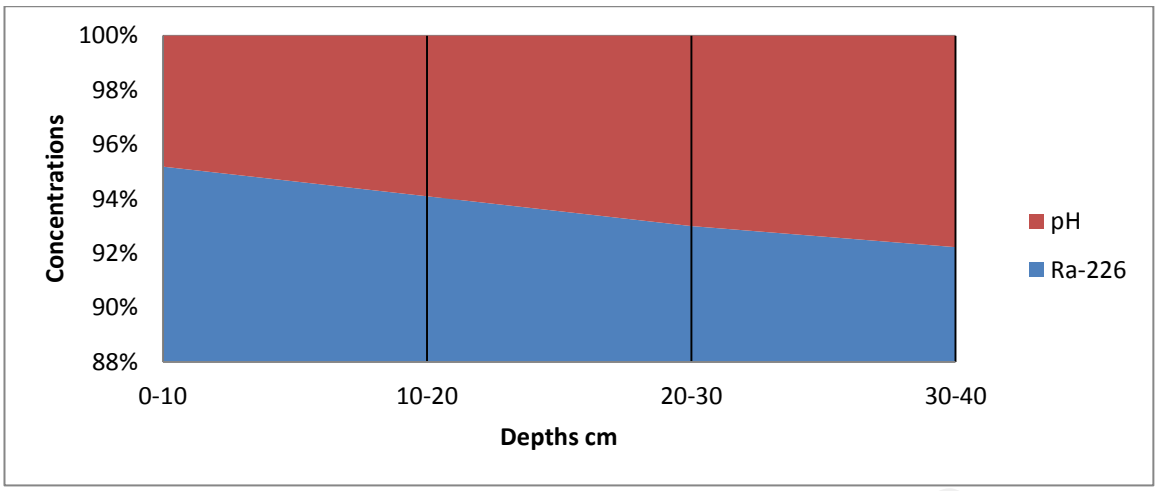

Figure 4.39: The trend contribution of ^{226}Ra Bq.kg $^{-1}$ and pH value across depth in the soil samples from Kedah

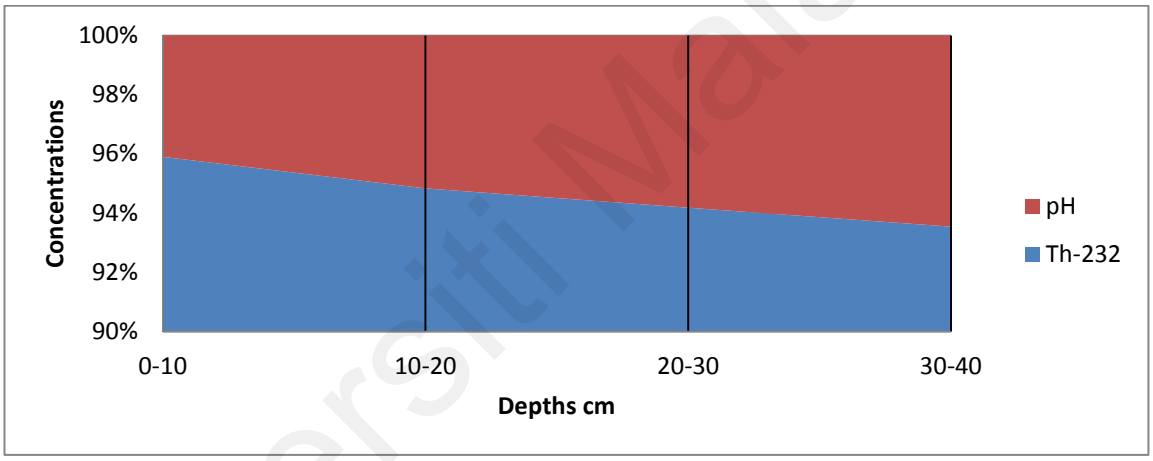

Figure 4.40: The trend contribution of ^{232}Th Bq.kg $^{-1}$ and pH value across depth in the soil samples from Kedah

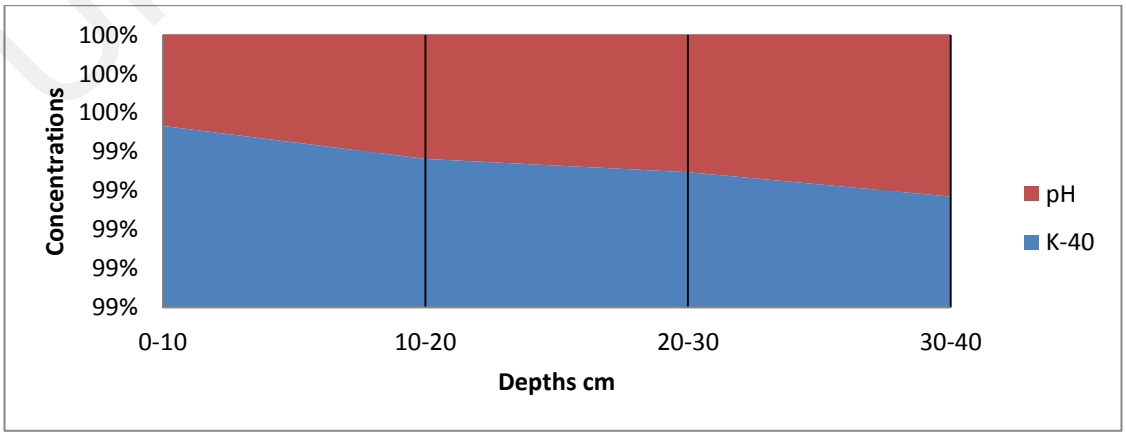

Figure 4.41: The trend contribution of ^{40}K Bq.kg $^{-1}$ and pH value across depth in the soil samples from Kedah

4.4 The vertical distribution of the stable metals in the soil matrix

4.4.1 The vertical distribution of the stable metals in Kedah

4.4.1.1 The vertical distribution of Phosphorus (P) in Kedah

Table 4.33 shows the essential stable metals in soil samples from Kedah. Table 4.34 depicts the vertical distribution of the elements. The mean value of P was found to be 21.7 mg/kg, with values ranging from 8.2 to 38.5 mg/kg.

Figure 4.42 depicts the vertical distribution of P. Generally, P movement decreased with soil depth. P content was highest in the top soil layer (0-10 cm) and steadily dropped deeper into the soil layer. Figure 4.42 depicts a pattern of vertical distribution within the soil matrix that suggests a steady progressive reduction with depth.

The associations between radionuclides (^{226}Ra, ^{232}Th, and ^{40}K) and P were found to be significant ($P \leq 0.01$). Positive associations ($P \leq 0.01$) were found between P and OM and Zn. P was negatively linked ($P \leq 0.01$) with pH, K, and Mn, Table 4.35.

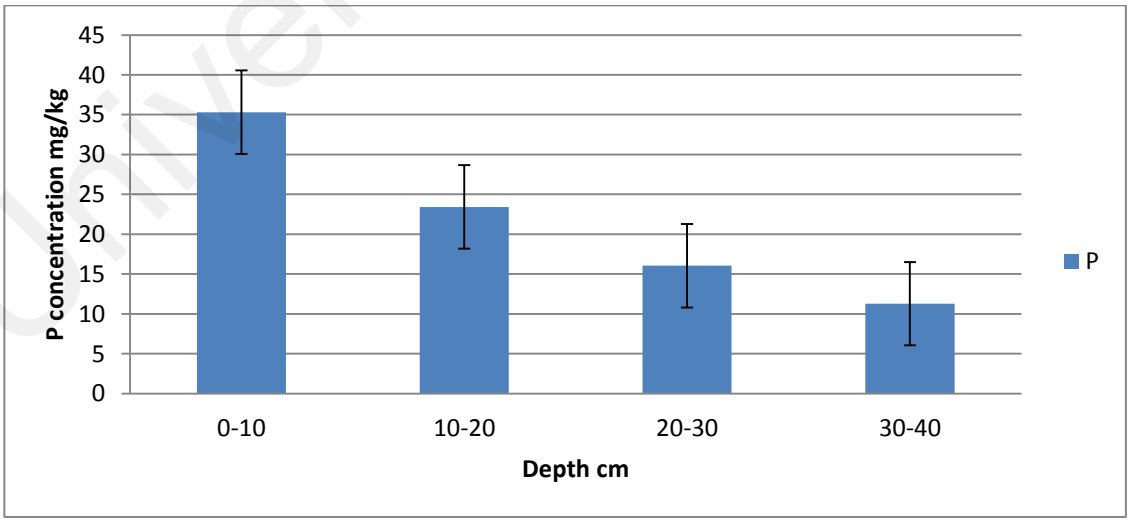

Figure 4.42: The vertical distribution of P in the soil from Kedah

Table 4.33: Concentrations of stable metals in the soil samples from Kedah

Sample ID	Depth cm	mg/kg								
		P	K	Ca	Mg	Cu	Zn	Mn	Fe	Al
AS1	10-20	20.5	18.3	15.2	13.2	1.8	2.6	10.5	675	756
AS2	20-30	18.2	20.2	17.5	6.2	1.2	1.7	9.5	555	643
AS3	0-10	34.4	17.2	14.2	12.3	2.2	3.5	8.3	893	943
AS4	10-20	23.5	19.4	15.5	14.5	1.7	2.6	9.2	572	767
AS5	30-40	8.5	20.3	17.5	16.0	2.3	1.3	15.3	875	1068
AS6	0-10	32.2	15.5	15.5	14.5	1.7	3.2	7.5	1575	1678
AS7	10-20	30.2	18.4	13.4	13.2	1.7	2.7	7.2	634	764
AS8	0-10	35.8	14.2	14.3	12.2	1.8	3.8	8.7	1404	1624
AS9	20-30	14.3	22.4	16.4	15.5	2.2	1.3	11.2	460	662
AS10	10-20	20.5	15.7	12.5	13.8	1.8	2.7	8.5	588	664
AS11	0-10	35.2	13.5	13.2	13.3	2.3	3.3	7.6	1617	1537
AS12	10-20	25.8	18.2	15.5	14.6	1.5	2.7	9.5	1275	1352
AS13	20-30	15.5	21.3	16.3	18.5	1.3	1.8	12.5	489	670
AS14	30-40	11.3	19.5	15.8	16.2	2.5	1.2	13.5	715	1054
AS15	0-10	38.5	15.2	13.3	11.5	2.2	3.5	8.2	1354	1592
AS16	20-30	12.7	18.7	17.5	15.5	1.5	1.5	12.5	704	1053
AS17	30-40	8.5	17.4	18.3	13.6	2.3	1.5	14.7	804	1072
AS18	20-30	14.3	21.4	15.4	16.2	1.3	2.8	11.4	688	943
AS19	10-20	22.2	18.8	15.6	14.2	1.3	2.8	9.6	1274	1312
AS20	30-40	11.7	19.2	6.5	3.5	2.2	1.8	12.3	1853	1978
AS21	10-20	18.5	17.5	14.4	13.2	1.7	2.6	9.5	658	743

AS22	30-40	12.3	18.5	18.5	17.7	2.5	1.5	15.8	1775	1895
AS23	20-30	18.5	19.2	15.5	13.5	1.3	1.4	12.4	511	645
AS24	30-40	8.2	17.5	12.7	2.3	2.6	1.8	15.2	1805	1974
AS25	0-10	34.3	16.5	12.2	11.5	2.5	3.7	8.5	735	989
AS26	30-40	18.5	17.5	3.7	17.5	2.4	1.6	7.2	822	543
AS27	10-20	24.5	18.4	16.2	12.6	1.7	2.6	9.5	745	954
AS28	20-30	17.5	22.5	16.5	15.7	1.2	1.5	12.8	495	585
AS29	30-40	11.4	18.5	17.5	15.5	2.5	1.5	16.5	1834	1987
AS30	20-30	16.8	18.5	18.2	16.5	1.4	1.7	12.4	507	656
AS31	10-20	18.0	15.7	14.5	13.5	1.8	2.5	8.2	677	832
AS32	0-10	31.7	14.5	13.4	11.8	2.3	2.8	6.8	778	812
AS33	10-20	28.4	18.3	13.5	14.5	1.7	2.6	9.6	658	785
AS34	0-10	38.2	15.4	14.2	11.5	1.8	2.8	8.4	345	643
AS35	20-30	16.7	17.6	16.5	15.8	1.3	1.8	11.3	430	552
AS36	30-40	13.2	19.5	17.7	16.2	2.5	1.4	16.8	831	1143
AS37	0-10	35.6	15.3	13.3	11.8	2.3	3.2	6.5	1432	1678
AS38	10-20	25.7	17.3	13.5	13.7	1.8	2.7	8.5	823	785
AS39	0-10	37.2	14.5	14.5	11.5	2.3	3.6	7.5	678	898
AS40	30-40	9.2	15.5	19.5	15.6	2.3	1.3	15.3	786	978
Mean		**21.7±9.5**	**17.8±2.2**	**14.8±2.9**	**13.5±3.3**	**2.15±1.5**	**2.2±0.7**	**10.5±3.1**	**874.58±457.6**	**1049.27±435.3**
Range		**30.3**	**9.0**	**15.8**	**16.2**	**10.3**	**2.6**	**13.3**	**1844.8**	**1444.0**

Table 4.34: The vertical distribution of the stable metals in the soil from Kedah

Depth	pH	OM%	P	K	Ca	Mg	Cu	Zn	Mn	Fe	Al
			mg/kg								
0-10	3.58	3.94	35.31	15.18	13.81	12.37	3.07	3.21	7.33	946.52	1215.6
10-20	4.23	3.06	23.43	17.81	14.52	13.72	1.68	2.645	9.07	779.90	883.09
20-30	4.34	2.67	16.05	20.20	16.64	14.82	1.41	1.72	11.77	537.66	712.11
30-40	4.65	2.35	11.28	18.34	14.77	13.41	2.41	1.49	14.26	1210.00	1369.20
Mean	**4.20**	**3.01**	**21.70**	**17.82**	**14.88**	**13.55**	**2.15**	**2.29**	**10.54**	**874.58**	**1049.27**

Table 4.35: Pearson correlation coefficients between the stable metals mg/kg and radionuclides Bq.kg^{-1} in the soil from Kedah

	^{226}Ra	^{232}Th	^{40}K	pH	OM%	P	K	Ca	Mg	Cu	Zn	Mn	Fe	Al
^{226}Ra	1													
^{232}Th	0.812**	1												
^{40}K	0.737**	0.596**	1											
pH	-0.634**	-0.554**	-0.860**	1										
OM%	0.535**	0.495**	0.762**	-0.828**	1									
P	0.738**	0.612**	0.869**	-0.919**	0.778**	1								
K	-0.493**	-0.415**	-0.558**	0.595**	-0.588**	-0.622**	1							
Ca	-0.124	-0.084	-0.219	0.249	-0.115	-0.304	0.260	1						
Mg	-0.106	-0.055	-0.165	0.216	-0.063	-0.142	0.230	0.368*	1					
Cu	-0.099	-0.136	0.052	-0.344*	0.189	0.260	-0.277	-0.145	-0.055	1				
Zn	0.746**	0.603**	0.835**	-0.773**	0.789**	0.837**	-0.597**	-0.299	-0.227	-0.031	1			
Mn	-0.587**	-0.409**	-0.768**	0.800**	-0.672**	-0.842**	0.519**	0.507**	0.157	-0.291	-0.716**	1		
Fe	-0.058	-0.019	0.001	0.120	-0.095	-0.101	-0.195	-0.155	-0.310	-0.175	0.120	0.258	1	
Al	-0.121	-0.099	0.016	-0.027	-0.003	-0.022	-0.246	-0.059	-0.335*	0.239	0.085	0.211	0.877**	1

**. Correlation is significant at the 0.01 level (2-tailed)
*. Correlation is significant at the 0.05 level (2-tailed)

4.4.1.2 **The vertical distribution of Potassium (K) in Kedah**

In Kedah, the mean value of K was determined to be 17.80 ±2.2 mg/kg, and the soil is generally low in K, ranging from 13.5 to 22.5 mg/kg (Table 4.33). Table 4.34 and Figure 4.43 show the vertical distribution of K. The K concentrations rose slightly and consistently with depth, and then dropped at lower depths of 30-40 cm, revealing a peak in the centre of the profile, indicating K mobility within the soil matrix in the studied region.

Figure 4.43 shows an irregular vertical distribution pattern of K within the soil matrix; K was significantly higher at 20-30 cm. It is evident that the concentrations of K continued to increase gradually downward with depth, before dropped at 30–40 cm.

Although K has limited movement in the soil, increasing soil moisture can lead to increased K transport through the soil matrix. This behavior may explain the anomaly of K vertical distribution through the soil, in the paddy fields from which samples were collected, where the plant is usually flooded with water during the period of plant growth. It is also assumed that low OM content played a key role in speeding the leaching of K through the soil. Moreover, the high K concentration of some depths may be attributed to presence of illite and mica in the alluvium deposited of the soil (Zakaria, 1979).

As indicated in Table 4.38, the relationships between the radionuclides (^{226}Ra, ^{232}Th, and ^{40}K) and K were found to be negative ($P \leq 0.01$). Negative correlations ($P \leq 0.01$) were also shown between K and OM, P, Z, and Mn, while the relationship was found to be a positive ($P \leq 0.01$) with pH (Table 4.35).

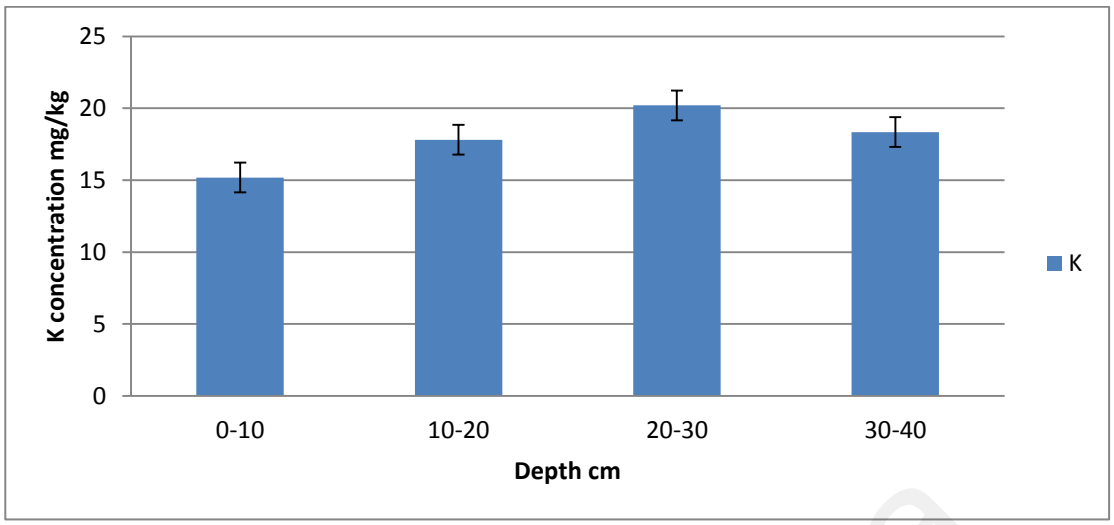

Figure 4.43: The vertical distribution of K in the soil from Kedah

4.4.1.3 The vertical distribution of Calcium (Ca) in Kedah

The mean value of Ca found to be 14.9±2.9 mg/kg in Kedah, while the average values vary from 2.5 to 14.9 mg/kg (Table 4.33). The vertical distribution of Ca is shown in Table 4.34. The estimated values indicate that the Ca concentrations gradually increased with depth before dropping at 20 cm. Figure 4.44 shows an irregular pattern of vertical distribution of Ca, where it recorded a gradual increase before decreasing at the lower depths 20-40 cm.

Relationships between the Ca and radionuclides ^{226}Ra, ^{232}Th, and ^{40}K were insignificant (Table 4.35). Insignificant correlations were also shown between Ca and (pH, OM, P, Cu, Zn, Fe and Al), while the relationships with Mn and Mg were positive at ($P \leq 0.01$) and ($P \leq 0.05$), respectively.

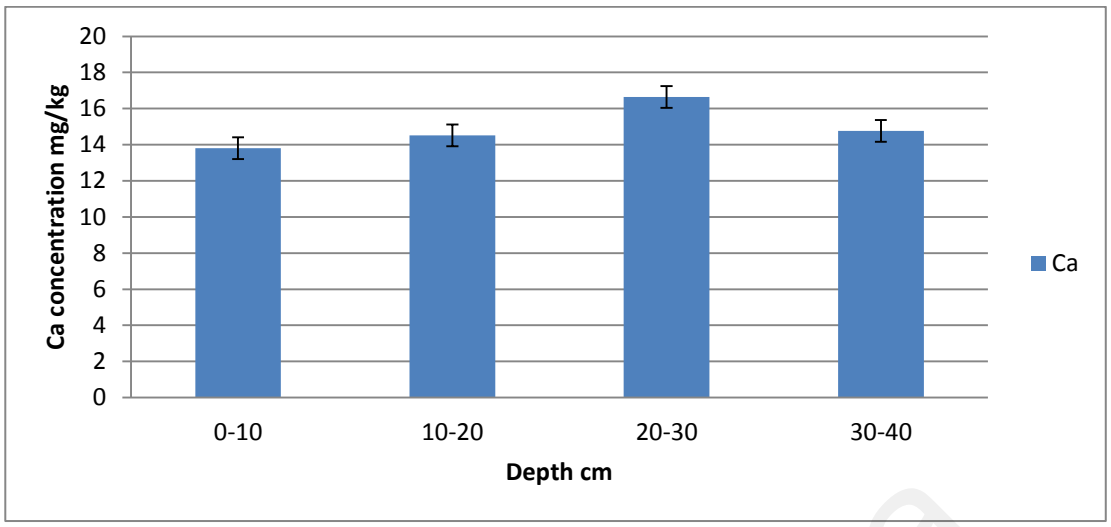

Figure 4.44: The vertical distribution of Ca in the soil from Kedah

4.4.1.4 The distribution of Magnesium (Mg) in Kedah

The mean value of Mg found to be 13.51±3.3 mg/kg in Kedah, while the average values vary from 2.30 to 18.50 mg/kg (Table 4.33). The vertical distribution of Mg is shown in Table 4.34. The calculated values indicate that the Mg movement is increasing through the depth Figure 4.45. The irregular distribution pattern of Mg within the soil matrix is shown in Figure 4.45. It is evident that the concentrations of Mg have increased regularly from 0-10 to 20-30 cm, and then decreased at 30-40 cm, to show a slight peak in the middle of the profile.

Insignificant relationships between Mg and radionuclides ^{226}Ra, ^{232}Th, and ^{40}K were shown in Table 4.35. Poor correlations were also shown between the Mg and pH, OM, P, K, Ca, Cu, Zn, Mn and Fe, while Al was negativly correlated with Mg at ($P \leq 0.05$).

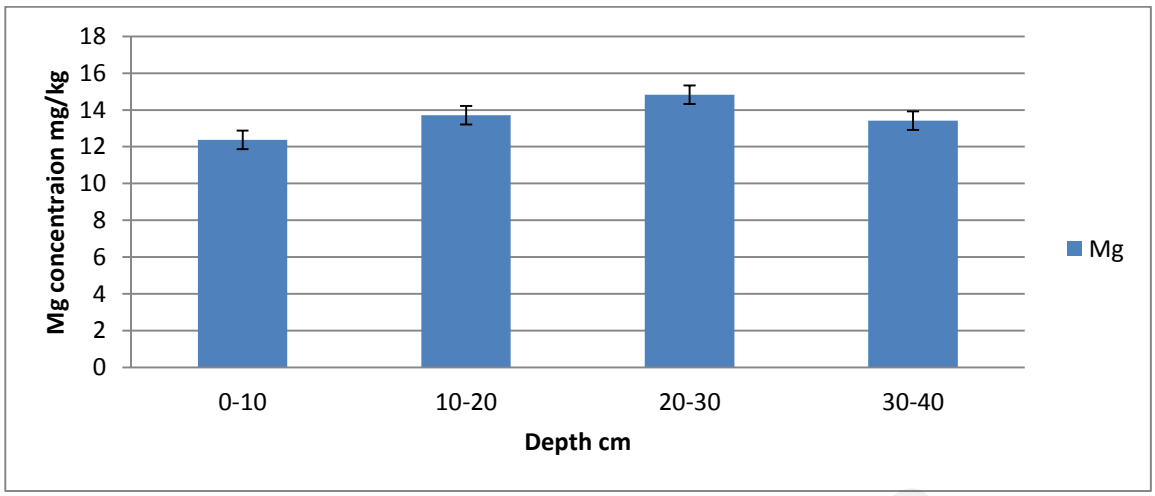

Figure 4.45: The vertical distribution of Mg in the soil from Kedah

4.4.1.5 **The vertical distribution of Copper (Cu) in Kedah**

The mean value of Cu was found to be 1.91±0.4 mg/kg in Kedah, while the average values vary from 1.20 to 2.60 mg/kg (Table 4.33). The vertical distribution of Cu is shown in Table 4.34.

The calculated values indicate a decrease in Cu concentrations with depth up to 20 cm before they increased again at 40 cm deep. The pattern of irregular distribution of Cu within the soil matrix is shown in Figure 4.46.

The relationships between Cu and the radionuclides ^{226}Ra, ^{232}Th and ^{40}K were shown to be insignificant (Table 4.35). Unimportant correlations were also shown between Cu with OM, P, K, Ca, Mg, Zn, Mn, Fe and Al. The soil pH negitivly correlated ($P \leq 0.05$) with Cu.

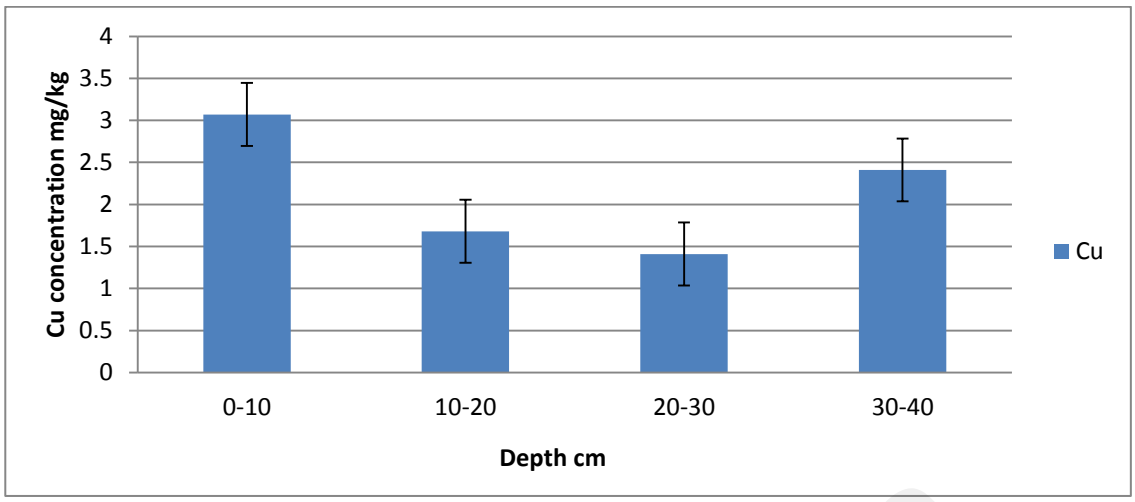

Figure 4.46: The vertical distribution of Cu in the soil samples from Kedah

4.4.1.6 The vertical distribution of Zinc (Zn) in Kedah

The mean value of Zn is found to be 2.32±0.7 mg/kg in Kedah, while the average values differ from 1.20 to 3.80 mg/kg (Table 4.33). The vertical distribution of Zn is shown in Table 4.34.

The calculated values indicate that Zn movement is decreased with the depth. The pattern of regular distribution of Zn within the soil matrix is shown in Figure 4.47.

Relashinship of Zn and the radionuclides ^{226}Ra, ^{232}Th and ^{40}K were positively correlated ($P \leq 0.01$). Positive correlations ($P \leq 0.01$) were also shown between Zn and OM, P and K, while, the Zn negatively correlated ($P \leq 0.01$) with soil pH and Mn (Table 4.35).

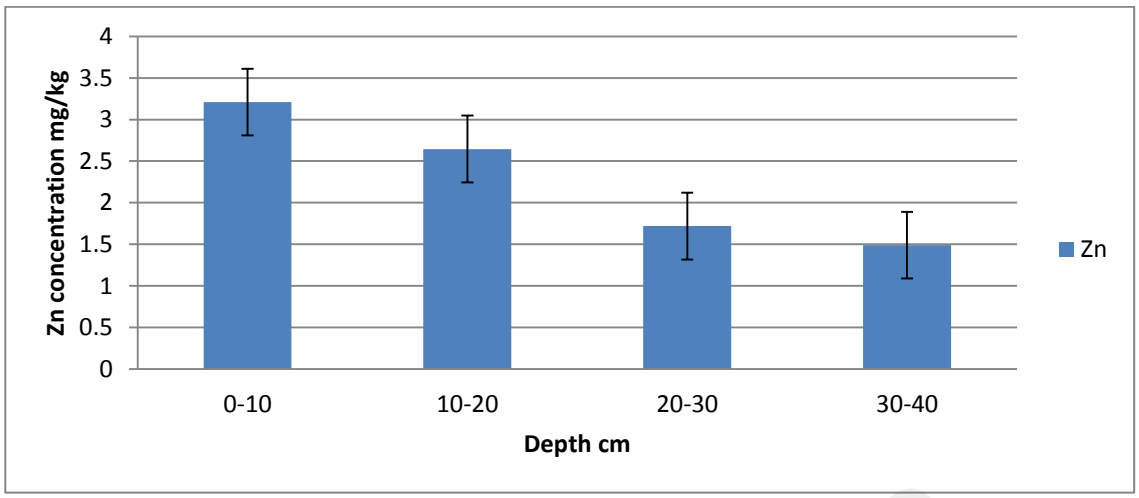

Figure 4.47: The vertical distribution of Zn in the soil samples from Kedah

4.4.1.7 The vertical distribution of Manganese (Mn) in Kedah

The mean value of Mn found to be 10.66±2.9 mg/kg in Kedah, while the average values differ from 6.50 to 16.80 mg/kg (Table 4.33). The vertical distribution of Mn is shown in Table 4.34and Figure 4.48.

The calculated values indicate that the Mn movement increased with the depth. The pattern of regular distribution of Mn within the soil matrix is shown in Figure 4.48.

Relationships between the Mn and the radionuclides ^{226}Ra, ^{232}Th and ^{40}K were negatively correlated ($P \leq 0.01$). Positive correlations ($P \leq 0.01$) were shown between to Mn with pH, K and Ca, and negative at ($P \leq 0.01$) with OM, P and Zn.

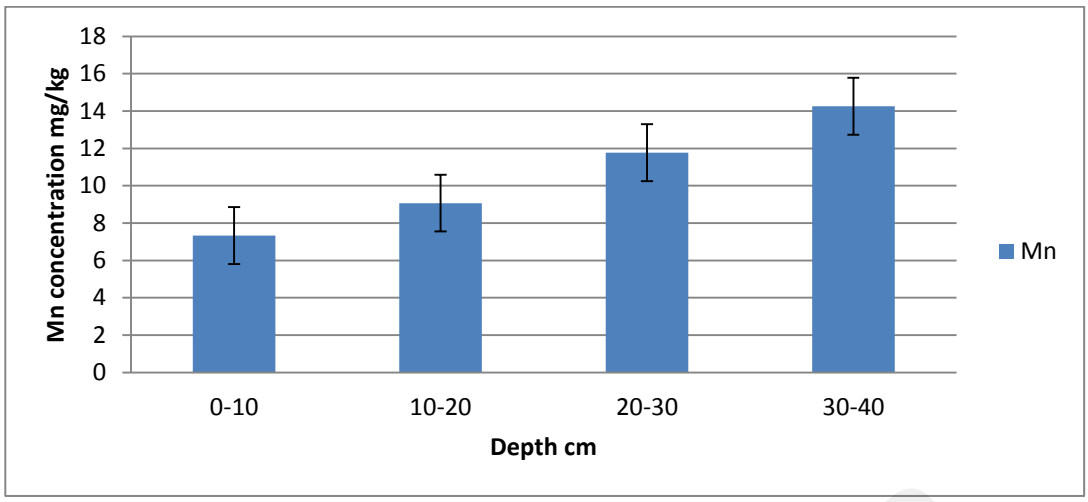

Figure 4.48: The vertical distribution of Mn in the soil samples from Kedah

4.4.1.8 The vertical distribution of Iron (Fe) in Kedah

The mean value of Fe found to be 908.22±41.2 mg/kg in Kedah, while the average values differ significantly from 345.00 to 1853.00 mg/kg (Table 4.33). The vertical distribution of Fe is shown in Table 4.34 and Figure 4.49.

The measured values indicate that the Fe movement is decreased with the depth, before increasing again at 20-30 cm depth. The pattern of irregular distribution of Fe within the soil matrix is shown in Figure 4.49.

Relationships between the Fe and the radionuclides ^{226}Ra, ^{232}Th and ^{40}K were found to be weak. Poor correlations were also shown between Fe and pH, OM, P, K, Ca, Mg, Cu, Zn, Mn and Al (Table 4.35).

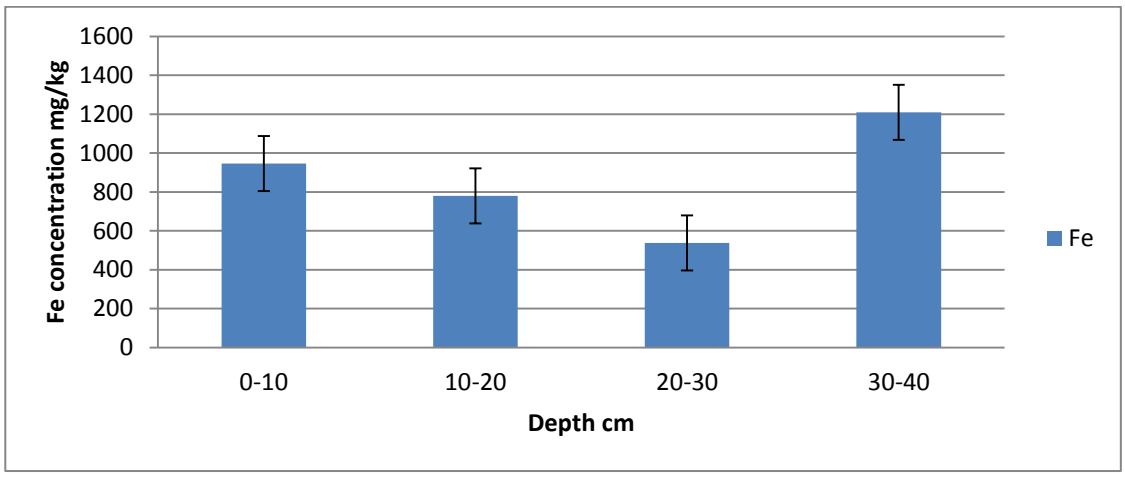

Figure 4.49: The vertical distribution of Fe in the soil samples from Kedah

4.4.1.9 **The vertical distribution of Aluminum (Al) in Kedah**

The mean value of Al found to be 1055.22±41.1 mg/kg in Kedah, while the average values differ significantly from 543.00 to 1987.00 mg/kg (Table 4.33). The vertical distribution of Al is shown in Figure 4.50.

The measured values indicate that the Al movement is decreased with the depth, before increasing again at 20-30 cm depth. The pattern of irregular distribution of Al within the soil matrix is shown in Figure 4.50.

Relationships between the Al and the radionuclides ^{226}Ra, ^{232}Th and ^{40}K were found to be weak. The relationship between Al and Fe was positively correlated at ($P \leq 0.01$), and negatively at ($P \leq 0.05$) with Mg Table 4.35.

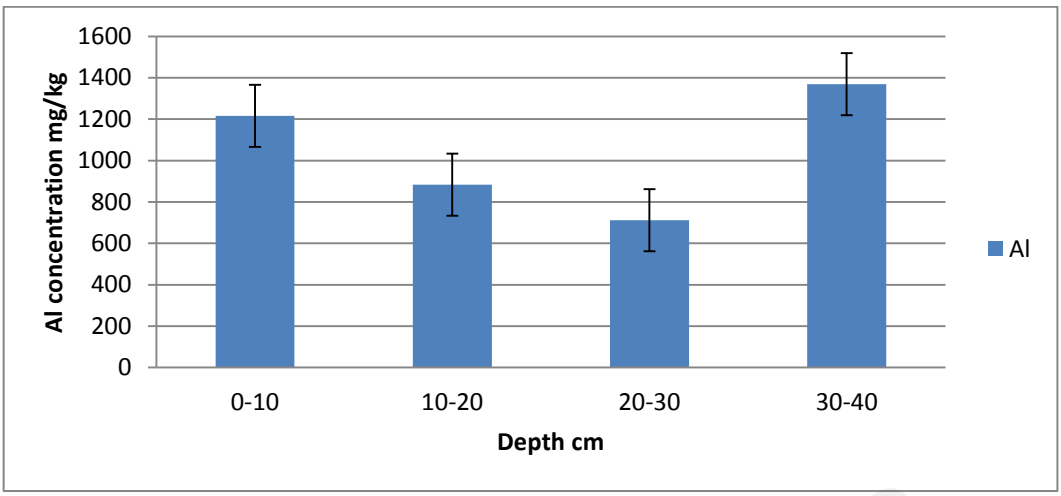

Figure 4.50: The vertical distribution of Al in the soil samples from Kedah

4.4.2 Distribution of stable metals in Selangor

4.4.2.1 The vertical distribution of Phosphorus (P) in Selangor

The mean value of P found to be 16.90±6.8 mg/kg in Selangor, while the average values differ from 6.2 to 32.8 mg/kg (Table 4.36). The vertical distrubutions of K shown in Table 4.37 and Figur 4.51, the results indicate that the K movement is decreasing with the depth; P was higher at 0-10 cm before declining at the lower depths. Figure 4.51 shows the distribution pattern of the P within the soil matrix, it is noticeable that concentrations tended to be stable at depths from 20 to 30 cm before falling again to depth 40 cm.

The relationships between the radionuclides ^{226}Ra, ^{232}Th, and ^{40}K and P were found to be positive ($P \leq 0.01$) Table 4.38. Positive correlations ($P \leq 0.01$) were also shown between P and OM, Zn, Cu, Mn, and Al, and positive at ($P \leq 0.05$) with Fe and Al, while negative relationships ($P \leq 0.01$) were seen between P and pH and Mg, a negative correlation at ($P \leq 0.05$) was also seen with Ca (Table 4.38).

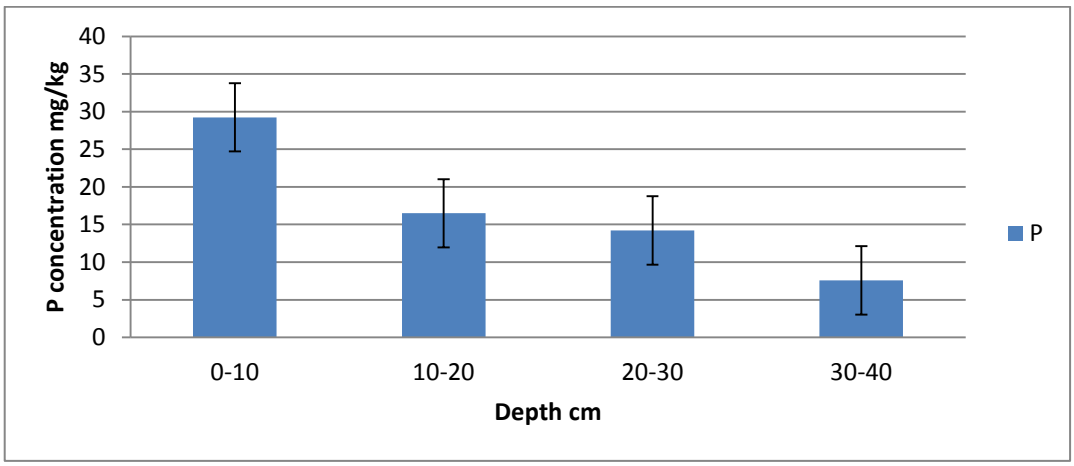

Figure 4.51: The vertical distribution of P in the soil samples from Selangor

Table 4.36: Concentrations of stable metals in the soil samples from Selangor

Sample ID	Depth cm	mg/kg								
		P	K	Ca	Mg	Cu	Zn	Mn	Fe	Al
S1	0-10	31.5	18.2	12.5	12.0	2.1	2.4	18.5	715.0	816.0
S2	10-20	16.3	25.2	13.5	15.2	2.2	2.2	15.5	626.0	745.0
S3	0-10	32.6	21.5	13.5	12.5	2.1	2.4	17.3	1572.0	1673.0
S4	0-10	30.5	21.2	12.3	13.5	1.8	2.6	17.6	1542.0	1637.0
S5	0-10	30.8	23.3	11.2	13.3	1.7	2.5	16.3	758.0	985.0
S6	10-20	18.2	26.5	15.3	14.7	1.2	2.3	14.5	786.0	871.0
S7	0-10	31.5	22.3	15.2	11.5	1.5	2.4	18.5	1544.0	1574.0
S8	20-30	15.5	26.5	17.2	18.5	0.7	1.3	5.7	584.0	697.0
S9	20-30	14.5	25.7	16.5	17.5	0.7	1.4	6.2	550.0	583.0
S10	10-20	15.7	25.3	14.7	15.3	1.2	2.1	13.5	6230	714.0
S11	20-30	15.5	28.5	15.5	17.5	0.6	1.3	15.5	423.0	547.0
S12	30-40	7.4	28.4	16.5	17.5	0.5	1.2	12.5	345.0	412.0
S13	30-40	6.5	26.8	17.8	16.8	0.5	1.1	13.3	478.0	523.0
S14	20-30	14.3	24.8	16.3	17.5	0.5	1.4	5.8	712.0	615.0
S15	10-20	14.6	25.3	14.2	13.5	0.9	2.3	13.5	634.0	782.0
S16	30-40	7.2	27.5	17.8	17.5	0.4	1.3	5.5	516.0	554.0

S17	20-30	13.5	22.7	16.5	16.5	0.6	1.5	6.7	415.0	575.0
S18	30-40	8.7	13.5	15.6	16.3	0.7	1.2	15.5	395.0	443.0
S19	10-20	15.5	25.5	13.5	13.2	0.9	2.2	15.2	752.0	802.0
S20	30-40	7.8	12.7	3.5	17.5	0.3	1.2	13.5	2755.0	2835.0
S21	20-30	13.7	27.6	16.4	16.2	0.7	1.2	5.5	398.0	542.0
S22	30-40	8.5	25.5	18.5	17.8	0.5	1.3	12.5	435.0	512.0
S23	30-40	6.2	26.4	17.5	16.5	0.6	1.2	12.5	321.0	405.0
S24	20-30	12.5	25.8	17.2	17.7	0.7	1.4	6.2	475.0	515.0
S25	0-10	32.8	21.5	13.2	12.5	2.2	2.5	17.5	1232.0	1519.0
S26	10-20	15.8	24.8	13.2	14.5	1.1	2.2	15.2	672.0	782.0
S27	0-10	31.5	21.5	14.2	12.3	2.1	2.3	16.5	743.0	827.0
S28	10-20	22.5	26.5	13.5	15.5	0.2	8.7	10.8	605.0	735.0
S29	0-10	28.3	22.3	15.3	13.5	2.1	2.4	18.3	1332.0	1432.0
S30	20-30	14.2	26.2	16.5	16.5	0.6	1.2	5.2	317.0	585.0
S31	0-10	13.7	23.2	13.5	13.5	1.2	2.2	14.8	682.0	712.0
S32	10-20	14.7	24.5	14.3	14.5	1.1	2.1	13.5	585.0	676.0
S33	30-40	8.5	28.5	17.3	16.5	0.4	1.5	12.5	314.0	480.0
S34	30-40	7.5	26.3	16.5	15.5	0.7	1.2	12.3	685.0	547.0
S35	10-20	15.2	22.7	14.2	16.3	1.3	2.2	13.2	710.0	803.0
Mean		**16.9±8.6**	**24.1±3.6**	**14.8±2.6**	**15.3±1.9**	**1.04±0.6**	**1.8±0.5**	**12.7±4.2**	**749.4±491.2**	**841.5±495.8**
Range		**26.6**	**15.8**	**15.0**	**7.0**	**2.0**	**1.6**	**13.3**	**2441.0**	**2430.0**

Table 4.37: The vertical distribution of the stable metals in the soil from Selangor

Depth	pH	OM%	P	K	Ca	Mg	Cu	Zn	Mn	Fe	Al
			Mg/kg								
0-10	3.54	2.38	29.24	21.66	13.43	12.73	1.86	2.41	17.25	1124.44	1241.66
10-20	4.09	1.60	16.50	25.14	14.04	14.74	1.12	2.25	13.87	665.88	767.77
20-30	4.34	0.98	14.21	25.97	16.51	17.23	.63	1.33	7.10	484.25	582.37
30-40	4.77	0.73	7.58	23.95	15.66	16.87	.51	1.24	12.23	693.77	745.66
Mean	**4.18**	**1.43**	**16.96**	**24.13**	**14.86**	**15.34**	**1.04**	**1.82**	**12.77**	**749.45**	**841.57**

Table 4.38: Pearson correlation coefficients between the stable metals mg/kg and radionuclides Bq.kg^{-1} in the soil from Selangor

	^{226}Ra	^{232}Th	^{40}K	pH	OM%	P	K	Ca	Mg	Cu	Zn	Mn	Fe	Al
^{226}Ra	1													
^{232}Th	0.943**	1												
^{40}K	0.784**	0.831**	1											
pH	-0.654**	0-.613**	-0.608**	1										
OM%	0.669**	0.629**	0.616**	-.904**	1									
P	0.536**	0.486**	0.467**	-.899**	0.835**	1								
K	0.049	.095	0.004	.251	-0.355*	-0.307	1							
Ca	-0.187	-0.178	-0.307	.384*	-0.404*	-0.342*	0.665**	1						
Mg	-0.628**	-0.579**	-0.558**	.833**	-0.856**	-0.792**	0.322	0.372*	1					
Cu	0.553**	0.546**	0.640**	-.815**	0.840**	0.819**	-0.338*	-0.308	-.789**	1				
Zn	0.688**	0.674**	0.629**	-.861**	0.844**	0.801**	-0.207	-.425*	-0.834**	0.736**	1			
Mn	0.333	0.388*	0.439**	-.557**	0.642**	0.556**	-0.428*	-.453**	-0.743**	0.679**	0.642**	1		
Fe	0.004	0.037	0.055	-0.360*	0.385*	0.418*	-0.637**	-.772**	-0.356*	0.342*	0.334	0.431**	1	
Al	0.037	0.058	0.093	-0.403*	0.401*	0.469**	-0.633**	-.795**	-0.384*	0.379*	0.375*	0.444**	0.987**	1

**. Correlation is significant at the 0.01 level (2-tailed)
*. Correlation is significant at the 0.05 level (2-tailed

4.4.2.2 **The vertical distribution of Potassium (K) in Selangor**

In Selangor, the mean value of K was determined to be 24.10±3.6 mg/kg, with average values vary from 12.7 to 28.5 mg/kg (Table 4.36). The majority of Malaysia's soil series are generally low in K, the mean value of Selangor with the exception levels. Table 4.37 shows the virtical distributions of K; the data show that the K movement decreases with depth, K was greater at 0-10 cm before dropping at 20-30 cm depth.

The vertical distributions of the K are shown in Figure 4.52. The concentrations of K generally increased slightly and regularry with depth, and then declined at lower depths of 30-40 cm, to show a slight peak at 20-30 cm, reflecting K mobility within the soil matrix. As shown in Figure 4.52 an irregular vertical distribution pattern of K within the soil matrix, and K was significantly higher at 20-30 cm. Although Selangor's mean K levels were significantly higher, it behaved in the soil matrix similarly to Kedah.

The associations between radionuclides (^{226}Ra, ^{232}Th, and ^{40}K) and K were determined to be inconsequential, as shown in Table 4.38. Negative correlations ($P \leq 0.01$) were discovered between K and OM, Cu, and Mn, and negative correlations ($P \leq 0.01$) with Fe and Al, whereas the association with Ca was found to be positive ($P \leq 0.01$) Table 4.38.

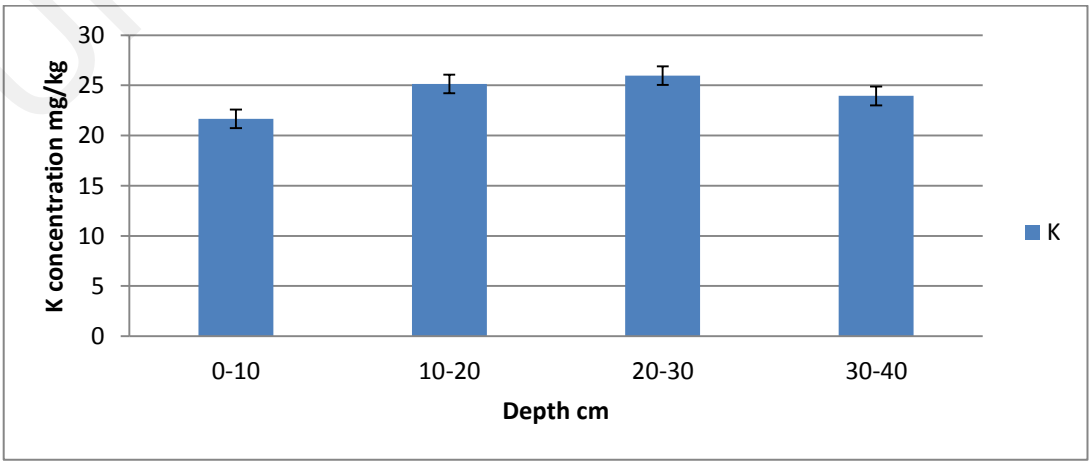

Figure 4.52: The vertical distribution of K in the soil samples from Selangor

4.4.2.3 **The vertical distribution of Calcium (Ca) in Selangor**

The mean value of the Ca was found to be 14.8±2.6 mg/kg in Selangor, while the average values significantly differ from 3.50 to 81.50 mg/kg (Table 4.36). The vertical distribution of the Ca is shown in Table 4.37. The estimated values indicate that the Ca concentrations gradually increased with depth before dropping at 20 cm. Figure 4.53 shows an irregular pattern of vertical distribution of Ca, which recorded a gradual increase before decreasing at the lower depths 20-40 cm.

Relationships between the Ca and the radionuclides (^{226}Ra, ^{232}Th, and ^{40}K) were insignificant. Negative correlations ($P \leq 0.05$) were showed between Ca and OM, P, and Zn, and negative at ($P \leq 0.01$) with Mn, Fe and Al, while the relationships with pH and Mg were positive ($P \leq 0.01$). Poor relationship was found between Ca and Cu (Table 4.38).

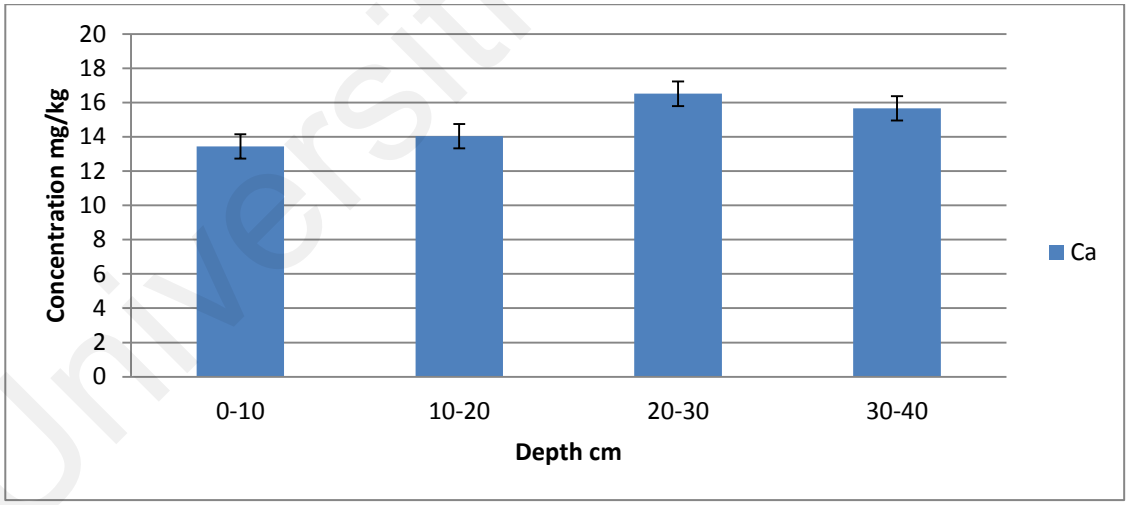

Figure 4.53: The vertical distribution of Ca in the soil samples from Selangor

4.4.2.4 **The vertical distribution of Magnesium (Mg) in Selangor**

Mg was found to have a mean value of 15.34±1.9 mg/kg in Selangor, with range values ranging from 11.50 to 18.50 mg/kg (Table 4.36). Figure 4.54 depicts the

irregular distribution pattern of Mg within the soil matrix. It is clear that Mg concentrations have begun to rise steadily from 0-10 to 20-30 cm in the soil layers, before settling at 30-40 cm depth (Table 4.37).

Relationships between Mg and radionuclides (^{226}Ra, ^{232}Th, and ^{40}K) were negatively correlated ($P \leq 0.01$). Negative correlations ($P \leq 0.01$) were also shown between Mg and OM, P, Cu, Mg, Zn, and Mn, and negative ($P \leq 0.05$) with Fe and Al, while the relationships with pH and Ca are positively correlated ($P \leq 0.01$) and ($P \leq 0.05$), respectively Table 4.38.

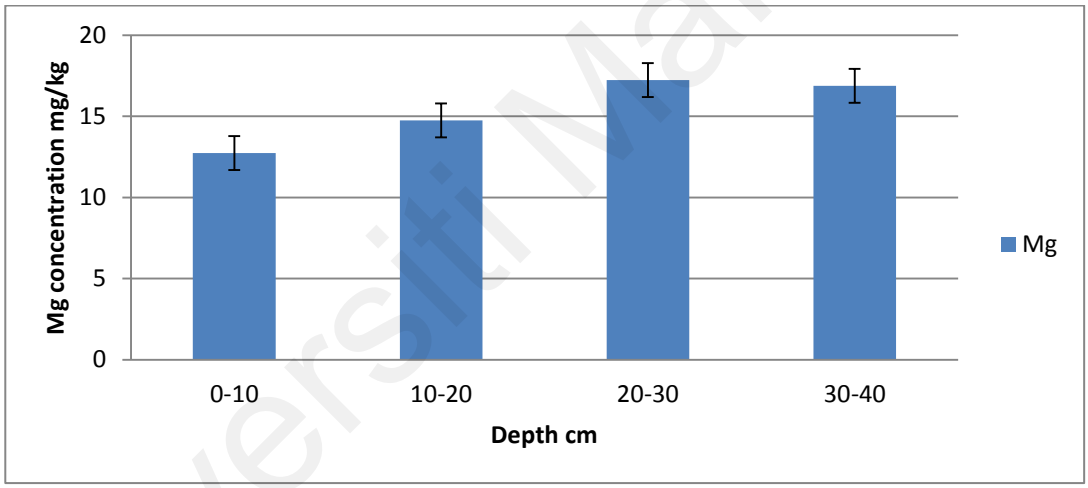

Figure 4.54: The vertical distribution of Mg in the soil samples from Selangor

4.4.2.5 The vertical distribution of Copper (Cu) in Selangor

The mean value of Cu determined to be 1.04±0.6 mg/kg in Selangor, whereas the average values varied from 0.20 to 1.20 mg/kg (Table 4.36). Table 4.37 depicts the vertical distribution of Cu. The measured values show that the Cu migration is decreasing with depth. Figure 4.55 depicts the pattern of uniform distribution of Cu inside the soil matrix.

Relationships between Cu and radionuclides (^{226}Ra, ^{232}Th, and ^{40}K) were positively c -orrelated at ($P \leq 0.01$). Positive correlations ($P \leq 0.01$) were also shown between Cu and OM, P, Zn and Mn, and positive ($P \leq 0.05$) with Fe and Al. Copper (Cu) negatively correlated with pH and Mg ($P \leq 0.01$) and ($P \leq 0.05$), respectively (Table 4.38).

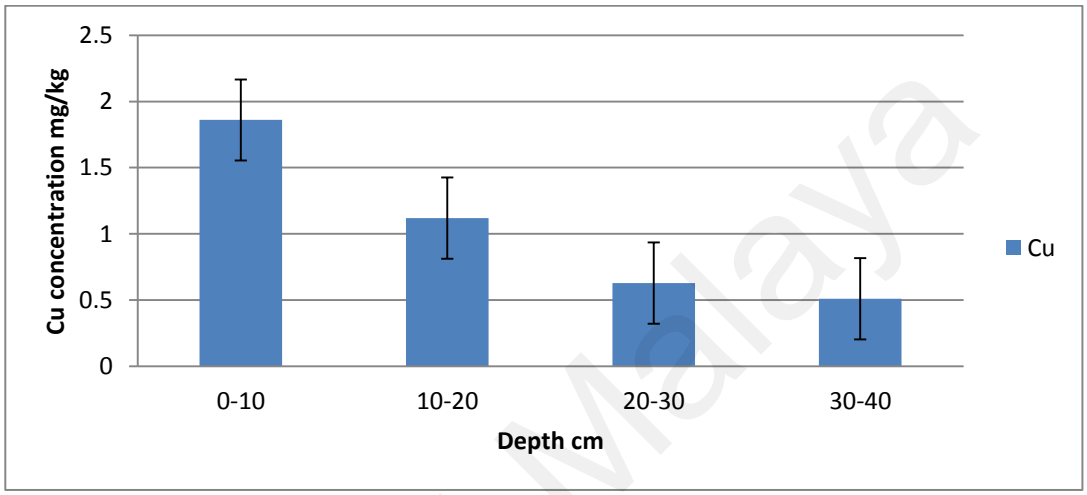

Figure 4.55: The vertical distribution of Cu in the soil samples from Selangor

4.4.2.6 The vertical distribution of Zinc (Zn) in Selangor

The mean value of the Zn found to be 1.99±1.2 mg/kg in Selangor, while the average values differ from 1.10 to 8.70 mg/kg (Table 4.36). The vertical distribution of Zn is shown in Table 4.37. The measured values indicate that the Zn movement is decreased with the depth. The distribution pattern of Zn within the soil matrix is shown in Figure 4.56.

Relationships between Zn and radionuclides (^{226}Ra, ^{232}Th and ^{40}K) were positively correlated ($P \leq 0.01$). Positive correlations ($P \leq 0.01$) were also shown between Zn and pH, OM, P, Cu, and Mn, and positive at ($P \leq 0.05$) with Al. While the relationships with Mg and Ca correlated negatively at ($P \leq 0.01$) and ($P \leq 0.05$), respectively (Table 4.38).

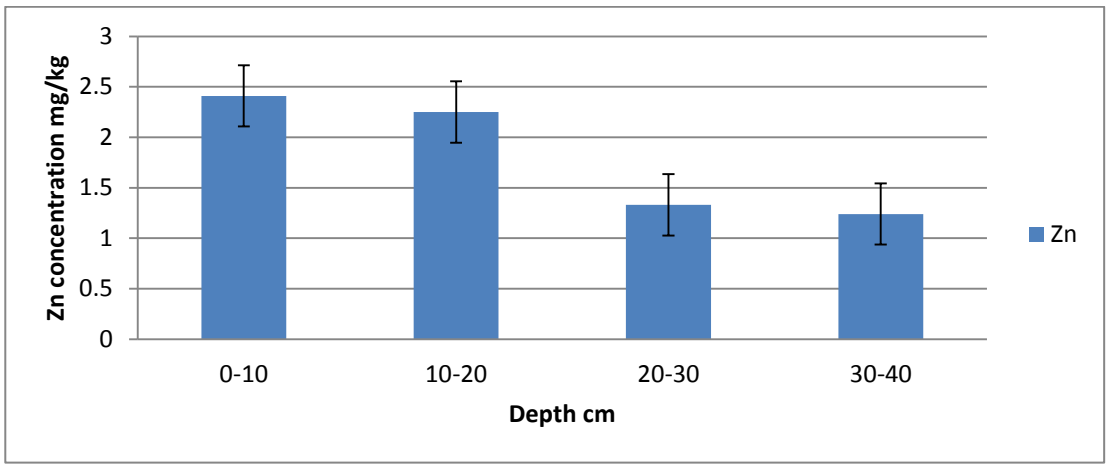

Figure 4.56: The vertical distribution of Zn in the soil samples from Selangor

4.4.2.7 **The vertical distribution of Manganese (Mn) in Selangor**

The mean value of the Mn found to be 12.77±4.2 mg/kg in Selangor, while the average values differ significantly from 5.20 to 18.50 mg/kg (Table 4.36). The vertical distribution of Mn is shown in Table 4.37.

The calculated values indicate that the Mn movement is decreased with the depth, before increasing again at 20-30 cm depth. The pattern of irregular distribution of Mn within the soil matrix is shown in Figure 4.57.

Relationships between the Mn and the radionuclides (^{232}Th and ^{40}K) were positively correlated at ($P \leq 0.05$) and ($P \leq 0.01$), respectively. A weak correlation was shown between Mn and ^{226}Ra. Positive correlations ($P \leq 0.01$) were shown between Mn and OM, P, Cu, and Zn, and positive at ($P \leq 0.05$) with Al. The correlations found to be negative ($P \leq 0.01$) between Mn and pH, Ca and Mg, and negative at ($P \leq 0.05$) with the K (Table 4.38).

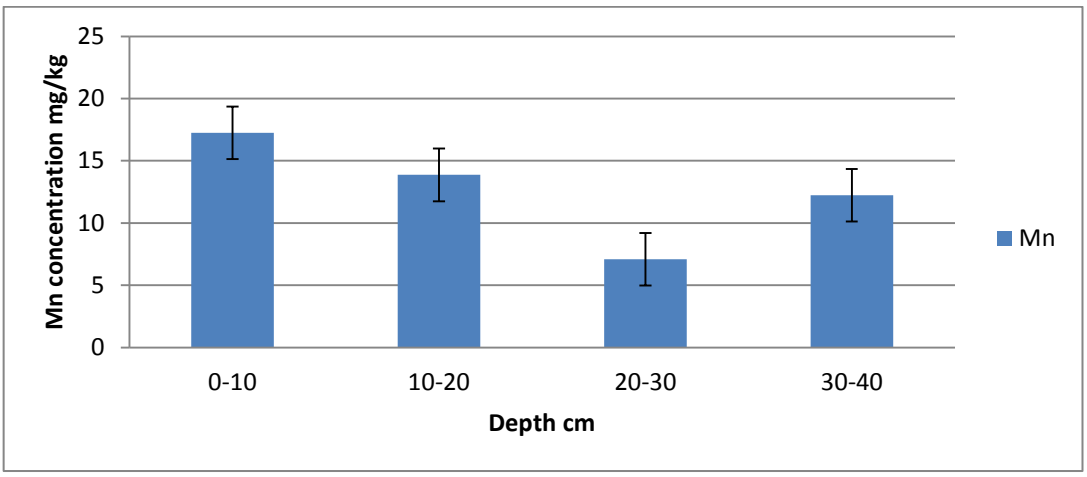

Figure 4.57: The vertical distribution of Mn in the soil samples from Selangor

4.4.2.8 The vertical distribution of Iron (Fe) in Selangor

The mean value of Mn found to be 749.45±49.2 mg/kg in Selangor, while the average values differ significantly from 314.00 to 2755.00 mg/kg (Table 4.36). The vertical distribution of Fe is shown in Table 4.37.

The measured values indicate that the Fe movement is decreased with the depth, before increasing again slightly at 20-30 cm depth. The pattern of irregular distribution of Fe within the soil matrix is shown in Figure 4.58.

Relationships between Fe and radionuclides (^{226}Ra, ^{232}Th and ^{40}K) were found to be insignificant. Positive correlations ($P \leq 0.01$) were shown between Fe and Mn and Al, and positive at ($P \leq 0.05$) with OM and P. The correlations between Fe and pH, Mg and Cu were found to be negative ($P \leq 0.05$), and negative at ($P \leq 0.05$) with K and Ca (Table 4.38).

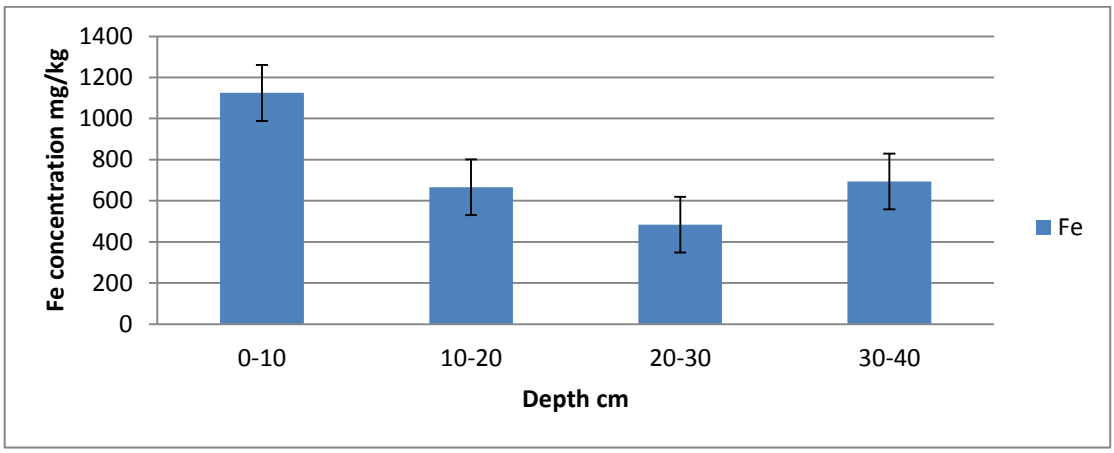

Figure 4.58: The vertical distribution of Fe in the soil samples from Selangor

4.4.2.9 The vertical distribution of Aluminum (Al) in Selangor

In Selangor, the mean value of Al was found to be 841.75±49.8 mg/kg, whereas the average values ranged from 405.00 to 2835.00 mg/kg (Table 4.36). Table 4.37 depicts the vertical distribution of Al. According to the observed results, the Al migration decreases with depth before rising again at 20-30 cm deep. Figure 4.59 depicts the pattern of irregular distribution of Al inside the soil matrix. Relationships between Al and radionuclides (^{226}Ra, ^{232}Th and ^{40}K) were shown to be weak. The relationships between Al and OM, P, Mn and Fe were positively correlated at ($P \leq 0.01$), and positively at ($P \leq 0.05$) with Cu and Zn. Al correlations with pH and Mg were found to be negative ($P \leq 0.05$) in Selangor (Table 4.38).

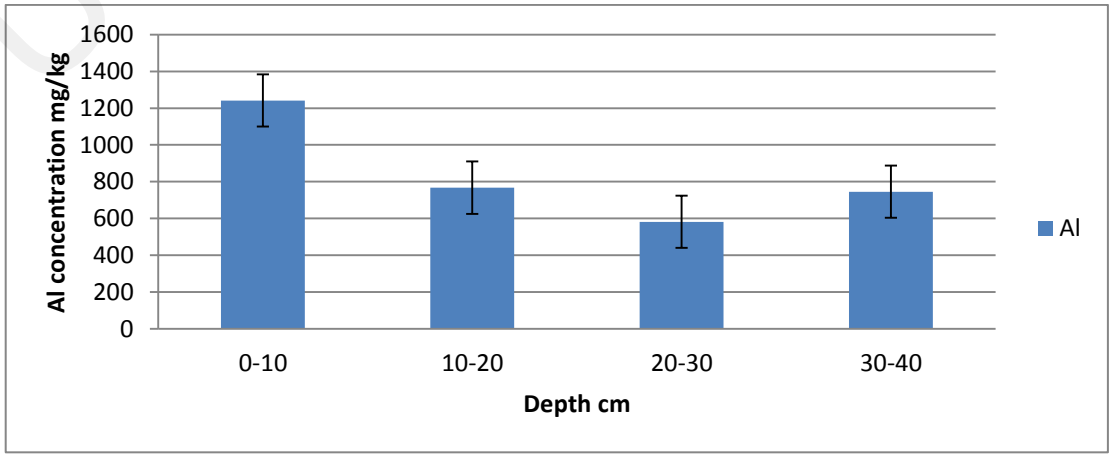

Figure 4.59: The vertical distribution of Al in the soil samples from Selangor

4.4.3 Distribution of stable metals in Malacca

4.4.3.1 The vertical distribution of Phosphorus (P) in Malacca

The mean value of P found to be 9.3± 6.5 mg/kg in Malacca, while the average values differ from 1.3 to 21.2 mg/kg (Table 4.39). The vertical distrubution of P is presented in Table 4.40 and Figur 4.60; the results indicate that the P movement is decreasing with the depth in the collected samples.

P was greater at 0-10 cm and gradually declined as depth increased. Figure 4.60 depicts the pattern of P distribution throughout the soil matrix. It is clear that P continued to decrease to a depth of 40 cm.

Significant positive relationships ($P \leq 0.01$) between the radionuclides (^{226}Ra, ^{232}Th, and ^{40}K) and P have been found. Positive correlations at ($P \leq 0.01$) were also shown between P and OM, K, Cu, Mn, Mg, Fe and Al, and negative ($P \leq 0.05$) with pH, while relationships with Ca and Zn were insignificant Table 4.41.

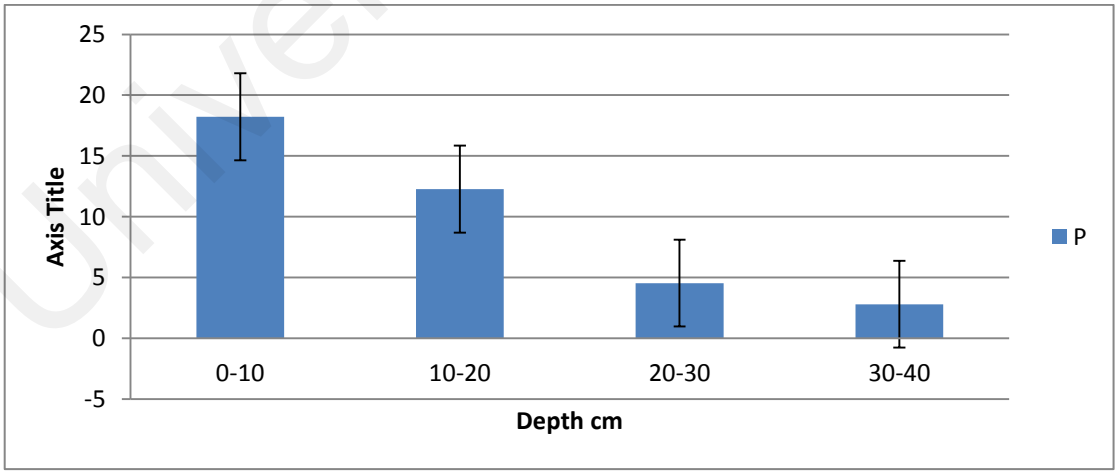

Figure 4.60: The vertical distribution of P in the soil samples from Malacca

Table 4.39: Concentrations of stable metals in the soil samples from Malacca

Sample ID	Depth cm	mg/kg								
		P	K	Ca	Mg	Cu	Zn	Mn	Fe	Al
M1	20-30	6.2	6.5	11.5	6.5	0.7	0.8	7.5	462.0	676.0
M2	0-10	18.4	12.5	11.2	8.2	1.2	1.7	12.5	1512.0	1673.0
M3	30-40	3.7	7.5	12.5	7.4	0.5	0.5	6.5	573.0	582.0
M4	20-30	4.3	7.2	8.5	5.5	0.7	1.1	0.7	453.0	593.0
M5	10-20	11.5	7.5	8.5	7.2	1.1	1.3	8.2	668.0	864.0
M6	30-40	2.5	7.5	16.5	7.5	0.5	0.2	6.2	485.0	543.0
M7	10-20	11.5	8.2	7.3	8.2	1.1	1.5	8.3	874.0	894.0
M8	20-30	5.8	6.5	9.5	7.5	0.6	1.2	6.7	572.0	693.0
M9	30-40	1.3	6.8	9.5	6.5	0.5	0.6	5.8	342.0	463.0
M10	10-20	17.0	9.5	8.5	7.2	1.1	1.3	7.1	763.0	884.0
M11	0-10	21.2	15.3	12.3	8.3	1.2	1.7	11.2	1427.0	1572.0
M12	20-30	7.5	7.3	8.5	8.6	0.6	1.2	7.5	555.0	655.0
M13	0-10	15.8	13.5	15.2	7.5	1.3	1.5	1.2	519.0	675.0
M14	10-20	11.5	7.8	9.5	6.2	1.2	1.2	7.5	625.0	884.0
M15	10-20	10.5	8.5	7.2	7.5	1.1	1.5	8.2	754.0	892.0
M16	0-10	15.7	14.2	12.2	7.8	1.2	1.5	12.3	1404.0	1573.0
M17	20-30	5.8	6.5	9.5	7.2	0.8	1.1	6.5	423.0	676.0
M18	30-40	2.3	8.5	12.5	6.7	0.7	0.5	5.7	485.0	523.0
M19	30-40	1.6	7.5	11.5	5.2	0.6	0.6	4.6	373.0	412.0

M20	30-40	2.5	7.3	8.5	5.5	0.6	0.7	4.7	332.0	378.0
M21	10-20	14.5	8.5	9.2	6.3	1.2	1.3	9.1	654.0	723.0
M22	10-20	13.5	8.5	7.5	7.2	1.1	1.2	8.2	643.0	895.0
M23	0-10	18.5	12.5	13.2	8.5	1.2	1.5	9.5	1621.0	1865.0
M24	20-30	5.2	6.2	12.5	7.0	0.8	1.2	7.3	432.0	534.0
M25	30-40	2.6	6.2	14.3	7.5	0.5	0.6	5.5	335.0	485.0
M26	20-30	1.5	7.5	11.3	8.7	0.7	15.4	6.2	422.0	642.0
M27	10-20	7.5	9.2	8.2	7.6	1.1	1.2	9.2	635.0	858.0
M28	0-10	16.3	13.5	14.3	8.7	1.4	1.7	11.5	778.0	912.0
M29	0-10	18.2	12.5	12.8	9.5	1.2	1.5	9.7	856.0	927.0
M30	20-30	1.8	7.5	9.5	7.5	0.7	1.2	6.5	462.0	656.0
M31	30-40	3.2	7.5	14.5	5.2	0.5	0.4	4.8	385.0	442.0
M32	0-10	21.7	12.5	13.5	7.5	1.2	1.5	11.3	1510.0	1702.0
M33	10-20	12.5	8.2	8.2	6.5	1.1	1.4	9.3	668.0	835.0
M34	0-10	18.2	13.3	12.3	7.5	1.2	1.7	12.4	1547.0	1782.0
M35	10-20	12.7	8.5	7.6	7.3	1.1	1.3	8.5	724.0	882.0
M36	20-30	2.8	7.6	8.5	8.2	0.7	0.8	7.5	532.0	663.0
M37	30-40	4.6	5.3	12.5	5.2	0.6	0.5	4.5	382.0	472.0
M38	30-40	3.7	6.5	11.7	6.7	0.5	0.4	6.3	375.0	525.0
Mean		**9.3±6.5**	**8.8±2.6**	**10.8±2.4**	**7.2±1.0**	**0.8±0.2**	**1.48±2.3**	**7.5±2.7**	**699.0±382.2**	**839.6±409.3**
Range		**20.4**	**10.0**	**9.3**	**4.3**	**0.9**	**15.2**	**11.8**	**1289.0**	**1487.0**

Table 4.40: The vertical distribution of the stable metals in the soil from Malacca

Depth	pH	OM%	P	K	Ca	Mg	Cu	Zn	Mn	Fe	Al
			Mg/kg								
0-10	3.60	3.88	18.22	13.31	13.00	8.16	1.23	1.58	10.17	1241.55	1409.0
10-20	3.91	3.54	12.27	8.44	8.17	7.12	1.12	1.32	8.36	700.80	861.10
20-30	4.15	2.81	4.54	6.97	9.92	7.41	0.70	2.66	6.26	479.22	643.11
30-40	4.71	2.29	2.80	7.06	12.40	6.34	0.55	0.50	5.46	406.70	482.50
Mean	**4.10**	**3.12**	**9.35**	**8.88**	**10.84**	**7.23**	**0.89**	**1.48**	**7.53**	**699.00**	**839.60**

Table 4.41: Pearson correlation coefficients between the stable metals mg/kg and radionuclides Bq.kg^{-1} in the soil from Malacca

	^{226}Ra	^{232}Th	^{40}K	pH	OM	P	K	Ca	Mg	Cu	Zn	Mn	Fe	Al
^{226}Ra	1													
^{232}Th	0.946**	1												
^{40}K	0.782**	0.815**	1											
pH	-0.641**	-0.585**	-0.366*	1										
OM	0.773**	0.765**	0.569**	-0.846**	1									
P	0.697**	0.699**	0.523**	-0.750**	0.837**	1								
K	0.553**	0.516**	0.313	-0.651**	0.725**	0.831**	1							
Ca	-0.214	-0.250	-0.210	0.045	-0.081	0.056	0.331*	1						
Mg	0.386*	0.267	0.036	-0.587**	0.437**	0.449**	0.521**	0.093	1					
Cu	0.794**	0.802**	0.668**	-0.784**	0.918**	0.900**	0.762**	-0.093	0.420**	1				
Zn	0.007	-0.002	-0.153	-0.436**	0.229	0-.047	0.043	-0.010	0.331*	0.050	1			
Mn	0.478**	0.493**	0.250	-0.522**	0.515**	0.680**	0.599**	-0.025	0.550**	0.620**	0.032	1		
Fe	0.496**	0.514**	0.210	-0.640**	0.681**	0.833**	0.819**	0.138	0.477**	0.684**	0.009	0.776**	1	
Al	00.540**	0.566**	0.249	-0.680**	0.723**	0.832**	0.800**	0.103	0.481**	0.706**	0.053	0.776**	0.987**	1

**. Correlation is significant at the 0.01 level (2-tailed).
*. Correlation is significant at the 0.05 level (2-tailed).

4.4.3.2 **The vertical distribution of Potassium (K) in Malacca**

The mean value of K in Malaca found to be 8.80 ± 2.6 mg/kg in Malacca, while the average significantly differs from 5.3 to 15.3 mg/kg (Table 4.39). The vertical distrubution of K is presented in Table 4.40; the values indicate that the K movement is generally decreased with the depth. The distribution pattern of K in Malacca was different from that of Kedah and Selangor, which are expected to contain valuable quantities of K, since they are known to contain some illite and mica in their clay minerals (Zakaria, 1979); in the absence of theses minrrals, soil such as Melaca is very poor in K content in the absence of these minerals. Figure 4.61 shows the distribution pattern of K within the soil matrix. It is evident that the concentrations of K continued to decrease gradually at the lowest depths.

The relationships between K and the radionuclides (^{226}Ra and ^{232}Th) were negatively correlated at ($P \leq 0.01$). Positive correlations ($P \leq 0.01$) were also shown between K and OM, Mg, Cu, Mu, Fe and Al, and positive ($P \leq 0.05$) with the Ca, while, the relationship was a negative ($P \leq 0.01$) with pH. Insignificant relationships were showed with ^{40}K and Zn (Table 4.41).

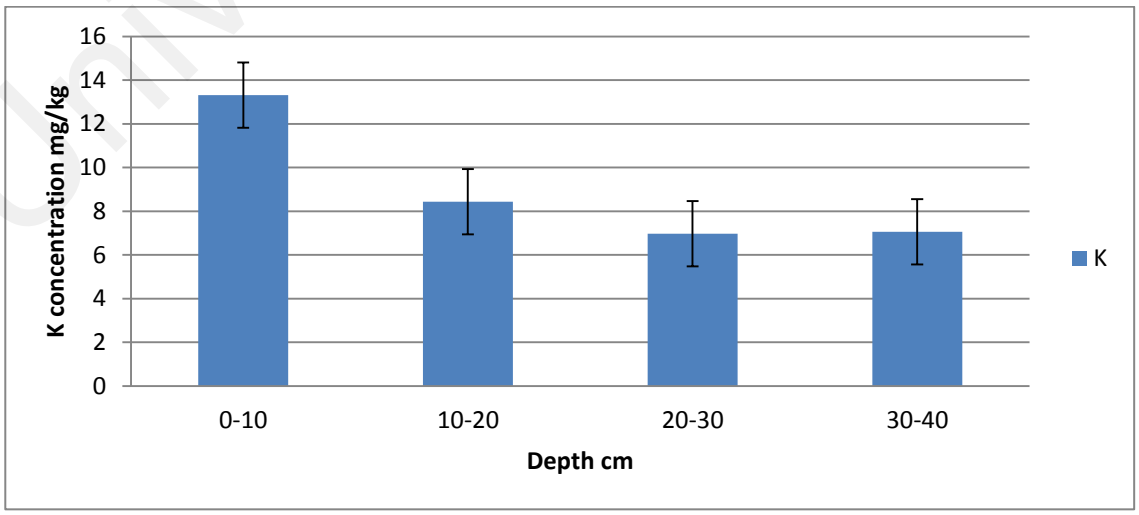

Figure 4.61: The vertical distribution of K in the soil samples from Malacca

4.4.3.3 **The vertical distribution of Calcium (Ca) in Malacca**

The mean value of Ca found to be 10.84±2.4 mg/kg in Malacca, while the average values differ from 7.20 to 16.50 mg/kg (Table 4.39). The vertical distributions of Ca are shown in Table 4.40. Ca concentrations declined with depth before rising again at 10-20 cm, and then progressively increasing to 30-40 cm depth. Figure 4.62 depicts the Ca distribution pattern inside the soil matrix. K concentrations have been continuously decreasing down to a depth of 0-10 to 30-40 cm, as can be shown.

Poor relationships was shown between the Ca and the radionuclides (^{226}Ra, ^{232}Th, and ^{40}K), as wel as with soil pH, OM, P, Mg, Cu, Zn, Mn, Fe and Al, while the correlation with K was a positive ($P \leq 0.05$) (Table 4.41).

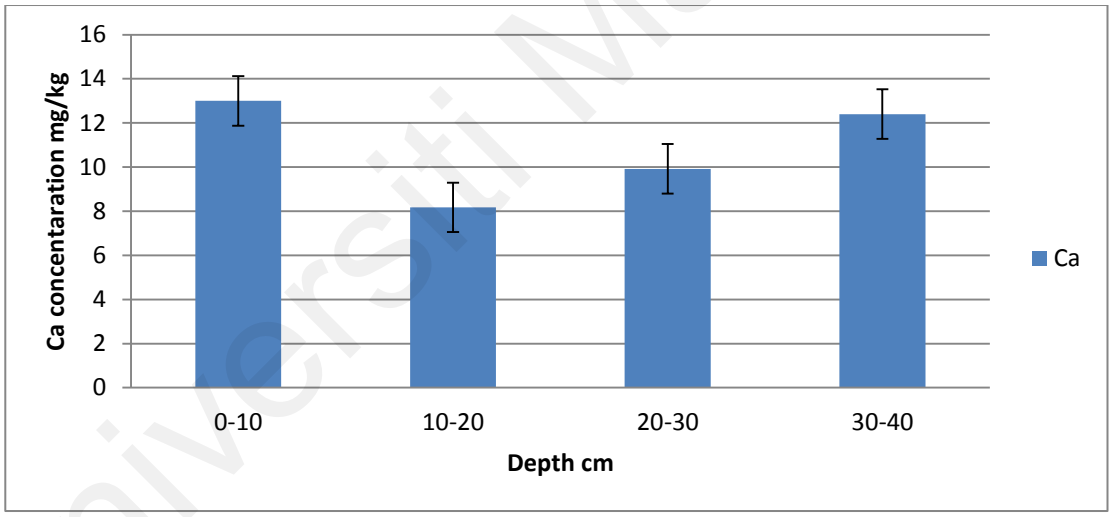

Figure 4.62: The vertical distribution of Ca in the soil samples from Malacca

4.4.3.4 **The vertical distribution of Magnesium (Mg) in Malacca**

The mean value of Mg found to be 7.23±1.0 mg/kg in Malacca, while the average values differ from 5.20 to 9.50 mg/kg (Table 4.39). The vertical distributions of Mg are shown in Table 4.40. The calculated values indicate that the Mg movement is decreasing through the depth. The distribution pattern of Mg within the soil matrix is

shown in Figure 4.63. It is evident that the concentrations of Mg decreased regularly from 0-10 to 30-40 cm in depth.

Relationship between the Mg and ^{226}Ra was a positive ($P \leq 0.05$), while the correlations with ^{232}Th, and ^{40}K were insignificant. Positive correlations ($P \leq 0.01$) were shown between Mg and OM, P, K, Cu, Mn, Fe and Al, while the relationship with Zn was a positive at ($P \leq 0.05$), and negative at ($P \leq 0.01$) with pH (Table 4.41).

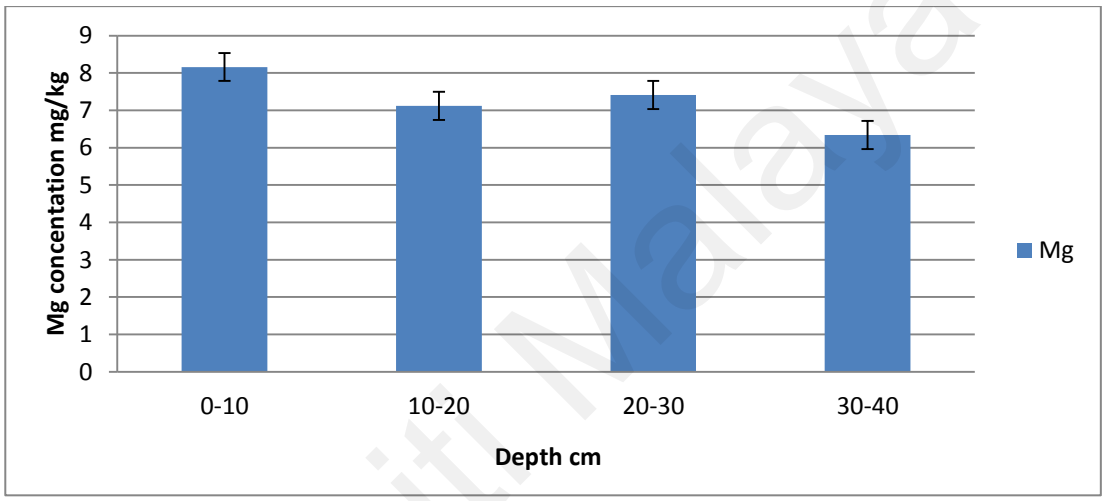

Figure 4.63: The vertical distribution of Mg in the soil samples from Malacca

4.4.3.5 The distribution of Copper (Cu) in Malacca

The mean value of Cu found to be 0.89 ± 0.2 mg/kg in Malacca, with average values ranging from 0.50 to 1.40 mg/kg (Table 4.39). Table 4.40 shows the vertical distribution of Cu. The movement of Cu was reduced through the depth, according to the estimated values. Figure 4.64 depicts the pattern of regular Cu decrease throughout the soil matrix.

Relationships between Cu and radionuclides (^{226}Ra, ^{232}Th and ^{40}K) were positively correlated at ($P \leq 0.01$). Positive correlations ($P \leq 0.01$) were also shown between Cu and OM, P, K, Mg, Zn, Mn, Fe and Al, the relationship between Cu and the soil pH is

positively correlated at ($P \leq 0.01$). A weak relationship was seen between Cu and Ca Table 4.41.

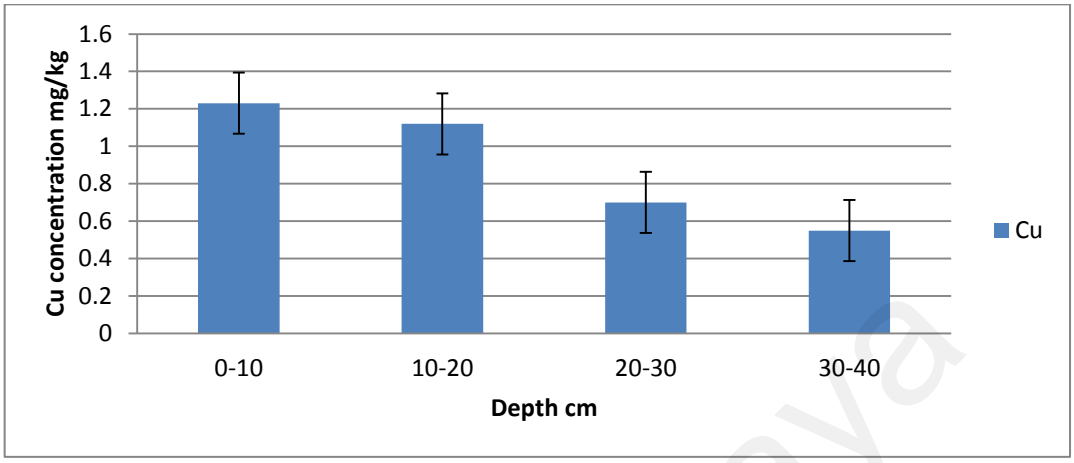

Figure 4.64: The vertical distribution of Cu in the soil samples from Malacca

4.4.3.6 The vertical distribution of Zinc (Zn) in Malacca

The mean value of Zn was found to be 1.48±0.3 mg/kg in Malacca, while the average values differ from 0.20 to 15.40 mg/kg (Table 4.39). The vertical distribution of Zn is shown in Table 4.40. The measured values indicate that the Zn movement was decreased with the depth 10-20 cm, before increasing again at 20-30 cm, and followed by a further decrease at 30-40 cm depth. The pattern of irregular distribution of Zn within the soil matrix is shown in Figure 4.65.

Relationships between Zn and radionuclides (^{226}Ra, ^{232}Th and ^{40}K) were weak. Poor correlations were also shown between Zn and OM, P, K, Ca, Cu, Mn, Fe and Al, while, the relationship with pH was negatively correlated at ($P \leq 0.01$). A positive correlation ($P \leq 0.05$) was observed between Zn and Mg (Table 4.41).

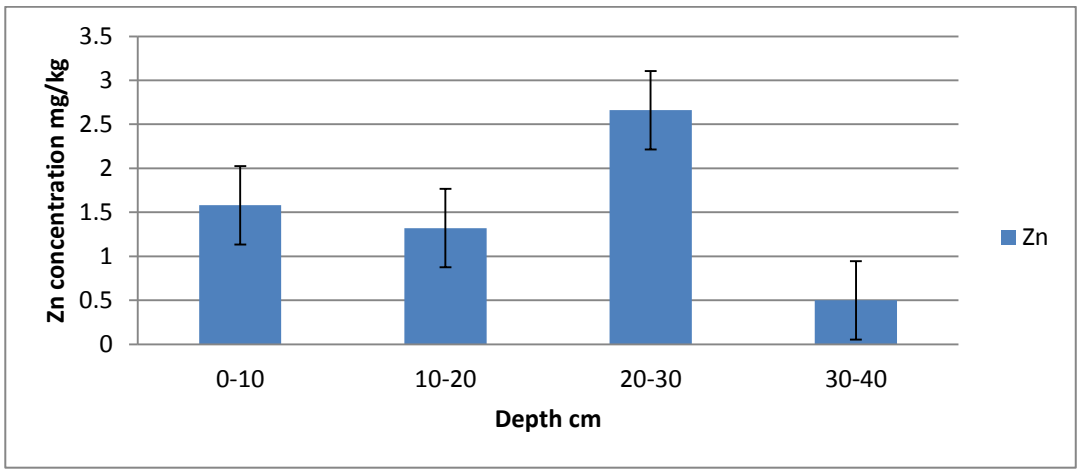

Figure 4.65: The vertical distribution of Zn in the soil samples from Malacca

4.4.3.7 The vertical distribution of Manganese (Mn) in Malacca

The mean value of Mn was found to be 7.53±2.7 mg/kg in Malacca, while the average values differ from 0.70 to 12.50 mg/kg (Table 4.39). The vertical distribution of Mn is shown in Table 4.40. The calculated values indicate that the Mn movement was decreased with the depth. The pattern of irregular distribution of Mn within the soil matrix is shown in Figure 4.66.

Relationships between Mn and radionuclides (^{226}Ra and ^{232}Th) were shown to be positively correlated (P ≤0.01), while a weak relationship was shown with ^{40}K. Positive correlations (P ≤0.01) were also shown between Mn and OM, P, K, Mg, and Cu, and negative (P ≤0.01) with the soil pH. Insignificant relationships were shown with Ca, Zn, Fe and Al (Table 4.41).

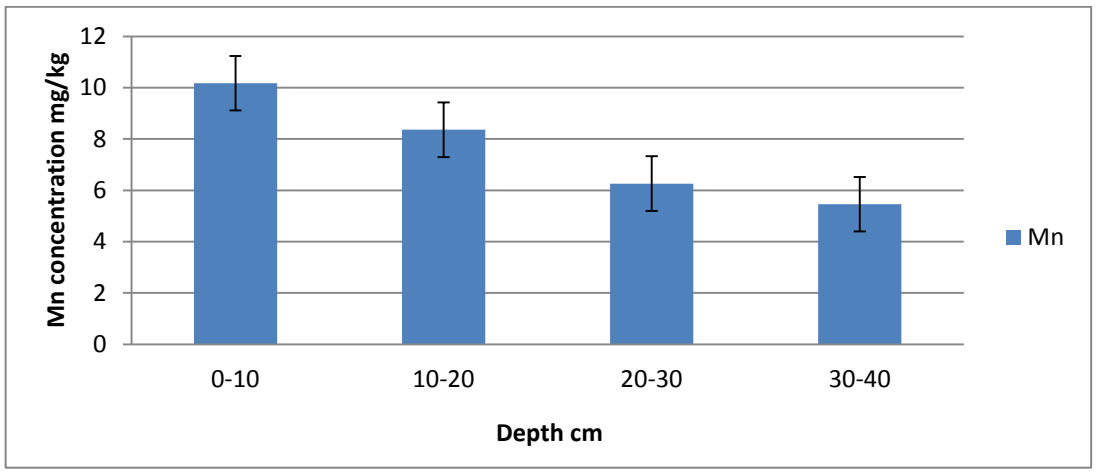

Figure 4.66: The vertical distribution of Mn in the soil samples from Malacca

4.4.3.8 The vertical distribution of Iron (Fe) in Malacca

In Malacca, the mean value of Fe was found to be 699.00±51.2 mg/kg, with average values ranging from 332.00 to 1612.00 mg/kg (Table 4.39).

Table 4.40 depicts the vertical distribution of Fe. The Fe migration was found to be decreasing with depth, based on the observed values. Figure 4.67 depicts the pattern of regular Fe distribution within the soil matrix.

Relationships between Fe and radionuclides (^{226}Ra and ^{232}Th) were positively correlated at ($P \leq 0.01$), while the correlation with ^{40}K was found to be insignificant. Positive correlations at ($P \leq 0.01$) were shown between Fe and OM, P, K, Mg, Cu, Mn and Al, while the correlation with pH was a negative ($P \leq 0.05$ (Table 4.41).

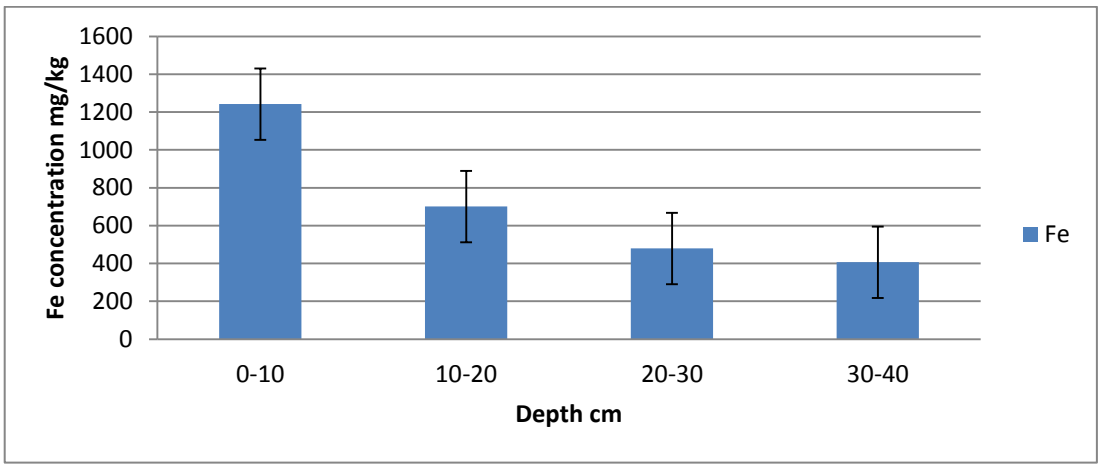

Figure 4.67: The vertical distribution of Fe in the soil samples from Malacca

4.4.3.9 The vertical distribution of Aluminum (Al) in Malacca

The mean value of Al was found to be 839.60±40.3 mg/kg in Malacca, while the average values differ significantly from 378.00 to 1865.00 mg/kg (Table 4.39). The vertical distribution of Al is shown in Table 4.40. The measured values indicate that the Al movement was decreased with the depth.

The pattern of irregular distribution of Al within the soil matrix is shown in Figure 4.68. Relationships between Al and radionuclides ^{226}Ra and ^{232}Th were positively correlated (P ≤0.01), while the correlation with ^{40}K was insignificant. The relationships between Al and OM, P, K, Mg, Cu, Mn and Fe were positively correlated at (P ≤0.01), and negatively at (P ≤0.01) with the soil pH (Table 4.41).

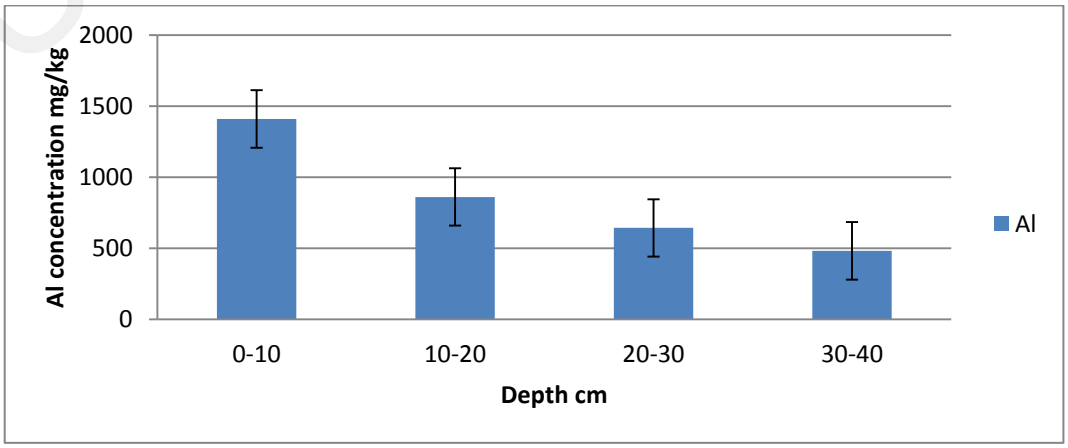

Figure 4.68: The vertical distribution of Al in the soil samples from Malacca

4.4.4 Distribution of stable metals in Johor

4.4.4.1 The vertical distribution of Phosphorus (P) in Johor

P was found with a mean value of 19.53±10.4 mg/kg in Johor, with range values ranging from 6.50 to 28.50 mg/kg (Table 4.42). Table 4.43 shows the vertical distributions of P, the concentrations of K dropped somewhat with depth. Figure 4.69 shows the distribution pattern of P within the soil matrix. It is evident that the concentrations of P show consistent decreasing with the depth, the concentrations were higher in the surface, and then regularly decreased with the depth. The downward movement of P was similar to the distribution pattern of Malacca.

The relationships between P and the radionuclides (^{226}Ra, ^{232}Th, and ^{40}K) were found to be positive ($P \leq 0.01$). Positive correlations ($P \leq 0.01$) were also shown between P and OM, P, K, Ca, Mg, Cu, Z, Mn, Fe and Al, while the relationship was negative at ($P \leq 0.01$) with pH (Table 4.44).

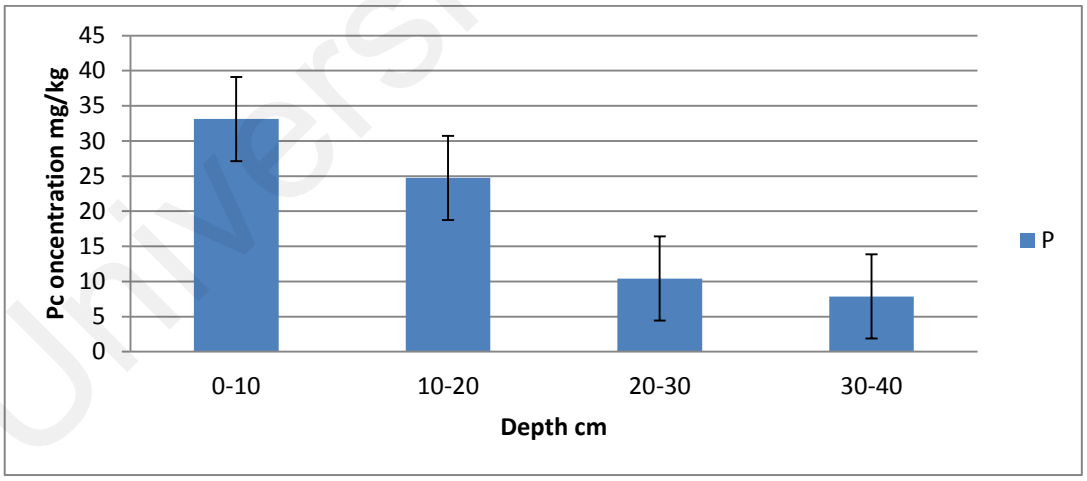

Figure 4.69: The vertical distribution of P in the soil samples from Johor

Table 4.42: Concentrations of stable metals in the soil samples from Johor

Sample ID	Depth cm	mg/kg								
		P	K	Ca	Mg	Cu	Zn	Mn	Fe	Al
JB1	0-10	32.3	28.2	15.2	12.5	1.6	2.3	14.5	1612.0	1656.0
JB2	10-20	28.0	18.5	12.5	13.2	2.2	2.2	12.5	673.0	885.0
JB3	30-40	9.5	7.5	7.5	7.3	3.5	0.8	11.3	423.0	544.0
JB4	30-40	8.5	7.5	7.3	8.5	2.7	0.9	9.2	332.0	466.0
JB5	20-30	12.5	11.2	8.5	8.3	2.8	1.5	9.3	568.0	582.0
JB6	30-40	7.0	8.5	8.3	11.5	3.6	1.1	8.5	385.0	508.0
JB7	10-20	23.5	18.5	15.5	12.2	2.2	2.4	13.5	1524.0	1564.0
JB8	10-20	23.8	21.3	16.3	11.3	2.2	2.8	14.7	517.0	532.0
JB9	20-30	12.3	16.5	8.5	7.5	2.5	0.8	8.2	1410.0	1652.0
JB10	0-10	31.0	28.5	15.5	12.8	1.8	2.2	14.5	1358.0	1584.0
JB11	20-30	9.2	8.5	7.6	7.3	2.6	2.8	8.2	415.0	471.0
JB12	0-10	29.5	27.5	15.5	9.6	1.5	1.8	12.5	745.0	962.0
JB13	30-40	7.5	9.2	8.2	7.5	3.5	1.1	7.3	326.0	454.0
JB14	30-40	8.5	7.5	7.5	6.5	3.7	0.9	8.4	332.0	492.0
JB15	20-30	11.7	12.5	10.2	8.3	2.8	1.5	8.5	457.0	543.0
JB16	10-20	25.3	21.3	12.5	12.6	2.4	2.2	12.2	711.0	872.0
JB17	10-20	25.2	19.5	16.5	8.2	2.3	2.2	13.5	423.0	783.0

JB18	20-30	11.5	9.5	9.5	8.5	2.5	1.5	11.7	433.0	578.0
JB19	0-10	32.5	23.7	14.2	11.0	1.7	2.2	13.5	1458.0	1486.0
JB20	30-40	7.3	8.5	12.8	8.5	3.5	1.1	7.5	325.0	464.0
JB21	10-20	23.2	17.5	13.2	12.5	2.3	2.1	14.2	767.0	791.0
JB22	30-40	7.2	7.5	7.5	7.5	3.6	1.2	8.5	285.0	424.0
JB23	20-30	9.2	8.7	7.2	6.5	2.5	0.8	7.5	345.0	395.0
JB24	0-10	35.5	28.5	14.3	11.5	1.5	2.5	13.2	1472.0	1573.0
JB25	20-30	8.5	9.2	8.7	7.3	2.7	1.2	8.5	285.0	484.0
JB26	0-10	32.5	27.2	15.5	9.7	1.6	2.5	14.2	685.0	815.0
JB27	20-30	8.2	8.6	11.5	7.5	2.8	1.4	9.3	434.0	587.0
JB38	10-20	25.2	15.5	13.5	14.3	2.3	2.1	12.5	607.0	856.0
JB39	10-20	22.5	17.5	14.3	12.2	2.2	2.1	13.5	435.0	742.0
JB30	30-40	7.5	6.5	8.5	7.3	3.5	1.2	8.5	358.0	426.0
JB31	0-10	38.5	25.7	16.3	11.7	1.5	1.7	13.2	1468.	15150
JB32	20-30	8.2	9.2	11.5	8.2	2.7	1.3	10.5	485.0	558.0
JB33	0-10	35.7	27.4	17.5	10.3	1.6	1.8	15.5	1384.0	1462.0
JB34	20-30	11.2	11.4	9.5	7.2	2.5	1.3	8.5	382.0	552.0
JB35	0-10	32.6	28.2	15.4	12.5	1.8	2.5	13.5	1268.0	1412.0
JB36	10-20	23.5	17.5	13.3	14.5	2.2	2.1	12.5	637.0	754.0
JB37	20-30	12.2	8.50	12.5	12.2	2.5	1.4	8.5	345.0	458.0
JB38	10-20	23.7	18.2	13.5	14.2	2.2	2.3	12.5	625.0	757.0
JB39	0-10	31.2	27.5	15.5	9.50	1.7	2.2	13.2	795.0	817.0
JB40	10-20	28.3	17.5	13.4	13.0	2.3	2.5	12.5	428.0	652.0
Mean		**19.5±10.4**	**16.2±7.7**	**12.0±3.2**	**10.0±2.4**	**2.4±0.6**	**1.7±0.6**	**11.2±2.5**	**697.9±428.9**	**827.7±419.1**
Range		**31.5**	**22.0**	**10.3**	**8.0**	**2.2**	**2.0**	**8.2**	**1327.0**	**1261.0**

Table 4.43: The vertical distribution of the stable metals in the soil from Johor

Depth	pH	OM%	P	K	Ca	Mg	Cu	Zn	Mn	Fe	Al
			mg/kg								
0-10	3.47	4.49	33.13	27.24	15.49	11.11	1.63	2.17	13.78	1224.50	1328.20
10-20	3.87	3.82	24.74	18.43	14.04	12.56	2.25	2.27	13.10	667.90	835.27
20-30	4.48	2.77	10.42	10.34	9.56	8.07	2.62	1.40	8.97	505.36	623.63
30-40	4.83	2.76	7.87	7.83	8.45	8.07	3.45	1.03	8.65	345.75	472.25
Mean	**4.13**	**3.49**	**19.53**	**16.29**	**12.05**	**10.06**	**2.44**	**1.76**	**11.24**	**697.92**	**827.70**

Table 4.44: Pearson correlation coefficients between the stable metals mg/kg and radionuclides Bq.kg^{-1} in the soil from Johor

	^{226}Ra	^{232}Th	^{40}K	pH	OM	P	K	Ca	Mg	Cu	Zn	Mn	Fe	Al
^{226}Ra	1													
^{232}Th	0.936**	1												
^{40}K	0.849**	0.858**	1											
pH	-0.532**	-0.520**	-0.452**	1										
OM	0.487**	0.482**	0.415**	-0.792**	1									
P	0.609**	0.577**	0.482**	-0.930**	0.855**	1								
K	0.575**	0.554**	0.479**	-0.888**	0.855**	0.959**	1							
Ca	0.562**	0.541**	0.441**	-0.800**	0.748**	0.853**	0.834**	1						
Mg	0.674**	0.644**	0.548**	-0.566**	0.656**	0.656**	0.568**	0.609**	1					
Cu	-0.493**	-0.473**	0-.441**	0.887**	-0.734**	-0.878**	-0.873**	-0.801**	-0.531**	1				
Zn	0.608**	0.581**	0.475**	-0.736**	0.655**	0.770**	0.734**	0.717**	0.644**	-0.691**	1			
Mn	0.589**	0.573**	0.510**	-0.843**	0.784**	0.900**	0.856**	0.856**	0.631**	-0.792**	0.765**	1		
Fe	0.297*	0.292	0.241	-0.597**	0.600**	0.711**	0.742**	0.570**	0.425**	-0.683**	0.425**	0.600**	1	
Al	0.329*	0.334*	0.259	-0.625**	0.614**	0.726**	0.753**	0.575**	0.445**	-0.678**	0.426**	0.607**	0.979**	1

**. Correlation is significant at the 0.01 level (2-tailed)
*. Correlation is significant at the 0.05 level (2-tailed)

4.4.4.2 **The vertical distribution of Potassium (K) in Johor**

The mean value of K was found to be 16.2±7.7 mg/kg in Johor, while the average values vary signifacntly from 6.5 to 28.50 mg/kg (Table 4.42). The vertical distributions of K are shown in Table 4.43, the results show that the K movement reduced irregularly with depth, with K being higher at 0-10 cm and then decreasing with depth. Figure 4.70 shows the distribution pattern of K within the soil matrix. The concentrations of K clearly continued to decline steadily downhill to a depth of 40 cm.

The relationships between K and the radionuclides (^{226}Ra, ^{232}Th, and ^{40}K) correlated positively at ($P \leq 0.01$). Positive correlations ($P \leq 0.01$) were also shown between K and OM, P, Ca, Mg, Cu, Zn, Mn, Fe and Al, while the relationship found to be negative ($P \leq 0.01$) with the soil pH in Johor Table 4.44.

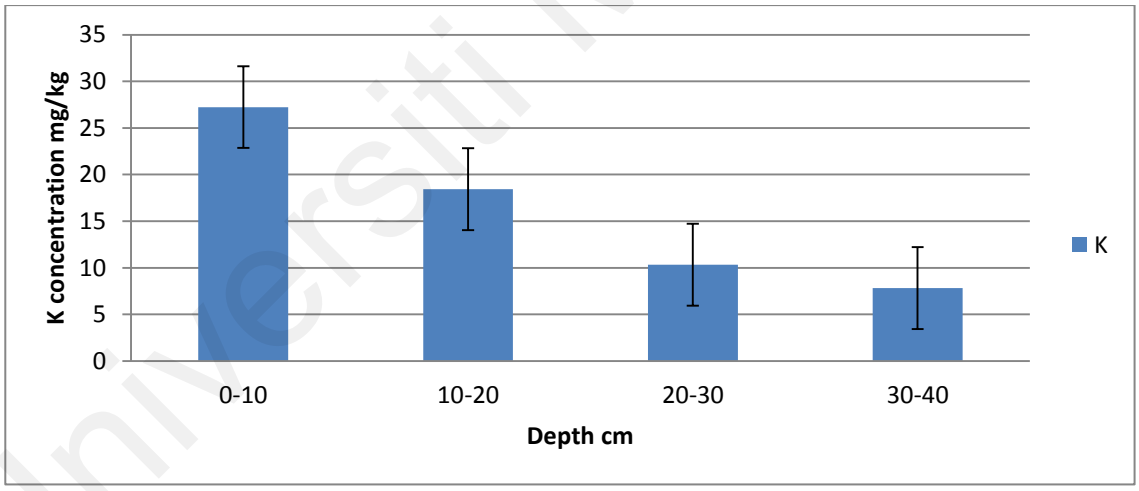

Figure 4.70: The vertical distribution of K in the soil samples from Johor

4.4.4.3 **The vertical distribution of Calcium (Ca) in Johor**

Ca was found with a mean value of 12.05±3.2 mg/kg in Johor, with average values ranging from 7.20 to 17.50 mg/kg. Table 4.43 depicts the vertical distribution of Ca. The computed figures show that the Ca migration reduced as depth increased. Ca levels were greater at 0-10 cm and gradually dropped as the soil profile progressed. Figure

4.71 depicts the Ca distribution pattern inside the soil matrix. Ca concentrations have clearly begun to slowly decline with depth from 0-10 cm, reaching 30-40 cm.

Relationships between Ca and radionuclides (^{226}Ra, ^{232}Th, and ^{40}K) were positively c orrelated at ($P \leq 0.01$). Positive correlations ($P \leq 0.01$) were also shown between Ca and OM, P, K, Mg, Zn, Mn, Fe and Al, and negative ($P \leq 0.05$) with pH and Cu (Table 4.44).

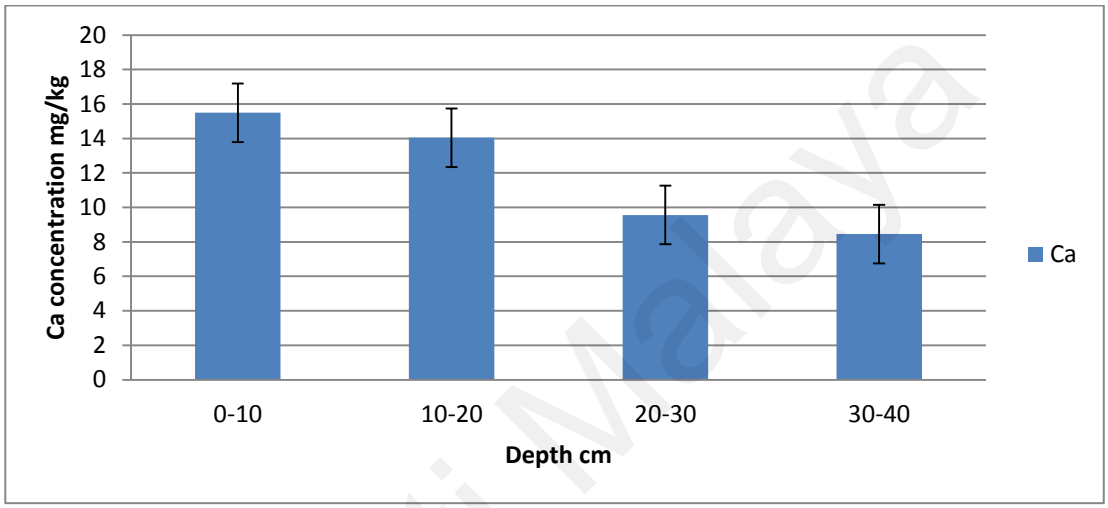

Figure 4.71: The vertical distribution of Ca in the soil samples from Johor

4.4.4.4 The vertical distribution of Magnesium (Mg) in Johor

The mean value of Mg was found to be 10.06±2.4 mg/kg in Johor, while the average values differ from 6.50 to 14.50 mg/kg (Table 4.42). The vertical distribution of Mg is shown in Table 4.43. The estimated figures show that concentrations grew with depth before decreasing at depth 20 cm and stabilising at this level in the lower depths. Figure 4.72 depicts the distribution pattern of Mg inside the soil matrix. The Mg concentrations indicated an irregular distribution pattern.

Mg and radionuclide relationships (^{226}Ra, ^{232}Th, and ^{40}K) were positively linked at ($P \leq 0.01$). Positive ($P \leq 0.01$) relationships were also found between Mg and OM, P, K, Ca, Zn, Mn, Fe, and Al. Mg and pH were shown to have a negative connection ($P \leq 0.01$) (Table 4.44).

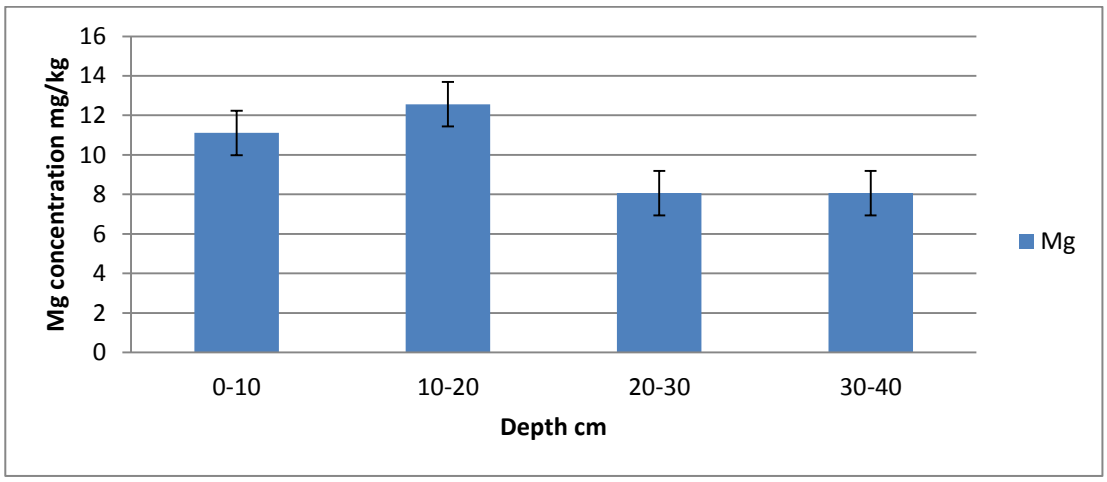

Figure 4.72: The vertical distribution of Mg in the soil samples from Johor

4.4.4.5 **The vertical distribution of Copper (Cu) in Johor**

Cu was found to have a mean value of 2.44±0.6 mg/kg in Johor, with range values ranging from 1.50 to 3.70 mg/kg (Table 4.42). Table 4.43 represents the vertical distribution of Cu. The computed data show that Cu migration increases with depth. Figure 4.73 shows the pattern of uniform distribution of Cu within the soil matrix.

Relationships between Cu and radionuclides (^{226}Ra, ^{232}Th and ^{40}K) were negatively correlated ($P \leq 0.05$). Negative correlations ($P \leq 0.01$) were also shown between Cu and OM, P, K, Ca, Zn, Mn, Fe and Al. A positive correlation ($P \leq 0.01$) was seen between Cu and soil pH (Table 4.44).

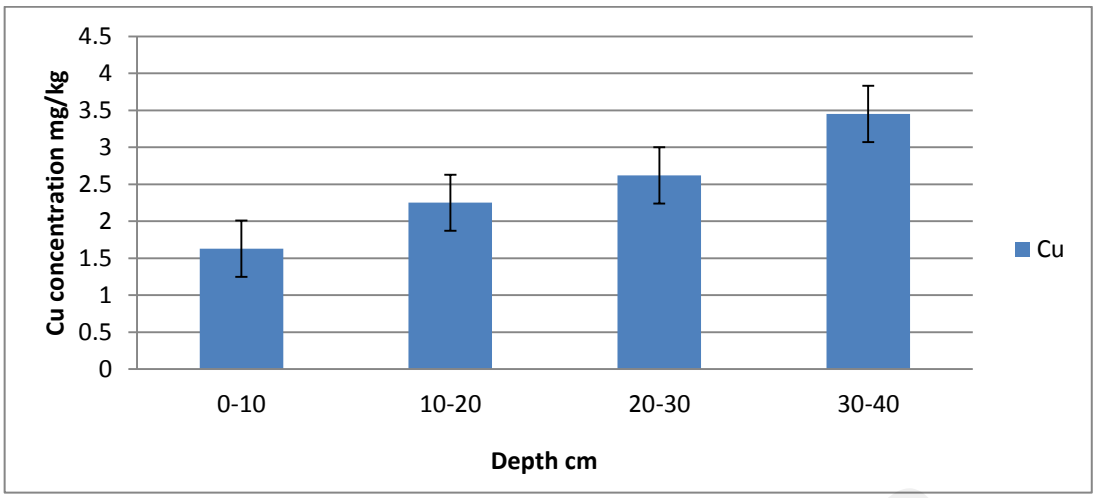

Figure 4.73: The vertical distribution of Cu in the soil samples from Johor

4.4.4.6 The vertical distribution of Zinc (Zn) in Johor

In Johor, the mean value of Zn was found to be 1.76±0.6 mg/kg, with range values differ from 0.80 to 2.80 mg/kg (Table 4.42). Table 4.43 shows the vertical distribution of Zn. According to the computed results, the Cu movement decreased with depth. Figure 4.74 depicts the pattern of Cu distribution throughout the soil matrix.

Relationships between Zn and radionuclides (^{226}Ra, ^{232}Th and ^{40}K) were correlated positively (P ≤0.01). Positive relationships (P ≤0.01) were also shown between Zn and OM, K, Ca, Mg, Mn, Fe and Al, and negative (P ≤0.01) with pH and Cu (Table 4.44).

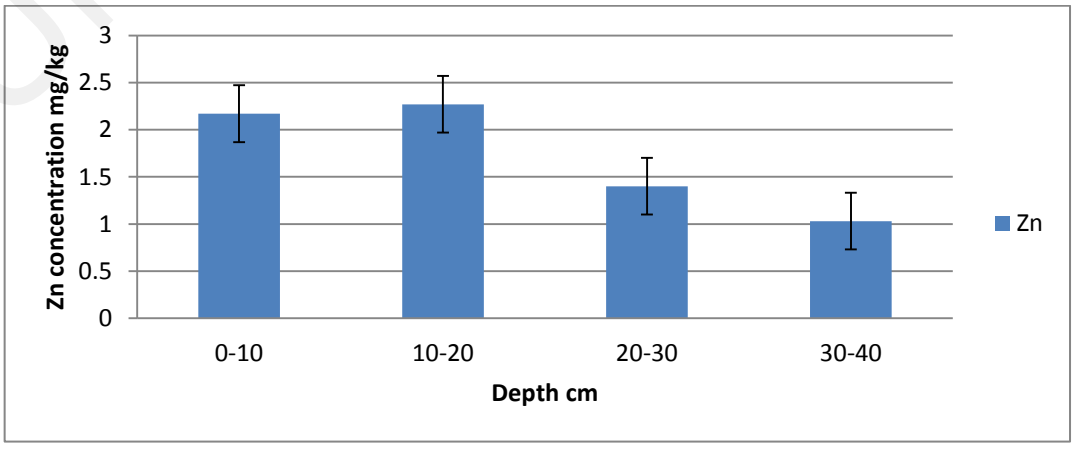

Figure 4.74: The vertical distribution of Zn in the soil samples from Johor

4.4.4.7 **The vertical distribution of Manganese (Mn) in Johor**

In Johor, the mean value of Mn was found to be 11.25±2.5 mg/kg, whereas the average values ranged from 7.30 to 15.50 mg/kg (Table 4.42). Table 4.43 represents the vertical distribution of Mn. The estimated results show that Mn mobility has been reduced within the soil profile. Figure 4.75 shows the pattern of uniform distribution of Mn inside the soil matrix.

Relationships between Mn and radionuclides (^{226}Ra, ^{232}Th and ^{40}K) were positively correlated (P ≤0.01). Positive correlations (P ≤0.01) were also shown between Mn and OM, P, K, Ca, Mg, Zn, Fe and Al, while the relationships correlated negatively (P ≤0.01) with pH and Cu (Table 4.44).

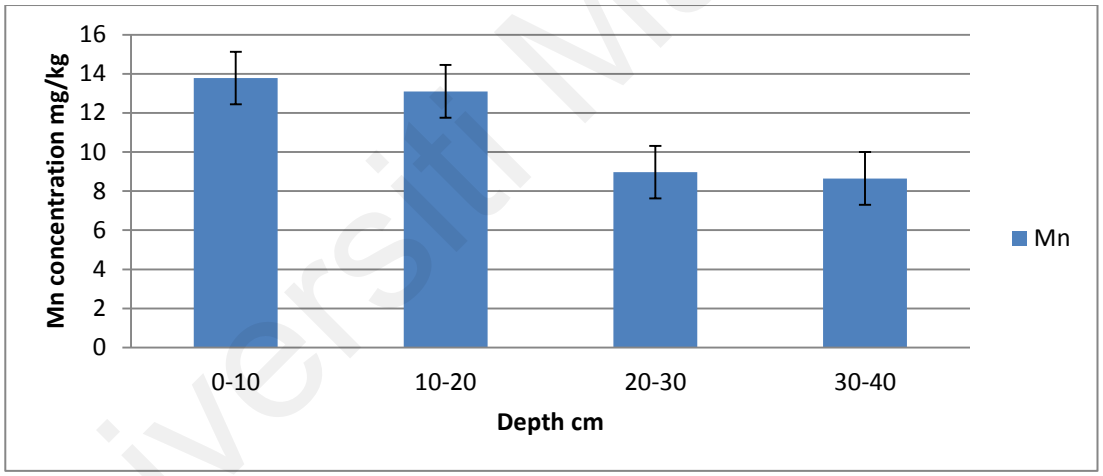

Figure 4.75: The vertical distribution of Mn in the soil samples from Johor

4.4.4.8 **The vertical distribution of Iron (Fe) in Johor**

In Johor, the mean value of Fe was determined to be 697.92±41.5 mg/kg, whereas the range values differ from 285.00 to 1612.00 mg/kg (Table 4.42). Table 4.43 shows the vertical distribution of Fe. The measured data show that the Fe mobility inside the profile was reduced. Figure 4.76 depicts the pattern of uniform distribution of Fe within the soil matrix.

The relationship between Fe and ^{226}Ra was found to be positive (P ≤0.05), whereas the correlations with ^{232}Th and ^{40}K were found to be insignificant. There was a positive (P ≤0.01) association between Fe and OM, P, K, Ca, Zn, Mn, and Al, and a negative relationship (P ≤0.01) between pH and Cu (Table 4.44).

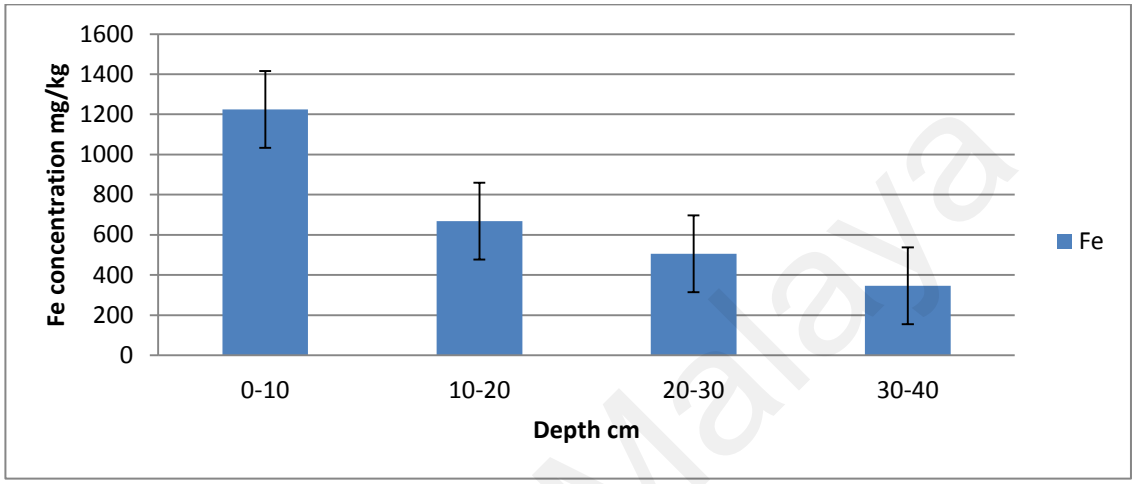

Figure 4.76: The vertical distribution of Fe in the soil samples from Johor

4.4.4.9 The vertical distribution of Aluminum (Al) in Johor

The mean value of Al was found to be 827.70±41.1 mg/kg in Johor, while the range values differ significantly from 395.00 to 1656.00 mg/kg (Table 4.42). The vertical distribution of Al is shown in Table 4.43. The measured data show that Al mobility within the soil profile has decreased. Figure 4.77 shows the pattern of regular Al distribution within the soil matrix.

Relationships between Al and the radionuclides ^{226}Ra and ^{232}Th were positively correlated (P ≤0.05). A weak correlation was shown between Al and ^{40}K. The relationships between Al and OM, P, K, Ca, Mg, Zn, Mn and Fe were positively correlated (P ≤0.01), and negatively at (P ≤0.01) with pH and Cu (Table 4.44).

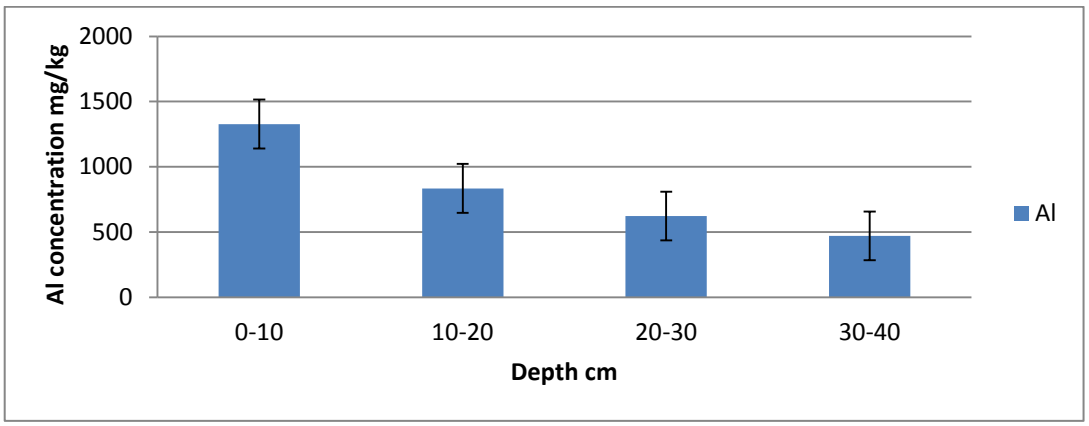

Figure 4.77: The vertical distribution of Al in the soil samples from Johor

4.4.5 Distribution of stable metals in Raub

4.4.5.1 The vertical distribution of Phosphorus (P) in Raub

P was found to have a mean value of 13.5±6.3 mg/kg in Raub, with range values differ from 5.3 to 25.5 mg/kg (Table 4.45). The vertical P distributions illustrated in Table 4.46 and Figure 4.78. The measured data show that P mobility within the soil profile has decreased. Figure 4.78 depicts the pattern of P distribution throughout the soil matrix. P continued to decline until it reached a depth of 40 cm. Raub showed no alteration in the distribution pattern of P concentrations. The relationships between P and the radionuclides (^{226}Ra, ^{232}Th and ^{40}K) were correlatrd positively at ($P \leq 0.01$). A positive correlations ($P \leq 0.01$) were also shown between P and OM, K, Ca, Mg, Cu, Zn, Mn, Fe and Al, while, relationship with pH negatively correlated ($P \leq 0.01$) (Table 4.47).

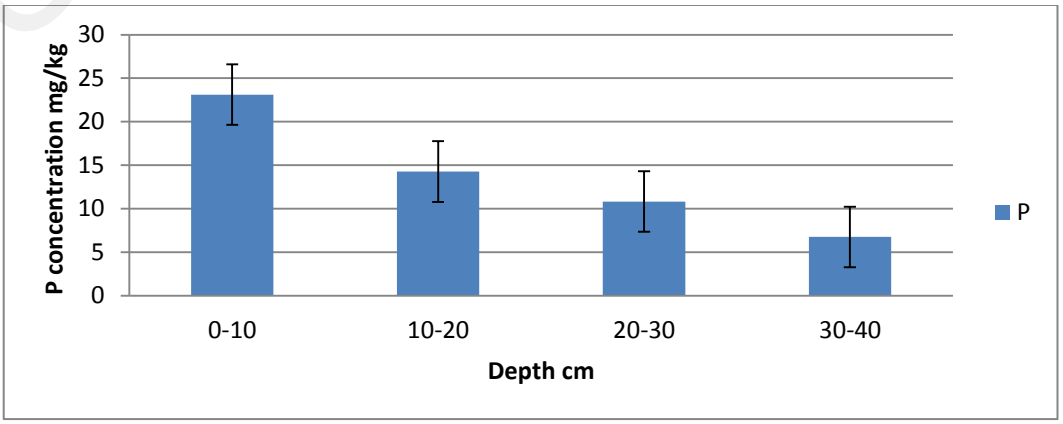

Figure 4.78: The vertical distribution of P in the soil samples from Raub

Table 4.45: Concentrations of stable metals in the soil samples from Raub

Sample ID	Depth cm	mg/kg								
		P	K	Ca	Mg	Cu	Zn	Mn	Fe	Al
PR1	30-40	8.2	6.7	14.3	14.3	0.6	1.1	6.2	388.0	411.0
PR2	30-40	7.2	8.5	12.5	15.5	0.7	1.2	6.5	353.0	470.0
PR3	0-10	22.3	17.2	9.5	12.2	1.5	2.8	10.5	1512.0	1764.0
PR4	20-30	12.6	12.4	13.3	8.5	1.2	2.2	8.2	546.0	625.0
PR5	30-40	5.5	8.7	15.4	15.3	0.8	1.5	5.5	685.0	862.0
PR6	0-10	24.5	17.6	8.5	13.3	1.6	2.8	11.5	1542.0	1573.0
PR7	30-40	7.5	9.5	13.5	12.5	0.8	1.1	4.5	325.0	372.0
PR8	10-20	16.5	14.5	12.4	9.5	1.1	2.1	8.6	640.0	817.0
PR9	0-10	23.5	18.5	7.4	12.5	1.7	2.5	11.5	1643.0	1757.0
PR10	10-20	15.5	13.6	10.2	11.5	1.2	2.1	9.5	712.0	831.0
PR11	10-20	15.5	13.0	11.5	9.2	1.3	2.2	9.5	625.0	758.0
PR12	20-30	8.4	5.5	14.3	12.5	1.1	1.7	7.5	523.0	575.0
PR13	10-20	13.7	14.2	12.2	9.5	1.2	2.3	9.5	858.0	886.0
PR14	20-30	11.2	9.5	11.5	11.5	0.8	2.2	7.2	530.0	632.0
PR15	0-10	22.5	19.6	9.4	11.7	1.5	2.8	11.2	784.0	983.0
PR16	20-30	8.5	11.5	13.7	10.8	0.8	1.6	9.5	342.0	585.0
PR17	10-20	13.7	15.7	11.3	9.5	1.1	2.8	8.5	763.0	804.0
PR18	20-30	12.2	9.4	12.7	9.2	0.8	2.7	8.5	343.0	584.0
PR19	10-20	14.5	12.5	12.5	11.5	1.2	2.3	9.5	523.0	774.0

PR20	20-30	11.4	8.5	12.7	11.6	0.7	2.5	7.5	331.0	453.0
PR21	30-40	7.6	8.5	14.5	13.2	0.6	1.2	4.3	354.0	412.0
PR22	30-40	6.5	7.2	13.2	14.8	0.7	1.3	5.5	435.0	482.0
PR23	10-20	12.7	15.8	12.2	11.3	1.2	2.4	9.5	675.0	783.0
PR24	20-30	11.5	8.4	9.5	13.6	0.7	2.8	7.5	436.0	546.0
PR25	30-40	7.5	8.5	12.7	14.2	0.8	1.3	5.3	352.0	386.0
PR26	30-40	6.2	7.5	14.4	13.2	0.6	1.2	4.6	432.0	495.0
PR27	10-20	13.8	14.5	13.5	11.2	1.2	2.2	9.2	1257.0	1442.0
PR28	20-30	9.5	8.7	12.8	8.5	1.1	1.8	7.5	452.0	585.0
PR29	10-20	12.7	13.2	11.5	9.5	1.2	2.1	9.3	735.0	876.0
PR30	0-10	18.5	15.8	7.6	11.5	1.5	2.2	10.2	1436.0	1521.0
PR31	0-10	25.5	17.5	11.5	12.5	1.7	2.6	12.3	1487.0	1564.0
PR32	0-10	22.3	16.5	9.3	12.2	1.7	2.5	11.5	835.0	945.0
PR33	30-40	5.5	6.2	14.5	15.5	0.8	1.1	5.2	478.0	525.0
PR34	20-30	9.5	9.5	12.7	13.5	1.3	1.7	7.6	322.0	512.0
PR35	30-40	5.3	11.5	14.2	14.2	0.7	1.1	5.5	395.0	432.0
PR36	30-40	7.5	7.5	12.5	13.2	0.7	1.1	4.5	483.0	587.0
PR37	0-10	25.5	16.7	8.5	12.2	1.6	2.3	11.5	1485.0	1586.0
PR38	20-30	13.5	8.6	12.5	11.2	1.1	2.5	7.4	455.0	484.0
PR39	0-10	22.2	16.5	9.2	11.8	1.4	1.8	11.7	1458.0	1642.0
PR40	0-10	24.3	15.8	8.2	12.3	1.5	2.2	12.5	788.0	873.0
Mean		**13.5±6.3**	**12.0±3.9**	**11.8±2.1**	**12.0±1.8**	**1.0±0.3**	**1.9±0.5**	**8.3±2.4**	**717.9±416.0**	**829.8±428.5**
Range		**20.2**	**14.1**	**8.0**	**7.0**	**1.1**	**1.7**	**8.2**	**1321.0**	**1392.0**

Table 4.46: The vertical distribution of the stable metals in the soil from Raub

Depth	pH	OM%	P	K	Ca	Mg	Cu	Zn	Mn	Fe	Al
			mg/kg								
0-10	3.48	3.13	23.11	17.17	8.91	12.22	1.57	2.45	11.44	1297.00	1420.80
10-20	3.87	2.65	14.28	14.11	11.92	10.30	1.188	2.27	9.23	754.22	885.66
20-30	4.55	2.03	10.83	9.20	12.57	11.09	0.96	2.17	7.84	428.00	558.10
30-40	4.61	1.60	6.77	8.20	13.79	14.17	0.70	1.20	5.23	425.45	494.00
Mean	**4.15**	**2.33**	**13.56**	**12.02**	**11.84**	**12.04**	**1.09**	**1.99**	**8.33**	**717.95**	**829.85**

Table 4.47: Pearson correlation coefficients between the stable metals mg/kg and radionuclides Bq.kg^{-1} in the soil from Raub

	^{226}Ra	^{232}Th	^{40}K	pH	OM%	P	K	Ca	Mg	Cu	Zn	Mn	Fe	Al
^{226}Ra	1													
^{232}Th	0.929**	1												
^{40}K	0.771**	0.753**	1											
pH	-0.521**	-0.487**	-0.464**	1										
OM	0.428**	0.389**	0.368*	0-.670**	1									
P	0.409**	0.351*	0.375*	-0.894**	0.705**	1								
K	0.529**	0.443**	0.473**	0-.865**	0.658**	0.860**	1							
Ca	-0.370*	-0.329*	-0.348*	0.780**	-0.556**	-0.853**	-0.763**	1						
Mg	-0.137	-0.049	-0.081	0.127	0-.379*	-0.205	-0.258	0.099	1					
Cu	0.585**	0.519**	0.431**	-0.861**	0.739**	0.905**	0.866**	-0.772**	-0.251	1				
Zn	0.472**	0.385**	0.430**	-0.636**	0.537**	0.723**	0.668**	-0.643**	-0.446**	0.658**	1			
Mn	0.547**	0.488**	0.432**	-0.857**	0.729**	0.921**	0.848**	-0.798**	-0.330*	0.896**	0.743**	1		
Fe	0.388**	0.275	0.262	-0.801**	0.569**	0.817**	0.811**	-0.739**	-0.025	0.814**	0.521**	0.758**	1	
Al	0.380**	0.269	0.236	-0.805**	0.578**	0.811**	0.821**	-0.731**	-0.070	0.814**	0.543**	0.781**	0.988**	1

**. Correlation is significant at the 0.01 level (2-tailed)

*. Correlation is significant at the 0.05 level (2-tailed)

4.4.5.2 **The vertical distribution of Potassium (K) in Raub**

The mean value of K was found to be 12.0±3.9 mg/kg in Raub, while the range values significantly differ from 5.5 to 18.5 mg/kg (Table 4.45). The vertical distrubutions of K are presented in Table 4.46. The values indicate that the K movement was decreased within the depths. Figure 4.79 shows the distribution pattern of K within the soil matrix. It is evident that the concentrations of K continued to decrease gradually downward to the depth of 40 cm.

The relationships between K and the radionuclides (^{226}Ra, ^{232}Th, and ^{40}K) were positively correlated ($P \leq 0.01$). Positive correlations ($P \leq 0.01$) were also shown between K and OM, P, Cu, Zn, Mn, Fe and Al. K was negatively correlated ($P \leq 0.01$) with the soil pH and Ca (Table 4.47).

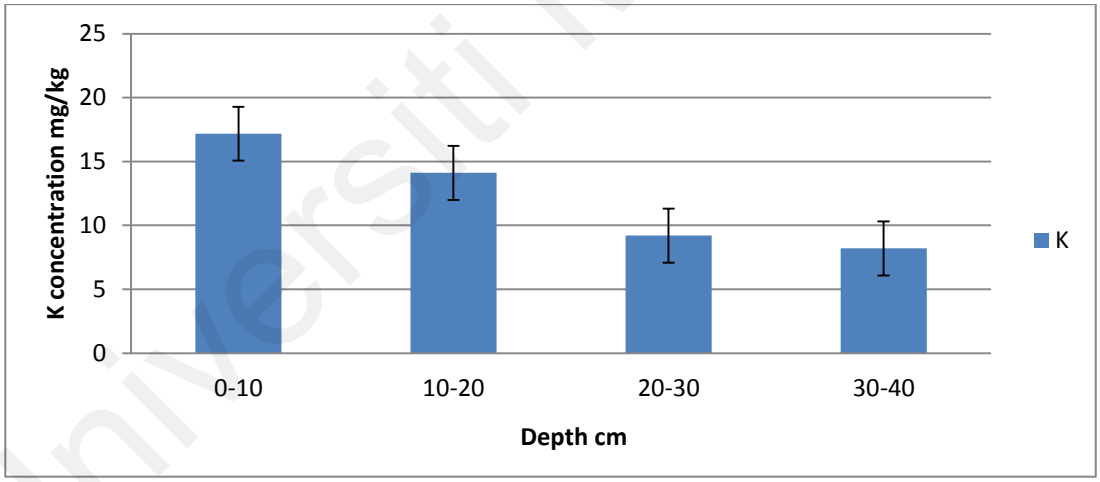

Figure 4.79: The vertical distribution of K in the soil samples from Raub

4.4.5.3 **The vertical distribution of Calcium (Ca) in Pahang Raub**

In Raub, the mean value of Ca was determined to be 11.84±2.3 mg/kg, with range values vary from 7.40 to 15.40 mg/kg (Table 4.45). The vertical distribution of Ca is shown in Table 5.46 and Figure 4.80. The estimated figures show that Ca mobility increased with depth in the soil matrix. Figure 4.80 depicts the vertical distribution

pattern of Ca throughout the soil profile. Ca concentrations have clearly begun to grow consistently from 0-10 to 30-40 cm. Relationships between Ca and the radionuclides (^{226}Ra, ^{232}Th, and ^{40}K) were negatively correlated at ($P \leq 0.05$). Negative correlations ($P \leq 0.01$) were also shown between Ca and OM, P, K, Cu, Zn, Mn, Fe and Al. However, the relationship was found to be a positive at ($P \leq 0.01$) with pH (Table 4.47).

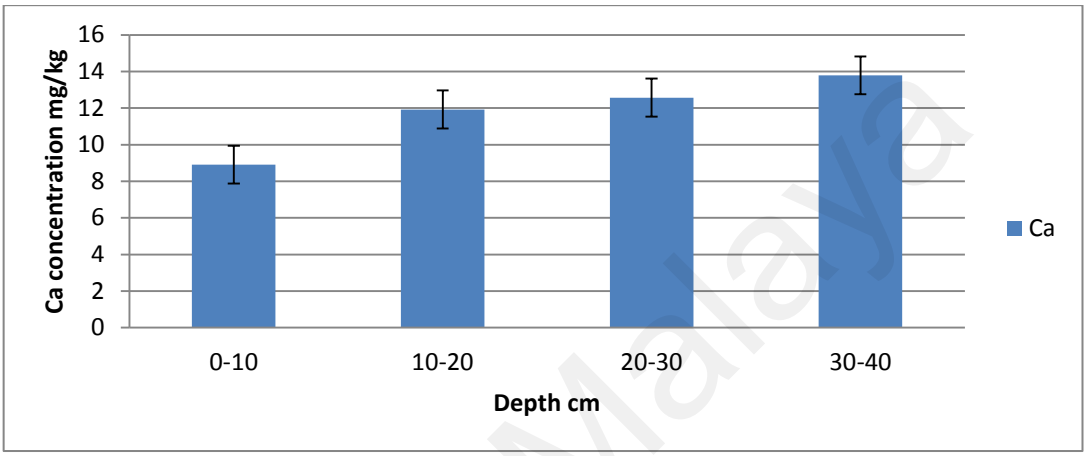

Figure 4.80: The vertical distribution of Ca in the soil samples from Raub

4.4.5.4 The vertical distribution of Magnesium (Mg) in Raub

The mean value of Mg was found to be 12.04±1.8 mg/kg in Raub, while the range values vary from 8.50 to 15.50 mg/kg (Table 4.45). The vertical distribution of Mg showing in Table 4.46, and Figure 4.81, the computed Mg values suggest that Mg movement was decreased through the soil up to 20 cm, and then rose consistently to a depth of 30-40 cm. Figure 4.81 depicts the irregular distribution pattern of Mg concentrations throughout the soil matrix. Relationships between Mg and radionuclides (226Ra, 232Th, and 40K) were found to be weak. Poor correlations ($P \leq 0.01$) were also shown between Mg and pH, P, K, Ca, Cu, Fe and Al. The correlations with OM and Zn were negative at ($P \leq 0.05$) and ($P \leq 0.01$), respectively. A positive relationship ($P \leq 0.05$) was shown between Mg and Mn (Table 4.47).

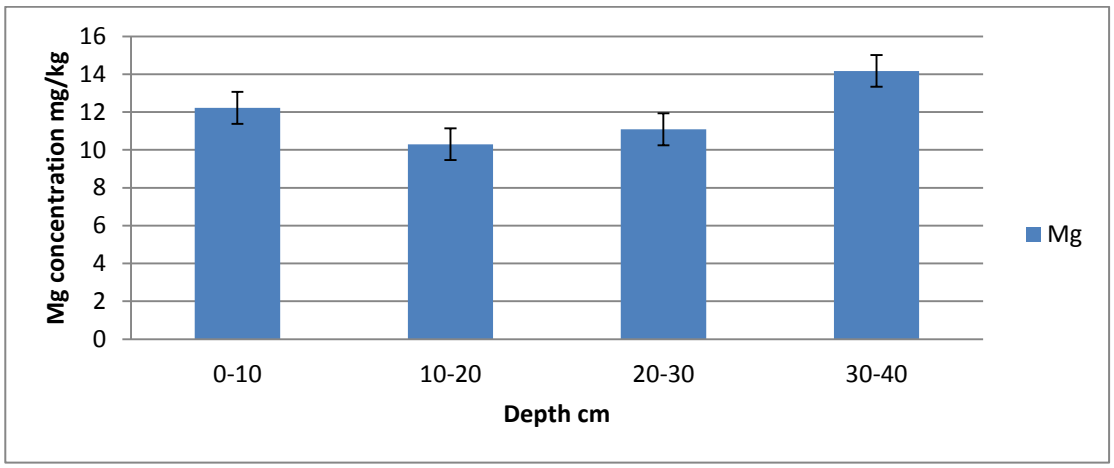

Figure 4.81: The vertical distribution of Mg in the soil samples from Raub

4.4.5.5 The vertical distribution of Copper (Cu) in Raub

The mean value of Cu was found to be 1.09±0.3 mg/kg in Raub, with range values differ from 0.60 to 1.70 mg/kg (Table 4.45). Table 4.46 illustrates the vertical distribution of Cu. The movement of Cu was decreased through the depth, according to the estimated values. Figure 4.82 depicts the pattern of uniform Cu distribution within the soil matrix. Cu and radionuclides (^{226}Ra, ^{232}Th, and ^{40}K) had a positive correlation ($P \leq 0.01$), and positive correlations ($P \leq 0.01$) with OM, P, K, Zn, Mn, Fe, and Al, while negatively correlated ($P \leq 0.01$) with pH and Ca (Table 4.47).

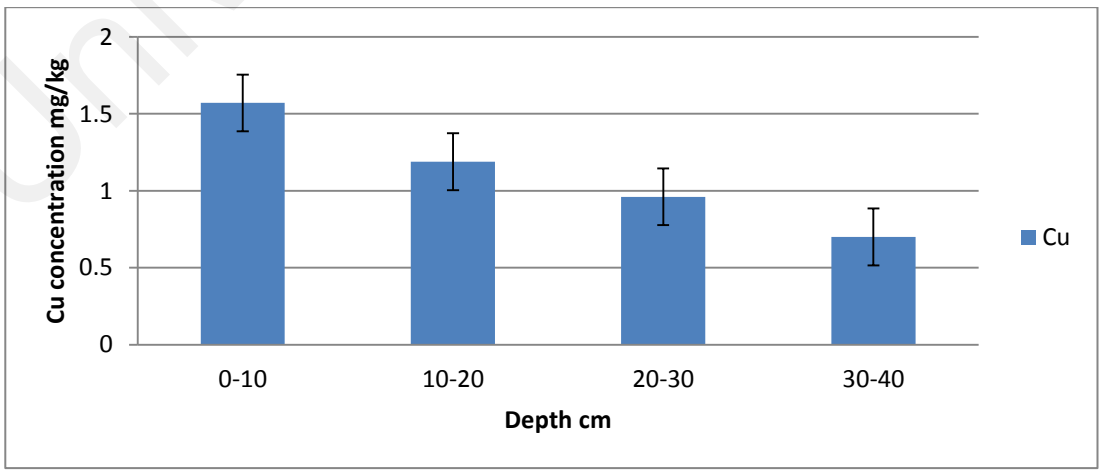

Figure 4.82: The vertical distribution of Cu in the soil samples from Raub

4.4.5.6 **The vertical distribution of Zinc (Zn) in Raub**

The mean value of Zn was found to be 1.99±0.5 mg/kg in Raub, while the range values differ from 1.10 to 2.80 mg/kg (Table 4.45). The vertical distributions of Zn are shown in Table 4.46. Cu movement was decreased inside the depths, according to the computed values. Figure 4.83 depicts the Zn distribution pattern inside the soil matrix.Relationships between Zn and radionuclides (^{226}Ra, ^{232}Th and ^{40}K) were positive ly correlated at (P ≤0.01). Positive correlations (P ≤0.01) were also shown between Zn and OM, P, K, Cu, Mn, Fe and Al. While, the relationships were negatively correlated (P ≤0.01) between Zn and pH, Ca and Mg (Table 4.47).

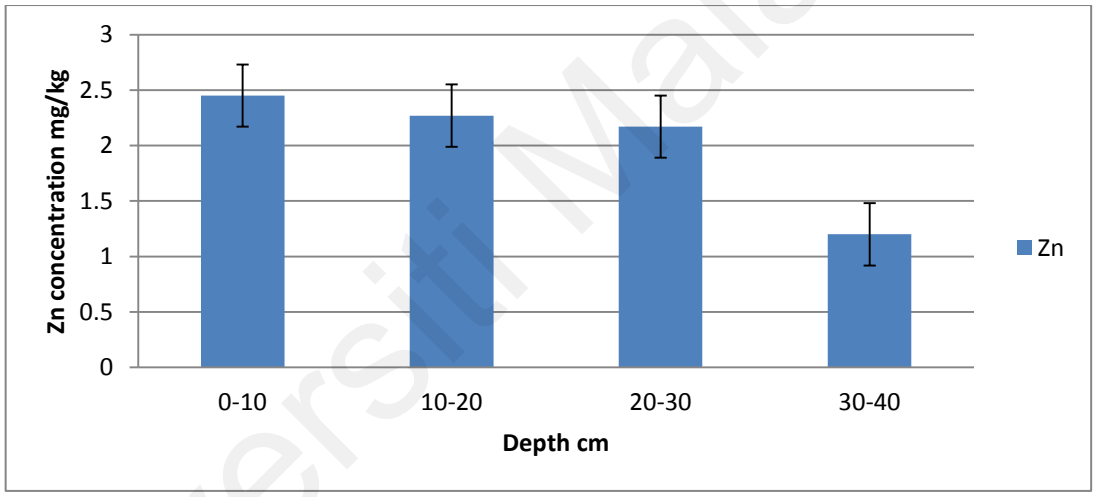

Figure 4.83: The vertical distribution of Zn in the soil samples from Raub

4.4.5.7 **The vertical distribution of Manganese (Mn) in Raub**

In Raub, the mean value of Mn was determined to be 8.33±2.4 mg/kg, with range values vary from 4.30 to 12.50 mg/kg (Table 4.45). Table 4.46 shows the vertical distribution of Mn. The movement of Mn has decreased across depths, according to the observed values. Figure 4.84 depicts the pattern of regular Mn distribution within the soil matrix.

The relationships between Mn and the radionuclides (^{226}Ra, ^{232}Th and ^{40}K) were positively correlated (P ≤0.01). Positive correlations (P ≤0.01) were also shown between Mn and OM, P, K, Cu, Zn Fe and Al, and negative (P ≤0.01) with the pH and Ca. The relationship between Mn and Mg is negatively correlated at (P ≤0.05) (Table 4.47).

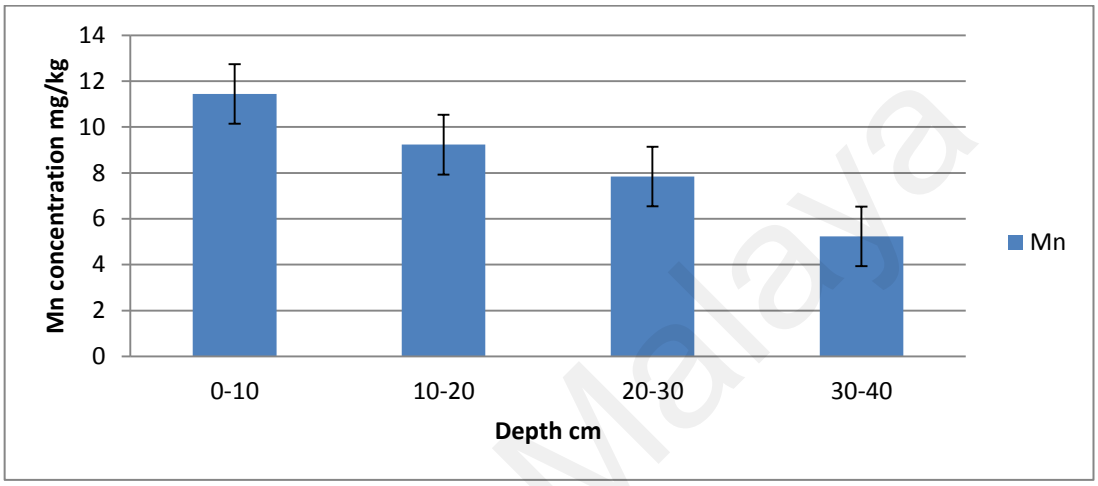

Figure 4.84: The vertical distribution of Mn in the soil samples from Raub

4.4.5.8 **The vertical distribution of Iron (Fe) in Raub**

The mean value of Fe was found to be 717.95±55.2 mg/kg in Raub, while the range values differ significantly from 322.00 to 1643.00 mg/kg (Table 4.45). The vertical distributions of Fe are shown in Table 4.46. The measured data show that the Fe movement within the soil profile has decreased. Figure 4.85 depicts the pattern of uniform distribution of Fe within the soil matrix.

The relationship between Fe and ^{226}Ra was positively correlated at (P ≤0.01), while the relationships with ^{232}Th and ^{40}K were found to be insignificant. Positive correlations (P ≤0.01) were shown between Fe and OM, P, K, Cu, Zn, Fe and Al, and negative (P ≤0.01) with pH and Ca (Table 4.47).

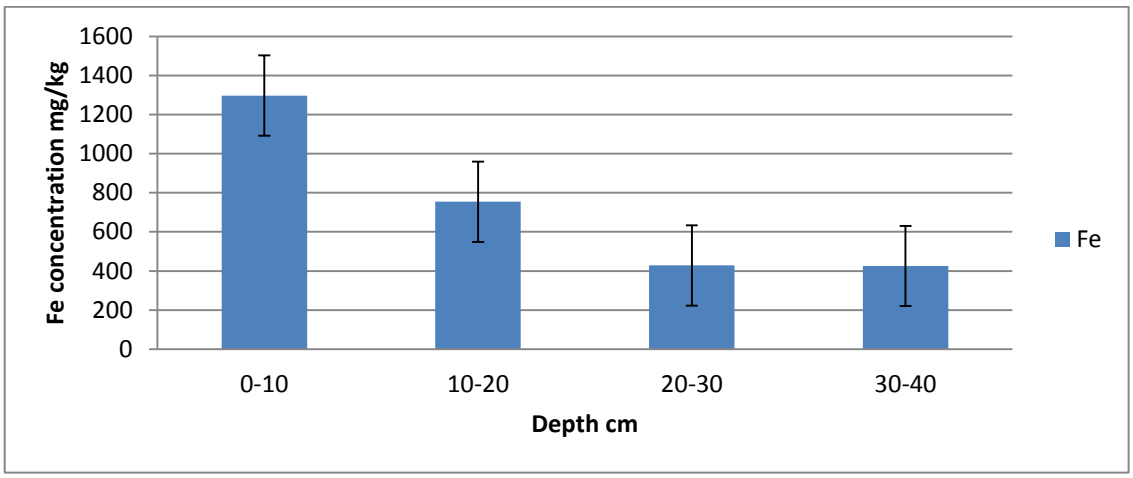

Figure 4.85: The vertical distribution of Fe in the soil samples from Raub

4.4.5.9 The vertical distribution of Aluminum (Al) in Raub

In Raub, the mean value of Al was determined to be 829.85±42.5 mg/kg, whereas the range values vary from 372.00 to 1764.00 mg/kg (Table 4.45). Table 4.46 depicts the vertical distribution of Al. The measured data show that the Al movement within the soil profile has decreased. Figure 4.86 depicts the pattern of uniform distribution of Al within the soil matrix. The relationship between Al and ^{226}Ra is positively correlated ($P \leq 0.05$), while the correlations with ^{232}Th and ^{40}K were found to be insignificant. The relationships between Al and OM, P, K, Cu, Zn, Mn and Fe were positively correlated ($P \leq 0.01$), and negativily ($P \leq 0.01$) with pH and Ca (Table 4.47).

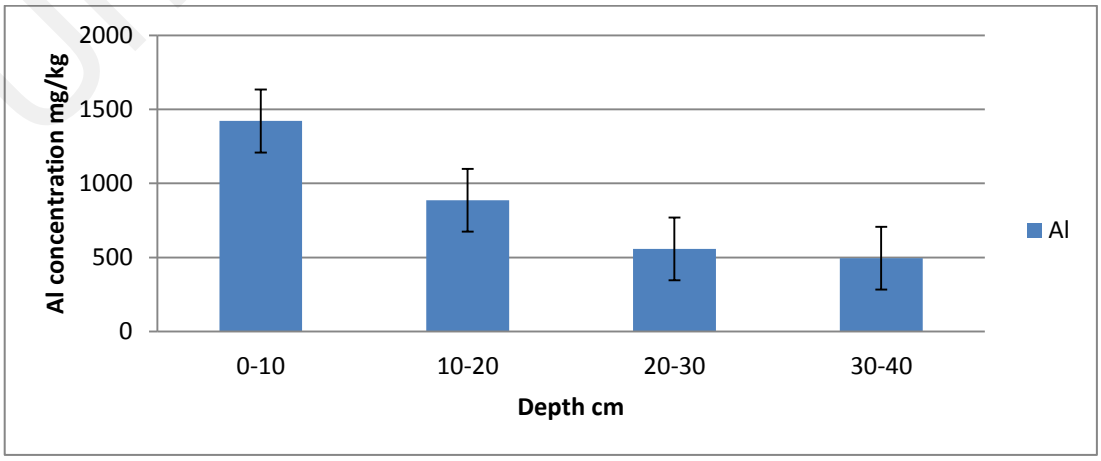

Figure 4.86: The vertical distribution of Al in the soil samples from Raub

4.4.6 Distribution of stable metals in Lanchang

4.4.6.1 The vertical distribution of Phosphorus (P) in Lanchang

The mean value of P was found to be 15.16±6.9 mg/kg in Lanchang, while the range values vary from 6.5 to 28.5 mg/kg (Table 4.48). The vertical distrubutions of P are shown in Table 4.49. The measured values indicate that the P movement has decreasd with depths. Figure 4.87 shows distribution pattern of P within the soil matrix, it is noticeable that the the concentrations tended to stabilize at the depth from 30 to 40 cm after a gradual decrease from 10 to 30 cm.

The relationships between P and the radionuclides ^{226}Ra, ^{232}Th, and ^{40}K were correlated positivly ($P \leq 0.01$). Positive correlations at ($P \leq 0.01$) were also shown between P and OM, K, Ca, Mg, Zn, Mn, Fe and Al, while P correlated negatively ($P \leq 0.01$) with pH (Table 4.50).

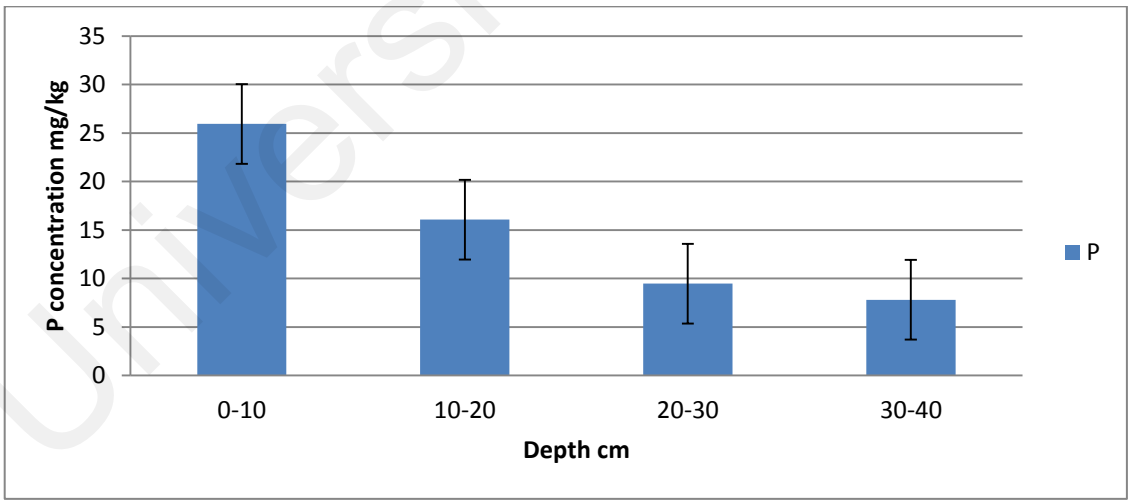

Figure 4.87: The vertical distribution of P in the soil samples from Lanchang

Table 4.48: Concentrations of stable metals in the soil samples from Lanchang

Sample ID	Depth cm	mg/kg								
		P	K	Ca	Mg	Cu	Zn	Mn	Fe	Al
PL1	10-20	17.5	18.5	14.2	12.5	1.2	1.7	9.5	712.0	755.0
PL2	0-10	24.5	21.2	18.5	15.5	1.2	2.5	10.5	1605.o	1648.0
PL3	10-20	15.5	17.3	13.5	12.5	1.2	1.7	11.5	696.0	711.0
PL4	10-20	17.2	15.5	15.5	13.3	1.1	1.6	10.2	568.0	722.0
PL5	20-30	12.7	13.3	8.3	9.5	0.8	2.1	8.5	438.0	575.0
PL6	10-20	15.2	16.5	14.3	11.2	1.1	1.6	9.3	675.0	727.0
PL7	0-10	26.2	18.2	18.5	15.2	1.3	2.4	11.5	1432.0	1637.0
PL8	10-20	16.2	17.2	15.2	12.3	1.1	1.6	11.4	611.0	784.0
PL9	0-10	24.3	18.5	17.5	13.5	1.2	2.4	10.5	1568.0	1627.0
PL10	20-30	9.0	12.2	13.5	10.8	0.8	2.3	8.3	448.0	5740
PL11	20-30	11.2	12.5	9.7	8.3	0.7	2.1	9.5	312.0	547.0
PL12	10-20	17.8	16.3	16.2	12.5	1.1	1.5	11.5	592.0	682.0
PL13	30-40	6.5	8.5	9.5	9.5	0.5	1.1	8.2	443.0	585.0
PL14	10-20	15.0	15.3	14.5	10.5	1.1	1.5	12.5	695.0	772.0
PL15	20-30	8.5	13.5	12.5	10.5	1.1	2.1	9.5	473.0	692.0
PL16	20-30	9.4	11.3	10.3	11.5	0.8	2.2	10.3	484.0	553.0
PL17	10-20	15.3	16.5	15.4	9.3	1.2	1.5	10.2	585.0	772.0
PL18	10-20	14.7	17.5	14.5	12.7	1.1	1.7	9.3	578.0	763.0

PL19	30-40	7.2	11.3	7.2	8.2	0.5	1.3	8.2	334.0	452.0
PL20	30-40	7.5	9.7	8.4	9.5	0.7	1.1	7.7	343.0	472.0
PL21	20-30	8.5	12.5	10.7	11.5	1.1	2.6	8.2	427.0	4830
PL22	30-40	8.3	11.2	9.5	7.5	2.5	1.2	9.2	383.0	495.0
PL23	10-20	16.5	17.3	13.5	11.5	1.1	1.8	12.4	583.0	6750
PL24	20-30	8.2	12.5	9.5	10.5	0.7	2.1	9.5	523.0	673.0
PL25	0-10	24.5	17.7	17.3	14.5	1.3	2.2	11.5	1485.0	1589.0
PL26	0-10	28.5	18.5	18.5	15.5	1.2	2.4	12.2	1572.0	1653.0
PL27	30-40	9.5	9.5	9.3	8.6	0.6	1.2	17.5	448.0	568.0
PL28	0-10	27.3	21.5	17.7	15.5	1.2	2.2	12.7	765.0	896.0
PL29	0-10	24.2	19.2	18.5	13.5	1.2	1.5	11.5	882.0	987.0
PL30	10-20	16.8	18.5	14.3	11.5	1.1	1.7	11.5	687.0	756.0
PL31	0-10	28.0	21.2	19.5	17.2	1.5	2.3	11.5	793.0	882.0
PL32	30-40	8.5	9.5	8.2	8.6	2.5	1.2	8.5	473.0	521.0
PL33	10-20	15.2	17.5	13.2	9.2	1.1	1.8	9.2	538.0	685.0
PL34	30-40	7.2	8.5	7.5	7.2	2.7	1.1	8.3	342.0	473.0
PL35	20-30	8.3	13.5	9.5	12.3	0.7	2.3	9.5	432.0	578.0
Mean		**15.16±6.9**	**15.12±3.7**	**13.2±3.7**	**11.5±2.5**	**1.15±0.5**	**1.8±0.4**	**10.3±1.9**	**683.5±377.9**	**798.9±367.2**
		22.0	**13.0**	**12.3**	**10.0**	**2.2**	**1.5**	**9.8**	**1293.0**	**1201.0**

Table 4.49: The vertical distribution of the stable metals in the soil from Lanchang

Depth	pH	OM%	P	K	Ca	Mg	Cu	Zn	Mn	Fe	Al
			mg/kg								
0-10	3.42	4.35	25.93	19.50	18.25	15.05	1.26	2.23	11.48	1262.75	1364.87
10-20	3.95	4.07	16.07	16.99	14.52	11.58	1.12	1.64	10.70	626.66	733.66
20-30	4.33	2.99	9.47	12.66	10.50	10.61	.83	2.22	9.16	442.12	584.37
30-40	4.53	2.43	7.81	9.74	8.51	8.44	1.42	1.17	9.65	395.14	509.42
Mean	**4.03**	**3.56**	**15.16**	**15.12**	**13.25**	**11.52**	**1.15**	**1.81**	**10.32**	**683.57**	**798.97**

Table 4.50: Pearson correlation coefficients between the stable metals mg/kg and radionuclides Bq.kg^{-1}in the soil from Lanchang

	^{226}Ra	^{232}Th	^{40}K	pH	OM5	P	K	Ca	Mg	Cu	Zn	Mn	Fe	Al
^{226}Ra	1													
^{232}Th	0.884**	1												
^{40}K	0.658**	0.697**	1											
pH	-0.505**	-0.483**	-0.624**	1										
OM%	0.666**	0.627**	0.630**	-0.869**	1									
P	0.462**	0.436**	0.573**	-0.959**	0.832**	1								
K	0.610**	0.594**	0.592**	-0.907**	0.907**	0.893**	1							
Ca	0.562**	0.511**	0.580**	-0.934**	0.911**	0.924**	0.899**	1						
Mg	0.347*	0.341*	0.396*	-0.884**	0.723**	0.859**	0.815**	0.859**	1					
Cu	-0.092	-0.107	0.076	-0.057	0.018	0.088	-0.013	0.033	-0.087	1				
Zn	0.206	0.226	0.212	-.0517**	0.401*	0.459**	0.483**	0.447**	0.629**	-0.228	1			
Mn	0.341*	0.136	0.163	-0.388*	0.390*	0.480**	0.380*	0.442**	0.364*	-0.112	0.052	1		
Fe	0.299	0.254	0.403*	-0.846**	0.671**	0.825**	0.664**	0.764**	0.735**	0.079	0.519**	0.345*	1	
Al	0.310	0.260	0.421*	-0.848**	0.669**	0.822**	0.656**	0.766**	0.724**	0.051	0.531**	0.338*	0.990**	1

**. Correlation is significant at the 0.01 level (2-tailed)
*. Correlation is significant at the 0.05 level (2-tailed)

The soil pH level has an effect on phosphorus availability, if soils are excessively acidic; P reacts with Fe and Al. That renders it inaccessible to plants. However, P interacts with Ca and becomes unavailable (Cerozi & Fitzsimmons, 2016). Negative correlation was also obtained by Khadka, Lamichhane, & Thapa, (2016).

The results show that phosphorous (P) mobility decreases with depth in all investigated areas. P was often highest at 0-10 cm and lowest at 30-40 cm. The presence of high P concentrations at the top surface may be due to frequent fertiliser application procedures in acidic tropical soils. Where, Al toxicity and low P availability are major constraints for crop production.

Phosphorous P mobilization is also affected by Al and Fe adsorption sites that protect P from microbial and enzymatic decomposition (Giesler *et al.*, 2004; Stutter *et al.,* 2015). The majority of P is occluded within Fe oxides, which implies that this P may be released and become available for plants at surface depths following the dissolution of Fe oxides in soil. However, some soil groups showed stability of P values at lower depths, this may be attributed to the P-bearing minerals that were present during soil evolution. The soil groups of Kedah and Johor showed the highest mean values of P at 21.7 and 19.5 mg/kg, respectively.

For all the study areas, the mean values of P are follow the order of Malacca (9.3±6.5) < Raub (13.5±6.3) < Lanchang (15.16±6.9) < Selangor (16.9±8.6) < Johor (19.5±10.4) < Kedah (21.7±9.5) mg/kg.

The relationships between P and the radionuclides ^{226}Ra, ^{232}Th and ^{40}K were correlated positively ($P \leq 0.01$) in all the soil groups. This could mainly be due the fact that phosphate rocks of sedimentary origin contain ^{238}U and ^{232}Th, and its decay products in addition to phosphate minerals (Roesseler, 1990). The soils in Kedah and Selangor are derived from sedimentary rocks of marine and continental deposits, while the soils in Johor Segamat are derived from sedimentary and volcanic rocks.

Sedimentary phosphate rocks, or phosphorites originating in a marine environment, are typically distinguished by concentrations of uranium activity far higher than those of volcanic rocks. Reported values of ^{238}U in rock phosphate range from1.0 to 5.7 Bq/g (Barišić, Lulić, & Miletić, 1992; Guimond & Hardin, 1989; Heijde, Klijn, & Passchier, 1988). These phos-phates are largely used for the production of phosphoric acid, fertilizers and hence phosphate fertilizers are considered to be a potential source of natural radionuclide contamination and show significant correlations.

Positive correlations ($P \leq 0.01$) were shown between P and Fe and Al, while, the relationship between P and pH was found to be a negative in all the ivestegated areas. The significant positive correlations between P and Fe and Al, could be due to the fact that Fe and Al are the most important binding partners for P in non-calcareous natural systems (Borovec, Kopáček, & Hejzlar, 2015). This leads to the conclusion that the amount of Fe and Al oxides that are characterized by high concentrations in tropical soils have a direct influence on P mobility, hence on ecosystem structure and function, and this could explain the close relationships between them.

The results are in agreement with Reddy *et al.,* (1996) findings that the behavior of P is strongly regulated by Al. Thus, the clay fraction was highly correlated with labile P fractions. Herlihy & McGrath, (2007) also found that P sorption in soil was mainly correlated with Al, clay content, and Fe.

This is consistent with earlier studies which suggested that the surface area and positive charge of of Fe and Al oxides affect their ability to bind phosphate and other anions, including organic molecules in sediments and soils (Kingston *et al.* 1972; Detenbeck & Brezonik 1991; De Vicente *et al.,* 2008).

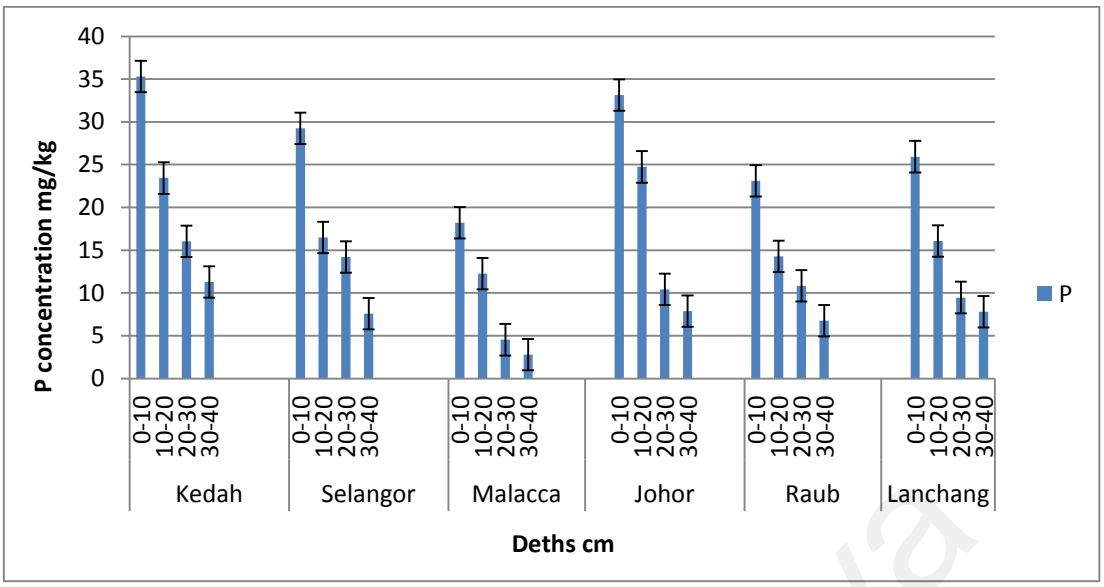

Figure 4.88: The vertical distribution of phosphorus P concentrations across the study areas

4.4.6.2 The vertical distribution of the Potassium (K) in Lanchang

The mean value of the K was found to be 13.25±3.7 mg/kg in Lanchang, while the range values vary from 7.20 to 19.50 mg/kg (Table 4.48). The vertical distribution of K is shown in Table 4.49. The measured values indicate that the K movement is decreasing with the depth through the soil profile. Figure 4.89 depicts the pattern of K distribution throughout the soil matrix. It is obvious that K concentrations have started to steadily decline down to a depth from 0-10 to 30-40 cm.

The correlations between K and the radionuclides ^{226}Ra, ^{232}Th, and ^{40}K were positive ($P \leq 0.01$). There were also significant correlations ($P \leq 0.01$) between K and OM, P, Ca, Mg, Zn, Fe, and Al, as well as positive correlations at ($P \leq 0.05$) with Mn. The association with pH, on the other hand, was shown to be negative ($P \leq 0.01$). The link between K and Cu was found to be insignificant (Table 4.50).

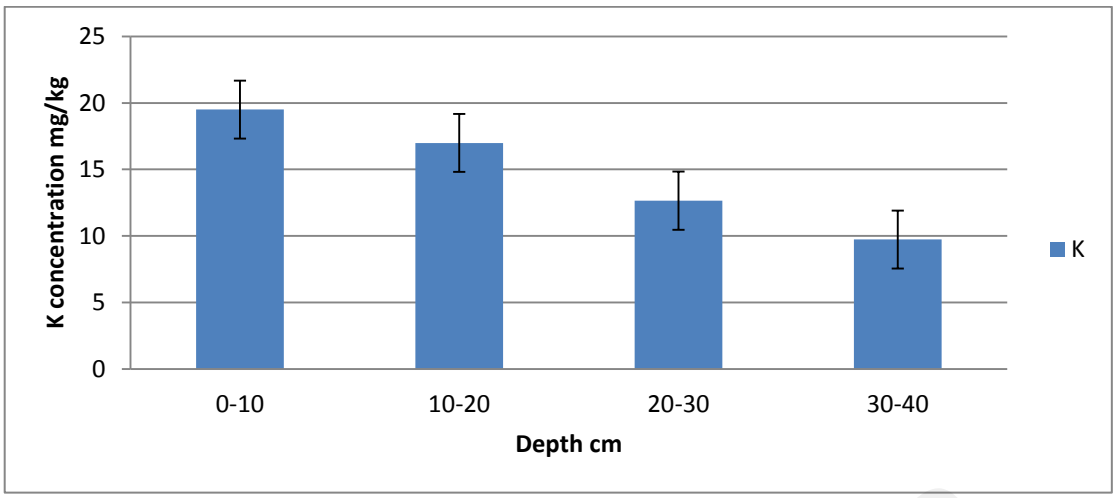

Figure 4.89: The vertical distribution of K in the soil samples from Lanchang

Generally, K decreased slightly with the depths in all the soil groups, reflecting its mobility within the soil profile. High concentrations of K in the top layer can be attributed to being an alkaline metal. The alkali metals are characterized as lithophile (or oxygen-loving) elements as they are hosted primarily in the silicate portion of the earth and therefore remain close to the Earth's surface because they combine readily with oxygen and so associate strongly with silica, forming relatively low-density minerals that do not sink down into the soil (Albarède, 2009).

Compared to the other study areas, soil from Kedah and Selangor exhibited high mean values of K at 17.80 and 24.10 mg/kg, respectively (Table 4.37 and 4.43).

The K mean values of the study areas follow the order of Malaca (8.8±2.6) < Raub (12.0±3.9) < Lanchang (15.12±3.7) < Johor (16.2±7.7) < Kedah (17.8±2.2) < Selangor (24.1±3.6) mg/kg.

The high K concentrations in Kedah and Selangor may be attributed to the present of illite and mica, because organic matter is not very retentive of K at such low pH levels, it is likely that alluvium deposited in these soils contains illite, mica, or other clay minerals.

Radionuclides showed negative relationships with K in Kadah, and it can be attributed to the vertical distribution of K in area, where the pattern of distribution showed an anomaly represented by an increase in K concentrations at the lower depths. This increase may be attributed to illite, and mica content.

With the exception of Kedah and Selangor, K showed positive relationships with radionuclides within the study areas; the positive relationships may be related in general terms to the behavior of radionuclides that are controlled by chemical environment and climate factors in the area. Dragović *et al.,* (2012) also revealed a positive relationship between K and ^{40}K in different soil types of Serbia. This is consistent with Wasserman *et al.,* (2002) finding that characteristics of tropical soils, such as acidity, poor nutrient availability, and low clay content 2:1, may be responsible for the high mobility of radionuclides.

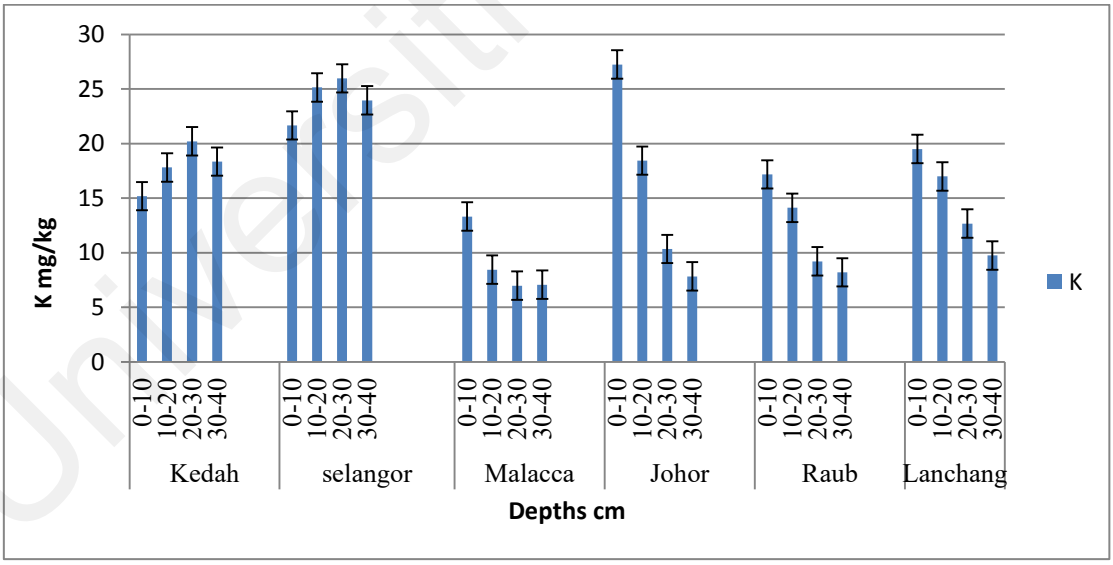

Figure 4.90: The vertical distribution of Potassium (K) concentrations across the study areas

4.4.6.3 The vertical distribution of Calcium (Ca) in Lanchang

The mean value of Ca was found to be 13.25±3.7 mg/kg in Lanchang, while the range values vary from 7.20 to 19.50 mg/kg (Table 4.48). The vertical distributions of

Ca are shown in Table 4.49. The estimated values indicate that the Ca movement is decreasing through the depths. The distribution pattern of Ca within the soil matrix is shown in Figure 4.91. It is evident that the concentrations of Ca decreased regularly starting from 0-10 depth up to 30-40 cm.

The relationships between Ca and the radionuclides ^{226}Ra, ^{232}Th, and ^{40}K were positively correlated at ($P \leq 0.01$). Positive correlations ($P \leq 0.01$) were also shown between Ca and OM, P, K, Mg, Zn, Mn, Fe and Al, while the correlation with pH was a negative ($P \leq 0.05$ (Table 4.50).

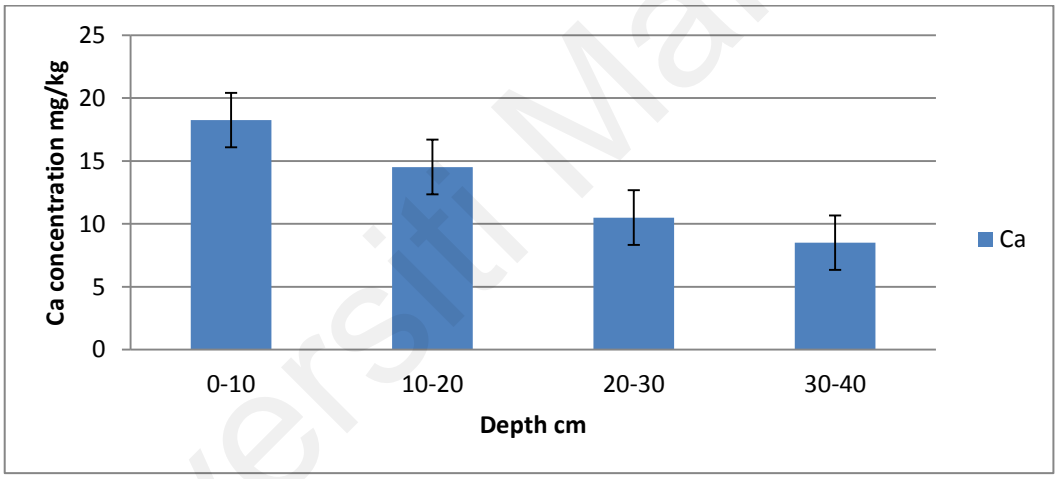

Figure 4.91: The vertical distribution of Ca in the soil samples from Lanchang

Soil profile in Selangor and Kedah exhibited high concentration of Ca with mean values of 14.80 and 14.90 mg/kg, respectively. High levels of Ca at the top surface of the soil profile may be reflecting the regular application of phosphate rock in the fertilizer program.

Calcium (Ca) mean values for the study areas follow the order of Malacca (10.8±2.4) < Raub (11.8±2.1) < Johor (12.0±3.2) < Lanchang (13.2±3.7) < Selangor (14.8±2.6) < Kedah (14.8±2.9) mg/kg.

The correlations between Ca and the specific activities of the radionuclides ^{226}Ra, ^{232}Th and ^{40}K were found to be positive ($P \leq 0.01$) in Johor and Lanchang, whereas, in Raub the correlations with ^{226}Ra, ^{232}Th and ^{40}K were shown to be negative ($P \leq 0.05$). No significant correlations between Ca and the radionuclides in soil groups of Kedah, Selangor and Malacca.

Usually Ca compounds are common in limestone and fossilized remains of early marine life; gypsum, anhydrite, fluorite, and apatite. The negative correlation of the radionuclides with Ca is in agreement the conclusion given by Navas *et al*. (2005) and Dragović *et al.,* (2012) where negative correlations ($P \leq 0.01$) were found between ^{226}Ra and ^{232}Th and Ca.

High Ca concentrations at the depths of 30-40 cm were shown in Kedah, Selangor and Pahang Raub soils. The increasing pattern of Ca concentrations with the depth was readily reflected in their pH values. However, in Johor, Malacca and Lanchang, this was not seen in the distribution patterns. The concentrations of Ca at the top surface layers were greater in Johor, Malacca and Lanchang. The high Ca at the top surface may be may be reflecting the regular application of rock phosphate of fertilizer, where additional Ca may be supplied when dolomite is used as Mg source. Distribution of Ca in these soils may be related to time of application as well as to OM and content of clay materials. The vertical distribution pattern of Ca was similar in Kedah and Selangor. The Ca concentrations also follow a uniform vertical distribution pattern in Johor and Raub.

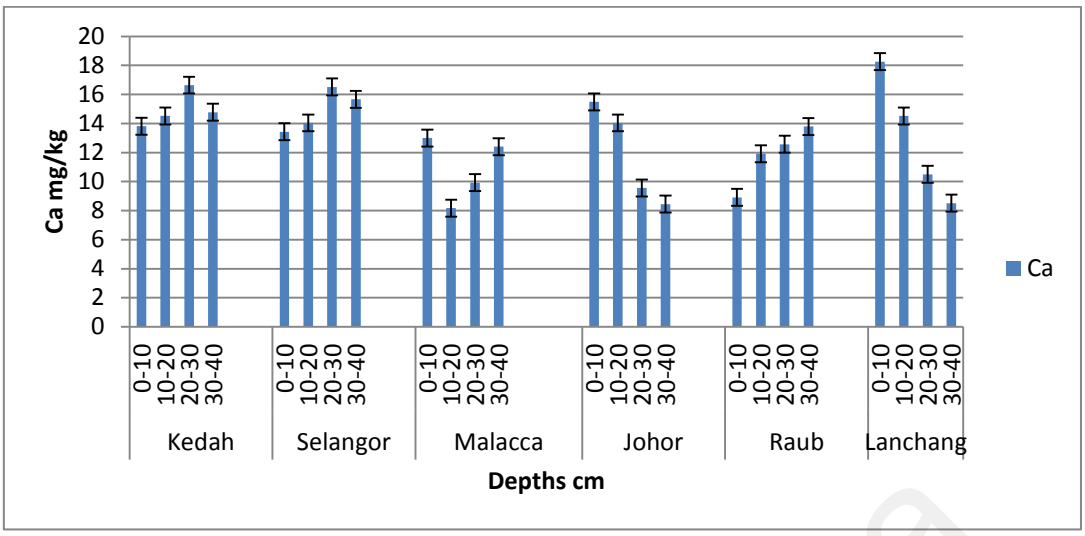

Figure 4.92: The vertical distribution of Ca concentrations across the study areas

4.4.6.4 The vertical distribution of Magnesium (Mg) in Lanchang

The mean value of Mg was found to be 11.52±2.5 mg/kg in Lanchang, while the range values differ significantly from 7.20 to 17.20 mg/kg (Table 4.48). The vertical distribution of Mg is shown in Table 4.49. The estimated values indicate that the Mg movement is decreasing through the depths. The distribution pattern of Mg within the soil matrix is shown in Figure 4.93. It is evident that Mg concentrations decreased regularly from 0-10 to 30-40 cm.

Relationships between Mg and the radionuclides ^{226}Ra, ^{232}Th, and ^{40}K were positively correlated ($P \leq 0.05$). Positive correlations ($P \leq 0.01$) were also shown between Mg and OM, P, K, Ca, Zn, Fe and Al, and positive at ($P \leq 0.05$) with the Mn, while the relationship with pH correlated negativly ($P \leq 0.01$) (Table 4.50).

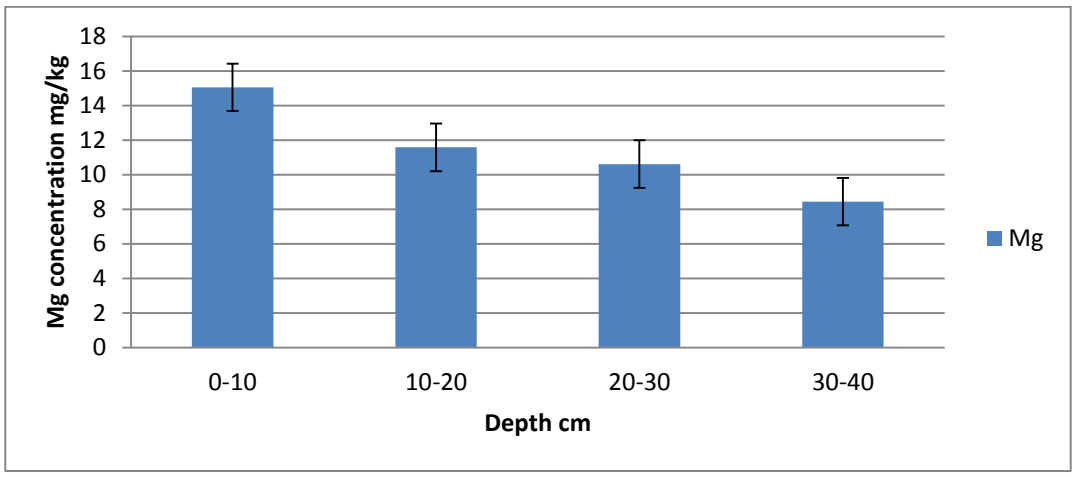

Figure 4.93: The vertical distribution of Mgin the soil samples from Lanchang

Magnesium (Mg) generally decreased with depth in Malacca, Johor and Lanchang soils. However, an increase in Mg content with depth was noted for Kedah, Selangor and Raub soils that may be associated with OM content and clay minerals. A low concentration of Mg was found in soils of Malacca. This soil was dominated with clay minerals indicating that it has proceeded to an advanced stage of weathering and a consequent loss of Mg-bearing minerals. Mg tends to be uniformly distributed throughout Kedah, Selangor, Johor and Raub soils suggesting a constant downward leaching of this element and return by plant cycling.

The mean values of Mg concentrations for all soil groups were found to be comparable, with the exception of soil from Malacca. The mean values of Mg for the study areas follow the order of Malacca (7.2±1.0) < Johor (10.0±2.4) < Lanchang (11.5±2.5) < Raub (12.0±1.8) < Kedah (13.5±3.3) < Selangor (15.3±1.9) mg/kg.

Strong negative correlations ($P \leq 0.01$) were observed between Mg and the natural radionuclides ^{226}Ra, ^{232}Th and ^{40}K in Selangor, and negative ($P \leq 0.05$) in Lanchang. The significant negative correlation between ^{40}K and Mg in the soil was also reported by Dragović *et al.,* (2012), while Mg correlated positively at ($P \leq 0.01$) with ^{226}Ra, ^{232}Th and ^{40}K in Johor, and positively ($P \leq 0.05$) with ^{226}Ra in Malacca. The

relationships between the radionuclides and the soil elements showed significant variations among the areas.

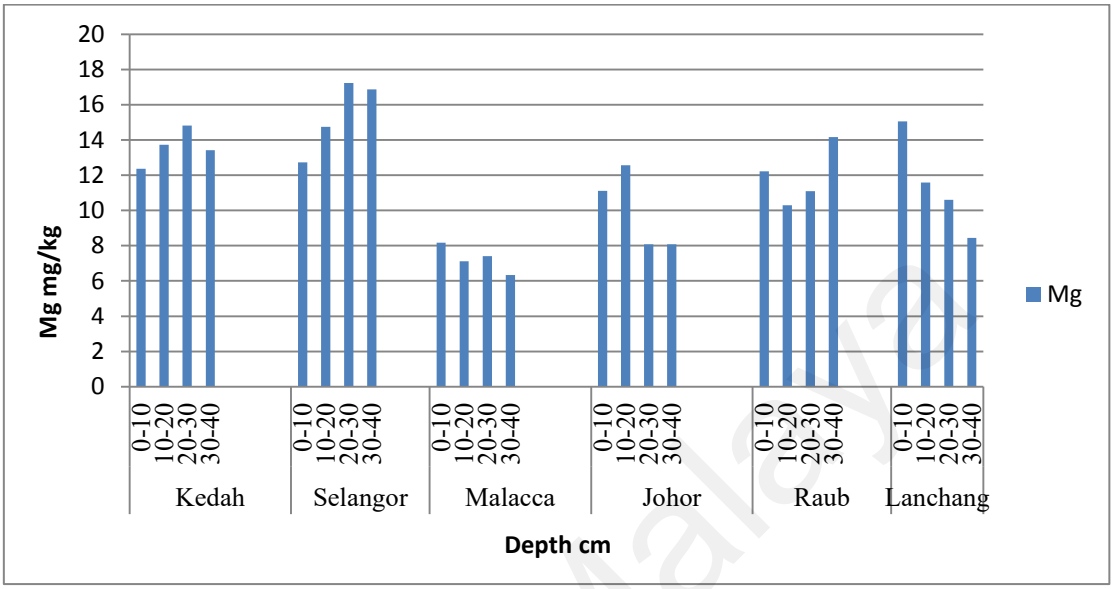

Figure 4.94: The vertical distripution of Mg concentrations across the study areas

4.4.6.5 **The vertical distribution of Copper (Cu) in Lanchang**

The mean value of Cu was found to be 1.15±0.5 mg/kg in Lanchang, while the range values differ from 0.50 to 2.70 mg/kg (Table 4.48). The vertical distribution of Cu is shown in Table 4.49. According to the observed results, the Cu movement reduced with depth before rising again at 20-30 cm. Figure 4.95 depicts the pattern of uneven distribution of Cu within the soil matrix.

Relationships between Cu and the radionuclides ^{226}Ra, ^{232}Th and ^{40}K were found to be weak. Poor correlations were also shown between Cu and pH, OM, P, K, Ca, Mg, Zn, Mn, Fe and Al (Table 4.50).

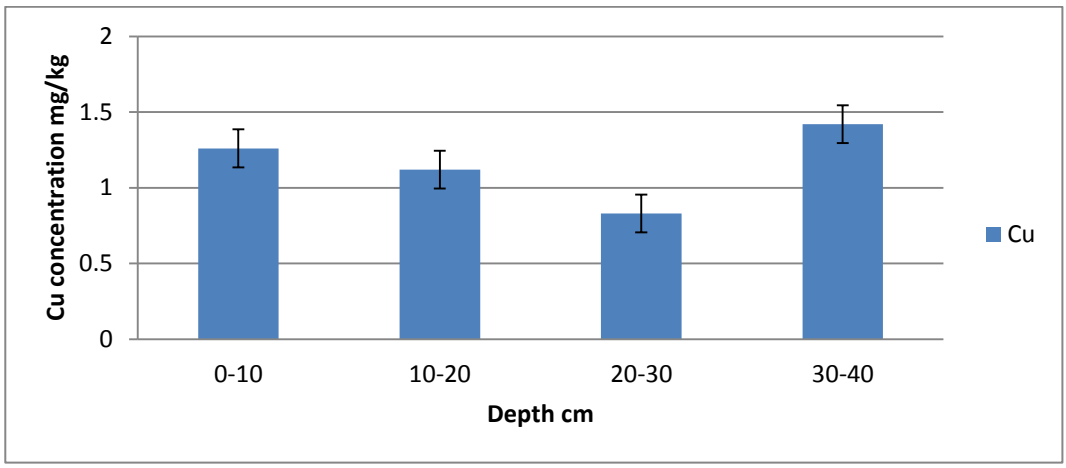

Figure 4.95: The vertical distribution of Cu in the soil samples from Lanchang

There was a general tendency of Cu to be uniformly distributed throughout the soils of Kedah and Lanchang. While at the lower depths, the soils of Selangor, Malacca and Raub showed a noticeable decrease in Cu concentrations.

The highest mean values of Cu were found in Johor and Kedah as 2.44 and 1.91 mg/kg, respectively, this observation could be attributed to the geochemical nature of the soil that was derived from marine alluvium.

An increase in Zn concentrations were observed at the same depths in Selangor, Malacca and Lanchang soils. Since there was a drop in pH, it is a probable that Cu and Zn bearing minerals in the form of sulfides occurred at that particular depth. The high concentrations of Cu in the top of the soil agree with Alexandre *et al.,* (1995) findings that Fe minerals and OM are responsible for the retention of Cu in in a tropical soil profile in Sao Paulo, Brazil. According to Alexandre *et al.,* (1995), Fe minerals (together with OM) were responsible for retaining Cu in a tropical soil profile in Sao Paulo, Brazil.

Copper (Cu) values of the study areas are follow the order of Malacca (0.8±0.2) < Selangor (1.04±0.6) < Raub (1.0±0.3) < Lanchang (1.15±0.5) < Kedah (2.15±1.5) < Johor (2.4±0.6) mg/kg.

The significant low of Cu concentrations may be related to the high OM content of these soils. The Cu deficiency frequently occurs in the soil rich in OM, particulary peat soils (Bolle, 1957).

The relationships between Cu and the radionuclides ^{226}Ra, ^{232}Th and ^{40}K were positively correlated ($P \leq 0.01$) in Selangor, Malacca and Raub, while, the Cu negatively correlated ($P \leq 0.01$) with the radionuclides in the soil from Johor. No significant correlations were observed in Kedah and Lanchang. Dragović *et al.,* (2012) also reported weak relationships between Cu and the radionuclide activites of ^{226}Ra, ^{232}Th, ^{40}K and ^{137}Cs.

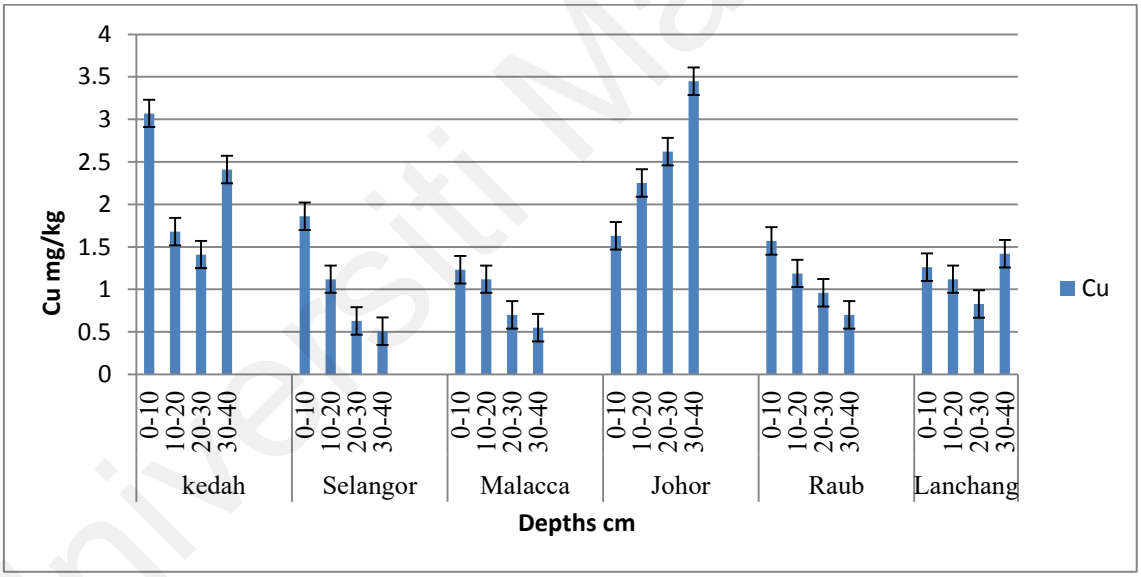

Figure 4.96: The vertical distribution of Cu concentrations across the study areas

4.4.6.6 The vertical distribution of Zinc (Zn) in Lanchang

The mean value of Zn was found to be 1.81±0.4 mg/kg in Lanchang, while the range values differ from 1.10 to 2.60 mg/kg (Table 4.48). The vertical distribution of Zn is shown in Table 4.49. The estimated values show that the Zn movement decreased with depth before increasing at 10-20 cm. Figure 4.96 depicts the pattern of irregular Zn distribution throughout the soil matrix.

The elationships between Zn and the radionuclides ^{226}Ra, ^{232}Th and ^{40}K were found to be weak. Positive correlations (P ≤0.01) were shown between Zn and P, K, Ca, Mg, Fe and Al, and positive (P ≤0.05) with OM. The correlation found to be a negative (P ≤0.01) between the Zn and the soil pH (Table 4.50).

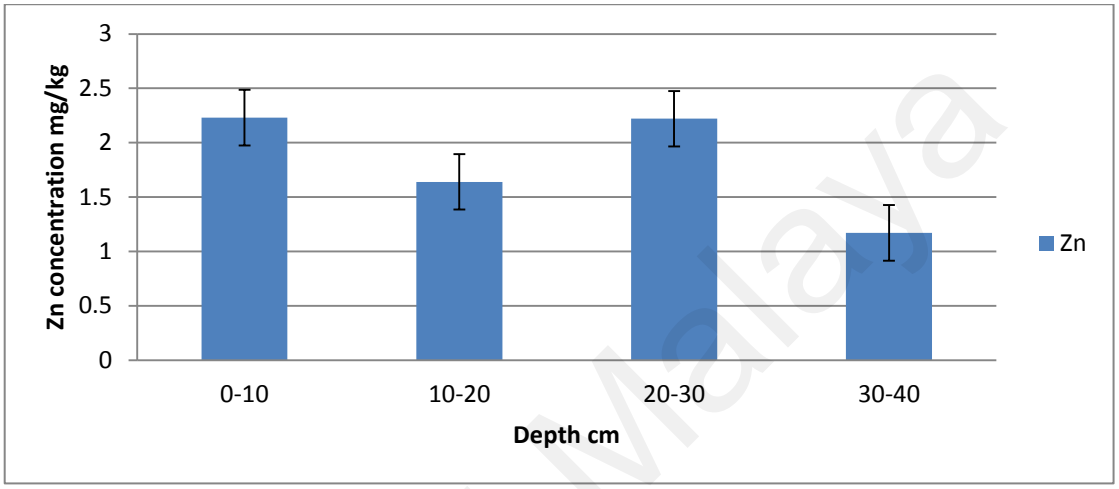

Figure 4.97: The vertical distribution of Zn in the soil samples from Lanchang

The trends of vertical distributions of Zn in Kedah, Selangor, Johor and Raub showed a clear tendency to decrease at lower depths. However, no clear tendency of Zn concentration within the vertical distribution of depths in Malacca and Lanchang. The variability of Zn distribution within the soil profile may be related to soil texture and the occurrence of Zn-bearing minerals. As well as, Fe distribution, many tropical soil studies have concluded that Fe and Al oxyhydroxides are important soil components for trace metal sorption. For instance, the distribution of trace metals (Cu, Ni, Pb and Zn) appeared to be correlated with that of free Fe oxides in an analysis of a tropical kaolinitic ultisol profile in Nigeria in a study counducted by Mbila *et al.*, (2001). The conclusion about the distribution of Zn bound to Fe oxides in tropical has been reported by other studies done by King (1988), Munkholm *et al.,* (1993), Appel *et al.,* (2003), Wilcke *et al.,* (1999), Zarcinas *et al.,* (2004). On the whole, the Zn concentrations were

low, averaging less than 3 mg/kg in most of samples. The highest mean values of Zn were shown in Kedah, Selangor and Pahang Ruab at 2.32, 1.99 and 1.99 mg/kg, respectively, while, the lowest value is found in Malacca. High levels of Zn concentration could be related to the soils derived from marine alluvium and organic enriched alluvial deposits that contain relatively higher levels of Zn throughout the soil.

Zinc (Zn) mean values of the study areas follow the order of Malacca (1.48±2.3) < Johor (1.7±0.6) < Lanchang (1.8±0.4) < Selangor (1.8±0.5) < Raub (1.9±0.5) < Kedah (2.2±0.7) mg/kg.

The correlations were shown to be positive ($P \leq 0.01$) between Zn and the activity of radionuclides ^{226}Ra, ^{232}Th and ^{40}K in the soils from Kedah, Selangor, Johor and Raub. While, insignificant correlations were shown in the soils from Malacca, and Lanchang. The positive relationship between Zn and radionuclides ^{226}Ra, ^{232}Th and ^{40}K was also reported by Dragović *et al.,* (2012).

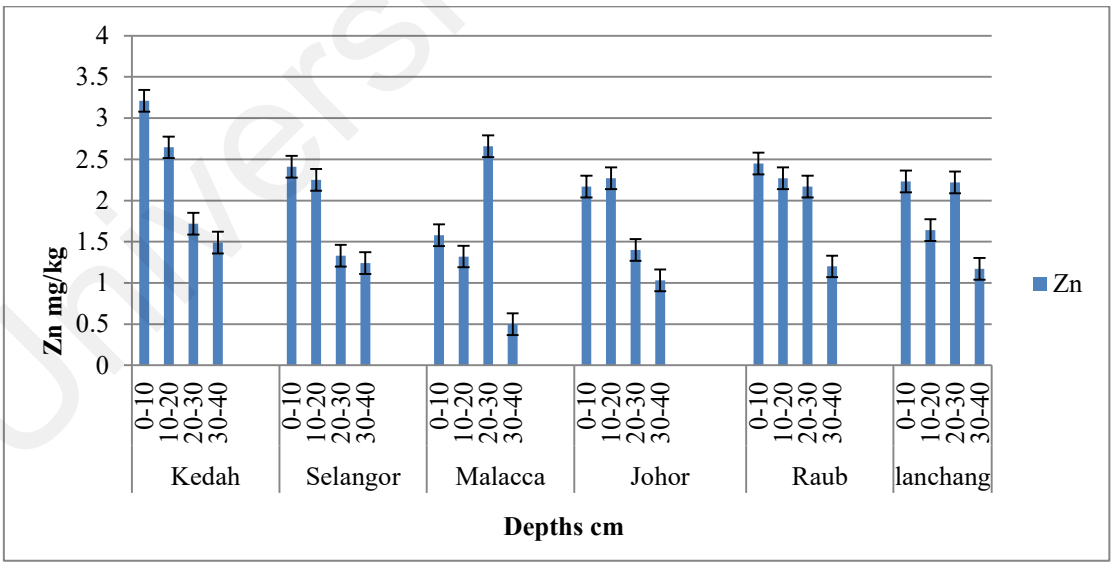

Figure 4.98: The vertical distribution of Zn concentrations across the study areas

4.4.6.7 **The vertical distribution of Manganese (Mn) in Lanchang**

Mn was found to have a mean value of 10.32±1.904 mg/kg in Lanchang, with range values differ from 7.70 to 17.50 mg/kg (Table 4.48). Table 4.49 illustrates the vertical distribution of Mn. According to the computed values, Zn migration decreased within depths before increasing again at 20-30 cm. Figure 4.99 depicts the pattern of uneven Mn distribution throughout the soil matrix.

The relationship between Mn and ^{226}Ra was a positive ($P \leq 0.05$), and a weak relationship with ^{232}Th and ^{40}K. Positive correlations ($P \leq 0.01$) were shown between Mn and P, Ca, Fe and Al, and positive ($P \leq 0.05$) with OM, K and Mg. The correlation found to be a negative ($P \leq 0.05$) between Mn and soil pH, while, insignificant relationships were shown with Cu and Zn (Table 4.50).

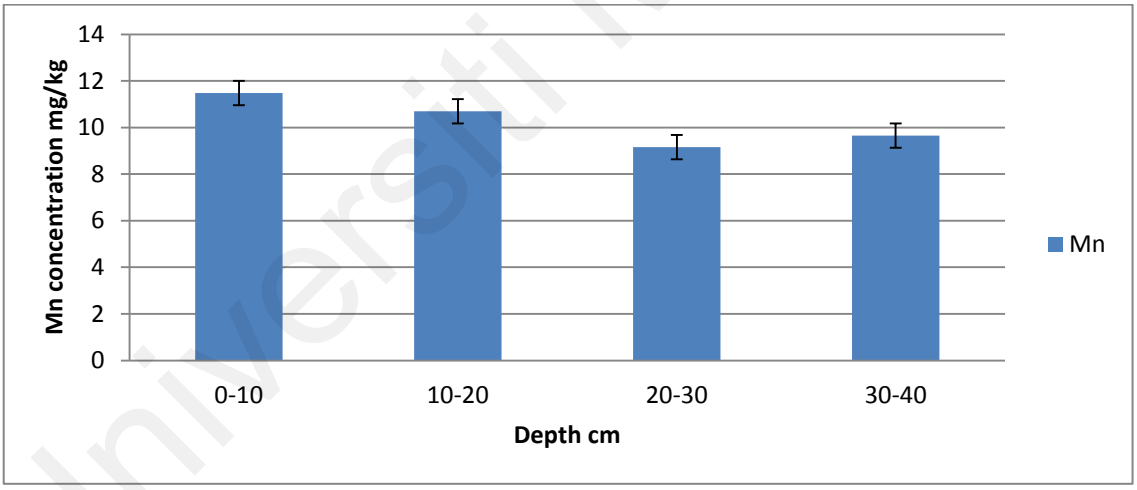

Figure 4.99: The vertical distribution of Mn in the soil samples from Lanchang

Distribution of Mn showed a regular decreasing of the concentration pattern with depths in soil from Malacca, Johor and Raub. In Kedah the vertical distribution pattern of Mn showed a regular increase within the soil depths. High Mn concentrations on the top of the soil profile may be attributed to the oxidation of Mn to less soluble forms not leached by rainfall at the soil surface. This process would likely occur on poorly drained soils in Malaysia. The accumulation of Mn in the surface of well-drained soils may be

associated with the OM content and nutrient recycling. However, the vertical distribution patterns of Mn in Selangor and Lanchang were irregular. The highest mean values of Mn concentrations were found in Selangor and Johor as 12.7±4.2 and 11.2±2.5 mg/kg, respectively. The lowest value was found in Malacca as 7.53 mg/kg.

Manganese (Mn) values of the study areas follow order of Malacca (7.5±2.7) < Raub (8.3±2.4) < Lanchang (7.5±2.7) < Kedah (10.5±3.1) < Johor (11.2±2.5) < Selangor (12.7±4.2) mg/kg.

In the coastel areas, such as Kedah, Selangor; whereas soils derived from sandstone parent material generally have higher micronutrient content, especially of Mn. Other soils that orginated from argillaceous, organic enriched alluvial deposits, and granite generally had low micronutrient reserves.

Manganese (Mn) is positively correlated ($P \leq 0.01$) with the radionuclides ^{226}Ra, ^{232}Th and ^{40}K in the soil from Malacca, Johor and Raub. This is consistent with earlier studies conducted by Dragović *et al.,* (2012), Navas *et al.,* (2005), and Chao & Chuang, (2011) where they reported significant correlations between Mn and ^{226}Ra and ^{232}Th. However, the Mn found to be negatively associated ($P \leq 0.01$) with the radionuclides ^{226}Ra, ^{232}Th and ^{40}K in Kedah.

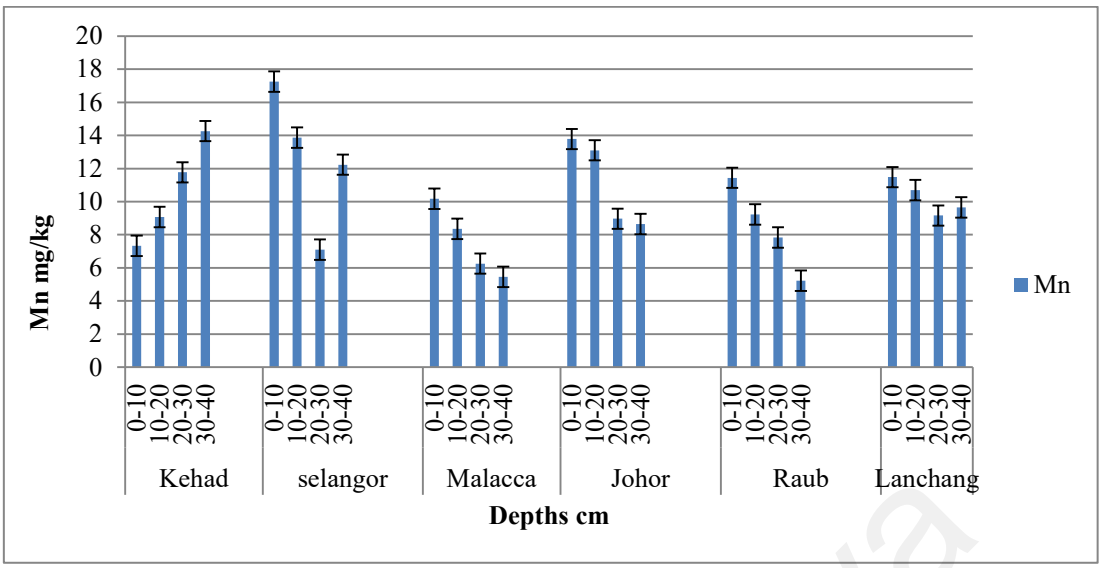

Figure 4.100: The vertical distribution of Mn concentrations across the study areas

4.4.2.6.8 The vertical distribution of Iron (Fe) in Lanchang

The mean value of Fe was found to be 683.57±38.6 mg/kg in Lanchang, while the range values differ significantly from 312.00 to 605.00 mg/kg (Table 4.48). The vertical distribution of Fe is shown in Table 4.49. The measured values indicate that the Fe movement gradually decreasing with depths. The pattern of regular distribution of Fe within the soil matrix is shown in Figure 4.101.

The relationship between Fe and ^{40}K is positively correlated ($P \leq 0.05$), while insignificant correlations were shown with ^{232}Th and ^{40}K. The relationships between Fe and OM, P, Ca, Mg, Zn and Al were positively correlated ($P \leq 0.01$), and positively at $P \leq 0.05$ with K and Mn. The relationship between Fe and pH was negativiley correlated ($P \leq 0.01$). Insignificant relationship was shown between Fe and Cu (Table 4.50).

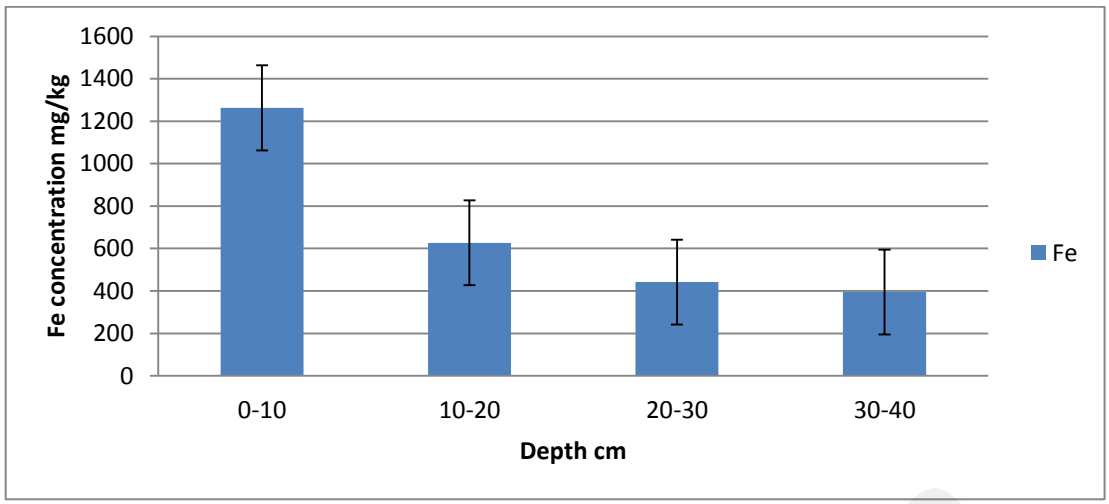

Figure 4.101: The vertical distribution of Fe in the soil samples from Lanchang

This is in agreement with Mbila *et al.,* (2001) findings that the distribution of trace metals is related to the distribution of free iron oxides.

The concentrations of Fe were generally high in all the investigated areas. High Fe content has been considered to be a distinguishing characteristic of highly weathered of tropical soils. There was gradual decrease in Fe concentrations in the horizon immediately below the surface as indicated in the soils groups of the study areas. Soils from Kedah and Selangor exhibited high mean values of Fe with 908.22 and 749.54 mg/kg, respectively.

Iron (Fe) values of the study areas follow the order of Lanchang (683.5±377.9) < Johor (697.9±428.9) < Malacca (699.0±382.2) < Raub (717.9±416.0) < Selangor (749.4±491.2) < Kedah (874.58±457.6) mg/kg.

Positive correlations ($P \leq 0.01$) were shown between Al and Fe in all the soil groups except for Kedah. Positive significant relationships were observed between Fe and the activity concentrations of ^{226}Ra in Malacca, Johor and Raub. This is consistent with earlier studies by Dragović *et al.,* (2012), Navas *et al.,* (2005), Chao & Chuang, (2011 reported significant correlations between Fe and ^{226}Ra and ^{232}Th.

The correlations between Fe and ^{232}Th were found to be significant in Malacca, while the correlation between Fe and ^{40}K was a significant in Lanchang. The relationships between Fe and the radionuclides ^{226}Ra, ^{232}Th and ^{40}K were shown to be insignificant in Kedah and Selangor.

The results reveal that radionuclides behavior depends on the elemental properties of radionuclides, the mineral, soil organic stocks and chemical reaction environment. This is consistent with the findings by Koch-Steindl & Pröhl, (2001) and Van Hullebusch *et al.*, (2005).

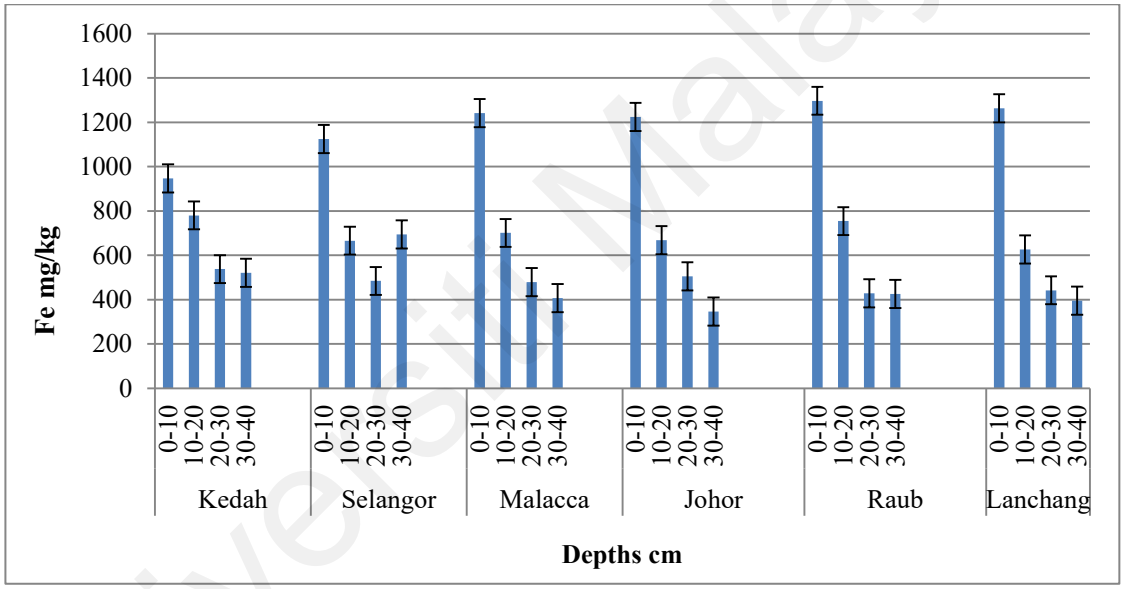

Figure 4.102: The vertical distribution of Fe concentrations across the study areas

4.4.6.8 The vertical distribution of Aluminum (Al) in Lanchang

In Lanchang, the mean value of Al was determined to be 798.97±36.2 mg/kg, whereas the range values vary from 452.00 to 1653.00 mg/kg (Table 4.48). Table 4.49 depicts the vertical distribution of Al. The computed figures show that the Al movement decreased as depth increased. Figure 4.103 depicts the pattern of uniform distribution of Al within the soil matrix.

Relationships between Al and the radionuclides ^{232}Th and ^{40}K were insignificant, while the correlation with ^{40}K was a positive ($P \leq 0.05$). The relationships with OM, P, Ca, Mg, Zn and Fe were positively correlated ($P \leq 0.01$), and positive at $P \leq 0.05$ with K and Mn (Table. 4.50). This is in agreement with Zarcinas *et al.,* (2004) finding that Zn concentrations are significantly correlated with soil Al and Fe.

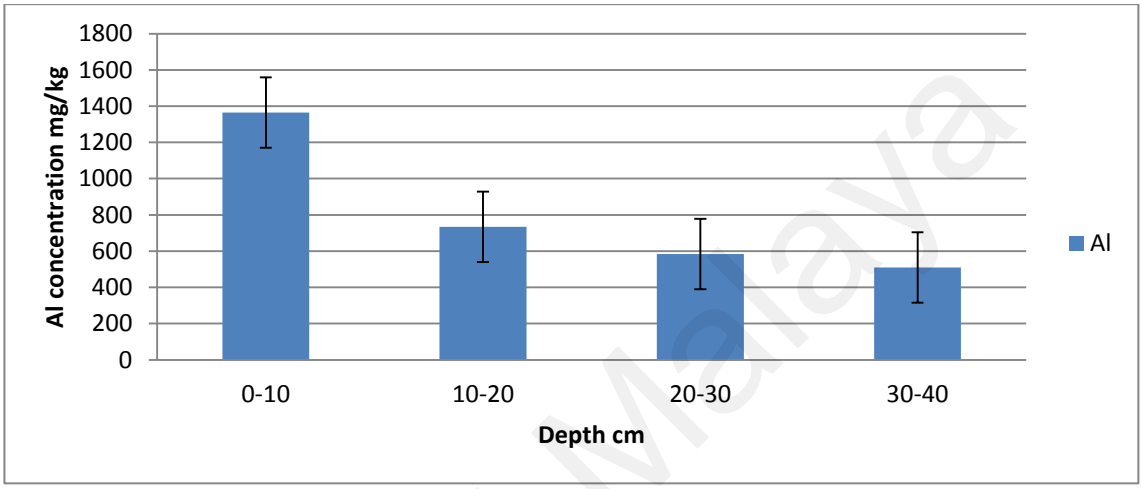

Figure 4.103: The vertical distribution of Al in the soil samples from Lanchang

The concentrations of Al were generally high in all the investigated soil groups. High Al content has been considered to be a distinguishing characteristic of highly weathered of tropical soils. There was gradual decrease in Fe concentrations in the horizon immediately below the surface as indicated in the soils groups in the study areas. However, high concentrations of Al at lower depths may occur due to severe weathering and leaching. Soils from Kedah and Selangor exhibited high mean values of Al with1055.22 and 841.57 mg/kg, respectively (Table 4.37 and 4.43). Aluminum (Al) values of the study areas follow the order of Lanchang (798.9±367.2 < Johor (827.7±419.1) < Raub (829.8±428.5) < Malacca (839.6±409.3) < Selangor (841.5±495.8) < Kedah (1049.27±435.3) mg/kg. Positive correlations ($P \leq 0.01$) were shown between Al and Fe in all the soil groups except for Kedah. Positive significant relationships were observed between Al and the activity concentrations of ^{226}Ra in

Malacca, Johor and Raub. This is consistent with earlier studies couducted by Dragović *et al.,* (2012), Navas *et al.,* (2005), and Chao & Chuang, (2011) where they reported significant correlations between Al and ^{226}Ra and ^{232}Th. The correlation between Al and ^{232}Th was shown to be a significant in Malacca and Johor, while significant correlation with ^{40}K was shown in Lanchang. The relationships between Fe and the radionuclides ^{226}Ra, ^{232}Th and ^{40}K were found to be insignificant in Kedah and Selangor.

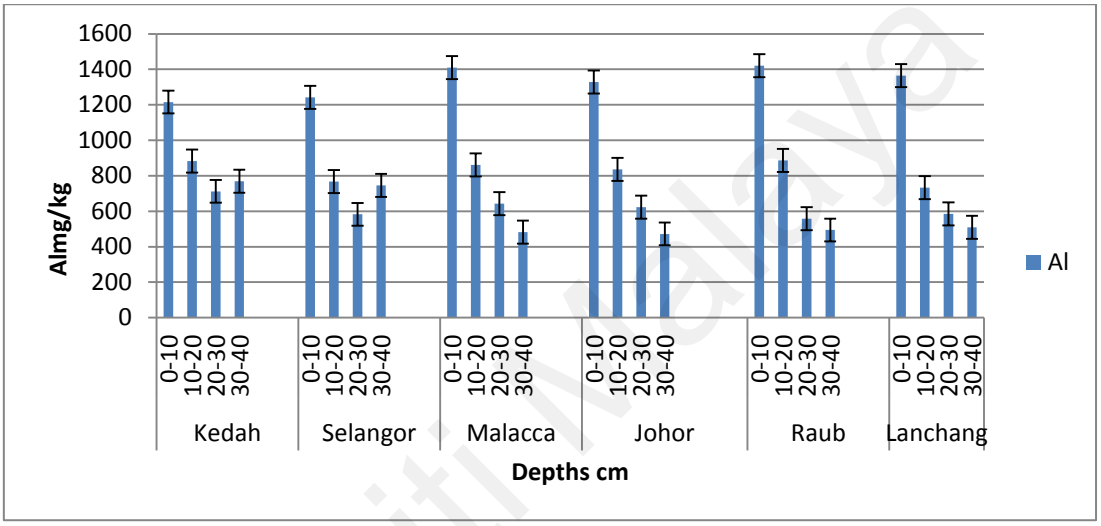

Figure 4.104: The vertical distribution of Al concentrations across the study areas

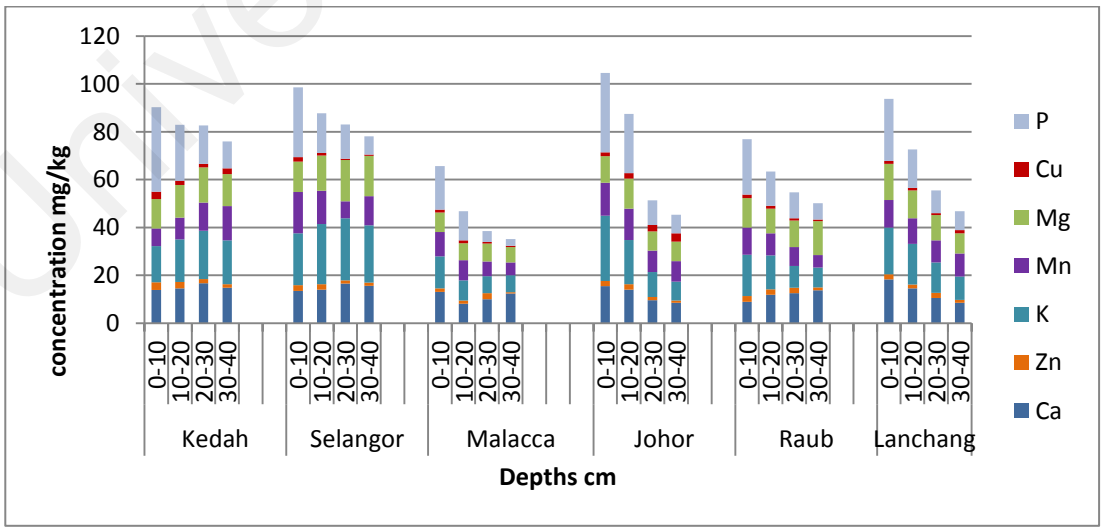

Figure 4.105: The vertical distribution of stable metals in the soil profile across the study areas

4.4.7 Seasonal changes of redox potential and microbial activity in tropical soils and implications for radionuclide availability

At the beginning and end of the growing season, this study compared two groups of microorganisms in their response to altered soil conditions, and the potential effect on the availability of radionuclides. The seasonal changes of the radionucldies ^{226}Ra, ^{232}Th, ^{40}K and ^{137}Cs activites, redox potential and activity of microorganisms are presented in Table 4.58 and Table 4.59.

4.4.7.1 Seasonal variations of radionuclide activities

The measurements of the seasonal changes of radionuclides activities are presented in Table 4.51 and 4.52. The mean values of ^{226}Ra, ^{232}Th, ^{40}K and ^{137}Cs were found to be 67.1±8.2, 69.1±11.0, 805.3±208.9 and 2.2±0.8 Bq kg^{-1} during the wet season, respectively. Whereas, the the mean values for the dry season were found to be 72.4±8.7, 68.2±7.5, 688.1±129.0 and 1.3±0.7 Bq kg $^{-1}$, respectively. The concentrations of the radionuclides ^{226}Ra, ^{228}Ra, ^{40}K and ^{137}Cs were slightly higher in the wet season than the dry season (Figure 4.106). Table 4.53 and 4.54 show the relationships between Fe and Mn oxides and the radionucldies ^{226}Ra, ^{232}Th, ^{40}K and ^{137}Cs. In the wet season, Fe and Mn oxides were positively correlated with the radionuclides ^{226}Ra ($P < 0.01$), ^{232}Th ($P < 0.01$), ^{40}K ($P < 0.01$), and ^{137}Cs ($P < 0.01$), while, in the dry season, Mn correlated in a positive significant relationship with the radionuclides ^{226}Ra ($P < 0.01$), ^{232}Th ($P < 0.01$), and ^{137}Cs ($P < 0.05$).

Fe correlated positively with ^{226}Ra ($P < 0.01$), and ^{137}Cs ($P < 0.05$). The results are consistent with the conclusion of Rieuwerts, (2007) that heavy metals tend to be relatively mobile in tropical soils and appear to be relatively bioavailable.

The Fe oxide content might have a proportionally greater importance in retention heavy metals such as thorium, uranium and radium. For example, it has been reported

that iron oxides are important in adsorbing uranium in tropical soils by Payne *et al.,* (1994).

In wet season of tropical environments, almost all organic material that reaches the soil surface decomposes rapidly, so the surface accumulation of soil organic matter is minimal. Consequently, there is rapid recycling of nutrients and contaminants into the vegetation. In temperate zones, the decomposition of organic debris is slower and the accumulation of soil organic matter is usually greater than the rate of decomposition, resulting in highly organic surface soil. In the tropics, due to the relatively highly aged soils and high mineral weathering rates, clays of low exchange activity, such as kaolinite, are more common than in temperate zones. This leads to soils that, despite having high clay content, have a low exchange capacity. Because rice plants grow in flooded conditions, the behaviour of redox-sensitive elements is different in paddy fields than in comparable dryland agriculture (Yanagisawa *et al.,* 2000; Uchida, 2007).

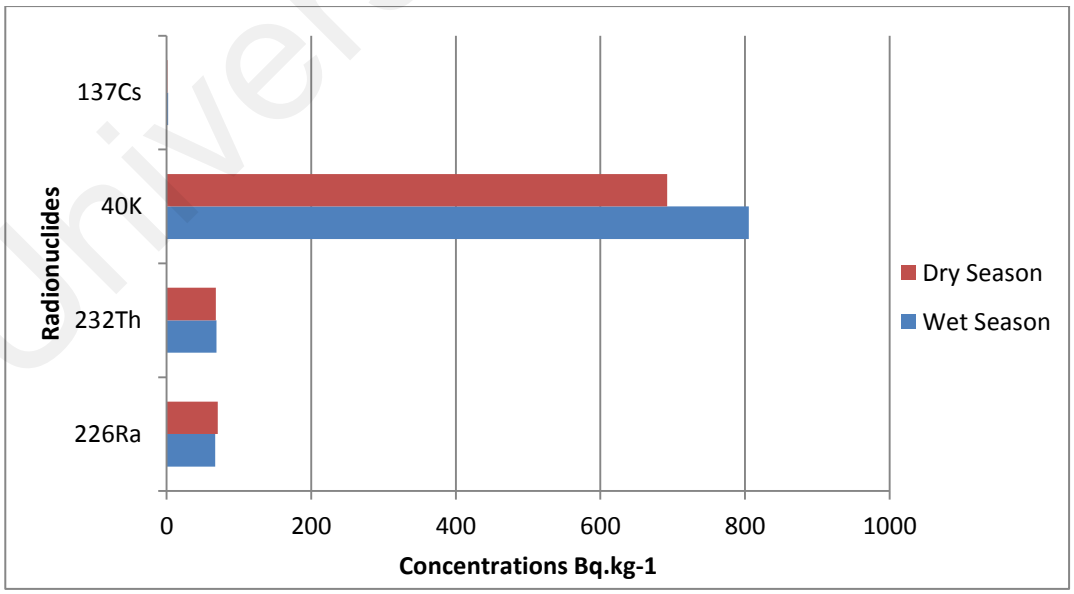

Figure 4.106: Concentration of the radionuclide activities (mean) in soil during the wet and dry season

Table 4.51: Values of Fe and Mn oxides, bacterial and fungal (CFU), and the radionuclides ^{226}Ra, ^{232}Th, ^{40}K and ^{137}Cs Bq.kg^{-1} of the soil in the wet season

Sample (wet) ID	Fe oxides mg/100g	Mn oxides mg/100g	Fungi CFU	Becteria CFU	^{226}Ra Bq.kg^{-1}	^{232}Th Bq.kg^{-1}	^{40}K Bq.kg^{-1}	^{137}Cs Bq.kg^{-1}
K1	774.00	11.50	5.50×10^{8}	3.00×10^{8}	66.2±5.5	76.2±3.5	723.2±58.4	2.7±0.02
K2	643.00	7.50	4.00×10^{8}	2.20×10^{8}	61.3±6.5	62.4±2.5	615.3±56.4	2.3±0.02
K3	1671.00	12.50	7.50×10^{8}	5.50×10^{8}	77.4±3.3	81.4±7.5	778.4±57.5	2.8±0.01
K4	432.00	7.80	5.00×10^{8}	3.20×10^{8}	57.2±3.5	55.5±3.5	652.4±58.5	2.2±0.03
K5	535.00	7.30	3.00×10^{8}	4.50×10^{8}	53.4±4.5	60.3±3.5	752.3±61.5	1.5±0.02
K6	422.00	7.50	6.50×10^{8}	5.00×10^{8}	68.2±2.3	62.5±2.5	674.3±71.5	1.4±0.03
K7	635.00	8.50	4.20×10^{8}	3.00×10^{8}	68.2±3.5	73.3±2.2	657.4±52.2	0.5±0.01
K8	778.00	10.30	5.00×10^{8}	6.20×10^{8}	69.2±2.3	92.3±3.5	1103.3±115.2	2.3±0.03
K9	886.00	10.50	3.50×10^{8}	2.00×10^{8}	75.4±5.5	59.5±3.3	814.5±78.6	3.5±0.02
K10	762.00	12.50	5.00×10^{8}	3.00×10^{8}	72.4±4.2	75.3±2.4	733.5±77.5	2.4±0.05
K11	385.00	6.20	6.50×10^{8}	4.00×10^{8}	58.2±5.2	55.4±4.5	676.8±78.3	0.7±0.01
K12	1410.00	14.50	3.80×10^{8}	2.00×10^{8}	72.3±2.5	80.3±4.3	1192.4±97.3	3.4±0.01
K13	768.00	10.20	3.00×10^{8}	4.30×10^{8}	75.3±2.5	77.5±5.5	653.4±88.5	1.2±0.03
K14	1747.00	13.50	4.20×10^{8}	4.60×10^{8}	82.2±2.2	58.3±6.5	785.4±97.7	2.8±0.03
K15	711.00	10.70	7.00×10^{8}	3.70×10^{8}	68.3±5.5	73.3±5.5	725.6±87.5	2.7±0.05
K16	588.00	8.20	5.70×10^{8}	2.10×10^{8}	68.2±2.4	65.5±5.3	832.5±78.3	1.5±0.01
K17	893.00	11.40	3.50×10^{8}	1.40×10^{8}	77.2±2.5	86.3±3.5	1264.3±118.5	3.3±0.03
K18	582.00	9.30	4.50×10^{8}	3.00×10^{8}	54.5±4.3	57.2±2.5	629.3±97.2	1.4±0.05
K19	752.00	12.50	4.50×10^{8}	2.70×10^{8}	65.3±2.2	76.2±2.5	1207.4±87.5	2.2±0.01
K20	674.00	8.70	3.00×10^{8}	1.40×10^{8}	57.3±6.5	60.2±3.5	642.4±87.5	3.2±0.05
Mean	**802.4±379.6**	**10.0±2.3**	**$(4.9\pm1.4)\times10^{8}$**	**$(4.24\pm1.2)\times10^{8}$**	**67.1±3.84**	**69.1±3.90**	**805.3±80.28**	**2.2±0.02**
Range	**385.0- 1747.0**	**6.2 -14.5**	**$(3.3\text{-}8.0)\times10^{8}$**	**$(2.4\text{-}6.2)\times10^{8}$**	**53.0 -82.0**	**55.0 - 92.0**	**615.0 -1264.0**	**0.5 -3.5**

Table 4.52: Values of Fe and Mn oxides, bacterial and fungal (CFU), and the radionuclides ^{226}Ra, ^{232}Th, ^{40}K and ^{137}Cs Bq.kg^{-1}of the soil in the dry season

Sample (dry) ID	Fe oxides mg/100g	Mn oxides mg/100g	Fungi CFU	Becteria CFU	^{226}Ra Bq.kg^{-1}	^{232}Th Bq.kg^{-1}	^{40}K Bq.kg^{-1}	^{137}Cs Bq.kg^{-1}
K1	582.0	5.50	3.70×10^{8}	2.20×10^{8}	72.2±3.5	64.2±2.5	814.4±77.5	0.8±0.05
K2	1225.00	10.30	5.80×10^{8}	4.80×10^{8}	82.3±8.2	85.1±3.5	623.4±82.5	2.8±0.02
K3	622.00	4.50	3.20×10^{8}	2.30×10^{8}	71.5±7.2	60.3±7.3	512.5±79.5	1.2±0.01
K4	542.00	4.90	4.40×10^{8}	4.20×10^{8}	82.5±6.5	75.2±5.5	802.5±78.5	0.8±0.01
K5	762.00	5.50	3.50×10^{8}	2.50×10^{8}	57.4±8.5	51.2±5.5	805.5±67.3	1.3±0.05
K6	525.00	8.30	5.00×10^{8}	4.20×10^{8}	72.3±5.5	78.3±7.3	712.8±91.5	0.9±0.03
K7	923.00	11.20	5.50×10^{8}	4.70×10^{8}	83.2±2.5	85.2±2.5	825.6±84.5	2.7±0.01
K8	642.00	7.80	4.50×10^{8}	4.20×10^{8}	62.2±8.5	65.4±1.5	565.3±92.5	2.2±0.04
K9	433.00	7.40	3.20×10^{8}	3.30×10^{8}	59.3±5.2	68.3±8.3	622.5±65.5	1.3±0.01
K10	487.00	8.20	3.80×10^{8}	2.30×10^{8}	75.5±8.5	66.2±2.5	508.7±62.5	2.1±0.05
K11	1244.00	10.20	5.70×10^{8}	3.80×10^{8}	87.5±8.5	75.1±8.3	758.5±71.5	2.5±0.01
K12	674.00	9.50	2.80×10^{8}	4.00×10^{8}	65.7±3.5	68.2±2.5	618.3±92.5	0.7±0.03
K13	618.00	10.20	4.70×10^{8}	3.20×10^{8}	77.5±7.2	62.3±5.5	767.4±102.5	0.5±0.05
K14	993.00	8.50	5.50×10^{8}	3.50×10^{8}	78.6±1.5	55.3±2.2	510.4±63.5	1.6±0.01
K15	642.00	7.20	4.20×10^{8}	2.50×10^{8}	73.8±8.7	75.5±3.5	714.3±86.5	2.5±0.01
K16	1303.00	11.30	5.50×10^{8}	4.50×10^{8}	85.4±8.5	88.5±8.2	710.4±68.7	2.8±0.04
K17	552.00	7.20	3.00×10^{8}	1.30×10^{8}	56.3±4.5	62.3±2.5	636.7±81.5	1.5±0.03
K18	564.00	6.50	4.30×10^{8}	2.00×10^{8}	57.3±7.5	60.3±7.5	996.5±83.5	0.7±0.01
K19	479.00	6.20	2.50×10^{8}	1.30×10^{8}	56.2±6.5	58.2±3.7	622.7±72.5	0.5±0.01
K20	582.00	6.30	2.80×10^{8}	2.20×10^{8}	63.4±6.7	58.2±6.5	734.8±85.2	0.8±0.01
Mean	**719.7±269.1**	**9.8±2.0**	**$(4.1\pm1.0)\times10^{8}$**	**$(3.1\pm1.1)\times10^{8}$**	**70.6±6.36**	**67.9±4.84**	**692.6±79.48**	**1.4±0.02**
Range	**433.0-1303.0**	**4.5-11.3**	**(3.0-6.0) 10^{8}**	**(1.0-5.0) $\times10^{8}$**	**56.0-87.0**	**51.0-88.0**	**508.0-996.0**	**0.5-2.8**

4.4.7.2 **Seasonal changes of oxidation potential**

The measured values of Fe and Mn oxides in the wet and dry season are presented in Table 4.51 and 4.52. The mean values of Fe and Mn were found to be 802.4±379.6 and 10.0±2.3 during the wet season, respectively. Whereas, the mean values for the dry season were 719.7±269.1 and 9.7±1.9, respectively, the concentrations were slightly higher during the wet season than in the dry season (Figure 4.107; 4.108). It is well understood that pH has a significant effect on the sorption of trace metals in soils. Where net negative surface charge of a tropical soil decreases with decreasing soil pH and OM content, the low surface charge density creates conditions conducive to increased mobility of metals. Low pH often stands alone as the parameter best able to predict trace metal solubility in an inverse correlation (Rieuwerts *et al.,* 2006). A low pH tends to lead to a decrease in sorption and a consequent increase in the bioavailability of radionuclides and trace metals. This could explain the increase in radionuclide concentrations and oxidative processes during the wet season as the soil pH decreases due to increased weathering and leaching.

Table 4.53 and 4.54 show the relationships between Fe and Mn oxides and the radionucldies ^{226}Ra, ^{232}Th, ^{40}K and ^{137}Cs. During the wet season, the Fe oxide correlated positively with the radionuclides ^{226}Ra ($P < 0.01$), ^{232}Th ($P < 0.01$), ^{40}K ($P < 0.01$) and ^{137}Cs ($P < 0.01$), while the Mn oxide correlated in a significant positive relationship with the radionuclides ^{226}Ra ($P < 0.01$) and ^{232}Th ($P < 0.05$), ^{40}K ($P < 0.01$) and ^{137}Cs ($P < 0.01$). During the dry season, the Fe oxide correlated positively with the radionuclides ^{226}Ra ($P < 0.01$) and ^{137}Cs ($P < 0.05$), while the Mn oxide correlated in a significant positive relationship with the radionuclides ^{226}Ra ($P < 0.01$), ^{232}Th ($P < 0.01$) and ^{137}Cs ($P < 0.05$).

The positive correlations can be due to the sensitivity of some elements to the oxidation and reduction conditions, including radionuclides. Heavy metals and radionuclides are absorbed by Fe and Mn oxides as an important immobilization reaction for immobilization of these compounds (Hohl & Stumm 1976; Means *et al.,* 1978a; Means *et al.,* 1978 b; Ainsworth *et al.,* 1994; Ames *et al.,* 1983; Dzombak *et al.,* 1990; Salomons *et al.*, 1984; Saunders *et al.,* 1997). Redox speciation variations in Fe and Mn play a significant role in the sorption and release of radionuclides and trace elements (Twining *et al.,* 2005). The important relationship between radionuclides and Fe and Mn oxides that was reached is in agreement with other studies carried out by Means *et al.,* (1978a), Lack *et al.,* (2002), Twining, *et al.,* (2005), Navas, *et al.,* (2005) which indicated that the radionuclides bind positively with the Fe and Mn oxides. Increased oxidation processes of Fe and Mn in wet soils have been reported by Wasserman, *et al.,* (1998), Schulze, *et al.,* (1995) and Twining, *et al.,* (2005). There are no previous local studies available that sought to investigate the relationship between radionuclide activities and oxidation and reduction processes in soil for comparison.

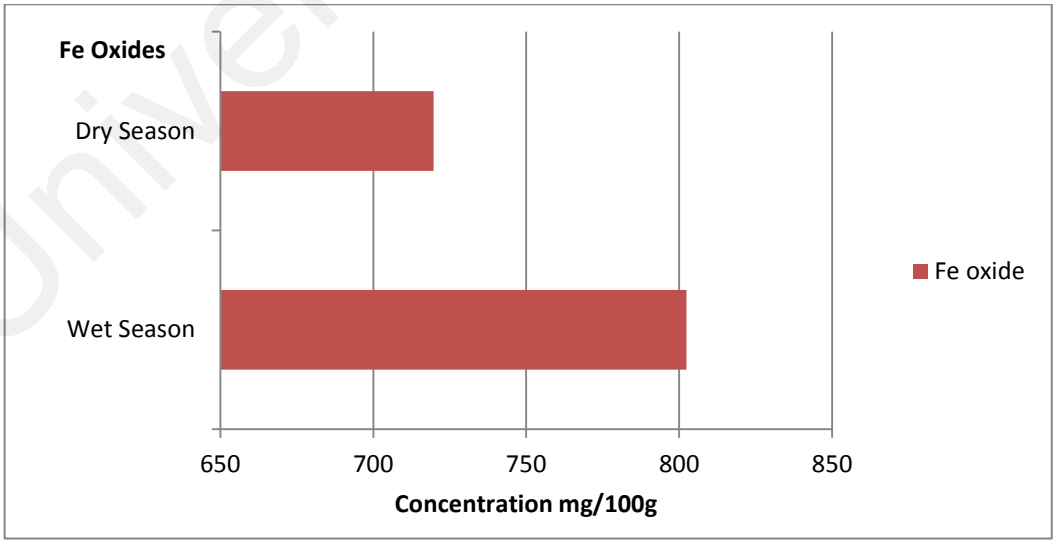

Figure 4.107: Concentration of Fe oxide in soil during the wet and dry season

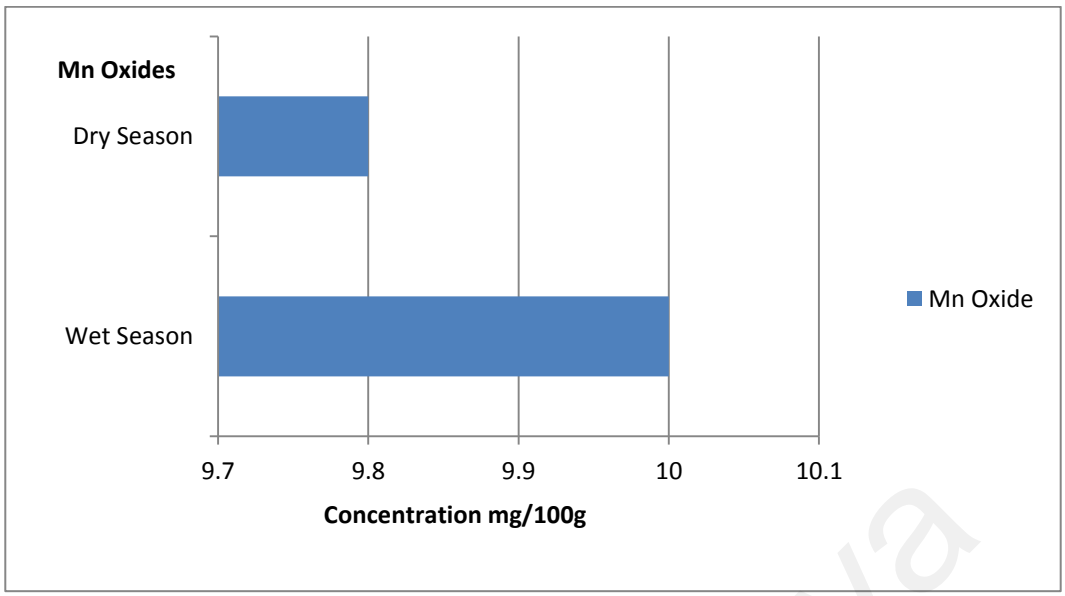

Figure 4.108: Concentration of Mn oxide in soil during the wet and dry season

Table 4.53: Pearson correlation coefficients between the the radionuclide activities, and Fe, Mn oxides and the activity of microorganisms in the soil in the wet season

Wet season	Fe	Mn	MEA (Fungi)	NA (Bacteria)	^{226}Ra	^{232}Th	^{40}K	^{137}Cs
Fe	1.000							
Mn	0.866**	1.000						
MEA (Fungi)	0.828**	0.865**	1.000					
NA (Bacteria)	0.686**	0.650**	0.732**	1.000				
^{226}Ra	0.801**	0.653**	0.622**	0.571**	1.000			
^{232}Th	0.605**	0.541*	0.544*	0.532*	0.531*	1.000		
^{40}K	0.568**	0.563**	0.688**	0.649**	0.541*	0.520*	1.000	
^{137}Cs	0.744**	0.649**	0.574**	0.360	0.459*	0.269	.451*	1.000

**. Correlation is significant at the 0.01 level (2-tailed)
*. Correlation is significant at the 0.05 level (2-tailed)

Table 4.54: Pearson correlation coefficients between the the radionuclide activities, and Fe, Mn oxides and the activity of microorganisms in the soil in the dry season.

Dry season	Fe	Mn	MEA (Fungi)	NA (Bacteria)	^{226}Ra	^{232}Th	^{40}K	^{137}Cs
Fe	1.000							
Mn	0.536*	1.000						
MEA (Fungi)	0.588**	0.659**	1.000					
NA (Bacteria)	0.536*	0.649**	0.721**	1.000				
^{226}Ra	0.569**	0.593**	0.792**	0.684**	1.000			
^{232}Th	0.251	0.594**	0.559*	0.738**	0.646**	1.000		
^{40}K	0.083	-0.102	0.179	-0.023	0.108	0.097	1.000	
^{137}Cs	0.520*	0.466*	0.524*	0.493*	0.471*	0.583**	-0.131	1.000

**. Correlation is significant at the 0.01 level (2-tailed)
*. Correlation is significant at the 0.05 level (2-tailed)

4.4.7.3 **Seasonal changes in the activity of microorganisms**

Results of seasonal of microbial counts are given in Table 4.51 and 4.52. The mean values MEA (Fungi) and NA (Bacteria) colonies/g soil during the wet season of were found to be 4.9±1.4 × 10^8 and 4.24±1.2 × 10^8, respectively, whereas the values for the dry were measured to be 4.1±1.0 × 10^8 and 3.1±1.1 × 10^8, respectively. The activities mass were shown to be slightly higher in the wet season than in the dry season. The results show slightly change in bacterial and fungal populations over the growing period or wet season (Figure 4.109).

The relationships between the fungi and bacteria biomass and the radionucldies ^{226}Ra, ^{232}Th, ^{40}K and ^{137}Cs are presented in Table 4.53 and 4.54.

During the wet season, the fungi activities correlated positively with the radionuclides ^{226}Ra ($P < 0.01$), ^{232}Th ($P < 0.01$), ^{40}K ($P < 0.01$) and ^{137}Cs ($P < 0.01$), while the bacteria activities were correlated in positive significant relationship with the radionuclides ^{226}Ra ($P < 0.01$) and ^{232}Th ($P < 0.05$), ^{40}K ($P < 0.01$). During the dry

season, fungi activities correlated in positive significant relationship with the radionuclides ^{226}Ra ($P < 0.01$), ^{232}Th ($P < 0.05$), and ^{137}Cs ($P < 0.05$), while the bacteria activities positively correlated with the radionuclides ^{226}Ra ($P < 0.01$), ^{232}Th ($P < 0.01$) and ^{137}Cs ($P < 0.05$).

Microorganisms play an important role in the biogeochemical cycling of radionuclides (Gadd, 2002; Morris & Raiswell, 2002; Lloyd & Renshaw, 2005), and can affect soil composition by a variety of mechanisms, such as changing the soil pH and this affects the rate of transfer of radionuclides from the solute to solid phase (Tamponnet *et al.,* 2001). This effect has been found to be particularly significant in organic and acid soils (Valcke & Cremers, 1994; Sanchez *et al.,* 2000). The presence of microorganisms may also increase radionuclide binding by increasing the surface area for binding in the organic matrix and clay minerals and by depleting the medium of competing ions (Parekh *et al.,* 2008).

The observed increase in microbial activity during the wet season may increase the exudates in the form of low-molecular-weight organic compounds formed during microbial metabolism and could serve as potential ligands for radionuclides. Microorganisms can also alter soil structure through the formation of mineral aggregates, thus affecting radionuclide binding sites. Radionuclides may also become attached to microbial cell walls or to extracellular polysaccharides of bacteria, and radionuclides may be actively taken up by microorganisms from soil solution.

It is understood that all types of cultivated plants are naturally associated with fungi. These associations typically improve the production of biomass and the supply of water and nutrients to the plant during the growing season by enhancing solubilizing scarcely soluble nutrients (Ek *et al*., 1994; Smith & Read, 1997). Fungal can also affect the absorption of inorganic contaminants, including radionuclides, by the same processes

(Riesen & Brunner, 1996; Brunner *et al.,* 1996; Nikolova *et al.,* 1997; Strandberg & Johansson 1998; Drissner *et al.,* 1998; Entry *et al.,* 1999). This could explain the increase shown by radionuclide concentrations during the growing season. Seasonal changes of microorganisms as factors affecting radionuclide behavior were also reported also by (Nishita *et al.,* 1961; Smolders & Shaw, 1995; Twining, *et al.,* 2005).

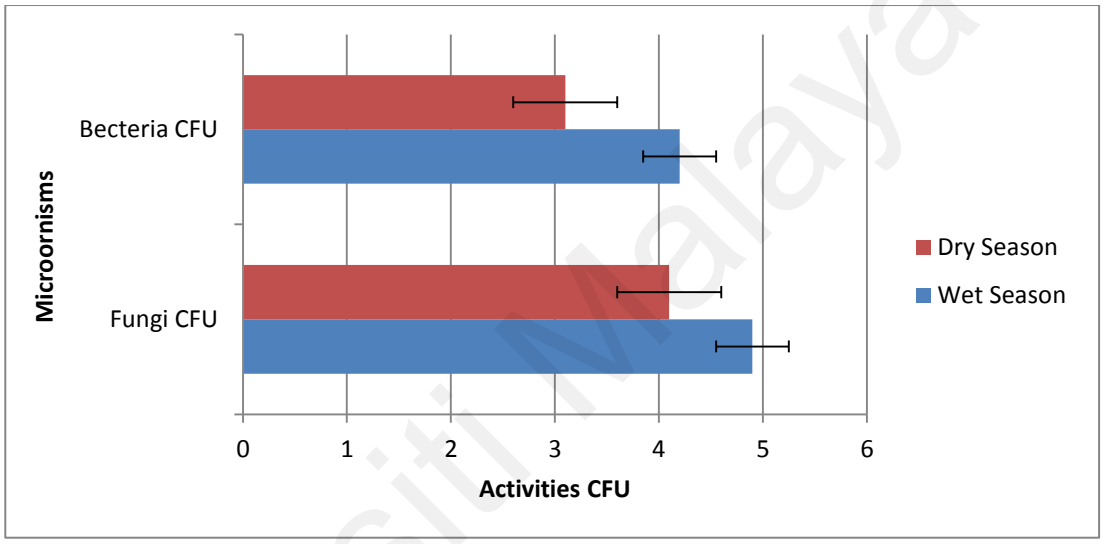

Figure 4.109: Fungi and Bacteria biomass activities (CFU) in soil in the wet and dry season

4.5 Radiological hazard assessment of the radionuclides

4.5.1 Radiation hazard assessment of radionuclides in Kedah

4.5.1.1 Evaluation of the radium equivalent activity (Ra_{eq}) in Kedah

The distribution of ^{226}Ra, ^{232}Th and ^{40}K in soil is usually non-uniform. To compare the specific activity of soils containing different amounts of ^{226}Ra, ^{232}Th and ^{40}K, uniformity with respect to exposure to radiation was specified in terms of radium equivalent activity (Ra_{eq}) in Bq kg^{-1}. It is calculated through the Equation 3.24 given in chapter 3. The estimated Ra_{eq} values for the samples collected from Kedah are shown in

Table 4.55. The Ra_{eq} range values differ from 175.69 to 323.86 Bq kg^{-1} with a mean value of 236.31±32.7 Bq kg^{-1}. The mean value did not exceed the permissible limit 370 $Bq.kg^{-1}$ recommended by OECD, (1979). This means that the use of soil in the area for agriculture or as building materials does not pose a significant radiation health risk.

4.5.1.2 **Evaluation of the absorbed dose rate (D) in Kedah**

The absorbed gamma dose rate DR (nGy h^{-1}) in air was calculated at 1 m above the ground surface to ensure uniform distribution of radionuclides, according to the guidance given by UNSCEAR, (2000). Any radiological hazard and radiation exposure from radionuclides in the soil can be measured using this parameter; the absorbed dose rate has been estimated using the Equation 3.23. The absorbed dose rate indicates the received dose outdoors from radiation emitted by radionuclides in environmental materials. Determination of this rate is the main step for evaluating health risk, and this parameter is expressed in Gray. Table 4.55 shows the absorbed dose rate calculated from the radioactivity concentrations of ^{226}Ra, ^{232}Th and^{40}K in the soil samples from Kedah.

The absorbed dose rate in soil samples ranged from 81.15 nGy h^{-1} to 207.34 nGy h^{-1}, with a mean value of 112.86±14.6 nGy h^{-1}, which is higher than the global mean value of (60 nGy h^{-1}) established by UNSCEAR, (2000). Differences in geological formation and geochemical structure of the sample locations may account for the variation in absorbed dose rate compared to UNSCEAR's value, this agrees with a statement of Nguelem *et al.,* (2016).

Table 4.55: The Radiological parameters of the soil samples from Kedah

Sample ID	Depth cm	D ($nGy.h^{-1}$)	AEDE ($\mu Sv.y^{-1}$)	Ra_{eq} ($Bq.kg^{-1}$)	H_{ex}
AS1	10-20	107.34	0.131	234.35	0.63
AS2	20-30	207.34	0.254	203.76	0.55
AS3	0-10	147.28	0.180	323.86	0.87
AS4	10-20	84.70	0.103	181.38	0.48
AS5	30-40	95.34	0.116	206.71	0.55
AS6	0-10	109.07	0.133	234.70	0.63
AS7	10-20	134.55	0.165	292.28	0.78
AS8	0-10	118.23	0.144	256.97	0.69
AS9	20-30	130.15	0.159	284.42	0.76
AS10	10-20	105.99	0.129	231.58	0.62
AS11	0-10	123.40	0.151	267.20	0.72
AS12	10-20	84.37	0.103	183.24	0.49
AS13	20-30	81.15	0.099	175.69	0.47
AS14	30-40	101.56	0.124	219.11	0.59
AS15	0-10	104.72	0.128	228.40	0.61
AS16	20-30	115.20	0.141	248.72	0.67
AS17	30-40	112.12	0.137	243.87	0.65
AS18	20-30	130.91	0.160	284.67	0.76
AS19	10-20	102.76	0.126	220.15	0.59
AS20	30-40	119.44	0.146	257.46	0.69
AS21	10-20	119.44	0.146	234.84	0.63
AS22	30-40	87.62	0.107	188.68	0.50
AS23	20-30	99.87	0.122	217.43	0.58
AS24	30-40	87.81	0.107	190.81	0.51
AS25	0-10	102.34	0.125	222.39	0.60
AS26	30-40	94.76	0.116	204.92	0.55
AS27	10-20	144.19	0.176	246.84	0.66
AS28	20-30	93.93	0.115	202.05	0.54
AS29	30-40	95.57	0.117	207.08	0.55
AS30	20-30	107.46	0.131	235.27	0.63
AS31	10-20	129.04	0.158	279.96	0.75
AS32	0-10	140.46	0.172	304.93	0.82
AS33	10-20	117.05	0.143	247.84	0.67
AS34	0-10	138.62	0.170	300.75	0.81
AS35	20-30	124.85	0.153	271.26	0.73
AS36	30-40	112.08	0.137	243.64	0.65
AS37	0-10	104.89	0.128	227.67	0.61
AS38	10-20	90.60	0.111	196.59	0.53
AS39	0-10	87.73	0.107	188.35	0.50
AS40	0-10	120.71	0.148	262.93	0.71
Mean		**112.86±14.6**	**0.138±0.01**	**236.31±32.7**	**0.63±0.08**
Range		**80.80 - 145.30**	**0.10 - 0.18**	**175.58 - 314.65**	**0.47- 0.84**

4.5.1.3 **Evaluation of the annual effective dose equivalent (AEDE) in Kedah**

Annual effective dose AEDE is calculated to assess the health effects of the absorbed dose by using a conversion coefficient (0.7 Sv Gy^{-1}) to transform absorbed dose in air to the effective dose received by humans, with an outdoor occupancy factor (0.2), which is in reference equivalent with an outdoor occupancy of 20% and 80% for indoors (OECD, 1979; UNSCEAR, 1993). This factor is suitable for determining the pattern of life in the studied area. Annual effective dose rate (AEDE $mSv.y^{-1}$) received by the population can be calculated using the Equation 3.27 given in chapter 3, (UNSCEAR, 1988; Cevik *et al.,* 2007). The estimated annual effective dose in the soil samples from Kedah ranged from 0.10 mSv y^{-1} to 0.25 mSv y^{-1}, with a mean value of 0.138±0.01 mSv y^{-1} (Table 4.55), the observed values for outdoor falls within the range of the recommended annual average for an individual member of the public by given the International Commission on Radiological Protection (ICRP) which is 1 $mSv.year^{-1}$.

4.5.1.4 **Evaluation of the external hazard index (H_{ex}) in Kedah**

The external hazard index for soil samples of the selected study areas was calculated using Equation (3.25). The range of calculated value of H_{ex} of Kedah soil samples vary from 00.47 to 0.84, with a mean value of 0.63±0.08 Table 4.55. All calculated values were found to be less than unity or less than the recommended universal value UNSCEAR, (2000).

4.5.2 Radiation hazard assessment of radionuclides in Selangor

4.5.2.1 **Evaluation of the radium equivalent activity (Ra_{eq}) in Selangor**

Table 4.56 presents the measured Ra_{eq} values for the samples obtained from Selangor. The range of the values varies from 170.86 to 332.56 $Bq.kg^{-1}$ with a mean

value of 245.55±39.0 Bq.kg^{-1}, which falls within the acceptable safe limit of 370 Bq kg^{-1} given by OECD, (1979), UNSCEAR, (1982), UNSCEAR, (1988).

4.5.2.2 **Evaluation of the absorbed dose rate (D) in Selangor**

The calculated values of the absorbed dose rate of samples from Selangor are presented in Table 4.56. The measured values ranged from 78.92 to 153.33, with a mean value of 113.30±18.1 nGy h^{-1} which is higher than the world average of 60 nGy h^{-1} given by UNSCEAR, (2000).

4.5.2.3 **Evaluation of the annual effective dose equivalent (AEDE) in Selangor**

Table 4.56 shows the estimated annual effective dose in the soil samples from Selangor, the measured values are found in the range from 0.10 mSv y^{-1} to 0.19 mSv year^{-1}, with a mean value of 0.138±0.02 mSv year^{-1}. The mean value for outdoor falls within the range of the recommended annual average for an individual member of the public given by the International Commission on Radiological Protection (ICRP) which is 1 mSv year^{-1}.

4.5.2.4 **Evaluation of external hazard index (H_{ex}) in Selangor**

The range of computed H_{ex} of Selangor soil samples vary from 00.46 to 0.89, with a mean value of 0.66±0.1 Table 4.56. Interestingly, 100% of the values are lower than unity, fitting well with the universal assigned value, showing that the concentration of these materials are safe for building construction and agriculture UNSCEAR, (2000), UNSCEAR, (1988).

Table 4.56: The Radiological parameters of the soil samples from Selangor

Sample ID.	Depth cm	D ($nGy.h^{-1}$)	AEDE ($\mu Sv.y^{-1}$)	Ra_{eq} ($Bq.kg^{-1}$)	H_{ex}
S1	0-10	131.43	0.161	282.60	0.76
S2	10-20	140.48	0.172	301.80	0.85
S3	0-10	129.66	0.159	279.61	0.75
S4	0-10	128.55	0.157	276.63	0.74
S5	0-10	122.61	0.150	264.90	0.71
S6	10-20	110.75	0.135	240.06	0.64
S7	0-10	111.10	0.136	242.61	0.65
S8	20-30	96.28	0.118	208.81	0.56
S9	20-30	117.48	0.144	252.90	0.68
S10	10-20	127.80	0.156	274.98	0.74
S11	20-30	112.34	0.137	242.53	0.65
S12	30-40	100.19	0.122	216.86	0.58
S13	30-40	91.11	0.111	197.01	0.53
S14	20-30	110.68	0.135	240.07	0.65
S15	10-20	126.72	0.155	273.94	0.73
S16	30-40	97.58	0.119	212.74	0.57
S17	20-30	108.70	0.133	235.76	0.63
S18	30-40	78.92	0.096	170.86	0.46
S19	10-20	153.33	0.188	332.56	0.89
S20	30-40	81.24	0.099	175.27	0.47
S21	20-30	89.64	0.109	193.88	0.52
S22	30-40	106.04	0.130	238.58	0.64
S23	30-40	100.04	0.122	215.87	0.58
S24	20-30	107.02	0.131	232.94	0.62
S25	0-10	128.84	0.158	278.88	0.75
S26	10-20	148.65	0.182	323.90	0.87
S27	0-10	130.68	0.160	284.18	0.76
S28	10-20	110.75	0.135	240.91	0.65
S29	0-10	110.66	0.135	240.23	0.64
S30	20-30	110.86	0.135	241.21	0.65
S31	0-10	121.45	0.148	263.17	0.71
S32	10-20	133.96	0.164	289.49	0.78
S33	30-40	91.43	0.112	196.76	0.53
S34	30-40	94.38	0.115	204.64	0.55
S35	10-20	104.47	0.128	227.14	0.61
Mean		**113.30±18.1**	**0.138±0.02**	**245.55±39.0**	**0.66±0.1**
Range		**78.92 - 153.33**	**0.10 -0.19**	**170.86 -332.56**	**0.46 - 0.89**

4.5.3 Radiation hazard assessment of radionuclides in Malacca

4.5.3.1 Evaluation of the radium equivalent activity (Ra_{eq}) in Malacca

The obtained value of radium equivalent Ra_{eq} (Bq kg^{-1}) in soils collected from Malacca are provided in Table 4.57. The measured values are found in the range of

146.52 to 296.65 Bq kg^{-1}, with a mean value of 224.74±41.7 Bq kg^{-1}. The mean value did not exceed the permissible limit (370 $Bq.kg^{-1}$) recommended by OECD, (1979).

4.5.3.2 **Evaluation of the absorbed dose rate (D) in Malacca**

Table 4.57 shows the absorbed dose rate calculated from the activity concentrations of ^{226}Ra, ^{232}Th and ^{40}K in the soil from Malacca. The range of the absorbed dose rate is vary from 68.01 nGy h^{-1} to 136.25 nGy h^{-1}, with a mean value of 103.26±19.1 nGy h^{-1}, which is higher than the global mean value of (60 nGy h^{-1}) established by UNSCEAR, (2000).

4.5.3.3 **Evaluation of the annual effective dose equivalent (AEDE) in Malacca**

The measured values of the annual effective dose of the samples from Malacca are presented in Table 4.57. The range value differs from 0.08 to 0.17 mSv y^{-1}, with a mean value of 0.126±0.02 mSv y^{-1}. The mean value falls within the range of the recommended annual average for individual members of the public provided by the International Commission on Radiological Protection (ICRP), which is 1 mSv $year^{-1}$.

4.5.3.4 **Evaluation of the external hazard index (H_{ex}) in Malacca**

The range value of the the external hazard index H_{ex} of Malacca vary from 0.39 to 0.80, with a mean value of 0.60±0.1, Table 4.57. All calculated values are found to be less than unity or less than the recommended universal value UNSCEAR, (2000).

Table 4.57: The Radiological parameters of the soil samples from Malaca

Sample ID	Depth cm	D ($nGy.h^{-1}$)	AEDE ($\mu Sv.y^{-1}$)	Ra_{eq} ($Bq.kg^{-1}$)	H_{ex}
M1	20-30	74.14	0.090	160.12	0.43
M2	0-10	102.10	0.125	222.36	0.60
M3	30-40	86.89	0.106	188.96	0.51
M4	20-30	87.17	0.106	195.93	0.52
M5	10-20	105.00	0.128	227.33	0.61
M6	30-40	83.30	0.102	179.86	0.48
M7	10-20	97.13	0.119	212.95	0.57
M8	20-30	106.59	0.130	232.30	0.62
M9	30-40	88.41	0.108	193.30	0.52
M10	10-20	129.41	0.158	283.32	0.76
M11	0-10	118.66	0.145	258.88	0.69
M12	20-30	85.62	0.105	186.61	0.50
M13	0-10	125.55	0.153	271.51	0.73
M14	10-20	132.54	0.162	288.12	0.77
M15	10-20	119.38	0.146	260.78	0.70
M16	0-10	118.68	0.145	259.10	0.69
M17	20-30	97.68	0.119	212.63	0.57
M18	30-40	97.06	0.119	206.15	0.55
M19	30-40	87.84	0.107	189.24	0.51
M20	30-40	68.01	0.083	146.52	0.39
M21	10-20	129.04	0.158	278.33	0.75
M22	10-20	133.38	0.163	289.93	0.78
M23	0-10	117.91	0.144	258.91	0.69
M24	20-30	93.60	0.114	202.71	0.54
M25	30-40	93.41	0.114	203.10	0.54
M26	20-30	84.38	0.103	184.91	0.49
M27	10-20	136.08	0.166	295.78	0.79
M28	0-10	115.15	0.141	252.77	0.68
M29	0-10	103.07	0.126	223.50	0.60
M30	20-30	99.47	0.121	216.35	0.58
M31	30-40	68.87	0.084	150.04	0.40
M32	0-10	108.87	0.133	237.90	0.64
M33	10-20	136.25	0.167	296.65	0.80
M34	0-10	117.02	0.143	256.79	0.69
M35	10-20	112.56	0.138	243.77	0.65
M36	20-30	88.01	0.107	191.94	0.51
M37	30-40	89.28	0.109	192.12	0.51
M38	30-40	86.66	0.106	188.98	0.51
Mean		**103.26±19.1**	**0.126±0.02**	**224.74±41.7**	**0.60±0.1**
Range		**68.01 136.25**	**0.08 -0.17**	**146.52 296.65**	**0.39-0.80**

4.5.4 Radiation hazard assessment of radionuclides in Johor

4.5.4.1 Evaluation of the radium equivalent (Ra_{eq}) in Johor

Table 4.58 shows the calculated values of the radium equivalent Ra_{eq} (Bq kg^{-1}) in the soil samples collected from Johor. The measured values of Ra_{eq} (Bq kg^{-1}) found in the range from 139.47 to 338.26 Bq kg^{-1}, with a mean value of 239.44±43.6 Bq kg^{-1}. The mean value did not exceed the permissible limit (370 Bq.kg−1) recommended by OECD, (1979).

4.5.4.2 Evaluation of the absorbed dose rate (D) in Johor

The measured mean value of the absorbed dose rate in the soil samples from Johor was shown to be 112.02±18.8 n Gy h^{-1} with a range from 81.93 nGy h^{-1} to 157.34 nGy h^{-1} Table 4.58. The estimated mean value is higher than the global mean value (60 nGy h−1) recommended by UNSCEAR, (2000).

4.5.4.3 Evaluation of the annual effective dose equivalent (AEDE) in Johor

Table 4.58 shows the estimated annual effective dose in the soil samples from Johor, the measured values are found in the range of 0.10 mSv y^{-1} to 0.19 mSv y^{-1}, with a mean value of 0.136 $\pm$0.02 mSv y^{-1}. The mean value for outdoor falls within the range of the recommended annual average for an individual member of the public given by the International Commission on Radiological Protection (ICRP) which is 1 mSv $year^{-1}$.

4.5.4.4 Evaluation of external hazard index (H_{ex}) in Johor

Table 4.58 shows the calculated values of the external hazard index of Johor. The calculated mean value of H_{ex} was 0.64±0.1, while the range values varied from 0.48 to 0.80. All calculated H_{ex} values are found to be less than unity or less than the recommended universal value given by UNSCEAR, (2000).

Table 4.58: The Radiological parameters of the soil samples from Johor

Sample No.	Depth	D ($nGy.h^{-1}$)	AEDE ($\mu Sv.y^{-1}$)	Ra_{eq} ($Bq.kg^{-1}$)	H_{ex}
JB1	0-10	124.71	0.152	270.12	0.72
JB2	10-20	138.59	0.169	299.87	0.80
JB3	30-40	106.03	0.130	228.08	0.61
JB4	30-40	97.75	0.119	211.94	0.57
JB5	20-30	116.96	0.143	251.20	0.67
JB6	30-40	99.12	0.121	213.90	0.57
JB7	10-20	128.16	0.157	277.76	0.75
JB8	10-20	133.52	0.163	288.24	0.77
JB9	20-30	103.06	0.126	221.53	0.59
JB10	0-10	126.65	0.155	273.40	0.73
JB11	20-30	88.88	0.109	190.93	0.51
JB12	0-10	114.07	0.139	246.18	0.66
JB13	30-40	98.98	0.121	214.20	0.57
JB14	30-40	85.67	0.105	183.81	0.49
JB15	20-30	110.72	0.135	139.47	0.64
JB16	10-20	157.34	0.192	338.26	0.91
JB17	10-20	127.34	0.156	274.98	0.74
JB18	20-30	87.11	0.106	187.17	0.50
JB19	0-10	110.94	0.136	240.56	0.64
JB20	30-40	98.49	0.120	213.89	0.57
JB21	10-20	109.90	0.134	237.92	0.64
JB22	30-40	91.69	0.112	198.88	0.53
JB23	20-30	90.37	0.110	195.94	0.52
JB24	0-10	114.56	0.140	246.14	0.66
JB25	20-30	131.27	0.160	282.79	0.76
JB26	0-10	117.71	0.144	254.14	0.68
JB27	20-30	103.26	0.126	222.63	0.60
JB28	10-20	112.62	0.138	243.94	0.65
JB29	10-20	103.69	0.127	225.24	0.60
JB30	30-40	81.93	0.100	177.83	0.48
JB31	0-10	94.14	0.115	203.80	0.55
JB32	20-30	87.08	0.106	187.18	0.50
JB33	0-10	123.42	0.151	265.95	0.71
JB34	20-30	91.57	0.112	198.02	0.53
JB35	0-10	113.01	0.138	244.98	0.66
JB36	10-20	154.65	0.189	330.58	0.89
JB37	20-30	126.04	0.154	272.65	0.73
JB38	10-20	146.06	0.179	315.30	0.85
JB39	0-10	115.19	0.141	250.20	0.67
JB40	10-20	118.69	0.145	258.01	0.69
Mean		**112.02±18.8**	**0.136±0.02**	**239.44±43.6**	**0.64±0.1**
Range		**81.93 - 157.34**	**0.10 - 0.19**	**139.47- 338.26**	**0.48 - 0.91**

4.5.5 Radiation hazard assessment of radionuclides in Raub

4.5.5.1 Evaluation of the radium equivalent activity (Ra_{eq}) in Raub

Table 4.59 shows the measured values of the radium equivalent Ra_{eq} (Bq kg^{-1}) in the soil samples collected from Raub. The estimated values of Ra_{eq} (Bq kg^{-1}) found in the range from 149.37 to 333.46 Bq kg^{-1}, with a mean value of 234.31Bq kg^{-1}. The mean value of study area did not exceed the permissible limit (370 Bq.kg^{-1}) recommended by OECD, (1979).

4.5.5.2 Evaluation of the absorbed dose rate (D) in Raub

The measured values of the absorbed dose rate in the soil samples from Raub are presented in Table 4.59. It was found that the measured mean value of the absorbed dose rate was 112.02 nGy h^{-1}, while the range values vary from 81.93 nGy h^{-1} to 157.34 nGy h^{-1}. The estimated mean value is higher than the global mean value (60 nGy h−1) g by UNSCEAR, (2000).

4.5.5.3 Evaluation of the annual effective dose equivalent (AEDE) in Raub

The calculated values of the annual effective dose in the soil samples from Raub are shown in Table 4.59. The measured values are found in the range of 0.09 mSv y^{-1} to 0.19 mSv y^{-1}, with a mean value of 0.134 $\pm$0.02 mSv y^{-1}. The mean value for outdoor lies within the range of the annual average suggested for individual members of the public as set out by the International Committee on Radiological Protection (ICRP) which is 1 mSv y^{-1}. The worldwide average annual effective dose rate is approximately 0.5 mSv y^{-1} UNSCEAR, (2000). Thus, the present values of the annual effective dose rates lie within the average values of reported worldwide.

4.5.5.4 **Evaluation of external hazard index (H_{ex}) in Raub**

Calculated values of the external hazard index (H_{ex}) in the soil samples from Raub are presented in Table 4.59. The obtained value of the external hazard index in the investigated soil ranged from 0.42 to 0.90, with a mean of 0.635 ± 0.10 which lies within the published value by UNSCEAR, (2000) for the protection of the public. The value of H_{ex} must be lower than unity to keep the radiation hazard insignificant

Table 4.59: The Radiological parameters of the soil samples from Raub

Sample ID	Depth cm	D ($nGy.h^{-1}$)	AEDE ($\mu Sv.y^{-1}$)	Ra_{eq} ($Bq.kg^{-1}$)	H_{ex}
PR1	30-40	102.03	0.125	222.23	0.60
PR2	30-40	114.99	0.141	249.52	0.67
PR3	0-10	89.07	0.109	192.51	0.51
PR4	20-30	124.90	0.153	270.04	0.72
PR5	30-40	106.85	0.131	231.50	0.62
PR6	0-10	127.72	0.156	275.65	0.74
PR7	30-40	89.14	0.109	191.35	0.51
PR8	10-20	96.69	0.118	208.54	0.56
PR9	0-10	131.55	0.161	283.21	0.76
PR10	10-20	113.37	0.139	245.23	0.66
PR11	10-20	106.75	0.130	229.79	0.62
PR12	20-30	110.21	0.135	237.43	0.64
PR13	10-20	102.13	0.125	221.45	0.59
PR14	20-30	86.89	0.106	186.17	0.50
PR15	0-10	133.61	0.163	287.01	0.77
PR16	20-30	112.71	0.138	243.15	0.65
PR17	10-20	145.54	0.178	306.87	0.82
PR18	20-30	115.68	0.141	228.79	0.61
PR19	10-20	132.49	0.162	284.43	0.76
PR20	20-30	84.73	0.103	182.90	0.49
PR21	30-40	72.82	0.089	155.67	0.42
PR22	30-40	99.97	0.122	215.89	0.58
PR23	10-20	146.03	0.179	311.4	0.83
PR24	20-30	97.24	0.119	209.54	0.56
PR25	30-40	88.57	0.108	190.93	0.51
PR26	30-40	83.81	0.102	181.12	0.48
PR27	10-20	114.52	0.140	149.37	0.67
PR28	20-30	107.82	0.132	233.73	0.63
PR29	10-20	118.34	0.145	256.10	0.69
PR30	0-10	126.81	0.155	274.31	0.74
PR31	0-10	113.43	0.139	244.65	0.66
PR32	0-10	155.08	0.190	333.46	0.90
PR33	30-40	116.91	0.143	249.82	0.67
PR34	20-30	99.66	0.122	221.94	0.59
PR35	30-40	119.15	0.146	256.07	0.69
PR36	30-40	89.92	0.110	192.76	0.52
PR37	0-10	102.58	0.125	221.32	0.59
PR38	20-30	121.43	0.148	260.61	0.70
PR39	0-10	95.13	0.116	205.28	0.55
PR40	0-10	107.60	0.131	230.70	0.62
Mean		**112.02±18.2**	**0.136±0.02**	**239.44±40.9**	**0.64±0.1**
Range		**72.82 - 155.08**	**0.09 - 0.19**	**149.37 - 333.46**	**0.42 - 0.90**

4.5.6 Radiation hazard assessment of radionuclides in Lanchang

4.5.6.1 Evaluation of the radium equivalent activity (Ra_{eq}) in Lanchang

The measured values of the radium equivalent activity (Ra_{eq}) in the soil samples from Lanchang are presented in Table 4.60. The calculated value of the radium equivalent activity (Ra_{eq}) varied from 175.58 to 314.65 Bq kg^{-1}, with a mean value of 240.79±32.7 Bq kg^{-1} which falls within the worldwide average value. The maximum value of Ra_{eq}, in building materials as well as geological material must be less than 370 $Bqkg^{-1}$ for the material to be considered safe for use ICRP (1996).

For all the study areas, the mean values of the radium equivalent activity (Ra_{eq}) follow the order of Malacca (224.74 $Bqkg^{-1}$) < Raub (234.31 $Bqkg^{-1}$) < Kedah (236.31 $Bqkg^{-1}$) < Johor (239.44 $Bqkg^{-1}$) < Lanchang (240.79 $Bqkg^{-1}$) < Selangor (245.55 $Bqkg^{-1}$).

It is observed values of Ra_{eq} in all the study areas were less than the acceptable safe limit of 370 $Bq.kg^{-1}$ (OECD, 1979; UNSCEAR, 1982; UNSCEAR, 1988). Levels of comparable values of the Ra_{eq} have been reported in local studies carried out by Ramli, Hussein & Wood, (2005), Omaret *et al.,* (2006), (2007), Ramli *et al.,* (2009), Lee *et al.,* (2009) and Alzubaidi *et al.,* (2016).

4.5.6.2 Evaluation of the absorbed dose rate (D) in Lanchang

The measured values of the absorbed dose rate (D) in the soil samples from Pahang Lanchang are presented in Table 4.60. The total absorbed dose rate in air varied from 80.8 nGy h^{-1} to 145.3 nGy h^{-1}, with a mean of 110.10±14.6 nGy h^{-1}. The estimated mean value is higher than the global mean value (60 nGy h^{-1}) recommended by UNSCEAR, (2000).

For all the study areas, the mean values of the absorbed dose rate are follow the order of Malacca (103.26 nGy h^{-1}) < Lanchage (110.10 nGy h^{-1}) < Raub (110.90 nGy h^{-1}) < Johor (112.02 nGy h^{-1}) < Kedah (112.86 nGy h^{-1}) < Selangor (113.30 nGy h^{-1}). According UNSCEAR, (2000), ^{232}Th contributes more to the absorbed dose rate in air, where the contribution of each primordial radionuclide to the average gamma absorbed is ^{226}Ra (25 nGy h^{-1}), ^{232}Th (45 nGy h^{-1}) and ^{40}K (30 nGy h^{-1}) for the average activites of ^{226}Ra (33 Bq kg^{-1}), ^{232} Th (45 Bq kg^{-1}) and ^{40}K (420 Bq kg^{-1}).

The mean values of the absorbed dose rate D (n Gy h^{-1}) of agricultural soil groups were higher than the global mean value of 60 nGy h^{-1}. However, the estimated mean values were comparable to the average value of Malaysian 92 nGy h^{-1} established by UNSCEAR, (2000), but higher to those reported in other countries.

The high absorbed dose rate D (n Gy h^{-1}) levels were also reported in other local studies conducted by Tajuddin *et al.,* (1994), Ramli, (1997), Ramli *et al.,* (2005), Ramli, Hussein & Wood, (2005), Omaret *et al.,* (2006), Abdul Rahman & Ramli, (2007), Ramli *et al.,* (2009), Lee *et al.,* (2009), Almayahi *et al.,* (2012a), Almayahi *et al.,* (2012b) and Alzubaidi *et al.,* (2016).

4.5.6.3 **Evaluation of the annual effective dose equivalent (AEDE) in Lanchang**

The measured values of the annual effective dose equivalent in the soil samples from Lanchang are presented in Table 4.60. The values of the outdoor annual effective dose in soil samples varied from 0.10 to 0.18 mSv.y^{-1}, with a mean value of 0.134±0.01 mSv.y^{-1}. For all the study areas, the mean values of the absorbed dose rate are follow the order of Malacca (0.126 mSv y^{-1}) < Raub (0.134 mSv y^{-1}) < Kedah (0.138 mSv y^{-1}) and Selangor (0.138 mSv y^{-1}) < Lanchage (0.340 mSv y^{-1}) < Johor (0.369 mSv.y^{-1}).

The mean value for outdoor lies within the range of the annual average suggested for individual members of the public recommended by the International Committee on Radiological Protection (ICRP) which is 1 mSv year^{-1}. The worldwide average annual effective dose rate is approximately 0.5 mSv year^{-1} UNSCEAR, (2000). Thus, the present values of the annual effective dose rates lie within the recommended levels. Similarly, annual effective dose values within previously recommended levels have been reported in local study couducted by Alias, *et al.,* (2008), Almayahi *et al.,* (2012a), Saat, et al., (2011, June), Hamzah, *et al.,* (2012), Kolo, *et al.,* (2015), Alzubaidi, *et al.,* (2016).

4.5.6.4 **Evaluation of the external hazard index (H_{ex}) in Lanchang**

The measured values of the external hazard index in the soil samples from Lanchang are presented in Table 4.60. The values of H_{ex} varied from 0.47 to 0.84, with a mean value of 0.64 ± 0.08. The obtained value of the external hazard index in the investigated soil of Lanchang falls within the recommended value given by UNSCEAR, (2000) for the protection of the public. The estimated value of H_{ex} must be lower than unity to keep the radiation hazard insignificant. The measured values of all the soil groups were less than the limit (H_{ex} less than or equal to one) established by ECRR**, (**1999); hence, soils from the study areas present low radiation exposure for people that can be used as a construction material without posing any significant radiological threat to the general population.

Local studies conducted by Almayahi, *et al.,* (2012a), Alias, *e al.,* (2008), Almayahi *et al.,* (2012b), Saat, *et al.,* (2011, June), Hamzah, *et al.,* (2012), Kolo, *et al.,* (2015), Alzubaidi, *et al.,* (2016) also reported H_{ex} vlues lower than unity (Table 4.61). For all the study areas, the mean values of the absorbed dose rate follow the order of Malacca

(0.60±0.1) < Kedah (0.63±0.08) < Raub (0.635 ± 0.10) < Lanchage (0.64±0.08) < Johor (0.64±0.1) < Selangor (0.66±0.1).

Table 4.60: The Radiological parameters of the soil samples from Lanchang

Sample ID	Depth cm	D ($nGy.h^{-1}$)	AEDE ($\mu Sv.y^{-1}$)	Ra_{eq} ($Bq.kg^{-1}$)	H_{ex}
PL1	10-20	120.9	0.148	264.40	0.71
PL2	0-10	105.52	0.129	230.78	0.62
PL3	10-20	106.57	0.130	232.73	0.62
PL4	10-20	117.12	0.143	254.53	0.68
PL5	20-30	99.46	0.121	214.74	0.57
PL6	10-20	105.75	0.129	229.06	0.61
PL7	0-10	114.34	0.140	247.02	0.66
PL8	10-20	119.46	0.146	260.43	0.70
PL9	0-10	120.11	0.147	256.92	0.69
PL10	20-30	95.00	0.116	207.21	0.55
PL11	20-30	119.97	0.147	260.67	0.70
PL12	10-20	122.64	0.150	266.51	0.71
PL13	30-40	80.80	0.099	175.58	0.47
PL14	10-20	125.59	0.154	272.21	0.73
PL15	20-30	99.06	0.121	213.75	0.57
PL16	20-30	116.06	0.142	253.92	0.68
PL17	10-20	136.93	0.167	300.20	0.81
PL18	10-20	127.06	0.155	275.43	0.74
PL19	30-40	94.69	0.116	206.52	0.55
PL20	30-40	96.10	0.117	207.40	0.56
PL21	20-30	104.43	0.128	227.25	0.61
PL22	30-40	92.00	0.112	199.61	0.53
PL23	10-20	104.79	0.128	288.74	0.61
PL24	20-30	105.33	0.129	229.63	0.62
PL25	0-10	110.59	0.135	240.85	0.65
PL26	0-10	126.91	0.155	275.02	0.74
PL27	30-40	84.70	0.103	184.76	0.49
PL28	0-10	107.29	0.131	232.43	0.62
PL29	0-10	125.01	0.153	268.94	0.72
PL30	10-20	145.3	0.178	314.65	0.84
PL31	0-10	113.47	0.139	245.22	0.66
PL32	30-40	89.86	0.110	194.74	0.52
PL33	10-20	120.76	0.148	262.33	0.70
PL34	30-40	97.26	0.097	209.90	0.56
PL35	20-30	102.84	0.126	223.75	0.60
Mean		**110.10±14.6**	**0.134±0.01**	**240.79±32.7**	**0.64±0.08**
Range		**80.80 - 145.30**	**0.10 - 0.18**	**175.58 -314.65**	**0.47 - 0.84**

Table 4.61: The average hazard indices of the primordial radionuclides in the worldwide agricultural soils

Location	D (nGy/h)	D_{eff} (mSv/y)	H_{ex}	Reference
Vietnam	71.72	0.54	0.43	Huy *et al.,* (2012)
India	97.47	0.12		Mehra *et al.,* (2011)
Saudi Arabia	23.3	0.14	0.13	Alaamer, (2008)
Malaysia	202.04	0.23	1.19	Musa *et al.,* (2011)
Jordan	51.50	0.06	0.28	Al-Hamarneh & Awadallah (2009)
Pakistan	68.83	0.34	0.39	Rafique *et al.,* (2001)
India	90.1	0.11	0.53	Zubair *et al.,* (2013)
Egypt (Rashid)	118.36	145.16	0.40	EL-Kameesy *et al.,* (2016)
India Karnataka State(	33.23	4.07	0.19	Chandrashekara *et al.,* (2014)
Malaysia	141.62	0.169	0.859	Alzubaidi *et al.,* (2016)
Worldwide	60	0.070	1	UNSCEAR, (2000)

CHAPTER 5: CONCLUSION

The aim of the study was to designe a methodology for investigating the behavior of natural radionuclides and stable metals in the tropics to reach a broader understanding by fill the gaps in the boundary of knowledge and realise the research aim.

The objectives of the research are listed below. All of these objectives were completed as part of the research. Furthermore, the results obtained as a direct consequence of meeting these objectives are stated.

Tropical soils are considered the products of interactions of unique climate and the parent geological materials of the Earth's crust. Weathering within the equatorial climatic regime is the major process contributing to the properties of tropical soils. Due to relatively high temperatures and high-intensity rainfall in parts of the region, weathering is rapid and the strong leaching leads to an abundance of highly stable minerals such as kaolinite and sesquioxides (Naidu *et al.,* 1998).

The distribution of radionuclides in the environment is determined by several main factors, including the source of radionuclides and the mechanism through which they enter; the processes of participation of radionuclides in chemical reactions and their association with other molecules; vertical and horizontal mixing mechanisms (primarily perturbed) may cause dilution and dispersion to parts distant from its place of origin; wet and dry deposition to the Earth's surface may result in its physical removal. Finally, radioactive decay, quantified by the radionuclide's half-life, acts as another removal mechanism.

The results in investigate the behavior of natural radionuclides ^{226}Ra, ^{232}Th and ^{40} K and stable metals in tropical soils indicate that the radionuclide activities of ^{226}Ra, ^{232}Th and ^{40}K of the study areas were found to be higher than the avarge global levels of ^{226}Ra, ^{232}Th, and ^{40}K which are 35, 30, and 400 Bq kg^{-1}, respectively, and higher than those reported in others countries. However, the concentrations were comparable with the values reported in local studies.

The mean ^{226}Ra activity concentrations for the research regions were in the order of Raub < Malacca < Kedah < Johor < Lanchang < Selangor, with a range of 61.811.8Bq kg^{-1} to 67.512.0 Bq kg^{-1}. There were no significant variations in ^{226}Ra concentrations between the study areas.

The mean values of ^{232}Th activity concentrations for the study areas were follow the order of Kedah < Malacca < Raub < Johor < Lanchang < Selangor, with values ranging from 74.9±10.1 Bq kg^{-1} to 84.7±11.2 Bq kg^{-1}. The values of ^{232}Th concentrations differed a slightly between the study areas.

The mean values of ^{40}K activity concentrations for the study areas were follow the order of Malacca < Kedah < Pahang Lanchang < Selangor < Pahang Raub < Johor, with a range differ from 625.1±118.9 Bq kg^{-1} to 759.3±147.3Bq kg^{-1}. There was a minor variance in the levels of ^{40}K concentrations between the research areas.

Before going to the conclusion, it must be emphasized that the tropics investigated were agricultural and homogenous, with identical climatic conditions and management approaches in each location.Therefore, it is assumed that the variance of the sample mean is insignificant. Given the homogeneity of the selected agricultural areas, any variation caused by factors affecting radionuclide distribution will be clearly evident.

Furthermore; the sites chosen had no or with little background information, where the obvious contaminated area does not exist, which reduced bias errors; each sample site was chosen independently of the others, and all subsets of the frame were assigned the same probability. As a consequence, each frame element had an equal chance of being chosen, each frame element had an equal probability of selection.

While spatial divergence factors limits the generalizability of the results, this approach provides new insight into tropical factors. In other word, it is clearly the study gives an opportunity for the emergence of spatial variation factors in the behavior of radionuclides and chemical elements, but it also raises the question of tropical factors.

However, based on the calculated data, the concentrations of ^{226}Ra, ^{232}Th, and ^{40}K were comparable and did not differ considerably between research regions. The lack of noticeable variance in data readings suggests that their behavior susceptible to the same interacting factors and that their paths are linked to unified environmental conditions.

The vertical distribution was regarded as a potential variation between the research groups. The behavior of radionuclides can be shown by vertical distribution, bioavailability, microbial and oxidation states, mineral distribution, soil pH, as well as soil organic components.

In the target tropical interaction environment, the response patterns of the radionuclides and the stable elements varied, but nevertheless, in all study regions they tended to have a common distribution behavior within the soil matrix, as none of the sites showed anomalies in element retention within the soil profiles. While vertical distribution concentrations of ^{226}Ra, ^{232}Th, and ^{40} K differed between research areas, they all showed a tendency to decrease with depth. In general, ^{226}Ra and ^{232}Th activities

showed a comparable tendency and predictable decreasing patterns with depth; however ^{40}K displayed an irregular decreasing pattern. The comparable values of radionuclide concentrations and stable elements, as well as vertical distribution trends, indicate that there is no clear spatial divergence across the research areas.

In tropical environments, almost all organic material that reaches the soil surface decomposes rapidly, so the surface accumulation of soil organic matter OM is minimal. Consequently, there is rapid recycling of nutrients and contaminants into the vegetation (Velasco *et al.,* 2008), There is direct competition between the elements that converge in their ionic radii (Carvalho *et al.,* 2006), and thus a common accumulation mechanism in the soil, and this explains the distribution patterns of radionuclides and the stable elements that showed a growing tendency to decrease within the depth in all study areas.

Regarding the relationships between the radionuclides, stable elements, and other chemical factors in the reaction environment within the soil profiles, the statistics indicated that soil pH was negatively correlated ($P \leq 0.01$) with the radionuclides ^{226}Ra, ^{232}Th and ^{40}K, while OM was positively correlated. The significant correlations between radionuclides and pH and OM reinforce the hypothesis that radionuclides mobility within the soil tropical profile is linked to its extreme factors.

All study areas showed high levels of aluminum (Al) and iron (Fe) concentrations, low soil pH and low organic matter (OM). More generally, these basic findings are consistent with Rieuwerts, (2007) that heavy metals in tropical soils are more mobile and more bioavailable.

The radionuclides ^{226}Ra, ^{232}Th, ^{40}K were positively correlated ($P \leq 0.01$) with P in all the soil groups. With the exception of Kedah and Selangor, K showed significant relationships with radionuclides across the study areas. The correlations between Ca and the radionuclides activities ^{226}Ra, ^{232}Th and ^{40}K were found to be significat in Johor, Lanchang and Raub.

Significant correlations ($P \leq 0.01$) were showed between the Mg and the radionuclides ^{226}Ra, ^{232}Th and ^{40}K in Selangor, Malacca, Johor, and Lanchang. The relationship between Cu and the radionuclides ^{226}Ra, ^{232}Th and ^{40}K were significantly correlated ($P \leq 0.01$) in Selangor, Malacca, Johor and Raub. The correlations were shown to be positive ($P \leq 0.01$) between Zn and the activities of ^{226}Ra, ^{232}Th and ^{40}K in the soils from Kedah, Selangor, Johor and Raub. Manganese (Mn) showed significant correlation with the radionuclides ^{226}Ra, ^{232}Th and ^{40}K in Kedah, Malacca, Johor and Raub. Positive significant relationships were observed between Fe and the activity concentrations of ^{226}Ra in Malacca, Johor and Raub. The correlation between Fe and ^{232}Th were found to be significant in Malacca, while the correlation between Fe and ^{40}K was significant in Lanchang. The correlation between Al and ^{232}Th was shown to be significant in Malacca and Johor, and significant with ^{40}K in Lanchang.

This is an important finding in the understanding of the behavior of radionuclides and stable metals in tropics. The significant correlations between radionuclides and soil physiochemical properties may represent uniform responses to reaction conditions. The rapid recycling of nutrients and pollutants in the vegetation cover due to the lack of organic matter as a result of severe weathering factors makes them participate in the

mechanisms of accumulation within the soil matrix and thus link in significant relationships with each other. This is consistent with Velasco *et al.,* (2008) conclusion that severe weathering, lack of organic matter, and low ion exchange capacity affect radionuclide transport factors in tropical environments.

In recent years, models of the behavior of potentially toxic elements in soils have been developed for temperate soils, which tend to have quite different characteristics to those of tropical soils. The findings of this work give a basis for developing environmental forecasting models in the tropics.

Seasonal changes might also be a possible variation factor since they offer materials that decompose and distributed vertically and horizontally in the soil. Thus, gaining a comprehensive understanding of what is going on and identifying sources of variance.

The oxisols and other highly weathered soil types, including alfisols and ultisols, which predominate in the humid tropics, are important for agriculture and occupy extensive areas of land used for crop and food production. These soils are dominated by low activity sesquioxide minerals (i.e. oxides and of iron and aluminium) (Naidu *et al.,* 1998; Twining & Baxter, 2012).

Based on study of seasonal changes of redox potential and microbial activity in tropical soils, it appeared that that the values of radionuclides concentrations ^{226}Ra, ^{232}Th, ^{40}K and ^{137}Cs were higher in the wet season (growing season) than the dry season (harvest season). During the wet season, microbial activity of fungus and bacteria were positively linked ($P < 0.05$) with radionuclides and (Fe and Mn) oxides. However, microorganisms and oxides are significantly associated with ^{226}Ra and ^{232}Th during the dry season as well.

Seasonal changes were assessed over one area and further data are required to confirm these observations as being consistent seasonal events or as being correlated with other seasonal factors. However, the findings obtained are not inconsistent with expectations and, hence, point to the potential for such factors to be involved.

Remaining issues are the subject of radiation hazard, the study data indicate that the calculated mean values of the radium equivalent activity (Ra_{eq}) for the study areas followed the order of Malacca < Raub < Kedah < Johor < Lanchang < Selangor, with a range values differ from 224.74 $Bqkg^{-1}$ to 245.55 $Bqkg^{-1}$. However, the observed values of Ra_{eq} in the study areas were less than the global average of 370 $Bq.kg^{-1}$. While the computed mean values of the absorbed dose rate (D) for the study locations were in the order of Malacca < Lanchage < Raub < Johor < Kedah < Selangor, with a range values vary from 103.26 nGy h^{-1} to 113.30 nGy h^{-1}. There were considerable discrepancies in the estimated values of the absorbed dose rate across the research regions, which may be attributed to variation in geology formation and geochemical compostion, as well as human activity. The mean values of the absorbed dose rate D (n Gy h^{-1}) in all the soil groups were higher than the global mean value of 60 nGy h^{-1}.

The computed mean annual effective dose equivalent (AEDE) values for the research regions are in the following order: Malaca < Raub < Kedah and Selangor < Lanchage < Johor, with a range of 0.126 $mSv.y^{-1}$ to 0.369 $mSv.y^{-1}$. The calculated mean values of the the external hazard index (H_{ex}) for the study areas followed the order of Malacca < Kedah < Pahang Raub < Pahang Lanchage < Johor < Selangor, with a range values differ from 0.60±0.1 to 0.66±0.1. The present findings confirm that the values of all the soil groups were less than the limit.

These findings provide a potential mechanism for for building forecasting models and support the physicochemical and bio-sorption techniques for the remediation in the tropics.

It is a contribution that can be considered by environmental policymakers to provide a more precise evaluation of the hazards and consequences of chemical exposure on humans and biota. In addition to monitoring the radionuclides in the environment and the paths they follow between soil, water, air, plants and animals. Where, the study approach lays out clear strategies for interpreting results and for more specialized analyses.

5.1 Future Work

Future studies could fruitfully explore these issues further by:

- Study the effect of seasonal changes on the activities of radionuclides in several tropical regions to ensure that the observations made by individual regions are consistent seasonal events and correlated with tropical environmental factors.
- Investigate the impact of root type and plant nutrition needs on radionuclide activity in tropical environments.

REFERENCES

Abdel, M. (2012). Cosmogenic Radionuclides in the Atmosphere: Origin and Applications, Radiation Physics & Protection Conference, Nasr City - Cairo, Egyp.

Adams, J. A., Osmond, J. K., & Rogers, J. J. (1959). The geochemistry of thorium and uranium. *Physics and Chemistry of the Earth*, *3*, 298-348.

Ademoroti, C. M. A. (1996). Environmental chemistry and toxicology. Ibadan: *Foludex Press Ltd*.

Ahad, A., ur Rehman, S., ur Rehman, S., & Faheem, M. (2004). Measurement of radioactivity in the soil of Bahawalpur division, Pakistan. *Radiation Protection Dosimetry*, *112*(3), pp.443-447.

Ahmad, N., Jaafar, M. S., Bakhash, M., & Rahim, M. (2015). An overview on measurements of natural radioactivity in Malaysia. *Journal of Radiation Research and Applied Sciences*, *8*(1), 136-141.

Ahmed, H., Young, S., & Shaw, G. (2012, April). Solubility and mobility of thorium and uranium in soils: The effect of soil properties on Th and U concentrations in soil solution. In *EGU General Assembly Conference Abstracts* (p. 2994).

Ahmed, N. K., & El-Arabi, A. G. M. (2005). Natural radioactivity in farm soil and phosphate fertilizer and its environmental implications in Qena governorate, Upper Egypt. *Journal of Environmental Radioactivity*, *84*(1), 51-64.

Ainsworth, C. C., Pilon, J. L., Gassman, P. L., & Van Der Sluys, W. G. (1994). Cobalt, cadmium, and lead sorption to hydrous iron oxide: residence time effect. *Soil Science Society of America Journal*, *58*(6), 1615-1623.

Akhtar, N., & Tufail, M. (2011). Cancer risk in Pakistan due to natural environmental pollutants. *International Journal of Environmental Research, 5*(1), 159-166.

Akhtar, N., Tufail, M., Ashraf, M., & Iqbal, M. M. (2005). Measurement of environmental radioactivity for estimation of radiation exposure from saline soil of Lahore, Pakistan. *Radiation Measurements*, *39*(1), 11-14.

Alam, M. N., Chowdhury, M. I., Kamal, M., Ghose, S., Banu, H., & Chakraborty, D. (1997). Radioactivity in chemical fertilizers used in Bangladesh. *Applied Radiation and Isotopes, 48(*8), 1165-1168.

Alam, M. N., Chowdhury, M. I., Kamal, M., Ghose, S., Islam, M. N., Mustafa, M. N., ... & Ansary, M. M. (1999). The ^{226}Ra, ^{232}Th and ^{40}K activities in beach sand minerals and beach soils of Cox's Bazar, Bangladesh. *Journal of Environmental Radioactivity, 46*(2), 243-250.

Albarède, F. (2009). Geochemistry: an introduction. Cambridge University Press.

Albrecht, A., Bernstein, G., Cahn, R., Freedman, W. L., Hewitt, J., Hu, W., ... & Suntzeff, N. B. (2006). Report of the dark energy task force. *arXiv preprint astro-ph/0609591*.

Aldrich, L. T., & Wetherill, G. W. (1958). Geochronology by radioactive decay. *Annual Review of Nuclear Science, 8*(1), 257-298.

Alencar, A. S., & Freitas, A. C. (2005). Reference levels of natural radioactivity for the beach sands in a Brazilian southeastern coastal region. *Radiation Measurements*, *40*(1), 76-83.

Alencar, A. S., & Freitas, A. C. (2005). Reference levels of natural radioactivity for the beach sands in a Brazilian southeastern coastal region. *Radiation Measurements, 40*(1), 76-83.

Alexandre, G. A. L., Szikszay, M., & Ligo, M. A. V. (2021). Behavior of copper from agricultural pesticides in the unsaturated and saturated zones in a tropical climate, State of São Paulo, Brazil. In *Water-Rock Interaction* (pp. 851-853).

Al-Hamarneh, I. F., & Awadallah, M. I. (2009). Soil radioactivity levels and radiation hazard assessment in the highlands of northern Jordan. *Radiation Measurements*, *44*(1), 102-110.

Alias, M., Hamzah, Z., Saat, A., Omar, M., & Wood, A. K. (2008). An assessment of absorbed dose and radiation hazard index from natural radioactivity. *Malaysian Journal of Analytical Sciences*, *12*(1), 195-204.

Alipour-Asll, M., Mirnejad, H., & Milodowski, A. E. (2012). Occurrence and paragenesis of diagenetic monazite in the upper Triassic black shales of the Marvast region, South Yazd, Iran. *Mineralogy and Petrology*, *104*(3), 197-210.

Al-Jundi, J. (2002). Population doses from terrestrial gamma exposure in areas near to old phosphate mine, Russaifa, Jordan. *Radiation Measurements, 35*(1), 23-28.

Al-Jundi, J., & Al-Tarazi, E. (2008). Radioactivity and elemental analysis in the Ruseifa municipal landfill, Jordan. *Journal of Environmental Radioactivity*, *99*(1), 190-198.

Al-Jundi, J., Al-Bataina, B. A., Abu-Rukah, Y., & Shehadeh, H. M. (2003). Natural radioactivity concentrations in soil samples along the Amman Aqaba Highway, Jordan. *Radiation Measurements*, *36*(1-6), 555-560.

Allisy, A. (1996). Henri Becquerel: the discovery of radioactivity. *Radiation protection dosimetry, 68*(1-2), 3-10.

Almayahi, B. (2015). NaI (Tl) Spectrometry to Natural Radioactivity Measurements of Soil Samples in Najaf City. *Iranica Journal of Energy Environment, 6*(3), 207-211.

Almayahi, B. A., Tajuddin, A. A., & Jaafar, M. S. (2012 b). Radiation hazard indices of soil and water samples in Northern Malaysian Peninsula. *Applied Radiation and Isotopes, 70*(11), 2652-2660.

Almayahi, B. A., Tajuddin, A. A., & Jaafar, M. S. (2012a). Effect of the natural radioactivity concentrations and $^{226}Ra/^{238}U$ disequilibrium on cancer diseases in Penang, Malaysia. *Radiation Physics and Chemistry, 81*(10), 1547-1558.

Almayahi, B. A., Tajuddin, A. A., & Jaafar, M. S. (2014). Measurements of natural radionuclides in human teeth and animal bones as markers of radiation exposure from soil in the Northern Malaysian Peninsula. *Radiation Physics and Chemistry*, 97, 56-67.

Al-Sulaiti, H., Nasir, T., Al Mugren, K. S., Alkhomashi, N., Al-Dahan, N., Al-Dosari, M., ... & Habib, A. (2012). Determination of the natural radioactivity levels in north west of Dukhan, Qatar using high-resolution gamma-ray spectrometry. *Applied Radiation and Isotopes*, *70*(7), 1344-1350.

Al-Trabulsy, H. A., Khater, A. E. M., & Habbani, F. I. (2011). Radioactivity levels and radiological hazard indices at the Saudi coastline of the Gulf of Aqaba. *Radiation Physics and Chemistry*, *80*(3), 343-348.

Alzubaidi, G., Hamid, F., & Abdul Rahman, I. (2016). Assessment of natural radioactivity levels and radiation hazards in agricultural and virgin soil in the state of Kedah, North of Malaysia. *The Scientific World Journal,* 2016.

Ames, L. L., McGarrah, J. E., Walker, B. A., & Salter, P. F. (1983). Uranium and radium sorption on amorphous ferric oxyhydroxide. *Chemical Geology, 40*(1-2), 135-148.

Amrani, D., & Tahtat, M. (2001). Natural radioactivity in Algerian building materials. *Applied Radiation and Isotopes, 54*(4), 687-689.

Appel, C., & Ma, L. (2002). Concentration, pH, and surface charge effects on cadmium and lead sorption in three tropical soils. *Journal of Environmental Quality*, *31*(2), 581-589.

Appel, C., Ma, L. Q., Rhue, R. D., & Reve, W. (2003). Selectivities of potassium-calcium and potassium-Lead exchange in two tropical soils. *Soil Science Society of America Journal, 67*(6), 1707-1714.

Apriantoro, N. H., Ramli, A. T., & Sutisna, S. (2013). Activity concentration of 238U, 232Th and 40K based on soil types in Perak State, Malaysia. *Earth Science Research, 2*(2), 122.

Arafa, W. (2004). Specific activity and hazards of granite samples collected from the Eastern Desert of Egypt. *Journal of Environmental Radioactivity, 75*(3), 315-327.

Arienzo, M., Christen, E. W., Quayle, W., & Kumar, A. (2009). A review of the fate of potassium in the soil–plant system after land application of wastewaters. *Journal of Hazardous Materials*, *164*(2-3), 415-422.

Arnold, W. D., & Crouse, D. J. (1965). Radium removal from uranium mill effluents with inorganic ion exchangers. *Industrial & Engineering Chemistry Process Design and Development, 4*(3), 333-337.

Ashraf, M. A., Othman, R., & Ishak, C. F. (Eds.). (2017). *Soils of Malaysia*. CRC Press.

Aswathanarayana, U. (1988). Natural radiation environment in the Minjingu phosphorite area, northern Tanzania. In *Health Problems In Connection With Radiation From Radioactive Matter In Fertilizers, Soils and Rocks 2(3), 200-230*.

Aswood, M. S., Jaafar, M. S., & Bauk, S. (2013). Assessment of radionuclide transfer from soil to vegetables in farms from Cameron Highlands and Penang,(Malaysia) using neutron activation analysis. *Applied Physics Research, 5*(5), 85

Atwood, D. A. (Ed.). (2013). *Radionuclides in the Environment*. John Wiley & Sons.

Avila, R., & Moberg, L. (1999). A systematic approach to the migration of 137Cs in forest ecosystems using interaction matrices. *Journal of Environmental Radioactivity*, *45*(3), 271-282.

Ažman, A., Moljk, A., & Pahor, J. (1968). Electron capture in potassium 40. *Zeitschrift Für Physik A Hadrons and Nuclei*, *208*(3), 234-237.

Baeza, A., Del Rio, M., Jimenez, A., Miro, C., & Paniagua, J. (1995). Influence of geology and soil particle size on the surface-area/volume activity ratio for natural radionuclides. *Journal of Radioanalytical and Nuclear Chemistry, 189*(2), 289-299.

Baeza, A., Del Rio, M., Miro, C., & Paniagua, J. (1994). Natural radionuclide distribution in soils of Cáceres (Spain): dosimetry implications. *Journal of Environmental Radioactivity, 23*(1), 19-37.

Baeza, A., Hernández, S., Guillén, F. J., Moreno, G., Manjón, J. L., & Pascual, R. (2004). Radiocaesium and natural gamma emitters in mushrooms collected in Spain. *Science of The Total Environment*, *318*(1-3), 59-71.

Bagshaw, M. (2008). Cosmic radiation in commercial aviation. *Travel Medicine and Infectious Disease, 6(*3), 125-127.

Bajoga, A. D., Alazemi, N., Regan, P. H., & Bradley, D. A. (2015). Radioactive investigation of NORM samples from Southern Kuwait soil using high-resolution gamma-ray spectroscopy. *Radiation Physics and Chemistry, 116*, 305-311.

Baranov, V. I., & Morozova, N. G. (1973). Behavior of natural radionuclides in soils. In Radioecology, Klechkowski, V.M., Polikarpov, G.G., Aleksakhin, R.M., Eds, Wiley, New York 3-29.

Baranov, V. I., Kunasheva, K. G., Morozova, N. G., Pavlotskaya, F. I., & Tyuryukanova, E. B. (1964). Some regularities of distribution and migration of radioactive elements in soil covering in soil covering, 28/P/385.

Baranov, V. I., Morozova, N. G., Kunasheva, K. G., Grigor'ev, G. I., & Vernadskii, V. I. (1963). Geochemistry of some natural radioactive elements in soils. Inst. of *Geochemistry and Analytical Chemistry,* USSR.

Barišić, D., Lulić, S., & Miletić, P. (1992). Radium and uranium in phosphate fertilizers and their impact on the radioactivity of waters. Water Research, 26(5), 607-611.

Barthel, F. H., & Tulsidas, H. (2014). Thorium occurrences, geological deposits and resources. IAEA International Symposium on Uranium Raw Material for Nuclear Energy.

Basham, I. R., & Kemp, S. J. (1994). A review of natural uranium and thorium minerals.

Baxter, M. S. (1991). Personal perspectives on radioactivity in the environment. *Science of the Total Environment*, *100*, 29-42.

Beck, H.L., 1972. The physics of environmental gamma radiation fields. In: *Proceedings 2nd International Symposium on Natural Radiation Environment,* pp.101-301. Houston, Springfield, VA.

Becquerel, H., & Curie, P. (1901). Action physiologique des rayons du radium. *Comptes Rendus*, 132, 1289-1291.

Becquerel, J., & Crowther, J. A. (1948). Discovery of radioactivity. *Nature, 161*(4094), 609.

Beer, J., Muscheler, R., Wagner, G., Laj, C., Kissel, C., Kubik, P. W., & Synal, H. A. (2002). Cosmogenic nuclides during Isotope Stages 2 and 3. *Quaternary Science Reviews*, 21(10), 1129-1139.

Belivermis, M., Kılıç, Ö., Çotuk, Y., Topçuoğlu, S., Coşkun, M., Çayır, A., & Küçer, R. (2008). Radioactivity concentrations in topsoil samples from the Thrace region of Turkey and assessment of radiological hazard. *Radiation Effects & Defects in Solids, 163*(11), 903-913.

Beneš, P., & Poliak, R. (1990). Factors affecting interaction of radiostrontium with river sediments. *Journal of Radioanalytical and Nuclear Chemistry*, *141*(1), 75-90.

Beneš, P., Borovec, Z., & Strejc, P. (1985). Interaction of radium with freshwater sediments and their mineral components: II. Kaolinite and montmorillonite. *Journal of Radioanalytical and Nuclear Chemistry*, *89*(2), 339-351.

Beneš, P., Strejc, P., & Lukavec, Z. (1984). Interaction of Radium with Freshwater Sediments and their Mineral Components. I. Ferric hydroxide and quartz. *Journal of Radioanalytical and Nuclear Chemistry*, *82*(2), 275-285.

Bennett, B. G. (1997). Exposure to natural radiation worldwide. In Proceedings of the Fourth International Conference on High Levels of Natural Radiation: *Radiation Doses and Health Effects,* Beijing, China, 1997 (pp. 15-23).

Beretka, J., & Mathew, P. J. (1985). Natural radioactivity of Australian building materials, industrial wastes and by-products. *Health physics, 48*(1), 87-95.

Berger, A., Gnos, E., Janots, E., Fernandez, A., & Giese, J. (2008). Formation and composition of rhabdophane, bastnäsite and hydrated thorium minerals during alteration: Implications for geochronology and low-temperature processes. *Chemical Geology, 254*(3-4), 238-248.

Bertoncini, E. I., Mattiazzo, M. E., & Rossetto, R. (2005). Sugarcane yield and heavy metal availability in two biosolid-amended Oxisols. *Journal of Plant Nutrition*, *27*(7), 1243-1260.

Bingham, F. T., Page, A. L., & Sims, J. R. (1964). Retention of Cu and Zn by H-montmorillonite. *Soil Science Society of America Journal*, *28*(3), 351-354.

Blake, L., Mercik, S., Koerschens, M., Goulding, K. W. T., Stempen, S., Weigel, A., ... & Powlson, D. S. (1999). Potassium content in soil, uptake in plants and the potassium balance in three European long-term field experiments. *Plant and Soil*, *216*(1), 1-14.

Boenzi, D., Dlouhy, Z., & Lenzi, G. (1965). A Study on the Sorption Properties of Natural Tuffs Occurring in the Lake Bracciano Region (Rome) (No. RT/PROT (65) 19). *Comitatio Nazionale per l'Energia Nucleare*, Rome (Italy).

Bohn, H. L. (1970). Comparisons of measured and theoretical Mn2+ concentrations in soil suspensions. *Soil Science Society of America Journal*, *34*(2), 195-197.

Bolle-Jones, E. W. (1957). Copper: Its effects on the growth and composition of the rubber plant (Hevea brasiliensis). *Plant and soil,* 160-178.

Boukhenfouf, W. (2018). *Concentration de l'uranium: application aux fertilisants agricoles* (Doctoral dissertation). Algeria.

Bréchignac, F., Moberg, L., & Suomela, M. (2000). Long-term environmental behaviour of radionuclides; Recent advances in Europe.

Brookins, D. G. (1988). Thorium. In *Eh-pH Diagrams for Geochemistry* (pp. 158-159). Springer, Berlin, Heidelberg.

Brookins, D. G. (1988). Uranium deposits in sandstones as analogs for spent fuel rod disposal. *Transactions of the American Nuclear Society*, *56*.

Brunner, I., Frey, B., & Riesen, T. K. (1996). Influence of ectomycorrhization and cesium/potassium ratio on uptake and localization of cesium in Norway spruce seedlings. Tree Physiology, 16(8), 705-711.

Burcham, W. E. (1973). Nuclear physics: an introduction, Longman, London.

Burns, P. C., & Finch, R. J. (1999). Wyartite: crystallographic evidence for the first pentavalent-uranium mineral. *American Mineralogist*, *84*(9), 1456-1460.

Butt, K. A., Ali, A., & Qureshi, A. A. (1998). Estimation of environmental gamma background radiation levels in Pakistan. *Health Physics, 75*(1), 63-66.

Cabala, P., & Fassbender, H. W. (1970). Forms of phosphorus in the cacao region of Bahia, Brazil. *Tunialba*, *20*, 439-444.

Campos, M. L., Pierangeli, M. A. P., Guilherme, L. R. G., Marques, J. J., & Curi, N. (2003). Baseline concentration of heavy metals in Brazilian Latosols. *Communications in Soil Science and Plant Analysis*, *34*(3-4), 547-557.

Carvalho, C., Anjos, R. M., Mosquera, B., Macario, K., & Veiga, R. (2006). Radiocesium contamination behavior and its effect on potassium absorption in tropical or subtropical plants. *Journal of Environmental Radioactivity, 86*(2), 241-250.

Carvalho, F., Chambers, D., Fernandes, S., Fesenko, S., Goulet, R., Howard, B., ... & Yankovich, T. (2014). The environmental behaviour of radium: revised edition.

Cathcart, J. B. (1978). Uranium in phosphate rock. University of Michigan.

Cecil, L. D., & Green, J. R. (2000). Radon-222. In Environmental tracers in subsurface hydrology (pp. 175-194). Springer, Boston, MA.

Cember, H. (2009). Interaction of radiation with matter. In "Introduction to Health Physics," ed by H. Cember and TE Johnson.

Cevik, U., Damla, N., Koz, B., & Kaya, S. (2007). Radiological characterization around the Afsin-Elbistan coal-fired power plant in Turkey. Energy & Fuels, 22(1), 428-432.

Chakraborty, S. R., Azim, R., Rahman, A. R., & Sarker, R. (2013). Radioactivity concentrations in soil and transfer factors of radionuclides from soil to grass and plants in the Chittagong city of Bangladesh. J*ournal of Physical Science, 24*(1), 95.

Chao, J. H., & Chuang, C. Y. (2011). Accumulation of radium in relation to some chemical analogues in Dicranopteris linearis. *Applied Radiation and Isotopes, 69*(1), 261-267.

Chew, D. M., & Spikings, R. A. (2015). Geochronology and thermochronology using apatite: time and temperature, lower crust to surface. *Elements*, *11*(3), 189-194.

Choi, Y. H., Lim, K. M., Choi, H. J., Choi, G. S., Lee, H. S., & Lee, C. W. (2005). Plant uptake and downward migration of 85Sr and 137Cs after their deposition on to flooded rice fields: lysimeter experiments with and without the addition of KCl and lime. Journal of Environmental Radioactivity, 78(1), 35-49.

Chougaonkar, M. P., Eappen, K. P., Ramachandran, T. V., Shetty, P. G., Mayya, Y. S., Sadasivan, S., & Raj, V. V. (2004). Profiles of doses to the population living in the high background radiation areas in Kerala, India. *Journal of Environmental Radioactivity, 71*(3), 275-297.

Chowdhury, M. I., Alam, M. N., & Hazari, S. K. S. (1999). Distribution of radionuclides in the river sediments and coastal soils of Chittagong, Bangladesh and evaluation of the radiation hazard. *Applied Radiation and Isotopes, 51*(6), 747-755.

Christophersen, O. A., Lyons, G., Haug, A., Steinnes, E., & Alloway, B. J. (2013). Heavy metals in soils: trace metals and metalloids in soils and their bioavailability.

Clint, G. M., & Dighton, J. (1992). Uptake and accumulation of radiocaesium by mycorrhizal and non-mycorrhizal heather plants. *New Phytologist, 121*(4), 555-561.

Coleman, N. T., Thorup, J. T., & Jackson, W. A. (1960). Phosphate-sorption Reactions That Involve Exchangeable A1. *Soil Science*, *90*(1), 1-7.

Cook, G. T., MacKenzie, A. B., McDonald, P., & Jones, S. R. (1997). Remobilization of Sellafield-derived radionuclides and transport from the north-east Irish Sea. *Journal of Environmental Radioactivity*, *35*(3), 227-241.

Cooper, J. R., Randle, K., & Sokhi, R. S. (2003). Radioactive releases in the environment: impact and assessment. Wiley, New York, United States.

Copplestone, D., Johnson, M. S., & Jones, S. R. (2001). Behaviour and transport of radionuclides in soil and vegetation of a sand dune ecosystem. *Journal of Environmental Radioactivity, 55*(1), 93-108.

Cornell, R. (1993). Adsorption of cesium on minerals: a review. *Journal of Radioanalytical and Nuclear Chemistry*, *171*(2), 483-500.

Coughtrey, P. J., Jackson, D., & Thorne, M. C. (1983). Radionuclide distribution and transport in terrestrial and aquatic ecosystems. *A Critical Review of Data*. Volume 3. AA Balkema.

Cumberland, S. A., Douglas, G., Grice, K., & Moreau, J. W. (2016). Uranium mobility in organic matter-rich sediments: A review of geological and geochemical processes. *Earth-Science Reviews*, *159*, 160-185.

Da Conceicao, F. T., & Bonotto, D. M. (2006). Radionuclides, heavy metals and fluorine incidence at Tapira phosphate rocks, Brazil, and their industrial (by) products. *Environmental Pollution, 139*(2), 232-243.

Dabin, B. (1980). Phosphorus deficiency in tropical soils as a constraint on agricultural output. *Priorities For Alleviating Soil-Related Constraints to Food Production in the Tropics,* 217-233.

Darvill, C. M. (2013). Cosmogenic nuclide analysis. Geomorphological Techniques. British Society for Geomorphology, London, 1-25.

Darwish, S. M., El-Bahi, S. M., Sroor, A. T., & Arhoma, N. F. (2013). Natural radioactivity assessment and radiological hazards in soils from Qarun Lake and Wadi El Rayan in Faiyum, Egypt. Open Journal of Soil Science, 3(07), 289.

Das, B. (2010). Genetic studies on human population residing in High Level Natural Radiation Areas of Kerala coast. BARC News letter, 28-37.

Davies, B. E. (1997). Deficiencies and toxicities of trace elements and micronutrients in tropical soils: limitations of knowledge and future research needs. *Environmental Toxicology and Chemistry: An International Journal*, *16*(1), 75-83.

Dawood, H. I. (2011). Measurement of radioactivity for radium226 isotopes in some soil samples from different regions in Karbala Governorate using gamma ray spectrometry. J. Babylon Univercity /Pure Appl. Sci, 2(19), 562.

De Alcantara, M. A. K., & De Camargo, O. A. (2004). Chromium movement in columns of two highly weathered soils. *Communications in Soil Science and Plant Analysis*, *35*(5-6), 599-613.

De Bortoli, M., & Gaglione, P. (1972). Radium-226 in environmental materials and foods. *Health Physics, 22(*1), 43-48.

De Jesus, A. S. M. (1984). Technological enhancement. In The Behaviour of Radium in Waterways and Aquifers (pp. 87-114).

De Jesus, A. S. M., Malan, J. J., & Basson, J. K. (1980). Movement of radium from South African gold/uranium mine dumps into the aqueous environment. progress report, Source, Distribution, Movement and Deposition of Radium in Inland Waterways and Aquifers (Proc. 4th Research Co-ordination Mtg Vienna, 1980), IAEA, Vienna, 3, 779-783.

De Matos, A. T., Fontes, M. P. F., Da Costa, L. M., & Martinez, M. A. (2001). Mobility of heavy metals as related to soil chemical and mineralogical characteristics of Brazilian soils. *Environmental pollution, 111*(3), 429-435.

De Vicente, I., Huang, P., Andersen, F. Ø., & Jensen, H. S. (2008). Phosphate adsorption by fresh and aged aluminum hydroxide. Consequences for lake restoration. *Environmental Science & Technology, 42*(17), 6650-6655.

Delpoux, M., Dulieu, H., Leonard, A., & Dalebroux, M. (1996). Experimental study of the genetic effects of high levels of natural radiation in South-France.

Dement'ev, V. S., & Syromyatnikov, N. G. (1968). Conditions of formation of a sorption barrier to the migration of uranium in an oxidizing environment. Inst. of Geological Sciences, Alma-Ata, USSR.

Dementyev, V. A., & Syromyatnikov, N. G. (1965). The Form of Thorium Isotopes in Ground Waters. *Geokhimiya _2,* 211.

Department of Agriculture Peninsular Malaysia, 1973. Map of Soil Types in Peninsular Malaysia L-40A Series first ed. Malaysia, Kuala Lumpur.

Department of Geological Survey, 1982. Map of Mineral Resources in Johore State, Malaysia, first ed. (Ipoh, Malaysia).

Derin, M. T., Vijayagopal, P., Venkatraman, B., Chaubey, R. C., & Gopinathan, A. (2012). Radionuclides and radiation indices of high background radiation area in Chavara-Neendakara placer deposits (Kerala, India). PloS One, 7(11), e50468.

Detenbeck, N. E., & Brezonik, P. L. (1991). Phosphorus sorption by sediments from a soft-water seepage lake. 1. An evaluation of kinetic and equilibrium models. *Environmental Science & Technology, 25*(3), 395-403.

Diener, A., & Neumann, T. (2011). Synthesis and incorporation of selenide in pyrite and mackinawite. *Radiochimica Acta, 99*(12), 791-798.

Diener, A., Neumann, T., Kramar, U., & Schild, D. (2012). Structure of selenium incorporated in pyrite and mackinawite as determined by XAFS analyses. *Journal of Contaminant Hydrology, 133*, 30-39.

Dighton, J., Clint, G. M., & Poskitt, J. (1991). Uptake and accumulation of 137Cs by upland grassland soil fungi: a potential pool of Cs immobilization. *Mycological Research, 95*(9), 1052-1056.

Dighton, J., Tugay, T., & Zhdanova, N. (2008). Fungi and ionizing radiation from radionuclides. *FEMS Microbiology Letters, 281*(2), 109-120.

Dlouhy, Z. (1968). Movement of Radinuclides in the Aerated Zone. *Nuclear Research Inst*., Rez, Czechoslovakia.

Dovlete, C., & Povinec, P. P. (2004). Quantification of uncertainty in gamma-spectrometric analysis of environmental samples. *Quantifying Uncertainty in Nuclear Analytical Measurements,* 103.

Dowdall, M., & O'Dea, J. (2002). 226Ra/238U disequilibrium in an upland organic soil exhibiting elevated natural radioactivity. *Journal of Environmental Radioactivity, 59*(1), 91-104.

Dowdall, M., Standring, W., Shaw, G., & Strand, P. (2008). Will global warming affect soil-to-plant transfer of radionuclides?. *Journal of Environmental Radioactivity, 99(*11), 1736-1745.

Dragović, S., Gajić, B., Dragović, R., Janković-Mandić, L., Slavković-Beškoski, L., Mihailović, N., ... & Ćujić, M. (2012). Edaphic factors affecting the vertical distribution of radionuclides in the different soil types of Belgrade, Serbia. *Journal of Environmental Monitoring, 14*(1), 127-137.

Dragović, S., Gajić, B., Janković-Mandić, L., Slavković-Beškoski, L., Mihailović, N., Momčilović, M., & Ćujić, M. (2011). Vertical distribution of radionuclides in soils of varying pedochemistry. *The Enviroment and the Industry,* 122.

Drichko, V. F., & Lisachenko, E. P. (1984). Background concentrations of 226 Ra, 228 Th, and 40 K in cultivated soils and agricultural plants. S*oviet Journal of Ecology, 15*(2), 81-85.

Drissner, J., Bürmann, W., Enslin, F., Heider, R., Klemt, E., Miller, R., ... & Zibold, G. (1998). Availability of caesium radionuclides to plants–classification of soils and role of mycorrhiza. *Journal of Environmental Radioactivity, 41*(1), 19-32.

Duggal, V., Rani, A., Mehra, R., & Ramola, R. C. (2013). Assessment of natural radioactivity levels and associated dose rates in soil samples from Northern Rajasthan, India. *Radiation Protection Dosimetry, 158*(2), 235-240.

Duggar, B. M. (1936). Biological Effects of Radiation: Mechanism and Measurement of Radiation, Applications in Biology, Photochemical Reactions, Effects of Radiant Energy on Organisms and Organic Products (Vol. 2). McGraw-Hill Book Company.

Dunai, T. J. (2010). Cosmogenic nuclides: principles, concepts and applications in the earth surface sciences. Cambridge University Press.

Dzombak, D. A., & Morel, F. M. (1990). Surface complexation modeling: hydrous ferric oxide. John Wiley & Sons.

Eadie, G. G., & Kaufmann, R. F. (1977). Radiological evaluation of the effects of uranium mining and milling operations on selected ground water supplies in the Grants Mineral Belt, New Mexico. *Health Physics, 32*(4), 231-241.

Echevarria, G., Sheppard, M. I., & Morel, J. (2001). Effect of pH on the sorption of uranium in soils. *Journal of Environmental Radioactivity, 53*(2), 257-264.

Echevarria, G., Sheppard, M. I., & Morel, J. (2001). Effect of pH on the sorption of uranium in soils. *Journal of Environmental Radioactivity, 53*(2), 257-264.

Eisenbud, M., & Gesell, T. F. (1997). Environmental radioactivity from natural, industrial and military sources: from *Natural, Industrial and Military Sources*. Elsevier.

Eisenbud, M., & Paschoa, A. S. (1989). Environmental radioactivity. Nuclear Instruments and Methods in Physics Research Section A: Accelerators, Spectrometers, *Detectors and Associated Equipment, 280(*2-3), 470-482.

Eisenbud, M., Gesell, T., & Whicker, F. W. (1997). Environmental Radioactivity from Natural, Industrial, and Military Sources. *Radiation Research, 148(*4), 402-402.

Eisenman, G. (1962). Cation selective glass electrodes and their mode of operation. *Biophysical Journal, 2*(2 Pt 2), 259.

Ek, H., Sjögren, M., Arnebrant, K., & Söderström, B. (1994). Extramatrical mycelial growth, biomass allocation and nitrogen uptake in ectomycorrhizal systems in response to collembolan grazing. *Applied Soil Ecology, 1*(2), 155-169.

El-Arabi, A. M. (2005). Natural radioactivity in sand used in thermal therapy at the Red Sea Coast. *Journal of Environmental Radioactivity, 81*(1), 11-19.

Elejalde, C., Herranz, M., Romero, F., & Legarda, F. (1996). Correlations between soil parameters and radionuclide contents in samples from Biscay (Spain). *Water, Air, and Soil Pollution, 89*(1-2), 23-31.

El-Taher, A., Abbady, A. G., & Uosif, M. A. M. (2006). The ^{226} Ra, ^{232} Th and ^{40} K activities and dose assessment in beach sand used in Climatotherapy From Safaga, Egypt.

Emsbo, P., McLaughlin, P. I., Breit, G. N., du Bray, E. A., & Koenig, A. E. (2015). Rare earth elements in sedimentary phosphate deposits: solution to the global REE crisis?. *Gondwana Research*, *27*(2), 776-785.

Entry, J. A., Watrud, L. S., & Reeves, M. (1999). Accumulation of 137Cs and 90Sr from contaminated soil by three grass species inoculated with mycorrhizal fungi. *Environmental Pollution, 104(*3), 449-457.

Evans, R. D., Keane, A. T., Kolenkow, R. J., Neal, W. R., & Shanahan, M. M. (1969). Radiogenic tumors in the radium and mesothorium ca studied at M.I.T. Massachusetts Inst. of Tech., Cambridge.

Faires, R. A., & Parks, B. H. (1958). Radioisotope laboratory techniques. George Newnes Limited; London.

Faulkner, K., & Vano, E. (2001). Deterministic effects in interventional radiology. Radiation Protection Dosimetry, 94(1-2), 95-98.

Faulkner, K., Järvinen, H., Butler, P., McLean, I. D., Pentecost, M., Rickard, M., & Abdullah, B. (2010). A clinical audit programme for diagnostic radiology: the approach adopted by the International Atomic Energy Agency. Radiation Protection Dosimetry, 139(1-3), 418-421.

Federle, T. W., Dobbins, D. C., Thornton-Manning, J. R., & Jones, D. D. (1986). Microbial biomass, activity, and community structure in subsurface soils. *Groundwater*, *24*(3), 365-374.

Felmlee, J. K., & Cadigan, R. A. (1978). Radium and uranium data for mineral springs in eight Western States. US Department of the Interior, Geological Survey.

Filippelli, G. M. (2011). Phosphate rock formation and marine hosphorus geochemistry: The deep time perspective. *Chemosphere*, *84*(6), 759-766.

Finkel, A. J., Miller, C. E., & Hasterlik, R. J. (1970). Radium-induced malignant tumors in man. *Journal of Occupational and Environmental Medicine, 12*(1), 39.

Finkl C.W. (1999) Tropical soils. In: Environmental Geology. Encyclopedia of Earth Science. Springer, Dordrecht.

Fisica, L. C., & Divisione Materiali, C. N. E. N. (1976). On the structure of highly hydrolyzed Thorium salt solutions. *Acta Chemica Scandinsvica A, 30*, 437-447.

Fitzgerald, W. F., Lamborg, C. H., Holland, H. D., & Turekian, K. K. (2014). Treatise on Geochemistry.

Föllmi, K. B. (1996). The phosphorus cycle, phosphogenesis and marine phosphate-rich deposits. *Earth-Science Reviews*, *40*(1-2), 55-124.

Frame, P. W. (2004). A history of radiation detection instrumentation. *Health Physics, 87*(2), 111-135.

Franca, E. P., Ribeiro, C. C., Teitakowski, M., Londres, H., Santos, P. L., & Albuquerque, H. A. (1965). Survey of radioactive content of food grown on Brazilian areas of high natural radioactivity. *Health Physics, 11*(12), 1471-1484.

Frankel, R. B., & Bazylinski, D. A. (2003). Biologically induced mineralization by bacteria. *Reviews in Mineralogy and Geochemistry, 54*(1), 95-114.

Freitas, A. C., & Alencar, A. S. (2004). Gamma dose rates and distribution of natural radionuclides in sand beaches—Ilha Grande, Southeastern Brazil. J*ournal of Environmental Radioactivity, 75*(2), 211-223.

Fry, C., & Thoennessen, M. (2013). Discovery of actinium, thorium, protactinium, and uranium isotopes. *Atomic Data and Nuclear Data Tables, 99*(3), 345-364.

Fujiyoshi, R., & Sawamura, S. (2004). Mesoscale variability of vertical profiles of environmental radionuclides (^{40}K, ^{226}Ra, ^{210}Pb and ^{137}Cs) in temperate forest soils in Germany. *Science of the Total Environment, 320*(2-3), 177-188.

Gabriel, S., Baschwitz, A., Mathonnière, G., Eleouet, T., & Fizaine, F. (2013). A critical assessment of global uranium resources, including uranium in phosphate rocks, and the possible impact of uranium shortages on nuclear power fleets. *Annals of Nuclear Energy*, *58*, 213-220.

Gadd, G. M. (1997, January). Roles of micro-organisms in the environmental fate of radionuclides. In Ciba Foundation Symposium (pp. 94-103). John Wiley & Sons LTD, United Kingdom.

Geering, H. R., & Hodgson, J. F. (1969). Micronutrient cation complexes in soil solution: III. Characterization of soil solution ligands and their complexes with Zn2+ and Cu2+. *Soil Science Society of America Journal*, *33*(1), 54-59.

Geissler, A., & SELENSKA-POBELL, S. (2005). Addition of U (VI) to a uranium mining waste sample and resulting changes in the indigenous bacterial community. *Geobiology, 3*(4), 275-285.

Gerzabek, M. H., Strebl, F., & Temmel, B. (1998). Plant uptake of radionuclides in lysimeter experiments. *Environmental Pollution, 99*(1), 93-103.

Ghiassi-Nejad, M., Mortazavi, S. M. J., Cameron, J. R., Niroomand-Rad, A., & Karam, P. A. (2002). Very high background radiation areas of Ramsar, Iran: preliminary biological studies. *Health physics, 82*(1), 87-93.

Ghiassi-Nejad, M., Mortazavi, S. M. J., Cameron, J. R., Niroomand-Rad, A., & Karam, P. A. (2002). Very high background radiation areas of Ramsar, Iran: preliminary biological studies. *Health Physics, 82*(1), 87-93.

Giblin, A. M., Batts, B. D., & Swaine, D. J. (1981). Laboratory simulation studies of uranium mobility in natural waters. *Geochimica Et Cosmochimica Acta, 45*(5), 699-709.

Giddings, J. C. (1973). Chemistry, man, and environmental change. San Francisco, Canfield Press.

Giesler, R., Satoh, F., Ilstedt, U., & Nordgren, A. (2004). Microbially available phosphorus in boreal forests: effects of aluminum and iron accumulation in the humus layer. *Ecosystems, 7*(2), 208-217.

Gilmore, G.R. (2008), Practical Gamma-ray Spectrometry (2nd edition), Chichester: John Wiley & Sons Ltd.

Ginzburg, V. L., & Syrovatskii, S. I. (2013). The origin of cosmic rays. Elsevier.

Gnandi, K., & Tobschall, H. (2002). Heavy metals distribution of soils around mining sites of cadmium-rich marine sedimentary phosphorites of Kpogame and Hahotoe (southern Togo). *Environmental Geology, 41*(5), 593-600.

Godoy, J. M., & Godoy, M. L. (2006). Natural radioactivity in Brazilian groundwater. *Journal of Environmental Radioactivity, 85*(1), 71-83.

Godoy, J. M., Carvalho, Z. L. D., Fernandes, F. D. C., Danelon, O. M., Godoy, M. L. D., Ferreira, A. C. M., & Roldão, L. A. (2006). 228Ra and 226Ra in coastal seawater samples from the Ubatuba region: Brazilian southeastern coastal region. *Journal of the Brazilian Chemical Society, 17*(4), 730-736.

Goh, K. J., Härdter, R., & Fairhurst, T. (2003). Fertilizing for maximum return. *Oil Palm: Management for large and sustainable yields*, 279-306.

Gomes, N. C. M., Heuer, H., Schönfeld, J., Costa, R., Mendonca-Hagler, L., & Smalla, K. (2001). Bacterial diversity of the rhizosphere of maize (Zea mays) grown in tropical soil studied by temperature gradient gel electrophoresis. *Plant and soil, 232*(1), 167-180.

Gonçalves, C. C., & Braga, P. F. (2019). Heavy mineral sands in Brazil: deposits, characteristics, and extraction potential of selected Areas. *Minerals, 9*(3), 176.

Górecka, H., & Górecki, H. (1984). Determination of uranium in phosphogypsum. *Talanta, 31*(12), 1115-1117.

Gorycki, T., Lasek, I., Kamiński, K., & Studniarek, M. (2014). Evaluation of radiation doses delivered in different chest CT protocols. *Polish Journal of Radiology, 79,* 1.

Gosse, J. C., & Phillips, F. M. (2001). Terrestrial in situ cosmogenic nuclides: theory and application. *Quaternary Science Reviews, 20*(14), 1475-1560.

Grancea, L., Mihalasky, M., Fairclough, M., Blaise, J. R., Boytsov, A., Hanly, A., ... & Vance, R. (2020). *Uranium Resources, Production and Demand 2020* (No. NEA--7551). Organisation for Economic Co-Operation and Development.

Grandia, F., Merino, J., & Bruno, J. (2008). Assessment of the radium-barium co-precipitation and its potential influence on the solubility of Ra in the near-field (No. SKB-TR--08-07). Swedish Nuclear Fuel and Waste Management Co.

Gray, S. N. (1998). Fungi as potential bioremediation agents in soil contaminated with heavy or radioactive metals. *Biochemical Society Transactions, 26*(4), 666-670.

Greeman, D. J., Rose, A. W., Washington, J. W., Dobos, R. R., & Ciolkosz, E. J. (1999). Geochemistry of radium in soils of the Eastern United States. *Applied Geochemistry, 14*(3), 365-385.

Grieβmeier, J. M., Stadelmann, A., Motschmann, U., Belisheva, N. K., Lammer, H., & Biernat, H. K. (2005). Cosmic ray impact on extrasolar Earth-like planets in close-in habitable zones. *Astrobiology, 5*(5), 587-603.

Grosch, D. (2012). Biological effects of radiations. Elsevier. Academic press, London.

Grubbé, E. H. (1933). Priority in the therapeutic use of X-rays. *Radiology, 21*(2), 156-162.

Guimond, R. J. (1978). Radiological aspects of fertilizer utilization (No. NUREG/CP-0001).

Guimond, R. J. (1990). Radium in fertilizers. Vienna: I*nternational Atomic Energy Agency (IAEA), Technical Report,* (310), 113-128.

Guimond, R. J., & Hardin, J. M. (1989). Radioactivity released from phosphate-containing fertilizers and from gypsum. International Journal of Radiation Applications and Instrumentation. Part C. *Radiation Physics and Chemistry, 34*(2), 309-315.

Guimond, R. J., & Windham, S. T. (1975). Radioactivity distribution in phosphate products, by-products, effluents, and wastes (No. ORP/CSD-75-3). Environmental Protection Agency, Washington, DC (USA). Office of Radiation Programs.

Haas, C. N., & Horowitz, N. D. (1986). Adsorption of cadmium to kaolinite in the presence of organic material. Water, *Air, and Soil Pollution, 27*(1), 131-140.

Haji-Djafari, S., Antommaria, P. E., & Crouse, H. L. (1981). Attenuation of radionuclides and toxic elements by in situ soils at a uranium tailings pond in central Wyoming. In Permeability and Groundwater Contaminant Transport. ASTM International.

Halperin, M. L., & Kamel, K. S. (1998). Potassium. The Lancet, 352(9122), 135-140.

Hamzah, Z., Karim, U. K. A., Saat, A., & Yunus, S. M. (2014). Assessment of naturally occuring radionuclide in the sediment core in southern of Kuala Selangor coastal area. *Malaysian Journal of Analytical Sciences, 18*(2), 284-298.

Hamzah, Z., Rahman, S. A. A., Ahmad Saat, M., & Hamzah, S. (2012). Evaluation of natural radioactivity in soil in district of Kuala Krai, Kelantan. *Malaysian Journal of Analytical Sciences, 16*(3), 335.

Hansen, R. O., & Huntington, G. L. (1969). Thorium movements in morainal soils of the High Sierra, California. *Soil Science, 108*(4), 257-265.

Hansen, R. O., & Stout, P. R. (1968). Isotopic distributions of uranium and thorium in soils. *Soil Science, 105,* pp. 44-50.

Hanson, J. B. (1984). The functions of calcium in plant nutrition. Advances in plant nutrition. *Nuclear Technology & Radiation Protection-1*, p26.

Harmsen, K., & De Haan, F. A. M. (1980). Occurrence and behaviour of uranium and thorium in soil and water. *Netherlands Journal of Agricultural Science, 28*, 40-62.

Hassan, N. M., Mansour, N. A., Fayez-Hassan, M., & Sedqy, E. (2016). Assessment of natural radioactivity in fertilizers and phosphate ores in Egypt. *Journal of Aibah University for Science, 10*(2), 296-306.

Havlik, B., Nycova, B., & Grafova, J. (1968). Radium-226 Liberation from Uranium Ore Processing Mill Waste Solids and Uranium Rocks Into Surface Streams-Ii The Effect of Different Chemical Composition of Surface Water. *Health Physics, 14*(5), 423-430.

Hazen, R. M., Ewing, R. C., & Sverjensky, D. A. (2009). Evolution of uranium and thorium minerals. *American Mineralogist*, *94*(10), 1293-1311.

Heal, O. W., & Horrill, A. D. (1983). Terrestrial ecosystems: an ecological content for radionuclide research. *In Ecological Aspects of Radionuclide Release 22*(1), 331-450.

Helus, F. (2019). Radionuclides Production: Volume 2 (Vol. 2). CRC Press.

Hem, J. D. (1992). Study and interpretation of the chemical characteristics of. *Natural Water-Geological Surwey—Water Suply Paper I*, 4, 73.

Henn, M. R., & Chapela, I. H. (2001). Ecophysiology of 13 C and 15 N isotopic fractionation in forest fungi and the roots of the saprotrophic-mycorrhizal divide. *Oecologia, 128*(4), 480-487.

Henriksen, T., & Maillie, H. D. (2003). Radiation and Health. London and New York: Taylor and Francis Group.

Herpin, U., Cerri, C. C., Carvalho, M. C. S., Markert, B., Enzweiler, J., Friese, K., & Breulmann, G. (2002). Biogeochemical dynamics following land use change from forest to pasture in a humid tropical area (Rondonia, Brazil): a multi-

element approach by means of XRF-spectroscopy. *Science of the Total Environment*, *286*(1-3), 97-109.

Hewamanna, R., Samarakoon, C. M., & Karunaratne, P. A. V. N. (1988). Concentration and chemical distribution of radium in plants from monazite-bearing soils. *Environmental and Experimental Botany, 28*(2), 137-143.

Hewamanna, R., Sumithrarachchi, C. S., Mahawatte, P., Nanayakkara, H. L. C., & Ratnayake, H. C. (2001). Natural radioactivity and gamma dose from Sri Lankan clay bricks used in building construction. *Applied Radiation and Isotopes, 54*(2), 365-369.

Hien, P. D., Hiep, H. T., Quang, N. H., Huy, N. Q., Binh, N. T., Hai, P. S., ... & Bac, V. T. (2002). Derivation of 137Cs deposition density from measurements of 137Cs inventories in undisturbed soils. *Journal of Environmental Radioactivity, 62*(3), 295-303.

Hien, P. D., Hiep, H. T., Quang, N. H., Luyen, T. V., Binh, N. T., Ngo, N. T., ... & Bac, V. T. (2002). Environmental radionuclides in surface soils of Vietnam. *The Scientific World Journal, 2*, 1127-1131.

Ho, C. H., & Miller, N. H. (1986). Adsorption of uranyl species from bicarbonate solution onto hematite particles. *Journal of Colloid and Interface Science, 110*(1), 165-171.

Hobbie, E. A. (2005). Using isotopic tracers to follow carbon and nitrogen cycling of fungi. *Mycology Series, 23*, 361.

Hodgson, J. F. (1963). Chemistry of the micronutrient elements in soils. *Advances in Agronomy*, *15*, 119-159.

Hodgson, J. F., Lindsay, W. L., & Trierweiler, J. F. (1966). Micronutrient cation complexing in soil solution: II. Complexing of zinc and copper in displaced solution from calcareous soils. *Soil Science Society of America Journal*, *30*(6), 723-726.

Hohl, H., & Stumm, W. (1976). Interaction of Pb2+ with hydrous γ-Al2O3. *Journal of Colloid and Interface Science, 55*(2), 281-288.

Holmgren, G. G. S., Meyer, M. W., Chaney, R. L., & Daniels, R. B. (1993). Cadmium, lead, zinc, copper, and nickel in agricultural soils of the United States of America. *Journal of Environmental Quality, 22*(2), 335-348.

Hong, F. D. L. (2002). Tritium, Carbon-14 in the environment [J]. *Radialization Protection, 1.*

Hooda, P. S., & Alloway, B. J. (1998). Cadmium and lead sorption behaviour of selected English and Indian soils. *Geoderma, 84*(1-3), 121-134.

Houtermans, H., Milosevic, O., & Reichel, F. (1980). Half-lives of 35 radionuclides. *The International Journal of Applied Radiation and Isotopes, 31*(3), 153-154.

Hsue, S. T., Langer, L. M., & Tang, S. M. (1966). Precise determination of the shape of the twice forbidden beta spectrum of ^{137}Cs. *Nuclear Physics, 86*(1), 47-55.

Hu, S. J., & Kandaiya, S. (1985). Radium-226 and 232Th concentration in amang. *Health physics, 49*(5), 1003-1007.

Hu, S. J., Chong, C. S., & Subas, S. (1981). 238 U and 232 Th in cassiterites and amang by-products. *Health Physics, 40(*2), 248-250.

Hu, S. J., Kandaiya, S., & Lee, T. S. (1995). Studies of the radioactivity of Amang effluent. *Applied Radiation and Isotopes, 46*(3), 147-148.

Hursh, J. B. (1957). The natural occurrence of radium in man and in waters in food. Brit J Radiol, 7, 45-53.

Hurst, A. (1990). Natural gamma-ray spectrometry in hydrocarbon-bearing sandstones from the Norwegian Continental Shelf. *Geological Society, London, Special Publications*, *48*(1), 211-222.

Hussein, E. M. (1994). Radioactivity of phosphate ore, superphosphate, and phosphogypsum in Abu-Zaabal phosphate plant, Egypt. *Health Physics, 67*(3), 280-282.

Batlle, J. V., Bryan, S., & McDonald, P. (2008). A process-based model for the partitioning of soluble, suspended particulate and bed sediment fractions of plutonium and caesium in the eastern Irish Sea. *Journal of Environmental Radioactivity*, *99*(1), 62-80.

IAEA, (2016). Protection of the Public against Exposure Indoors due to Radon and Other Natural Sources of Radiation. Specific Safety Guide No. SSG-32, Vienna International Centre.

IAstrebov, M. T. (1976). migration uranium 238, radium 226, thorium 232 and potassium 40 into the flood plain soils of superaquatic landscapes of Bityug River. *Vestnik. Seriia VI. Biologiia, pochvovedenie, 83-86.*

Ibrahiem, N. M., el Ghani Abd, A. H., Shawky, S. M., Ashraf, E. M., & Farouk, M. A. (1993). Measurement of radioactivity levels in soil in the Nile Delta and middle Egypt. *Health Physics, 64*(6), 620-627.

Igwe, J. C., Nnororm, I. C., & Gbaruko, B. C. (2005). Kinetics of radionuclides and heavy metals behaviour in soils: Implications for plant growth. *African Journal of Biotechnology, 4*(13).

International Atomic Energy Agency (IAEA) 2004, soil sampling for environmental contaminants. IAEA-TECDOC-1415., Vinna: IAEA.

International Atomic Energy Agency (IAEA), 1979. Gamma-ray surveys in uranium exploration. Technical Report Series No. 186, International Atomic Energy Agency.

International Atomic Energy Agency (IAEA), soil sampling for environmental contaminants. IAEA-TECDOC-1415. 2004, Vinna: IAEA.

International Atomic Energy Agency. The Environmental Behaviour of Radium, Technical Reports Series No. 310, IAEA, Vienna (1990).

International Atomic Energy Agency, The Environmental Behaviour of Radium: Revised Edition, Technical Reports Series No. 476, IAEA, Vienna (2014).

Ioannides, K. G., Mertzimekis, T. J., Papachristodoulou, C. A., & Tzialla, C. E. (1997). Measurements of natural radioactivity in phosphate fertilizers. *Science of the Total Environment, 196*(1), 63-67.

Ion, A. (2014, May). Uranium-238, Thorium-232, Potassium-40 and Cesium-137 in the surface layers of soils from Lehliu area, Romania. *In EGU General Assembly Conference Abstracts* (p. 955).

Iskandar, I. K. (1992). Restoration of metals contaminated soil. *Environmental Restoration of Metals Contaminated Soil, Lewis Publishers*, 59.

Islam, M. R., Lahermo, W. P., Salminen, R., Rojstaczer, S., & Peuraniemi, V. (2000). Lake and reservoir water quality affected by metals leaching from tropical soils, Bangladesh. *Environmental Geology*, *39*(10), 1083-1089.

Iurian, A. R., Phaneuf, M. O., & Mabit, L. (2015). Mobility and bioavailability of radionuclides in soils. *In Radionuclides in the Environment* (pp. 37-59). Springer, Cham.

Iyengar, M. A. R. (1990). The natural distribution of radium. *The environmental Behaviour of Radium, 1,* 59-128.

Izrael, Y. A. (2002). *Radioactive fallout after nuclear explosions and accidents*. Elsevier. Page 260

Jaffey, A. H., Flynn, K. F., Glendenin, L. E., Bentley, W. T., & Essling, A. M. (1971). Precision measurement of half-lives and specific activities of U 235 and U 238. *Physical Review* C, 4(5), 1889.

Jenkins, J. H. (1972). Evaluation of the factors involved in bioaccumulation of gamma-emitting radionuclides in white-tailed deer (Odocoileus virginianus). *Fourth Technical Progress Report, February 1, 1972--January 31, 1973* (No. SRO-642-3). Georgia Univ., Athens. School of Forest Resources.

Johnston, H. M., & Gillham, R. W. (1980). A review of selected radionuclide distribution coefficients of geologic materials. Atomic Energy of Canada Limited Technical Record, TR-90.

Jordan, C., Higgins, A., Hamill, K., & Cruickshank, J. G. (1997). The soil geochemical atlas of Northern Ireland. *Department of Agriculture for Northern Ireland. Belfast. UK*.

Joshi, S. R. (1987). Determination of Lead-210, Radium-226, Thorium-228 and Uranium-238 in Five CCRMP Reference Samples by Gamma-Ray Spectrometry. *Geostandards Newsletter*, *11*(2), 199-201.

Joshi, S. R. (1987). Early Canadian results on the long-range transport of Chernobyl radioactivity. *Science of the total environment*, *63*, 125-137.

Justyn J., Stanek Z., (1968). Investigation of streams contamination by natural radioactive substances (in Czech), Final Report No. S-R-30-238/4, Water Research Institute, Prague.

Kabata-Pendias, A. (2010). *Trace elements in soils and plants*. CRC press. Boca Raton, London.

Kabata-Pendias, A., & Pendias, H. (1992). Trace metals in soils and plants. 2nd Edition, CRC Press, Boca Raton.

Kabata-Pendias, A., Pendias, H., 2001. Trace elements in soils and plants. 3rd ed. CRC. p. 413. Boca Raton, London.

Kalpage, F. S. C. P. (1979). Soils and fertilizers for plantations in Malaysia, *Chemical and Physical Properties of Soils.*

Kaplan, D. I., Seme, R. J., & Piepkho, M. G. (1995). Geochemical factors affecting radionuclide transport through near and far fields at a low-level waste disposal site (No. PNL-10379). Pacific Northwest Lab., Richland, WA (United States).

Karahan, G., & Bayulken, A. (2000). Assessment of gamma dose rates around Istanbul (Turkey). *Journal of Environmental Radioactivity, 47*(2), 213-221.

Karmakar, R., Das, I., Dutta, D., & Rakshit, A. (2016). Potential effects of climate change on soil properties: a review. *Science International, 4*(2), 51-73.

Kathren, R. L. (1984). Radioactivity in the Environment: Sources. Distribution, and Surveillance," Harwood Academic Publishers, London.

Kathren, R. L. (1998). NORM sources and their origins. *Applied Radiation and Isotopes, 49*(3), 149-168.

Kato, K., Konoplev, A., & Kalmykov, S. N. (2020). Behavior of Radionuclides in the Environment I. Springer Singapore.

Kato, K., Nagaosa, K., Kinoshita, T., Kastsuyama, C., Nazina, T. N., Ohnuki, T., & Kalmykov, S. N. (2020). Microbial ecological function in migration of radionuclides in groundwater. In Behavior of Radionuclides in the Environment I (pp. 1-34). Springer, Singapore.

Katyal, J. C., & Sharma, B. D. (1991). DTPA-extractable and total Zn, Cu, Mn, and Fe in Indian soils and their association with some soil properties. *Geoderma*, *49*(1-2), 165-179.

Katz, J. J., Seaborg, G. T., & Morss, L. R. (Eds.). (1987). *The Chemistry of the Actinide Elements: Volume 2*. Springer Netherlands.

Kaufman, R. F., & Bliss, J. D. (1977). Effects of phosphate mineralization and phosphate industry on ^{226}Ra in ground water of central Florida. In Rept. EPA/520-66-77-010. US EPA, Off. of Rad. Program Las Vegas, Nev.

Khater, A. E., & Al-Sewaidan, H. A. (2008). Radiation exposure due to agricultural uses of phosphate fertilizers. *Radiation Measurements, 43*(8), 1402-1407.

Khoo, T. T., & Tan, B. K. (1983, September). Geological evolution of peninsular Malaysia. In Proceedings of the Workshop on Stratigraphic Correlation of Thailand and Malaysia (Vol. 1, pp. 253-290). Geol. Soc. Thailand and Geol. Soc. Malaysia Bangkok.

Kiefer, J. (2012). Biological radiation effects. Springer Science & Business Media. Berlin, Germany.

King, L. D. (1988). Retention of metals by several soils of the southeastern United States (Vol. 17, No. 2, pp. 239-246). American Society of Agronomy, Crop Science Society of America, and Soil Science Society of America.

Kingston, F. J., Posner, A. M., & QUIRK, J. T. (1972). Anion adsorption by goethite and gibbsite: I. The role of the proton in determining adsorption envelopes. *Journal of Soil Science, 23*(2), 177-192.

Kirchmann, R., Darcheville, M., & Koch, G. (1980). Accumulation of radium-226 from phosphate fertilizers in cultivated soils and transfer to crops (No. CONF-780422-(VOL. 2)).

Kirchmann, R., Fagniart, E., & Van Puymbroeck, S. (1966). Studies on foliar contamination by radiocaesium and radiostrontium. *Radiological Concentration Processes*, 475-483.

Kiss, J. J., De Jong, E., & Bettany, J. R. (1988). The distribution of natural radionuclides in native soils of southern Saskatchewan, Canada. *Journal of Environmental Quality, 17*(3), 437-445.

Knoll, G. F. (2000). Radiation Detection and Measurement3rd edition John Wiley and Sons. New York.

Knoll, G. F. (2010). Radiation detection and measurement. John Wiley & Sons. Inc. ISBN: 0-471-07338-5.

Knox, A. S., Seaman, J. C., Mench, M. J., & Vangronsveld, J. (2000). Remediation of metal-and radionuclides-contaminated soils by in situ stabilization techniques. *Environmental Restoration of Metals-Contaminated soils*, 21-60.

Koch-Steindl, H., & Pröhl, G. (2001). Considerations on the behaviour of long-lived radionuclides in the soil. Radiation and environmental biophysics, 40(2), 93-104. uclides in the soil. *Radiation and Environmental Biophysics, 40*(2), 93-104.

Kochupillai, N., Verma, I. C., Grewal, M. S., & Ramalingaswami, V. (1976). Down's syndrome and related abnormalities in an area of high background radiation in coastal Kerala. *Nature, 262*(5563), 60-61.

Koczy, F. F. (1961). Ratio of thorium-230 to thorium-232 in deep-sea sediments. Science, 134(3494), 1978-1979.

Kogan, R. M., Nazarov, I. M., & Fridman, S. D. (1971). *Gamma spectrometry of natural environments and formations: Theory of the method applications to geology and geophysics*. Israel Program for Scientific Translations;[available from the US Department of Commerce, National Technical Information Service, Springfield, Va.].

Kolo, M. T., Aziz, S. A. B. A., Khandaker, M. U., Asaduzzaman, K., & Amin, Y. M. (2015). Evaluation of radiological risks due to natural radioactivity around Lynas Advanced Material Plant environment, Kuantan, Pahang, Malaysia. *Environmental Science and Pollution Research, 22*(17), 13127-13136.

Komura, K., Yanagisawa, M., Sakurai, J., & Sakanoue, M. (1985). Uranium, thorium and potassium contents and radioactive equilibrium states of the uranium and thorium series nuclides in phosphate rocks and phosphate fertilizers. *Radioisotopes, 34*(10), 529-536.

Konoplev, A., Kato, K., & Kalmykov, S. N. (Eds.). (2020). *B*ehavior of Radionuclides in the Environment II: Chernobyl. Springer, *Nature.* Page 265.

Kookana, R. S., & Naidu, R. (1998). Effect of soil solution composition on cadmium transport through variable charge soils. *Geoderma*, *84*(1-3), 235-248.

Kopp, P. M., Burkart, W., & Goerlich, W. (1983). Studies on the uptake of Ra-226 by edible plants under various experimental conditions. Dosimetry, Radionuclides and Technology. Martinus Nijhoff, Amsterdam.

Krane, K. S., & Halliday, D. (1988). Introductory nuclear physics (Vol. 465). New York: Wiley.

Kreuzer, O. P., Markwitz, V., Porwal, A. K., & McCuaig, T. C. (2010). A continent-wide study of Australia's uranium potential: Part I: GIS-assisted manual prospectivity analysis. *Ore Geology Reviews*, *38*(4), 334-366.

Kribek, B. (1979). Sorption of Radionuclides on Natural Sorbents, Faculty of Natural Science, Charles University, Prague (Czech), Rep. P-09–125.

Krishnaswami, S., & Cochran, J. K. (1978). Uranium and thorium series nuclides in oriented ferromanganese nodules: growth rates, turnover times and nuclide behavior. *Earth and Planetary Science Letters, 40*(1), 45-62.

Królak, E., & Karwowska, J. (2010). Potassium-40 and Cesium-137 in the Surface Layers of Arable Soils and Food Supplies. *Polish Journal of Environmental Studies, 19*(3).

Królak, E., Krupa, B., Sarnowska, K., & Karwowska, J. (2008). Isotopes: caesium-137 and potassium-40 in soils of the powiat of Garwolin [Province of Mazowsze]. *Journal of Elementology,* 13(1).

Krupka, K. M. (1999). Review of geochemistry and available Kd values, for cadmium, cesium, chromium, lead, plutonium, radon, strontium, thorium, tritium (3H), and uranium. Understanding Variation in Partition Coefficient, Kd, Values, 2.

Kumar, A., Kumar, M., Singh, B., & Singh, S. (2003). Natural activities of 238U, 232Th and 40K in some Indian building materials. *Radiation Measurements, 36*(1-6), 465-469.

Kumara, P. A. R. P., Mahakumara, P., Jayalath, A., & Jayalath, C. P. (2018). Estimating natural radiation exposure from building materials used in Sri Lanka. *Journal of Radiation Research and Applied Sciences, 20,* 320-433.

Kurnaz, A., Küçükömeroğlu, B., Keser, R., Okumusoglu, N. T., Korkmaz, F., Karahan, G., & Çevik, U. (2007). Determination of radioactivity levels and hazards of soil and sediment samples in Fırtına Valley (Rize, Turkey). *Applied Radiation and Isotopes, 65*(11), 1281-1289.

Lack, J. G., Chaudhuri, S. K., Kelly, S. D., Kemner, K. M., O'Connor, S. M., & Coates, J. D. (2002). Immobilization of radionuclides and heavy metals through anaerobic bio-oxidation of Fe (II). *Applied and Environmental Microbiology, 68*(6), 2704-2710.

Lambert, R., Grant, C., & Sauvé, S. (2007). Cadmium and zinc in soil solution extracts following the application of phosphate fertilizers. *Science of the Total Environment, 378*(3), 293-305.

Langmuir, D., & Herman, J. S. (1980). The mobility of thorium in natural waters at low temperatures. *Geochimica et Cosmochimica Acta, 44*(11), 1753-1766.

Langmuir, D., & Riese, A. C. (1985). The thermodynamic properties of radium. G*eochimica et Cosmochimica Acta, 49*(7), 1593-1601.

L'Annunziata, M. F. (2016). Radioactivity: introduction and history, from the quantum to quarks. Elsevier.

Lapp, R. E., & Andrews, H. L. (1954). Nuclear radiation physics. London: Sir Isaac Pitman and Sons Ltd.

Laul, J. C., & Smith, M. R. (1988). Disequilibrium study of natural radionuclides of uranium and thorium series in cores and briny groundwaters from Palo Duro Basin, Texas (No. PNL/SRP-5783). Pacific Northwest Lab., Richland, WA (USA).

Laul, J. C., Smith, M. R., & Hubbard, N. (1984). Behavior of natural uranium, thorium and radium isotopes in the Wolfcamp brine aquifers, Palo Duro Basin, Texas. MRS Online Proceedings Library Archive, 44.

Lauria, D. C., Ribeiro, F. C. A., Conti, C. C., & Loureiro, F. A. (2009). Radium and uranium levels in vegetables grown using different farming management systems. *Journal of Environmental Radioactivity, 100*(2), 176-183.

Lee, S. K., Wagiran, H., Ramli, A. T., Apriantoro, N. H., & Wood, A. K. (2009). Radiological monitoring: terrestrial natural radionuclides in Kinta District, Perak, Malaysia. J*ournal of Environmental Radioactivity, 100*(5), 368-374.

Leiterer, A., Berard, P., & Menetrier, F. (2010). Thorium and health: state of the art; Thorium et sante. L'état de l'art, French.

Leiterer, A., Berard, P., & Ménétrier, F. (2010). Thorium and health: state of the art (No. CEA-R--6251). CEA Fontenay-aux-Roses.

Leutz, H., Schulz, G., & Wenninger, H. (1965). The decay of potassium-40. *Zeitschrift Für Physik, 187*(2), 151-164.

Lewu, F. B., Volova, T., Thomas, S., & Rakhimol, K. R. (Eds.). (2020). *Controlled release fertilizers for sustainable agriculture*. Academic Press. Page 36.

Ligero, R. A., Ramos-Lerate, I., Barrera, M., & Casas-Ruiz, M. (2001). Relationships between sea-bed radionuclide activities and some sedimentological variables. *Journal of Environmental Radioactivity, 57*(1), 7-19.

Lilley, J. (2013). Nuclear physics: principles and applications. John Wiley & Sons.

Lim, S. E. (2004). The Concentration of Uranium and Thorium in Amang and Ilmenite Samples Collected from Industry (Doctoral dissertation, Universiti Teknologi Malaysia).

Lima, V. T., & Penna-Franca, E. (1988). Uptake of endogenous and exogenous 226Ra by vegetables from soils of a highly radioactive region. *Radiation Protection Dosimetry, 24*(1-4), 123-126.

Lindsay, W. L. (1972). Inorganic phase equilibria of micronutrients in soils. *Micronutrients in Agriculture., 41*-57.

Livens, F. R., & Baxter, M. S. (1988). Particle size and radionuclide levels in some west Cumbrian soils. *Science of the Total Environment, 70*, 1-17.

Lloyd, J. R., & Renshaw, J. C. (2005). Bioremediation of radioactive waste: radionuclide–microbe interactions in laboratory and field-scale studies. *Current Opinion in Biotechnology, 16*(3), 254-260.

Loneragan, J. F. (1975). The availability and absorption of trace elements in soil-plant systems and their relation to movement and concentrations of trace elements in plants. *Trace Elements in Soil-Plant-Animal Systems*, 109-134.

Lopatkina, A. P. (1967). Conditions of accumulation of uranium in peat. Geochem. Int.(Engl. Transl.), 4: 577-88 (1967).

Lorenz, E. (1944). Radioactivity and lung cancer; a critical review of lung cancer in the miners of Schneeberg and Joachimsthal. *Journal of the National Cancer Institute, 5*(1), 1-15.

Lubkowski, K. (2016). Environmental impact of fertilizer use and slow release of mineral nutrients as a response to this challenge. *Polish Journal of Chemical Technology, 18*(1), 72-79.

Lütz, G. (2007). Semiconductor radiation detectors: Device physics. Lutz, Berlin.

Luxin, W., Deqing, C., & Yongling, Y. (1993). Epidemiological Investigation in High Background Radiation Areas of Yangjiang, China. *High Levels of Natural Radiation*, 523.

Maiti, T. C., Smith, M. R., & Laul, J. C. (1989). Sorption of uranium, thorium, and radium on matrices under oxic environments. *Radioactive Waste Management and the Nuclear Fuel Cycle, 11*(3), 269-278.

Makki, N. F., Kadhim, S. A., Alasadi, A. H., & Almayahi, B. A. (2014). Natural Radioactivity Measurements in different regions in Najaf city, Iraq. International *Journal of Computer Trends and Technology, 9*(6), 286-289.

Malanca, A., Gaidolfi, L., Pessina, V., & Dallara, G. (1996). Distribution of 226Ra, 232Th, and 40K in soils of Rio Grande do Norte (Brazil). Journal of *Environmental Radioactivity, 30*(1), 55-67.

Malanca, A., Pessina, V., & Dallara, G. (1993). Assessment of the natural radioactivity in the Brazilian state of Rio Grande do Norte. *Health Physics, 65*(3), 298-302.

Malik, J. A. (Ed.). (2021). *Handbook of Research on Microbial Remediation and Microbial Biotechnology for Sustainable Soil*. IGI Global.

Manning, D. A. (2010). Mineral sources of potassium for plant nutrition. A Review. *Agronomy for Sustainable Development, 30*(2), 281-294.

Mar, S. S., & Okazaki, M. (2012). Investigation of Cd contents in several phosphate rocks used for the production of fertilizer. *Microchemical Journal*, *104*, 17-21.

Marsh, J. W., Blanchardon, E., Gregoratto, D., Hofmann, W., Karcher, K., Nosske, D., & Tomášek, L. (2012). Dosimetric calculations for uranium miners for epidemiological studies. *Radiation Protection Dosimetry, 149*(4), 371-383.

Marshall Cavendish Corporation. (2008). Inventors and Inventions (Vol. 2). Marshall Cavendish.

Martin, A., Harbison, S., Beach, K., & Cole, P. (2018). An introduction to radiation protection. CRC Press (37).

Mason, C. F. V., Turney, W. R. J. R., Thomson, B. M., Lu, N., Longmire, P. A., & Chisholm-Brause, C. J. (1997). Carbonate leaching of uranium from contaminated soils. *Environmental Science & Technology, 31*(10), 2707-2711.

Masters, G. M., & Ela, W. P. (1991). Introduction to environmental engineering and science (Vol. 3). Englewood Cliffs, NJ: Prentice Hall.

Mayfield, D. B., & Lewis, A. S. (2013, April). Environmental review of coal ash as a resource for rare earth and strategic elements. In Proceedings of the 2013 World of Coal Ash (WOCA) Conference, Lexington, KY, USA (Vol. 2013, pp. 22-25).

Mazzilli, B., Palmiro, V., Saueia, C., & Nisti, M. B. (2000). Radiochemical characterization of Brazilian phosphogypsum. *Journal of Environmental Radioactivity, 49*(1), 113-122.

Mbila, M. O., Thompson, M. L., Mbagwu, J. S., & Laird, D. A. (2001). Distribution and movement of sludge-derived trace metals in selected Nigerian soils. *Journal of Environmental Quality, 30*(5), 1667-1674.

McKinley, J. P., Zachara, J. M., Smith, S. C., & Turner, G. D. (1995). The influence of uranyl hydrolysis and multiple site-binding reactions on adsorption of U (VI) to montmorillonite.

McLennan, S. M., & Murray, R. W. (1999). Geochemistry of sediments. In 'Encyclopedia of geochemistry'.(Eds CP Marshall, RW Fairbridge) pp. 282–292.

Means, J. L., Crerar, D. A., & Duguid, J. O. (1978a). Migration of radioactive wastes: radionuclide mobilization by complexing agents. *Science, 200*(4349), 1477-1481.

Means, J. L., Crerar, D. A., Borcsik, M. P., & Duguid, J. O. (1978b). Adsorption of Co and selected actinides by Mn and Fe oxides in soils and sediments. *Geochimica et Cosmochimica Acta, 42*(12), 1763-1773.

Megumi, K. (1979). Radioactive disequilibrium of uranium and actinium series nuclides in soil. Journal of Geophysical Research: *Solid Earth, 84*(B7), 3677-3682.

Megumi, K., & Mamuro, T. (1977). Concentration of uranium series nuclides in soil particles in relation to their size. *Journal of Geophysical Research, 82*(2), 353-356.

Mehra, O. P. (1960). Ion oxide removal from soils and clays by a dithionite-citrate system buffered with sodium bicarbonate in Clays and Clay Minerals. In Proc. 7th Natl. Conf., Washing-ton, DC, 1958. Pergamon Press.

Meinrath, A., Schneider, P., & Meinrath, G. (2003). Uranium ores and depleted uranium in the environment, with a reference to uranium in the biosphere from the Erzgebirge/Sachsen, Germany. *Journal of Environmental Radioactivity, 64*(2-3), 175-193.

Mengel, K., Kirkby, E. A., Kosegarten, H., & Appel, T. (2001). Potassium. *In Principles of Plant Nutrition* (pp. 481-511). Springer, Dordrecht.

Meriwether, J. R., Beck, J. N., Keeley, D. F., Langley, M. P., Thompson, R. H., & Young, J. C. (1988). *Radionuclides in Louisiana soils* (Vol. 17, No. 4, pp. 562-568). American Society of Agronomy, Crop Science Society of America, and Soil Science Society of America.

Meriwether, J. R., Beck, J. N., Keeley, D. F., Langley, M. P., Thompson, R. H., & Young, J. C. (1988). Radionuclides in Louisiana soils. *Journal of Environmental Quality, 17(*4), 562-568.

Mielke, J. E. (1979). Composition of the Earth's crust and distribution of the elements. In: Siegel, F.R. (Ed.), Review of Research on Modern Problems in Geochemistry. UNESCO Report, Paris, pp. 13–37.

Million, J. B., Sartain, J. B., Gonzalez, R. X., & Carrier III, W. D. (1994). Radium-226 and Calcium Uptake by Crops Grown in Mixtures of Sand and Clay Tailings from Phosphate Mining. *Journal of Environmental Quality, 23*(4), 671-676.

Milodowski, A. E., & Zalasiewicz, J. A. (1991). Redistribution of rare earth elements during diagenesis of turbidite/hemipelagite mudrock sequences of Llandovery age from central Wales. *Geological Society, London, Special Publications*, *57*(1), 101-124.

Milodowski, A. E., Pearce, J. M., Basham, I. R., & Hyslop, E. K. (1991). The uranium source-term mineralogy and geochemistry at the Broubster Natural Analogue Site, Caithness (No. EUR--13280). Commission of the European Communities.

Mireles, F., Davila, J. I., Quirino, L. L., Lugo, J. F., Pinedo, J. L., & Rios, C. (2003). Natural soil gamma radioactivity levels and resultant population dose in the cities of Zacatecas and Guadalupe, Zacatecas, Mexico. *Health physics, 84*(3), 368-372.

Mishra, U. C., & Sadasivan, S. (1971). NATURAL RADIOACTIVITY LEVELS IN INDIAN SOILS. Bhabha Atomic Research Centre, Bombay.

Möller, T., Burmeister, S., Ehresmann, B., Heber, B., Labrenz, J., Panitzsch, L., ... & Berger, T. (2012). Altitude Dependence of the Dose Rate from Ground up to the Stratosphere. Verhandlungen der Deutschen Physikalischen Gesellschaft.

Moore, W. (1972). Radium: element and geochemistry. *The Encyclopedia of Geochemistry and Environmental Sciences.* NJ, Van Nostrand Reinhold, 1006-7.

Morris, K., & Raiswell, R. (2002). Biogeochemical cycles and remobilisation of the actinide elements. In Radioactivity in the Environment (Vol. 2, pp. 101-141). Elsevier.

Morrison, S. J., Spangler, R. R., & Tripathi, V. S. (1995). Adsorption of uranium (VI) on amorphous ferric oxyhydroxide at high concentrations of dissolved carbon (IV) and sulfur (VI). *Journal of Contaminant Hydrology, 17*(4), 333-346.

Mouhamad, R., Atiyah, A., & Iqbal, M. (2016). Behavior of Potassium in Soil: A mini review. *Chemistry International, 2*(1), 58-69.

Muhammad, B. G., Jaafar, M. S., Rahman, A. A., & Ingawa, F. A. (2012). Determination of radioactive elements and heavy metals in sediments and soil from domestic water sources in northern peninsular Malaysia. *Environmental Monitoring and Assessment, 184*(8), 5043-5049.

Munkholm, L. J., Esu, I., & Moberg, J. P. (1993). Trace elements in some northern Nigerian soils. *Communications in Soil Science and Plant Analysis, 24*(7-8), 657-672.

Murray, E. G., & Adams, J. A. (1958). Thorium, uranium and potassium in some sandstones. *Geochimica et Cosmochimica Acta, 13*(4), 260-269.

Naeem, M., Ansari, A. A., & Gill, S. S. (Eds.). (2020). *Contaminants in agriculture: sources, impacts and management*. Springer Nature. Page 31.

Naidu, R., Sumner, M. E., & Harter, R. D. (1998). Sorption of heavy metals in strongly weathered soils: an overview. *Environmental Geochemistry and Health, 20*(1), 5-9.

Nair, K. R. R., Nair, M. K., Gangadharan, P., Jayadevan, S., & Jayalakshmy, P. (2000). Natural Background Radiation Level Measurement in Karunagappally taluk, Kerala, India. In Proceedings of the 5th International Conference on High Levels of Natural Radiation & Radon Areas: Munich, Germany(pp. 79-82).

Nathwani, J. S., & Phillips, C. R. (1978). Rates of leaching of radium from contaminated soils: An experimental investigation of radium bearing soils from Port Hope, Ontario. *Water, Air, and Soil Pollution, 9*(4), 453-465.

Nathwani, J. S., & Phillips, C. R. (1979). Adsorption of 226Ra by Soils (I). *Chemosphere, 8*(5), 285-291.

National Council on Radiation Protection and Measurements (NCRP). 1993. Limitation of Exposure to Ionizing Radiation. Report No. 116, NCRP Publications, Bethesda, Maryland. Nations. ISBN: 9211422426.

Navas, A., Machín, J., & Soto, J. (2005). Mobility of natural radionuclides and selected major and trace elements along a soil toposequence in the central Spanish Pyrenees. *Soil Science, 170*(9), 743-757.

Navas, A., Soto, J., & Machın, J. (2002). ^{238}U, ^{226}Ra, ^{210}Pb, ^{232}Th and ^{40}K activities in soil profiles of the Flysch sector (Central Spanish Pyrenees). *Applied Radiation and Isotopes, 57*(4), 579-589.

Navas, A., Soto, J., & Machín, J. (2002). Edaphic and physiographic factors affecting the distribution of natural gamma-emitting radionuclides in the soils of the Arnás catchment in the Central Spanish Pyrenees. *European Journal of Soil Science, 53*(4), 629-638.

Nelson, G., & Reilly, D. (1991). Gamma-ray interactions with matter. *Passive Nondestructive Analysis of Nuclear Materials*, 27-42.

Nelson, J. L., & Melsted, S. W. (1955). The chemistry of zinc added to soils and clays. *Soil Science Society of America Journal*, *19*(4), 439-443.

Ngachin, M., Garavaglia, M., Giovani, C., Njock, M. K., & Nourreddine, A. (2007). Assessment of natural radioactivity and associated radiation hazards in some Cameroonian building materials. *Radiation Measurements, 42*(1), 61-67.

Nguelem, E. J. M., Ndontchueng, M. M., & Motapon, O. (2016). Determination of ^{226} Ra, ^{232} Th, ^{40} K, ^{235} U and ^{238} U activity concentration and public dose assessment in soil samples from bauxite core deposits in Western Cameroon. Springer Plus, 5(1), 1253.

Nierop, K. G., Tonneijck, F. H., Jansen, B., & Verstraten, J. M. (2007). Organic matter in volcanic ash soils under forest and páramo along an Ecuadorian altitudinal transect. *Soil Science Society of America Journal*, *71*(4), 1119-1127.

Nikolova, I., Johanson, K. J., & Dahlberg, A. (1997). Radiocaesium in fruitbodies and mycorrhizae in ectomycorrhizal fungi. *Journal of Environmental Radioactivity, 37*(1), 115-125.

Nishita, H., Romney, E. M., & Larson, K. H. (1961). Uptake of radioactive fission products by crop plants. *Journal of Agricultural and Food Chemistry, 9*(2), 101-106.

Norvell, W. A., & Lindsay, W. L. (1969). Reactions of EDTA complexes of Fe, Zn, Mn, and Cu with soils. Soil Sci. Soc. Am. Proc. 33:86-91.

Nuclear Energy Agency. (1979). Exposure to radiation from the natural radioactivity in building materials: report. OECD.

Nyamangara, J., & Mzezewa, J. (1999). The effect of long-term sewage sludge application on Zn, Cu, Ni and Pb levels in a clay loam soil under pasture grass in Zimbabwe. *Agriculture, Ecosystems & Environment, 73*(3), 199-204.

OECD, 1979. Organization for economic cooperation and development exposure to radiation from natural radioactivity in building materials. Report by a group of experts of the OECD Nuclear Energy Agency, OECD, Paris

Ogunsanwo, F. O., Olowofela, J. A., Okeyode, I. C., Idowu, O. A., & Olurin, O. T. (2019). Aeroradio spectrometry in the spatial formation characterization of Ogun State, south-western, Nigeria. *Scientific African, 6*, e00204.

Ogunsanwo, F. O., Olurin, O. T., Ogunsanwo, B. T., Okeyode, I. C., & Olowofela, J. A. (2019). Correlations between airborne and terrestrial gamma-ray spectrometric data in the bitumen deposit area, Ogun State, Nigeria. *Scientific African, 5,* e00133.

Ohno, T., Muramatsu, Y., Miura, Y., Oda, K., Inagawa, N., Ogawa, H., ... & Sato, M. (2012). Depth profiles of radioactive cesium and iodine released from the Fukushima Daiichi nuclear power plant in different agricultural fields and forests. *Geochemical Journal, 46(*4), 287-295.

Omar, M., Ali, H. M., Abu, M. P., Kontol, K. M., Ahmad, Z., Ahmad, S. H. S. S., ... & Hamzah, R. (2004). Distribution of radium in oil and gas industry wastes from Malaysia. *Applied Radiation and Isotopes, 60*(5), 779-782.

Omar, M., Hassan, A., & Sulaiman, I. (2006). Radiation exposure during travelling in Malaysia. *Radiation Protection Dosimetry, 121*(4), 456-460.

Onyatta, J. O., & Huang, P. M. (1999). Chemical speciation and bioavailability index of cadmium for selected tropical soils in Kenya. *Geoderma*, *91*(1-2), 87-101.

Örgün, Y., Altınsoy, N., Gültekin, A. H., Karahan, G., & Celebi, N. (2005). Natural radioactivity levels in granitic plutons and groundwaters in Southeast part of Eskisehir, Turkey. *Applied Radiation and Isotopes, 63*(2), 267-275.

Osburn, W. S. (1965). Primordial radionuclides: their distribution, movement, and possible effect within terrestrial ecosystems. *Health Physics, 11*(12), 1275-1295.

Osburn, W. S. (1967). Ecological concentration of nuclear fallout in a Colorado mountain watershed. *In Radioecological Concentration Processes* (pp. 675-709). Pergamon.

Östhols, E. (1994). Some processes affecting the mobility of thorium in natural ground waters (No. TRITA-OOK--1038). Royal Inst. of Tech.

Palm, C., Sanchez, P., Ahamed, S., & Awiti, A. (2007). Soils: A contemporary perspective. Annu. Rev. Environ. *Resour., 32,* 99-129.

Paramananthan, S., Fairhurst, T., & Härdter, R. (2003). Oil palm–Management for large and sustainable yields. Singapore: Potash & Phosphate Institute/Potash & Phosphate Institute of Canada (PPI/PPIC) and International Potash Institute (IPI), 27-57.

Paramanathan, S. (1978). Register of Soils-Peninsular Malaysia. Soils and Analytical Services Bulletin-Kementerian Pertanian (Malaysia).

Parekh, N. R., & Bardgett, R. D. (2002). The characterisation of microbial communities in environmental samples. *In Radioactivity in the Environment* (Vol. 2, pp. 37-60). Elsevier.

Parekh, N. R., Poskitt, J. M., Dodd, B. A., Potter, E. D., & Sanchez, A. (2008). Soil microorganisms determine the sorption of radionuclides within organic soil systems. *Journal of Environmental Radioactivity, 99*(5), 841-852.

Paschoa, A. S., Mafra, O. Y., Cardoso, D. O., & Rocha, A. C. S. (1984). Application of SSNTD to the Brazilian phosphate fertilizer industry to determine uranium concentrations. *Nuclear Tracks and Radiation Measurements* (1982), 8(1-4), 469-472.

Paul, A. C., Pillai, P. M. B., Haridasan, P. P., Radhakrishnan, S., & Krishnamony, S. (1998). Population exposure to airborne thorium at the high natural radiation areas in India. *Journal of Environmental Radioactivity, 40*(3), 251-259

Pavlidou, S., Koroneos, A., Papastefanou, C., Christofides, G., Stoulos, S., & Vavelides, M. (2006). Natural radioactivity of granites used as building materials. *Journal of Environmental Radioactivity, 89*(1), 48-60.

Payne, T. E., & Edis, R. (2012). Mobility of radionuclides in tropical soils and groundwater. *In Radioactivity in the Environment* (Vol. 18, pp. 93-120). Elsevier.

Payne, T. E., Davis, J. A., & Waite, T. D. (1994). Uranium retention by weathered schists-the role of iron minerals. *Radiochimica Acta, 66*, 297-297.

Payne, T. E., Hatje, V., Itakura, T., McOrist, G. D., & Russell, R. (2004). Radionuclide applications in laboratory studies of environmental surface reactions. *Journal of Environmental Radioactivity*, *76*(1-2), 237-251.

Pereira, C. E., Vaidyan, V. K., Sunil, A., Ben Byju, S., Jose, R. M., & Jojo, P. J. (2011). Radiological assessment of cement and clay based building materials from southern coastal region of Kerala. *Indian Journal of Pure & Applied Physics, 49*, 372-376.

Peterson, J., MacDonell, M., Haroun, L., Monette, F., Hildebrand, R. D., & Taboas, A. (2007). Radiological and chemical fact sheets to support health risk analyses for contaminated areas. *Argonne National Laboratory Environmental Science Division,* 133.

Petigara, B. R., Blough, N. V., & Mignerey, A. C. (2002). Mechanisms of hydrogen peroxide decomposition in soils. *Environmental Science & Technology*, *36*(4), 639-645.

Pettersson, H. B. L., Hallstadius, L., Redvall, R., & Holm, E. (1988). Radioecology in the vicinity of prospected uranium mining sites in a subarctic environment. *Journal of environmental radioactivity, 6*(1), 25-40.

Poinssot, C., & Geckeis, H. (2012). Overview of radionuclide behaviour in the natural environment. *In Radionuclide Behaviour in the Natural Environment* (pp. 1-10).

Porcelli, D., Andersson, P. S., Wasserburg, G. J., Ingri, J., & Baskaran, M. (1997). The importance of colloids and mires for the transport of uranium isotopes through the Kalix River watershed and Baltic Sea. *Geochimica et Cosmochimica Acta, 61*(19), 4095-4113.

Post, J. E. (1999). Manganese oxide minerals: Crystal structures and economic and environmental significance. *Proceedings of the National Academy of Sciences,* 96(7), 3447-3454.

Pratt, P. F. (1965). Potassium. Methods of Soil Analysis: Part 2 *Chemical and Microbiological Properties,* 9, 1022-1030.

Pufahl, P. K., & Groat, L. A. (2017). Sedimentary and igneous phosphate deposits: formation and exploration: an invited paper. *Economic Geology*, *112*(3), 483-516.

Quindos, L. S., Fernandez, P. L., Soto, J., Rodenas, C., & Gómez, J. (1994). Natural radioactivity in Spanish soils. *Health physics, 66*(2), 194-200.

Rahman, A. A., & Ramli, A. T. (2007). Radioactivity levels of 238U and 232Th, the α and β activities and associated dose rates from surface soil in Ulu Tiram, Malaysia. *Journal of Radioanalytical and Nuclear Chemistry, 273*(3), 653-657.

Rahman, M. M., Koddus, A., Ahmad, G. U., & Voigt, G. (2005). Soil-to-plant transfer of radiocaesium for selected tropical plant species in Bangladesh. *Journal of Environmental Radioactivity*, *83*(2), 199-211.

Rahman, Z. A., Gikonyo, E. W., Silek, B., Goh, K. J., & Soltangheisi, A. (2014). Evaluation of phosphate rock sources and rate of application on oil palm yield grown on peat soils of Sarawak, Malaysia. *Italian Journal of Agronomy*, *13*(1), 12-22.

Ramadan, K. A., Badran, H. M., Seddeek, M. K., & Sharshar, T. (2009). Radiological Studies in the Hot Spring Region of Oyoun Mossa and Hammam Faraun Thermal Spring Areas in Western Sinai.

Ramasamy, V., Sundarrajan, M., Suresh, G., Paramasivam, K., & Meenakshisundaram, V. (2014). Role of light and heavy minerals on natural radioactivity level of high background radiation area, Kerala, India. A*pplied Radiation and Isotopes, 85*, 1-10.

Ramasamy, V., Suresh, G., Meenakshisundaram, V., & Ponnusamy, V. (2011). Horizontal and vertical characterization of radionuclides and minerals in river sediments. *Applied Radiation and Isotopes, 69*(1), 184-195.

Ramli, A. T. (1997). Environmental terrestrial gamma radiation dose and its relationship with soil type and underlying geological formations in Pontian District, Malaysia. *Applied Radiation and Isotopes, 48*(3), 407-412.

Ramli, A. T., Apriantoro, N. H., & Wagiran, H. (2009 a). Assessment of radiation dose rates in the high terrestrial gamma radiation area of Selama District, Perak, Malaysia. *Applied Physics Research, 1*(2), 45.

Ramli, A. T., Apriantoro, N. H., Wagiran, H., Wood, A. K., & Kuan, L. S. (2009 b). Health risk implications of high background radiation dose rate in Kampung Sungai Durian, Kinta District, Perak, Malaysia. *Global Journal of Health Science,* 1(2), 140

Ramli, A. T., Hussein, A. W. M., & Lee, M. H. (2001). Geological influence on terrestrial gamma radiation dose rate in the Malaysian State of Johore. *Applied Radiation and Isotopes, 54*(2), 327-333.

Ramli, A. T., Hussein, A. W. M., & Wood, A. K. (2005 a). Environmental 238U and 232Th concentration measurements in an area of high level natural background radiation at Palong, Johor, Malaysia. *Journal of Environmental Radioactivity,* 80(3), 287-304.

Ramli, A. T., Sahrone, S., & Wagiran, H. (2005 b). Terrestrial gamma radiation dose study to determine the baseline for environmental radiological health practices in Melaka state, Malaysia. *Journal of Radiological Protection, 25*(4), 435.

Ramli, S. H., & Samsudin, A. R. (2014, September). Study of movement of the western and central belts of Peninsular Malaysia using GPS data analysis. In AIP Conference Proceedings (Vol. 1614, No. 1, pp. 750-755). American Institute of Physics.

Reddy, K. R., O Connor, G. A., & Gale, P. M. (1998). Phosphorus sorption capacities of wetland soils and stream sediments impacted by dairy effluent. *Journal of Environmental Quality, 27*(2), 438-447.

Reddy, M. R., & Perkins, H. F. (1974). Fixation of zinc by clay minerals. *Soil Science Society of America Journal*, *38*(2), 229-231.

Reeves, R. D. (2003). Tropical hyperaccumulators of metals and their potential for phytoextraction. *Plant and Soil*, *249*(1), 57-65.

Richardson, K. A. (1968). Thorium, uranium, and potassium in the Conway granite, New Hampshire, USA. Rice Univ., Houston, Tex.

Riesen, T. K., & Brunner, I. (1996). Effect of ectomycorrhizae and ammonium on 134Cs and 85Sr uptake into Picea abies seedlings. *Environmental Pollution,* 93(1), 1-8.

Rieuwerts, J. S. (2007). The mobility and bioavailability of trace metals in tropical soils: a review. *Chemical Speciation & Bioavailability, 19*(2), 75-85.

Rieuwerts, J. S., Ashmore, M. R., Farago, M. E., & Thornton, I. (2006). The influence of soil characteristics on the extractability of Cd, Pb and Zn in upland and moorland soils. *Science of the total Environment, 366*(2-3), 864-875.

Robison, W., Conrado, C., Hamilton, T., & Stoker, A. (2000). The effect of carbonate soil on transport and dose estimates for long-lived radionuclides at a US Pacific Test Site. *Journal of Radioanalytical and Nuclear Chemistry, 243*(2), 459-465.

Roessler, C. E. (1990). Control of radium in phosphate mining, beneficiation and chemical processing. *The environmental behaviour of radium, 2*, 270-279.

Roessler, C. E., Smith, Z. A., Bolch, W. E., & Prince, R. J. (1979). Uranium and radium-226 in Florida phosphate materials. *Health Physics, 37*(3), 269-277.

Rogers, J. J. W., & Adams, J. A. S. (1969). Handbook of geochemistry. Springer, Berlin, II/3, sections, 90.

Röster, H. J.; Lange, H. (Geochemische Tabellen, Verlag Grundstoffind., Leipzig 1965, pp. 1/328).

Roto, R., Kartini, I., Motuzas, J., Triyana, K., Siswanta, D., Wahyuningsih, T. D., & Kusumaatmaja, A. (Eds.). (2019). *Symposium of Materials Science and Chemistry*. Trans Tech Publications Ltd.

Ruess, L., Häggblom, M. M., Langel, R., & Scheu, S. (2004). Nitrogen isotope ratios and fatty acid composition as indicators of animal diets in belowground systems. *Oecologia, 139*(3), 336-346

Ruess, L., Tiunov, A., Haubert, D., Richnow, H. H., Häggblom, M. M., & Scheu, S. (2005). Carbon stable isotope fractionation and trophic transfer of fatty acids in fungal based soil food chains. *Soil Biology and Biochemistry, 37*(5), 945-953.

Rusanova, G. V. (1962). Study of leaching and migration of radium in soils. *Soviet Soil Sci, 9*, 962-964.

Rutherford, P. M., Dudas, M. J., & Samek, R. A. (1994). Environmental impacts of phosphogypsum. *Science of the Total Environment, 149*(1-2), 1-38.

Saad, H. R., & Al-Azmi, D. (2002). Radioactivity concentrations in sediments and their correlation to the coastal structure in Kuwait. *Applied Radiation and Isotopes,* 56(6), 991-997.

Saat, A., Kassim, N., & Hamzah, Z. (2011, June). Measurement of natural radioactivity levels in soil samples in research station at National Park area in Malaysia. In Sustainable Energy & Environment (ISESEE), 2011 3rd *International Symposium & Exhibition* in (pp. 177-180). IEEE

Sachett, I. A. (2002). Caracterização da radiação gama ambiental em áreas urbanas utilizando uma unidade móvel de rastreamento. Rio de Janeiro: Instituto de Biociências Nucleares, Universidade do Estado do Rio de Janeiro.

Sahoo, S. K., Hosoda, M., Kamagata, S., Sorimachi, A., Ishikawa, T., Tokonami, S., & Uchida, S. (2011). Thorium, uranium and rare earth elements concentration in weathered Japanese soil samples. Prog. Nucl. Sci. *Technol, 1*, 416-419.

Sahoo, S. K., Mohapatra, S., Sethy, N. K., Patra, A. C., Shukla, A. K., Kumar, A. V., ... & Puranik, V. D. (2010). Natural radioactivity in roadside soil along Jamshedpur- Musabani road: a mineralised and mining region, Jharkhand and associated risk. *Radiation Protection Dosimetry, 140*(3), 281-286.

Sahoo, S., Yonehara, H., Kurotaki, K., Shiraishi, K., Ramzaev, V., & Barkovski, A. (2001). Determination of rare earth elements, thorium and uranium by inductively coupled plasma mass spectrometry and strontium isotopes by thermal ionization mass spectrometry in soil samples of Bryansk region contaminated due to Chernobyl accident. *Journal of Radioanalytical and Nuclear Chemistry, 247*(2), 341-345.

Saleh, H. E. D. M., & Rahman, R. O. A. (2018). Principles and Applications in Nuclear Engineering-Radiation Effects, Thermal Hydraulics, Radionuclide Migration in the Environment. IntechOpen.

Saleh, H., & Shayeb, M. A. (2014). Natural radioactivity distribution of southern part of Jordan (Ma′ an) Soil. *Annals of Nuclear Energy, 65*, 184-189.

Saleh, M. A., Ramli, A. T., Alajerami, Y., & Aliyu, A. S. (2013). Assessment of natural radiation levels and associated dose rates from surface soils in Pontian District, Johor, Malaysia. J Ovonic Res, 9(1), 17-27.

Salomons, W., & Forstner, U. (1984). Metals in the Hydrocycle Springer-Verlag. Berlin. Heidelberg New York, 349.

Sample, E. C., Soper, R. J., & Racz, G. J. (1980). Reactions of phosphate fertilizers in soils. The role of phosphorus in agriculture, (theroleofphosph), 263-310.

Sanchez, A. L., Parekh, N. R., Dodd, B. A., & Ineson, P. (2000). Microbial component of radiocaesium retention in highly organic soils. Soil Biology and Biochemistry, 32(14), 2091-2094.

Sanchez, P. A. (2019). Properties and Management of Soils in the Tropics. Cambridge University Press.

Sanchez, P. A., Ahamed, S., Carré, F., Hartemink, A. E., Hempel, J., Huising, J., ... & Zhang, G. L. (2009). Digital Soil Map of the World. *Science, 325*(5941), 680-681.

Sanderman, J., & Amundson, R. (2014). 10.7-Biogeochemistry of decomposition and detrital processing. *Treatise Geochem, 2nd edn. Elsevier Ltd*, 217-272.

Santos Júnior, J. A. D., Cardoso, J. J. R. F., Silva, C. M. D., Silveira, S. V., & Amaral, R. D. S. (2005). Analysis of the 40K levels in soil using gamma spectrometry. *Brazilian Archives of Biology and Technology, 48*(SPE2), 221-228.

Santos, I. R., Burnett, W. C., & Godoy, J. M. (2008). Radionuclides as tracers of coastal processes in Brazil: review, synthesis, and perspectives. *Brazilian Journal of Oceanography*, *56*(2), 115-130.

Saunders, J. A., Pritchett, M. A., & Cook, R. B. (1997). Geochemistry of biogenic pyrite and ferromanganese coatings from a small watershed: a bacterial connection?. *Geomicrobiology Journal, 14*(3), 203-217.

Saw, S. H. (2007). The population of Malaysia. Institute of Southeast Asian Studies. Malaysia.

Sawhney, B. L., & Brown, K. W. (1989). *Reactions and movement of organic chemicals in soils*. Soil Science Society of America.

Scholten, L. C., & Timmermans, C. W. M. (1995). Natural radioactivity in phosphate fertilizers. *Fertilizer Research, 43*(1-3), 103-107.

Schroeder, D. (1978). Structure and weathering of potassium containing minerals. *IPI Research topics*, 5-25.

Schroeyers, W. (Ed.). (2017). Naturally Occurring Radioactive Materials in Construction: Integrating Radiation Protection in Reuse (Cost Action Tu1301 NORM4BUILDING). Woodhead Publishing.

Schwarcz, H. P., Gascoyne, M., & Ford, D. C. (1982). Uranium-series disequilibrium studies of granitic rocks. *Chemical Geology, 36*(1-2), 87-102.

Schwertmann, U. (1964). Differenzierung der eisenoxide des bodens durch extraktion mit ammoniumoxalat-Lösung. Zeitschrift Für Pflanzenernährung, *Düngung, Bodenkunde, 1*05(3), 194-202.

Shahbazi-Gahrouei, D. (2003). Natural background radiation dosimetry in the highest altitude region of Iran. *Journal of Radiation Research, 44*(3), 285-287.

Shamshuddin, J., & Auxtero, E. A. (1991). Soil solution compositions and mineralogy of some active acid sulfate soils in Malaysia as affected by laboratory incubation with lime. *Soil Science, 152*(5), 365-376.

Shamshuddin, J., & Ismail, H. (1995). Reactions of ground magnesium limestone and gypsum in soils with variable-charge minerals. *Soil Science Society of America Journal, 5*9(1), 106-112.

Shamsuddin, S. A., Yusop, Z., & Noguchi, S. (2014). Influence of plantation establishment on discharge characteristics in a small catchment of tropical forest. *International Journal of Forestry Research,* 2014.

Sheppard, M. I., & Thibault, D. H. (1988). Migration of technetium, iodine, neptunium, and uranium in the peat of two minerotrophic mires. *Journal of Environmental Quality, 17*(4), 644-653.

Sheppard, M. I., & Thibault, D. H. (1990). Default soil solid/liquid partition coefficients, Kdsmallcap˜ S, for four major soil types: a compendium. *Health Physics, 59*(4), 471-482.

Sheppard, S. C., & Sheppard, M. I. (1988). Modeling estimates of the effect of acid rain on background radiation dose. *Environmental Health Perspectives, 78*, 197.

Sheppard, S. C., Evenden, W. G., & Pollock, R. J. (1989). Uptake of natural radionuclides by field and garden crops. *Canadian Journal of Soil Science, 69*(4), 751-767.

Shishkunova, L. V., Grashchenko, S. M., & Strukov, V. N. (1989). Entry of uranium, thorium, and radium isotopes into plants from soils and fertilizers. *Soviet Radiochemistry* (English Translation), 30(3), 362-367.

Shleien, B., Slaback, L. A., & Birky, B. K. (Eds.). (1998). Handbook of health physics and radiological health. Baltimore: Williams & Wilkins.

Sill, C. W. (1977). Determination of thorium and uranium isotopes in ores and mill tailings by alpha spectrometry. *Analytical chemistry, 49*(4), 618-621.

Simon, S. L., & Ibrahim, S. A. (1987). The plant/soil concentration ratio for calcium, radium, lead, and polonium: Evidence for non-linearity with reference to substrate concentration. *Journal of Environmental Radioactivity, 5*(2), 123-142.

Singh, S., Rani, A., & Mahajan, R. K. (2005). ^{226}Ra, ^{232}Th and ^{40}K analysis in soil samples from some areas of Punjab and Himachal Pradesh, India using gamma ray spectrometry. *Radiation Measurements, 39*(4), 431-439.

Smolders, E., Kiebooms, L., Buysse, J., & Merckx, R. (1996). 137Cs uptake in spring wheat (Triticum aestivum L. cv. Tonic) at varying K supply. II. A potted soil experiment. *Plant and Soil, 181*(2), 211-220.

Sodré, F. F., Lenzi, E., & Costa, A. C. S. D. (2001). Utilização de modelos físico-químicos de adsorção no estudo do comportamento do cobre em solos argilosos. *Química Nova, 24*(3), 324-330.

Sohrabi, M. (1998). The state-of-the-art on worldwide studies in some environments with elevated naturally occurring radioactive materials (NORM). *Applied Radiation and Isotopes, 49*(3), 169-188.

Spalding, R. F., & Sackett, W. M. (1972). Uranium in runoff from the Gulf of Mexico distributive province: anomalous concentrations. *Science*, *175*(4022), 629-631.

Steiner, M., Linkov, I., & Yoshida, S. (2002). The role of fungi in the transfer and cycling of radionuclides in forest ecosystems. *Journal of Environmental Radioactivity, 58*(2-3), 217-241.

Stoulos, S., Manolopoulou, M., & Papastefanou, C. (2003). Assessment of natural radiation exposure and radon exhalation from building materials in Greece. *Journal of Environmental Radioactivity, 69*(3), 225-240.

Strain, C. D., Watson Jr, J. E., & Fong, S. W. (1979). An evaluation of 226 Ra and 222 Rn concentrations in ground and surface water near a phosphate mining and manufacturing facility. *Health physics, 37*(6), 779-783.

Strandberg, M., & Johansson, M. (1998). 134Cs in heather seed plants grown with and without mycorrhiza. Journal of Environmental Radioactivity, 40(2), 175-184.

Stranden, E. R. L. I. N. G. (1976). Some aspects on radioactivity of building materials. Phys. Norv, 8(3), 163-167.

Sturchio, N. C., Banner, J. L., Binz, C. M., Heraty, L. B., & Musgrove, M. (2001). Radium geochemistry of ground waters in Paleozoic carbonate aquifers, midcontinent, USA. *Applied Geochemistry, 16(*1), 109-122.

Sully, M. J., Flocchini, R. G., & Nielsen, D. R. (1987). Linear distribution of naturally occurring radionuclides in a mollic xerofluvent. S*oil Science Society of America Journal, 51*(2), 276-281.

Sunta, C. M. (1993, August). A review of the studies of high background areas of the SW coast of India. In Proceedings of the International Conference on High Levels of Natural Radiation, Ramsar, IAEA (pp. 71-86).

Tajuddin, A. A., Hu, S. J., & Sakanoue, M. (1994). Continuous measurements of radiation levels along the west coast highway of Peninsular Malaysia. *Applied Radiation and Isotopes, 45*(11), 1117-1119.

Tajuddin, A. A., Hu, S. J., & Sakanoue, M. (1994). Continuous measurements of radiation levels along the west coast highway of Peninsular Malaysia. *Applied Radiation and Isotopes, 45*(11), 1117-1119.

Tamponnet, C., Martin-Garin, A., Gonze, M. A., Parekh, N., Vallejo, R., Sauras-Yera, T., ... & Shaw, G. (2008). An overview of BORIS: bioavailability of radionuclides in soils. *Journal of Environmental Radioactivity, 99*(5), 820-830.

Tamponnet, C., Plassard, C., Parekh, N., & Sanchez, A. (2001). Impact of micro-organisms on the fate of radionuclides in rhizospheric soils (pp. 175-185). EDP Science.

Taskayev, A. I., Ovchenkov, V. Y., Aleksakhin, R. M., & Shuktomova, I. I. (1977). Uptake of radium-226 by plants and change in its state in the soilplant tops-litterfall system. *Soviet Soil Science, 9*, 79-85.

Taskin, H., Karavus, M., Ay, P., Topuzoglu, A., Hidiroglu, S., & Karahan, G. (2009). Radionuclide concentrations in soil and lifetime cancer risk due to gamma radioactivity in Kirklareli, Turkey. *Journal of Environmental Radioactivity, 100*(1), 49-53

Taylor, M. D. (2007). Accumulation of uranium in soils from impurities in phosphate fertilisers. *Landbauforschung Volkenrode, 57*(2), 133.

Taylor, S. R. (1964). Trace element abundances and the chondritic earth model. *Geochimica et Cosmochimica Acta, 28*(12), 1989-1998.

Teixera, V.S., Penna Franca, E., "Distribution of 226Ra into six fractions of agricultural soils from Pocos de Caldas, Minas Gerais State, Brazil, contaminated in the laboratory", Annals of the 8th Annual Congr. of the *Brazilian Biophysical Society*, Rio de Janeiro (1979).

Temgoua, E., Pfeifer, H. R., & Bitom, D. (2003). Trace element differentiation in ferruginous accumulation soil patterns under tropical rainforest of southern Cameroon, the role of climatic change. *Science of the Total Environment, 303*(3), 203-214.

Temminghoff, E. J., Van der Zee, S. E., & de Haan, F. A. (1997). Copper mobility in a copper-contaminated sandy soil as affected by pH and solid and dissolved organic matter. *Environmental Science & Technology, 31*(4), 1109-1115.

Tesoriero, A. J., & Pankow, J. F. (1996). Solid solution partitioning of Sr^{2+}, Ba^{2+}, and Cd^{2+} to calcite. *Geochimica et Cosmochimica Acta, 60*(6), 1053-1063.

Thomas, G. W., & Swoboda, A. R. (1962). Cation exchange in kaolinite-iron oxide systems. *Clays and Clay Minerals*, *11*(1), 321-326.

Titaeva, N. A., & Taskaev, A. I. (1983). Review of investigations on U, Tr, Ra isotopes migration in biosphere. In Migration of heavy natural radionuclides in conditions of humid zone.

Trudell, S. A., Rygiewicz, P. T., & Edmonds, R. L. (2004). Patterns of nitrogen and carbon stable isotope ratios in macrofungi, plants and soils in two old-growth conifer forests. *New Phytologist, 164(*2), 317-335.

Tsai, T. L., Liu, C. C., Chuang, C. Y., Wei, H. J., & Men, L. C. (2011). The effects of physico-chemical properties on natural radioactivity levels, associated dose rate and evaluation of radiation hazard in the soil of Taiwan using statistical analysis. J*ournal of Radioanalytical and Nuclear Chemistry, 288*(3), 927-936.

Tufail, M. (2012). Enhancement of natural radioactivity in fertilized soil of Faisalabad, Pakistan. *Environmental Science and Pollution Research, 19*(8), 3327-3338.

Tufail, M., Akhtar, N., & Waqas, M. (2006). Measurement of terrestrial radiation for assessment of gamma dose from cultivated and barren saline soils of Faisalabad in Pakistan. *Radiation Measurements, 41*(4), 443-451

Twining, J. R., & Baxter, M. (Eds.). (2012). Tropical Radioecology (Vol. 18). Elsevier.

Twining, J. R., Payne, T. E., & Itakura, T. (2004). Soil–water distribution coefficients and plant transfer factors for 134Cs, 85Sr and 65Zn under field conditions in tropical Australia. *Journal of Environmental Radioactivity*, *71*(1), 71-87.

Twining, J. R., Zaw, M., Russell, R., & Wilde, K. (2004). Seasonal changes of redox potential and microbial activity in two agricultural soils of tropical Australia: some implications for soil-to-plant transfer of radionuclides. *Journal of Environmental Radioactivity, 76*(1-2), 265-272.

Tyuryukanova, E. B., & Kalugina, V. A. (1971). behavior of thorium in soils. Ecology NY.

Tzortzis, M., Svoukis, E., & Tsertos, H. (2004). A comprehensive study of natural gamma radioactivity levels and associated dose rates from surface soils in Cyprus. *Radiation Protection Dosimetry, 109*(3), 217-224.

Uchida, S. (2007). Radionuclides in tropical and subtropical ecosystems. *Radioactivity in the Environment, 10*, 193-209.

Uchida, S. (2007). Radionuclides in tropical and subtropical ecosystems. *Radioactivity in the Environment*, *10*, 193-209.

Udom, B. E., Mbagwu, J. S. C., Adesodun, J. K., & Agbim, N. N. (2004). Distributions of zinc, copper, cadmium and lead in a tropical ultisol after long-term disposal of sewage sludge. *Environment International, 30*(4), 467-470.

United Nations. Scientific Committee on the Effects of Atomic Radiation. (2000). Sources and effects of ionizing radiation: sources (Vol. 1). United Nations Publications.

United Nations. Scientific Committee on the Effects of Atomic Radiation. (2008). Effects of ionizing radiation: UNSCEAR 2006 Report to the General Assembly, with scientific annexes (Vol. 2). United Nations Publications.

United Nations. Scientific Committee on the Effects of Atomic Radiation. (1994). Sources and Effects of Ionizing Radiation: United Nations Scientific Committee on the Effects of Atomic Radiation: UNSCEAR 1994 Report to the General Assembly, with Scientific Annexes (Vol. 49). United Nations Publications.

United Nations. Scientific Committee on the Effects of Atomic Radiation. (1977). Sources and Effects of Ionizing Radiation; 1977 Report to the General Assembly with Annexes. UN.

UNSCEAR, "Effects of Atomic Radiation to the General Assembly" in United Nations Scientific Committee on the Effect of Atomic Radiation. (UNSCEAR) (2000) United Nations: New York.

UNSCEAR, "Exposure from natural sources of radiation," in United Nations Scientific Committee on the Effect of Atomic Radiation. (1993) United Nations: New York.

UNSCEAR, "Ionising Radiation: Sources, and Biological Effect." United Nations Scientific Committee on the Effect of Atomic Radiation. (1982) New York: United Nations. ISBN: 9211422426.

UNSCEAR, "Sources and Effects of Ionizing Radiation." in United Nations Scientific Committee on the Effect of Atomic Radiation. (1977) United Nations: New York.

UNSCEAR, "Sources, Effect and Risk of Ionising Radiation," in United Nations Scientific Committee on the Effect of Atomic Radiation. (1988) United Nations: New York. ISBN: 92- 1-142143-8.

UNSCEAR, 1993. Exposure from natural sources of radiation, in United Nations Scientific Committee on the Effect of Atomic Radiation., United Nations: New York.

UNSCEAR, 2000. Sources effects and risks of ionizing radiation. United Nations Scientific Committee on the effects of Atomic Radiation, Report to the general Assembly, with annexes, United Nations, New York.

UNSCEAR, A. (2000). United Nations Scientific Committee on the Effects of Atomic Radiation. Sources and effects of ionizing radiation, 2.

UNSCEAR, S. (1988). Effects and Risks of Ionizing Radiation. United Nations, New York, 565-571.

UNSCEAR, United Nations Scientific Committee on the Effect of Atomic Radiation, 1988. Sources, effects and risk of ionizing radiation, United Nations, New York.

UNSCEAR, United Nations Scientific Committee on the Effect of Atomic Radiation, 1993. Exposure from natural sources of radiation, United Nations, New York.

UNSCEAR. Sources, Effects and Risks of Ionizing Radiations; Report to the General Assembly, with Scientific Annexes; United Nations: New York, NY, USA, 1998; pp. 42–85.

Valcke, E., & Cremers, A. (1994). Sorption-desorption dynamics of radiocaesium in organic matter soils. Science of the Total Environment, 157, 275-283.

Valcke, E., & Cremers, A. (1994). Sorption-desorption dynamics of radiocaesium in organic matter soils. Science of the Total Environment, 157, 275-283.

Valkovic, V. (2000). Radioactivity in the environment: physicochemical aspects and applications. Elsevier.

Van Hullebusch, E. D., Lens, P. N., & Tabak, H. H. (2005). Developments in bioremediation of soils and sediments polluted with metals and radionuclides. 3. Influence of chemical speciation and bioavailability on contaminants immobilization/mobilization bio-processes. *Reviews in Environmental Science and Bio/Technology, 4*(3), 185-212.

Vandenhove, H., & Van Hees, M. (2007). Predicting radium availability and uptake from soil properties. *Chemosphere, 69*(4), 664-674.

Vandenhove, H., Eyckmans, T., & Van Hees, M. (2005). Can barium and strontium be used as tracers for radium in soil–plant transfer studies?. *Journal of Environmental Radioactivity, 81*(2-3), 255-267.

Vandenhove, H., Gil-García, C., Rigol, A., & Vidal, M. (2009). New best estimates for radionuclide solid–liquid distribution coefficients in soils. Part 2. Naturally

occurring radionuclides. *Journal of Environmental Radioactivity, 100*(9), 697-703.

Vasconcellos, L. M. H., Amaral, E. C. S., Vianna, M. E., & Franca, E. P. (1987). Uptake of 226Ra and 210Pb by food crops cultivated in a region of high natural radioactivity in Brazil. *Journal of Environmental Radioactivity, 5*(4), 287-302.

Veiga, R., Sanches, N., Anjos, R.M., Macario, K., Bastos, J., Iguatemy, M., Aguiar, J.G., Santos, A.M.A., Mosquera, B., Carvalho, C. and Baptista Filho, M., 2006. Measurement of natural radioactivity in Brazilian beach sands. *Radiation Measurements, 41*(2), pp.189-196.

Velasco, H., Ayub, J. J., & Sansone, U. (2008). Analysis of radionuclide transfer factors from soil to plant in tropical and subtropical environments. *Applied Radiation and Isotopes, 66*(11), 1759-1763.

Vinogradov, A. P. (1957). Biological role of potassium-40. *Nature, 180*(4584), 507-508.

Von Uexkull, H. R. (1986). Efficient fertilizer use in acid upland soils of the humid tropics (No. 10). Food & Agriculture Org.

Vučić, N., & Ilić, Z. (1989). Extraction and spectrophotometric determination of uranium in phosphate fertilizers. *Journal of Radioanalytical and Nuclear Chemistry, 129*(1), 113-120.

Vukasinovic, I., Djordjevic, A., Rajkovic, M., Todorovic, D., & Pavlovic, V. (2010). Distribution of natural radionuclides in anthrosol-type soil. *Turkish Journal of Agriculture and Forestry, 34*(6), 539-546.

Waite, T. D., Davis, J. A., Payne, T. E., Waychunas, G. A., & Xu, N. (1994). Uranium (VI) adsorption to ferrihydrite: Application of a surface complexation model. *Geochimica et Cosmochimica Acta*, *58*(24), 5465-5478.

Wasserman, M. A., Pérez, D. V., & Bourg, A. C. (2002). Behavior of cesium-137 in some Brazilian oxisols. *Communications in Soil Science and Plant Analysis, 33*(7-8), 1335-1349.

Wasserman, S. R., Soderholm, L., & Staub, U. (1998). Effect of surface modification on the interlayer chemistry of iron in a smectite clay. *Chemistry of Materials, 10*(2), 559-566.

Weber, J. B., & Miller, C. T. (1989). Organic chemical movement over and through soil. *Reactions and Movement of Organic Chemicals in Soils, 22*, 305-334.

Wedepohl, K H. (1978). Handbook of Geochemistry: Volume II/5 Elements La(57) to U(92). Springer-Verlag, Berlin, Heidleberg & New York.

Wedepohl, K. H. (1995). The composition of the continental crust. *Geochimica et Cosmochimica Acta, 59*(7), 1217-1232.

Wei, L., & Sugahara, T. (2000). An introductory overview of the epidemiological study on the population at the high background radiation areas in Yangjiang, China. *Journal of Radiation Research, 41*(Suppl), S1-S7.

Wei, L., & Sugahara, T. (2000). An introductory overview of the epidemiological study on the population at the high background radiation areas in Yangjiang, China. *Journal of Radiation Research, 41*(Suppl), S1-S7.

Wilcke, W., Kretzschmar, S., Bundt, M., & Zech, W. (1999). Metal concentrations in aggregate interiors, exteriors, whole aggregates, and bulk of Costa Rican soils. *Soil Science Society of America Journal, 63*(5), 1244-1249.

Wilcke, W., Müller, S., Kanchanakool, N., Niamskul, C., & Zech, W. (1999). Urban soil contamination in Bangkok: concentrations and patterns of polychlorinated biphenyls (PCBs) in topsoils. *Soil Research, 37*(2), 245-254.

Willett, I. R., & Bond, W. J. (1995). Sorption of manganese, uranium, and radium by highly weathered soils (Vol. 24, No. 5, pp. 834-845). American Society of Agronomy, Crop Science Society of America, and Soil Science Society of America.

Willett, I. R., & Bond, W. J. (1995). Sorption of manganese, uranium, and radium by highly weathered soils. *Journal of Environmental Quality, 24*(5), 834-845.

Witkamp, M. (1968). Accumulation of 137Cs by Trichoderma viride relative to 137Cs in soil organic matter and soil solution. *Soil Science, 106*(4), 309-311.

Wong, C. L., Venneker, R., Uhlenbrook, S., Jamil, A. B. M., & Zhou, Y. (2009). Variability of rainfall in Peninsular Malaysia. *Hydrology and Earth System Sciences Discussions, 6*(4), 5471-5503.

Wu, S., Wang, L., Zhao, L., Zhang, P., El-Shall, H., Moudgil, B., ... & Zhang, L. (2018). Recovery of rare earth elements from phosphate rock by hydrometallurgical processes–A critical review. *Chemical Engineering Journal*, *335*, 774-800.

Yamazaki, I. M., & Geraldo, L. P. (2003). Uranium content in phosphate fertilizers commercially produced in Brazil. *Applied Radiation and Isotopes, 59*(2-3), 133-136.

Yanagisawa, K., Takeda, H., Miyamoto, K., & Fuma, S. (2000). Transfer of technetium from paddy soil to rice seedling. *Journal of Radioanalytical and Nuclear Chemistry, 243*(2), 403-408.

Yang, Y. X., Wu, X. M., Jiang, Z. Y., Wang, W. X., Lu, J. G., Lin, J., ... & Hsia, Y. F. (2005). Radioactivity concentrations in soils of the Xiazhuang granite area, China. *Applied Radiation and Isotopes, 63*(2), 255-259.

Yasir, M. S., Ab Majid, A., & Yahaya, R. (2007). Study of natural radionuclides and its radiation hazard index in Malaysian building materials. Journal of *Radioanalytical and Nuclear Chemistry, 273*(3), 539-541.

Zach, R., Hawkins, J. L., & Mayoh, K. R. (1989). Transfer of fallout cesium-137 and natural potassium-40 in a boreal environment. *Journal of Environmental Radioactivity, 10*(1), 19-45.

Zakeri, F., Rajabpour, M. R., Haeri, S. A., Kanda, R., Hayata, I., Nakamura, S., ... & Ahmadpour, M. J. (2011). Chromosome aberrations in peripheral blood lymphocytes of individuals living in high background radiation areas of Ramsar, Iran. *Radiation and Environmental Biophysics, 50*(4), 571-578.

Zarcinas, B. A., Ishak, C. F., McLaughlin, M. J., & Cozens, G. (2004). Heavy metals in soils and crops in Southeast Asia. *Environmental Geochemistry and Health, 26*(3), 343-357.

Zaw, M., Szymczak, R., & Twining, J. (2002). Application of synchrotron radiation technique to analysis of environmental samples. Nuclear Instruments and Methods in Physics Research Section B: *Beam Interactions With Materials and Atoms,* 190(1-4), 856-859.

Zechmeister, H. G., Hohenwallner, D., Riss, A., & Hanus-Illnar, A. (2003). Variations in heavy metal concentrations in the moss species Abietinella abietina (Hedw.) Fleisch. according to sampling time, within site variability and increase in biomass. *Science of the Total Environment, 301*(1-3), 55-65.

Zhdanova, N. N., Tugay, T., Dighton, J., Zheltonozhsky, V., & Mcdermott, P. (2004). Ionizing radiation attracts soil fungi. *Mycological Research, 108*(9), 1089-1096.

Zimdahl, R. L., & Skogerboe, R. K. (1977). Behavior of lead in soil. *Environmental Science & Technology, 11*(13), 1202-1207.